

Studies in Systems, Decision and Control 418

Alla G. Kravets  
Alexander A. Bolshakov  
Maxim Shcherbakov *Editors*

# Cyber-Physical Systems: Modelling and Industrial Application

 Springer

# **Studies in Systems, Decision and Control**

Volume 418

## **Series Editor**

Janusz Kacprzyk, Systems Research Institute, Polish Academy of Sciences,  
Warsaw, Poland

The series “Studies in Systems, Decision and Control” (SSDC) covers both new developments and advances, as well as the state of the art, in the various areas of broadly perceived systems, decision making and control—quickly, up to date and with a high quality. The intent is to cover the theory, applications, and perspectives on the state of the art and future developments relevant to systems, decision making, control, complex processes and related areas, as embedded in the fields of engineering, computer science, physics, economics, social and life sciences, as well as the paradigms and methodologies behind them. The series contains monographs, textbooks, lecture notes and edited volumes in systems, decision making and control spanning the areas of Cyber-Physical Systems, Autonomous Systems, Sensor Networks, Control Systems, Energy Systems, Automotive Systems, Biological Systems, Vehicular Networking and Connected Vehicles, Aerospace Systems, Automation, Manufacturing, Smart Grids, Nonlinear Systems, Power Systems, Robotics, Social Systems, Economic Systems and other. Of particular value to both the contributors and the readership are the short publication timeframe and the world-wide distribution and exposure which enable both a wide and rapid dissemination of research output.

Indexed by SCOPUS, DBLP, WTI Frankfurt eG, zbMATH, SCImago.

All books published in the series are submitted for consideration in Web of Science.

More information about this series at <https://link.springer.com/bookseries/13304>

Alla G. Kravets · Alexander A. Bolshakov ·  
Maxim Shcherbakov  
Editors

# Cyber-Physical Systems: Modelling and Industrial Application

 Springer

*Editors*

Alla G. Kravets  
Volograd State Technical University  
Volograd, Russia

Alexander A. Bolshakov  
Peter the Great St. Petersburg  
Polytechnic University  
St. Petersburg, Russia

Maxim Shcherbakov   
Volograd State Technical University  
Volograd, Russia

ISSN 2198-4182

ISSN 2198-4190 (electronic)

Studies in Systems, Decision and Control

ISBN 978-3-030-95119-1

ISBN 978-3-030-95120-7 (eBook)

<https://doi.org/10.1007/978-3-030-95120-7>

© The Editor(s) (if applicable) and The Author(s), under exclusive license to Springer Nature Switzerland AG 2022

This work is subject to copyright. All rights are solely and exclusively licensed by the Publisher, whether the whole or part of the material is concerned, specifically the rights of translation, reprinting, reuse of illustrations, recitation, broadcasting, reproduction on microfilms or in any other physical way, and transmission or information storage and retrieval, electronic adaptation, computer software, or by similar or dissimilar methodology now known or hereafter developed.

The use of general descriptive names, registered names, trademarks, service marks, etc. in this publication does not imply, even in the absence of a specific statement, that such names are exempt from the relevant protective laws and regulations and therefore free for general use.

The publisher, the authors and the editors are safe to assume that the advice and information in this book are believed to be true and accurate at the date of publication. Neither the publisher nor the authors or the editors give a warranty, expressed or implied, with respect to the material contained herein or for any errors or omissions that may have been made. The publisher remains neutral with regard to jurisdictional claims in published maps and institutional affiliations.

This Springer imprint is published by the registered company Springer Nature Switzerland AG  
The registered company address is: Gewerbestrasse 11, 6330 Cham, Switzerland

# Preface

This book discusses the open questions regarding the modelling of cyber-physical systems and their application in different industries. The industry needs new approaches to improve its competitiveness. These approaches, on the one hand, should ensure the execution of current business processes, and on the other hand, ensure a quick speed of reactions to changes. The concept of cyber-physical systems supports such changes, with the need to find new modelling tools becoming a key challenge.

The book contains five-section covering the following topics. In the section, Cyber-Physical Systems Modelling, the authors present concepts and results of fundamental research for complex systems modelling and simulation in different domains. Multiple representations and formal descriptions of cyber-physical systems help to improve modelling and simulation processes. The section IoT and Signal Processing present new findings on information measuring systems in the framework of cyber-physical systems, optimization of operation and transferring data between systems. Cyber-Physical Systems Intelligent Control section presents control methods of a closed-loop system with incomplete information. In addition, the control methods for a group of cyber-physical systems are proposed. The section Cyber-Physical Systems Industrial implementation shows the results of deploying cyber-physical systems on industrial enterprises, metal processing, petrochemical facilities, etc. The last section New Materials Production for Cyber-Physical Systems includes chapters proposing how new materials help to improve the quality of cyber-physical systems, and how cyber-physical systems are used for the production of new materials.

This book is directed to researchers, practitioners, engineers, software developers, professors and students. We do hope the book will be useful for them.

The edition of the book is dedicated to 2021, the Year of Science and Technology in Russia and technically supported by the Project Laboratory of Cyber-Physical Systems of Volgograd State Technical University.

Volgograd, Russia  
St. Petersburg, Russia  
Volgograd, Russia  
October 2021

Alla G. Kravets  
Alexander A. Bolshakov  
Maxim Shcherbakov

# Contents

## Cyber-Physical Systems Modelling

<b>Algebraic Means of Heterogeneous Cyber-Physical Systems Design</b> . . . .	3
Serge P. Kovalyov	
<b>Computer System for Resource-Saving Design of Industrial Processes of Secondary Oil Refining</b> . . . . .	15
Tamara Chistyakova and Dmitriy Furaev	
<b>Verification of Numerical Three-Dimensional Models of Auger Centrifugal Stages for Cavitation Calculation Using the Rayleigh-Plesset Model</b> . . . . .	25
Oleg Chistyakov, Alexei Petrov, and Mikhail Fomin	
<b>On the Qualitative Study of Phase Portraits for Some Categories of Polynomial Dynamic Systems</b> . . . . .	39
Irina Andreeva and Tatiana Efimova	
<b>Model of Organization of Software Testing for Cyber-Physical Systems</b> . . . . .	51
Dmitriy Tobin, Alexey Bogomolov, and Mikhail Golosovskiy	
<b>Digital Twin of Building Heating Substation: An Example of a Digital Twin of a Cyber-Physical System</b> . . . . .	61
Oleg Yu. Maryasin	
<b>Generalized Formalization of Multiplicatively Release and Isolating Functions and Locally Approximating Functions in the Formation of a Single Analytical Function in the Cut-Glue Method</b> . . . . .	75
Nikita Kudinov, Nikita Gamayunov, and Asya Atayan	
<b>Local Fragmentary Functions' Smooth and Monotonic Docking in "Cut-Glue" Approximation of Experimental Data</b> . . . . .	85
N. V. Kudinov, A. S. Drepin, and S. V. Protsenko	



## **IoT and Signal Processing**

- Automatic Compensation of Thermal Deformations of the Carrying Structures of Cyber-Physical Information Measuring Systems** ..... 97  
 Michail Livshits, Boris Borodulin, Aleksei Nenashev, and Yulia Savelieva
- Solving the Problem of Optimizing the Modes of Operation of the Combined Heat and Power Systems, Depending on the Chosen Method** ..... 107  
 A. V. Andryushin, E. K. Arakelyan, A. V. Neklyudov, N. S. Dolbikova, and Y. Y. Yagupova
- Testing a Ground-Based Radar Station as a Cyber-Physical System Using a Carrier and On-Board Equipment** ..... 117  
 A. L. Kalabin and A. K. Morozov
- Algorithm for Determining Distributed Subsurface Layers Based on Ultra-Wideband GPR** ..... 129  
 S. L. Chernyshev, M. V. Rodin, and I. B. Vlasov
- Formant Frequencies Estimation Based on Correlogram Method of Spectral Analysis and Binary-Sign Stochastic Quantization** ..... 137  
 Vladimir Yakimov, Petr Lange, and Ekaterina Yaroslavkina
- Estimation of the Influence of the Supply Voltage Non-sinusoidally on the Results of Measuring the Parameters of Powerful Submersible Electric Motors** ..... 147  
 Evgenii Melnikov, Ekaterina Yaroslavkina, and Vladimir Yakimov
- Cyber-Physical Systems Intelligent Control**
- On the Possibilities of the Cyber-Physical Approach to Study the Frequency Properties of a Closed-Loop System with Incomplete Information About the Control Plant Model** ..... 161  
 E. G. Krushel, E. S. Potafeeva, T. P. Ogar, I. V. Stepanchenko, and I. M. Kharitonov
- Combined Control of Technological Processes with Delay** ..... 177  
 I. V. Gogol, O. A. Remizova, V. V. Syrokvashin, and A. L. Fokin
- Robust Control Objects with Delayed Admission by the Extended Model** ..... 189  
 I. V. Gogol, I. V. Zhukov, O. A. Remizova, and A. L. Fokin
- Study the Algorithm of Paths Calculation Parallelization in the Problem of Group Control of Robots** ..... 199  
 Alexandr Krashennnikov and Serge Popov

<b>Research of Methods of Decentralized Control of a Group of Robots in the Liquidation of Technogenic Accidents</b> .....	213
Leonid M. Kurochkin and Igor R. Muhamedshin	
<b>Cyber-Physical Systems Industrial Implementation</b>	
<b>Impact of Preventive Measures on Conditions of Risk Insurance in Cyber-Physical System of Industrial Enterprise</b> .....	235
Mikhail Geraskin and Elena Rostova	
<b>A Combined Method for Solving the Problem of Optimizing the Production Schedule of Metal Structure Processing for Use in a Cyber-Physical Control System of a Metallurgical Enterprise</b> .....	243
Alexander A. Bolshakov, Lilia Slobodyanyuk, Olga Shashikhina, and Yana Kovalchuk	
<b>Redmine-Based Approach for Automatic Tasks Distribution in the Industrial Automation Projects</b> .....	261
Alla G. Kravets, Alexey Seelantiev, Natalia Salnikova, and Irina Medintseva	
<b>Development of a Tool for Extracting and Analyzing Software Development Process Models</b> .....	275
Aleksandr Kushchenko and Aleksandr Samochadin	
<b>Models and Algorithms for Determining the Safety Valves Critical Flow at Petrochemical Facilities</b> .....	287
A. V. Nikolin and E. R. Moshev	
<b>New Materials Production for Cyber-Physical Systems</b>	
<b>Analysis of the Efficiency of the Rotary Method for Producing a Mixture of Granular Raw Materials in the Preparation of a Cyber-Physical Platform</b> .....	299
A. B. Kapranova, D. V. Stenko, D. D. Bahaeva, A. A. Vatagin, and A. E. Lebedev	
<b>Optimization of Ingredients of a Polymeric Composition Under the Conditions of a Paired Interaction of Active Additives</b> .....	311
I. V. Germashev, E. F. Feoktistov, E. V. Derbisher, and V. E. Derbisher	
<b>Mathematical Model of the Heat Transfer Process in Multilayer Fencing Structures</b> .....	323
Fail Akhmadiev, Renat Gizzyatov, and Ilshat Nazipov	
<b>Calculation Features for the Heat and Power Balance in the Cyber-Physical System of Pellets Roasting on the Roasting Machine Conveyor</b> .....	337
Vladimir Bobkov and Maksim Dli	

# **Cyber-Physical Systems Modelling**

# Algebraic Means of Heterogeneous Cyber-Physical Systems Design



Serge P. Kovalyov 

**Abstract** Algebraic means are proposed to rigorously describe and eventually automate the design of cyber-physical systems based on digital twins, as Industry 4.0 demands. Following recent trends, we employ category theory as a mathematical framework. It allows rigorously composing and verifying system models using the universal construction of colimit. For example, we show how to compose a discrete-event simulation of the robotic production line by a suitable colimit. Further, the paper introduces a novel construction of multicomma category, the objects of which describe possible system architectures with a fixed structural hierarchy represented from a certain viewpoint, and morphisms denote actions associated with the parts selection and replacement during the system design. The multicomma category can be built using the universal constructions of product, exponent, and pullback. We present applications of the multicomma in solving direct and inverse problems of heterogeneous cyber-physical systems design. In particular, suitable subcategories of the multicomma apply as generative design spaces for automatic search for (sub-, Pareto-) optimal system architectures.

**Keywords** Cyber-physical system · Digital twin · Architecture viewpoint · Category theory · Colimit · Multicomma category

## 1 Introduction

A technical system is called cyber-physical whenever it integrates the digital world and the physical world [1]. Cyber-physical systems include heterogeneous equipment with attached digital sensors and actuators, and software and hardware for monitoring and/or control. E.g., an automated production system encompasses machines, power supply networks, controllers, telecommunication channels, servers, software programs, etc. [2].

---

S. P. Kovalyov (✉)

V. A. Trapeznikov Institute of Control Sciences RAS, Moscow, Russia

e-mail: [kovalyov@sibnet.ru](mailto:kovalyov@sibnet.ru)

© The Author(s), under exclusive license to Springer Nature Switzerland AG 2022  
A. G. Kravets et al. (eds.), *Cyber-Physical Systems: Modelling and Industrial Application*,  
Studies in Systems, Decision and Control 418,  
[https://doi.org/10.1007/978-3-030-95120-7\\_1](https://doi.org/10.1007/978-3-030-95120-7_1)

The Industry 4.0 paradigm recommends establishing the bidirectional link between the two worlds through the digital twin, viz. a virtual model of a physical asset that displays and alters its properties, status, and behavior in real time [3]. Thus, the cyber-physical system designer deals mostly with digital models, in accordance with the systems engineering methodology. Alternative system architectures are composed in the course of virtual parts selection and replacement process. The typical “direct” design problem amounts to assembling the system model from the models of selected components and its verification against stakeholder requirements. Very important is the inverse design problem that amounts to the search for part sets and parameters that are (sub-, Pareto-) optimal wrt the objective functions that account for the system stakeholder quality requirements, such as cost of ownership, performance, reliability, and power consumption. The requirements bound the design space across which the search optimization performs. The automatic composition along with the implementation of the system architecture through such optimization is called the generative design [4].

For a complex physical asset, the cyber-physical control system design problems are substantially complicated due to the heterogeneity of models caused by the inherently diverse nature of the parts [5]. In essence, the designer has to reproduce the asset life cycle virtually on heterogeneous information and mathematical models. Numerous software tools apply to automate such a reproduction: MATLAB, Simulink, Modelica, Ptolemy II, and others. However, they often turn out to be either too general in purpose and therefore time-consuming in use, or too narrow in scope and therefore capable to handle only a small fragment of the system. Consequently, multicomponent toolchains integrated on the basis of a formal semantic representation and verification of systems engineering knowledge are in demand [6].

In this paper, we propose a formal basis for a wide class of means to automate solving both direct and reverse heterogeneous cyber-physical systems design problems. Following recent trends [7–9], we employ category theory as a mathematical framework to achieve a sufficiently high level of generality and scalability. Indeed, category theory is a branch of higher algebra specifically aimed at a unified representation of objects of different nature and relationships between them [10]. Its application to systems engineering is based on representing a system structure as a diagram in the category that works like a virtual “product catalog”. Objects of such a catalog category are algebraic models of all possible units of all structural hierarchy levels (ranging from elementary parts to systems of systems), and morphisms describe, in the language of models, the actions associated with assembling higher-level units from components [11]. The well-known universal algebraic construction called the colimit of a diagram represents assembling the system from units. Observe that there are other, more narrow-scope approaches to leverage category theory in systems modeling, e.g., the representation of signal flow diagrams by string diagrams in a suitable monoidal category [12].

The paper is composed as follows. Section 2 provides an overview of some category-theoretic concepts and constructions applicable in systems engineering.

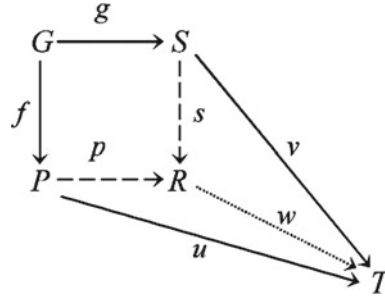
Section 3 is devoted to the multicomma category and its applications in cyber-physical systems design. Section 4 presents the properties of the multicomma as a universal construction in the “category of all categories” **CAT**. Some conclusions and directions for further research are outlined in Sect. 5.

## 2 Applying Category Theory to Systems Engineering

We use category-theory concepts and constructions introduced in [10, 11, 13]. As stated above, the representation of a system units catalog as a category is a starting point to apply them in systems engineering. Indeed, a catalog is a category since it has the composition of morphisms (sequential execution of actions) and identity morphisms (idle “doing nothing” action with any model). In many known applications, models are sets equipped with some structure (algebras, graphs, transition systems, vector spaces, manifolds, and so on), so the catalog is a concrete category over the category **Set** of all sets and maps.

Suitable diagrams in a catalog category represent possible system structures. Recall that a diagram in a category  $C$  is a functor  $\Delta : I \rightarrow C$  where  $I$  is a small category that is generated by the diagram graph and called a scheme of  $\Delta$ . Given a system structure diagram, category theory allows rigorously composing and verifying the model of the system as a whole, applying the universal construction called the colimit of the diagram. The concept of a colimit expresses in algebraic terms the common-sense view of a system as a “container” that includes all parts, respecting their structural interconnections, and nothing else. Formally, a colimit is an object endowed with morphisms from each vertex of the diagram that satisfy certain naturality and universality conditions.

The simple non-trivial colimit, called a pushout, is constructed for a span-shaped diagram  $f : P \leftarrow G \rightarrow S : g$ . This diagram can be interpreted as the structure of a system comprised from parts  $P$  and  $S$  joined by a “glue”  $G$ . Clearly, the system should include both parts and respect the glue in a sense that tracing the glue inclusion through either part amounts to the same action (the naturality condition). Moreover, the system should contain nothing except two glued parts, i.e., it should be unambiguously identified within any arbitrary unit that contains the parts and respects the glue (the universality condition). The colimit that represents such a system algebraically is an object  $R$  along with morphisms  $p : P \rightarrow R$  and  $s : S \rightarrow R$  that satisfy the following two conditions: (i)  $p \circ f = s \circ g$ ; (ii) for any object  $T$  and morphisms  $u : P \rightarrow T, v : S \rightarrow T$ , there exists a unique morphism  $w : R \rightarrow T$  such that  $w \circ p = u$  and  $w \circ s = v$  whenever  $u \circ f = v \circ g$ .



It is easy to verify that the colimit object  $R$ , provided that it exists, is unique up to an isomorphism. Under mild technical conditions, a colimit of any finite diagram can be calculated by a sequence of pushouts. See below example colimits that appear in the cyber-physical production systems design process (Fig. 1 and 2).

When dealing with heterogeneous systems, means to relate and combine multiple categories are often needed. The “category” **CAT**, which consists of all categories and functors, provides an appropriate context for such means. **CAT** has sums, products, exponents, and other universal constructions similar to these in **Set**. For instance, we will use the exponential functor  $C^{(-)} : \mathbf{CAT}^{op} \rightarrow \mathbf{CAT} : X \mapsto C^X$ . Some categories are particularly close to sets: they don’t contain any non-identity morphisms and therefore are called discrete. A single-object discrete category is denoted by  $1$ . Any category  $C$  has the largest discrete subcategory  $|C|$  that essentially coincides with the class of all its objects.

Of course, category theory also offers much more involved constructions to apply to systems engineering. Yet, they are out of the scope of the present paper.

### 3 Multicomma Category for Cyber-Physical Systems Design

The cyber-physical systems designer could compose catalog categories separately by unit kinds: equipment, power supply devices, sensors and controllers, control algorithms, and so on. However, it is a priori unclear what terms are appropriate

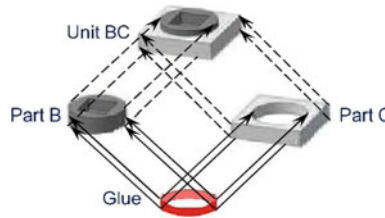


**Fig. 1** Gluing two mechanical parts represented as a pushout

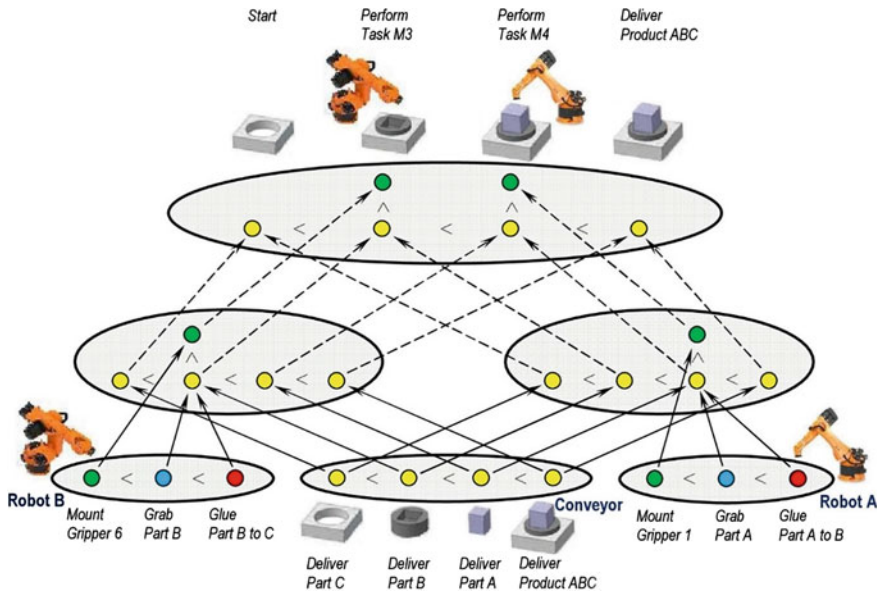


Fig. 2 Composing a production line scenario by a colimit

for rigorous and semantically consistent description of the composition of holistic systems from such heterogeneous units [5]. The designer can only fix the product structure, viz. the system hierarchy graph determined by the nature of units. To compose the architecture, one needs to map the structure to different architectural viewpoints on the system, such as:

- spatial location (a geometric shape);
- behavior;
- stakeholder quality;
- material;
- control;
- security;
- diagnostics;
- other relevant viewpoints.

A viewpoint-based approach to architecture design is established by the ISO/IEC/IEEE 42,010:2011 standard “Systems and software engineering—Architecture description”.

Algebraic descriptions of all possible units of all kinds from a certain fixed viewpoint form a category of their own with morphisms expressing the viewpoint on assembly actions. For example, the geometric shape of any unit is algebraically represented as a subset of  $\mathbb{R}^3$  which is bounded, regular (i.e., it coincides with the closure of its interior wrt the standard topology), and semi-analytical (i.e., it admits a representation as a finite Boolean combination of sets of the kind



$\{(x, y, z) | F_1(x, y, z) \leq 0, F_2(x, y, z) \leq 0, \dots\}$  where  $F_i : \mathbb{R}^3 \rightarrow \mathbb{R}$  is a real analytic function for any index  $i$  [14]. To provide a capability to specify unit joining such as gluing together by surface fragments, all bounded regular semi-analytical subsets of  $\mathbb{R}^n, 0 \leq n \leq 3$ , are considered. Then, the quotient is formed: any two such sets that can be turned into one another by affine isometries and stretches are identified with one another. Morphisms of such equivalence classes, which describe assembly actions from the shape viewpoint, are generated by isometric embeddings and stretches. This way, the subcategory of **Set** emerges, which we will denote by **SBM** (from Solid Body Modeling).

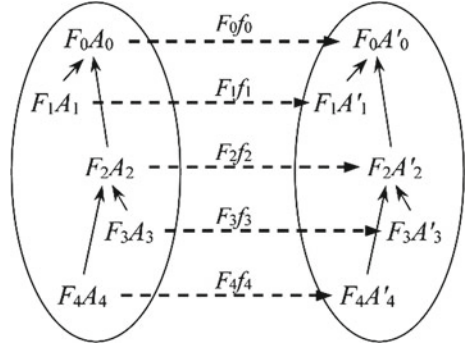
As an illustrative example of representing the system assembly by a colimit, consider a pushout in **SBM** that represents gluing together two parts (Fig. 1) [11]. The glue is a thin layer of a red-colored chemical adhesive applied to parts' contact 2D surface.

To describe manufacturing and other systems from the behavior viewpoint, discrete-event simulation is widely used [15]. A simulation virtually represents an operational scenario, viz. a fragment of the imagined history of the system behavior described as a stream of events of various types. Descriptions of actions used to build a complex system's behavior scenario specify the contribution of the components' behavior. E.g., the production line operational scenario is composed of machines' operational scenarios linked together according to the production process. Algebraically, a scenario is a set of events partially ordered by causal dependencies and labeled by event types. Since neither events nor dependencies, nor labels could be "lost" when composing a complex system behavior scenario, actions involved in assembling scenarios are defined as maps that preserve the order and the labeling [16]. All scenarios and actions comprise a category called **Pomset**. This category comes equipped with a functor to the category **Set** that "forgets" the order and the labeling.

Colimits and other universal constructions in **Pomset** formalize techniques for composing complex simulations. As a simplified example, consider a scenario intended for execution by a cyber-physical control system of an automatic production line [11]. The line consists of three units of the lowest structural level: two assembly robots and a conveyor. The production plan assigns a scenario of interaction with the conveyor to each robot, generating two intermediate-level units (tasks M3 and M4). The top-level production scenario is constructed from these scenarios via a colimit in the category **Pomset** (Fig. 2). The calculation of this colimit boils down to a pushout.

Let  $C$  be a category of a certain viewpoint. Representing a system architecture from the viewpoint  $C$  boils down to composing a diagram in  $C$  whose vertices are the representations of units, and arrows represent actions for assembling the system from units. Let  $I$  be a scheme (shape) of this diagram,  $D_i, i \in |I|$ , be catalogs of unit models of different kinds. For the  $i$ -th unit, there is a rule of representation from the viewpoint  $C$ , which is specified as a functor of the form  $F_i : D_i \rightarrow C$  to ensure consistency (we will denote by  $F$  such a family of functors indexed by the set of scheme vertices). Thus, compose the category-theoretic architecture description of some specific system from a family of objects  $A_i \in D_i, i \in |I|$ , and a diagram

**Fig. 3** A structurally consistent transformation of the architecture descriptions



$\Delta : I \rightarrow C$  that satisfies the condition  $\Delta i = F_i A_i, i \in |I|$ . Observe that a many-faceted architecture description from several viewpoints at once has the same form: given a set  $Q$  and a family of viewpoint categories  $C_q, q \in Q$ , obtain the integral description by substituting the product of the categories  $\prod_{q \in Q} C_q$  instead of  $C$ .

The virtual parts selection and replacement actions that comprise the design process are described algebraically by certain transformations of architecture descriptions. Specifically, such transformations shall preserve the system structure and all unit representation rules. Hence, natural transformations (in a categorical sense) of architecture description diagrams naturally serve as such transformations, provided that they are induced by actions from the unit catalogs. A morphism of a description  $((A_i, i \in |I|), \Delta : I \rightarrow C)$  to a description  $((A'_i, i \in |I|), \Delta' : I \rightarrow C)$  is any family of morphisms  $f_i : A_i \rightarrow A'_i, i \in |I|$  (where each morphism  $f_i$  belongs to the category  $D_i$ ), such that for every two vertices  $i, j \in |I|$  and every arrow  $s : i \rightarrow j$  the following naturality condition holds:  $F_j f_j \circ \Delta s = \Delta' s \circ F_i f_i$ . It is this condition that expresses categorically the structural consistency of the architecture transformation caused by part replacements [17] (Fig. 3).

For any fixed  $I$  and  $F$ , all architecture descriptions and their transformations comprise a category. We will denote it by  $\Downarrow_I F$  and call it a *multicomma* category [17]. The name stems from the fact that the multicomma turns into the well-known comma category [2, § II.6] whenever the scheme  $I$  consists of two vertices and a single non-identical arrow directed from one vertex to another. The pair  $\langle I, F \rangle$  is called the *multicomma shape*; it describes algebraically the structure of the system of interest along with the unit representation rules.

We describe algebraically systems design procedures as suitable functors acting on the category  $\Downarrow_I F$ . For example, if any diagram with the scheme  $I$  in  $C$  has a colimit, then the colimit object calculation, i.e., the solution to a direct design problem, is a functor from  $\Downarrow_I F$  to  $C$ . Checking various properties of the colimit, one verifies the architecture against requirements posed on the system of interest as a whole.

For solving inverse problems, the multicomma category serves as a convenient “raw material” for the design space since the objective functions of the optimal parts selection can be specified as functors. Indeed, the range of any objective function

is a linearly ordered set, so it admits well-known representation as a category [10, § I. 2]: objects of such a category are elements of the set, and morphisms are all pairs  $(x, y)$  such that  $x \leq y$  (so that there is at most one morphism between any two objects). Of particular interest is the situation when the objective function is the object-part of a functor that takes values in such a category and arguments in a suitable nontrivial (morphism-rich) subcategory of  $\Downarrow_I F$  or of its dual  $(\Downarrow_I F)^{op}$ . In this case, optimization algorithms of gradient descent type are reasonable to employ, which navigate along the subcategory morphisms calculating the path by means of computer algebra. Performant category-theory solvers for such calculations are available [18].

For example, when designing energy-efficient production systems, power consumption of production processes is minimized while maintaining acceptable performance. To evaluate the consumption by simulation, the simulation model comes equipped with the consumption values associated with events that denote the operations. Let  $\Downarrow_I F$  be a multicomma category that represents the cyber-physical production systems architecture from the behavior viewpoint (e.g., it has **Pomset** as  $C$ ). The design space is defined as a subcategory of  $(\Downarrow_I F)^{op}$  with morphisms satisfying the following condition: the total energy consumption of events contained in the domain's colimit is not greater than the consumption of the codomain's colimit. Calculation of the consumption defines a functor from this subcategory to the category of real numbers.

Notice that category theory allows representing the cyber-physical system structure not only as a small category. For example, the structure defined as a block diagram, that describes the control and data flows between parts, is convenient to represent by a string diagram in a suitable monoidal category  $\mathbf{W}$  [19]. One introduces a functor  $F : \mathbf{W} \rightarrow \mathbf{CAT}$  that maps each part to its catalog so that a system architecture description is obtained by selecting an object in the category  $F X$  for each block  $X$  and linking the selected objects using functors  $F f$  for each inter-block connection  $f$ . One poses and eventually verifies requirements to the system by specifying constraints on block inputs and outputs in the language of category theory. However, the resulting architecture representations express only a limited (albeit very important) subset of viewpoints on the system: the behavior and semantically close to it. It is unclear how to specify, e.g., the geometric shape as a block diagram.

## 4 Properties of a Multicomma

The multicomma category can be built using the universal constructions of product, exponent, and pullback: it is isomorphic to the upper left vertex of the following pullback (dual of a pushout) in  $\mathbf{CAT}$  [17] (Fig. 4).

We will refer to this pullback as *generating* the multicomma  $\Downarrow_I F$ . It allows establishing several multicomma category properties that make sense in the context of heterogeneous cyber-physical systems design. For example, if the system has no structure at all, i.e.,  $I \cong 1$ , then the multicomma shape contains exactly one functor

**Fig. 4** The universal constructions of product, exponent, and pullback

$$\begin{array}{ccc}
 \Downarrow_I F & \dashrightarrow & C^I \\
 \downarrow & & \downarrow C^{(|I| \dashv n)} \\
 \prod_{i \in |I|} D_i & \xrightarrow{\quad} & C^{I^I} \\
 & \prod_{i \in |I|} F_i &
 \end{array}$$

$F_0 : D_0 \rightarrow C$ ; yet, the category  $\Downarrow_1(F_0)$  is isomorphic to the catalog of a single “part”  $D_0$  regardless of the choice of the functor. Indeed,  $|1| \cong 1$ , so the right vertical arrow of the generating pullback becomes an isomorphism. Since the edge of any pullback parallel to an isomorphism is itself an isomorphism [13, Proposition 11.18], the left vertical arrow of the pullback generating  $\Downarrow_1(F_0)$  is an isomorphism as well:

$$\Downarrow_1(F_0) \cong D_0. \quad (1)$$

Another illustrative special case of a multicomma is obtained when every functor  $F_i, i \in |I|$ , is an isomorphism. Such a choice of representation functors means that all system units are described accurately (i.e., with neither omissions nor extra data) from the viewpoint  $C$ . Therefore, systems assembled from such units are essentially homogeneous, the assembly process is completely specifiable in  $C$ , and any diagram with the scheme  $I$  represents a valid system architecture. In this case, the lower horizontal arrow of the generating pullback is an isomorphism; hence, the upper horizontal arrow is an isomorphism as well:  $\Downarrow_I F \cong C^I$ .

Now consider the situation when the system consists of several subsystems that do not interact with each other, i.e. when the scheme  $I$  is the sum (the disjoint union) of subschemes:  $I \cong \coprod_{s \in S} I_s$  for some set  $S$ . The architecture of such a system can be composed of an arbitrary set of subsystem architectures: it is easy to see that

$$\Downarrow_I F \cong \prod_{s \in S} \Downarrow_{I_s}(F_i, i \in |I_s|). \quad (2)$$

To verify this statement, one composes a “term-wise” product of the pullbacks that generate the multicommas representing each subsystem and takes advantage of the fact that the exponent sends products into sums (i.e.,  $C^X \times C^Y \cong C^{X \sqcup Y}$  [13, Proposition 27.8(3)]). Formulas (1) and (2) together imply that the multicomma is isomorphic to a product of unit catalogs whenever the system structure is discrete (i.e., its units are agnostic of each other).

The term-wise product of generating pullbacks also occurs while modeling complexes of systems consisting of different parts from different viewpoints. If all systems have the same structural scheme, then one obtains a category of the whole complex architecture descriptions with this scheme using the product of pullbacks. Formally, it turns out that the construction of the multicomma category sends the

products of functors into products of categories, i.e., it “covariantly” depends on the unit representation rules. Indeed, for an arbitrary scheme  $I$ , a set  $Q$ , and a family of functors  $F_i^{(q)} : D_i^{(q)} \rightarrow C_q, i \in |I|, q \in Q$ , the term-wise product of the generating pullbacks for each multicomma  $\Downarrow_I F^{(q)}$  yields the following isomorphism:

$$\Downarrow_I \left( \prod_{q \in Q} F_i^{(q)} : \prod_{q \in Q} D_i^{(q)} \rightarrow \prod_{q \in Q} C_q, i \in |I| \right) \cong \prod_{q \in Q} \Downarrow_I F^{(q)}. \quad (3)$$

Likewise, for an arbitrary small category  $J$ , one verifies the following statement by exponentiating the generating pullback to the power of  $J$  term-wise.

$$(\Downarrow_I F)^J \cong \Downarrow_I (F_i^J : D_i^J \rightarrow C^J, i \in |I|). \quad (4)$$

## 5 Conclusion

Category theory demonstrates significant potential for practical application in Industry 4.0 technologies, in particular for the digital design of heterogeneous cyber-physical systems. Presently, we are exploring options of employing the proposed category-theoretic methods on the prototype software tool for generative design and verification of power systems [20]. Further development and deployment of the tool will call for further theoretical and applied research in numerous directions.

**Acknowledgements** This work was supported by the Russian Foundation for Basic Research (Grant 19-011-00799).

## References

1. Khaitan, S.K., McCalley, J.D.: Design techniques and applications of cyber physical systems: a survey. *IEEE Syst. J.* **9**(2), 350–365 (2015)
2. Rossit, D.A., Tohmé, F., Frutos, M.: Production planning and scheduling in Cyber-Physical Production Systems: a review. *Int. J. Comput. Integr. Manuf.* **32**(4–5), 385–395 (2019)
3. Tao, F., Qi, Q., Wang, L., Nee, A.Y.C.: Digital twins and cyber-physical systems toward smart manufacturing and Industry 4.0: correlation and comparison. *Engineering* **5**, 653–661 (2019)
4. Sun, H., Ma, L.: Generative design by using exploration approaches of reinforcement learning in density-based structural topology optimization. *Designs* **4**(2), 10 (2020)
5. Rajhans, A., et al.: Supporting heterogeneity in cyber-physical systems architectures. *IEEE Trans. Autom. Control* **59**(12), 3178–3193 (2014)
6. Larsen, P.G., et al.: Integrated tool chain for model-based design of Cyber-Physical Systems: The INTO-CPS project. In: *Proceedings of the 2nd International Workshop on Modelling, Analysis, and Control of Complex CPS (CPS Data)*, pp. 1–6. IEEE Computer Society, Vienna (2016)

7. Breiner, S., Subrahmanian, E., Jones, A.: Categorical foundations for system engineering. In: Madni, A., et al. (eds.) *Disciplinary Convergence in Systems Engineering Research*, pp. 449–463. Springer, Heidelberg (2018)
8. Watson, M.D.: Future of systems engineering. *IncoSE Insight* **22**(1), 8–12 (2019)
9. Mordecai, Y., Fairbanks, J.P., Crawley, E.F.: Category-theoretic formulation of the model-based systems architecting cognitive-computational cycle. *Appl. Sci.* **11**, 1945 (2021)
10. Mac Lane, S.: *Categories for the Working Mathematician*, 2nd edn. Springer, New York (1998)
11. Kovalyov, S.P.: Leveraging category theory in model based enterprise. *Adv. Syst. Sci. Appl.* **20**(1), 50–65 (2020)
12. Baez, J.C., Erbele, J.: Categories in control. *Theory Appl. Categ.* **30**(24), 836–881 (2015)
13. Adámek, J., Herrlich, H., Strecker, G.E.: *Abstract and Concrete Categories*. Wiley, New York (1990)
14. Requicha, A.G.: Representations for rigid solids: theory, methods, and systems. *J. ACM Comput. Surv.* **12**(4), 437–464 (1980)
15. Prajapat, N., Tiwari, A.: A review of assembly optimisation applications using discrete event simulation. *Int. J. Comput. Integr. Manuf.* **30**(2–3), 215–228 (2017)
16. Pratt, V.R.: Modeling concurrency with partial orders. *Int. J. Parallel Prog.* **15**(1), 33–71 (1986)
17. Kovalyov, S.P.: Methods of the category theory in digital design of heterogeneous cyber-physical systems. *Inf. Appl.* **15**(1), 23–29 (2021)
18. Gross, J., Chlipala, A., Spivak, D.I.: Experience implementing a performant category-theory library in Coq. In: Klein, G., Gamboa, R. (eds.) *5th Conference (International) on Interactive Theorem Proving*. LNCS, vol. 8558, pp. 275–291. Springer, Heidelberg (2014)
19. Bakirtzis, G., Fleming, C.H., Vasilakopoulou, C.: Categorical semantics of cyber-physical systems theory. [arXiv:2010.08003](https://arxiv.org/abs/2010.08003) [cs.LO] (2021)
20. Kovalyov, S.P.: An approach to develop a generative design technology for power systems. In: Massel, L., et al. (eds.) *VI International Workshop “Critical Infrastructures: Contingency Management, Intelligent, Agent-Based, Cloud Computing and Cyber Security” (IWCI 2019)*, *Advances in Intelligent Systems Research*, vol. 169, pp. 79–82 (2019)

# Computer System for Resource-Saving Design of Industrial Processes of Secondary Oil Refining



Tamara Chistyakova and Dmitrij Furaev

**Abstract** The structure of a computer system for the design and practice-oriented training of specialists in the field of solving industrial engineering problems, including issues of design and resource-saving management of oil recycling facilities, is presented. Testing of the system carried out on the example of designing a catalytic cracking unit, confirmed its operability.

**Keywords** Industrial engineering · Computer system · Resource-saving design · Management · Oil recycling

## 1 Introduction

The main condition for improving the economic efficiency of production in the field of petrochemicals and oil refining is the introduction of energy and resource-saving technologies [1–8]. Around the world actively the technologies of the industrial revolution the Industry of 4.0 (Industry 4.0) directed to digitalization and automation of the industry [9–11] develop.

In particular, in Russia in 2012, the Plan for the development of gas and petrochemicals of Russia for the period until 2030 was adopted, the main methodological position of this plan was the creation of oil and gas chemical clusters, which include projects for the modernization of existing and construction of new capacities for the production of basic petroleum products and large-capacity petrochemicals and polymers, facilities of engineering and social infrastructure, as well as organizations for educational and scientific support of projects.

---

T. Chistyakova (✉) · D. Furaev  
Saint-Petersburg State Institute of Technology, Saint-Petersburg 190013, Russia  
e-mail: [nov@technolog.edu.ru](mailto:nov@technolog.edu.ru)

D. Furaev  
e-mail: [d.furaev@pmpspb.ru](mailto:d.furaev@pmpspb.ru)

These programs aim to modernize existing production facilities or create new ones in accordance with modern world requirements for productivity, energy efficiency, and environmental friendliness, which, in turn, requires the training of highly qualified personnel for the design of these industries [12–14].

The goal of the authors is to create a computer system that would solve the issues of resource-saving design and design training.

The complexity of the design of oil refineries is due to the heterogeneity of physical and chemical processes of processing of raw materials and materials, the assortment of products, environmental requirements, expensive catalysts, numerous technological connections, complex laws of chemical reactions, variety of types of equipment and complexity of the layout, limitations imposed by terrain characteristics and availability of resources, strict requirements for environmental indicators of production and requirements for recycling and disposal of waste [15–18].

Despite the significant complexity of the design task, there are a large number of design solutions for individual oil recycling processes that can be integrated into a single design system.

There are quite a number of design environments used to design individual disciplines. The leaders used in the oil and gas industry of Russia are the companies: Intergraph, AVEVA, Autodesk, Bentley, Trimble [19, 20].

Digital doubles of industrial production are being created. Directly in the field of design, digital doubles are information 3D models that are a virtual copy of an industrial object with maximum detail and access to all project documentation.

All the above prerequisites make it possible to realize the idea of creating a single computer system combining existing design solutions, digital doubles, and 3D models [21, 22].

Thus, the task was set to develop a single computer system that would allow, based on the technical assignment for design or reconstruction, to form design solutions for the resource-saving energy-saving design of petrochemical oil recycling enterprises. In addition, which will allow for the training of qualified specialists to form scenarios for training in the design of various types of industrial oil recycling processes.

When implementing such a computer system, the following problems are solved:

1. Computer system information support has been developed, consisting of databases of standard process equipment, pipeline parts, and valves, a database of raw material characteristics of various suppliers, regulatory documents for the design and operation of oil recycling plants, and existing technological design solutions.
2. Mathematical support is formed, which includes mathematical models of oil recycling processes (cracking, visbreaking, hydrocracking, reforming, hydrotreating, and isomerization), mathematical models of estimating product quality, productivity, energy consumption, and cost, environmental characteristics.
3. The designer interfaces have been developed, which allow obtaining design solutions for equipment layout and routing of process pipelines based on the terms of reference; trainee interfaces allowing to pass different training



scenarios; instructor interfaces that allow you to define design training scenarios for different configurations of the design object, as well as analyze training protocols.

4. Software was developed and selected that implements various stages of design—selection and layout of process equipment, piping, as well as implementing the formation of a design solution, which includes 3D information model and design documentation. The software is integrated and includes various environments of the applied software (Intergraph Smart 3D, NanoCAD, Start).

## 2 Problem Statement

A design environment, varying parameters, and output characteristics or design criteria characterize the design object. The design object model allows you to solve a design problem for a given environment in a given range of variations, that is, to calculate and obtain output characteristics on which criterion restrictions are set.

The design environment  $X = \{X_1, \dots, X_M\}$  includes input parameters—a type of oil recycling process, types and composition of raw materials, dimensions of the workshop, rooms, and output parameters—indicators of productivity, energy efficiency, environmental safety.

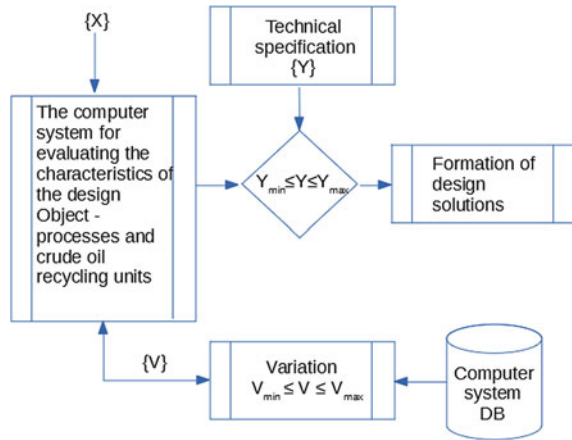
The design environment, as an object of study and control, is characterized by a set of the following components (variable parameters): characteristics of raw materials, reagents, fuel and energy resources  $M = \{M_1, \dots, M_{mn}\}$ , set and types of process equipment  $E = \{E_1, \dots, E_{en}\}$ , pipelines and valves  $P = \{P_1, \dots, P_{pn}\}$ , variants of specified dimensions of production sites and terrain characteristics  $G = \{G_1, \dots, G_{gn}\}$ , design rules  $R = \{R_1, \dots, R_m\}$ .

Thus necessary for a given design environment  $X = \{X_1, \dots, X_M\}$  based on engineering or reconstruction specification  $Y = \{Y_1, \dots, Y_L\}$ , varying parameters  $V = \{V_1, \dots, V_N\}$ ,  $V_{\min} \leq V \leq V_{\max}$  from the available information support (database of process equipment, pipelines, layout variants), to select the optimal design solution for output parameters. The outline of the general design task is shown in Fig. 1.

The task of designing the installation of a complex industrial facility of productivity and energy efficiency is not lower than acceptable, with quality indicators within the specified limits: productivity  $Pr \geq Pr_{ad.}$ , energy consumption  $Er \leq Er_{ad.}$ , cost  $Sr \leq Sr_{ad.}$ , environmental characteristics  $Kr \geq Kr_{ad.}$ , quality characteristics  $Cr \geq Cr_{\text{дон ад.}}$ . Criteria requirements ( $Pr_{ad.}$ ,  $Er_{ad.}$ ,  $Sr_{ad.}$ ,  $Kr_{ad.}$ ,  $Cr_{ad.}$ ), are usually specified in the terms of reference and are alternatives of the Customer when solving the design task.

To design an X plant with the specified performance, environmental, and energy efficiency inputs, the project team needs to:

1. Select suitable composition of feedstock  $M_1$ , catalyst  $M_2$ , reagents  $M_3$ , resources  $M_4$ , providing the required quality products according to the design specification.

**Fig. 1** General design task

2. Calculate equipment layout variant according to available dimensions and terrain characteristics  $G$ , as well as select process equipment  $E$  according to required characteristics. Equipment is selected from the process equipment database.
3. Form the binding of equipment  $E$  with pipeline  $P$  in accordance with the current standards and design rules  $R$ . Pipelines are selected from the pipeline and valve parts database.
4. Check the compliance of the selected equipment and strapping with the criteria restrictions.
5. Formation of documentation for the design object.

The extended stages of solving the design problem using the example of petrochemical industry facilities are given in Fig. 2.

Thus, the problems of variation are solved—various options for the layout of equipment and pipeline tracing are calculated, the total productivity, energy consumption, and estimated cost are determined.

The system was tested on the example of a catalytic cracking unit.

Catalytic cracking is one of the main processes of secondary oil refining. The goal is to obtain the necessary compounds used as valuable components of gasoline, increasing its octane number [23].

In Russia, there are quite a large number of catalytic cracking plants, some of which are subject to modernization.

Currently, when designing or upgrading, they are trying to solve the problems of recycling or processing the heaviest products remaining after the primary and secondary processes. Thus, there are studies of the composition and properties of the spent cracking catalyst, indicating the possibility of its complex processing to produce compounds of rare earth elements, lanthanum and metal ion sorbent [24].

The catalytic cracking process is characterized by the following main parameters: raw material consumption per unit  $R_s$ , raw material temperature  $T_s$ , total water

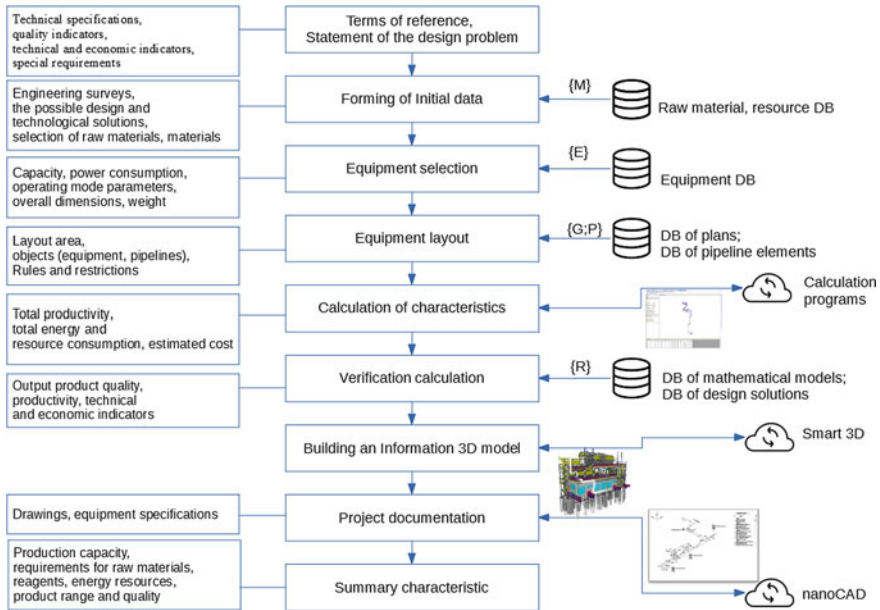


Fig. 2 Stages of solving the design problem

vapor flow rate  $R_p$ , steam flow rate to the reactor dome  $R_v$ , operating temperature  $T_p$ , pressure in the settling zone of the reactor  $P_r$ , catalyst circulation multiplicity  $C_r$ .

Technological equipment is characterized by the following parameters: working volume  $V_x$ , geometric characteristics  $G_x$ , operating and design pressures  $P_{workE}$ ,  $P_{calcE}$ , working temperature  $T_{workE}$ , rated flow  $R_x$ .

Process pipelines are characterized by the pipeline material  $M_x$ , operating and design pressures  $P_{workP}$ ,  $P_{calcP}$ , wall thickness  $S_x$ , nominal diameter  $D_x$ .

### 3 Description of the Computer System

The computer system is built based on mathematical models of the technological process, models of the equipment layout.

The technical specification for the design, which is set in the computer system by the designer, includes the following characteristics: performance, product quality requirements, resource consumption, energy efficiency, environmental indicators, weight and size characteristics of the main equipment, and the maximum dimensions of the installation.

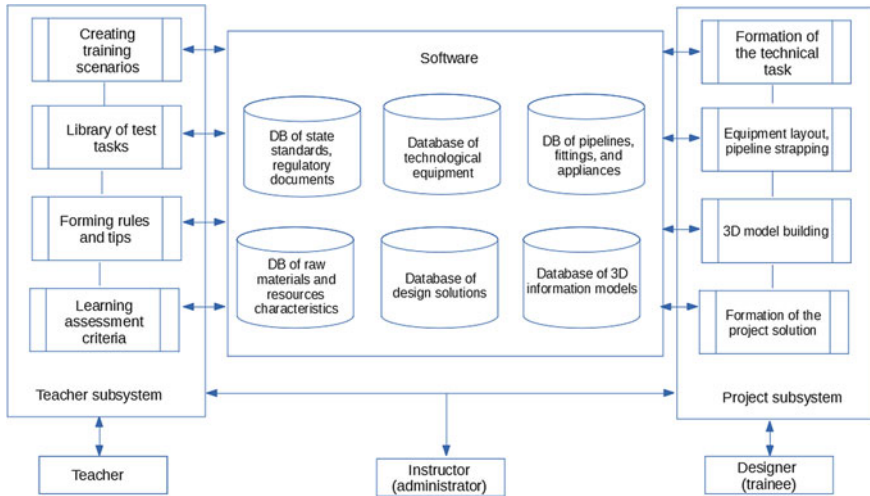


**Fig. 3** Computer system architecture

The computer system includes a database of available design solutions, a database of equipment, aggregates, pipeline parts and fittings, a database of regulatory documentation, modules for equipment placement and layout, pipeline tracing, verification of calculations, and design solutions. The architecture of the computer system is shown in Fig. 3.

Currently, the knowledge base of the system contains a large amount of information, including regulatory documentation and standards, instructions for working in the computer-aided design systems used, calculation systems, design solutions, internal instructions, and operating rules.

A big plus is the fact that the number of documents and instructions in paper form has been significantly reduced, which has allowed almost unlimited access to them, while the remote access option is available.

The library of test tasks is a testing system containing questions on the database of normative and technical documents, in particular, it contains the classification of technological processes and requirements for them, design standards, classification of pipelines and methods of their laying and design, information about pipes and parts of technological pipelines, about the types of connections, fasteners, and rules for their selection, information about the types of fittings and their purpose, methods of management, selection, materials used. In addition, a separate test block is devoted to industrial safety issues in accordance with Federal standards and regulations.

The computer system includes various functional modules, in particular, the module for calculating and searching for technological equipment.

Based on the design specification, which includes the main characteristics: productivity, product quality, resource intensity, energy efficiency, environmental indicators, the analysis of the basic (standard) project is carried out, from which the necessary technological equipment is selected.

The initial data for the task of equipment layout are the flow diagram of the technological process, the results of calculations, the number and size of the equipment.

The output data are the overall dimensions of the workshops, the coordinates of the equipment, the location of the service areas and evacuation routes, as well as the configuration of pipelines and the location of pipeline fittings and devices [22].

Based on the analysis of the master plan of the installation, the design and operating characteristics of the equipment are determined, according to which the most suitable equipment is selected from the database.

This equipment database contains the main types of technological equipment, as well as 3D models. The presence of such a database allows you to reduce time, as well as provide a conditional 3D model at the pre-design stage, or provide the Customer with several layout options.

The search for the optimal layout option is associated with the analysis of a variety of possible options for placing equipment and tracing pipelines, each of which must be checked for compliance with the restrictions of the mathematical model: structural restrictions (maximum permissible room dimensions, service, and repair areas, weight and dimensions of equipment), technological restrictions (flow rate in the pipeline, transportation time, pipeline slope), conditions for non-intersection of objects.

At the first stage, the equipment is arranged according to the design specification and the results of calculating the mathematical model of the optimal equipment placement. A base of geometric primitives for building equipment has been developed.

The next stage is the tracing of technological pipelines, taking into account the initial data: the requirements for the transportation of substances according to their physical and chemical properties, the dimensions of the equipment. For the possibility of tracing pipelines, a database of standard sizes of pipes and pipeline elements (tees, bends, and transitions), some fittings, and a database of geometric parametric fragments have been developed.

After the initial tracing, the pipeline system is transferred to the calculation module, which analyzes the characteristics of the pipelines and the correctness of the decisions made. If the calculation results do not meet the required standards, then the pipeline routing is revised or a different version of the equipment layout is proposed.

The simulation module is a virtual environment that simulates the interface of a computer-aided design system, and, in turn, consists of a system for the placement and layout of industrial equipment and a pipeline tracing system.

After working with this system, specialists can design complex industrial complexes in the field of petrochemistry and oil refining, an example of a model of a catalytic cracking plant is shown in Fig. 4. The model base is the initial data for use in designing and performing verification calculations.



**Fig. 4** Example of a 3D model of a catalytic cracking plant

## 4 Conclusion

The proposed computer system allows us to solve the design problem for the resource-saving design of petrochemical enterprises of secondary oil processing from the formation of the technical specification to the formation of the object information model and project documentation.

The architecture of the computer system is flexible and customizable, as it has augmented databases of technological equipment, pipelines, regulatory documentation, and replenished libraries of mathematical models of technological processes.

The computer system for resource-saving design of industrial processes was tested on the basis of the Russian company JSC “PMP” on the example of a high-performance catalytic cracking plant of 2500 thousand tons/year and power consumption of 23 thousand kW., where it showed its effectiveness, as well as during training of specialists at the Department of CAD SPSIT (TU). The work was carried out at the expense of a grant from the Russian Science Foundation (project No. 21-79-30,029).

## References

1. Gartman, T.N., Sovetin, F.S.: Procedure for the synthesis of resource-saving integrated complex large-capacity chemical-technological systems of continuous operation. *Izvestiya Sankt-Peterburgskogo gosudarstvennogo tekhnologicheskogo instituta (tekhnicheskogo universiteta)*

- 17(43), 103–106 (2012)
2. Dozorcev, V.M.: Digital transformation in oil refining. *Mir nefteproduktov* no. 2, p. 34–41 (2020)
  3. Meshalkin, V.P.: Introduction to the Engineering of Energy-Resource-Saving Chemical-Technological Systems, 208 p. RHTU im. D.I. Mendeleeva, Moscow (2020)
  4. Meshalkin, V.P., Hodchenko, S.M.: The essence and types of engineering of energy-resource-efficient chemical-technological systems. *Enciklopedicheskij spravochnik*, no. 6, p. 210 (2017)
  5. Dvoretiskii, D., Dvoretiskii, S., Ostrovskii, G.: Integrated design of power- and re-source-saving chemical processes and process control systems: strategy, methods, and application. *Theory Found. Chem.* **42**, 26–36 (2008)
  6. Meshalkin, V.P., Vagramyan, T.A., Mazurova, D.V., Grigoryan, N.S., Abrashov, A.A., Khodchenko, S.M.: Development of a power-and-resource-saving combined low-temperature chemical engineering process of crystalline phosphatizing. *Dokl. Chem.* **490**(1), 19–21 (2020)
  7. Chistyakova, T.B., Novozhilova, I.V., Kozlov, V.V.: Computer system of industrial data mining for resource-saving control of steel-smelting converter production. In: Proceedings 1st International Conference on Control Systems, Mathematical Modelling, Automation and Energy Efficiency, SUMMA 2019, pp. 523–526 (2019)
  8. Chistyakova, T.B., Polosin, A.N.: Computer modeling system of industrial extruders with adjustable configuration for polymeric film quality control. In: Proceedings of 2017 IEEE II International Conference on Control in Technical Systems. St. Petersburg, Saint Petersburg Electrotechnical University “LETI”, pp. 47–50 (2017)
  9. Dalenogare, L.S., Benitez, G.B., Frank, A.G., Ayala, N.F.: The expected contribution of Industry 4.0 technologies for industrial performance. *Int. J. Prod. Econ.* **204**, 383–394 (2018)
  10. Ghobakhloo, M.: Industry 4.0, digitization, and opportunities for sustainability. *J. Clean Prod* **252**, 2–18 (2020)
  11. Kohlert, M., Hissmann, O.: Applied industry 4.0 in the polymer film industry. In: Proceedings of the 16th TAPPI European PLACE Conference, Basel, pp 183–190 (2017)
  12. Dozorcev, V.M.: New industrial safety challenges will computer simulators help? *Bezopasnost' truda v promyshlennosti*, no. 9, p. 31–38 (2019)
  13. Norenkov, I.P., Sokolov, N.K., Uvarov, M.Y.: Ontologies in tools for creating electronic educational resources. *SHkol'nye tekhnologii*, no. 3, pp. 26–29 (2010)
  14. Chistyakova, T.B., Furaev, D.N.: A computer system for training of specialists in design of industrial facilities for petrochemistry and oil processing. In: Planning and Teaching Engineering Staff for the Industrial and Economic Complex of the Region (PTES): XVII Russian Scientific and Practical Conference. Saint Petersburg, pp. 92–94 (2018)
  15. Glinushkin, A.P., Vershinin, V.V., Kovaleva, T.N., Chelnokov, V.V., Meshalkin, V.P., Matasov, A. V., Makarova, A.S., Glushko, A.N., Nikulina, E.A., Makarenkov, D.A.: Energy resource efficient and environmentally friendly land use planning principles for intensive remediation of solid waste landfills.: IOP conference series. *Earth Environ. Sci.* **663**, 1–7 (2021)
  16. Menshikov, V., Meshalkin, V., Obratsov, A.: Heuristic algorithms for 3D optimal chemical plant layout design. In: Proceeding of the 19th International Congress of Chemical and Process Engineering (CHISA-2010), Prague, Czech Republic, vol. 4, pp. 14–25 (2010)
  17. Mokeddem, D., Khellaf, A.: Optimal solutions of multiproduct batch chemical process using multiobjective genetic algorithm with expert decision system. *J. Autom. Methods Manag. Chem.* **3**, 1–9 (2009)
  18. Mokrozub, V.G., Neminov, V.A., Mokrozub, A.V.: Procedural model for designing multi-product chemical plants. *Chem. Pet. Eng.* **53**(5–6), 326–331 (2017)
  19. Holí, P., Park, S.S., Patil, A.K., Kumar, G.A., Chai, Y.H.: Intelligent reconstruction and assembling of pipeline from point cloud data in smart plant 3D. In: *Advances in Multimedia Information Processing*, vol. 9315. Springer, Cham (2015)
  20. Lee, J.M., Lee, K.H., Kim, D.S., Kim, C.H.: Active inspection supporting system based on mixed reality after design and manufacture in an offshore structure. *J. Mech. Sci. Technol.* **24**, 197–202 (2010)

21. Meshalkin, V.P., Panchenko, S.V., Dli, M.I., Panchenko, D.: Analysis of the thermophysical processes and operating modes of electrothermic reactor using a computer model. *Theor. Found. Chem. Eng.* **52**(2), 166–174 (2018)
22. Mokrozub, V.G., Nemtinov, V.A.: An approach to smart information support of decisionmaking in the design of chemical equipment. *Chem. Pet. Eng.* **51**(7), 487–492 (2015)
23. Lappas, A.A., Iatridis, D.K., Papapetrou, M.C., Kopalidou, E.P., Vasalos, I.A.: Feedstock and catalyst effects in fluid catalytic cracking comparative yields in bench-scale and pilot plant reactors. *Chem. Eng. J.* **278**, 140–149 (2015)
24. Likhterova, N.M.: Trends: in development of exhaustive refining of crude oil in Russia. *Chem. Technol. Fuels Oils* **40**(3), 121–127 (2004)



# Verification of Numerical Three-Dimensional Models of Auger Centrifugal Stages for Cavitation Calculation Using the Rayleigh-Plesset Model



Oleg Chistyakov, Alexei Petrov, and Mikhail Fomin

**Abstract** When creating digital twins of circulation loops of nuclear power installation, the simulation of the operation of a centrifugal pump is implemented using pre-calculated characteristics. This chapter considers the issues of the numerical prediction of cavitation curves and modeling of cavitation using a homogeneous Zwart-Gerber-Belamri mass transfer model based on the Rayleigh-Plesset equation with the possibility of further application of the results in the development of a super-computer twin of a nuclear power installation. To validate three-dimensional discrete models of centrifugal pumps with upstream axial inducers, experimental studies of the pump performance and cavitation curves were carried out. The work carried out a preliminary study of the effectiveness of the turbulence models  $k-\varepsilon$  and SST as applied to the calculations of cavitation in pumps with standard model settings. The main purpose of the work is to study the influence of the empirical coefficients of the cavitation model, which are responsible for the rate of vaporization and condensation, on the shape of the resulting characteristic Head versus NPSH and, as a result, the NPSH<sub>3</sub> value. Comparison with experiment was carried out. Based on the results of the preliminary study, the advantage of the  $k-\varepsilon$  turbulence model was determined by a combination of factors of calculation speed and accuracy, therefore it was used in the main study. The main research made it possible to obtain model settings for the investigated geometry of the auger centrifugal pump, consistent with the results obtained from other researchers and with experimental data.

**Keywords** Digital twin · Nuclear installation · CFD · Rayleigh-Plesset equation · Cavitation · Centrifugal pump · Auger-centrifugal stage · Experimental investigations

---

O. Chistyakov (✉) · A. Petrov  
BMSTU, ul. Baumanskaya 2-ya, 5, Moscow 105005, Russia

A. Petrov  
e-mail: [alex\\_i\\_petrov@mail.ru](mailto:alex_i_petrov@mail.ru)

O. Chistyakov · M. Fomin  
JSC “Afrikantov OKBM”, Burnakovsky proyezd, 15, Nizhny Novgorod 603074, Russia  
e-mail: [mikxail@list.ru](mailto:mikxail@list.ru)

## 1 Introduction

At the stages of nuclear power installation in order to decrease the length and high cost of full-scale tests for the development of individual units, systems, and equipment in recent years, digital twins have begun—analogs of equipment and systems of reactor installation [1, 2]. Most of the main loops and hydraulic systems use centrifugal pumping units. When simulating the operation of a pump in a circulation loop system, pre-calculated characteristic curves are utilized. Such characteristic curves are obtained by the following ways at the stage of design of a centrifugal pump: either by calculation based on empirical or semi-empirical methods or a providing numerical experiment using CFD codes.

Currently, the last of the above approaches using CFD codes are widely used. Issues related to obtaining a general hydrodynamic picture of the flow are not of interest, since are well studied (as evidenced by the works [3, 4]):

- the use of CFD codes has a large validation and verification base, as evidenced by, for example, works in which verification of numerical discrete models for calculating integral characteristics was carried out [3, 5–8];
- there are developed and verified in practice methods for the application of three-dimensional calculations, described, for example, in [3, 9];
- the influence of the choice of an approach to turbulence modeling on the characteristics of pumping units has been studied in papers [10–13];
- the methods of optimization of the flow paths of pumps are applied, which are reflected in [9, 14–16].

An insufficiently studied area is the problem of reliable calculation of cavitation in the flow path of centrifugal pumps. In the literature, individual attempts by researchers to calculate the cavitation curves of the pump  $NPSH_3(Q)$  (net positive suction head on 3% drop of the pump head vs. flow rate), cavitation curves  $H(NPSH)$  (Head vs. net positive suction head) using cavitation models based on the Rayleigh-Plesset equation are presented, as providing an adequate level of agreement with the experiment, presented in [17–20] and not: [21–25]. It should be noted that in most works the stage is represented by only one element—an axial or radial impeller.

The main focus of works on three-dimensional numerical calculations of cavitation of interest is the choice of the optimal values of the empirical coefficients of the cavitation model. The Zwart-Gerber-Belamri cavitation model of interest is based on the Rayleigh-Plesset equation and includes several empirical coefficients. However, as shown in [21], the main influence on the shape of the  $H(NPSH)$  curves is exerted by the coefficients responsible for the mass transfer rate of condensation and vaporization.

Based on the above facts, it is of interest to validate three-dimensional numerical models for:

- calibration of the coefficients of the cavitation model, responsible for the rate of condensation and vaporization, for a given case;
- expansion of the calculation base;

- in particular, the validation of the geometry models of the auger and wheel system.

The results of experimental studies of models of auger centrifugal stages, as well as a comparison with the results of numerical modeling, are presented in this chapter to:

1. Choose a turbulence model from the point of view of minimizing the design time for constructing cavitation curves  $H(NPSH)$  and maintaining the calculation accuracy.
2. Calibrate the coefficients of the cavitation model for the investigated geometries of the auger centrifugal stages.

Thus, the results of this work can be used to numerically calculate the NPSH curves at the stage of design a centrifugal pump and further be used to simulate the pump operation in the circulation loop, which is recreated in the digital twin of the nuclear power installation.

## 2 Experimental Studies

As the investigated geometries, we used the geometries of the auger centrifugal stages shown in Fig. 1.

Experimental studies were carried out at JSC “Afrikantov OKBM”. The research aimed to obtain the auger centrifugal stages characteristic curves and cavitation characteristics. The experiments investigations were carried out on the water. Figure 2 shows the layout of the experimental setup.

To measure water parameters, the following instrumentation was used, presented in Table 1. Based on the data in Table 1, we can conclude that the maximum errors of the quantities of interest will be:

- for the pump head  $H$ : 0.84 m;
- for the pump flow rate  $Q$ : 0.3 m<sup>3</sup>/h;
- for the net positive suction head available NPSH: 0.1 m.

**Fig. 1** a Geometry of Model 1, b Geometry of Model 2

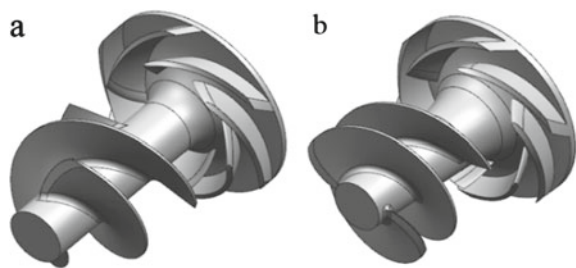


**Table 1** Instrumentation of measuring the parameters of the stand

Parameter	Instrument	Absolute error in the working range
Pump inlet pressure	Technical vacuum gauge “МТИ”	$\pm 0.015 \text{ kgf/cm}^2$
Pump outlet pressure	Technical pressure gauge “МПТИ-У2”	$\pm 0.006 \text{ MPa}$
Pressure in the tank	Technical vacuum gauge “МВПТИ-У2”	$\pm 5 \text{ kPa}$
Pump flow rate	Flowmeter “СИМАГ 11-100”	$\pm 0.2 \text{ m}^3/\text{h}$
Temperature at the pump inlet	Thermocouple “ТМПК-1-Л”	$\pm 1 \text{ }^\circ\text{C}$
Atmosphere pressure	Aneroid barometer “МД-49-2”	$\pm 0.8 \text{ mmHg}$

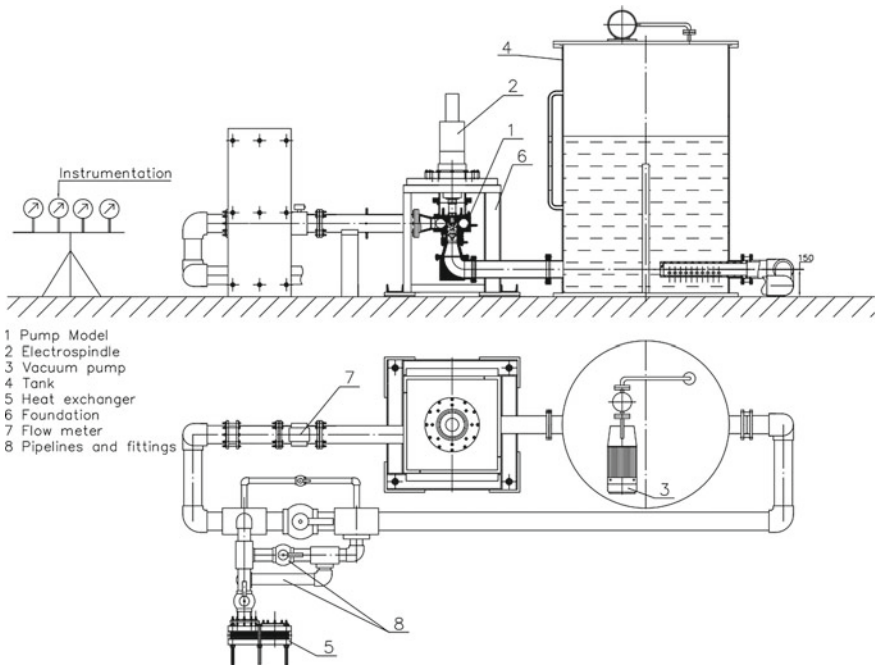


**Fig. 2** General view of the experimental setup

### 3 Numerical Discrete Model

The simplified 3D geometry was created based on the geometry of the experimental setup. ANSYS CFX is used as the calculation code. Figure 3 shows a schematic of the calculated 3D geometry.

It should be noted that in work [5] it is declared that the presence of an element that models an impeller shroud to pump housing clearance is not necessary to assess the amount of leakage. However, the presence of this element makes it possible to more accurately describe the hydrodynamics of the flow at the inlet to the impeller, where reverse flows often exist. The flow entering into this area can cause additional fluid flow disturbances. In the region of the auger, there is a radial clearance between the shroud and the blade, which is considered in the discrete model.

The solution to the problem is classically divided into three main stages:

1. Achievement of the steady-state solution in a single-phase flow
2. Achievement of the unsteady solution in a single-phase flow
3. Achievement of the unsteady solution in a double-phase flow.

For the unsteady single-phase problem time  $\tau_n$  (in a sec) is selected corresponding to a rotation angle of  $3^\circ$ :

$$\tau_n = \frac{3 \cdot 60}{n \cdot 360}, \tag{1}$$

where  $n$  is rotational speed, rev/min. Such value provides the value of the Courant number over the computational regions of the order of 1.

As a mass transfer model for a two-phase setting, as indicated earlier, the standard Rayleigh–Plesset model is used, described in [26], and implemented in CFX in the following general form:

$$\dot{m}_{fg} = F \frac{3r_g \rho_g}{R_{nuc}} \sqrt{\frac{2}{3} \frac{|p_v - p|}{\rho_f}} \text{sgn}(p_v - p), \tag{2}$$

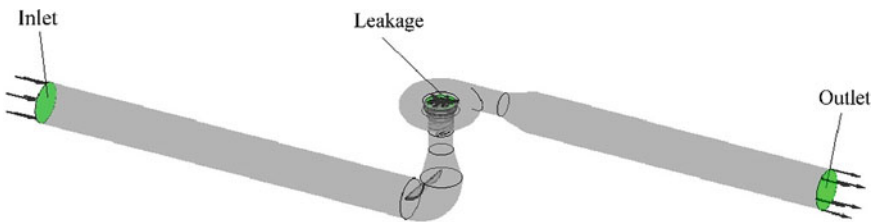


Fig. 3 Discrete model configuration

where  $\dot{m}_{fg}$  is interphase mass transfer rate per unit volume;  $F$  is the empirical factor that may differ for condensation and vaporization;  $\rho_g$  is steam density in a cavitation bubble;  $R_{nuc}$  is nucleation site radius;  $p_v$  is saturation pressure;  $p$  is pressure in the liquid surrounding the bubble;  $\rho_f$  is liquid density. For vaporization:  $F = F_{vap}$  and  $r_g$  is replaced by  $r_{nuc}(1 - r_g)$ , where  $r_{nuc}$  is the volume fraction of the nucleation sites. For condensation:  $F = F_{cond}$ .

The boundary conditions are set as follows:

- The inlet into the model is defined by the Total Pressure option. The value of the Total Pressure in Pa was chosen based on the required value of NPSH;
- The outlet is defined by the pump flow rate—Mass Flow Rate in kg/s. It was defined according to the experimental value;
- Leakage into the region behind the impeller hub is defined in the same way as for the outlet—using the Mass Flow Rate option. It was set according to the experimental value.

To determine the turbulence model, which is less expensive in terms of computational resources, two series of calculations were carried out at rated flow rates:

- Calculations of the Model 1(V1) and the Model 2(V2) using standard values of the F factor (FD) using the k- $\epsilon$  turbulence model(KE);
- Calculations of the Model 1(V1) and the Model 2(V2) using standard values of the F factor(FD) using the SST turbulence model(SST).

As a result, based on the mesh independence study by the head value H in the cavitation-free mode the dimension of the mesh averaged 4 million elements for the k- $\epsilon$  model and 6 million elements for the SST model. Also, the value of the  $y^+$  for the mesh used in the calculation with the k- $\epsilon$  model lies in the range from 45 to 72 on the surface of the impeller and auger. For the calculation using the SST model, the  $y^+$  value ranges from 1 to 3. In order to calibrate the coefficients of the Rayleigh-Plesset cavitation model, calculations of the Model 2 model were carried out with different values of the F coefficient presented in Table 2.

**Table 2** Model 2 cavitation calculations

Calculation code name	F factor value
F1	$F_{vap} = 0.5; F_{cond} = 1$
F2	$F_{vap} = 0.5; F_{cond} = 0.1$
F3	$F_{vap} = 250; F_{cond} = 0.001$
F4	$F_{vap} = 500; F_{cond} = 0.001$
FD	$F_{vap} = 50; F_{cond} = 0.01$

## 4 Results

### 4.1 Turbulence Model Choice

The calculation results for Model 1 are shown in Fig. 4, and for Model 2 are shown in Fig. 5.

Average deviations from the experimental data are summarized in Table 3.

The deviation is calculated from the values of the head  $H$  at the points of the curves with the corresponding NPSH, falling into the range of values of the experimental curve.

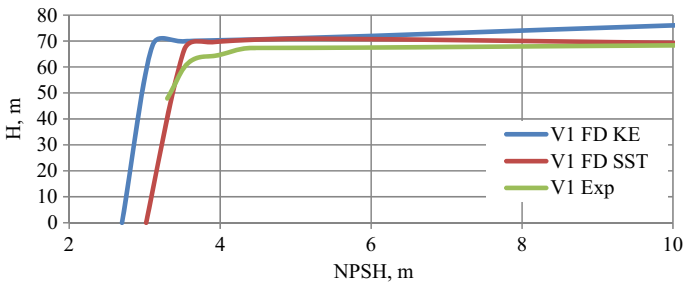


Fig. 4 Calculation results using various turbulence models. Model 1

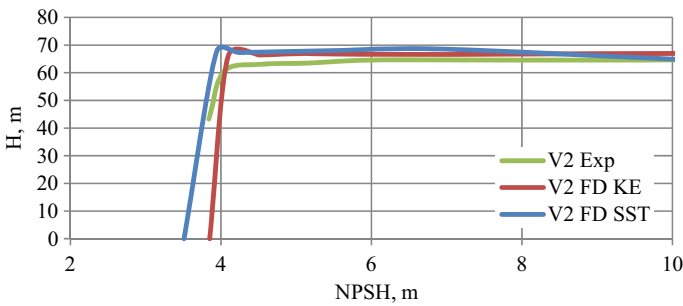


Fig. 5 Calculation results using various turbulence models. Model 2

Table 3 Deviations based on the calculation results with standard F coefficients

Calculation code name	Deviation, %	Qualitative compliance with cavitation stall prediction
V1 FD SST	5.39	Qualitatively correct
V1 FD KE	10.03%	Qualitatively incorrect
V2 FD SST	5.38%	Qualitatively incorrect
V2 FD KE	4.99%	Qualitatively correct

Both  $k-\epsilon$  and SST models give the same results, but the SST model gives on average the best match at all points of the characteristics. However, if we talk about the total calculation time, then the model  $k-\epsilon$  is a lower time spent on calculating 1 point of the curve. For further research, the  $k-\epsilon$  turbulence model is selected.

### 4.2 Calibration of Cavitation Model Coefficients

In order to calibrate the coefficient  $F$ , as noted above, the  $k-\epsilon$  turbulence model was used. The results of the  $F$  factor calibration are shown in Fig. 6.

Speaking in general about the qualitative influence of the  $F$  factor on the form of the characteristic, the following can be noted:

- an increase of  $F_{vap}$  with a simultaneous decrease of  $F_{cond}$  leads to an earlier onset of cavitation, with the same value of NPSH;
- an increase of  $F_{vap}$  with a simultaneous decrease of  $F_{cond}$  leads smoother breakdown of the cavitation curve  $H(NPSH)$ .

In this case, it is clearly seen that qualitative agreement with the experiment is observed in the calculations FD, F3, and F4. In this case, it is more logical to compare the value of the NPSH3.

The values of NPSH3 and deviations of the calculated data from the experiment value are shown in Table 4.

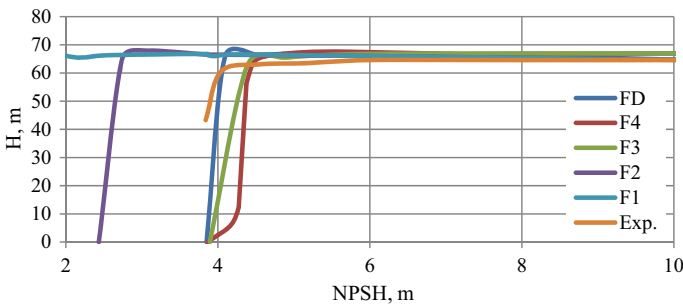


**Fig. 6** Comparison of the calculation results with different values of the coefficient  $F$  of the Model 2

**Table 4** Calibration results of the  $F$  coefficient values

Calculation	NPSH3, m	Deviation, %
Experiment	4.32	–
F3	4.5	4.17
F4	4.45	3.01
FD	4.088	5.56



The fact that the value of the deviation of the NPSH3 for the calculation with the standard values of the factor F (FD) does not exceed a value of 10%, indicates a satisfactory agreement between the calculation and experiment. It can be concluded that for a given geometry of an auger centrifugal pump and a fluid flow regime, the use of the standard Rayleigh-Plesset cavitation model is satisfactory. However, for geometry Model 2, the values of the coefficients F3 are preferable:  $F_{vap} = 250$ ;  $F_{cond} = 0.001$  with the expected level of deviation of the NPSH3, about 4%. The choice was made not in favor of the F4 coefficients, which is explained by the fact that they are less close to the preferred range of standard values  $F_{vap}$  and  $F_{cond}$  (FD).

### 4.3 Visualization of the Flow in the Blade Channels of the Auger

The distribution of the vapor volume fraction between the blades of the auger for each calculation in accordance with Table 2 for different values of NPSH is shown in Fig. 7. It is clearly seen that with a simultaneous increase in the value of  $F_{vap}$  and a decrease of  $F_{cond}$  at similar values of NPSH, the vapor volume fraction between the blades increases, and the length of the part of the blade, on which the vapor volume fraction is present, also increases. At the same time, it is worth noting the fact that qualitatively the stall of the pump occurs in different ways:

- the lower  $F_{vap}$  and higher  $F_{cond}$ , the more the vapor fraction tends to uniformly occupy the areas between the blades. At higher  $F_{vap}$  and lower  $F_{cond}$ , the channel cross-section, on the contrary, is not completely occupied by the vapor. In this case, the vapor is concentrated around the blade profile;
- calculations with lower  $F_{vap}$  and higher  $F_{cond}$ , provide lower values of the average and maximum vapor volume fraction in the auger channels;
- the lower  $F_{vap}$  and higher  $F_{cond}$  provide cavitation less loaded the pressure side of the blade, both in non-cavitation and install operation.

## 5 Conclusion

In this work, experimental and numerical studies were carried out in order to investigate curves Head versus NPSH of two models of auger centrifugal stages. Comparing the results of CFD calculations using the k- $\epsilon$  and SST turbulence models with the Rayleigh-Plesset cavitation model and experiment, a good coincidence was found, as evidenced by the average deviations on the curves of the order of 7,5% for k- $\epsilon$  and 5,4% for SST. However, as noted above, in terms of computational resources, the k- $\epsilon$  model is preferable to the SST model. Based on this, in further studies, it is

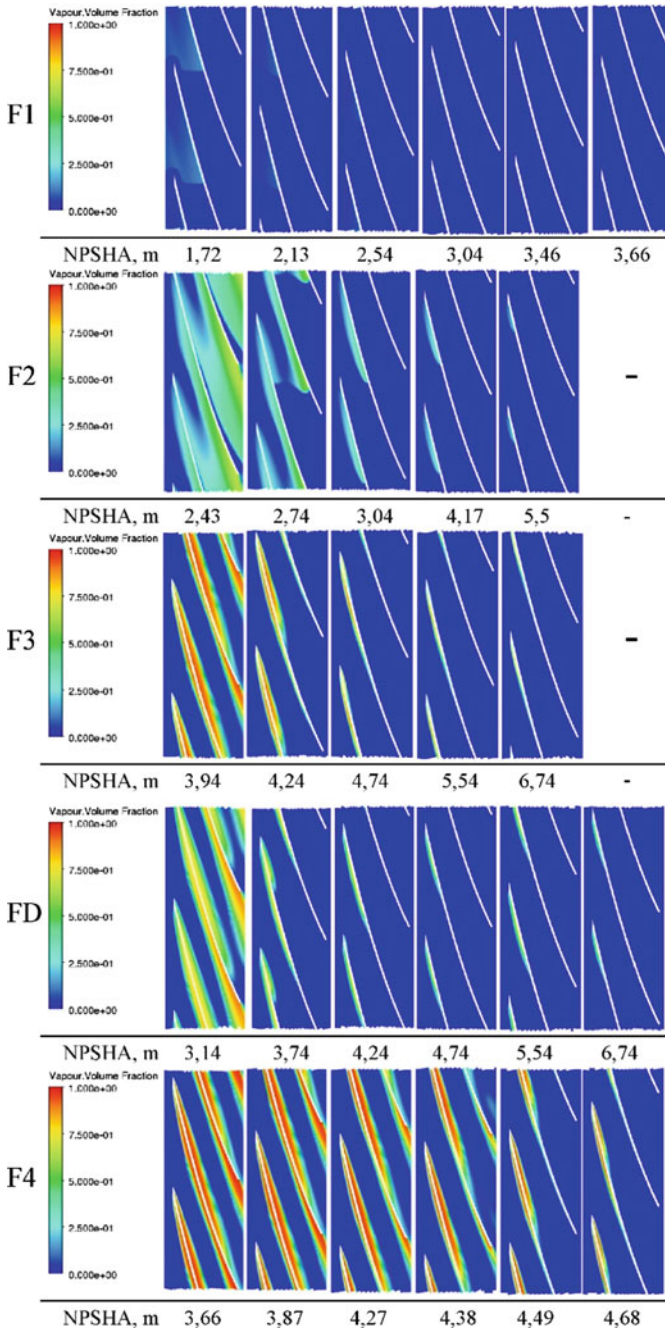


Fig. 7 Vapor volume fraction distribution

recommended to use the standard  $k-\varepsilon$  model, or models of this class, such as RNG  $k-\varepsilon$  and Realizable  $k-\varepsilon$ .

The extension of the results obtained using the  $k-\varepsilon$  model to other turbulence models of this class is fair. The latter is confirmed by the fact that there are a large number of works that affirm the similarities of the results of applying such class models when calculating pumping units, for example [11, 12, 24].

Calibration of the factor responsible for the rate of condensation and vaporization,  $F$  of the Rayleigh-Plesset model, showed that for this case considered in the work, it is expedient to choose the values:  $F_{vap} = 250$  and  $F_{cond} = 0.001$ . It is also worth noting that using the default  $F_{vap} = 50$ ;  $F_{cond} = 0.01$  in the general case can give qualitatively satisfactory results. The results of this work are in qualitative agreement with the results of the work [21].

Analysis of the visualization of the distribution of the vapor volume fraction showed that the results obtained are adequate. The results agree with the meaning of the coefficients  $F_{vap}$  and  $F_{cond}$ , which control the mass transfer rate of the vapor fraction to the water fraction and vice versa. Higher  $F_{vap}$  values intensify the formation of the vapor fraction, so this leads to the fact that the vapor fraction increases, as mentioned above. Lower values of the factor  $F_{cond}$  lead to the fact that the generated fraction of vapor will remain and “live” in the flow for a longer time, as evidenced by the propagation of vapor along the blade length.

The question of choosing the best settings for the cavitation model based on the Rayleigh-Plesset equation for other operating regimes and pump geometries remains open. Strictly speaking, it is incorrect to state the comprehensive applicability of the results obtained to other geometries and modes different from the rated one. For this, as noted earlier, it is necessary to verify and validate a larger number of discrete models.

Also, this chapter did not study the influence of the presence or absence of a leakage an impeller shroud to pump housing clearance on the calculation results, which is also a question for further research. Of particular interest is also the study of the effect on the final result of modeling the tip between the auger blade and auger shroud surface.

An important issue is the study of the effect of the mesh independence by the pressure drop value, which is not done in works on calculating cavitation using CFD codes. From the practice of calculations, we can say that the refinement of the mesh at the leading edge can significantly affect the magnitude of the pressure drop and, as a consequence, the intensity and development of cavitation.

In conclusion, it should be noted that the results of this work can be applied in the modernization of the digital twin of the RITM-200 nuclear power installation, which is being developed at JSC “Afrikantov OKBM” [2]. The obtained values of the coefficients  $F_{vap} = 250$  and  $F_{cond} = 0.001$  are planned to be used to calculate the cavitation characteristics of a centrifugal pump of one of the circulation circuits of a power installation. There is also an additional interest in the development of the topics of work and the formation of a technique for modeling cavitation curves to implement it into the technology of creating supercomputer twins of nuclear power installations.

## References

1. Varé, C., Morilhat, P.: Digital twins, a new step for long term operation of nuclear power plants. In: Liyanage, J., Amadi-Echendu, J., Mathew, J. (eds.) *Engineering Assets and Public Infrastructures in the Age of Digitalization. Lecture Notes in Mechanical Engineering*. Springer, Cham. (2020). [https://doi.org/10.1007/978-3-030-48021-9\\_11](https://doi.org/10.1007/978-3-030-48021-9_11)
2. Bolshukhin, M.A., Bolnov, V.A., Budnikov, A.V., et al.: Digital twin of nuclear power plants. Development technology and application experience. *Atomic Energy* **129**(2), 74–79 (2020). <https://doi.org/10.1007/s10512-021-00717-8>
3. Gülich, J.F.: *Centrifugal Pumps*, 3rd edn. Springer, Heidelberg, Berlin (2014)
4. Shah, S.R., Jain, S.V., Patel, R.N., Lakhera, V.J.: CFD for centrifugal pumps: a review of the state-of-the-art. *Procedia Eng.* **51**, 715–720 (2013). <https://doi.org/10.1016/j.proeng.2013.01.102>
5. Lomakin, V.O.: Investigation of two-phase flow in axial-centrifugal impeller by hydrodynamic modeling methods. In: 2015 International Conference on Fluid Power and Mechatronics (FPM), pp. 1204–1206. IEEE (2015). <https://doi.org/10.1109/FPM.2015.7337302>
6. Dick, E., Vierendells, J., Serbruyns, S., Voorde, J.V.: Performance and prediction of centrifugal pumps with steady and unsteady CFD-methods. *WIT Trans. Eng. Sci.* **36**, 559–568 (2002)
7. Prunieres, R., Inoue, Y., Nagahara, T.: Investigation of the flow field and performances of a centrifugal pump at part load. In: IOP Conference Series: Earth and Environmental Science, vol. 49, p. 032015 (2016). <https://doi.org/10.1088/1755-1315/49/3/032015>
8. Kaewnai, S., Chamaoot, M., Wongwises, S.: Predicting performance of radial flow type impeller of centrifugal pump using CFD. *J. Mech. Sci. Technol.* **23**, 1620–1627 (2009). <https://doi.org/10.1007/s12206-008-1106-1>
9. Skrzypacz, J., Szulc, P.: The CFD calculations as a main tool for the mixed-flow pump modernization. In: IOP Conference Series: Materials Science and Engineering, vol. 233, p. 012008 (2017). <https://doi.org/10.1088/1757-899x/233/1/012008>
10. Liu, H., Wang, Y., Liu, D., et al.: Assessment of a turbulence model for numerical predictions of sheet-cavitating flows in centrifugal pumps? *J. Mech. Sci. Technol.* **27**, 2743–2750 (2013). <https://doi.org/10.1007/s12206-013-0720-8>
11. Liu, H.L., Liu, M.M., Dong, L., Ren, Y., Du, H.: Effects of computational grids and turbulence models on numerical simulation of centrifugal pump with CFD. In: IOP Conference Series: Earth and Environmental Science, vol. 15, p. 062005 (2012). <https://doi.org/10.1088/1755-1315/15/6/062005>
12. Zhou, S.P., et al.: Numerical Simulation and Impeller Optimization of a Centrifugal Pump. In: *AMR*, vol. 472–475, pp. 2195–2198 (2012). <https://doi.org/10.4028/www.scientific.net/amr.472-475.2195>
13. Feng, J., Benra, F.-K., Dohmen, H.J.: Application of different turbulence models in unsteady flow simulations of a radial diffuser pump. *Forsch Ing.* **74**, 123–133 (2010). <https://doi.org/10.1007/s10010-010-0121-4>
14. Zhang, Y.L., Yuan, S.Q., Zhang, J.F., Feng, Y.N., Lu, J.X.: Numerical investigation of the effects of splitter blades on the cavitation performance of a centrifugal pump. In: IOP Conference Series: Earth and Environmental Science, vol. 22, p. 052003 (2014). <https://doi.org/10.1088/1755-1315/22/5/052003>
15. Wu, D., Yuan, S., Ren, Y., et al.: CFD investigation of the influence of volute geometrical variations on hydrodynamic characteristics of circulator pump. *Chin. J. Mech. Eng.* **29**, 315–324 (2016). <https://doi.org/10.3901/CJME.2015.1224.154>
16. Thakkar, S., Vala, H., Patel, V.K., et al.: Performance improvement of the sanitary centrifugal pump through an integrated approach based on response surface methodology, multi-objective optimization and CFD. *J. Braz. Soc. Mech. Sci. Eng.* **43**, 24 (2021). <https://doi.org/10.1007/s40430-020-02753-0>
17. Lomakin, V.O., Bibik, O.Y.: The influence of empirical rates (values) in the Releya-Plesett’s model on the cavitation calculated characteristics of the centrifugal pump. *Gidravlika.* **1**(3), 26–38 (2017)

18. Zhang, N., Gao, B., Li, Z., Jiang, Q.: Cavitating flow-induced unsteady pressure pulsations in a low specific speed centrifugal pump. *R. Soc. Open Sci.* **5**, 180408 (2018). <https://doi.org/10.1098/rsos.180408>
19. Ocepek, M., Peršin, Z., Kern, I., Djelić, V., Muhić, S., Lipej, A.: Experimental and numerical analysis of cavitation and pressure fluctuations in large high head propeller turbine. In: *IOP Conference Series: Earth and Environmental Science*, vol. 405, p. 012032 (2019). <https://doi.org/10.1088/1755-1315/405/1/012032>
20. Li, W.-G.: Modeling viscous oil cavitating flow in a centrifugal pump. *J. Fluids Eng.* **138** (2015). <https://doi.org/10.1115/1.4031061>
21. Liu, H., Wang, J., Wang, Y., Zhang, H., Huang, H.: Influence of the empirical coefficients of cavitation model on predicting cavitating flow in the centrifugal pump. *Int. J. Naval Archit. Ocean Eng.* **6**, 119–131 (2014). <https://doi.org/10.2478/ijnaoe-2013-0167>
22. Limbach, P., Skoda, R.: Numerical and experimental analysis of cavitating flow in a low specific speed centrifugal pump with different surface roughness. *J. Fluids Eng.* **139** (2017). <https://doi.org/10.1115/1.4036673>
23. Cao, L., Wang, Z.W., Xiao, Y.X., Yao, Y.Y., Zhu, W.: Numerical research on the cavitation characteristics for typical conditions of a centrifugal pump with whole flow passage. In: *IOP Conference Series: Materials Science and Engineering*, vol. 72, p. 032027 (2015). <https://doi.org/10.1088/1757-899x/72/3/032027>
24. Liu, H., Wang, Y., Liu, D., Yuan, S., Wang, J.: Assessment of a turbulence model for numerical predictions of sheet-cavitating flows in centrifugal pumps? *J. Mech. Sci. Technol.* **27**, 2743–2750 (2013). <https://doi.org/10.1007/s12206-013-0720-8>
25. Hanimann, L., Mangani, L., Casartelli, E., Widmer, M.: Cavitation modeling for steady-state CFD simulations. In: *IOP Conference Series: Earth and Environmental Science*, vol. 49, p. 092005 (2016). <https://doi.org/10.1088/1755-1315/49/9/092005>
26. Zwart, P.J., Gerber, A.G., Belamri, T.: A two-phase flow model for predicting cavitation dynamics. In: *Fifth International Conference on Multiphase Flow*, Yokohama, Japan (2004)
27. Paul, D., Agarwal, H., Ponangi, B.R.: CFD analysis of two-phase cavitating flow in a centrifugal pump with an inducer. In: *Lecture Notes in Mechanical Engineering*, pp. 17–31. Springer Singapore (2020). [https://doi.org/10.1007/978-981-15-7779-6\\_2](https://doi.org/10.1007/978-981-15-7779-6_2)
28. Franc, J.-P.: The Rayleigh-Plesset equation: a simple and powerful tool to understand various aspects of cavitation. In: *Fluid Dynamics of Cavitation and Cavitating Turbopumps*, pp. 1–41. Springer Vienna (2007). [https://doi.org/10.1007/978-3-211-76669-9\\_1](https://doi.org/10.1007/978-3-211-76669-9_1)

# On the Qualitative Study of Phase Portraits for Some Categories of Polynomial Dynamic Systems



Irina Andreeva  and Tatiana Efimova

**Abstract** A chapter is devoted to the results of the original study of some extended dynamic systems families with reciprocal polynomial right parts. It describes especially invented for the aims of this study research methods, fruitful for further investigations in the field, and useful for a wide range of applications. Dynamic systems play an important role in different areas of contemporary science, computing, and engineering, such as mathematical modeling of physical processes, the broad spectrum of complicated problems of modern cybernetics, for example, in fundamental studies of computing and producing systems, as well as in modeling of technical, geophysical, biological, sociological and economical events. Dynamic systems serve as a powerful mathematical apparatus under conditions if statistical events, or fluctuations, may be disregarded. Having the strictly outlined mathematical features, but in principle infinite, the family of dynamic systems under consideration was subdivided into several naturally appeared hierarchical levels. Thus, they were thoroughly investigated using the terms and methods of the qualitative theory of ordinary differential equations. The full set of about 250 their topologically different phase portraits was revealed, constructed, and described. The close-to-coefficient criteria of the realization of existing for this dynamic systems family phase portraits were found. The absence of limit cycles for all the systems belonging to the considered family was strictly proved.

**Keywords** Dynamic system · Cybernetics · Fluctuation · Reciprocal polynomials · Trajectory · Separatrix · Phase space · Phase portrait · Singular point · Poincare circle · Poincare transformation · Poincare sphere

---

I. Andreeva (✉) · T. Efimova

Peter the Great St.Petersburg Polytechnic University, 29 Polytechnicheskaya, St.Petersburg 195251, Russia

e-mail: [irandr@inbox.ru](mailto:irandr@inbox.ru)

# 1 Introduction

Challenges offered by the development of modern high technologies pose tasks for researchers to use new methods of mathematical modeling. A broad spectrum of contemporary scientific areas cannot develop without the involvement of mathematical apparatus such as dynamic systems. Mathematical modeling of any processes occurring in time with certain speed and possible acceleration is based on differential equations and systems of differential equations. This provision applies to investigation of geophysical and space processes [3, 9, 10, 24, 31, 32], to study of seismic stability of constructions and buildings [11–14], to practical and theoretical research and development in the fields of computing and producing systems [28], cybernetics and artificial intelligence systems, neural networks [21–23], mathematical modeling of biological processes [17, 29, 30], including virus distribution, population, sociological [15] and economical events [25–27]. All of these research fields are mathematically based on dynamic systems and their qualitative and also computational studies.

And one of the primary moments in a dynamic system investigation is the identification, enlisting, and classification of equilibrium positions of a system with a study of their stability.

The present chapter is devoted to the results and methods of the original study of some broad class, or family, of dynamic systems, characterized by their polynomial right parts (a cubic form for the first equation of the considered system, and a quadratic one for the second equation). Those right parts are taken as reciprocal polynomial forms. That means they won't have common multipliers being decomposed into polynomials of lower degrees.

Foundations of the qualitative theory of ordinary differential equations (and thus of the theory of dynamic systems) were laid by the great French mathematician and physicist Jules H. Poincare (1854–1912), who is considered to be one of the last encyclopedists of modern science (together with David Hilbert, 1862–1943). H. Poincare proved, that every normal autonomous second-order polynomial differential system considered on the real extended plane of its phase variables  $R_{x,y}^2$ , allows in principle its comprehensive qualitative investigation [1, 4–6].

Qualitative studies of dynamic systems were continued by later researchers, and features of some special classes of them were successfully described. The important contribution in this field was done by mathematicians belonging to Russian and even to St.Petersburg mathematical school. Among them were, for example, Dr. Victor A. Pliss and Dr. Alexey F. Andreev from the Differential Equations Department of the Faculty of Mathematics and Mechanics of St.Petersburg State University [2].

## 2 Initial Mathematical Formulation and Research Methods Survey

In the present work we study some specific, but rather a broad category, or family, of polynomial second-order differential dynamic systems on the arithmetical phase plane  $x, y$ :

$$\frac{dx}{dt} = X(x, y), \frac{dy}{dt} = Y(x, y), \tag{1}$$

in which  $X(x, y), Y(x, y)$  are taken as reciprocal polynomials (they haven't common multipliers in their decompositions into lower-order forms). Here the polynomial  $X$  is considered to be a cubic, while polynomial  $Y$  is a quadratic form, satisfying to the conditions that do not detract from the generality of reasoning:

$$X(0, 1) > 0, Y(0, 1) > 0. \tag{2}$$

With the help of a method of consequent mappings introduced by H. Poincare— firstly a central mapping and then an orthogonal one, which is performed via the two Poincare transformations, it becomes possible to obtain a detailed qualitative pattern of trajectories for the dynamic systems, belong to the (1)–family, in a Poincare circle. That leads to the construction and description of all possible for this family of systems (different in the topological meaning) phase portraits.

A sequence of steps in this study is as follows.

With the use of a central Poincare mapping, we display a phase plane  $\overline{R}_{x,y}^2, \overline{R}_{x,y}^2$  of a differential system under consideration onto a Poincare sphere  $\Sigma$  (from the center  $(0, 0, 1)$  of the Poincare sphere  $\Sigma$ ):

$$X^2 + Y^2 + Z^2 = 1 \tag{3}$$

(assuming the diametrically opposite points of the Poincare sphere to be identified).

With the use of an orthogonal Poincare mapping, we display a lower enclosed semi-sphere of a Poincare sphere onto an enclosed Poincare  $\underline{\Omega}$ :

$$x^2 + y^2 \leq 1 \tag{4}$$

(similar, assuming diametrically opposite points of a boundary  $\Gamma$  of a Poincare circle as identified ones) [1, 4–6].

We introduce special polynomials of key importance, related to the system (1):



$$\begin{aligned} P(u) &:= X(1, u) \equiv p_0 + p_1u + p_2u^2 + p_3u^3, \\ Q(u) &:= Y(1, u) \equiv a + bu + cu^2. \end{aligned} \tag{5}$$

For all dynamic systems of the (1)–family, the following common features have been revealed.

1. Real roots of the special polynomial  $Q(u)$  are in fact angular coefficients of isoclines of zero.
2. Real roots of the special polynomial  $P(u)$  represent angular coefficients of isoclines of infinity.

Further, we consider and always write out roots of both the abovementioned special polynomials  $P(u)$ ,  $Q(u)$  in ascending order. Among the roots of different polynomials, we never have equal ones, because the right parts of system (1) equations are reciprocal. Hence, polynomials  $P(u)$ ,  $Q(u)$  are also turn out to be reciprocal.

We study and describe all possible topological types, which appear to be possible for a finite singular point  $O(0,0)$ , as well as for all existing infinitely remote singularities of systems, which belong to the (1)–systems family [7, 16, 18].

During further investigation, the whole broad family (1) is split into subfamilies of several consequent levels and sublevels of hierarchy (up to four sequent levels for some cases). The principles of splitting depend, at the first step of this process, on the details of the decompositions of polynomials  $P(u)$ ,  $Q(u)$  to the lower degree forms, and on the presence (or absence) multiple roots for each one of these special characteristic polynomials. In the next steps of the work, the splitting continues depending on properties of the trajectories' qualitative pattern; in particular, depending on the fact, if the continuation of a given separatrix from a small neighborhood of a singular point to all the length of this separatrix appears to be unique or not unique. As a result, all possible for the whole (1)–family of dynamic systems phase portraits were constructed and fully investigated. There appeared to be about 250 topologically different qualitative types of them. Also were revealed criteria of their realization in a close to coefficient form.

In particular, there was strictly proved, that (1)–systems cannot have limit cycles [18, 19].

### 3 Subfamilies of the First Hierarchical Level and Splitting of them into Subfamilies of the Next Levels

The clear examples of subfamilies, related to the first hierarchical level, are given by some following variants.

Firstly, we mention the case of existence of three different roots of the special characteristic polynomial  $P(u)$ , and two different roots of the polynomial  $Q(u)$ , correspondingly. The right parts of the dynamic system (1) will in this case look like the follows:

$$X(x, y) = p_3(y - u_1x)(y - u_2x)(y - u_3x),$$

$$Y(x, y) = c(y - q_1x)(y - q_2x), \tag{6}$$

where  $p_3 > 0, c > 0, u_1 < u_2 < u_3, q_1 < q_2, u_i \neq q_j$  for each pair of  $i$  and  $j$ .

Clearly, under these conditions, we obtain ten independent variants of the order of different roots, belonging to both characteristic polynomials  $P(u), Q(u)$ , since

$$C_5^2 = \frac{5!}{3!2!} = 10. \tag{7}$$

And those ten different orders of roots could bring us also ten subfamilies of the next hierarchical level. Meanwhile, the detailed research reveals, that for real only 6 of those possible subfamilies are really independent one from another.

One of the key notions for the whole presented research is the notion of the *RSP (RSQ)*—be a sequence of all real roots, enlisted in the ascending order, of the characteristic specially introduced for these dynamic systems polynomial  $P(u)$  ( $Q(u)$ ), and a conjugated notion of the *RSPQ*—be a sequence of all real roots (in the ascending order) of both polynomial forms  $P(u), Q(u)$ .

Further, we introduce a notion of a DC-transformation—be a double replacement (or change) of variables:  $(t, y) \rightarrow (-t, -y)$ . Such a change of variables serves to transform the system under consideration to another similar differential system. But it is clear, that for the newly obtained system signs and numberings of real roots of its characteristic forms  $P(u), Q(u)$ , together with directions of its motion along trajectories (with the growth of  $t$ ) change to the opposite. Two different systems will further be named the mutually inversed pair (regarding the DC-transformation), in the case when the DC-transformation transmutes one of them into the other, and the independent pair (regarding the DC-transformation), oppositely.

Namely, the DC-transformation of (6)–systems allows concluding: 6 ones among them actually form independent DC-pairs, but every taken system among the remaining four has the mutually DC-inversed system-companion among the first 6 systems. Thus, it makes sense to assign a definite number  $r \in \{1, \dots, 10\}$  to the possible root sequences of characteristic polynomials of (6)–systems, so that systems with  $(RSPQ)_r, r = 1, 6$ , appear to be independent pairwise, and the same time systems, whose root sequences get the numbers  $r = 7, 10$ , turned out to be mutually DC-inversed to the systems obtained numbers  $r = \bar{1}, 4$ , correspondingly.

After the abovementioned comments, it is natural to introduce the notion of a  $(6)_r$ –sub subfamily of (6)–subfamily of dynamic systems:

$(6)_r$ –sub subfamily of (6)–subfamily := a totality of all dynamic systems of the (6)–subfamily of (1)–systems, such as for each of the ascending sequence of real roots of characteristic polynomials of the dynamic system  $P(u), Q(u)$ :  $RSPQ = (RSPQ)_r$ .

According to a single plan, we will step-by-step investigate  $(6)_r$ –sub subfamilies of (6)–subfamily of (1)–systems,  $r = \bar{1}, 6$ . Upon revealing their detailed features and constructing their phase portraits in the Poincare circle, we will be able to obtain

similar data for the  $(6)_r$ -sub subfamilies,  $r = \underline{7, 10}$ , using the DC-transformation for the investigated already  $(6)_r$ -families,  $r = \underline{1, 4}$ .

For every subfamily among the six DC-independent ones, we introduce a common program of their further investigation. This program includes several important items.

All singular points of the taken subfamily of dynamic systems in the enclosed Poincare circle are identified. They appeared to be the finite singular point  $O(0, 0) \in \Omega$  together with infinitely remote singular points  $O_i^\pm(u_i, 0) \in \Gamma$ ,  $i = \underline{0, 3}$ ,  $u_0 = 0$ . We introduce and apply to their notions of a nodal ( $N$ ) and saddle ( $S$ ) bounds of semi trajectories; of a separatrix and of a topo-dynamical type of a taken singular point [16, 18].

For every given singular point, we study the behavior of its separatrices. First of all, during this part of the study, we take into consideration a question of the uniqueness of this separatrix continuation from some tiny neighborhood of the singular point to the full length of the separatrix. Also, we consider a mutual arrangement of separatrices in the Poincare  $\Omega$ . All mentioned questions are fully answered for all the existing subfamilies of (1)-systems family [19].

All possible for the taken subfamily phase portraits we construct and describe together with criteria of their appearance [16, 18, 19]. In particular, for the subfamily (6) appeared to exist as many as 93 different phase portraits, independent under topological understanding [1, 16, 18].

Secondly, we mention another good example of the subfamily, belonging to the first hierarchical level of subfamilies. It is the case of a multiple roots existing for the cubic form.

$$\begin{aligned} X(x, y) &= p(y - u_1x)^{k_1}(y - u_2x)^{k_2}, \\ Y(x, y) &= q(y - q_1x)(y - q_2x), \end{aligned} \tag{8}$$

where  $p, q, u_1, u_2, q_1, q_2 \in R$ ,  $p > 0, q > 0, u_1 < u_2, q_1 < q_2, u_i \neq q_j$  for every pair of  $i, j \in \{1, 2\}$ ,  $k_1, k_2 \in N$ ,  $k_1 + k_2 = 3$ .

Such a case brings us the two subclasses of systems (8). First of them we'll call the A-class, and this class includes systems, for which  $k_1 = 1, k_2 = 2$ , and the second class we call the B-class, for the systems of which oppositely  $k_1 = 2, k_2 = 1$ .

So, the characteristic polynomials  $P(u), Q(u)$  will have forms:

$$P(u) := X(1, u) \equiv p(u - u_1)(u - u_2)^2, \quad Q(u) := Y(1, u) \equiv q(u - q_1)(u - q_2),$$

for the A-class dynamic systems, and

$$P(u) := X(1, u) \equiv p(u - u_1)^2(u - u_2), \quad Q(u) := Y(1, u) \equiv q(u - q_1)(u - q_2),$$

for the B-class systems. Possible different combinations for their roots orders we will see for each of these cases  $C_4^2 = \frac{4!}{2!2!} = 6$  correspondingly. But systems, belonging to these different classes *A* and *B*, have to be and were studied independently [18, 20].

For the aim of the detailed study of the (8)–subfamily a notion of a (8)<sub>*r*</sub>–family of the (8)<sub>*A*</sub>–systems (i.e. (8)–systems belonging to the *A*-class) has been introduced:

(8)<sub>*r*</sub>–family of the (8)<sub>*A*</sub>–systems be a totality of all the (8)<sub>*A*</sub>–systems with the same root sequence RSPQ number *r*, which is taken from the abovementioned list of possibilities.

After this, we undertake the sequential study of (8)<sub>*r*</sub>–families of (8)<sub>*A*</sub>–systems.

The study progress for every taken (8)<sub>*r*</sub>–family follows the main pattern. For each singular point of a given subsystem belonging to the taken family were introduced and applied important notions of the bundles *N* (the node bundle) and *S* (the saddle bundle) of semi trajectories of this subsystem, which appear to be adjacent to the considered singular point; of this singular point’s separatrix and also of its topological (TD) type. The following phases of an investigation are enlisted below.

A (8)<sub>*r*</sub>–family is split into (8)<sub>*r,s*</sub>–sub subfamilies (they are, obviously, belong to the third hierarchical level), where  $s = \underline{1, 5}$ .  $\forall s \in \{1, \dots, 5\}$  we reveal the topological dynamical types of the singular points of the (8)<sub>*r,s*</sub>–systems, and investigate their separatrices.

$\forall s \in \{1, \dots, 5\}$  the behavior of their singularities’ separatrices has been studied for the systems belonging to the (8)<sub>*r,s*</sub>–sub subfamily. Here the main questions that arise to answer them are about: (1) is a global continuation of each taken separatrix from some small neighborhood of a given singular point into all the lengths of this separatrix in the Poincare circle  $\Omega$  unique or not unique; (2) what is the relative position in the Poincare circle  $\Omega$  of all existing separatrices. The matter is that if for a taken number *s* the global continuation of each separatrix of singular points of (8)<sub>*r,s*</sub>–systems appear to be unique, which means, that their relative position in a Poincare circle  $\Omega$  is stable (invariable), therefore, all (8)<sub>*r,s*</sub>–systems will have one common phase portrait in a Poincare circle ( $PP_{r,s}$ ). Otherwise, if for some taken number *s* (8)<sub>*r,s*</sub>–systems will have several, e.g. *m* separatrices, for which their global continuations will not be unique, then (8)<sub>*r,s*</sub>–family has to be split into subfamilies of the next, already fourth hierarchical level denoted as (8)<sub>*r,s,l*</sub>–families,  $l = \underline{1, m}$ . For each of them, as it was proved during the further study of these subfamilies, the global continuations of each separatrix are unique, while their relative positions inside the circle  $\Omega$  appeared to be invariable. Thus, a phase portrait of all such a subfamily of systems inside the  $\Omega$  the circle is one and common for all the given subfamily:  $PP_{r,s,l}$ .

All revealed phase portraits inside the circle  $\Omega$  for the whole totality of systems of (8)<sub>*r*</sub>–families,  $r = \underline{1, 6}$ , were constructed in two forms of representation (in a graphical form and also in a table, or descriptive, form). Simultaneously formulated the (close to coefficient) criteria for each portrait realization [16].

The summary of phase portraits for the class *A* families is as follows. They show in a total of 45 topologically different types of phase portraits accordingly to the number of sub subfamilies into which the whole subfamily of the first hierarchical level has been split. Similarly, the *B*-class of subfamilies shows 52 different types

of phase portraits due to the fact that the number of sub subfamilies of the next hierarchical levels for them appeared to be 52.

The third representative example of subfamilies from the first hierarchical level comes from the interesting subfamily of (1)–systems

$$\frac{dx}{dt} = p_3(y - u_1x)(y - u_2x)(y - u_3x), \frac{dy}{dt} = c(y - q_1x)^2, \tag{9}$$

where  $p_3 > 0, c > 0, u_1 < u_2 < u_3, q_i (\in R) \neq u_i \ i = \underline{1, 3}$ .

Now the investigation process will include such items:

For the beginning, we split the (9)–subfamily into (9)<sub>r</sub>–sub subfamilies, with  $r = \underline{1, 4}$ . It is clear, that they represent the second hierarchical level of systems under investigation already.

Every appeared on the scene sub subfamily represents an (infinite in principle) set of dynamic systems having a proper sequence of real roots of characteristic polynomials  $P(u), Q(u)$ , which we later denote as  $RSPQ = (RSPQ)_r$ , where  $r$  means the number in the list of all existing  $RSPQ$ ’s:

$$\begin{aligned} &u_1, u_2, u_3, q, \\ &u_1, u_2, q, u_3, \\ &u_1, q, u_2, u_3, \\ &q, u_1, u_2, u_3. \end{aligned} \tag{10}$$

Using for the dynamic system of (9)–subfamily a double change of its variables (we call this important study instrument the DC-transformation):  $(t, y) \rightarrow (-t, -y)$ , we conclude, that the (9)<sub>r</sub>–sub subfamilies,  $r = 1, 2, 3, 4$ , to the (9)<sub>r</sub>–families,  $r = 4, 3, 2, 1$ , correspondingly (and, obviously, backward). This observation states, that sub subfamilies of systems (9)<sub>1</sub>and(9)<sub>2</sub> are not connected one to another via the DC-transformation; while families (9)<sub>3</sub>and(9)<sub>4</sub> appear to be connected (mutually inversed) via the DC-transformation to the sub subfamilies (9)<sub>2</sub>and(9)<sub>1</sub>, correspondingly.

For the second step, we investigate (9)<sub>r</sub>–families of systems,  $r = 1, 2$ , in turn, based on a single abovementioned program [7, 19], namely:

2<sub>1</sub>. After fixing the number  $r \in \{1, 2\}$ , we further subdivide the taken (9)<sub>r</sub>–family into (9)<sub>r,s</sub>–sub subfamilies [16, 18, 19],  $s = \underline{1, 9}$ , belonging to the third hierarchical level this time, for which we investigate their singular points and as a result, find out topo dynamical types (TD-types) of those singular points of (9)<sub>r,s</sub>–systems.

2<sub>2</sub>.  $\forall s \in \{1, \dots, 9\}$  we make up and draw the so-called “Off-Road Map” (ORM) for (9)<sub>r,s</sub>–systems [1, 16, 18, 19], and with its help define the  $\alpha(\omega)$ –limit set of each and every  $\alpha(\omega)$ –separatrix, together with the mutual disposition of all existing separatrices belong to this sub subfamilies of systems inside the Poincare circle  $\underline{\Omega}$ .

23. Eventually, it becomes possible to obtain, construct and describe all various in the topological understanding phase portraits possible for  $(9)_r$ -dynamic systems.

After the subfamilies of the second level of our hierarchy, having numbers  $r \in \{1, 2\}$ , our research moves on to  $(9)_r$ -subfamilies of systems,  $r = 3, 4$ . Now, through the DC-transformation, and taking into consideration the results for  $(3.1)_r$ -families,  $r = 2, 1$ , we eventually obtain all different phase portraits for  $(3.1)_3$  and  $3.1_4$ -subsystems.

Summing up the results of the conducted research in this item, it is possible to outline: for the totality of dynamic systems belong to the  $(9)_r$ -subfamilies,  $r = 1, 4$ , we revealed  $15 + 11 + 11 + 15 = 52$  different phase portraits in the Poincare circle  $\underline{\Omega}$  correspondingly.

The fourth representative example of subfamilies is given by the following category of systems:

$$\begin{aligned} \frac{dx}{dt} &= p_0x^3 + p_1x^2y + p_2xy^2 + p_3y^3 \equiv p_3(y - u_1x)^2(y - u_2x), \\ \frac{dy}{dt} &= x^2 + bxy + cy^2 \equiv c(y - qx)^2, \end{aligned} \tag{11}$$

where  $p_3 > 0, c > 0, u_1 < u_2, q(\in R) \neq u_{1,2}$ .

Investigation of this category of systems in principle repeats the previous sequence of research steps.

For every taken into consideration (11)-subsystem  $P(u), Q(u)$ -it's polynomials  $P, Q$ :

$$P(u) := X(1, u) \equiv p_3(u - u_1)^2(u - u_2), Q(u) := Y(1, u) \equiv c(u - q)^2,$$

a consequence of all existing real roots of these characteristic polynomials (the  $RSPQ$ ) can show us in this case three independent variants of it.

And in this case, was revealed, that for every  $(11)_r$ -sub subfamily of  $(11)$ -subsystems seven topologically different phase portraits appear to be possible, so for all categories of dynamic systems from  $(11)$ -subfamilies,  $r = 1, 3$ , the total amount of topologically different phase portraits reaches 21.

All possible for the discussed families and subfamilies of investigated systems phase portraits were described and constructed in the two convenient forms—in a graphical form and a table (or descriptive) form as well. For the table form of a phase portrait, the following scheme was accepted. A table, describing every portrait, includes 5 or 6 lines. A taken single line is used to describe features of an invariant cell of the phase portrait, i.e., its boundary, a source, and also a sink of the corresponding phase flow [1, 16, 18].

Fine mathematical details and clarifying points in relation to investigations of cubic and quasi quadratic dynamic systems are given in the sources and articles [2, 7, 16, 18, 19].

## 4 Conclusion

The chapter represents research methods and strict mathematical conclusions of the original fundamental investigation of a broad family of polynomial dynamical systems. This study has been undertaken and conducted in the field of the qualitative theory of ordinary differential equations and is based on the methodology of this theory. Precise research methods, a lot of notions and attitudes, directly invented especially for the goals of this work, being new and effective, would be useful for further research of applied dynamic systems, especially of dynamic systems with polynomial right parts of different orders.

Due to that strict fact, that dynamic systems represent the main instrument of mathematical modeling in all fields and branches of modern theoretical and applied science and technology, and especially in the fields of cybernetic systems development, artificial intelligence, and neural networks, as well as in theoretical and practical studies of computing and producing systems, of connections between the notions of energy and information, in the mathematical modeling of geophysical and biological processes, etc., this research work has the sharp actuality.

Its key goal was to reveal, depict and describe all topologically different phase portraits in a Poincare circle, possible for the numerical subfamilies, belonging to several levels of their hierarchy, of a broad initial family of the polynomial differential dynamical systems. All such portraits were eventually enlisted, counted, described, and constructed [8]. This means that qualitative features of all the infinite set of dynamic systems belonging to the considered family are finally investigated.

Thankfully to the new investigation methods, mentioned above, the work will be useful for applied studies of dynamic systems with polynomial right parts. The chapter could be interesting for advanced students and postgraduates as well as for researchers.

## References

1. Andronov, A., Leontovich, E., Gordon, I., Maier, A.: *Qualitative Theory of Second-Order Dynamic Systems*. Wiley, New York (1973)
2. Andreev, A., Andreeva, I., Detchenya, L., Makovetskaya, T., Sadovskii, A.: Nilpotent centers of cubic systems. *Differ. Equ.* **53**(8), 1003–1008 (2017)
3. Krivtsov, A.: The ballistic heat equation for a one-dimensional harmonic crystal. *Dyn. Proc. Gen. Cont. Struct.* **103**, 345–358 (2019)
4. Poincare, H.: *On Curves Defined by Differential Equations*. OGIS, Moscow (1947)
5. Poincare, H.: *Les methodes nouvelles de la mecanique celeste*, Paris (1892–99)
6. Poincare, H.: *Proceedings of the Royal Society, London*, vol. 91, pp. 5–16 (1915)
7. Andreeva, I., Efimova, T.: Phase portraits of a special class of dynamic systems in a Poincare circle. In: *IOP Journal of Physics: Conference Series*, vol. 1236, p. 012053. (2019)
8. Zakharov, V.: *Vibroengineering procedia*, vol. 25, pp. 143–150 (2019)
9. Aksenova, O., Khalidov, I.: *Rarefied Gas Dynamics AIP Conference Proceedings*, vol. 1786, pp. 1000091–1000097. American Institute of Physics, Melville, NY (2016)



10. Aksenova, O., Khalidov, I.: Rarefied Gas Dynamics AIP Conference Proceedings, vol. 1786, pp. 1000071–1000078. American Institute of Physics, Melville, NY (2016)
11. Fahmi, K., Kolosov, E., Fattah, M.: *J. Eng. Appl. Sci.* **14**(4), 1162–1168 (2019)
12. Kolosov, E., Agishev, K., Kolosova, N.: MATEC Web of Conferences, vol. 107, p. 00032 (2017)
13. Kolosova, N., Kolosov, E., Agishev, K.: MATEC Web of Conferences, vol. 107, p. 00065 (2017)
14. Rashid, D., Kolosov, E., Kolosova, N., Soldatenko, T.: Advances and trends in engineering sciences and technologies II. In: Proceedings of the 2nd International Conference on Engineering Sciences and Technologies: ESaT (2016)
15. Zakharov, V.: Optimization mathematical model of the peaceful subordinating interaction of two States. In: IOP Journal of Physics: Conference Series, vol. 1391, p. 012040 (2019)
16. Andreeva, I., Efimova, T.: Investigation of phase portraits belonging to polynomial dynamic systems in a Poincare disk. In: IOP Journal of Physics: Conference Series, vol. 1425, p. 012040, 7 p. (2019)
17. Egorov, V., Maksomova, O., Koibuchi, H., Andreeva, I., Rieu, J., et al.: Stochastic fluid dynamics simulations of the velocity distribution in protoplasmic streaming. *Phys. Fluids* **32**, 121902, 17 p. (2020)
18. Andreeva, I.: Notes on the behaviour of trajectories of polynomial dynamic systems. In: MATEC Web of Conferences, vol. 313, p. 00014, 7 p. (2020)
19. Andreeva, I.: Several classes of plain dynamic systems qualitative investigation. In: IOP Journal of Physics: Conference Series, vol. 1730, p. 012053, 8 p. (2021)
20. Aleksandrova, A.S., Shumikhin, A.G., Kavalerov, B.V.: Identification of a technological process with application of neural network modeling. In: Cyber-Physical Systems. Digital Technologies and applications. Studies in Systems Design and Control, vol. 350, pp. 71–82 (2021)
21. Lyasheva, S., Morozov, O., Shlyemovich, M.: Analysis of energy characteristics for issuing areas of significance when compressing images in cyber-physical systems. In: Cyber-Physical Systems. Digital Technologies and applications. Studies in Systems, Decision and Control, vol. 350, pp. 259–270 (2021)
22. Neydorf, R., Gaiduk, A., Gamayunov, N.: The multiplicative-isolating principle of significantly nonlinear mathematical models creation. In: Cyber-Physical Systems. Digital Technologies and applications. Studies in Systems, Decision and Control, vol. 338, pp. 23–32 (2021)
23. Neydorf, R., Gaiduk, A., Kapustyan, S., Kudinov, N.: Conversion of CGA models to Jordan controlled form for design significantly nonlinear control systems. In: Cyber-Physical Systems. Digital Technologies and applications. Studies in Systems, Decision and Control, vol. 338, pp. 125–138 (2021)
24. Andreev, A., Demina, N., Nefedyev, Y., Petrova, N., Arthur Zagidullin, A.: Creation of a Simulation Model of Spacecrafts' Navigation Referencing to the Digital Map of the Moon. In: Cyber-Physical Systems. Digital Technologies and applications. Studies in Systems, Decision and Control, vol. 338, pp. 193–204 (2021)
25. Bolshakov, A., Veshneva, I., Lushin, D.: Mathematical model of integration of cyber-physical systems for solving problems of increasing the competitiveness of the regions of the Russian Federation. In: Cyber-Physical Systems. Digital Technologies and applications. Studies in Systems, Decision and Control, vol. 333, pp. 129–140 (2020)
26. Galkin, A., Sysoev, A.: Controlling traffic flows in intelligent transportation system. In: Cyber-Physical Systems. Digital Technologies and applications. Studies in Systems, Decision and Control, vol. 333, pp. 91–102 (2020)
27. Bolshakov, A., Nikitina, M., Kalimullina, R.: Intelligent system for determining the presence of falsification in meat products based on histological methods. In: Cyber-Physical Systems. Digital Technologies and applications. Studies in Systems, Decision and Control, vol. 333, pp. 179–204 (2020)
28. Zakharov, V.: General mathematical model for energetic and informatics evaluated over natively producing surrounded systems. In: IOP Journal of Physics: Conference Series, vol. 1730, p. 012040 (2021)



29. Okumura, M., Homma, I., Noro, S., Koibuchi, H.: Finsler geometry modeling of complex fluids: reduction of viscosity resistance. In: IOP Journal of Physics: Conference Series, vol. 1730 (2021)
30. Koibuchi, H., Okumura, M., Noro, S.: Finsler geometry modeling of anisotropic diffusion in Turing patterns. In: IOP Journal of Physics: Conference Series, vol. 1730 (2021)
31. Kuzkin, V., Krivtsov, A.: Fast and slow thermal processes in harmonic scalar lattices. *J. Phys. Condens. Matter* **29**(50), 14 (2017)
32. Krivtsov, A., Kuzkin, V.: Enhanced vector-based model for elastic bonds in solids. *Lett. Math.* **7**(4), 455–458 (2017)

# Model of Organization of Software Testing for Cyber-Physical Systems



Dmitriy Tobin , Alexey Bogomolov , and Mikhail Golosovskiy 

**Abstract** The chapter presents a model for organizing software testing of cyber-physical systems and an algorithm for forming test scenarios that optimize the cost of software testing, increase labor productivity and reduce the time required to put software into operation, and increase the reliability of cyber-physical systems that implement the developed software.

**Keywords** Cyber-physical system · Software · Software testing · Software testing organization · Test scenarios · Automated generation of test scenarios

## 1 Introduction

One of the priorities of the development of information technologies is the development of the information technology concept of cyber-physical systems, which implies the integration of computing resources into physical entities [1–3]. The computational component of cyber-physical systems is distributed throughout the physical system (called its carrier) and is synergistically linked to its constituent elements [4–6]. The elements of cyber-physical systems are linked and interact with each other using standard Internet protocols implemented using software [7–9].

Software development lifecycle management in modern information infrastructure involves the use of test models and algorithms for organizing software tests [10, 11]. Any software tests are limited by the time and resources allocated for testing, as well as the duration of the work of experts, so they can not guarantee an exhaustive check of the software for compliance with the requirements for its functions and characteristics.

---

D. Tobin (✉) · A. Bogomolov · M. Golosovskiy  
St. Petersburg Federal Research Center Russian Academy of Sciences, 39, 14th line of  
Vasilievsky Island, St. Petersburg 199178, Russia  
e-mail: [dtobin@mail.ru](mailto:dtobin@mail.ru)

M. Golosovskiy  
e-mail: [golosovskiy@yandex.ru](mailto:golosovskiy@yandex.ru)

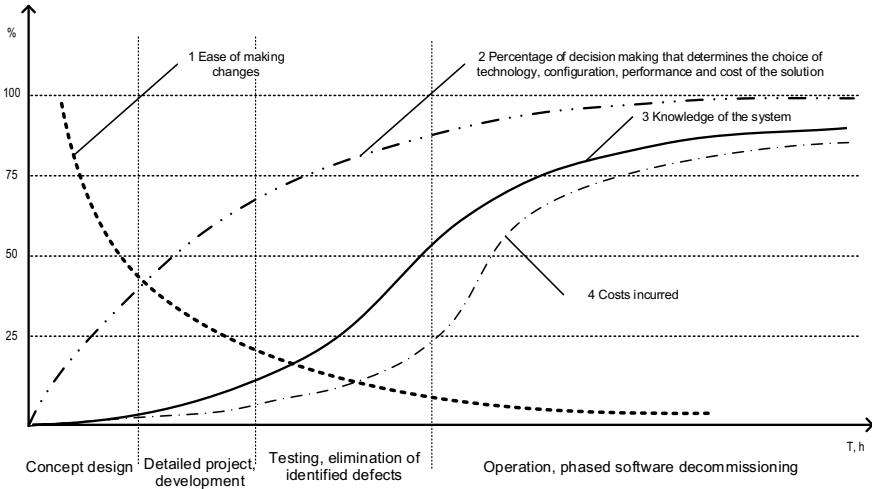


**Fig. 1** The dependence of various indicators of the software development process on the stage of the software life cycle

To increase the reliability of the definition and improve the evaluation of the characteristics after internal software tests, an algorithm for performing test scenarios for organizing tests of cyber-physical systems at the stage of presenting working versions of the software to the customer's representatives has been developed.

The use of test scenarios at the initial stages of software development makes it possible to make changes in a timely manner, reducing the likelihood of defects and errors at further stages of software development [12–14].

According to [15], the later changes are made to the software, the greater the costs are borne by its customer (Fig. 1).

Curve 2 (Fig. 1) shows the percentage of decisions made that determine the choice of technology, configuration, performance, and cost of the solution. At the beginning of the process, the curve increases sharply, and then the growth slows down—that is, the key decisions are made at the initial stage, and they dictate the logic of further implementation of the software development project. Curve 4 (cost growth) is s-shaped, since the costs are minimal at the design stage, but they increase dramatically after the software is put into operation. Curve 3 (the amount of knowledge about the system) is also s-shaped, although the stage of rapid growth on this curve is less pronounced.

## **2 Generalized Model of the Organization of Software Testing of Cyber-Physical Systems, Taking into Account Various Models of the Software Life Cycle**

Agile methodologies, such as Scrum, Kanban, OpenUP, and others, have gained the greatest popularity in software engineering to reduce the risks associated with incompleteness or changes in requirements.

These software development methodologies are primarily based on iterative, iterative-incremental, and pipelined software lifecycle models. In the modern standards of the Russian Federation (GOST 19 and 34 series), software tests are considered in the context of the cascade software model. In the SWEBOK v3 software engineering knowledge base [16] and ISTQB materials [17], the description of the test organization process is given in the form of a list of recommendations or practices, without forming a connection between these practices, taking into account the context of the software lifecycle model used by the team, which makes it relevant to create a generalized model for organizing software testing of cyber-physical systems, taking into account various software lifecycle models.

One of the most common methods for developing test scenarios based on specifications that include private implementations of the relationships between source and result data (“black box methods”) [18–20].

The description of the expected results of the test scenarios should be a necessary part of the test coverage of the software requirements. Test coverage of requirements is formed on the basis of the analysis of input functional specifications and is implemented by the methods of equivalent partitioning, analysis of boundary conditions, and functional diagrams [21–24].

When developing test scenarios for software testing, the following requirements are taken into account:

- the tests being developed must be ready by the time a particular software module is implemented;
- the set of previously created test scenarios must (with the same requirements) be executed at each test on all software versions;
- if changes are made to the software requirements, the test scenarios should be changed accordingly [15].

The methodological reliability of software tests is determined by the following factors:

- the completeness of the test program and the correctness of testing methods to cover possible scenarios for the functioning of both software components and in general, as well as the initial requirements for the software;
- the reliability and accuracy of the reference values of the software functionality characteristics, which serve as a reference for calculating the performance estimates recorded in the terms of reference and requirements specifications (they should compare the characteristics of the tested software);

- the adequacy and accuracy of the algorithms and models used to generate test scenarios;
- the accuracy and correctness of processing the results and generated reports on software tests, as well as comparing the data obtained with the requirements and standards of the terms of reference and specifications.

The use of automated tools and automated test scenarios reduces the time spent on organizing software tests.

Taking into account the stated requirements, a generalized model of the organization of software testing of cyber-physical systems is formed, taking into account various models of the software life cycle (Fig. 2) in the UML-activity diagram notation.

It is shown in [25, 26] that the development model often combines both an iterative and an incremental approach in flexible methodologies.

For example, although the Scrum methodology requires a product to be developed at the end of each iteration that is potentially ready for trial operation, teams often transfer to the production environment a set of changes obtained during several iterations, due to the need to implement more complete implementation of complex functions that cannot be implemented in one iteration. In the proposed model, this feature is taken into account. The iterative-incremental model is taken as a basis, but if there is only one iteration in one increment, the model degenerates into an iterative one. If the life cycle consists of only one iteration and one increment, then the model degenerates into a classic waterfall model.

To support pipeline-type methodologies, such as Kanban, the model uses the UML mechanism-branch nodes, after which control flows can be executed in parallel. This allows the model to implement each individual requirement independently.

One requirement in one iteration and one increment goes through all the stages of the life cycle, from the development of the requirement to the transfer to commercial operation. If necessary, such increments that implement individual requirements can be performed in parallel, if resources are available.

The model can be divided into three parts. The first part consists of activities aimed at creating a test model. It includes:

- selection of requirements for increment and a further selection of requirements for iteration;
- analysis of the selected requirements in terms of the completeness of the description and the formed acceptance criteria and other characteristics. As a result of the requirements analysis, a test plan is formed for testing the software that implements the selected requirements, taking into account the previously implemented functionality;
- development of test scenarios: it can include both the development of test scenarios for new functionality and previously implemented as a result of analyzing defects or analyzing relationships between elements;

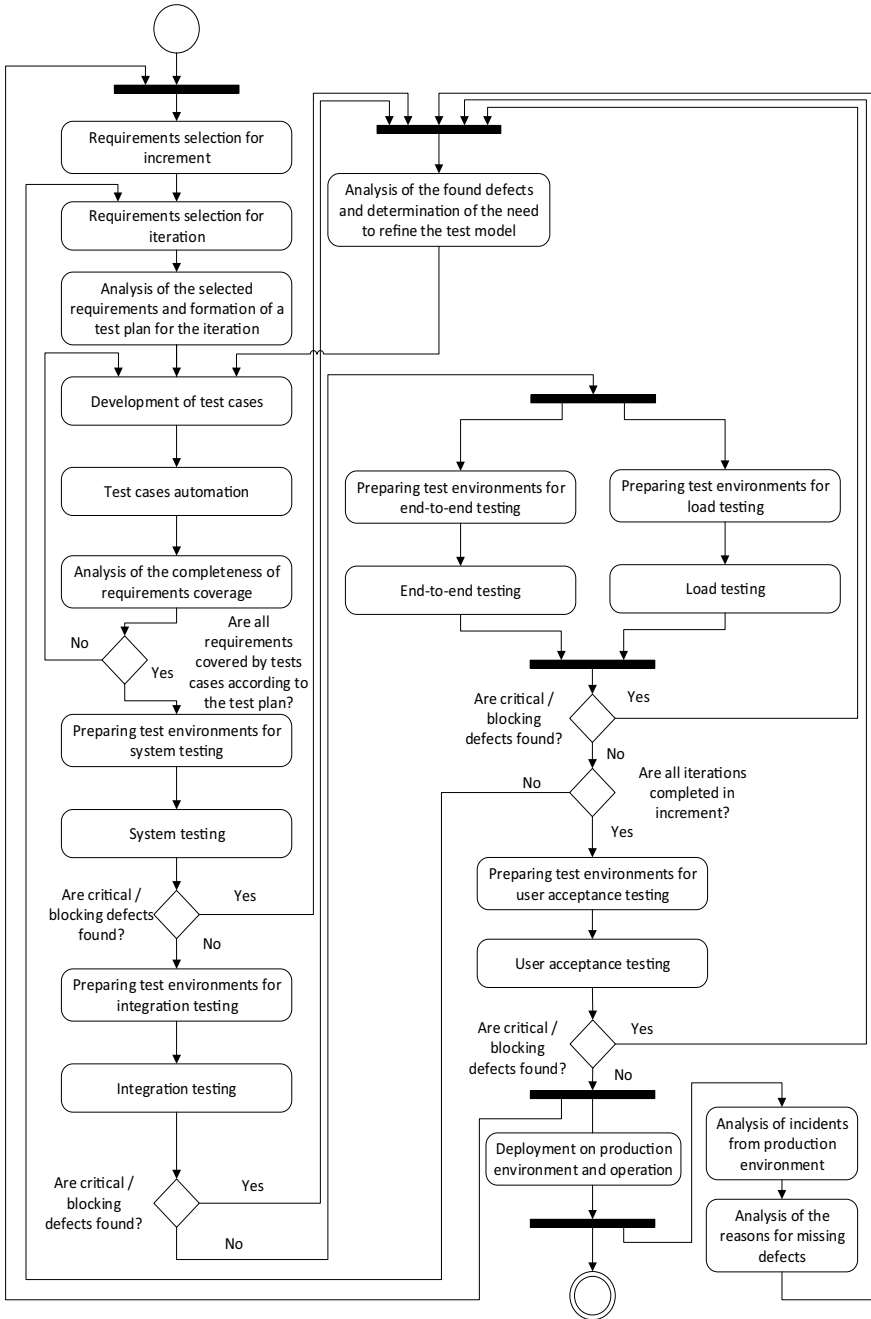


Fig. 2 Generalized model of the organization of software testing of cyber-physical systems, taking into account various models of the software life cycle

- selection and automation of test scenarios: depending on the availability of resources/capabilities, not all test scenarios can be automated. In testing practices, it is recommended to make the percentage of automated tests as large as possible, but this figure is left to the discretion of the teams;
- analysis of the completeness of the requirements coverage, in accordance with the test plan.

The second part consists of activities aimed at preparing test environments, which consist in preparing stands, test environments, test data, and activities for direct testing [26]. In total, the model identifies the following types of tests:

- system testing—testing the implementation of requirements in general, in which all integrations with adjacent systems are tested on emulators.
- system-integration testing—testing of integrations with external systems.
- end-to-end testing is a test aimed at verifying the implementation of business processes as a whole. Full integration and involvement of participants of related systems in the process of organizing tests may be required;
- load testing—a test performed to evaluate the behavior of a component or system under increasing load;
- acceptance test—a test conducted to determine whether the system meets the acceptance criteria, which allows users, customers, or other authorized persons to determine whether to accept the developed software or not.

The third part of the model consists of activities aimed at analyzing the reasons for missing defects identified during industrial operation and analyzing defects identified during testing. As a result of these activities, the test model is adjusted [27].

### 3 Interpretation and Discussion of Research Results

The details of the block for generating test scenarios are shown in the diagram (Fig. 3). Using this algorithm is important because successive software development cycles require multiple executions of the same set of test scenarios. The application of the developed algorithm will allow you to automate testing at the stage of preparing the software for testing.

Test scenarios of load testing will collect indicators and determine the performance and response time of the software in response to an external request in order to establish compliance with the requirements for the software being developed [2].

A comprehensive approach to the organization of test scenarios will allow you to create a test model with the division of tests into groups “Performance tests”, “New Functionality”, “Regression”. A test model is a reflection of the structure and behavior of the system. The test model can be described in terms of the state of the system, input effects on it, end states, data flows and control flows, results returned by the system, etc.

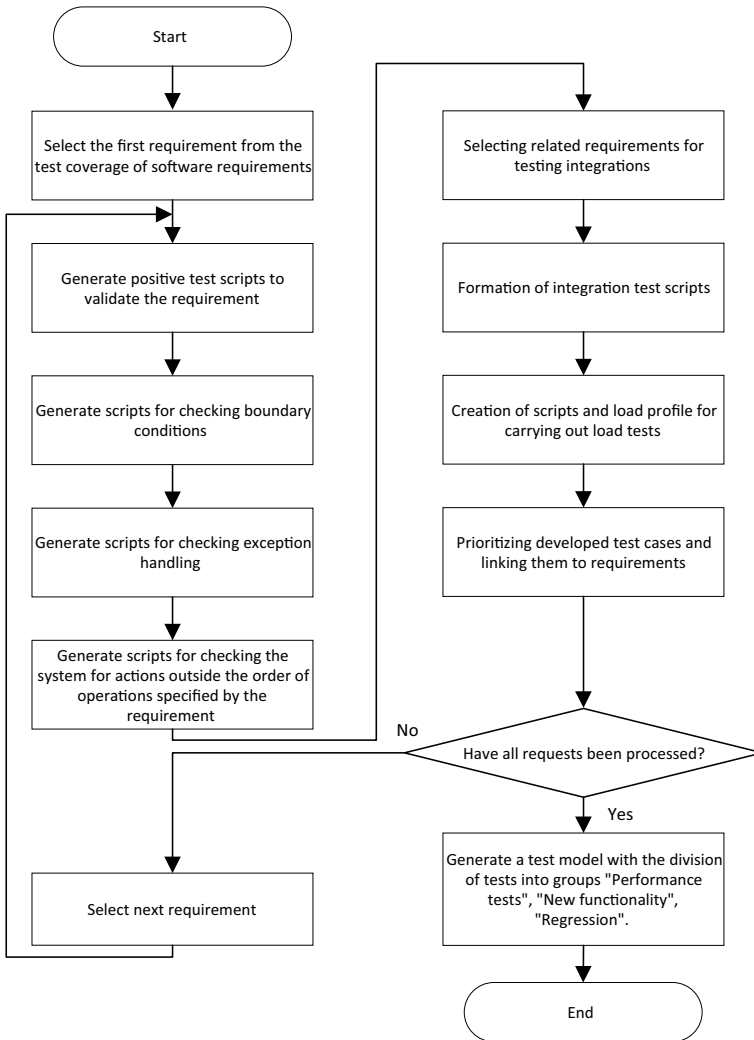


Fig. 3 Algorithm for forming test scenarios when organizing software tests

For a consistent software development lifecycle model, the first increment and iteration contain the entire scope of work for the main part of the project, and no changes are allowed. The increment will be implemented when all the iteration requirements are met. In this way, a sequential check of the fulfillment of all requirements is performed based on test scenarios.

It is shown in [28] that the duration of iterative and pipelined LC models strongly depends on the time of regression testing, the size of the test model, the software



developed, and the number of re-tested requirements. This determines the effectiveness of the application of the algorithm for generating test scenarios when organizing software tests.

The use of test scenarios in the early stages of the software life cycle is a means of monitoring the functioning of the software, allows you to check the software for the correctness of the requirements (expected result), as well as to reduce the number of critical errors and errors caused by the human factor.

## 4 Conclusion

The developed model of the organization of software testing of cyber-physical systems allows you to form and effectively apply test scenarios in the organization of software testing, providing the possibility of maximum test coverage, which leads to optimization of software testing costs, increased labor productivity, and reduced software commissioning time, and to increase the reliability of cyber-physical systems that implement the developed software.

**Acknowledgements** This work was supported by a grant from the President of the Russian Federation for state support of leading scientific schools of the Russian Federation (NSh-2553.2020.8).

## References

1. Zelentsov, V.A., Potryasaev, S.A., Pimanov, I.J., Nemykin, S.A.: Creation of intelligent information flood forecasting systems based on service oriented architecture. *Autom. Control Theory Perspect. Intell. Syst. Adv. Intell. Syst. Comput.* **466**, 371–381 (2016)
2. Balunov, A.I., Smirnov, M.A., Boykov, S.Yu.: Software application for modeling the fractionation process based on the principle of maximum entropy. In: Kravets, A.G., Bolshakov, A.A., Shcherbakov, M.V. (eds.) *Studies in Systems, Decision and Control*, vol. 350 *Cyber-Physical Systems: Digital Technologies and Applications*, pp. 63–70. Springer (2021). <https://doi.org/10.1007/978-3-030-67892-0>
3. Kravets, A.G., Salnikova, N.A., Shestopalova, E.L.: Development of a module for predictive modeling of technological development trends. In: *studies in systems, decision and control*, vol. 350. In: Kravets, A.G., Bolshakov, A.A., Shcherbakov, M.V. (eds.), *Cyber-Physical Systems: Digital Technologies and Applications*, pp. 125–136. Springer (2021). <https://doi.org/10.1007/978-3-030-67892-0>
4. Merkuryeva, G., Merkuryev, Y., Sokolov, B.V., Potriasaev, S.A.: Advanced river flood monitoring, modelling and forecasting. *J. Comput. Sci.* **10**, 77–85 (2015)
5. Soldatov, E., Bogomolov, A.: Decision support models and algorithms for remote monitoring of the equipment state. In: *Proceedings of the International Scientific and Practical Conference “Information Technologies and Intelligent Decision Making Systems” (ITIDMS 2021)* (2021). <http://ceur-ws.org/Vol-2843/shortpaper016.pdf>
6. Korobkin, D., Fomenkov, S., Fomenkova, M., Vayngolts, I., Kravets, A.: The software for computation the criteria-based assessments of the morphological features of technical systems. In: Kravets, A.G., Bolshakov, A.A., Shcherbakov, M.V. (eds.), *Studies in Systems, Decision and*

- Control, vol. 350 Cyber-Physical Systems: Digital Technologies and Applications, pp. 161–172. Springer (2021). <https://doi.org/10.1007/978-3-030-67892-0>
7. Larkin, E.V., Bogomolov, A.V., Privalov, A.N., Dobrovolsky, N.N.: Discrete model of paired relay-race. *Bull. South Ural State Univ. Seri. Math. Modell. Programm. Comput. Softw.* **11**(3), 72–84 (2018). <https://doi.org/10.14529/mmp180306>
  8. Davydenko, A., Sai, C., Shcherbakov, M.: Forecast evaluation techniques for i4.0 systems. in: studies in systems, decision and control, vol. 338 In: Kravets, A.G., Bolshakov, A.A., Shcherbakov, M.V. (eds.), *Cyber-Physical Systems: Modelling and Intelligent Control*, pp. 79–102. Springer (2021). <https://doi.org/10.1007/978-3-030-66077-2>
  9. Shulga, T., Sytnik, A., Danilov, N., Palashevskii, D.: Ontology-based model of user activity data for cyber-physical systems. in: studies in systems. In: Kravets, A.G., Bolshakov, A.A., Shcherbakov, M.V. (eds.) *Decision and Control*, vol. 259 *Cyber-Physical Systems: Advances in Design & Modelling*, pp. 205–216. Springer (2021) <https://doi.org/10.1007/978-3-030-32579-4>
  10. Larkin, E., Akimenko, T., Bogomolov, A., Krestovnikov, K.: Mathematical model for evaluating fault tolerance of on-board equipment of mobile robot. *Smart Innov. Syst. Technol.* **187**, 383–393 (2021). [https://doi.org/10.1007/978-981-15-5580-0\\_31](https://doi.org/10.1007/978-981-15-5580-0_31)
  11. Buldakova, T.I., Suyatinov, S.I.: Assessment of the state of production system components for digital twins technology. In: Kravets, A.G., Bolshakov, A.A., Shcherbakov, M.V. (eds.) *Studies in Systems, Decision and Control*, vol. 259 *Cyber-Physical Systems: Advances in Design & Modelling*, pp. 253–262. Springer (2021) <https://doi.org/10.1007/978-3-030-32579-4>
  12. Garousi, V., Felderer, M., Karapıçak, C.M., Yılmaz, U.: What we know about testing embedded software. *IEEE Softw.* **35**(4), 62–69 (2018). <https://doi.org/10.1109/MS.2018.2801541>
  13. Wnuk, K., Garrepalli, T.: Knowledge management in software testing: a systematic snowball literature review. *E-Informatica Software Eng. J.* **12**(1), 51–78 (2018). <https://doi.org/10.5277/e-Inf180103>
  14. Lonetti, F., Marchetti, E.: Emerging software testing technologies. *Adv. Comput.* **108**, 91–143 (2018). <https://doi.org/10.1016/bs.adcom.2017.11.003>
  15. Lipaev V.V.: *Reliability and Functional Safety of Real-Time Software Complexes*. Moscow: Institute for System Programming of the Russian Academy of Sciences, 348 p.
  16. *Guide to the Software Engineering Body of Knowledge Version 3.0*. (2013) IEEE Computer Society, 335 p. (2013)
  17. *Certified Tester Foundation Level Syllabus Version* (2018) International Software Testing Qualifications Board, 96 p. (2018)
  18. Garousi, V., Felderer, M., Karapıçak, C.M., Yılmaz, U.: Testing embedded software: a survey of the literature. *Inf. Softw. Technol.* **104**, 14–45 (2018). <https://doi.org/10.1016/j.infsof.2018.06.016>
  19. Idrus, H.M., Ali, N.: Towards development of software testing competency framework to empower software testers' profession. *Int. J. Eng. Technol. (UAE)* **7**(4), 749–754 (2018). <https://doi.org/10.14419/ijet.v7i4.35.23101>
  20. Cockburn, L.: Using both incremental and iterative development. *Cross Talk* **5**, 27–30 (2018)
  21. Bychkov, E.V., Bogomolov, A.V., Kotlovanov, K.Yu.: Stochastic mathematical model of internal waves. *Bull. South Ural State Univ Series: Math. Modell. Programm. Comput. Softw.* **13**(2), 33–42. (2018). <https://doi.org/10.14529/mmp200203>
  22. Han, X., Zhang, N., He, W., Zhang, K., Tang, L.: Automated warship software testing system based on Loadrunner automation API. 2018 IEEE International Conference on Software Quality, Reliability and Security Companion (QRS-C), Lisbon, Portugal, pp. 51–55. (2018). <https://doi.org/10.1109/QRS-C.2018.00023>
  23. Sánchez-Gómez, N., Torres-Valderrama, J., García-García, J.A., Gutiérrez, J.J., Escalona, M.J.: Model-based software design and testing in blockchain smart contracts: a systematic literature review. *IEEE Access* **8**, 164556–164569. (2020). <https://doi.org/10.1109/ACCESS.2020.3021502>
  24. Yenigun, H., Yevtushenko, N., Cavalli, A.R.: Guest editorial: special issue on testing software and systems. *Software Qual. J.* **27**(2), 497–499 (2019). <https://doi.org/10.1007/s11219-019-09447-4>

25. Larkin, E.V., Bogomolov, A.V., Privalov, A.N., Dobrovolsky, N.N.: Relay races along a pair of selectable routes. *Bull. South Ural State Univ. Ser. Math. Modell. Programm. Comput. Softw.* **11**(1), 15–26 (2018). <https://doi.org/10.14529/mmp180102>
26. Khatibsyarbini, M., Isa, M.A., Jawawi, D.N., Hamed, H.N., Mohamed, M.D.: Test case prioritization using firefly algorithm for software testing. *IEEE Access* **7**, 132360–132373 (2019). <https://doi.org/10.1109/ACCESS.2019.2940620>
27. Chen, L., Fan, G., Yu, H.: Modeling and optimizing CPS software testing based on Petri nets. *Int. J. Performability Eng.* **13**(8), 1183–1194 (2017). <https://doi.org/10.23940/ijpe.17.08.p2.11831194>
28. Golosovsky, M.S.: Algorithms for automated identification of connections between elements of a software development project. *Cybern. Program.* **6**, 38–49 (2017)

# Digital Twin of Building Heating Substation: An Example of a Digital Twin of a Cyber-Physical System



Oleg Yu. Maryasin 

**Abstract** This chapter dwells upon developing and implementing a digital twin of a building heating substation. The real-world prototype in the case presented is a laboratory bench. A building heating substation equipped with an intelligent control system integrated into the building management system can be presented as a cyber-physical system. A building heating substation computer model has been developed in OpenModelica using the IBPSA library. The author-developed DTTool suite was used to implement the digital twin. FMITool is an application within the suite that can load computer models made in various modeling systems to run simulations and parametric optimization, as well as to identify the parameters of loaded models. The suite applications can be used in combination to implement a real-time digital twin, exchange data with the laboratory equipment, and identify the parameters of the digital twin from time to time. The DTTool suite presented herein can be used as a platform to implement and run digital twins of various cyber-physical objects.

**Keywords** Digital twin · HVAC · Building heating substation · Cyber-physical system · DTTool · OpenModelica · IBPSA

## 1 Introduction

Digital breakthroughs have multiplied the available computing power and enabled the processing of big data in real time. Coupled with the fourth industrial revolution, they led to the emergence of digital twins (DT) [1]. Most experts agree that DT as a concept was first introduced by Michael Grieves of the University of Michigan in 2003 [2]. The concept was furthered and first used in practice in NASA laboratories [3]. The concept implies that the virtual model is not discarded after the creation of a physical object; instead, it accompanies its real-world counterpart throughout its

---

O. Yu. Maryasin (✉)

Yaroslavl State Technical University, Yaroslavl 150023, Russia

e-mail: [maryasin2003@list.ru](mailto:maryasin2003@list.ru)

lifecycle, as it is used for testing, refinements, operation, and disposal. The physical object uses sensors that provide real-time measurements to be further sent to the DT. The data is used to refine the digital model that in its turn helps optimize the operation and maintenance of the real-world object [4, 5].

DT is not yet a clear-cut concept even if publications on the topic are numerous [6]. Besides DT, there are such concepts as a digital model and digital shadow. Modeling and data specialists may interpret these terms differently. For instance, paper [7] states that if a virtual DT model is unable to automatically communicate with the real object, it is a digital model. If the model can automatically receive data from its real-world counterpart, then it is a digital shadow. Only the models capable of automated bidirectional communication can be called digital twins.

Other researchers use the concept of dimensionality to describe the differences in DT architectures [8, 9]. A 3D DT contains a physical object, a virtual object, and a module for their interaction. A 4D architecture also incorporates local or cloud storage; a 5D one will also include data analysis and decision-making module; finally, a 6D structure offers a user interface, including augmented- or virtual-reality interface.

There are two basic approaches to making DTs [6, 10]. The first approach uses real-object data such as sensor readings or other sources. Data-based DTs use digital or data-driven models (black-box models), the building of which involves statistical methods, machine learning, deep learning, and other methods. The second approach relies on conventional multiphysical or system models that apply known physical, chemical, biological, and other laws of the functioning of the real object. They are computer-aided implementations of mathematical models based on the systems of differential and/or algebraic equations (white-box models). The advantage of the second approach is that DTs based on it are applicable to the entire class of similar physical objects rather than one specific object.

In recent years, building engineering systems, and in particular heating, ventilation, and air conditioning (HVAC) have come to make use of DTs. The substantial experience of developing various HVAC models contributes to this trend. For instance, paper [11] overviews all sorts of ways to make data-driven HVAC models. These include frequency-based methods, machine learning, fuzzy logic, statistical methods, state-space models, etc. Energy recovery ventilation DT is an example of a HVAC DT based on a system Modelica model [12].

This chapter dwells upon creating a DT of a building heating substation (BHS). BHSs are nowadays commonly used in heating systems in both newly constructed and renovated buildings. A BHS comprises process equipment, instrumentation, and automation. BHSs have evolved from based PI and PID controller-based systems to complex systems that provide optimal and adaptive control, model predictive control (MPC), and intelligent control [13]. When an intelligent control system of a BHS is integrated into the building management system (BMS), this BHS becomes a cyber-physical system. DTs help expand the capabilities of an intelligent control system, save more energy, prolong the service life, and make the BHS easier to maintain.

## 2 DT Implementation Tools

Various science and engineering suites such as MATLAB, SCILAB, Modelica-based suite (SimulationX, Dymola, MapleSim, OpenModelica), etc. are used to make DTs. However, such simulation systems focus on user interaction, which makes implementing DTs difficult. They are designed for the user to first configure the model, then run a simulation and analyze the output. The simulation uses model time rather than real-time. Processes that take hours can be simulated in a matter of seconds. The use of DTs often requires real-time modeling, at the rate of data coming from the physical object. However, this mode is not possible in all simulation systems, and where possible, for example, in MATLAB/Simulink, a special environment configuration and several specialized libraries are required to make it work.

Recently, there have been created special DT-making tools such as ANSYS Twin Builder as well as cloud platforms for the Internet of Things (IoT) and Industrial Internet of Things (IIoT), which support DTs [14]. ANSYS Twin Builder provides ample opportunities to create, validate, and deploy DTs [15]. Twin Builder combines an extensive set of model libraries for various applications, 3D solvers, and lower-order models. It can import Simulink models and export Modelica models via the FMI interface. It is possible to change variables in real time, conduct complex parametric optimization, and make Python or Visual Basic scripts to automate modeling processes. Twin Builder can be easily integrated with IIoT platforms to connect a DT model with test data or real-time instrumentation readings. It also supports exporting models to create an inter-platform cloud infrastructure for SAP, PTC ThingWorx, and GE Predix IIoT platforms. An extensive selection of graphic and table reports is available for output visualization. The tool can export diagrams, graphs, and tables to Microsoft Excel or in various image formats.

GE Predix, Siemens MindSphere, and PTC ThingWorx are the prominent IIoT cloud platforms that support DTs [16]. PTC and Siemens offer in-house software for modeling. Besides, these platforms can be integrated with third-party simulation software such as ANSYS, and so can GE Predix. IIoT cloud platforms are not yet extensively used to make DTs, but their application is becoming more frequent [7, 17].

This chapter uses the author-developed DTTTool software platform to implement a DT. DTTTool is designed to implement DTs of buildings and other energy facilities. Some components of this digital platform have already been used to automate energy modeling and optimize the energy consumption of buildings [18].

DTTTool contains a suite of interrelated applications coded in Python with specialized libraries. BEMTool is an application designed to comprehensively automate energy modeling, optimize energy consumption, and build digital models based on the EnergyPlus system. FMITool is an application that has the following main functions: importing models created in various simulation systems; running the imported models as configured by the user; visualizing the model output; export of simulation

results in csv files; optimizing the variables of the loaded model for the given objective function providing for the specified constraints; performing standard operations to automate the modeling process.

OPCTool is designed to run the following functions: connecting to an OPC UA server; viewing the data structure of the OPC UA server and its tag attributes; subscription to change the tag values of the OPC UA server; reading OPC UA server tags into ScriptTool variables; writing ScriptTool variables into OPC UA server tags. OntoTool operates with ontologies and interacts with external systems using the semantic web. ScriptTool is an application designed to create, delete, and edit internal ScriptTool variables; edit the operation variables of all DTTool applications; create, edit, and execute arbitrary Python scripts.

Using these applications in combination helps automate model operations, run simulations, process the model output, and communicate with physical objects in real time. BEMTool, FMITool, OPCTool, OntoTool operations and ScriptTool scripts can communicate their data bi-directionally. On the one hand, model inputs and outputs can be fed to scripts for further processing. On the other hand, OPCTool and ScriptTool can receive, process, and transmit data of the physical object to adjust model variables and parameters. The built-in tools of the applications can be used to visualize data as tables or graphs. Connecting an external SCADA system via the OPC interface provides enhanced DT data visualization and a human-machine interface.

Functionally, DTTool is close to ANSYS Twin Builder, the difference being that DTTool is focused more on digital construction, HVAC systems and energy facilities. At the moment the author is developing an application to enable DTTool communication with IoT and IIoT devices using MQTT and AMQP protocols.

### 3 BHS Computer Model

The considered physical object of the DT is a laboratory bench, a small physical BHS model located at the Cybernetics Department, Yaroslavl State Technical University. Figure 1 shows the bench external view. The core equipment of the laboratory BHS includes an electric water heater, soldered plate heat exchangers, circulation pumps, membrane expansion tanks, and a sectional radiator. This BHS can use different heating systems (HS) and hot water supply (HWS) connection schemes.

The BHS computer model was developed in OpenModelica [19] using the standard Modelica v3.2.2 library as well as the IBPSA library [20]. IBPSA is a library that incorporates many components to simulate different HVAC units: heaters, heat exchangers, chillers, radiators, pumps, a variety of sensors, shutoff and control valves, etc. Figure 2 shows a fragment of the BHS OpenModelica model with a dependent HS connection and a single-stage HWS connection.

In Fig. 2, **bou** and **bou1** are model sources and drainage of cold and hot water, **hea** is the heating boiler, **hex** is the hot-water heat exchanger, **pump** and **pump1** are HS and HWS pumps, **res** and **res2** simulate hydraulic resistance in HS and

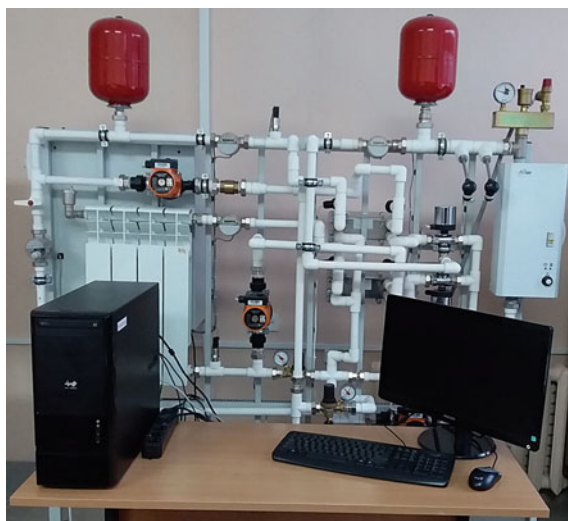


Fig. 1 Laboratory BHS

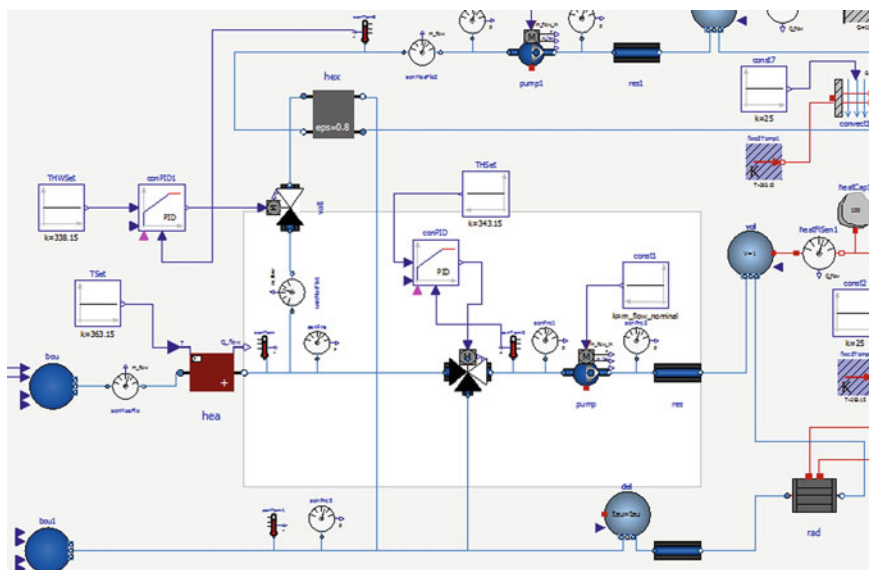
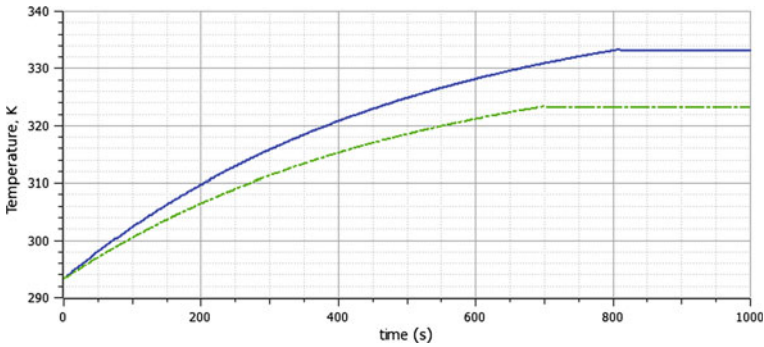


Fig. 2 Fragment of OpenModelica BHS model





**Fig. 3** Curves of HS and HWS water temperature

HWS, **val** simulates the hydraulic and thermal capacity of the HS, **val** is a three-way control valve of the HS, **val1** is the HWS control valve, **conPID** and **conPID1** are automatic HS and HWS controllers; **senTem**, **senTem1**, **senTem2**, and **senTem3** are temperature sensors; **senMasFlo**, **senMasFlo1**, and **senMasFlo2** are flow meters; **senPre**, **senPre1**, ..., **senPre5** are pressure sensors.

Each component of the BHS computer model is based on a mathematical model that includes a system of differential and/or algebraic equations. The correctness of the implementation of the library components was checked using various verification procedures, such as the International Energy Agency Building Energy Simulation Test (IEA BESTEST) [21] and ASHRAE Standard 140 [22].

The BHS is heated by an electric water heater that sustains an output temperature of 70 °C. The control system keeps the HS temperature at 60 °C and the HWS temperature at 50°C. For simplicity, PID controllers are used as automatic controllers in both the laboratory BHS and the computer model. However, more complex controls are implementable as well. Figure 3 shows the HS and HWS water temperature curves (in K) obtained as a result of modeling in the OpenModelica system.

The developed BHS computer model has several features in comparison with the models of building and district heating substations known from the literature. So, for example, unlike [23], it takes into account not only the heat consumption through the radiators of the heating system but also the heat loss through the walls of the pipelines. Compared to [24], the BHS model implements the mixing of water in the heating system using a three-way valve and takes into account the possibility of changing the direction of water flow to the opposite (reverse).

OpenModelica supports exporting models via the functional mockup interface (FMI) [25]. FMI was developed as an independent standard for model exchange and co-simulation. To date, it is supported by over 100 software systems including Adams, ANSYS, MATLAB/Simulink, NI LabVIEW, Dymola, SimulationX, MapleSim, etc. FMI-based models can be exported to functional mockup units (FMU) to be used by other systems for model exchange and co-simulation.

### 4 DT Implementation in DTTool

FMITool imports the OpenModelica FMU module with the BHS model. The imported FMU model then functions as a virtual model of the BHS DT. Figure 4 shows the FMITool home screen with the loaded BHS model. It also shows the HS temperature curve produced by FMITool simulation. This curve coincides with the one shown as a solid line in Fig. 3.

DT can run in real time. This can be done by using the following FMITool operations: Start modeling, Get the variable value, Set the variable value, Simulate. Start modeling is an operation the user only runs once when starting the modeling procedure. Get the variable value reads variables from the virtual BHS DT model, visualizes them in FMITool, or sends them via OPCTool or ScriptTool to a SCADA system for visualization. Set the variable value can be used to set BHS DT variables for the values received from the laboratory bench or a SCADA system via OPCTool and ScriptTool. From time to time, the laboratory bench communicates the following measurements to the DT: temperature and pressure of water received by the heating boiler; temperature and pressure of water fed to the HWS heat exchanger; water flow rate in the circuits of a heating boiler, heat exchanger, and HWS; indoor temperature, etc. Therefore, all the major disturbances affecting the laboratory bench will affect the DT as well.

“Simulate” runs a simulation for a certain period of time with a given step. The simulation time for the DT should match the operations startup period. The actual simulation time should be less than the operations startup period. Once the operation is complete, the model state is stored as an internal variable and used in the next run. Therefore, with periodic execution of the operations, it is possible to organize a continuous process of simulation in real-time.

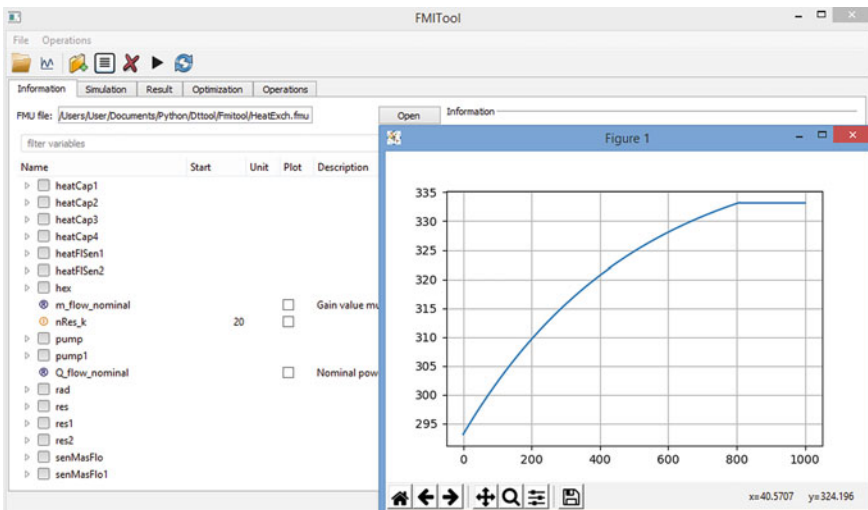
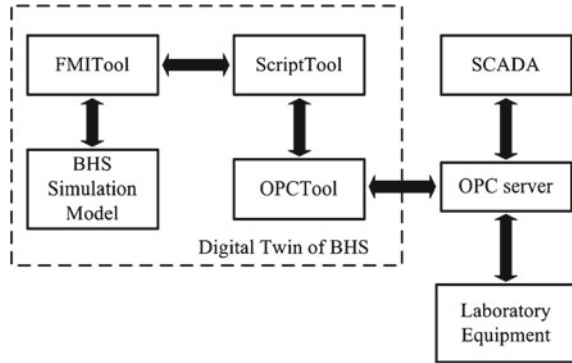


Fig. 4 FMITool home screen

**Fig. 5** DT communication flowchart



The simulation parameters must be configured in a way for the model to remain numerically stable. OPCTool and ScriptTool parameters should be configured in a way to enable timely data transmission. All of this provides for the functioning of BHS DT in real time while exchanging data with the laboratory bench and the SCADA system. Figure 5 shows how the laboratory BHS and DT interact, including the FMITool, ScriptTool, and OPCTool applications of DTTool.

The author is not known about the implementation of BHS DT based on ANSYS Twin Builder or using cloud platforms from GE, Siemens and PTC. The closest in functionality to the BHS DT implementation considered in the chapter is the cloud-based HVAC control system for an office building, described in [26]. It uses the Modelica model as the base model for the HVAC system including thermal equipment. The nonlinear Modelica model is linearized and used by the optimal control algorithm implemented in the MATLAB package. MATLAB communication with HVAC equipment is carried out through the cloud-based SCADA system Mervis. It should be noted that when using a cloud system, the communication between the virtual DT model and the physical object is highly dependent on the Internet connection. This can lead to delays in data transmission and reduce the reliability of the system. In contrast to this, BHS DT based on the DTTool platform supports communication both over the Internet and over a local network.

MATLAB was also used in [27] to implement a virtual building model in a building energy management system. At the same time, the HVAC equipment of the building was simulated using the EnergyPlus building energy modeling system. The control system database was used to communicate between the virtual model and the physical world. The disadvantage of this approach is that the EnergyPlus software uses simplified HVAC equipment models. This significantly reduces the accuracy of the simulation. In addition, the BCVTB software that is used to exchange data between MATLAB and EnergyPlus does not support newer versions of MATLAB and EnergyPlus. Another disadvantage of the systems described in [26] and [27] is that they do not have periodic identification of the HVAC system model.

## 5 Identifying the Virtual Model

In the course of time, the DT must remain an adequate replica of its physical prototype. Therefore, the virtual model parameters must be matched to real-world data on the go from time to time. FMITool has this function, as it includes the optimization of the parameters of the FMU model. Any variables of the loaded FMU model can be the inputs to optimize. Besides, any variables of the FMU model can be defined as the outputs and used to calculate the objective function. Any permissible Python operators can be used to define the objective function as a function of the output variables.

Parametric optimization and identification can be done manually or automatically from time to time using the corresponding operations. Usually, only the initial model identification has to be done manually. For the initial identification of the laboratory BHS parameters, we run a series of experiments with the automatic controls off. Experimental results are further used to identify various model parameters. The identification routines are conducted as follows: first one identifies the parameters to adjust the temperature in the heating boiler circuit; further—the parameters to adjust the HS temperature and pressure; then, the parameters to adjust the HWS temperature and pressure are identified. Figure 6 shows the Optimization tab of FMITool during identification.

The optimality criterion for identification is the sum of squared deviations of model output variables from their “experimental” values. “Experimental” data in Fig. 6 are shown as a table in the Identification tab. They can be entered manually

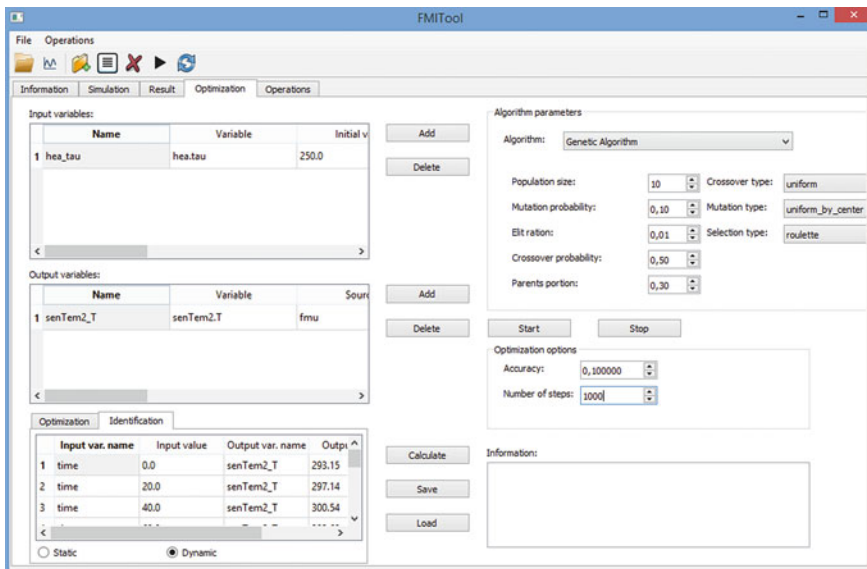
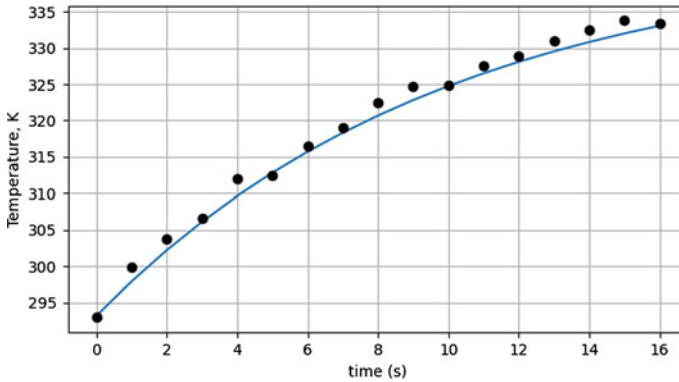


Fig. 6 Optimization tab of FMITool



**Fig. 7** Change in HS water temperature against “experimental” values

or loaded from a csv file. Identification can be switched from static to dynamic data using the corresponding switches in the Identification tab. Figure 7 shows the results of adjusting the HS water temperature. Figure 7 shows the “experimental” values (black dots) and the simulated HS temperature curve (solid line). In the case of automatic identification, the required data file can be generated by OPCTool and ScriptTool using the real-world data from the laboratory bench.

To run parametric optimizations, FMITool uses a variety of optimum search methods based on calculating the objective function. At the moment, it supports local Nelder-Mead and Powell methods, global brute-force search, the genetic algorithm, and the particle swarm optimization algorithm.

## 6 BHS DT Applications

BHS troubleshooting can be one of the most critical DT applications. The evidence of BHS operations shows that the crucial failure causes include [28] clogged filters, stopped mixing and circulation pumps, and increased hydraulic resistance of heat exchangers due to limescale. All these factors reduce the water flow rate in HS and HWS circuits, causing the heated water to lose temperature. Changes in the process parameters can be tracked by comparing the real object with its DT. A normally functioning BHS will not differ significantly from its DT in terms of the process parameters. A failure will cause a gradual increase in the deviations between corresponding process variables. The BHS control system can detect and analyze such trends.

DTs can also be used to develop and configure BHS control systems. A DT is far safer, faster, and more convenient than its real-world counterpart when it comes to configuring automatic controllers. It also allows using such configuration methods that would not be advisable in case of a real object due to risk of equipment damage or unacceptable operating modes. For instance, the author used FMITool’s built-in

parametric optimization functionality to optimize the parameters of HS and HWS circuit controllers. Figures 3 and 4 show the quality of transients under optimal settings. These configurations were tested on the laboratory bench, and the results were good. Notably, a digital twin, unlike computer models, can be used to assess the behavior of automatic control systems in real-time when exposed to real-world disturbances.

DTs show promise for implementing complex optimal and adaptive control systems. For instance, the BHS DT can be used as part of a two-level system for optimal control of the thermal regime of a building [29]. It can therefore be used as an internal model of the MPC controller or a reference model for implementing adaptive control systems. Other applications of BHS DT are also possible, among the applications of DT considered in [6].

## 7 Conclusions

This chapter dwells upon developing and implementing a BHS DT. The real-world prototype in the case considered is a laboratory bench. The BHS computer model has been developed in OpenModelica using the IBPSA library, then exported to the FMU module. DTTTool suite was used to implement the BHS DT. The suite's application FMITool can load computer models made in various modeling systems to run simulations and parametric optimization, as well as to identify the parameters of loaded models. Suite applications (FMITool, OPCTool, and ScriptTool) can be used in combination to implement a real-time DT, exchange data with the laboratory equipment via the OPC interface, and identify the parameters of the DT virtual model from time to time.

Under the classification presented in Section I, the DTTTool BHS DT has a 4D architecture with ontologies serving as local data storage. OntoTool provides the interaction of DT with ontologies. Adding a SCADA system to the suite will transform the DT into a 5D system.

DTTool can be used to implement any other DT whose computer model is an FMU module and that is capable of interacting with its real-world counterpart via the OPC interface. This is why the DTTTool suite presented herein can be used as a platform to implement and run digital twins of various cyber-physical objects.

## References

1. Rodic, B.: Industry 4.0 and the new simulation modelling paradigm. *Organizacija* **50** (3), 193–207 (2017)
2. Grieves, M., Vickers, J.: Digital twin: Mitigating unpredictable, undesirable emergent behavior in complex systems. In: *Transdisciplinary Perspectives on Complex Systems*. Springer, Cham, pp. 85–113 (2017). [https://doi.org/10.1007/978-3-319-38756-7\\_4](https://doi.org/10.1007/978-3-319-38756-7_4)
3. Glaessgen, E., Stargel, D.: The digital twin paradigm for future NASA and U.S. Air force vehicles. In: *53rd Structures Dynamics Materials Conference*, pp. 1–14 (2012)

4. Kitain, L.: Digital Twin—The New age of Manufacturing (2018) <https://medium.com/data-driveninvestor/digital-twin-the-new-age-of-manufacturing-d964eeba3313>
5. Pires, F., Souza, M., Ahmad, B., Leitao, P.: Decision support based on digital twin simulation: a case study. In: Service Oriented, Holonic and Multi-Agent Manufacturing Systems for Industry of the Future. Studies in Computational Intelligence, vol. 952, pp. 99–110. Springer, Cham (2020). [https://doi.org/10.1007/978-3-030-69373-2\\_6](https://doi.org/10.1007/978-3-030-69373-2_6)
6. Liu, M., Fang, S., Dong, H., Xu, C.: Review of digital twin about concepts, technologies, and industrial applications. *J. Manuf. Syst.* **58**, 346–361 (2021)
7. Kritzinger, W., Karner, M., Traar, G., Henjes, J., Sihn, W.: Digital Twin in manufacturing: a categorical literature review and classification. *IFAC-PapersOnLine*. **51**(11), 1016–1022 (2018)
8. Redelinghuys, A.J.H., Basson, A.H., Kruger, K.: A six-layer architecture for the digital twin: a manufacturing case study implementation. *J. Intell. Manuf.* **31**, Springer, 1383–1402 (2020). <https://doi.org/10.1007/s10845-019-01516-6>
9. Redelinghuys, A.J.H., Kruger, K., Basson, A.H.: A six-layer architecture for digital twins with aggregation. In: Service Oriented, Holonic and Multi-agent Manufacturing Systems for Industry of the Future. Studies in Computational Intelligence, vol. 853, pp. 171–182. Springer, Cham (2019). [https://doi.org/10.1007/978-3-030-27477-1\\_13](https://doi.org/10.1007/978-3-030-27477-1_13)
10. Adamenko, D., Kunnen, S., Pluhnau, R., Loibl, A., Nagarajah, A.: Review and comparison of the methods of designing the Digital Twin. *Procedia CIRP*. **91**, 27–32 (2020)
11. Afram, A., Janabi-Sharifi, F.: Review of modeling methods for HVAC systems. *Appl. Thermal Eng.* **67**, 507–519 (2014)
12. Vering, C., Mehrfeld, P., Nürenberg, M., Coakley, D., Lauster, M., Müller, D.: Unlocking Potentials of building energy systems’ operational efficiency: application of digital twin design for HVAC systems. In: 16th IBPSA Conference, pp. 1304–1310 (2019)
13. Afram, A., Janabi-Sharifi, F.: Theory and applications of HVAC control systems—a review of model predictive control (MPC). *Build. Environ.* **72**, 343–355 (2014)
14. Adamenko, D., Kunnen, S., Nagarajah, A.: Comparative analysis of platforms for designing a digital twin. In: Advances in Design, Simulation and Manufacturing III. Lecture Notes in Mechanical Engineering, pp. 3–12. Springer, Cham (2020). [https://doi.org/10.1007/978-3-030-50794-7\\_1](https://doi.org/10.1007/978-3-030-50794-7_1)
15. Ansys Twin Builder. <https://www.ansys.com/products/digital-twin/ansys-twin-builder>. Accessed 14 October 2021
16. Becue, A., Maia, E., Feeken, L., Borchers, P., Praca, I.: A new concept of digital twin supporting optimization and resilience of factories of the future. *Appl. Sci.* **10**(4482), 1–32 (2020)
17. Zidek, K., Pitel, J., Adamek, M., Lazorik, P., Hosovsky, A.: Digital twin of experimental smart manufacturing assembly system for industry 4.0 concept. *Sustainability* **12**(3658), 1–16 (2020)
18. Maryasin, O.Yu.: A system for automation of energy modeling, optimization of energy consumption and preparation of digital models. In: 33th International Conference on Mathematical Methods in Engineering and Technology, vol. 12 (2), pp. 140–147 (2020)
19. Welcome to OpenModelica—OpenModelica. <https://www.openmodelica.org/index.php>. Accessed 14 October 2021
20. GitHub—ibpsa/modelica-ibpsa: Modelica library for building and district energy systems developed within IBPSA Project 1. <https://github.com/ibpsa/modelica-ibpsa>. Accessed 14 October 2021
21. Jorissen, F., Reynders, G., Baetens, R., Picard, D., Saelens, D., Helsen, L.: Implementation and verification of the IDEAS building energy simulation library. *J. Build. Perform. Simul.* **11**(6), 669–688 (2018). <https://doi.org/10.1080/19401493.2018.1428361>
22. Yuan, S., O’Neill, Z.: Testing and validating an equation-based dynamic building program with ASHRAE standard method of test. In: Proceedings of the 3rd SimBuild Conference, Berkeley, USA, pp. 45–52 (2008)
23. Filonenko, K., Arendt, K., Jradi, M., Andersen, S., Veje, C.: Modeling and simulation of a heating mini-grid for a block of buildings. In: 16th IBPSA Conference, vol. 16, pp. 1–8 (2019)
24. Stinner, S., Schumacher, M., Finkbeiner, K., Streblow, R., & Müller, D. FastHVAC: A library for fast composition and simulation of building energy systems. In: Proceedings of the International Modelica Conference, pp. 921–927 (2015). <https://doi.org/10.3384/ecp15118921>

25. Functional Mock-up Interface. <http://fmi-standard.org/>. Accessed 14 October 2021
26. Drgona, J., Picard, D., Helsen, L.: Cloud-based implementation of white-box model predictive control for a GEOTABS office building: a field test demonstration. *J. Process Control* **88**, 63–77 (2020)
27. Kwak, Y., Huh, J., Jang, C.: Development of a model predictive control framework through real-time building energy management system data. *Appl. Energy* **155**, 1–13 (2015)
28. Vitaliev, V.P., Nikolaev, V.B., Seldin, N.N.: *Operation of Heat Points and Heat Consumption Systems*. Stroyizdat, Moscow (1988)
29. Maryasin, O.Yu., Kolodkhina, A.S.: Control of the thermal regime of buildings using predictive models. *Bull. SamGTU*. **1** (53), 122–132 (2017)



# Generalized Formalization of Multiplicatively Release and Isolating Functions and Locally Approximating Functions in the Formation of a Single Analytical Function in the Cut-Glue Method



Nikita Kudinov , Nikita Gamayunov , and Asya Atayan 

**Abstract** The chapter deal with the fragmentary multiplicative-additive approximation method, which is written in the language of linear algebra. This makes it possible to use standard mathematical libraries in programs using approximation. It is proved that the quasi-linearizability condition and the least-squares method in polynomial regression are compatible, which allows us to obtain a single analytical function in a quasilinear form with an arbitrary arrangement of experimental data and fragment boundaries. The advantages of using the matrix formalism for the polynomial approximation of fragments and the Cut-Glue approximation are shown.

**Keywords** Multiplicatively additive approximation · Cut-glue method · Mathematical model · Experimental data · Fragmentariness · Quasilinear form · Least square method · Polynomial regression

## 1 Problem Statement

Currently, there is an increase in requirements for the quality of management of many objects. It is impossible to solve the problem without full consideration of properties with a minimum depth of assumptions. The adequacy of the models to the processes increases because the intensive development of computer technologies allows applying symbolic methods for the synthesis of complex nonlinear control

---

N. Kudinov (✉) · N. Gamayunov · A. Atayan  
Don State Technical University, 1 Gagarin Sq., Rostov on Don 344000, Russia  
e-mail: [kudinov\\_nikita@mail.ru](mailto:kudinov_nikita@mail.ru)

N. Gamayunov  
e-mail: [mangal.harry@yandex.ru](mailto:mangal.harry@yandex.ru)

A. Atayan  
e-mail: [atayan24@mail.ru](mailto:atayan24@mail.ru)

laws. Quite a lot of methods have been developed for the analytical solution of synthesis problems for nonlinear control systems, such as the feedback linearization method, the transformation method, the backstepping method, the position-trajectory control method, and many others [1].

Analytical methods for the synthesis of control systems assume the presence of a mathematical model (MM) of objects and control processes, which are usually a certain set of algebraic and differential, including essentially nonlinear, equations. The application of most of these methods requires the implementation of certain mathematical transformations of the MM equations, for which it is necessary that MM has analytical properties, and its equations are presented in a given form, for example, quasilinear.

Cut-Glue approximation method [2–5] allows obtaining an analytical model as an approximation of experimental data in a quasilinear form. The most difficult and irregular stage in the use of this method is the optimization of the number and position of the fragments into which the experimental data (ED) are divided. In the course of designing an optimizing program, in order to minimize the role of the human factor, it is advisable to use unified algorithms that implement numerical methods. Therefore, it is desirable that the equation of a quasilinear form does not change structurally with variations in the number of fragments, the amount of data on each fragment from the degree of the approximating polynomials. Our research is focused on the construction of such a unified record of Cut-Glue approximation.

Thus, the systematization problems are formulated for a deeper study of the most important properties of the multiplicative transformation of polynomial functions and the proof of the possibility of writing the Cut-Glue approximation formula in a single expression. The structure of this expression does not depend on the number of fragments, the amount of data in each fragment, and the degree of the polynomials approximating the fragments. Determine the quasi-linearizability condition for reducing the MM to the so-called quasilinear model. It is necessary to prove the existence of an algorithm for solving the Cut-Glue approximation problem, the structure of which does not depend on the above factors, which, in turn, will allow parametric optimization of the approximation error.

## 2 Obtaining, Recording, and Fragmentation of Experimental Data

The first stage in the approximation of experimental data by the Cut-glue method [6] is data fragmentation (Fig. 1). In general, the purpose of such fragmentation is to select a set of segments and positions of their joining so that in each segment the approximating ED model does not deviate strongly from the polynomial dependence (linear with respect to the basis of power functions) and the complexity of calculating the polynomials is minimal. Such a criterion should lead to the fact that the boundaries of the segments should coincide with the break points (trend changes) of the

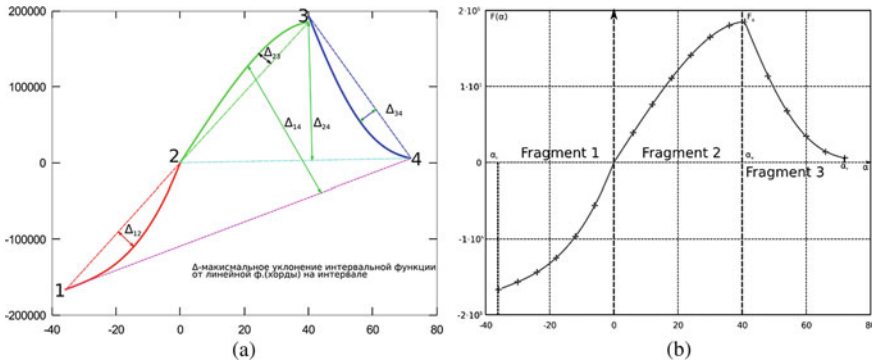


Fig. 1 ED fragmentation result

dependence (Fig. 1a). The influence of the position of the boundaries of fragments in the approximation of a nonlinear function by a polynomial on the approximation error is apparently indirectly related to the statement contained in the Weierstrass approximation theorem [7] about the possibility of approximating a continuous functional dependence of a polynomial.

Approximation of experimental data over the entire domain of the factor definition or on its segments by a mathematical function saves on expensive experiments. Such modeling is advisable when information about the internal structure of the object is not available to the researcher. Thus, the experimental study of the object is carried out in accordance with the «black box» principle.

At the early stages of the Cut-Glue approximation method, subsets of the impact values are identified in the factor space, and information about the response of the object under study is put through different channels. In the computer memory, “action-response” connections, called fragments of experimental data (FED), are formed. Let us assume that the clustering of experimental data on which it is necessary to construct the dependence  $L(x)$  so that the result of the Cut-Glue method [6] describes the set ED with a minimum error has already been performed (Fig. 1b). Also assume that the ED values (responses) in the slices are independent of each other in the sense of linear regression. Then the subsets of the values of the argument-factor parameter of the experiment are conveniently represented by a two-dimensional array of numbers—the matrix

$$X = \begin{pmatrix} x_1 & \cdots & x_{k_{n-1}+1} \\ \vdots & \ddots & \vdots \\ x_{k_1} & \cdots & x_{k_n} \end{pmatrix},$$

where  $k_i$ —the amount of ED for the  $i$ -th section,  $x_j$ —the value of the determining parameter (factor) in the experiment. Matrix X has as many rows as the maximum number of experiments performed in the  $i$ -th interval. On intervals with fewer dimensions, the blank elements of the array are equal to the special value NaN.

### 3 Multifragment Polynomial Regression and the Quasi-Linearizability Condition

Let us assume that for each section of the experimental data a polynomial or harmonic approximation of the dependence of the responses on factors is possible and adequate, the same as in the spline method or the Prony's method.

For definiteness, a polynomial approximation is chosen. The parameters of power polynomials, due to random measurement errors and measurement noises, are related to unknown measured values not functionally, but in regression. With such a connection, mutually compensated fluctuations of the measured value are possible, which should not affect the assessment. One of the methods of mathematical regression, in particular the LSM, allows estimating the coefficients of the linear expansion—the real coefficients of the polynomial. The preliminary adoption of the polynomial assumption leads to choosing a basis of monomials  $x_0, x_1, x_2 \dots x_n$ . For this basis, the problem of orthogonal expansion is solved by the classical LSM on each fragment of experimental data:

$$J = \sum_{i=1}^n (y_i - \beta_1 x_i - \dots - \beta_n x_i^n)^2 \rightarrow \min_{\beta_1, \dots, n \in R} . \quad (1)$$

$J$  is minimized independently on each interval. The general solution to the problem of polynomial regression by the LSM method [8] with respect to vectors whose components are equal to monomials is given by the linear dependence  $Y = X\beta + \varepsilon$ [9]. Thus, the vector of estimates  $\beta$  on each interval can be found as a solution to the matrix equation  $X'X\hat{\beta} = X'Y$ ,  $\hat{\beta} = X'X \setminus X'Y$ [10]. The general solution to the regression problem on all intervals can be conventionally written in the form of a composition of interval solutions, which are the expansion coefficients

$$B = \begin{pmatrix} \beta_1^1 & \dots & \beta_1^j \\ \vdots & \ddots & \vdots \\ \beta_{n_j}^1 & \dots & \beta_{n_j}^j \end{pmatrix},$$

where  $j$ -number of the fragment ED,  $n_j$ -max maximum degree of the interpolation polynomial. For the possibility of further multiplicative decomposition of the mathematical model into a quasilinear factor [11–13] (by quasilinear is meant linear, with an infinitely small change in the independent argument  $x$ ) and the argument of the function  $x$ , it is assumed that when minimizing (1)  $\beta_0$  is almost equal to zero, more strictly  $\beta_0 = 0$ .

## 4 Cut-Glue Conversion of Polynomial Functions from the Sum of Arguments

Suppose that modal control is used to control the deviation from the equilibrium state, and nonzero static characteristics (parameters of the object in the equilibrium position) can be reduced to 0 by shifting the argument by a constant value, in such problems the constant displacement is not essential when the object is stabilized in the transient process [14–17]. Then, taking into account the small deviation of  $\Delta x$  from the control goal  $x_0$  the dependence  $L(x)$ ,  $x = x_0 + \Delta x$  can be written for one fragment in the form of a binomial structure corresponding to the complete equation of polynomial regression [18]:

$$L(\Delta x, x_0) = \beta_n(\Delta x + x_0)^n + \dots + \beta_2(\Delta x + x_0)^2 + \beta_1(\Delta x + x_0)^1 + \beta_0(\Delta x + x_0)^0. \quad (2)$$

For example, for  $n = 3$

$$L(\Delta x, x_0) = \beta_3\Delta x^3 + (3\beta_3x_0 + \beta_2)\Delta x^2 + (3\beta_3x_0^2 + 2\beta_2x_0 + \beta_1)\Delta x + \beta_3x_0^3 + \beta_2\beta_0^2 + \beta_1x_0 + \beta_0. \quad (3)$$

It is appropriate to use the matrix formalism for the polynomial approximation of the FED, this makes it possible to vary the degrees of the polynomials and the sizes of the FED with the equations written unchanged, which turns out to be important for minimizing the approximation error while minimizing the error in these parameters and providing algorithmic support for this possibility. Expression (2) can be written in the multiplicative matrix form, which is the initial one for the methods of synthesis of the control law:

$$L(\Delta x) = V_{n,n}(\Delta x)T = a(\Delta x)\Delta x + a(x_0), \quad (4)$$

where

$$T = (B_{i,j}S_{i,j})V_{n,n}(\alpha_0) \quad (5)$$

the vector representing the coefficients of the polynomial (3), in this formula  $V$ —the Vandermonde matrix [9]. The main pragmatic meaning of the transition from (2) to (4–5) is that the additive shift of the argument of the function  $L$  is equivalent to the product of matrices (change of the basis). It is important that the elements of one of them depend only on the variable value  $\Delta x$ , and the elements of the other are constant, associated with an unchanged parameter— $x_0$ .

$$V_{n,n}(x) = \begin{pmatrix} 1 & x & x^2 & \dots & x^n \\ 1 & x & x^2 & \dots & x^n \\ 1 & x & x^2 & \dots & x^n \\ 1 & x & x^2 & \dots & x^n \end{pmatrix}. \quad (6)$$

Constant coefficients of the polynomial (3) do not depend on  $\Delta x$  and  $x$  form a Pascal matrix, in the particular case when  $n = 5$ ,

$$S^5 = \begin{pmatrix} 1 & 0 & 0 & 0 & 0 \\ 1 & 1 & 0 & 0 & 0 \\ 1 & 2 & 1 & 0 & 0 \\ 1 & 3 & 3 & 1 & 0 \\ 1 & 4 & 6 & 4 & 1 \end{pmatrix},$$

a B—lower triangular matrix of binomial coefficients of the full polynomial in argument  $I = \begin{pmatrix} 1 & 0 \\ 0 & -1 \end{pmatrix}$  in expression (3)

$$B = (b_{ij}) = \begin{pmatrix} \beta_n & 0 & 0 & 0 & 0 \\ \beta_{n-1} & \beta_n & 0 & 0 & 0 \\ \dots & \dots & \ddots & 0 & 0 \\ \beta_1 & \beta_2 & \dots & \beta_n & 0 \\ \beta_0 & \beta_1 & \dots & \beta_{n-1} & \beta_n \end{pmatrix}.$$

The structure of expression (5) allows its multiplicative decomposition of the form (4) by placing  $\Delta x$  for the Vandermonde matrix (6) due to the renumbering of column indices in it. Such a multiplicative matrix expression is quasilinear  $\Delta x$ . Thus, the additive shift of the argument in the polynomial representation of the fragmentary dependence can be expressed by the product of the Vandermonde matrix whose elements depend on  $x$  by a matrix with constant elements. In this way, it is proved that the constant addition of a constant to the argument of the required Cut-Glue function can be expressed in matrix notation by a product of matrices.

The Gut-Glue approximation method ED defines a method for obtaining a single analytical functional characteristic, the composite (main) element of which are fragmentary functions of the form (4–5), in which the matrix B characterizes the behavior of fragmentary functions (FF) on each of the fragments [19, 20]. In accordance with the Cut-Glue method, FFs are combined into a common dependence by an additive convolution with a weight function called a multiplicative-separating function, which can be written in «matrix language» in a linear space, the dimension of which is equal to the number of fragments ED—k:

$$K(x, x_b) = \begin{bmatrix} M_1(x, x_b) \\ \vdots \\ M_j(x, x_b) \end{bmatrix}, \text{ where } M(x, x_b) = \prod_{i=1}^n \frac{N_i(x, x_b)I_{ii} + \sqrt{N_i(x, x_b)^2 + E}}{2\sqrt{N(x, x_b)^2 + E^2}}$$

$$I = \begin{pmatrix} 1 & 0 \\ 0 & -1 \end{pmatrix},$$

$$E = (\varepsilon \dots \varepsilon)^T, N_i(x, x_b) = x(1 \dots 1)^T - (1 \dots 1)^T x_b, x_b = (x_l \ x_r), \quad (7)$$

where  $K(x)$ —vector whose components are the IMF of ED fragments. In the same vector space, we represent fragmentary functions—vector components. Column vectors E,K,N have dimension k, M—vector has dimension k,  $n = 2$ —number of boundaries of the ED fragment,  $x_b$ — vector whose components are equal to the position of the fragment’s boundaries, in particular  $x_l$  и  $x_r$ , I—vector specular reflection matrix.

$$J(x, x_0) = \begin{pmatrix} L_1(\Delta x, x_0) \\ \vdots \\ L_j(\Delta x, x_0) \end{pmatrix},$$

then the Cut-Glue gluing of the fragmentary functions is written as the scalar product of K by J— $L = K(\Delta x + x_0) \cdot J(x, x_0)$ . The part of the fragmentary functions  $L_i(x)$  linear in  $\Delta x$  is determined by the vector

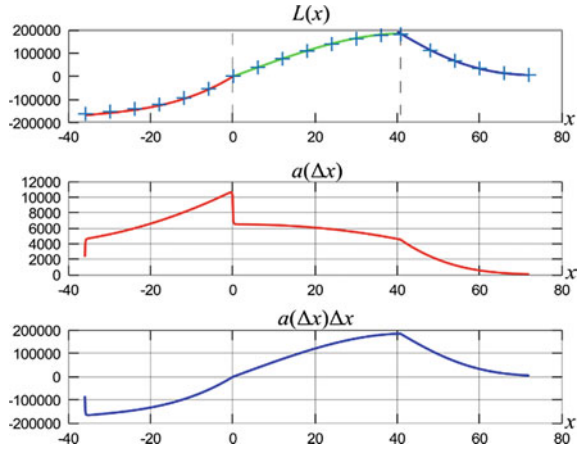
$$W(x) = \begin{pmatrix} 1 & x & x^2 & \dots & x^{n-1} \\ 1 & x & x^2 & \dots & x^{n-1} \\ 1 & x & x^2 & \dots & x^{n-1} \\ 1 & x & x^2 & \dots & x^{n-1} \end{pmatrix} (B_{i,j} S_{i,j}) V_{n,n}(x_0),$$

and the linear in  $\Delta x$  part of the  $W(x)$  function combined by the Cut-Glue method is expressed by the scalar product of W and  $K(\Delta x)$ . Therefore, the function  $a(\Delta x)$  can be considered as an eigenvalue in the differential equation of motion of a technical object recorded with respect to the increments of the state variable  $m \Delta x = a(\Delta x, x_0)\Delta x = L(\Delta x + x_0)$ . The transformation results are shown in Fig. 2.

## 5 Conclusion

The Cut-Glue approximation method can be used to approximate physical functional dependencies, geo- meteorological data, integral characteristics of the interaction of

**Fig. 2** Result of fragmentary approximation (a), part of  $L(x)$  linear in  $\Delta x$  (b), quasi-linearized function (c)



solids with liquid and gas. The result is presented as an analytical function, which allows it to be used in problems of forecasting, diagnostics, and automatic control in conjunction with sim-free analytical methods of mathematics.

Mathematical methods for processing estimates of the least-squares method are considered, which guarantees obtaining the results of polynomial approximation of the controlled parameter of the model in deviations from the nominal (position of stability) and, as a consequence, a unified analytical function in the quasilinear form obtained in the course of the investigated method of fragmentary approximation. The condition of quasi-linearizability is determined. The possibility of using the matrix formalism for the polynomial approximation of the FED is revealed, which allows, with the constant writing of equations, to vary the degrees of polynomials and the sizes of the FED, which is important for minimizing the approximation error in the course of minimizing the error in these parameters and providing algorithmic support for this possibility. It has been experimentally confirmed that the approach developed within this project (using Cut-Glue approximation and quasilinear models) can be used to create high-quality control systems for nonlinear objects with substantially nonlinear characteristics. Expands this conclusion about the possibilities of the method in the problems of mathematical modeling of the dynamics of any technical objects with nonlinearities, the construction of an algorithm capable of approximating experimental data with an arbitrary number of experimental factors.

**Acknowledgements** The reported study was funded by RFBR, project number 18-08-01178 in DSTU.

## References

1. Gaiduk, A.R., Neydorf, R.A., Kudinov, N.V., Polyakh, V.V.: Analytical problem solution of



- synthesis of a nonlinear stabilization system based on a mathematical CGA model. *Eng. J. Don* **7**(58) (2019)
2. Neydorf, R., Gaiduk, A., Gamayunov, N.: The multiplicative-isolating principle of significantly nonlinear mathematical models creation. In: Kravets, A.G., Bolshakov, A.A., Shcherbakov, M. (eds.) *Cyber-Physical Systems: Modelling and Intelligent Control*. Studies in Systems, Decision and Control, vol. 338, Springer, Cham (2021). [https://doi.org/10.1007/978-3-030-66077-2\\_3](https://doi.org/10.1007/978-3-030-66077-2_3)
  3. Gaiduk, A.R., Neydorf, R.A., Kudinov, N.V.: Application of cut-glue approximation in analytical solution of the problem of nonlinear control design. In: Kravets, A., Bolshakov, A., Shcherbakov, M. (eds.) *Cyber-Physical Systems: Industry 4.0 Challenges*. Studies in Systems, Decision and Control, vol. 260, Springer, Cham (2020). [https://doi.org/10.1007/978-3-030-32648-7\\_10](https://doi.org/10.1007/978-3-030-32648-7_10)
  4. Neydorf, R.A.: Approximating mathematical model development according to point experimental data through “cut-glue” method. *Vestnik Don State Techn. Univ.* **14**(1), 45–58 (2014). <https://doi.org/10.12737/3503>
  5. Neydorf, R.A.: Prospects of using multiplicative-additive approximation for constructing mathematical models of dynamic objects. *Bulletin of St PbsIT(TU)*. №30 (2015). <https://doi.org/10.15217/issn1998984-9.2015.30.713>
  6. Kudinov, N.V., Neydorf, R.A.: Optimization of the linking of local fragmentary functions in the implementation of “cut-glue” approximation of experimental data. *Proceedings of the XXXII International Scientific Conference Mathematical Methods in Engineering and Technology-MMET-32*. 12(1), 17–20 (2019)
  7. Alexeichick, M.I.: Approximative properties of polyharmonic processes. *Eng. Autom. Problems*. No **1**, 34–38 (2009)
  8. Selyutin, A.D.: Approximation of n-degree polynomials by the least squares method. *Young Scientist* **16**(202), 91–96 (2018)
  9. *The Method of Least Squares*. In: *Data Analysis Using the Method of Least Squares*. Springer, Berlin, Heidelberg (2006) [https://doi.org/10.1007/3-540-31720-1\\_2](https://doi.org/10.1007/3-540-31720-1_2)
  10. Egorshin, A.O.: On linear differential equation discretization. *Vestnik YuUrGU. Ser. Mat. Model. Progr.* **14**, 59–72 (2012)
  11. Krivec, R., Mandelzweig, V., Tabakin, F.: Quasilinear approximation and WKB. *Few-Body-Syst.* **34**, 57–62 (2004). <https://doi.org/10.1007/s00601-004-0045-3>
  12. Bakunin, O.G.: Diffusion equations and the quasilinear approximation. In: *Turbulence and Diffusion*. Springer Series in Synergetics. Springer, Berlin, Heidelberg (2008). [https://doi.org/10.1007/978-3-540-68222-6\\_5](https://doi.org/10.1007/978-3-540-68222-6_5)
  13. Adewole, M.O.: Approximation of quasilinear hyperbolic problems with discontinuous coefficients: an optimal error estimate. *Bull. Iran. Math. Soc.* **47**, 307–331 (2021). <https://doi.org/10.1007/s41980-020-00384-8>
  14. Moothedath, S., Chaporkar, P., Belur, M.N.: Minimum cost feedback selection for arbitrary pole placement in structured systems. *IEEE Trans. Autom. Control* **63**(11), 3881–3888 (2018)
  15. Mei, W., Friedkin, N.E., Lewis, K., Bullo, F.: Dynamic models of appraisal networks explaining collective learning. *IEEE Trans. Autom. Control* **63**(9), 2898–2912 (2018)
  16. Xia, M., Rahnema, A., Wang, S., Antsaklis, P.J.: Control design using passivation for stability and performance. *IEEE Trans. Control* **63**(9), 2987–2993 (2018)
  17. Šeda, V.: Quasilinear and approximate quasilinear method for generalized boundary value problems, 1 (1992). [https://doi.org/10.1142/9789812798893\\_0038](https://doi.org/10.1142/9789812798893_0038)
  18. Totik, V.: Orthogonal polynomials. *Surv. Approx. Theory* **1**, 70–125 (2005)

19. Neydorf, R., Chernogorov, I., Vucinic, D.: Universal generator of irregular multidimensional multiextremal functions. Proceedings of IEEE East-West Design & Test Symposium (EWDTS'2017), Novi Sad, Serbia, pp. 253–256 (2017)
20. Neudorf, R.A.: Prospects for using the multiplicative-additive approximation for constructing mathematical models of dynamic objects. Proceedings of SPbGTI (TU), No. 30 (2015). <https://doi.org/10.15217/issn1998984-9.2015.30.71>

# Local Fragmentary Functions' Smooth and Monotonic Docking in “Cut-Glue” Approximation of Experimental Data



N. V. Kudinov , A. S. Drepin , and S. V. Protsenko

**Abstract** To build adequate nonlinear models of natural phenomena and technical systems, the method of experimental modeling and a set of experimental data corresponding to an active study of the relationship of factors and responses are applied. In many cases, the experimental data used for model creation are well approximated only by complex nonlinear dependences. Regression description methods are well suited for approximating such data in certain segments. However, when the nonlinearity of such dependencies is quite significant and a good approximation is achieved in the segments, the nodal smoothness and approximation error in the regions of fragment boundaries can be affected. By the example of the problem of height stabilization during airship surfacing, the mathematical experimental modeling additive-multiplicative method “Cut-Glue” parameters’ influence on the smoothness and monotonicity of the experimental data approximation is investigated. To study the dependence of approximation quality on “Cut-Glue” method parameters, the influence of fragment boundary location on the smoothness of docking of local approximating functions, and varying degrees and substructures of the approximating polynomial to study the behavior of accuracy, monotonicity, and approximation quality are investigated.

**Keywords** Experimental data · Fragmentary approximation · Mathematical model · Regression analysis

---

N. V. Kudinov (✉) · A. S. Drepin · S. V. Protsenko  
Don State Technical University, 1 Gagarin Square, Rostov-on-Don 344000, Russia  
e-mail: [kudinov\\_nikita@mail.ru](mailto:kudinov_nikita@mail.ru)

S. V. Protsenko  
e-mail: [rab555552@rambler.ru](mailto:rab555552@rambler.ru)

© The Author(s), under exclusive license to Springer Nature Switzerland AG 2022  
A. G. Kravets et al. (eds.), *Cyber-Physical Systems: Modelling and Industrial Application*,  
Studies in Systems, Decision and Control 418,  
[https://doi.org/10.1007/978-3-030-95120-7\\_8](https://doi.org/10.1007/978-3-030-95120-7_8)

## 1 Problem Statement

The mathematical models' construction is the control systems development integral part for aerodynamic processes and devices that use them. The constructing mathematical models' main aspect is the experimental data processing that characterizes the process under study, however, such data may consist of complex nonlinear dependencies. The computationally economical mathematical models construction based on such dependencies becomes even more complex when the output parameter changes very significantly in the input parameters' narrow zones, or the dependencies are nonmonotonic [1]. These dependencies include the lift force dependence on the attack angle, which is studied experimentally for a wing or other streamlined body [2]. To construct models with similar properties, the "Cut-Glue" experimental modeling method is developed and described [3].

One of the most important method's steps is the smooth fragments experimental data approximation. The experimental modeling method "Cut-Glue", allows to select and combine the approximated fragments into a single analytical function (SAF) [4]. It differs from other fragment-by-fragment description experimental data methods because it uses an alternative method of combining locally approximating functions into an analytical function by multiplicative selection and additive unification of the changing regions [5, 6]. The method characteristic feature is the leveling changes method in the function beyond the limits of the fragment essential for the model (masking). It is implemented by multiplying by a special multiplicative isolating function (MIF).

The single analytical function can be represented as follows:

$$f(x) = \sum_{i=1}^n f_i(x) = \sum_{i=1}^n \varphi_i(x) \cdot \lambda(x, x_{i-1}, x_i, \varepsilon_i) \quad (1)$$

where  $f_i(x)$  are the cut out local sections,  $\lambda(x, x_{i-1}, x_i, \varepsilon_i)$  is the MIF, which is represented by the following expression:

$$\lambda(x, x_{i-1}, x_i, \varepsilon_i) = \frac{\left[ x - x_{i-1} + \sqrt{(x - x_{i-1})^2 + \varepsilon^2} \right] \cdot \left[ x_i - x + \sqrt{(x_i - x)^2 + \varepsilon^2} \right]}{4\sqrt{[(x - x_{i-1})^2 + \varepsilon^2] \cdot [(x_i - x)^2 + \varepsilon^2]}} \quad (2)$$

The function  $\varphi(x)$  is an approximating model and in this study, the least-squares method is used:

$$\varphi(x) = b_0 + \sum_{i=1}^k b_i x^i \quad (3)$$

where  $k$  is the approximating polynomial order,  $b_i$  are the interpolation coefficients,  $x^i$  are the interpolation nodes.

An important step is the experimental data fragments approximation that are well approximated by analytical functions. Fragment boundaries can be varied, and the settings related to the same border, but different fragments may differ. These factors affect the approximation smoothness and monotonicity at their junctions. In addition, within the fragment and at the boundary, the approximation quality can also be affected by the approximating polynomial parameters, such as its maximum degree and its members' structure. Within the fragment and at the boundary, the approximation quality can also be affected by the parameters of the approximating polynomial, such as its maximum degree and its members' structure [7].

The research is aimed at achieving a compromise between the smoothness and monotonicity of the locally approximating functions (LAF) docking on the one hand and the polynomials' values calculating complexity on the other.

## 2 The Boundary Smoothness Violation in the Trend Change Areas Approximation

Consider the problem of airship flight conditions modeling [3] based on experimental data (ED) obtained by CFD-simulation of the airflow around solid-state airship model through the pitch-lifting channel as an example of using the "Cut-Glue" method, which allows considering the breaking the boundary smoothness problem. In the problem conditions, an extended "Cut-Glue" lifting force dependence approximation (lifting) on 3 parameters—the pitch angle ( $\alpha$ ), the flight altitude ( $h$ ), and the incoming flow velocity ( $v$ ) is investigated. Figure 1 a-c show the approximated functions graphs on 2 fragments. Figure 1b shows the non-monotonous behavior of the function between nodes, which is associated with fragment boundary position incorrect choice.

The maximum approximating polynomial degree order determines the points (nodes) number of the experimental data through which the interpolating curve passes without error (deviation) [8]. Figure 2 shows the approximation error behavior. The approximation error behavior analysis with variations of the maximum degree shows that with experimental data finite amount, the total approximation error should decrease and then increase. Moreover, with an increase in the magnitude order, the error in the nodes for determining the ED decreases, and with further increase in the polynomial degree, the maximum function deviation of the polynomial dependence on the piecewise linear approximation increases [9–11].

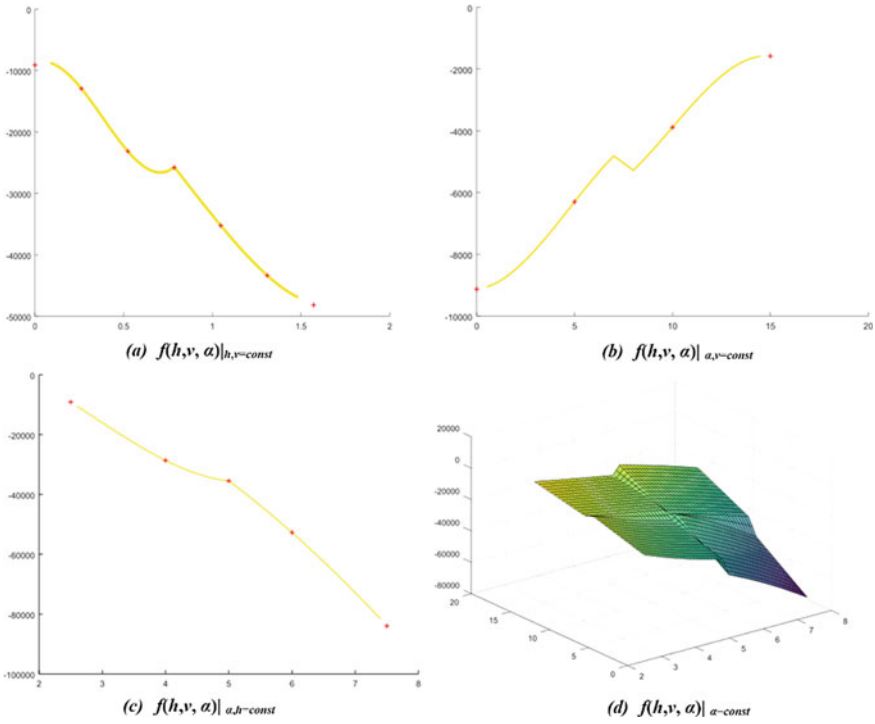
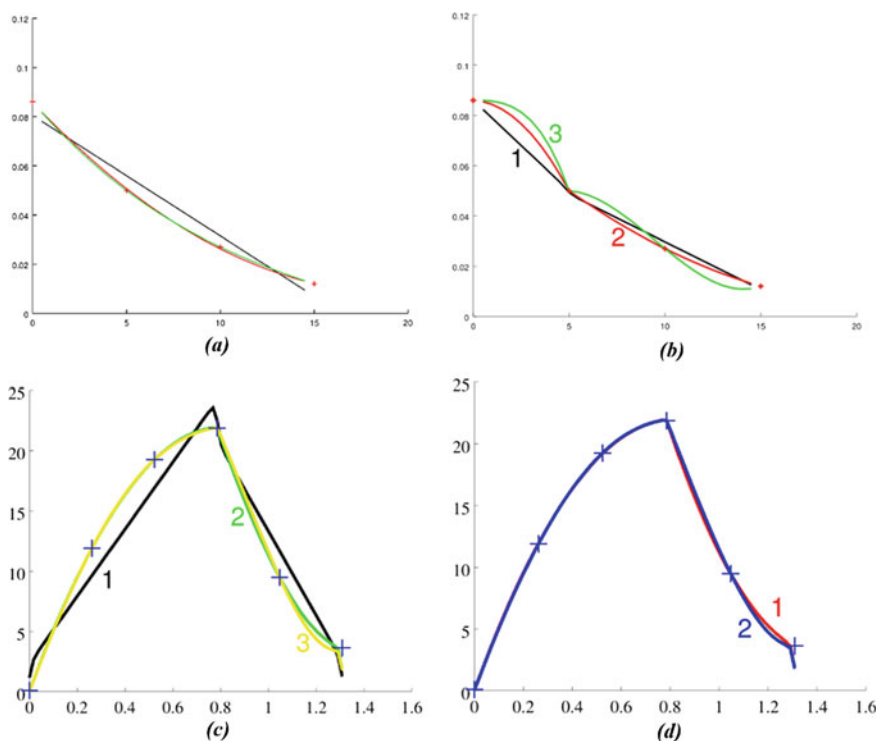


Fig. 1 SAF graphs for “Cat-Glue” three-parameter experimental dependence approximation: the thrust force on the flight altitude, the incoming flow velocity, and the pitch angle

### 3 The Structural Variations Effect on the Docking Smoothness

The structural constraints influence the terms in the polynomial regression [12–15] problems in the experimental data approximation on 2 fragments were studied [16]. For the study, the real model of the lateral displacement force of the balloon dependence on the flight conditions was chosen [17]. The complex three-parameter dependence cross-section is selected at  $v = 2.5$  m/s,  $h = 0$  m. The model peculiarity is the measurement that fixes the characteristic divides fracture the set of measurement results at different  $\alpha$  into two unequal parts of 4 and 2 ED nodes. Studies show that even in such an unfortunate situation, an experimental mathematical model can be constructed that reflects the trends of the studied dependence.

SAF is obtained by applying the Least-Squares Method to experimental data fragments. Various analytical functions can serve as candidate models for fragments in the regression problem, but power and harmonic polynomials occupy a special place due to the good information about the properties of such approximations and the relatively small computational cost.



**Fig. 2** SAF graphs for “Cut-Glue” experimental data various amounts approximation on fragments 1 and 2 by polynomials from 1 to 5°: **a** SAF approximating 4 ED without fragment separation for polynomials of 1, 2, 3°; **b** SAF approximating 4 ED with fragment separation for polynomials of 1, 2, 3°; **c** SAF approximating 6 ED with fragment separation for polynomials of 1, 2, 3°; **d** SAF approximating 6-ED with fragment separation for 3, 5° polynomials

An approach, which consists in sorting out the signs of the approximating function polynomial members presence was chosen for the study, which was represented as a binary mask of the polynomial terms' presence. Next comes the standard procedure for minimizing the least-squares by solving a system of linear equations [18], with the only exception that columns are excluded from the Vandermonde matrix according to the mass presence, which allows to eventually get an incomplete interpolation polynomial, which is then multiplied by the MIF in each fragment. At the final stage, the interpolating function values are added between all the fragments to get the final result.

All possible complete degree 4 polynomial substructures for approximating two fragments simultaneously have been studied. The results of the study show that the complex nonlinear technical system dependence [3] must be approximated by polynomials containing at least three terms containing different degrees of independent argument, but this is not a sufficient condition. In Table 1 possible structures of polynomials for which the error of the polynomial approximation by the LSM does

**Table 1** Possible structures of polynomials

Structure type number	Polynomial structure type	Approximation error on two fragments
15	$x^3+x^2+x^1+x^0$	0,00%
23	$x^4+x^2+x^1+x^0$	0,00%
27	$x^4+x^3+x^1+x^0$	0,00%
29	$x^4+x^3+x^2+x^0$	0,00%
31	$x^4+x^3+x^2+x^1+x^0$	0,00%
7	$x^2+x^1+x^0$	0,09%
14	$x^3+x^2+x^1$	0,20%
22	$x^4+x^2+x^1$	0,20%
26	$x^4+x^3+x^1$	0,20%
28	$x^4+x^3+x^2$	0,20%
11	$x^3+x^1+x^0$	1,04%
19	$x^4+x^1+x^0$	1,87%
30	$x^4+x^3+x^2+x^1$	2,58%
13	$x^3+x^2+x^0$	6,49%
21	$x^4+x^2+x^0$	7,95%
6	$x^2+x^1$	9,52%
3	$x^0+x^1$	10,31%
25	$x^4+x^3+x^0$	10,62%
10	$x^3+x^1$	12,29%
18	$x^4+x^1$	14,71%
5	$x^2+x^0$	20,51%
12	$x^3+x^2$	21,94%
20	$x^4+x^2$	25,84%
9	$x^3+x^0$	26,17%
17	$x^4+x^0$	29,65%
24	$x^4+x^3$	36,00%
2	$x^1$	41,55%
1	$x^0$	53,49%
4	$x^2$	61,12%
8	$x^3$	71,59%
16	$x^4$	80,19%

not exceed 2% are highlighted in green (Fig. 3a), the approximating polynomial smoothness is good, there are no interstitial oscillations.

The full polynomial approximating of the fourth degree shows an exceptional situation arising of the degeneracy of the inverse matrix transformation of the LSM (Fig. 3e) [19]. Blue shows the error of third-degree polynomials approximation, which does not exceed the threshold of 11%, when using such polynomials, the approximating function smoothness is preserved when passing through nodes (experimental data) is required (Fig. 3b). The yellow color shows the results of the approximation experiment when the discrepancy is insignificant at the nodes, but strong smooth distortions are observed in the area of the fragment junction (Fig. 3c). The worst results of the “Cut-Glue” approximation are observed when the polynomial is a power monomial (the lines corresponding to the experiments are highlighted in red), and there is no approximation on one of the fragments (Fig. 3d).



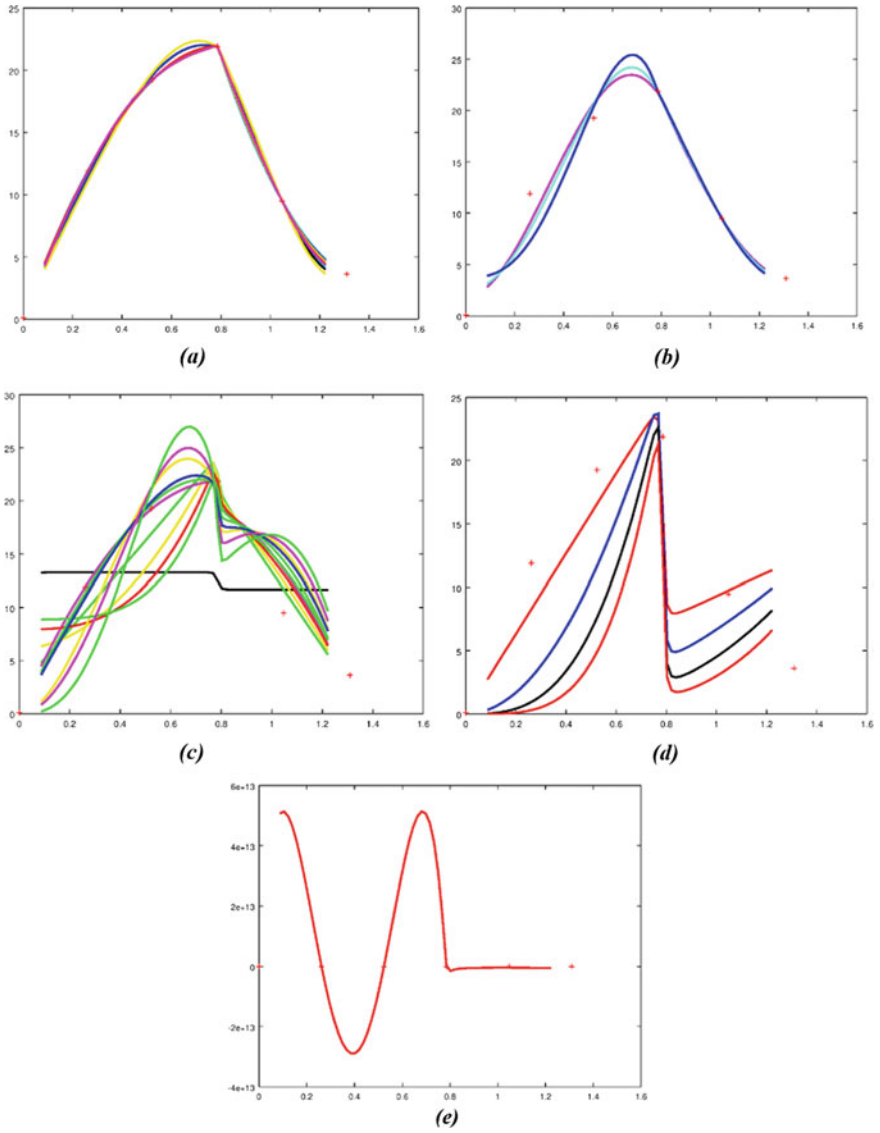


**Fig. 3** Cut-Glue graphs approximation for various polynomial structures. SAF obtained by “Cut-Glue” approximation with polynomials structure: **a** allows not to exceed an error of more than 2%; **b** allows not to exceed the error from 2 to 11%; **c** corresponds to a strong Rook smoothness violation; **d** power-law monomial, there is no approximation on the right fragment; **e** with complete fourth-degree polynomial, degenerate case

## 4 Conclusion

The described “Cut-gluе” approximation is limited by the original polynomial regression models. The fragmentary and polynomial approximation models synthesis allowed to develop algorithms for estimating the model parameters and structure in the analytical form that interpolates experimental data. The results of the study were obtained using a multiparameter “Cut-Gluе” approximation program created in the environment of the GNU Octave computer mathematics system [20]. It allows to study the various constraints and parameters variations influence on the approximation quality and to obtain quasioptimum approximation models with a given tolerance for the approximation error. The approximating polynomial degree influence and its structure on the interfacial conjugation quality is studied. It is shown that the criterion for evaluating the quality of the approximation by the residual in the approximation nodes is insufficient, so should resort to the average integral estimates of the difference of the  $i$ -th and  $i + 1$ -th degree polynomial on the approximation interval covering all fragments of experimental data. Assuming that the experimental data are fragmented, the criterion for the “Cut-Gluе” approximation quality in general and on one fragment in particular can be considered a polynomial of minimum degree and maximum simplicity, containing at least three power monomials, giving a 0-th discrepancy in the determining the experimental data nodes. At the same time, it is important that for geometrically nonlinear dependencies with clearly defined maximum, the fragment boundary is located at the maximum point and is not located between neighboring measurement results.

**Acknowledgements** The reported study was funded by RFBR, project number 18-08-01178, 19-31-90091, and 20-01-00421 A in DSTU.

## References

1. Neydorf, R., Neydorf, A.: Technology of cut-gluе approximation method for modeling strongly nonlinear multivariable objects. Theoretical Bases and Prospects of Practical Application. SAE Technical Paper 2016–01–2035, <https://doi.org/10.4271/2016-01-2035> (2016)
2. Neydorf, R., Gaiduk, A., Gamayunov, N.: The multiplicative-isolating principle of significantly nonlinear mathematical models creation. In: Kravets, A.G., Bolshakov, A.A., Shcherbakov, M. (eds.) *Cyber-Physical Systems: Modelling and Intelligent Control*. Studies in Systems, Decision and Control, vol. 338. Springer, Cham. [https://doi.org/10.1007/978-3-030-66077-2\\_3](https://doi.org/10.1007/978-3-030-66077-2_3) (2021)
3. Gaiduk, A.R., Neydorf, R.A., Kudinov, N.V.: Application of Cut-Gluе Approximation in Analytical Solution of the Problem of Nonlinear Control Design . *Cyber-Physical Systems: Advances in Design & Modelling*. Springer International Publishing, 2020, vol. 259 (2020)
4. Neydorf, R., Gaiduk, A., Kapustyan, S., Kudinov, N.: Conversion of CGA models to Jordan controlled form for design significantly nonlinear control systems. In: Kravets, A.G., Bolshakov, A.A., Shcherbakov, M. (eds.) *Cyber-Physical Systems: Modelling and Intelligent Control*. Studies in Systems, Decision and Control, vol. 338. Springer, Cham. [https://doi.org/10.1007/978-3-030-66077-2\\_10](https://doi.org/10.1007/978-3-030-66077-2_10) (2021)

5. Neydorf, R.: "Cut-Glue" approximation in problems on static and dynamic mathematical model development. Proc ASME Intl Mechan Eng Congr Expos (IMECE), 1. <https://doi.org/10.1115/IMECE2014-37236> (2014)
6. Neydorf, R.: Approximating creation of mathematical models on dot experimental data by cut-glue method. DSTU Bull **14**(75), 45–58 (2014)
7. Kudinov, N.V., Neydorf, R.A.: Local fragmentary functions' docking optimization in implementation of "cut-glue" experimental data approximation . XV International Scientific Conference "Mathematical Methods in Engineering and Technology": Proceedings/TSTU. SPb, 2019. T.12 (2014)
8. Light, W., Wayne, H.: Error estimates for approximation by radial basis functions. In: Singh, S.P. (eds.) Approximation Theory, Wavelets and Applications. NATO Science Series (Series C: Mathematical and Physical Sciences), vol. 454. Springer, Dordrecht (1995)
9. Garkavi, A. L.: "Best approximation theory in linear normed spaces", Results of Science. Series Mathematics. Mathematical Analysis 1967, VINITI, Moscow, 1969, 75–132; Progr. Math., 8, 83–150 (1970)
10. Singer, M.Y.: Elements of differential theory of Chebyshev approximations. Moscow, Nauka, 1975, 172 p. (1975)
11. António, M.G., Ghanbari, P., Ghanbari, M.: Piecewise approximation of contours through scale-space selection of dominant points. IEEE Trans. Image Process. **19**(6), 1442–1450 (2010)
12. Drapper, N, Smith, J.: Applied Regression Analysis, vol. 1, p. 366. Wiley, New York (1981)
13. Drapper, N, Smith, J.: Applied Regression Analysis, vol. 2, p. 351 S. Wiley, New York (1981)
14. Bates, D, Watts, D.: Nonlinear Regression Analysis and its Applications, p. 365. Wiley, New York (1988)
15. Rawlings, J., Pantula, S., Dickey, D.: Applied Regression Analysis: a Research Tool, 2nd edn. Springer, New York, 671p. ISBN 0–387–98454–2, SPIN 10660129 (1998)
16. Neydorf, R.: Bivariate: "Cut-Glue" approximation of strongly nonlinear mathematical models based on experimental data. SAE Int. J. Aerosp. 1, 47–54 (2015)
17. Neydorf, R., Neydorf, A., Vučinić, D.: "Cut-Glue" approximation method for strongly nonlinear and multidimensional object dependencies modeling. In: Öchsner, A., Altenbach, H. (eds) Improved Performance of Materials. Advanced Structured Materials, vol. 72. Springer, Cham. [https://doi.org/10.1007/978-3-319-59590-0\\_13](https://doi.org/10.1007/978-3-319-59590-0_13) (2018)
18. Fichtenholz, G.M.: Course of differential and integral calculus. **3**, 734 (1984)
19. Kudinov, N.V.: Parameter identification of ordinary differential equations using the least-squares method on an equidistant difference grid XVIII International Scientific Conference "Mathematical Methods in Engineering and Technology". Proceedings /KSTU. Kazan. 2005. VOL. 2, pp. 166–168 (2005)
20. Alexeev, E.R., Chesnokova, O.V.: Introduction to Octave for engineers and mathematicians. ALT Linux, 368 p. (2012)

# **IoT and Signal Processing**

# Automatic Compensation of Thermal Deformations of the Carrying Structures of Cyber-Physical Information Measuring Systems



Michail Livshits , Boris Borodulin, Aleksei Nenashev, and Yulia Savelieva

**Abstract** The ways of creation, possible algorithms of operation of the system of automatic control of thermal modes of supporting structures of information-measuring system of autonomous objects is considered. The problem of synthesis of the system of automatic stabilization of the temperature field of cyber-physical information-measuring systems by means of discretely distributed control is solved. The system provides an essential decrease of the thermo-deformation measurement error level, which is caused by deformation of supporting structures due to unstable and nonuniform heat release from information-measuring devices, placed on a structure. For the compensation of thermal deformations, an appropriate system of thermal mode support is used. The system consists of controlled heat sources used to compensate for the thermal gradients of the supporting structure arising under the influence of the heat generated by the information and measuring system devices and of the external thermal radiation on the structure. An effective economical algorithm of control of the controlled heat sources specially placed on the structure is suggested. This algorithm provides the compensation of the load-carrying structure thermal gradient up to the admissible level. The thermal deformation component of the information and measurement error, which is the cause of distortion of the operating and service information of an autonomous object, is reduced by compensation of the thermal gradient by an automatic control system of the operating modes of the distributed controlled heat sources. The control algorithm and structure of the system are implemented by special software of the onboard computer.

**Keywords** Autonomous object · Thermal deformation compensation · Controlled heat sources · Thermal regime

---

M. Livshits (✉) · B. Borodulin · A. Nenashev · Y. Savelieva  
Samara State Technical University, 244, Molodogvardeyskaya st., Samara 443100, Russia  
e-mail: [usat@samgtu.ru](mailto:usat@samgtu.ru)

© The Author(s), under exclusive license to Springer Nature Switzerland AG 2022  
A. G. Kravets et al. (eds.), *Cyber-Physical Systems: Modelling and Industrial Application*,  
Studies in Systems, Decision and Control 418,  
[https://doi.org/10.1007/978-3-030-95120-7\\_9](https://doi.org/10.1007/978-3-030-95120-7_9)

## 1 Introduction

The relevance of improving the quality of optoelectronic complexes of autonomous objects, primarily of the spacecraft, is constantly growing, which is associated, among other things, with their intensive usage in such areas as mapping, creation of geoinformation systems, etc. [1, 2]. These science-based areas provide the chances of strategic intensification of economic activity for many years. The development and operation of optoelectronic complexes are impossible without increasing the accuracy of the information-measuring systems (IMS) comprising optical devices. A significant part of the optical measurement error is the thermal deformation error, which is caused by the thermal deformation of the IMS carrying structures of the cyber-physical system due to the unstable and uneven temperature distribution in them [2, 3]. The temperature fields of the carrying structures are uneven and unstable due to non-stationary heat release from IMS devices, due to the effect of radiation from planets and stars through the corresponding access ports and openings of spacecraft, etc.

To compensate for thermal deformations, an appropriate system for providing a thermal mode is used, said system includes controlled heat sources (CHS) by which the thermal gradients of the carrying structure are compensated for, that arise under the influence of heat release from the IMS and external heat sources on the structure [1, 2].

Ways of creating, possible algorithms for the operation of an automatic control system (ACS) of thermal modes of carrying structures of cyber-physical information measuring systems of IMS autonomous objects are considered.

## 2 Function-Based Modeling

An example with the arrangement of IMS and CHS on a carrying structure in the form of a rectangular prism made of isotropic material is further considered. By means of the corresponding standardizing function [2–14]:

$$\omega(x, y, z, \tau) = Q_{X_1}(0, y, z, \tau) + Q_{X_2}(R_x, y, z, \tau) + Q_{Y_1}(x, 0, z, \tau) + Q_{Y_2}(x, R_y, z, \tau) + Q_{Z_1}(x, y, 0, \tau) + Q_{Z_2}(x, y, R_z, \tau), \quad (1)$$

temperature distribution  $\Theta(x, y, z, \tau)$  can be presented in the form of a non-homogeneous differential equation:

$$\begin{aligned} \partial\Theta(x, y, z, \tau)/\partial\tau - a[\partial\Theta^2(x, y, z, \tau)/\partial x^2 + \partial\Theta^2(x, y, z, \tau)/\partial y^2 + \\ + \partial\Theta^2(x, y, z, \tau)/\partial z^2] = \omega(x, y, z, \tau), \end{aligned} \quad (2)$$

$$\tau \in [0, \infty), \quad x \in [0, R_x], \quad y \in [0, R_y], \quad z \in [0, R_z],$$

with homogeneous boundary conditions

$$\begin{aligned} \partial\Theta(x, y, z, \tau)/\partial x|_{x=0} &= \partial\Theta(x, y, z, \tau)/\partial y|_{y=0} = \\ &= \partial\Theta(x, y, z, \tau)/\partial z|_{z=0} = 0, \quad \partial\Theta(x, y, z, \tau)/\partial\tau|_{\tau=0} = 0 \end{aligned} \quad (3)$$

Here  $\Theta(x, y, z, \tau)$ —relative temperature of the structure,  $a$ —temperature conductivity coefficient;

$$\begin{aligned} Q_{X_1}(0, y, z, \tau) &= q_{X_1}(y, z, \tau) \cdot \delta(x), \quad Q_{Y_1}(x, 0, z, \tau) = q_{Y_1}(x, z, \tau) \cdot \delta(y), \\ Q_{Z_1}(x, y, 0, \tau) &= [q_{Z_1}(x, y, \tau) + q_A(x, y, \tau) \cdot V_A(x, y)] \cdot \delta(z), \\ Q_{X_2}(R_x, y, z, \tau) &= q_{X_2}(y, z, \tau) \cdot \delta(x - R_x), \\ Q_{Y_2}(x, R_y, z, \tau) &= q_{Y_2}(x, z, \tau) \cdot \delta(y - R_y), \\ Q_{Z_2}(x, y, R_z, \tau) &= [q_{Z_2}(x, y, \tau) + q_B(x, y, \tau) \cdot V_B(x, y)] \cdot \delta(z - R_z) \end{aligned}$$

—heat flows on the corresponding edges of the prism;  $R_x, R_y, R_z$ —prism dimensions;  $q_A(x, y, \tau), q_B(x, y, \tau)$ —heat release intensity of controlled and uncontrolled heat sources arranged on the corresponding edges  $z = R_z$  and  $z = 0$ ;  $V_A(x, y) = \delta(x - x_A) \cdot \delta(y - y_A), V_B(x, y) = \delta(x - x_B) \cdot \delta(y - y_B)$ —areas of influence of the concentrated heat flows from the corresponding heat sources;  $q_{X_1}(y, z, \tau), q_{X_2}(y, z, \tau), q_{Y_1}(x, z, \tau), q_{Y_2}(x, z, \tau), q_{Z_1}(x, y, \tau), q_{Z_2}(x, y, \tau)$ —intensity of external heat exchange on the corresponding prism edges;  $\delta(\cdot)$ —Dirac delta function.

By means of the Laplace transforming the corresponding Green's function of the boundary value problem (2), it is possible to obtain the transfer functions over the control channels  $q_A(x, y, z, \tau) - \Theta(x, y, z, \tau)$  and disturbance  $\{q_{X_1}, q_{X_2}, q_{Y_1}, q_{Y_2}, q_{Z_1}, q_{Z_2}, q_B\} - \Theta(x, y, z, \tau) - \Theta(x, y, z, \tau)$  for the object subjected to control (1)–(2) [2, 10–18].

On this basis, it is possible to solve the problem of synthesizing the corresponding system for automatic stabilization of the structure temperature field by using a discretely distributed control  $q_A(x, y, \tau)$ . The synthesis technique is based on a finite-dimensional approximation of the infinite-dimensional Laplace transform of the corresponding Green's function and a formulation of the transfer function of the object with distributed parameters for synthesizing the controller in view of said basis [15, 16, 19, 20].

The transfer function can be presented as a parallel connection of the integrating link and an infinite number of aperiodic links, which, however, can be limited in practical applications.

The transfer function coefficients depend on the spatial location of the disturbance and the control point, reflect the influence of the characteristic of the heat transfer channels from one object to another. In this example, there are four possible transfer channels: “Point  $\rightarrow$  Point”, “Point  $\rightarrow$  Area”, “Area  $\rightarrow$  Point” and “Area  $\rightarrow$  Area”.

The objects “Point” represent conventional points of control of the structure surface temperature, points of applying the power of heat-releasing elements, attachment points, and other relatively small heat-releasing or absorption regions. The

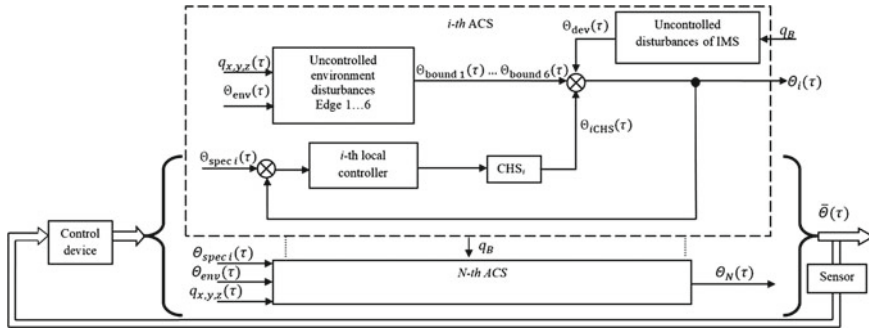


**Fig. 1** Automatic control system for compensation of thermal deformations: CHS—controlled heat source;  $\Theta_i(\tau)$ —temperature of  $i$ -th from  $N$  controlled points;  $\Theta_{spec i}(\tau)$ —temperature predetermined by the algorithm of the control device system in every of  $N$  controlled points;  $\Theta_{bound i}(\tau)$ —an average temperature of edges;  $\Theta_{iCHS}(\tau), \Theta_{dev}(\tau)$ —components of the temperature field, determined by the CHS operation, uncontrolled disturbances and heat release of the measuring equipment;  $\Theta_{env}(\tau)$ —temperature of the environment surrounding the structure

objects “Area” are the areas of the structure edges surface, the surface area of the water cooling structure, the surface area of the equipment seats, and etc.

Figure 1 shows the ACS of the temperature field of the structure by using discretely distributed local controllers.

The temperature controller of each  $i$ -th  $\Theta_i(\tau) = \Theta(x_i, y_i, z_i, \tau) = \{\Theta_i\}_1^N$  from  $N$  control points has a proportional-integral structure combined with a relay one. In this case, the control law has the form:

$$q_i(\tau) = \begin{cases} q_{max}, q_i(\tau) > q_{max} \\ K_i(\Theta_{spec}(\tau) - \Theta_i(\tau)) \\ + 1/T_{ui} \cdot \int_0^{\infty} [\Theta_{spec}(\tau) - \Theta_i(\tau)] \partial \tau, 0 \leq q_i(\tau) \leq q_{max} \\ 0, q_i(\tau) < 0 \\ i = \overline{1, N} \end{cases} \quad (4)$$

wherein  $K_i, T_{ui}$ —parameters of the controller settings;  $q_{max}$ —maximum installed power of CHS.

### 3 Interpretation and Discussion of Research Results

Description of an economical algorithm for thermo-gradient stabilization of the structure:



1. Diagnostics of technical means
  - a. at each step of the algorithm operation, sensor failures are diagnosed. Checking the sensor for failure is determined by polling the zero signal. An indication of the sensor failure is the absence of a current signal, which may be due to a broken communication line or a sensor defect. If a said indication of the sensor failure is detected, then the corresponding pair of heaters is forcibly turned off.
  - b. diagnostics of heater failure. Diagnostics of heater failures are carried out at each step of the algorithm operation. Checking the heater for failure is conducted by detecting a zero current signal. An indication of the heater failure is the absence of a current signal, which may be due to a broken communication line or a heater defect. If a said indication of the heater failure is detected, then the corresponding pair of heaters is forcibly turned off.
  - c. diagnostics of the measuring unit failure. Diagnostics of the measuring unit failures are carried out at each step of the algorithm operation. If an indication of a failure is detected (a break in the communication line or short circuit (SC)), then the corresponding control unit along with heaters is turned off.

As soon as said indication of failure of the sensor, heater, measuring, or control unit is eliminated, the heaters and the control channel are included in the algorithm accordingly.

## 2. Sensor polling.

At this step, the reading of the  $j$ -th sensor  $\Theta_{i,j}$  is carried out and said information is written into the microcontroller's memory.

3. Checking whether the parameter value is within the specified range of variation.
  - a. If the current temperature value in the sensor  $\Theta_{i,j} < \Theta_{\min}$ , then the power level of the corresponding heater is increased by 1 ( $k_{i+1,j+32} = k_{i,j+32} + 1$ ), i.e. the power of the  $j + 32$ th heater at the next  $(i + 1)$ -th step of operation will become equal to  $P_{i+1,j+32} = 0.5 \cdot (k_{i+1,j+32} - 1)$ . In this case, it is checked whether the power level of the heater does not exceed the maximum possible, if  $k_{i+1,j+32} > 8$ , then the power level of the heater is set equal to  $k_{i+1,j+32} = 8$ .
  - b. If the current temperature value in the sensor  $\Theta_{i,j} > \Theta_{\max}$ , then the power level of the corresponding heater decreases by 1 ( $k_{i+1,j} = k_{i,j} - 1$ ), i.e. the power of the  $j$ -th heater at the next  $(i + 1)$ -th step of operation will become equal to  $P_{i+1,j} = 0.5 \cdot (k_{i+1,j} - 1)$ . In this case, it is checked whether the power level of the heater does not exceed the minimum possible, if  $k_{i+1,j} < 1$ , then the power level of the heater is set equal to  $k_{i+1,j} = 1$ .
  - c. If the current temperature value in the sensor  $\Theta_{i,j+32} > \Theta_{\max}$ , then the power level of the corresponding heater decreases by 1 ( $k_{i+1,j+32} = k_{i,j+32} - 1$ ), i.e. the power of the  $j + 32$ th heater at the next  $(i + 1)$ -th step of operation will become equal to  $P_{i+1,j+32} = 0.5 \cdot (k_{i+1,j+32} - 1)$ . In this case, it is checked whether the heater power level does not exceed the minimum possible, if  $k_{i+1,j+32} < 1$ , then the heater power level is set equal to  $k_{i+1,j+32} = 1$ .

- d. If the current temperature value in the sensor is  $(\Theta_{i,j})_{\max/\min}$ , then the power level of the corresponding heater at the next  $(i + 1)$ -th step of operation does not change, i.e.  $k_{i+1,j} = k_{i,j}$ ,  $P_{i+1,j} = P_{i,j}$ .
- e. If the current temperature value in the sensor  $(\Theta_{i,j+32})_{\max/\min}$ , then the power level of the corresponding heater at the next  $(i + 1)$ -th step of operation does not change, i.e.

$$k_{i+1,j+32} = k_{i,j+32}, P_{i+1,j+32} = P_{i,j+32}.$$

4. Determination of the difference value in the thickness of the structure.

At each step of the algorithm operation, the value of the temperature difference across the thickness of the structure in the pair of opposite sensors is determined (Fig. 2). The value of the difference  $d\Theta_i > \Theta_{i,j} - \Theta_{i,j+32}$  is calculated.

5. Checking for finding the value of the temperature difference in the specified range and forming control actions

- a. If the absolute value of the difference  $|\Theta_i| \leq D$ , then no control actions are required, the heater power remains at the same level, i.e.  $k_{i+1,j} = k_{i,j}$ ,  $P_{i+1,j} = P_{i,j}$ ,  $k_{i+1,j+32} = k_{i,j+32}$ ,  $P_{i+1,j+32} = P_{i,j+32}$ .
- b. If the absolute value of the difference  $|\Theta_i| > D$ , then, depending on the sign of the value  $d\Theta_i$ , the following laws of variation of the heater power are established:

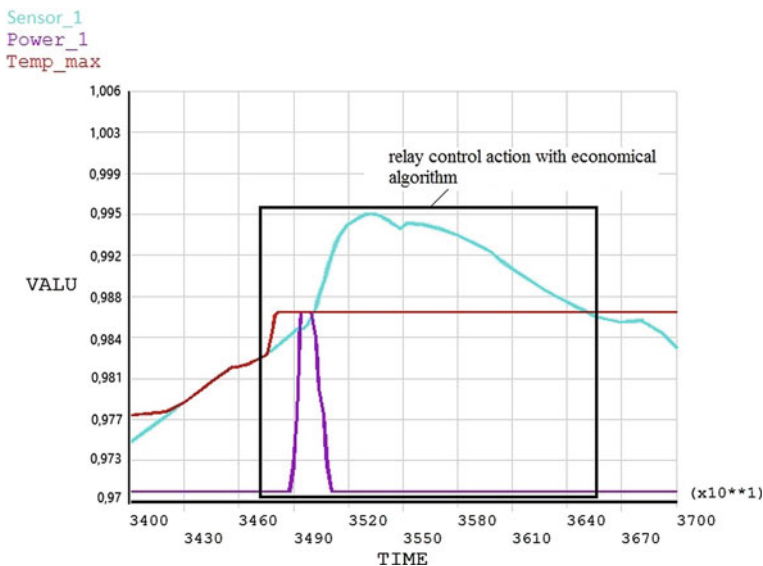


**Fig. 2** Temperature in the region of sensor No. 1, heater power (Power\_1) and the current set maximum temperature of the structure (Temp\_max) with an economical algorithm of operation of the ACS of thermo-gradient stabilization of the structure

- (1) If  $d\Theta_i > 0$  (i.e.  $\Theta_{i,j} > \Theta_{i,j+32}$ ), then the number of variants are possible:
    - i. If  $k_{i,j} \geq k_{i,j+32}$ ,  $k_{i,j} > 1$  th step, then the power level of the heater remains as minimal possible, if  $k_{i+1,j} < 1$ , then the power level of the heater is set equal  $k_{i+1,j} = 1$ ,  $P_{i+1,j} = 0.5 \cdot (k_{i+1,j} - 1)$  at the side of the structure, wherein the temperature is lower, the power of the heater remains at the same level  $k_{i+1,j} = k_{i,j}$ ,  $P_{i+1,j} = P_{i,j}$ .
    - ii. If  $k_{i,j} \leq k_{i,j+32}$  or  $k_{i,j+32} = 1$ , then at the side wherein the temperature is higher, the power of the heater remains at the minimum level without any changes  $k_{i+1,j+32} = k_{i,j+32}$ ,  $P_{i+1,j+32} = P_{i,j+32}$ , and power of the heater at the opposite side increases on 1 level:  $k_{i+1,j} = k_{i,j} + 1$ , it is checked whether the level of the heat power does not exceed the maximum possible, if  $k_{i+1,j} > 8$ , then the level of heat power is set equal to  $k_{i+1,j} = 8$ ,  $P_{i+1,j} = 0.5 \cdot (k_{i+1,j} - 1)$ .
  - (2) If  $d\Theta_i = 0$ , then the changes are not required, i.e.  $k_{i+1,j} = k_{i,j}$ ,  $P_{i+1,j} = P_{i,j}$ ,  $k_{i+1,j+32} = k_{i,j+32}$ ,  $P_{i+1,j+32} = P_{i,j+32}$ .
6. Check for reaching the limit number of polled sensors
    - a. If  $j = N$ , then the transition to the 8th step of the algorithm is carried out.
    - b. If  $j < N$ , then the transition to the 7th step of the algorithm is carried out
  7. Transition to the next sensor and the corresponding heater  $j = j + 1$ .  
Transition to step 1, diagnostics of the next pair sensor-heater.
  8. Checking to exit the algorithm
    - a. If  $i < n$ , then transition to the next step of the algorithm  $i = i + 1$  operation is carried out.
    - b. If  $i = n$ , then the exit the algorithm is carried out.

Thus, the economical algorithm for thermo-gradient stabilization of the structure is quite simple to implement, it has a small information memory resource, and it provides total low energy consumption for heating the temperature control elements. The disadvantages of this algorithm are a long time and low control accuracy.

The main disadvantage of the economical algorithm is a long time for control, which is explained by the fact that the algorithm can change the power of each temperature control element only once in one operation cycle. Therefore, the following is suggested.

At each step of the algorithm, the value of the difference  $\Delta\Theta_i$  between the maximum  $\Delta\Theta_{\max}$  or minimum  $\Delta\Theta_{\min}$  temperature and the current one  $\Theta_{i,j}$ ,  $\Theta_{i,j+32}$  are determined and stored (see steps 3.a and b).

If, for example,  $\Delta\Theta_i \geq 2K$ , then the power level of the heater at the next step is set equal to  $k_{i+1,j} = k_{i,j} \pm 2$ , where the operator is determined depending on the values of the current temperature ( $\Theta_{i,j} < \Theta_{\min}$  or  $\Theta_{i,j} > \Theta_{\max}$ , respectively). That is, indeed, changes are introduced into steps 3.a and b of the economical algorithm (Fig. 2).

## 4 Conclusion

Figures 3 and 4 represents the results of finite element modeling of the ACS in the ANSYS environment, with typical disturbances for this object and taking into account the structural features of the carrying structure of cyber-physical information measuring systems.

In operating mode, the average temperature difference  $\Delta\Theta$  between the controlled points is 0.0752 (up to 29600 s). When using the proposed ACS  $\Delta\Theta = 0.0262$ , which indicates a significant decrease in thermal deformation of the carrying structure of cyber-physical information measuring systems and the probability of unsatisfactory operation of the IMS.

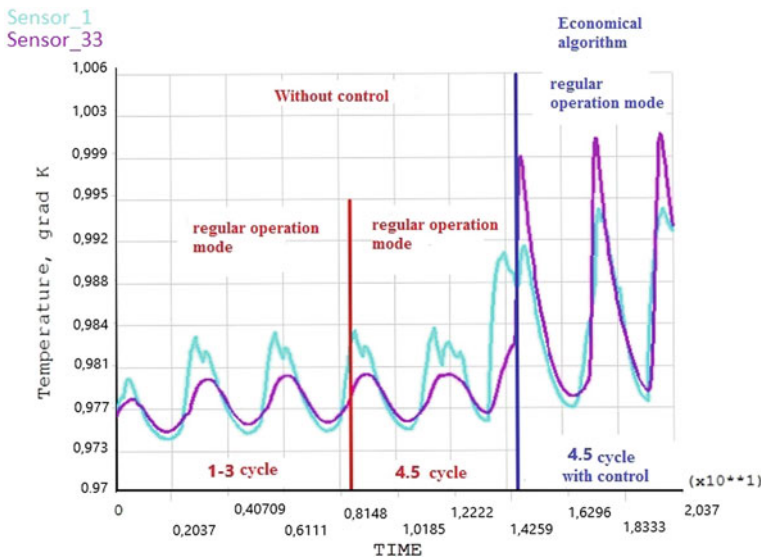


**Fig. 3** Temperature of the structure in the regions of sensors No. 1, No. 33 with an economical algorithm of operation of the ACS of thermo-gradient stabilization of the structure

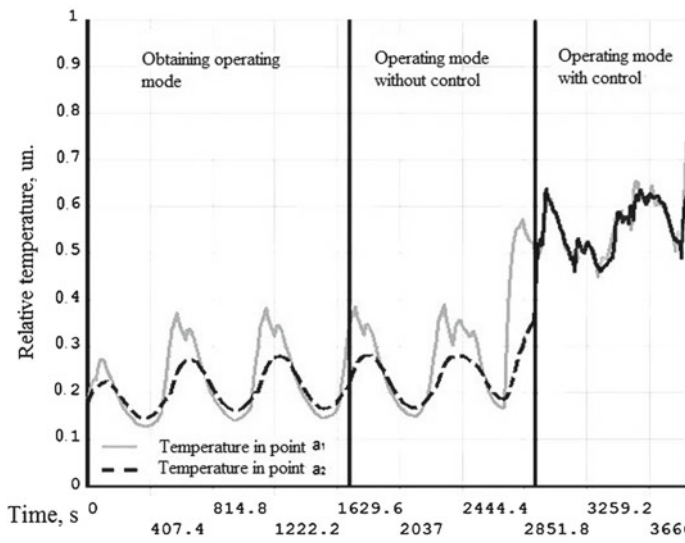


**Fig. 4** Temperature of the carrying structure in the controlled points

**Acknowledgements** This research was partially supported by the Russian Foundation for Basic Research, grant No. 20-08-00240.

## References

1. Borodulin, B.B., Livshits, M.Y.: Optimal control of temperature modes of the instrumental constructions of autonomous objects. In: EPJ Web of Conferences, volume 110. Thermophysical Basis of Energy Technologies (2016)
2. Meseguer, J., Pérez-Grande, I. and Sanz-Andrés, A.: Spacecraft Thermal Control, p. 413. Woodhead Publishing Limited (2012)
3. Demin, S., Panishev, O., Yunusov, V., Timashev, S.: The Application of Statistical Methods for the Analysis of Multi-Parameter Data of Complex Composite Objects in the Field of Cyber-Physical Systems: Studies in Systems. Springer International Publishing, Decision and Control (2021)
4. Lions, J.: Control of Distributed Singular Systems, p. 552. Gauthier-Villars, Paris (1985)
5. Warga, J.: Optimal Control of Differential and Functional Equations, vol. Xiii, p. 531. Academic Press, New York (1972)
6. Di Loreto, M., Damak, S., Eberard, D., Brun, X.: Approximation of linear distributed parameter systems by delay systems. *Automatica*, 162–168 (2016). <https://doi.org/10.1016/j.automatica.2016.01.065>
7. Felgenhauer, U., Jongen, H.T., Twilt, F., Weber, G.: Semi-infinite optimization: structure and stability of the feasible set. *J. Optim. Theory Appl.* **3**, 529–452 (1992)
8. Buttazzo, G., Kogut, P.: Weak optimal controls in coefficients for linear elliptic problems. *Rev. Mat. Comput.* **24**, 83–94 (2018)
9. Gogol, I.V., Remizova, O.A., Syrokvashin, V.V., Fokin, A.L.: Robust autonomous control of a multiply connected technological object with input delays. In: Cyber-Physical Systems:

- Modelling and Intelligent Control, Studies in Systems, Decision and Control, p. 338. [https://doi.org/10.1007/978-3-030-66077-2\\_7](https://doi.org/10.1007/978-3-030-66077-2_7)
10. Pleshivtseva, Y., Rapoport, E.: Parametric optimization of systems with distributed parameters in problems with mixed constraints on the final states of the object of control. *J. Comput. Syst. Sci. Int.* **57**, 723 (2018). <https://doi.org/10.1134/S1064230718050118>
  11. Gill, F., Murray, W., Wright, M.: *Practical Optimization*, p. 509. Academic Press, New York (1981)
  12. Cialkowski, M., Grysa, K.: Sequential and global method of solving an inverse problem of heat conduction equation. *J. Theor. Appl. Mech.* **48**(1), 111–134 (2010)
  13. Ramm, A.G.: *Inverse problems*. Springer Science, Business Media Inc., Mathematical and Analytical Techniques with Applications to Engineering. Boston (2005)
  14. Jing, L., Youjun, X.: An inverse coefficient problem with nonlinear parabolic equation. *J. Appl. Math. Comput.* **34**, 195–206 (2010)
  15. Livshits, M.Y., Borodulin, B.B., Nenashev, A.V.: *Efficient Computational Procedure for the Alternance Method of Optimizing the Temperature Regimes of Structures of Autonomous Objects Cyber-Physical Systems: Industry 4.0 Challenges*. Springer International Publishing (2020)
  16. Xiong, Q., Cai, W.-J., He, M.-J.: Equivalent transfer function method for PI/PID controller design of MIMO processes. *J. Process Control.* **17**, 665–673 (2007)
  17. Xiong, Q., Cai, W.-J.: Effective transfer function method for decentralized control system design of multi-input multi-output processes. *J. Process Control.* **16**, 773–784 (2006)
  18. Lian, T., Fan, Z., Li, G.: Lagrange optimal controls and time optimal controls for composite fractional relaxation systems. *Adv. Differ. Equ.* **1**, 233 (2017). <https://doi.org/10.1186/s13662-017-1299-7>
  19. Li, R., Liu, W., Ma, H., Tang, T.: Adaptive finite-element approximation for distributed elliptic optimal control problems. *SIAM J. Contr. Optim.* **4**, 1244–1265 (2003)
  20. Murat, F., Tartar, L.: On the control of the coefficients in partial equations. *SIAM J. Contr. Optim.* **4**, 1244–1265 (2003)

# Solving the Problem of Optimizing the Modes of Operation of the Combined Heat and Power Systems, Depending on the Chosen Method



A. V. Andryushin, E. K. Arakelyan, A. V. Neklyudov, N. S. Dolbikova, and Y. Y. Yagupova

**Abstract** The task of choosing the optimal operating modes of the station equipment includes two interrelated tasks: compilation of generating equipment and electrical load with a known composition of generating equipment. At present, various methods and software systems have been developed for the internal optimization of the equipment operating mode, including in relation to the problem of optimal distribution of the current load, but there is a significant proportion of manual input of initial data to select the optimal mode for each change in the task. It is necessary to improve the methodological and cyber-physical system at the plant for the practical implementation of the tasks of controlling the operating modes of the equipment of the power plant. The chapter discusses approaches to solving the problem of load distribution at a combined heat and power plant with a complex composition of equipment. Various optimization methods are described, as well as a station model within which the problem is being solved. The substantiation of the choice of the optimization method is given.

**Keywords** Optimization · Thermal power station · Optimization methods · Programming · Operating modes · Reliability · Economics

---

A. V. Andryushin (✉) · E. K. Arakelyan · A. V. Neklyudov · N. S. Dolbikova · Y. Y. Yagupova  
National Research University Moscow Power Engineering Institute, Moscow, Russia  
e-mail: [AndriushinAV@mpei.ru](mailto:AndriushinAV@mpei.ru)

E. K. Arakelyan  
e-mail: [ArakelianEK@mpei.ru](mailto:ArakelianEK@mpei.ru)

A. V. Neklyudov  
e-mail: [NekliudovAIV@mpei.ru](mailto:NekliudovAIV@mpei.ru)

N. S. Dolbikova  
e-mail: [DolbikovaNS@mpei.ru](mailto:DolbikovaNS@mpei.ru)

Y. Y. Yagupova  
e-mail: [YagupovaYY@mpei.ru](mailto:YagupovaYY@mpei.ru)

## 1 Introduction

Determining the optimal operating mode of an electric power plant remains an urgent task of modern power engineering. When solving this problem, it is necessary to find a method for optimizing the operating modes of the equipment and the plant, which will ensure the maximum efficiency of the production of thermal and electrical energy. Usually, the efficiency criterion is the margin profit value, but other optimality criteria can also be considered.

High price volatility in the electricity market leads to the need for regular planning of equipment operating modes at the power plant. Depending on the planning of the plant operation modes: short-term or long-term perspective, the requirements are taken into account, such as the production and distribution of a given amount of electricity between generating units, the release of a given capacity and heat by the planned schedule (with planning from several hours to several weeks) and the reduction of annual costs for the operation of equipment, ensuring reliable operation of the power system (with long-term planning). All this creates a limit on the optimization execution time [1–3].

There are many methods for solving the problems of optimizing the operating modes of units at a thermal station. It is always necessary to pay attention to the features of the optimization method because the choice of mathematical approach depends on the types of turbine installations, the ways of representing the energy characteristics of turbines, the structure of heat release from the station. Analytical methods for finding optimal solutions for thermal power plants are unsuitable due to many data, variables, and constraints on them [4–7].

To effectively solve the optimization problem of load distribution, it is necessary to correctly apply one or another optimization method corresponding to the problem being solved, both from the point of view of the possibility of its application, the complexity of calculations, the complexity of programming and universality of application, and from the point of view of modeling the physical process itself, based on the use of cyber-physical systems to quickly set up equipment and improve the quality of work. [8–12].

The analyzed optimization methods allow us to obtain a set of optimized parameters (electrical and thermal loads of power units, thermal loads of boilers, and other parameters) with a certain accuracy that satisfies the extremum of the target function [13–15].

The following optimization methods will be compared below.

1. The Monte Carlo method.
2. Dynamic programming method.
3. Methods of mixed-integer linear programming.
4. The inner point method.

The choice of the first three methods is determined by the fact that they can be used both for optimization problems with arbitrary function definition domains. Since the problem is not generally convex [16, 17].



The inner point method was added to demonstrate the effects that can be observed when using gradient methods in solving the optimization problem.

## 2 Test Model

As an example of a technological process for conducting numerical experiments, we take a test model of the station [18].

When developing an optimization model, the entire equipment composition is divided into groups of elements, after which each group of elements is described as a separate element of the optimization model. The main elements are boilers, turbines, steam collectors of the high, medium, and low pressure, and the heating equipment can be considered in the form of an adjustment for the characteristics [19, 20].

For simplicity of experiments, it is proposed to consider the optimization of turbine operating modes. The solution of the problem of minimizing the consumption of hot steam for a group of turbines is performed at a given total load of generation  $N$ , thermal selection  $Q_t$ , industrial selection  $Q_p$ , a given set of equipment: PT turbines operate in PT mode, T turbine-in a single-stage model.  $N = 150$  MW,  $Q_t = 120$  Gcal,  $Q_p = 80$  Gcal.

## 3 The Monte Carlo Method

The Monte Carlo method is a method of statistical testing. It is necessary to define the rules for conducting tests:

Step 1: Randomly distribute the  $Q_p$  between the two PT turbines  $Q_{p1}$  and  $Q_{p2}$ .

Step 2: it is necessary to determine the range of permissible values of  $Q_{t1}$  and  $Q_{t2}$  for turbines 1 and 2, considering the values of heat extraction  $Q_{p1}$  and  $Q_{p2}$  obtained in step 1. The volume of total heat extraction  $Q_t$  is distributed randomly among the three turbines, considering their possible ranges.

Step 3: it is necessary to determine the range of permissible values of turbine generation, considering the values of thermal and industrial selection. Then randomly distribute the total generation volume between the turbines.

Step 4: Calculate the hot steam flow rate for each of the turbines and its total value.

Next, you need to conduct  $N$  experiments and get the minimum value of the total heat removal  $Q_0$ .

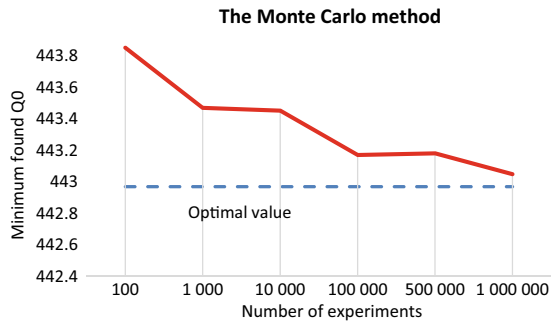
The experimental results are listed in Table 1.

As the number of experiments increases, the accuracy of the method increases. Figure 1 shows the dependence of the calculation execution time in proportion to the number of experiments.

**Table 1** Experimental results calculated by the Monte Carlo method

Number of experiments $n$	Minimum value $Q_0$	Calculation execution time, sec	% Points	Deviation from the optimal value
100	443,8514	0,01	62	0,88 Gcal
1 000	443,47	0,015	54	0,5 Gcal
10 000	443,4524	0.089	56,8	0,48 Gcal
100 000	443,1708	0.824	57,28	0,20 Gcal
500 000	443,1812	4,27	57,16	0,21 Gcal
1 000 000	443,049	8,9	57,06	0,08 Gcal

**Fig. 1** Dependence of the accuracy of the Monte Carlo method on the number of experiments



## 4 Dynamic Programming Method

The task is solved in several steps:

Step 1. To solve this problem, it is necessary to construct a generalized characteristic of turbines T1 and T2 for possible operating modes, provided that their total industrial selection is equal to the value of  $Q_p$ .

Step 2. It is necessary to form a generalized characteristic of the T3 turbine with the generalized characteristic obtained in the previous step for all possible variants of turbine operation, provided that the total volume of thermal extraction is equal to  $Q_t$ , and the total generation is equal to  $N$ .

To determine all possible variants of turbine operation, a table is formed linking the parameters  $Q_t$ ,  $Q_p$ ,  $N$ ,  $Q_0$ .

For each of the directions ( $Q_t$ ,  $Q_n$ ,  $N$ ), a step is set, a list of values from minimum to maximum. The final table contains all possible combinations of values on the axes  $Q_t$ ,  $Q_n$ ,  $N$ .

Below is Table 2 with the dependence for determining the optimal parameters of the optimization model.

**Table 2** Numerical experiments using the dynamic programming method

Step by Qp	Step by Qt	Step by N	Minimum Q0 value	Checkout time	Deviation from the optimal value
20 Gcal	10 Gcal	5 MW	443,062	1,4 s	0,092 Gcal
20 Gcal	10 Gcal	2,5 MW	443,061	3,4 s	0,091 Gcal
10 Gcal	10 Gcal	2,5 MW	443,061	9,3 s	0,091 Gcal

When the step of the calculated grid is reduced to a certain value, the accuracy of the optimization model increases, but the further reduction of the grid step does not bring any effect.

### 5 Integer Linear Programming Method

To solve the problem using the method of mixed-integer linear programming (MILP), [21–23] the parameterization of the object’s characteristics is first performed, that is, its representation occurs in the form of linear constraints such as equalities and inequalities. In the three-dimensional case, the surface is divided into a set of simplices, each of which is described by linear constraints, as shown in Fig. 2.

When solving a problem with the help of the most important role is played by the library that performs the solution (solver). Several solvers are compared: GLPK, SCIP, and GUROBI.

The result of calculating the task is presented in Table 3.

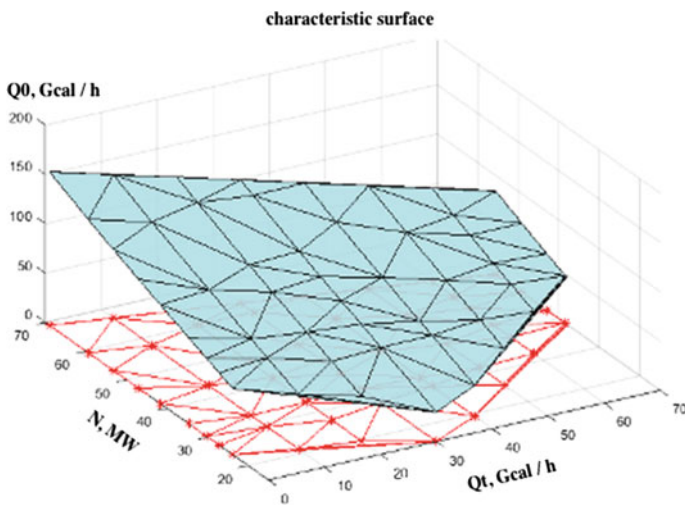
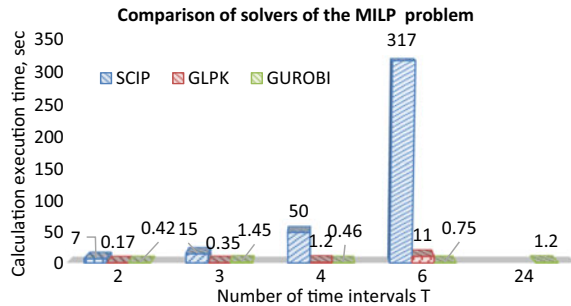


**Fig. 2** An example of representing a surface as a set of simplices

**Table 3** Result of calculation by the method MILP

Calculation library name	Minimum value of Q0, Gcal	Calculation execution time, sec	Deviation from the optimal value
SCIP	442,97	57	Less than 0.001 Gcal
GLPK	442,97	24	Less than 0.001 Gcal
GUROBI	442,97	5,045	Less than 0.001 Gcal

**Fig. 3** Comparison of Solvers of the MILP problem



One way to speed up the calculations MILP is to reduce the number of points at which the surface is formed. To reduce the number of reference points, you need to set the acceptable error criterion. For example, you can set an error of 0.05 Gcal in the direction of Q0.

It is interesting to conduct numerical experiments that allow us to construct the dependence of the calculation time on the number of variables in an empirical way.

Consider this problem not for one, but for several points in time T.

Each moment within the framework of the task is independent. However, the problem is solved in one iteration (the solver is called once).

The graphical representation of the results in Fig. 3 demonstrates the dependence of the calculation execution time on the complexity of the problem (the complexity is proportional to the number of time intervals considered).

From the table above, it can be seen that the Gurobi solver shows the best results on large-dimensional problems. Below is a graph of the calculation execution time depending on the number of calculated time intervals.

## 6 Gradient Methods

Even though the use of gradient methods has a high probability of finding local optima, it is interesting to make a numerical experiment using them. In the Matlab mathematical package, there is a calculation module “fmin”, which allows you to choose one of the optimization algorithms: ‘interior-point’ (default).

As a result of calculations for a different number of time intervals of the optimization problem, it was found that with an increase in the dimension of the problem, the found solution is removed from the optimal one using the inner point method.

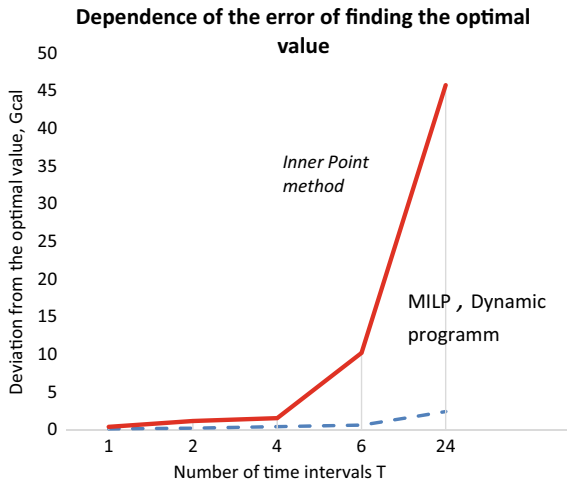
Below is Table 4 with the results of calculations for a different number of time intervals of the optimization task.

From the table above, it can be seen that with an increase in the dimension of the problem, the solution found is removed from the optimal one using the interior point method. Based on the results of the analysis of optimization calculations presented in Fig. 4, it can be concluded that for high-dimensional problems, the deviation of the found solution using the internal point method is much higher than for solutions found by Dynamic programming or MILP.

**Table 4** Calculation results for a different number of time intervals

Algorithm	Minimum value of Q0, Gcal	Calculation time, sec	Number of time intervals T	Deviation from the optimal value
'interior-point' (interior point method)	443,33	2,7	1	0,36 Gcal
	887,09	2,7	2	1,15 Gcal
	1773,4	3,05	4	1,52 Gcal
	2668	3,7	6	10,18 Gcal
	10,677	11,8	24	45,7 Gcal

**Fig. 4** Error of the optimization model depending on the method used



## 7 Conclusions

The Monte Carlo method is the most expensive in terms of the ratio of calculation time/accuracy of the result.

In the case when the problem is considered for a single moment in time, the found values of the minimum flow rate of sharp steam are comparable for the methods of MILP and Dynamic programming, and the method of the internal point.

In the case of solving the optimization problem in time, convex optimization methods show a result that is located further from the optimal one in comparison with the methods of MILP and Dynamic Programming.

The fastest solution was found using Mixed Integer Linear Programming (MILP) and the Dynamic Programming method.

The MILP concept allows you to flexibly modify the optimization model, as well as supplement it with new elements of the technological process. Using a modern solver allows you to perform an optimization calculation with the required accuracy in a fairly short period (seconds).

One of the disadvantages of MILP is the fact that not every process can be linearized (parameterized) with the required accuracy. Nevertheless, the MILP approach is very interesting from the point of view of the prospects of using it for the formation of optimization models of thermal power plants.

The dynamic programming method is called sequentially for each moment, however, to account for the maneuverability of the turbines, the number of calculations may increase. Taking into account additional integral constraints will require a serious refinement of the method implementation.

**Acknowledgements** The research is supported by the Russian Foundation for Basic Research, grant № 20-38-90146 \ 20.

## References

1. Arakelyan, A.V. Andryushin, V.A., Makarchyan, et al.: Methodological approaches to optimal control of the modes of operation of a combined heat and power plant with a complex composition of equipment. *Teploenergetika* **10**, (2012)
2. Dincer, I., Rosen, M.A., Ahmadi, P.: Modeling and optimization of power plants. *Optim. Energy Syst.* (2017). <https://doi.org/10.1002/9781118894484.ch9>
3. Arakelyan, E.K., Minasyan, S.A., Agababyan, G.E.: Methodical principles of multicriterial optimization of daily operating conditions of power equipment at thermal power stations. *Therm. Eng.* **53**, 767–771 (2006)
4. Arakelyan, E.K., Pikina, G.A.: Optimization and optimal management: studies, Manual, 2nd edn. In: Shchederkina, T.E. (ed.) Moscow: Publishing House of the Moscow Power Engineering Institute (2008). (Reprint and add)
5. Cole, W.J., Powell, K.M., Edgar, T.F.: Optimization and advanced control of thermal energy storage systems. In: Gruyter, D. (ed.) (2012). <https://doi.org/10.1515/revce-2011-0018>. Last accessed 1 July 2012

6. Sjelvgren, D., Andersson, S., Andersson, T., Nyberg, U., Dillon, T.S.: Optimal Operations Planning in a Large Hydro-Thermal Power System. *IEEE Trans. Power Appar. Syst.* PAS **102**(11) (1983)
7. Vinnikov, A.: Features of Selection of the Included Generating Equipment in the Russian Energy Market (2018)
8. Chernyshev, S.: Cyber-physical principles of information processing in ultra-wideband systems. *Cyber-Phys. Syst. Ind. 4 Chall.* (2020) <https://doi.org/10.1007/978-3-030-32648-7>
9. Ledukhovskiy, G.V., Pospelov, A.A.: Calculation and Rationing of Thermal Efficiency of Thermal Power Plant Equipment (2015)
10. Gorlach, I., Wessel, O.: Optimal level of automation in the automotive industry. *Eng. Lett.* **16**(1), 141–149 (2008)
11. Borodin, V.A., Protalinskiy, O., Khanova, A.: Developing an energy provider's knowledge base of flow charts. *Cyber-Phys. Syst. Ind. 4 Chall.* (2021) <https://doi.org/10.1007/978-3-030-66081-9>
12. Ustyugov, N.: Forecast of the cost of electricity and choice of voltage level for the enterprise. *Cyber-Phys. Syst. Ind. 4 Chall.* (2021). <https://doi.org/10.1007/978-3-030-66081-9>
13. Urin, V.D., Kutler, P.P.: Energy characteristics for optimizing the regime of power plants and power systems—M. Energy (1974)
14. Gronstein, V.M., Gronstein, V.M. (eds.): Methods for optimizing power system modes—M. Energy (1981)
15. Ivanov, N.S.: Theoretical and practical prerequisites for creating software for optimizing load distribution at thermal power plants. In: Materials of the All-Russian Conference on the Results of the Competition of Young Specialists of the NPK Organizations of JSC RAO, pp. 88–103. UES of Russia, Moscow (2005)
16. Andryushin, A.V., Arakelyan, E.K., Neklyudov, A.V., Yagupova, Y.Y., Drobyshev, T.O.: A Formation of an Approach to Solving the Problem of Selecting the Composition of the Included Generating Equipment (2019)
17. Andryushin, A.V., Arakelyan, E.K., Neklyudov, A.V., Yagupova, J.Y., Dolbikova, N.S., Kokhova, O.K.: Method of the Optimal Distribution of Heat and Electrical Loads (2020)
18. Vanderplas, J.: Python for complex tasks: data science and machine learning, p. 576. SPb (2018)
19. Ivashchenko, V.A., Fomin, I.N., Shulga, T.E.: Mathematical Model and Algorithm of Operational Control of TPP Generating Equipment (2020)
20. Hart, W.E., Laird, K.D., Watson, J.-P., Woodruff, L.D.: Pyomo—Optimization Modeling in Python (2017)
21. Qiu, G.X., Wang, S.Y., Wang, W.B.: Data Mining in Optimization of the Targeted Value for Thermal Power Plant, p. 116026. Dalian Maritime University Automation Research Institute, Dalian, China (2020)
22. Sheila Samsatlia, N.J., Samsatlib, S.: General Model of Mixed Integer Linear Programming for the Design and Operation of Integrated Urban Energy Systems (2018)
23. Cavalieri, F., Roversi, A., Ruggeri, R.: Use of mixed integer programming to investigate optimum running conditions for a thermal power station and possible extension to capacity. *J. Oper. Res. Soc.* **22**, 221–236 (1971)

# Testing a Ground-Based Radar Station as a Cyber-Physical System Using a Carrier and On-Board Equipment



A. L. Kalabin and A. K. Morozov

**Abstract** In the work, the radar station is considered as a cyber-physical system. The cyber-physical system, in particular the radar, needs to be tested during production, commissioning, and operation. The chapter proposes the modernization of the laboratory test method using an unmanned aerial vehicle, which houses a programmable generator with an onboard computer and other necessary auxiliary equipment. Radar testing is performed as in the flyby method, without using real targets. The essence of the method is to control the movement of the carrier and the signal from the output of the onboard generator in such a way that the emitted signal corresponds to the actual operating conditions of the radar. The digital representation of the test signal is calculated by the onboard computer and a radio signal corresponding to the current operating mode of the station is emitted by means of a generator and an antenna. By changing the coordinates and structure of the emitted signal, it is possible to control the angular coordinates, range, and number of targets for the tested radar. The proposed method can be used to test, for example, air traffic control radars with lower resource costs, in comparison with field tests due to the use of an unmanned aerial vehicle and onboard equipment instead of airplanes.

**Keywords** Imitation of a radar target · Computer simulation · Unmanned aerial vehicle · Bench tests · Semi-natural tests

## 1 Introduction

To test and confirm the performance of cyber-physical systems, in particular radars, test benches are often used [1–10]. The use of test benches allows obtaining the necessary information about the product at an acceptable cost of resources [11–13]. The task of the stand is to form the operating conditions for a cyber-physical system close to real ones by generating test signals [7–10]. When testing radar receivers (radar), test signals are formed on the basis of a mathematical model that takes

---

A. L. Kalabin (✉) · A. K. Morozov  
Tver State Technical University, Tver 170026, Russia  
e-mail: [akalabin@yandex.ru](mailto:akalabin@yandex.ru)

© The Author(s), under exclusive license to Springer Nature Switzerland AG 2022  
A. G. Kravets et al. (eds.), *Cyber-Physical Systems: Modelling and Industrial Application*,  
Studies in Systems, Decision and Control 418,  
[https://doi.org/10.1007/978-3-030-95120-7\\_11](https://doi.org/10.1007/978-3-030-95120-7_11)

117



into account the main factors [14, 15]. But there are factors that require significant computing power to account for. For example, reflections from the ground, terrain features, the influence of weather conditions, the electromagnetic environment at the deployment point, and others. Therefore, it is proposed to place equipment for simulating the target signal on an unmanned aerial vehicle (UAV) for testing ground-based pulse radars. In this case, the signal emitted from the carrier is received by the radar antenna with the influence of all the factors present.

## 2 Coordinates of the Simulated Target

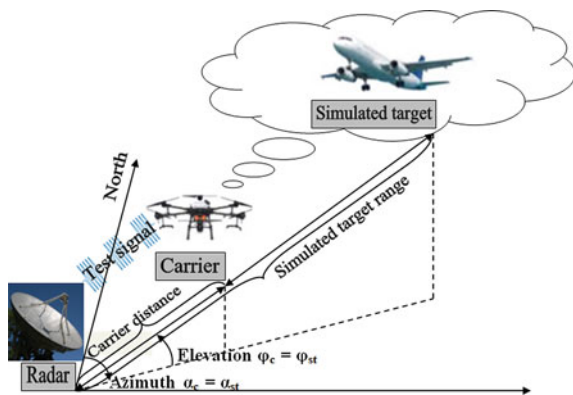
The purpose of this chapter is to describe a method for determining the capabilities of measuring the range of detected targets for ground-based pulse radars, using test signals generated from the UAV. The required target environment will consist of one simulated target, the range of which varies from a certain minimum to a maximum range within the studied range. The range of the simulated target will change with a constant step at regular intervals. As the station under study, we will consider a pulsed ground radar with a passive response. In the course of measurements, it is planned that the angular coordinates of the simulated target will remain unchanged and are determined by the position of the carrier, its angular coordinates.

$$\alpha_{st} = \alpha_c; \varphi_{st} = \varphi_c; \alpha_{st} = const; \varphi_{st} = const; \quad (1)$$

where  $\alpha_{st}$ —azimuth of simulated target;  $\varphi_{st}$ —elevation angle of simulated target;  $\alpha_c$ —carrier azimuth;  $\varphi_c$ —carrier elevation angle.

As can be seen from Fig. 1, the range of the simulated target is the sum of the measurement distance and the range added by the onboard equipment. With regard to the situation presented in Fig. 1, the range of the simulated target is calculated as [15–17].

**Fig. 1** Coordinates of the simulated target



$$r_{st} = r_{st \min} + \frac{t_{zg}c}{2} \quad (2)$$

where  $r_{st}$ —range of simulated target;  $r_{st \min}$ —minimum possible range of the simulated target;  $t_{zg}$ —onboard generator delay time;  $c$ —speed of light.

The minimum possible range of the simulated target is the sum of the current distance at which the carrier with the onboard equipment is located and the pause introduced by the computer and the synchronization scheme of the onboard equipment with the radar emitter and is calculated by the formula (3).

$$r_{st \min} = r_c + \frac{t_p c}{2} \quad (3)$$

where  $r_c$ —current removal of the carrier from the radar;  $t_p$ —pause introduced by the delay of the synchronization signal and the work of the calculator.

Thus, from (2, 3) it follows that the control of the range of the simulated target can be carried out by adding the delay time for the pulse emitted by the onboard generator.

$$t_{zg} = \frac{2(r_t - r_c)}{c} - t_p \quad (4)$$

### 3 Step of Changing the Range of the Simulation Target

Changes in the range of the simulated target are discrete, therefore, it is necessary to determine the step in range. The minimum possible step size will be related to the range resolution of the simulated targets, which the equipment used is capable of. The range of the simulated target is the sum of the position of the carrier and the delay time generated by the onboard generator.

The removal of the carrier from the radar  $r_c$  is determined by the data of the sensors. For example, using a GPS receiver, latitude and longitude are determined and using a barometric sensor, atmospheric pressure and temperature are determined, which are then converted into altitude. Usually, the position by the sensors is determined with some error, we will assume that the error is a random variable distributed according to the normal law. Let us assume that the value of the standard deviation  $\sigma_r$  of the measured value  $r_c$  is known, then the position of the carrier in accordance with the data will be located with a probability of more than 0.99 within the interval [9, 10].

$$-3\sigma_{r_c} < \xi_{r_c} < 3\sigma_{r_c} \quad (5)$$

where  $\xi_{r_c}$ —distance error  $r_c$ ;  $\sigma_{r_c}$ —range error standard deviation.

The airborne generator generates the required delay time discretely, generating an analog signal from digital samples, the value of which can be changed after a specified time interval (sampling time) associated with the sampling frequency. The sampling time [18] is determined by the formula (6).

$$t_{dg} = \frac{1}{f_{dg}} \quad (6)$$

where  $t_{dg}$ —onboard generator sampling time;  $f_{dg}$ —onboard generator sampling rate.

The accuracy of control of the output signal is carried out with an accuracy of one digital reading. If we assume that the required pulse pause in the signal is formed with an error distributed according to the normal law, then, similarly, as with the position of the UAV, the error of the formed pause in the signal will be with a probability of more than 0.99 within the interval [19].

$$-3\sigma_{t_{zg}} < \xi_{t_{zg}} < 3\sigma_{t_{zg}} \quad (7)$$

where  $\sigma_{t_{zg}}$ —value of the standard deviation of the pause error of the signal generated by the onboard generator;  $\xi_{t_{zg}}$ —pause error of the signal generated by the airborne generator.

Then the error in controlling the range of the simulated target [20] is calculated by the formula (8).

$$\sigma_{rst} = \sqrt{\left(\frac{\sigma_{tst}C}{2}\right)^2 + \sigma_{rc}^2} \quad (8)$$

where  $\sigma_{rst}$ —the value of the standard deviation of the error in controlling the range of the simulated target.

From (5, 7, 8) we determine the value of the distance step in terms of range for the generator of the target situation by the formula (9).

$$\Delta r_{st} = 3\sigma_{rst} \quad (9)$$

where  $\Delta r_{st}$ —the minimum step of changing the range of the simulated target.

Thus, the size of the step of changing the range of the simulated target depends on the accuracy of the positioning sensors and the onboard generator.

#### 4 Assessment of the Feasibility of the Measurement Plan

To determine the initial range and final range of the simulated target, the step size, and the period of its change, it is necessary to have an idea of how long the flight will take, i.e. the limitation on the available flight time.

On the one hand, the flight time will be calculated in accordance with (10).

$$T_c = t_{tk} + T_m + t_{ld} \quad (10)$$

where  $T_c$ —time taken to fly;  $t_{tk}$ —time required to fly from the take-off point to the first point of the measuring trajectory;  $t_{ld}$ —time required to fly to the landing point from the last point of the measuring trajectory;  $T_m$ —time spent on the measuring path.

The measurement plan will be realizable if the condition is met (11).

$$T_c \leq T_{\max} \quad (11)$$

where  $T_{\max}$ —maximum possible flight time for the carrier used.

On the other hand, the time required to execute the simulation of the target is calculated according to the Eq. (12).

$$T_m = \sum_{i=1}^n t_i \quad (12)$$

where  $n$ —number of positions of the simulated target;  $t_i$ —time spent by the simulated target at a given range.

For the situation of an all-round looking radar, the time spent by the target at a given range can be tied to the antenna rotation period and set for each position of the simulated target equal to an integer number of radar antenna turns  $k$ , then the measurement time will be calculated by the formula (13).

$$T_m = nkT_{radar} \quad (13)$$

where  $T_{radar}$ —radar antenna rotation period;  $k$ —an integer number of turns of the radar antenna, the same for each position of the simulated target;  $n$ —number of positions of the simulated target.

The number of positions of the simulated target depends on the step of changing its range and the investigated range segment, then the number of positions of the simulated target can be calculated by the formula (14).

$$n = \left\lceil \frac{r_{\max} - r_{\min}}{h \Delta r_{st}} + 1 \right\rceil \quad (14)$$

where  $r_{\min}$ —minimum range of simulated target;  $r_{\max}$ —maximum range of simulated target;  $h$ —integer coefficient that determines the step size of the range of the simulated target. The number of positions of the simulated target, by meaning, must be an integer greater than zero.

As a result, we obtain a system of Eq. (15) for calculating the range of detected targets for the formation of test signals on the carrier.

$$\left\{ \begin{array}{l} \Delta r_{st} = 3\sigma_{r_{st}} \\ n = \left\lceil \frac{r_{\max} - r_{\min}}{h\Delta r_{st}} + 1 \right\rceil \\ T_m = nkT_{radar} \\ T_c = t_{tk} + T_m + t_{ld} \\ T_c \leq T_{\max} \\ h\Delta r_{st} \leq \Delta r_{\min} \\ k \geq 1; h \geq 1; n \geq 2 \\ n \rightarrow \max; h \rightarrow \min; T_c \rightarrow T_{\max} \end{array} \right. \quad (15)$$

The solution to this system will be the values  $(k, h, n)$  that determine the sets of realizable measurement plans with fixed parameters of the test equipment  $\Delta r_{st}$ ,  $T_{\max}$ ,  $\sigma_{rc}$ ,  $\sigma_{t_{zg}}$ ,  $t_p$ ; station parameters  $T_{radar}$ ; measurement conditions  $r_{\min}$ ,  $r_{\max}$ .

## 5 Example and Software Implementation

Let us consider an example of solving system (15) to illustrate the obtained solution. After fixing the chosen solution  $(k, h, n)$ , the plan of measurements is calculated. The measurement plan includes the coordinates of the trajectory of the carrier and the range of the simulated target, since the on-board generator is only able to change the range through the change in the pulse delay time, and the angular coordinates of the simulated target will coincide with the angular coordinates of the carrier. Since the flight time of the carrier is limited, it is proposed to conduct a range study not in all possible directions, but at one selected azimuth and elevation angle.

The onboard computer in the process of measurements must keep a log of the coordinates of the carrier and the simulated target. The radar maintains a log of the recorded target situation. The coordinates of the simulated and detected targets are compared, as in the flyby method.

Suppose that the shaper has the following characteristics: the accuracy of determining the position in space  $\sigma_{rc} = 1, 5$  m; response delay time accuracy  $\sigma_{t_{zg}} = 50$  ns; delay introduced by the synchronization circuit and the calculator  $t_p = 5$   $\mu$ s; maximum carrier flight time  $T_{\max} = 30$  min; the coordinates of the station, the takeoff/landing point of the carrier and the measuring trajectory are such that the takeoff and landing time takes  $t_{tk} = t_{ld} = 30$  s. The investigated station has the

following characteristics (only those that are used for example are shown): radar antenna rotation period  $T_{radar} = 10$  s. The purpose of the measurements is to investigate the possibility of detecting targets at a distance from  $r_{min} = 5$  km to  $r_{max} = 50$  km, maximum step size  $\Delta r_{max} = 500$  m.

To search for and select solutions, consider the nature of the dependencies between the values of  $T_m$ ,  $n$ ,  $h$ .

Let us first consider the system (16).

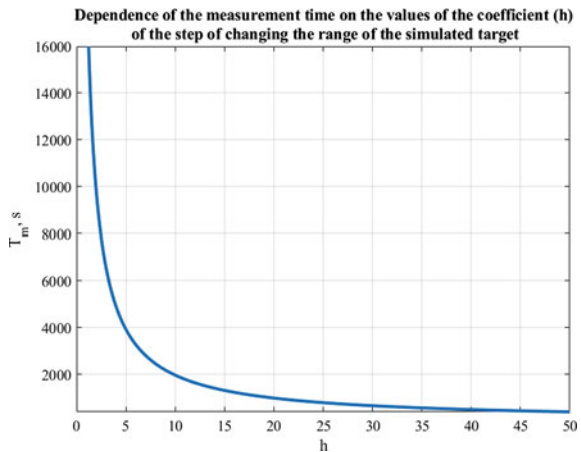
$$\begin{cases} h = 1, \dots, h_{max} \\ h_{max} = \frac{r_{max} - r_{min}}{(n_{min} - 1)\Delta r_{st}}; n_{min} = 2 \\ n = \frac{r_{max} - r_{min}}{h\Delta r_{st}} + 1 \\ T_m = nkT_{radar} \end{cases} \tag{16}$$

where  $h_{max}$ —maximum coefficient value  $h$ ;  $n_{min}$ —the minimum number of positions of the simulated target.

Consideration of system (16) is necessary to establish the dependence  $T_m(h)$ ,  $n(h)$ . For this, the value of  $h$  will go from 1 to some maximum value. The maximum value of  $h$  is reached at  $n = 2$ . From the point of view of planning measurements, this situation arises when the simulated target has 2 positions: at the beginning and at the end of the investigated range segment, then the coefficient  $h$ , which determines the step of changing the range between the positions of the simulated target, will have a maximum value, at which the step size will be equal to the length of the investigated distance segment. Figure 2 shows a graph illustrating the nature of the dependence of the value  $T_m(h)$ .

Now consider the system (17).

**Fig. 2** Illustration of the dependence of the measurement time on the coefficient that determines the step of changing the range of the simulated target



$$\begin{cases} n = 2, \dots, n_{\max} \\ n_{\max} = \frac{r_{\max} - r_{\min}}{(h_{\min} - 1)\Delta r_{st}} + 1; h_{\min} = 1 \\ h = \frac{r_{\max} - r_{\min}}{(n - 1)\Delta r_{st}} \\ T_m = nkT_{radar} \end{cases} \quad (17)$$

where  $n_{\max}$ —the maximum number of positions of the simulated target;  $h_{\min}$ —minimum value of coefficient h.

Similarly as system (16) system (17) for definitions of dependence  $T_m(n)$ ,  $h(n)$ . In this, the number of positions of the simulated target is brute-forced from the minimum possible value to a certain maximum value. The minimum number of positions of the simulated target is 2: at the beginning of the segment of the studied ranges and at the end. The variant with one position of the simulated target is not considered in the work. Similarly, to the previous reasoning, the maximum number of positions of the simulated target is achieved at the minimum step. The minimum possible step of changing the range of the simulated target is achieved when  $h = 1$ . Figure 3 shows a graph showing the nature of the dependence of the value  $T_m(n)$ .

From the point of view of searching for and choosing suitable solutions to the system (15), the most interesting solutions are those that provide the most information. According to the graphs in Figs. 2 and 3, it can be concluded that with the smallest step coefficient h of changing the range of the simulated target and the largest number of positions of the simulated target n, one can obtain the largest amount of information for further analysis.

Thus, for system (15), the largest value of n is attained at the smallest values of h, so we will find solutions as follows: first, we fix h, then we iterate over all k for

**Fig. 3** Illustration of the dependence of the measurement time on the number of positions of the simulated target

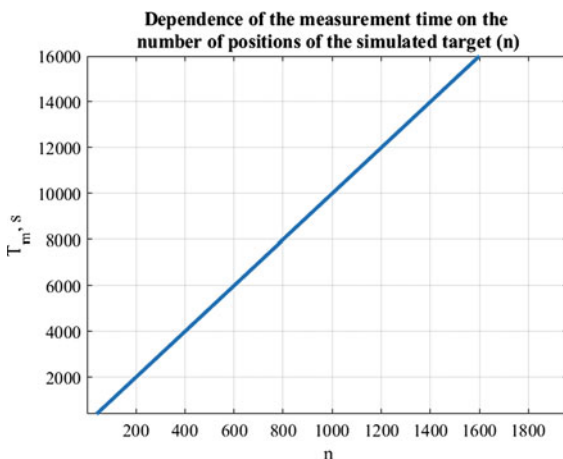


**Table 1** The solutions of the system

No.	h	n	$T_H$
1	10	168	1740
2	11	153	1590
3	12	140	1460
4	13	130	1360
5	14	121	1270
6	15	113	1190
7	16	106	1120
8	17	100	1060
9	18	94	1000

which the system is resolved, if for a fixed  $h$  there is no  $k$  for which the system has a solution, then we increase  $h$  and also iterate over  $k$ .

Table 1 shows the solutions of the system (15), by the characteristics of the test equipment, the station, and the test conditions.

Table 1 is a list of solutions of system (15) that satisfy the conditions for carrying out measurements, the characteristics of the station under study, and the equipment used for  $k = 1$ .

The search for solutions was carried out taking into account the fact that the values of the quantities  $h$  and  $n$  are integers. The number of positions of the simulated target  $n$  is meaningfully an integer. In addition, the coefficient  $h$  is an integer, since the used implementation of the target situation generator has errors in positioning, registration of its own coordinates, control of the range of the simulated target, therefore, for it, the step of changing the range of the simulated target is a discrete multiple of the minimum possible step of the simulated target  $\Delta r_{st}$ .

Of all the solutions, it is most advantageous to use the first one, since the smallest step of changing the range and a larger number of positions of the simulated target is achieved, which will provide more information for analysis.

To automate calculations and build a measurement plan, a program was written in C++. Figure 4 shows the result of planning by the obtained solution of the system (15).

The program also implements simulation of the course of measurements. Figure 5 shows images of the radar indicator at different simulation times. For the 9th minute, the simulated target mark is displayed almost at the maximum range displayed by the indicator, and at 24 min, the simulated target mark is not observed, but the simulated target signal is still generated.

The situation for the 24th minute of the simulation can be interpreted as exceeding the detection range for the station under study. At the 9th minute, the range of the detected target practically corresponds to the maximum for the software model of the radar indicator. When logging at the station and on-board computer, after comparing and analyzing the data, it is possible to conclude the maximum target detection range by the same analysis methods as in the flyby method.



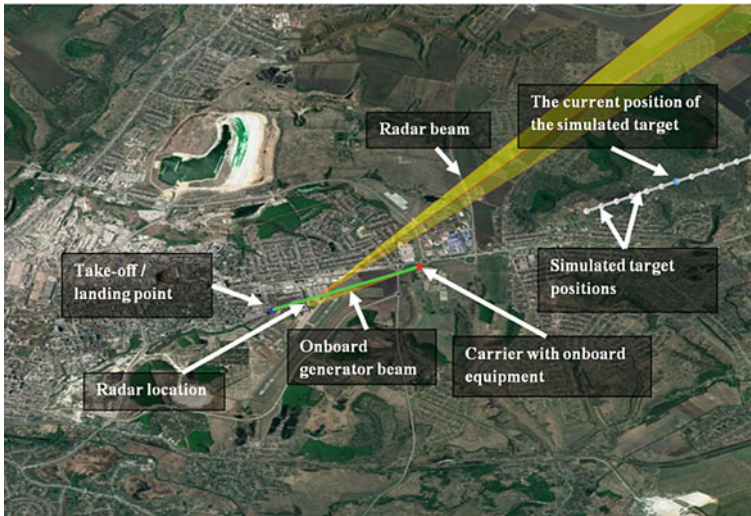


Fig. 4 Measurement planning

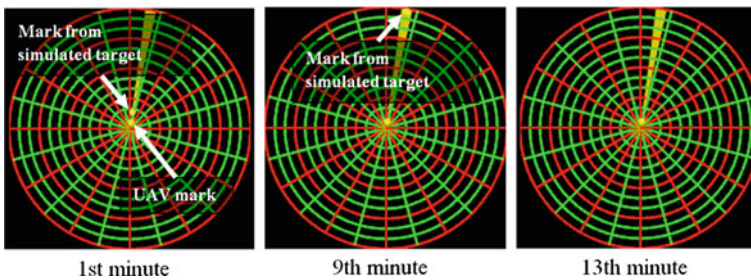


Fig. 5 Image of the radar indicator at the 1st, 9th, 24th minute

## 6 Conclusion

The chapter considers the issue of planning tests for the detection range for a cyber-physical system, namely, a ground-based all-round looking radar, using a carrier and onboard equipment. A system of equations has been obtained for planning tests to determine the range of detected targets, which takes into account: the error in controlling the range of simulated targets; range control error by the carrier; removal of the carrier from the radar; pause error of the signal generated by the on-board generator; the time spent on the flight; time spent on the measuring trajectory; antenna rotation period; the value of the discrete in range for the target situation generator; the number of turns of the radar antenna; the number of positions of the simulated target. To automate calculations and build a measurement plan, a C++ program was developed, with a flyby visualization tied to a real satellite map of the area.

Performance assessments are performed on the fly at the station deployment point without engaging real-world targets, potentially reducing test costs compared to real-world technology. Other characteristics of the radar can be investigated in a similar manner. For example, the accuracy of determining the coordinates and the resolution of detected targets, changing the trajectory of the carrier and the structure of the test signal. Testing of automobile radars is carried out in a similar way when debugging autopilot algorithms based on sensor readings [6]. The proposed method can be used to test the operation of other cyber-physical systems, for example, air traffic control radars, by setting the trajectory of simulated targets corresponding to the trajectory of one or more aircraft. And based on the result of processing the test signals, calculate the value of the tested characteristic.

## References

1. Fahmy, H.M.A.: Testbeds for WSNs. In: *Wireless Sensor Networks. Signals and Communication Technology*. Springer, Singapore (2016). [https://doi.org/10.1007/978-981-10-0412-4\\_5](https://doi.org/10.1007/978-981-10-0412-4_5)
2. Zemany, P., Gaughan, M.: Challenge problem testbed. In: Lesser, V., Ortiz, C.L., Tambe, M. (eds) *Distributed Sensor Networks. Multiagent Systems, Artificial Societies, and Simulated Organizations (International Book Series)*, vol. 9. Springer, Boston, MA (2003). [https://doi.org/10.1007/978-1-4615-0363-7\\_3](https://doi.org/10.1007/978-1-4615-0363-7_3)
3. Ergezer, H., Furkan Keskin, M., Gunay, O.: Real-time radar, target, and environment simulator. In: Obaidat, M., Ören, T., Kacprzyk, J., Filipe, J. (eds.) *Simulation and Modeling Methodologies, Technologies and Applications. Advances in Intelligent Systems and Computing*, vol 402. Springer, Cham (2015). [https://doi.org/10.1007/978-3-319-26470-7\\_11](https://doi.org/10.1007/978-3-319-26470-7_11)
4. Cosenza, C., Morante, Q., Corvo, S., Gottifredi, F.: GNSS bit-true signal simulator. A test bed for receivers and applications. In: Re, E.D., Ruggieri, M. (eds.) *Satellite Communications and Navigation Systems. Signals and Communication Technology*. Springer, Boston, MA (2008). [https://doi.org/10.1007/978-0-387-47524-0\\_34](https://doi.org/10.1007/978-0-387-47524-0_34)
5. Chan, C.C., Kurnia, F.G., Al-Hourmani, A., et al.: Open-Source and Low-Cost Test Bed for Automated 5G Channel Measurement in mmWave Band. *J. Infrared Milli. Terahz. Waves* **40**, 535–556 (2019). <https://doi.org/10.1007/s10762-019-00587-z>
6. Gadringer, M.E., Schreiber, H., Gruber, A., et al.: Virtual reality for automotive radars. *Elektrotech. Inftech.* **135**, 335–343 (2018). <https://doi.org/10.1007/s00502-018-0620-9>
7. Anritsu Company, Application Note, Radar Testing with Simulation Signals, Literature Number 11410–00752 (2013)
8. Keysight Technologies E6950 eCall/ERA-GLONASS Conformance Test Solution, Literature Number 5992–1823EN (2017)
9. Payment, T.: A low power, ultra-wideband radar testbed. In: *Ultra-Wideband, Short-Pulse Electromagnetics* vol. 5. Springer, Boston, MA (2002). [https://doi.org/10.1007/0-306-47948-6\\_28](https://doi.org/10.1007/0-306-47948-6_28)
10. Vorderderfler, M., Gadringer, M.E., Schreiber, H., et al.: Frequency dividers in radar target stimulator applications. *Elektrotech. Inftech.* **135**, 344–351 (2018). <https://doi.org/10.1007/s00502-018-0626-3>
11. Jarrar, A., Balouki, Y.: Formal modeling of a complex adaptive air traffic control system. *Complex Adapt. Syst. Model* **6**, 6 (2018). <https://doi.org/10.1186/s40294-018-0056-4>
12. Murthy, S., Murthy, M., Kumar, P.: Estimation of radar alignment parameters in multi sensor data fusion systems using MLE technique. In: Sobh, T., Elleithy, K., Mahmood, A., Karim, M.A.

- (eds.) *Novel Algorithms and Techniques In Telecommunications, Automation and Industrial Electronics*. Springer, Dordrecht (2008). [https://doi.org/10.1007/978-1-4020-8737-0\\_85](https://doi.org/10.1007/978-1-4020-8737-0_85)
13. Merkulov, V.I., Sadovskii, P.A.: Estimation of the range and its derivatives in an active two-position radar system. *J. Commun. Technol. Electron.* **63**, 346–353 (2018). <https://doi.org/10.1134/S1064226918040083>
  14. Costanzo, S., Spadafora, F., Borgia, A., Moreno, O.H., Costanzo, A., Di Massa, G.: High resolution software defined radar system for target detection. In: Rocha, Á., Correia, A., Wilson, T., Stroetmann, K. (eds.) *Advances in Information Systems and Technologies. Advances in Intelligent Systems and Computing*, vol. 206. Springer, Berlin, Heidelberg (2013). [https://doi.org/10.1007/978-3-642-36981-0\\_94](https://doi.org/10.1007/978-3-642-36981-0_94)
  15. Agilent Technologies, Application Note 1303, Radar Measurements, Literature Number 5989–7575EN (2009)
  16. Skolnik, M.I.: *Introduction to Radar Systems*, 2nd edn. McGraw-Hill, New York, NY (1980)
  17. Botov, M.I., Vyakhirev, V.A.: *Osnovy teorii radiolokatsionnykh sistem i kompleksov*. Krasnoyarsk, SFU, 530 s (2013)
  18. Richard, G.L.: *Understanding Digital Signal Processing*, 3rd edn. Pearson (2011)
  19. Tret'yak, L.N.: *Obrabotka rezul'tatov nablyudenii*. Orenburg, GOU OGU, 171 s (2004)
  20. Denisenko, V.V.: *Komp'yuternoe upravlenie tekhnologicheskim protsessom, ehksperimentom, oborudovaniem*. Moskva, Telekom, 608 s (2009)

# Algorithm for Determining Distributed Subsurface Layers Based on Ultra-Wideband GPR



S. L. Chernyshev, M. V. Rodin, and I. B. Vlasov

**Abstract** The ultra-wideband GPR signal penetrates the subsurface environment and is reflected from its different layers. The reflected signal carries information about the structure of the distributed subsurface medium. However, the shape of this signal depends on all layers, since information about them is mixed in this signal. Therefore, an algorithm has been developed that ensures the processing of this information. The algorithm makes it possible to determine the composition of a distributed multilayer medium based on the reflected ultrawideband signal received by the GPR. The algorithm uses the temporal realization of the signal and takes into account its values with a clock period equal to the duration of the probing ultra-wideband signal. These time values of the signal depend on many coefficients of reflection from the joints of different layers. Reflection coefficients depend on the characteristics of the layers. The algorithm allows the extraction of information about individual reflection coefficients from the values of the reflected ultra-wideband signal. In the developed algorithm, according to the found reflection coefficients from the connection of layers, their characteristics are determined: dielectric constants, specific attenuation, and the thickness of these layers are determined by time delays. An example of determining the characteristics of layers and their identification by the reflected signal from a multilayer distributed medium containing ice, water, and clay is considered.

**Keywords** GPR · Ultrawideband reflected signal · Layered medium · Reflection coefficient · Dielectric constant · Algorithm

---

S. L. Chernyshev (✉) · M. V. Rodin · I. B. Vlasov  
Bauman Moscow State Technical University, 5, 2-nd Baumanskaya str., Moscow, Russia  
e-mail: [chernshv@bmstu.ru](mailto:chernshv@bmstu.ru)

M. V. Rodin  
e-mail: [mvrodin@bmstu.ru](mailto:mvrodin@bmstu.ru)

I. B. Vlasov  
e-mail: [vlasovbmstu@mail.ru](mailto:vlasovbmstu@mail.ru)

## 1 Introduction

GPR is used to study subsurface objects in solving archaeological problems, searching for mines, cables, and other objects, layers of ice, water, etc. [1–19]. Such subsurface sensing uses ultra-wideband signals. In the case of a complex structure of an inhomogeneous soil, the UWB signal reflected from it has a shape that significantly differs from the shape of the emitted signal and depends on the above-mentioned structure. The main task is to obtain information about the composition of soil or ice from the reflected signal. However, this task is very difficult, since the reflected signal is formed not by a superposition of reflected signals from different layers, but also by a multitude of mutual reflections. Spectral research methods are of little use in this case, and it is necessary to study the temporal realization of the signal. This chapter is devoted to the algorithm for processing such information.

## 2 Reflected Wave Model

An inhomogeneous medium consists of layers with different dielectric constants. In reality, power is absorbed in these layers, as a result of which electromagnetic waves are attenuated in them. Table 1 shows the examples of characteristics of some media.

The characteristics of other media can be found in the respective reference books.

Consider a certain environment consisting of several different layers (Fig. 1).

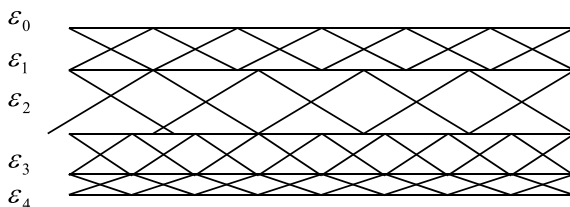
We will assume that it is possible to neglect the dispersion of the electromagnetic wave when propagating through the layers. When the wave falls perpendicular to the surface the reflection coefficient from the junction of  $i-1$ -th and  $i$ -th layers is determined as

$$S_i = (\sqrt{\varepsilon_{i-1}} - \sqrt{\varepsilon_i}) / (\sqrt{\varepsilon_{i-1}} + \sqrt{\varepsilon_i})$$

**Table 1** Examples of characteristics

Medium	Relative dielectric constant, $\varepsilon$	Specific attenuation, q dB/m	Wave propagation speed, V m/c $\times 10^{-8}$
Air	1	0	3
Wet sand	20–30	0,5–5	0,55–0,67
Dry sand	4–6	0,01–1,5	1,22–1,5
Wet clay	19–27	25–110	0,58–0,69
Dry clay	2–7	3–14	1,13–2,12
Dry concrete	3–7	1–7	0,9–1,13
Dry asphalt	3–6	2–15	1,22–1,73
Unleavened ice	4	0,1–3,5	1,5
Fresh water	81	0,10	0,33

**Fig. 1** Layered medium



If we imagine that an ideal single pulse of infinitely short duration falls on such a medium perpendicular to its surface, the signal reflected from it will be a sequence of pulses of different amplitudes:

$$b_{refl}(k) = S_1; S_2(1 - S_1^2)r_1^2; S_3(1 - S_1^2)(1 - S_2^2)r_1^2r_2^2 - (1 - S_1^2)S_1S_2r_1^4; \dots,$$

where  $r_i = 10^{-q_i l_i / 20}$ ,  $q_i$ —specific attenuation in the  $i$ -th layer,  $l_i$ —layer thickness.

As can be seen, the components of the reflected signal generally depend on the properties of many layers, and with an increase in the delay time, this dependence increases, since the number of terms in these components is equal to  $2^{n-1}$ .

When using a real UWB sounding signal, the signal reflected from the medium will have an even more complex composition:

$$u_{refl}(t) = S_1u(0); S_1u(2\tau) + (1 - S_1^2)S_2r_1^2u(0); S_1u(4\tau) + (1 - S_1^2)S_2r_1^2u(2\tau) + (1 - S_1^2)(1 - S_2^2)r_1^2r_2^2u(0) - (1 - S_1^2)S_1S_2r_1^4u(0); \dots,$$

where  $u(0); u(0), u(2\tau), u(4\tau), \dots$ —samples sounding signal through a double sampling period  $2\tau$ .

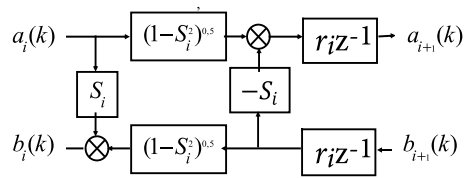
At first glance, these expressions can be used to determine the properties of different layers, since from the first sample it is possible to find  $S_1$ . After that, the characteristics of the first layer are determined. Then from the second sample, we find  $S_2$ , and so on. However, the expression for further samples is becoming more complex, and to find analytical expressions for the more distant in time samples of the reflected signal is not possible.

Earlier, a mathematical model of an irregular system was found through which an electromagnetic wave propagates [20]. This model assumed that such a system is nondissipative. This model is inapplicable for propagation through a lossy medium, so it needs to be modified.

Figure 2 shows a block scheme describing the formation of reflected  $b_i(k), b_{i+1}(k)$  and transmitted waves  $a_i(k), a_{i+1}(k)$  in one  $i$ -th layer.

In this scheme,  $z$  is the parameter of the  $Z$ -transform. Element  $z^{-1}$  is a link delaying the signal by one time period. Using this scheme, you can write the following equations linking the  $Z$ -images of the incident and reflected waves:

**Fig. 2** Block scheme of  $i$ -th layer



$$b_i(z) = a_i(z)S_i + b_{i+1}(z)r_i z^{-1} \sqrt{1 - S_i^2}$$

$$a_{i+1}(z) = \left[ a_i(z) \sqrt{1 - S_i^2} - S_i b_{i+1}(z) r_i z^{-1} \right] r_i z^{-1}$$

These equations can be transformed to the following form:

$$b_i(z) = a_i(z)s_i + b_{i+1}(z) \sqrt{1 - s_i^2} r_i z^{-1}$$

$$a_{i+1}(z) = r_i z^{-1} [a_i(z) - b_i(z)s_i] / \left[ \sqrt{1 - s_i^2} \right]$$

Let's apply the inverse Z-transform to the left and right sides of these equations:

$$b_i(k) = a_i(k)s_i + r_i b_{i+1}(k-1) \sqrt{1 - s_i^2} \quad (1)$$

$$a_{i+1}(k) = [a_i(k-1)r_i - r_i b_i(k-1)s_i] / \sqrt{1 - s_i^2} \quad (2)$$

These equations formed the basis of the algorithm for determining the layers of the subsurface medium.

### 3 Description of the Algorithm

The algorithm assumes the following sequence of actions.

So, the dielectric constant of the first layer can be determined immediately:

$$S_1 = \frac{b_1(0)}{a_1(0)}, \varepsilon_1 = \varepsilon_0 \left[ \frac{a_1(0) - b_1(0)}{a_1(0) + b_1(0)} \right]^2 = \varepsilon_0 \left[ \frac{u(0) - u_{omp}(0)}{u(0) + u_{omp}(0)} \right]^2.$$

By the dielectric constant, we identify the medium of the first layer and determine its specific attenuation and wave propagation speed. Then from Eq. (2) we find

$$a_2(1) = [a_1(0)r_1 - S_1b_1(0)r_1] / \sqrt{(1 - S_1^2)}$$

and from Eq. (1) we obtain

$$b_2(1) = [b_1(2) - S_1a_1(2)] / (r_1\sqrt{(1 - S_1^2)})$$

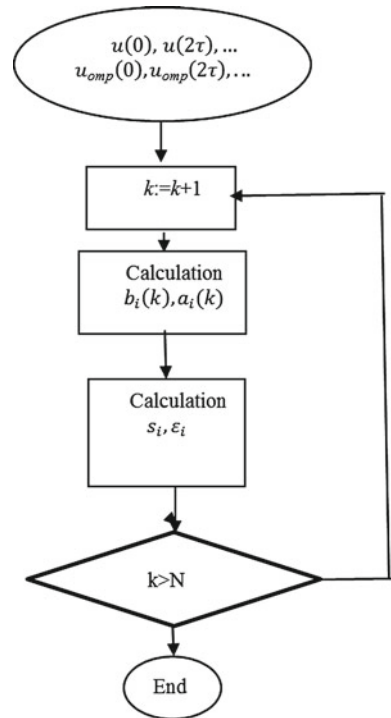
where  $b_1(2) = u_{OTP}(2\tau)$ ,  $a_1(2) = u(2\tau)$ .

The dielectric constant of the next layer is defined as

$$\varepsilon_2 = \varepsilon_1 \left[ \frac{a_2(1) - b_2(1)}{a_2(1) + b_2(1)} \right]^2$$

The dielectric constants and other characteristics of other layers are determined in the same way. And, thus, the problem of determining the structure of an inhomogeneous medium is solved. Figure 3 shows a simplified block scheme of the described algorithm.

**Fig. 3** The simplified scheme of the algorithm





The algorithm carries out  $N$  cycles of calculations, during which the characteristics of the layers are determined. The geometric length of the probing ultra-wideband pulse is less than the depth of the layers, and therefore the time delay of signals reflected from different layers is a multiple of this length. With the sequential determination of the characteristics of the layers, it is possible to determine the depth of each layer by this delay, taking into account the speed of wave propagation in the corresponding medium.

#### 4 Example of Defining Layers

Figure 4 shows an example of an ultra-wideband signal  $u_{refl}(t)$  reflected from layered medium. UWB sounding signal with duration  $\tau = 1$  ns and an amplitude of 50 mV was vertically applied to the layered medium. The external environment is air ( $\varepsilon_0 = 1$ ).

This signal has significant spikes at times 0 ns, 6 ns, 12 ns, and 18 ns. Using the program based on the developed algorithm, we found the coefficients of reflection from the joints of the layers:  $-0.333$ ;  $-0.636$ ;  $0.286$ .

The dielectric constant of the first layer is found from the expression:

$$\varepsilon_1 = \varepsilon_0 \left[ \frac{1 + 0.333}{1 - 0.333} \right]^2 = 4$$

This layer is identified as 0.45 m thick fresh ice.

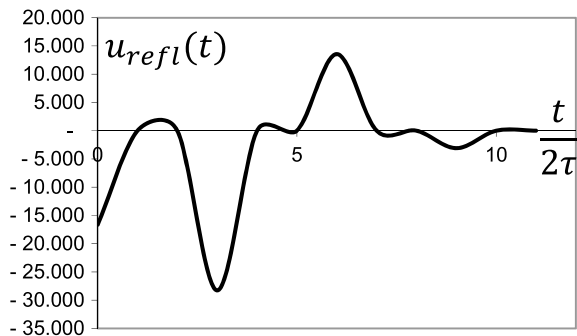
The dielectric constant of the second layer is found from the expression:

$$\varepsilon_2 = \varepsilon_1 \left[ \frac{1 + 0.636}{1 - 0.636} \right]^2 = 80,9$$

This layer is identified as 0.1 m thick freshwater.

The dielectric constant of the third layer is found from the expression:

**Fig. 4** The signal reflected from layered medium



$$\varepsilon_3 = \varepsilon_2 \left[ \frac{1 - 0.286}{1 + 0.286} \right]^2 = 24.3$$

This layer is identified as wet clay.

Thus, all layers were identified by the reflected UWB signal.

## 5 Conclusion

The developed algorithm makes it possible to determine the composition of the distributed layered medium based on the reflected ultra-wideband signal received by the GPR. The algorithm uses the temporal realization of the signal and takes into account its samples with a sampling period equal to the duration of the probing signal.

According to the found reflection coefficients from the joints of the layers, the characteristics of these layers are determined: dielectric constant, specific attenuation and the thickness of these layers is found from the time delays.

## References

1. Grinev, A.Y.: Subsurface radar issues. Collective monograph. Radiotekhnika, 416 (2005)
2. Vladov, M.L., Starovoitov, A.V.: Introduction to GPR, p. 153. Moscow, Moscow State University Publishing House (2004)
3. Grinev, A.Y., et al.: Diagnostics of mediums and line objects, probing with ultra-wideband short-pulse signals. In: Proceedings of the Progress in Electromagnetics Research Symposium, p. 294–299. Moscow, Russia (2009)
4. Lambot, S., Slob, E.C., Bosch, I.: Modeling of GPR for accurate characterization of subsurface electric properties. In: IEEE Transactions on Geoscience and Remote Sensing, vol. 42, No. 11, pp. 2555–2567 (2004)
5. Benedetto, A., Pajewski, L.: Civil Engineering Applications of Ground Penetrating Radar, p. 371. Springer, Switzerland (2015)
6. Daniels, D.J.: Ground Penetrating Radar, p. 419. London (2004)
7. Ground-penetrating radar for archaeology, 3rd edn. In: Conyers, L.B., Kvamme, K.L. (eds.) Geophysical Methods for Archaeology No. 4. AltaMira Press, Lanham, MD 241 (2013)
8. Persico, R.: Introduction to Ground Penetrating Radar: Inverse Scattering and Data Processing, p. 392. Wiley & Sons (2014)
9. Jol, H.M.: Ground Penetrating Radar Theory and Applications, p. 544. Elsevier (2008)
10. Davis, J.L., Annan, A.P.: Ground-penetrating radar for high-resolution mapping of soil and rock stratigraphy. *Geophys. Prospect.* **37**, 531–551 (1989)
11. Jol, H.M., Young, R., Fisher, T.G., Smith, D.G., Meyers, R.A.: Ground penetrating radar of eskers, kame terraces, and moraines: Alberta and Saskatchewan, Canada. In: 1996, 6th International Conference on Ground Penetrating Radar (GPR'96), p. 439–443. Sendai, Japan (1996)
12. Arcone, S.A., Lawson, D.E., Delaney, A.J., Strasser, J.C., Strasser, J.D.: Ground-penetrating radar reflection profiling of groundwater and bedrock in an area of discontinuous permafrost. *Geophysics* **63**(5), 1573–1585 (1998)

13. Cornick, M., Koechling, J., Stanley, B. and Zhang, B.: Localizing ground penetrating RADAR: A step toward robust autonomous ground vehicle localization. *J. Field Robot.* **33**(1), 82–102 (2016)
14. Ivashov, S.I., Razevig, V.V., Vasiliev, I.A., Zhuravlev, A.V., Bechtel, T.D., Capineri, L.: Holographic subsurface radar of RASCAN type: development and application (PDF). *IEEE J. Sel. Top. Appl. Earth Obs. Remote Sens.* **4**(4), 763–778 (2011)
15. Lowe, K.M., Wallis, L.A., Pardoe, C., Marwick, B., Clarkson, C., Manne, T., Smith, M.A. and Fullagar, R.: Ground-penetrating radar and burial practices in western Arnhem Land, Australia. *Archaeol. Ocean.* **49** (3), 148–157 (2014)
16. Grinev, A.Y., Bagno, D.V., Zaikin, A.E., Nikishov, D.V., Andriianov, A.V.: Multi-channel ground penetrating radar based on ultra-wideband short-pulse signal: hardware and software. In: 13th International Conference on Ground Penetrating Radar, GPR 2010, p. 1–6. Lecce (2010)
17. Grinev, A.Y., Gigolo, A.I., Andrianov, A.V.: Subsurface imaging using spectral methods. In: 12th International Conference Microwave and Telecommunication Technology, Conference Proceedings, vol. 12, pp. 581–582 (2002)
18. Grinev, A.Y., Chebakov, I.A., Gigolo, A.I.: Solution of the inverse problems of subsurface radiolocation. In: 4th International Conference on Antenna Theory and Techniques, ICATT 2003, vol. 4, pp. 523–526 (2003)
19. Ékes, C.; Neduczka, B.; Takacs, P.: Proceedings of the 15th International Conference on Ground Penetrating Radar, pp. 368–371 (2014)
20. Chernyshev, S.L.: Analysis and synthesis of UWB filters and shapers in time domain. In: 2013 IEEE International Conference on Microwave Technology & Computational Electromagnetics. Proceedings, No. 6812452, pp. 127–130. Qingdao, China (2013)

# Formant Frequencies Estimation Based on Correlogram Method of Spectral Analysis and Binary-Sign Stochastic Quantization



Vladimir Yakimov , Petr Lange , and Ekaterina Yaroslavkina 

**Abstract** The chapter considers the problem of calculating digital estimates of the formant frequencies of complex signals. This problem is solved using stochastic digital processing for continuous signals. A mathematical model is used to represent the result of binary-sign stochastic quantization in time. The conceptual basis of this model is the concept of a sign function and the theory of discrete-event modeling. In this case, events are understood as a sequential change in the values of the result for this quantization type. Estimates of the lower and upper boundaries of the formant frequencies and estimates of the spectral peak widths are calculated based on the Taylor series expansion of the power spectral density function (PSD). Mathematical equations for calculating the estimates of PSD and its second-order derivative are developed based on the correlogram method. The discrete-event model of binary-sign stochastic quantization made it possible to analytically calculate continuous integration operators when switching to signal processing in discrete form. The main operations of these equations are the arithmetic operations of addition and subtraction, as well as the operations of the logical processing of the calculated PSD estimates. At the same time, the total number of multiplication operations has been reduced. The practical implementation of the obtained equations provides a decrease in the multiplicative complexity of computational algorithms and an increase in the computational efficiency of estimating formant frequencies.

**Keywords** Formant · Power spectral density · Spectral peak · Bandwidth · Binary stochastic quantization · Timing

## 1 Introduction

One of the most important applications of spectral analysis is the localization and study of resonant frequency components in complex signals. Resonant frequencies are called formants. Formants are spectral peaks (maxima of the frequency spectrum

---

V. Yakimov (✉) · P. Lange · E. Yaroslavkina  
Samara State Technical University, 244, Molodogvardeiskaya Street, Samara 443100, Russia

envelope) of a certain width. The number of formants and their position in the spectrum is determined by the physical nature of the signal under study. Formants can be thought of as the distinctive frequency components of a signal. Formant analysis is used as a passive technique that can provide information about the current state of the emitting signal source. Formants are characterized by their frequency and spectral width. By this, the task of spectral analysis is reduced to determining the formant frequencies and identifying the corresponding frequency bands in the spectrum.

There are various approaches to localizing formant frequencies. Formant frequencies can be estimated directly from the frequency spectrum of the observed signal realization. In general, classical methods of spectral analysis developed based on the direct Fourier transform can be used to estimate the frequency spectrum itself. An approach based on the control of frequency bands of the spectrum with a pronounced formant characteristic is used. In this case, sections of frequency bands are identified according to certain rules, taking into account the typical behavior of the source emitting a signal. Within each such frequency band, the spectrum is calculated and pronounced maxima are selected. Formant frequencies are determined based on the analysis of these maxima. A method based on linear prediction signal coding is also used. By this method, the current samples of the signal can be approximated by a linear combination of the previous samples. This approximation leads to a linear system of equations. As a result of solving this system, the prediction parameters are obtained. The resulting solution is used to construct a spectral envelope, which is used to identify the formant frequencies. Here, the main task is to determine the prediction parameters that minimize the variance of the approximation error of signal segments [1–5].

Currently, signal processing is mainly carried out in a digital form. There are two main reasons for this. First, digital engineering allows you to create high-tech measurement systems. The practical implementation of such systems can be performed both in the form of specialized measuring devices and based on universal computing systems using protected metrologically significant software that performs the functions of collecting, transmitting, processing, and presenting measurement information. Second, the digital spectral analysis provides reproducibility, repeatability, and computational accuracy when processing discrete signal values. The need to fulfill these conditions is an important requirement for solving complex measurement problems, which include the problem of monitoring the position in the spectrum of formant frequencies. However, as a rule, the representation of a continuous signal in digital form occurs using the classical analog-to-digital conversion [6, 7]. In this case, uniform sampling in time and multi-level quantization of the analyzed signal is performed. This leads to the fact that when digitally processing multi-bit discrete samples of a signal, algorithms for obtaining estimates of the frequency spectrum require a significant amount of computational operations. At the same time, one of the mass operations in such algorithms is the operation of digital multiplication, which is the most computationally time-consuming. It is depending on the number of multiplication operations that must be performed that determine the computational complexity of the digital algorithm and call it the multiplicative complexity [8–11].

Thus, of particular interest is the development of digital algorithms for analyzing the location of formants in the spectrum and determining their frequency boundaries, which provide a reduction in computational costs when processing complex multicomponent signals.

## 2 Formant Estimation Method

In signal processing, in most cases, there is statistical measurement uncertainty. This is due to the influence of random factors that have a distorting effect on the measurement result. Signals can also be exposed to external noise, which can lead to a significant reduction in the signal-to-noise ratio. The consequence of this may be the loss of informative frequency components when determining the spectral composition of the signal. Therefore, the frequency analysis of such signals will be associated with the estimation of the power spectral density (PSD). It characterizes the distribution of the average signal power, which falls on a unit frequency interval [12].

By definition, PSD is a continuous function of frequency. Based on this, we represent the PSD in the vicinity of the formant frequency  $F_m$  in the form of a Taylor power series and restrict ourselves to its first three terms. In this case, we will take into account that the values of the first derivative at the extremum points of the PSD will be equal to zero. Accordingly, we will have:

$$S_{XX}(f) = S_{XX}(F_m) + \frac{1}{2}S''_{XX}(F_m)(f - F_m)^2, \quad (1)$$

where  $m = 1, 2, 3, \dots, M$ .

Equation (1) is a complete quadratic equation for frequency. Let us bring this equation to the canonical form:

$$S_{XX}(F_m)f^2 - 2F_m S_{XX}(F_m)f + S_{XX}(F_m)F_m^2 + 2S_{XX}(F_m) - 2S_{XX}(f) = 0. \quad (2)$$

For the sake of certainty, we write (2) in the general form:

$$af^2 + bf + c = 0,$$

$$a = S''_{XX}(F_m),$$

$$b = -2F_m S''_{XX}(F_m),$$

$$c = S''_{XX}(F_m)F_m^2 + 2S_{XX}(F_m) - 2S_{XX}(f).$$

As a result of finding the roots of Eq. (2), we obtain mathematical equations for calculating estimates of the lower and upper boundaries of the formant frequencies in the signal spectrum:

$$f_{Lo,m} = F_m - \sqrt{2 \frac{S_{XX}(f_{Lo,m}) - S_{XX}(F_m)}{S''_{XX}(F_m)}}, \quad (3)$$

$$f_{Hi,m} = F_m + \sqrt{2 \frac{S_{XX}(f_{Hi,m}) - S_{XX}(F_m)}{S''_{XX}(F_m)}}. \quad (4)$$

Equations (3) and (4) allow us to calculate the estimates  $f_{Lo,m}$  and  $f_{Hi,m}$  for the given values  $S_{XX}(f_{Lo,m})$  and  $(f_{Hi,m})$ , assuming that the values  $S_{XX}(F_m)$  and  $S''_{XX}(F_m)$  are known. In the limiting case, we assume that  $S_{XX}(f_{Lo,m}) = S_{XX}(f_{Hi,m}) = 0$ . Then, taking into account the fact that, according to the definition, the second derivative of the function at the maximum point will have a negative value, i.e.  $S''_{XX}(F_m) < 0$ , we get:

$$f_{Lo,m} = F_m - \sqrt{2 \frac{S_{XX}(F_m)}{|S''_{XX}(F_m)|}}, \quad (5)$$

$$f_{Hi,m} = F_m + \sqrt{2 \frac{S_{XX}(F_m)}{|S''_{XX}(F_m)|}}. \quad (6)$$

The bandwidth estimate for the formant frequencies will be:

$$\Delta f_m = f_{Hi,m} - f_{Lo,m} = 2 \sqrt{2 \frac{S_{XX}(F_m)}{|S''_{XX}(F_m)|}}. \quad (7)$$

From Eqs. (5)–(7) it follows that the task of developing algorithms for estimating the band of formant frequencies and determining their lower and upper boundaries has been reduced to the development of an algorithm for estimating the PSD and its second derivative.

### 3 PSD Estimation Algorithm

The approach based on the use of binary-sign stochastic quantization as the primary transformation of signals into a digital code allows the development of computationally efficient digital algorithms [13–17]. The basis of such quantization is the randomization of the procedure for representing the signal in digital form. It was shown in [14] that deliberate addition of independent uniformly distributed noise and

signal sampling are statistically equivalent. The result of the binary-sign stochastic quantization has the form:

$$z(t) = +1, \text{ если } \overset{o}{x}(t) \geq \xi(t); z(t) = -1, \text{ если } \overset{o}{x}(t) < \xi(t). \quad (8)$$

In Eq. (8),  $\overset{o}{x}(t)$  is the central implementation of the analyzed signal;  $\xi(t)$  is the auxiliary randomizing signal.

The auxiliary signal  $\xi(t)$  has a uniform distribution in the range from  $-\xi_{\max}$  to  $+\xi_{\max}$ , where  $\xi_{\max} \geq |\overset{o}{x}(t)|_{\max}$ .

Let the signal analysis time be equal to  $T$ . The PSD estimate within this time interval will be calculated based on the correlogram method [18]:

$$\hat{S}_{XX}(f) = 2 \int_0^T \hat{R}_{XX}(\tau) \cos 2\pi f \tau d\tau, \quad (9)$$

where  $\hat{R}_{XX}(\tau)$  is the estimate of the correlation function of the analyzed signal.

As  $\hat{R}_{XX}(\tau)$ , we take the following estimate [24, 25]:

$$\hat{R}_{XX}(\tau) = \frac{\xi_{\max}^2}{T} \int_{\tau}^T z_1(t) z_2(t - \tau) dt, \quad (10)$$

In Eq. (10),  $z_1(t)$  and  $z_2(t)$  represent the results of two independent binary-sign stochastic quantization procedures. According to [19, 20], they should be obtained using two homogeneous and statistically independent auxiliary signals  $\xi_1(t)$  and  $\xi_2(t)$ . Each of these signals should have a uniform distribution ranging from  $-\xi_{\max}$  to  $+\xi_{\max}$ .

The estimate of PSD (9), taking into account the Eq. (10), will take the form:

$$\hat{S}_{XX}(f) = 2 \frac{\xi_{\max}^2}{T} \int_0^T z_1(t) \int_0^t z_2(\tau) \cos 2\pi f(t - \tau) d\tau dt. \quad (11)$$

It follows from (8) that the result of binary-sign stochastic quantization takes only two values: “-1” and “+1”. The change of these values occurs sequentially at discrete points in time. Based on the discrete-event modeling theory, we can say that they are those points in time at which significant events occur in the process of performing this quantization type [21]. With this in mind, a discrete-event mathematical model for binary-sign stochastic quantization was developed. According to this model, for  $z_1(t)$  and  $z_2(t)$ , it is sufficient to know only the values at the initial



time of quantization  $t_0$  and the time counts at which the current values change. By this, we will have  $z_1(t_0)$ ,  $z_2(t_0)$  and two sets of time count:

$$\left\{ t_i^{Z_1} : 1 \leq i \leq I-1 \right\} \text{ и } \left\{ t_j^{Z_2} : 1 \leq j \leq J-1 \right\}. \quad (12)$$

Note that  $t_0^{Z_1} = t_0^{Z_2} = t_0 = 0$  and  $t_I^{Z_1} = t_J^{Z_2} = T$ .

Within the time intervals  $t \in [t_i^{Z_1}; t_{i+1}^{Z_1}]$  and  $t \in [t_j^{Z_2}; t_{j+1}^{Z_2}]$ , the values of the binary-sign quantization results  $z_1(t)$  and  $z_2(t)$  are equal to “−1” or “+1” and remain constant. As a consequence, the integrals in (11) can be represented as a sum of integrals, for which the limits of integration will be determined by the time counts  $[t_i^{Z_1}; t_{i+1}^{Z_1}]$  and  $[t_j^{Z_2}; t_{j+1}^{Z_2}]$ . These integrals are definite and calculated analytically. Taking this into account, mathematical equations were obtained for calculating the PSD estimate by the correlogram method [22, 23]. Adapted to the solution of the problem, the modified version of these equations has the form:

$$\hat{S}_{XX}(f) = \frac{\xi_{\max}^2}{2T(\pi f)^2} z(t_0) \sum_{i=1}^I (-1)^i \lambda_i \sum_{j=0}^{r(i)+1} (-1)^j v_j \cos 2\pi f \Delta t_{j,i}^{Z_i}, \quad (13)$$

$$\lambda_i = \begin{cases} 1, & i = I; \\ 2, & k = 1, 2, \dots, I-1. \end{cases}$$

$$v_j = \begin{cases} 1, & j = 0, j = r(1) + 1; \\ 2, & j = 1, 2, \dots, r(i). \end{cases}$$

$$z(t_0) = z_1(t_0)z_2(t_0), \quad \Delta t_{j,i}^Z = t_i^{Z_1} - t_j^{Z_2}, \quad t_{r(i)+1}^{Z_2} = t_i^{Z_1}.$$

It should be noted that the analytical calculation of the integrals in Eq. (11) eliminates the error inherent in digital algorithms when the integration operations are calculated numerically.

Equation (13) defines in the mathematical form an algorithm for performing operations for calculating  $\hat{S}_{XX}(f)$  estimates in a discrete form.

According to Eqs. (5)–(7), to calculate  $f_{Lo,m}$ ,  $f_{Hi,m}$  and  $\Delta f_m = f_{Hi,m} - f_{Lo,m}$ , it is necessary to have an estimate for the second-order derivative  $\hat{S}_{XX}''(f)$ . It follows from Eq. (13) that the mathematical equation for calculating this estimate can be obtained analytically. Operating simple double differentiation of the PSD estimate determined by Eq. (13), we obtain:

$$\hat{S}_{XX}''(f) = -\frac{2\xi_{\max}^2}{Tf^2} z(t_0) \sum_{i=1}^I (-1)^i \lambda_i \sum_{j=0}^{r(i)+1} (-1)^j v_j (\Delta t_{j,i}^Z)^2 \cos 2\pi f \Delta t_{j,i}^Z. \quad (14)$$

We will calculate the estimates (13) and (14) at discrete frequencies  $f_k = k\Delta f$  with a frequency resolution  $\Delta f = 1/T$ . Then these estimates will be equal:

$$\hat{S}_{XX}(f_k) = \frac{\xi_{\max}^2}{2\pi^2 k^2 \Delta f} z(t_0) \sum_{i=1}^I (-1)^i \lambda_i \sum_{j=0}^{r(i)+1} (-1)^j v_j \cos 2\pi k \Delta f \Delta t_{j,i}^Z, \quad (15)$$

$$\hat{S}_{XX}''(f_k) = -\frac{2\xi_{\max}^2}{k^2 \Delta f} z(t_0) \sum_{i=1}^I (-1)^i \lambda_i \sum_{j=0}^{r(i)+1} (-1)^j v_j (\Delta t_{j,i}^Z)^2 \cos 2\pi k \Delta f \Delta t_{j,i}^Z. \quad (16)$$

The resulting equations for calculating estimates  $\hat{S}_{XX}(f_k)$  and  $\hat{S}_{XX}''(f_k)$  are identical in their structural organization. This ensures the uniformity of the metrological characteristics of the procedures for calculating these estimates.

Equations (15) and (16) can be written in a generalized form:

$$\hat{A}(f_k) = \frac{b}{k^2} \sum_{i=1}^I (-1)^i \lambda_i \sum_{j=0}^{r(i)+1} (-1)^j v_j D_{j,i}. \quad (17)$$

For  $\hat{S}_{XX}(f_k)$  we will have:

$$b = z(t_0) \frac{\xi_{\max}^2}{2\pi^2 \Delta f}, \quad D_{j,i} = \cos 2\pi k \Delta f \Delta t_{j,i}^Z.$$

For  $\hat{S}_{XX}''(f_k)$  we will have:

$$b = -z(t_0) \frac{2\xi_{\max}^2}{\Delta f}, \quad D_{j,i} = (\Delta t_{j,i}^Z)^2 \cos 2\pi k \Delta f \Delta t_{j,i}^Z.$$

The algorithm for organizing the process of calculating the estimates  $\hat{S}_{XX}(f_k)$  and  $\hat{S}_{XX}''(f_k)$  can be represented as nested loops. At the same time, it follows from (15) that the calculation of the  $\hat{S}_{XX}(f_k)$  estimate does not require performing numerous multiplication operations. This reduces the multiplicative complexity of the procedure for calculating this estimate. Calculating the estimate of the second-order derivative  $\hat{S}_{XX}''(f_k)$  leads to the need to perform a multiplication operation to calculate the product  $D_{j,i} = (\Delta t_{j,i}^Z)^2 \cos 2\pi k \Delta f \Delta t_{j,i}^Z$ . However, the procedure for calculating the estimate  $\hat{S}_{XX}''(f_k)$  is performed only for the assumed formant frequencies  $F_m$ . This means that it is performed a limited number of times during the analysis of the frequency composition of the signal.

Equations (17) together with Eqs. (3)–(7) define the mathematical procedures for calculating the estimates  $\hat{S}_{XX}(f_k)$ ,  $\hat{S}_{XX}''(f_k)$ ,  $f_{Lo,m}$ ,  $f_{Hi,m}$ ,  $\Delta f_m = f_{Hi,m} - f_{Lo,m}$  in a discrete form with frequency resolution  $\Delta f = 1/T$ . These equations became the basis for the development of computationally efficient algorithmic support for evaluating the formant frequencies and their characteristics. The practical implementation of such algorithmic support involves the following computational procedures:

1. the estimates  $\hat{S}_{XX}(f_k)$  are calculated with the highest possible frequency resolution  $\Delta f = 1/T$  within a given frequency band with lower  $f_{\min}$  and upper  $f_{\max}$  boundaries;
2. the estimates  $\hat{S}_{XX}(f_k)$  are analyzed to determine the frequency bands of the presence of formants and their corresponding frequencies  $F_m$ ;
3. the estimates  $S''_{XX}(F_m)$  are calculated for  $m = 1, 2, 3, \dots, M$ ;
4. the estimates of the lower  $f_{Lo,m}$  and upper  $f_{Hi,m}$  frequency bounds of the formants are calculated, which are used to calculate the  $\Delta f_m = f_{Hi,m} - f_{Lo,m}$  estimates.

Note that all of the above computational procedures can be performed in a parallel mode of operation as the initial and intermediate data necessary for their execution arrive and are ready.

In practice, the developed algorithmic support can be implemented as a functionally independent software module [24]. In this case, the requirements for the metrologically significant software for measuring instruments must be taken into account. Separate sections of executable code or critical sections of a given module can be developed in assembler. This approach to the development of a software module can provide quick access to the software and hardware components in the computing devices and speed up the data exchange between them. This approach to the development of a software module can provide fast access to software and hardware as part of multicomponent computing devices and speed up data exchange between them. This will provide an additional increase in computational efficiency for the digital processing of the analyzed signal.

## 4 Conclusion

This chapter deals with the problem of developing mathematical and algorithmic support for analyzing the location of formants in the frequency spectrum of complex multicomponent signals. The procedures for calculating the estimates of the lower and upper bounds of the formant frequencies are developed on the expansion basis of the continuous PSD function into the Taylor series. Mathematical equations for calculating estimates of the PSD and its second-order derivative are obtained based on the correlogram method and binary-sign stochastic quantization. In this case, a discrete-event model was used to mathematically represent the procedure of binary-sign quantization of a continuous signal in time. This provided the analytical computation of integral operators in the transition to discrete computational procedures. The resulting mathematical equations provide an identical structural organization of the computational process. The main operations performed in the course of the practical implementation of these equations are simple algebraic addition and subtraction operations, as well as operations of the logical processing of computed PSD estimates. At the same time, the total number of multiplication operations has

been reduced. All this provides a reduction in computational costs when processing complex multicomponent signals in the process of estimating formant frequencies.

The developed mathematical and algorithmic support can be implemented as a functionally independent software module. This module can be used as a functionally independent component within the integrated metrologically significant software of multifunctional systems for operational time–frequency analysis of complex multi-component signals [25].

**Acknowledgements** The authors are grateful to the Russian Foundation for Basic Research (RFBR). This work was supported by the RFBR under initiative research project No. 19-08-00228-A.

## References

1. Madisetti, V.K. (editor-in-chief): *The Digital Signal Processing Handbook*, Second edition: *Digital Signal Processing Fundamentals*, 904 p. CRC Press, Taylor and Francis Group (2010)
2. Madisetti, V.K. (editor-in-chief): *The Digital Signal Processing Handbook*, Second edition: *Video, Speech, and Audio Signal Processing and Associated Standards*, 616 p. CRC Press, Taylor and Francis Group (2010)
3. Allen, R.L., Mills, D.W.: *Signal Analysis: Time, Frequency, Scale, and Structure*, 937 p. IEEE Press; Wiley-Interscience (2004)
4. Manolakis, D.G., Ingle, V.K.: *Applied Digital Signal Processing: Theory and Practice.*, XV, 991 p. Cambridge University Press (2011)
5. Rabiner, L.R., Schafer, R.W.: *Theory and Applications of Digital Speech Processing*, XIV, 1042 p. Pearson (2011)
6. Kester, W. (ed.): *Analog-Digital Conversion. Analog Devices*, 1138 p. (2004)
7. Pelgrom, M.: *Analog-to-Digital Conversion*, 548 p. Springer (2017)
8. Oberguggenberger, M., Ostermann, A.: *Analysis for Computer Scientists Foundations, Methods, and Algorithms*, 378 p. Springer (2018)
9. Ul'janov, M.V.: *Resource-Efficient Computer Algorithms [Development and Analysis]*, 304 p. Moscow, Publishing House "Fizmatlit" (2008)
10. Blahut, R.E.: *Fast Algorithms for Signal Processing*, 453 p. Cambridge University Press (2010)
11. Britanak, V., Rao, K.R.: *Cosine-/Sine-Modulated Filter Banks: General Properties, Fast Algorithms, and Integer Approximations*, 645 p. Springer. (2018)
12. Marple, S.L., Jr.: *Digital Spectral Analysis with Applications*, 2nd edn., 432 p. Dover Publications Inc. (2019)
13. Gorbunov, Y.N., Kulikov, G.V., Shpak, A.V.: *Radar: A Stochastic Approach*, 520 p. Publishing House "Gorjachaja Linija-Telekom", Moscow (2016)
14. Max, J.: *Methodes et techniques de traitement du signal et applications aux mesures physiques. Tome 1: Principes generaux et methodes classiques*, Paris, Masson, 354 p. 1996
15. Papadopoulos, H.C., Wornell, G.W., Oppenheim, A.V.: *Sequential signal encoding from noisy measurements using quantizers with dynamic bias control*. *IEEE Trans. Inf. Theory* **47**(3), 978–1002 (2001)
16. Zhai, Q., Wang, Y.: *Noise effect on signal quantization in an array of binary quantizers*. *Sig. Process.* **152**, 265–272 (2018)
17. Wang, G., Zhu, J., Blum, R.S., Willett, P., Marano, S., Matta, V., Braca, P.: *Signal amplitude estimation and detection from unlabeled binary quantized samples*. *IEEE Trans. Sig. Process.* **66**(16), 4291–4303 (2018)

18. Bendat, J.S., Piersol, A.G.: *Random Data: Analysis and Measurement Procedures*, 4th edn., 621 p. Wiley (2010)
19. Yakimov, V.N.: Correlation analysis based on interval representation result of sign-function for random processes. *Pribory i Sistemy Upravleniya*. **11**, 61–66 (2001)
20. Lange, P.K., Yakimov, V.N., Yaroslavkina, E.E., Muratova, V.V.: Method of operational determination of amplitudes of odd harmonics of voltages and currents in power supply circuits of powerful electrical installations. *cyber-physical systems: design and application for industry 4.0. Studies in Systems, Decision and Control*, vol. 342, pp. 311–312. Springer International Publishing (2021). [https://doi.org/10.1007/978-3-030-63563-3\\_11](https://doi.org/10.1007/978-3-030-63563-3_11), pp. 10
21. Hadjicostis, C.N.: *Estimation and Inference in Discrete Event Systems: A Model-Based Approach with Finite Automata*, XVIII, 346 p. Springer (2020)
22. Yakimov, V.N.: Digital spectral analysis based on sign two-level transformation of continuous random processes and asymptotically unbiased estimation of the correlation function. *Meas. Tech.* **48**(12), 1171–1178 (2005). <https://doi.org/10.1007/s11018-006-0040-9>
23. Yakimov, V.N.: Numerical estimation of a spectral power density (SPD) based on the signed stochastic quantization of continuous processes. *Pribory i Sistemy Upravleniya*. **12**, 60–64 (2001)
24. Stepanov, A.A., Rose, D.E.: *From Mathematics to Generic Programming*, 292 p. Addison-Wesley Professional (2015)
25. Yakimov, V.N., Zaberzhinskij, B.E., Mashkov, A.V., Bukanova, Y.V.: Multi-threaded approach to software high-speed algorithms for spectral analysis of multi-component signals. In: *Proceedings of IEEE XXI International Conference on Complex Systems: Control and Modeling Problems (CSCMP)*, pp. 698–701 (2019)

# Estimation of the Influence of the Supply Voltage Non-sinusoidally on the Results of Measuring the Parameters of Powerful Submersible Electric Motors



Evgenii Melnikov , Ekaterina Yaroslavkina , and Vladimir Yakimov 

**Abstract** The design of a stand for carrying out acceptance and periodic tests of submersible pumps electric motors (SEM) using a frequency converter (FC) as a source of supply voltage is described. The methodological problems of measuring the electrical parameters of electric motors of submersible pumps in the process of bench tests are considered, the normative base of tests is given. The errors of measurements of current, voltages of the power factor, active power arising in the process of testing are considered. A significant part of these errors is caused by the influence of the non-sinusoidality of the supply voltage to the SEM. It was found that the number of detected harmonics (more than 500) significantly exceeds the GOST requirement for power quality. An analysis of the errors associated with this influence was carried out, it was found that their contribution to the total measurement error can significantly exceed the standardized test errors. To reduce the errors caused by the influence of non-sinusoidality of the supply voltage, it is proposed to abandon voltage transformers and use exemplary dividers, measure the current by the method of root-mean-square values (True RMS), divide the measurement range into a series that excludes falling into the zone of large errors. The theoretical results of studies of the influence of non-sinusoidality of the supply voltage on the measurement results were confirmed by experimental tests on a stand manufactured and introduced into the technological process in an organization engaged in the repair of oil-producing equipment.

**Keywords** Submersible electric motor · Harmonic distortion · Phase error · Conversion nonlinearity · Acceptance tests · Calculation method

---

E. Melnikov (✉) · E. Yaroslavkina · V. Yakimov  
Samara State Technical University, 244, Molodogvardeiskaya Street, Samara 443100, Russia

© The Author(s), under exclusive license to Springer Nature Switzerland AG 2022  
A. G. Kravets et al. (eds.), *Cyber-Physical Systems: Modelling and Industrial Application*,  
Studies in Systems, Decision and Control 418,  
[https://doi.org/10.1007/978-3-030-95120-7\\_14](https://doi.org/10.1007/978-3-030-95120-7_14)

## 1 Introduction

In the oil industry, in the technology of oil extraction and pumping of reservoir fluid, engineers commonly use electric-driven centrifugal pumps with submersible electric motors (SEM) of vertical design.

Russian manufacturers produce a wide range of SEM with different pressure-flow and power characteristics. At the same time, the SEM operating power (for different models) varies in the range from 8 to 300 kW. To reduce voltage losses on the supply cable with hard limits on the conductor diameter, manufacturers have to increase SEM supply voltage, which can reach 5 kV for powerful models.

SEM performance is controlled by the frequency method. During the SEM operation in various modes, power frequency can be changed in the range from 20 to 100 Hz.

Currently, the oil industry is adopting brushless DC SEM, which has improved energy characteristics in comparison with traditional asynchronous motors. However, increased requirements apply to the brushless DC SEM testing process, including the accuracy of measuring individual characteristics.

The average service life of the submersible motor in the well is two to three years, after which the engine is sent for repair and subsequent tests to ensure that its characteristics correspond to the passport values.

Also, new SEMs are tested for compliance with the technical requirements of the manufacturer's plant and as part of the incoming inspection of the enterprise. Periodic tests should be carried out at least once a year on one electric motor of each type that has passed the acceptance tests [1–4].

In total, during the testing process, more than thirty parameters are controlled, some of which directly depend on the supply voltage. These parameters include:

- (1) voltage of the start of SEM acceleration,  $U_{st}$ ;
- (2) dielectric strength of the inter-turn insulation of the stator winding,  $U_{ds}$ ;
- (3) SEM short-circuit current, in the locked state of the shaft,  $I_{sc}$ ;
- (4) SEM short-circuit power,  $P_{sc}$ ;
- (5) SEM starting power,  $P_{st}$ ;
- (6) test in modes of overload on torque and current, up to 30% of the nominal,  $N/m$ , and  $A$ ;
- (7) nominal mechanical power,  $kW$ ;
- (8) SEM nominal current,  $I_n$ ;
- (9) SEM no-load current,  $I_{nl}$ ;
- (10) SEM no-load loss,  $W$ ;
- (11) SEM efficiency factor, %;
- (12) power factor (for asynchronous SEM), %;
- (13) slip (for asynchronous SEM), %;
- (14) ratio of the initial starting torque to the nominal;
- (15) ratio of maximum torque to nominal torque;
- (16) SEM load curves, %.

Measurement of most of the above SEM characteristics requires high-precision measurement of the values of the consumed current, voltage, power factor with the calculation of active, reactive, and apparent energy.

## 2 Problem Statement

By the requirements of the existing state standard [5–8] for testing asynchronous and synchronous electric motors, the SEM must be connected during the tests to a sinusoidal voltage source, which does not allow testing its performance at frequencies other than 50 Hz.

The next problem in the development of equipment for testing these electric motors is associated with the need to form the SEM supply voltage in the range from 5 to 130% of the nominal value. For this, high-power induction voltage regulators were previously used, which are currently out of production. Induction regulators are designed for a frequency of 50 Hz, are difficult to control, and do not allow maintaining the required output voltage with a given accuracy during the SEM test under load.

In this regard, an SEM control station equipped with a frequency converter was used to form the supply voltage of the tested electric motor. The use of a frequency converter allows, in addition to generating the required motor control frequency, to form the required volt-frequency characteristic.

The SEM connection diagram on the test bench (see Fig. 1). The engine control station generates the SEM supply voltage in the range from 10 to 380 V with a frequency of 20–100 Hz. In series, through the output choke and step-up transformer, the supply voltage is applied to the tested SEM. In Fig. 2 shows the appearance of

**Fig. 1** Power supply diagram of SEM

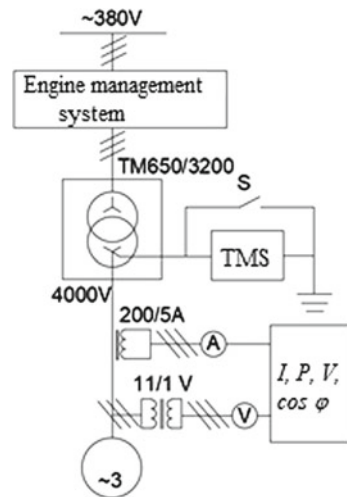




**Fig. 2** The appearance of test bench control cabinets



the test bench control cabinets.

Federation and models were carried out in works. The development of test equipment for SEM testing is complicated due to the lack of certified methods for measuring power supply parameters in frequency control conditions, as well as by the lack of current and voltage transformers certified for operation in this frequency band [12–14].

The chapter presents developments on the creation and certification of a test bench working with a control station and testing both asynchronous and valve motors with a frequency of up to 100 Hz.

### **3 Analysis of Causes of Power Measurement Error and Power Factor of SEM**

The error in determining the power factor, active and reactive power is the sum of the phase and current errors of the current transformer, phase errors and errors of voltage transmission for voltage transformers, errors of the measuring transducer of electrical quantities.

The frequency converter of the control station operates under scalar control conditions with a variable ratio of the SEM supply voltage to the supply frequency ( $U/F$ ). To generate these modes, pulse-width modulation with a carrier frequency of 2500 Hz is used. The consequence of these operating modes of the frequency converter is the formation of a large number of harmonics in the generated power supply voltage of the SEM, which leads to measurement errors.

The scheme to measure the amplitudes  $U_{nh}$  and phases  $\varphi_n$  of the harmonics of the SEM power supply is shown in Fig. 3. The spectrum and root-mean-square values (RMS) of the phase currents were calculated with an R&SHMO1002 digital

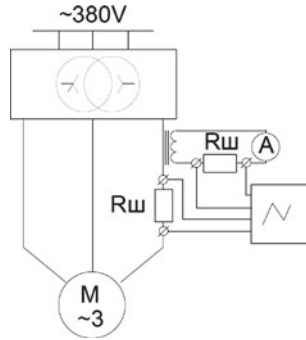


Fig. 3 Power supply diagram of SEM

oscilloscope. Figure 4 shows the spectral composition of harmonics obtained during the experiment.

As can be seen from Fig. 4, it is practically impossible to calculate the distortion coefficients of the supply network according to the requirements [9]. This is because the number of harmonics with an amplitude of more than 0.1% of the fundamental harmonic can reach 500 or more (with the required 40). The installation of a motor choke and the presence of a step-up transformer in the SEM power supply circuit did not radically improve the situation.

The distortion factor of the sinusoidal voltage waveform was determined using the standard formula for all significant harmonics:

$$K_{U,h} = \frac{\sqrt{U_{1h}^2 + U_{3h}^2 + \dots + U_{nh}^2}}{U_{fund,h}}$$



Fig. 4 The appearance of test bench control cabinets

**Table 1** Values sinusoidity coefficient

Control station output frequency	20	30	35	40	45	50
The voltage at the output of the control station	380/30	380/30	380/30	380/30	380/30	380/30
Distortion factor of the generated voltage sinusoidal	78/98	64/90	55/88	47/87	36/80	27/69

where  $U_{fund.h}$ —the effective value of harmonic, the level of which is  $>0.1\%$ .

The Table 1 shows the calculated values of the sinusoidality distortion coefficient obtained by changing the supply frequency and supply voltage of the SEM. As can be seen in the presented table, the U/F ratio is not constant.

To calculate the error in determining the electrical parameters of the SEM caused by the non-sinusoidal shape of the supply voltage, it is necessary to determine [3, 4, 10–12] errors of current transformers caused by a change in the transmission coefficient and phase error for each harmonic, determined by the following expressions:

$$k_{tt} = \left( \frac{I_2 N}{I_1} - 1 \right) * 100\%$$

where  $N$ —current transformation ratio;  $I_2$ —RMS of the secondary current;  $I_1$ —RMS primary current;

$$\varphi_{avr} = \frac{\sum_{j=1}^n (\varphi_1 - \varphi_2)}{n}$$

where  $\varphi_1$ —harmonic phase of the current in the primary circuit;  $\varphi_2$ —phase of the current harmonic in the secondary circuit,  $n$ —number of harmonics.

The total error  $\delta$  of the current transformer can be determined as follows:

$$\delta = \frac{100}{I_1} \sqrt{\frac{1}{T} \int_0^T (Ni_2 - i_1)^2 dt}$$

The results of calculating the error of a current transformer during current transfer are shown in Fig. 5 and phases in Fig. 6. The X-axis shows the current values, in percent of the nominal. Y-axis for graph (a) is the error of the current transfer in %, and graph (b) is the phase shift error in degrees.

Errors in determining the SEM electrical parameters caused by the error of voltage transformers [13–15] can be calculated by the expression:

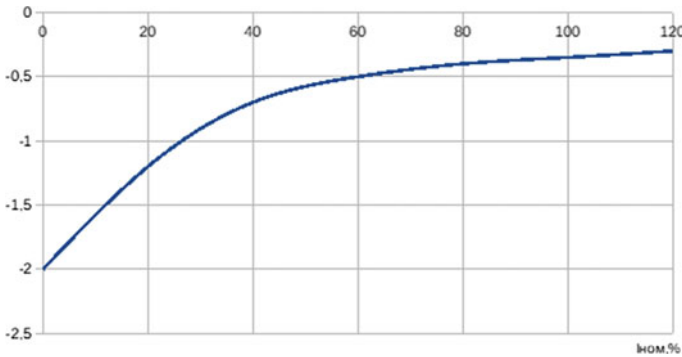


Fig. 5 Power supply diagram of SEM

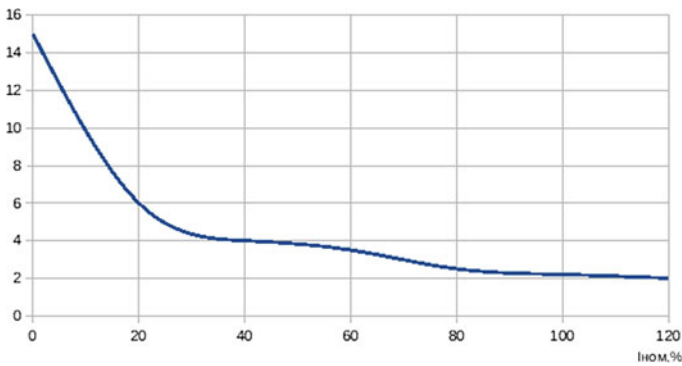


Fig. 6 The appearance of test bench control cabinets

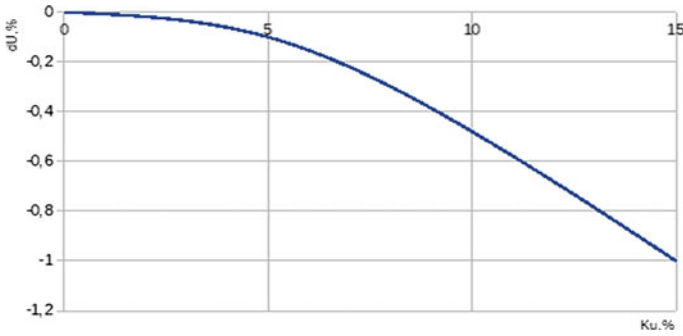
$$\delta U = 1 - (1 + k_{zero}^2 + k_{rev}^2) - \sum_{n=1}^{500} \frac{K_{Un}^2 z}{\sqrt{r^2 n + jx^2 n^2}} \frac{\sqrt{U_{1h}^2 + U_{3h}^2 + \dots + U_{nh}^2}}{U_{fund.h}}$$

where  $k_{zero}$  and  $k_{rev}$ —voltage unbalance coefficients for reverse and zero sequences, respectively;  $k_{Un}$ —coefficient of the  $n$ -th harmonic of the SEM supply voltage;  $r$ —active resistance of the secondary circuit of the voltage transformer;  $x$ —inductive reactance;  $z$ —impedance.

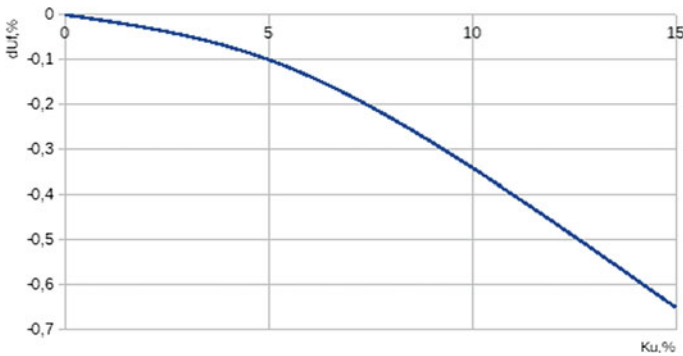
The results of calculating the error of the voltage transformer by the transfer coefficient (Fig. 7) and the change in the angle (Fig. 8).

Figure 9 shows the results of an SEM load test. As can be seen from this figure, the range of power factor variation during SEM tests is in the range from 0.4 to 0.95. In this case, the nature of the load changes from inductive at the beginning of the test to active when the motor is loaded at full power.

Because the SEM supply voltage is different for different models, it is set using the control station. At the same time, in the overlocking test, the voltage rises smoothly



**Fig. 7** Dependence of voltage and phase transmission error on the value of sinusoidality distortion coefficient by transmission coefficient



**Fig. 8** Dependence of voltage and phase transmission error on the value of sinusoidality distortion coefficient by the angle change Current transformer error during phase transfer

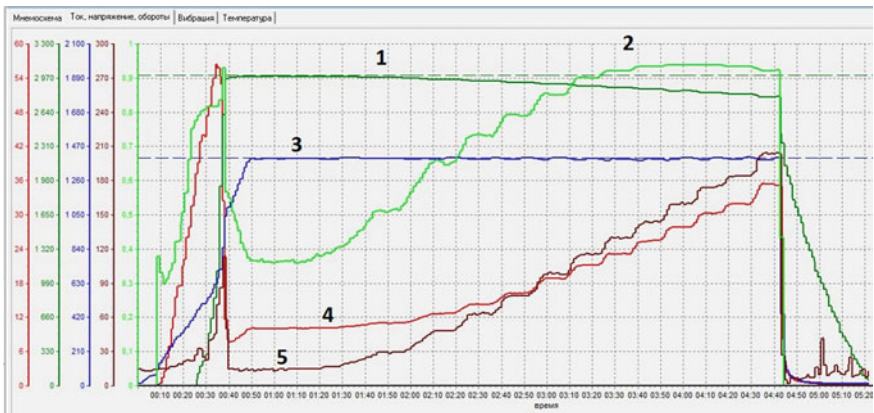


**Fig. 9** Load tests SEM. 1—speed of SEM rotor rotation; 2—the power factor of the SEM; 3—power supply voltage of SEM; 4—average current consumed by the SEM; 5—load percentage of nominal power

from zero volts to the nominal value for a particular SEM. As a result, the coefficient of sinusoidality distortion can vary from 20 to 45% (according to the data of the manufacturer of the control station).

Assuming the errors are statistically independent, the expression for determining the error in measuring the power factor takes the form:

$$\delta = \frac{\sqrt{3(\delta_U^2 + \delta_I^2 + \delta_\varphi^2)}}{3}$$

where  $\delta_U$ —voltage transformer error,  $\delta_I$ —current transformer error,  $\delta_\varphi$ —angle transmission error.

The value of the error in determining the power factor caused by the angular error of the transformers is in the range from  $0.5^\circ$  to  $8.1^\circ$ . It should be noted that the error of the measuring device connected to the primary current and voltage transformers, not exceeding 0.1% in the absence of non-standard harmonics, can also reach large values [16–21].

Error in measuring active power is:

$$\delta_{Pa} = \sqrt{3}$$

The magnitude of this error can be up to 10% in the worst case of measurement. Proposed solutions to improve measurement accuracy: The error of current transformers and voltage transformers is directly related to the value of the distortion factor of the output voltage of the motor control station. To reduce this error, the following actions should be taken:

- (1) to reduce current errors—split the measurement range into subranges by switching current transformers during testing. Attention must be taken that unused current transformers must not be short-circuited, but closed on current-limiting resistors to prevent their overload;
- (2) to reduce voltage errors—eliminate the error caused by voltage transformers by installing standard dividers with subsequent galvanic isolation of the measuring device from the data interface;
- (3) reduce the voltage regulation range using a frequency converter by switching the windings of a step-up transformer.

Further improvement of the measurement accuracy can be achieved by switching to the measurement of active and apparent power with root mean square values (True RMS) sensors, followed by the calculation of the power factor. The disadvantage of this solution is that there is currently no sensor data for the required voltages and the lack of a method for calibrating sensors for the required frequency range.

## 4 Conclusion

When designing and verifying test equipment using a frequency drive, it is necessary to take into account the influence of harmonics on measuring transducers and measuring instruments.

The use of high-precision power meters is impractical due to the large errors of the primary converters.

Current transformers and voltage transformers existing on the market are not certified for operation in a wide frequency band, there are no methods for their certification.

It is necessary to use sensors that correctly measure RMS current and voltage for a non-sinusoidal signal.

**Acknowledgements** This research was partially supported by the Russian Fund of Basic Research (grant No. 19-08-00228-A, 18-08-00253 -A).

## References

1. State Standard IEC 60092–301 Electrical installations in ships. Part 301: Equipment—Generators and motors, 38 p. (1980)
2. State Standard 29322–2014 (IEC 60038:2009) Standard Voltages, 13 p. Standartinform Publication, Moscow (2015)
3. State Standard 32144–2013 (EN 50160:2010) Electric energy. In: Electromagnetic Compatibility of Technical Equipment. Power Quality Limits in the Public Power Supply Systems, 20 p. Standartinform Publication, Moscow (2014)
4. State Standard 30331.1–2013 (IEC 60364–1:2005) Low-voltage electrical installations. In: Part 1: Fundamental Principles, Assessment of General Characteristics, Definitions, 46 p. Standartinform Publication, Moscow (2014)
5. Melent'ev, V.S., Gubanov, N.G., Latukhova, O.A., Smolin, A.M.: Improvement of methods of measuring the parameters of two-terminal electric circuits. *Measur. Techn.* **56**(6), 691–694 (September 2013). <https://doi.org/10.1007/s11018-013-0266-2>
6. Muratova, V.V., Yaroslavkina, E.E., Orlov, S.P.: Information-measuring system for rapid determination of power electrical equipment parameters. In: International Conference on Industrial Engineering, Applications and Manufacturing (ICIEAM), 25–29 March 2019, Sochi, Russia. <https://doi.org/10.1109/ICIEAM.2019.874293>, doi:<https://doi.org/10.1109/ICIEAM.2019.8742934>
7. Yang, J.-Z., Yu, C.-S., Liu, C.-W.: A new method for power signal harmonic analysis. *IEEE Trans. Power Deliv.* **20**(2), 1235–1239 (2005). <https://doi.org/10.1109/TPWRD.2004.834311>
8. Chen, X., Zhang, Y.: Detection and analysis of power system harmonics based on FPGA. In: Proceedings of First International Conference: Wireless Communications and Applications, ICWCA, Sanya, China, pp. 445–454 (2011). [https://doi.org/10.1007/978-3-642-29157-9\\_43](https://doi.org/10.1007/978-3-642-29157-9_43)
9. Heydt, G.T., Fjeld, P.S., Liu, C.C., Pierce, D., Tu, L., Hensley, G.: Applications of the windowed FFT to electric power quality assessment. *EEE Trans. Power Deliv.* **14**(4), 1411–1416 (1999)
10. Gu, Y.H., Bollen, M.H.J.: Time-frequency and time-scale domain analysis of voltage disturbances. *IEEE Trans. Power Deliv.* **15**(4), 1279–1284 (2000)
11. State Standard 30804.4.30–2013 (IEC 61000–4–30:2008) Electric energy. In: Electromagnetic Compatibility of Technical Equipment. Power Quality Measurement Methods, 58 p. Standartinform Publication, Moscow (2014)

12. State Standard 30804.4.7–2013 (IEC 61000–4–7:2009) Electromagnetic compatibility of technical equipment. In: General Guide on Harmonics and Interharmonics Measuring Instruments and Measurement for Power Supply Systems and Equipment Connected Thereto, 40 p. Standartinform Publication, Moscow (2013)
13. Xue, H., Yang, R.: A novel algorithm for harmonic measurement in power system. Proc. IEEE Int. Conf. Power Syst. Technol. **1**, 438–442 (2002). <https://doi.org/10.1109/ICPST.2002.1053581>
14. Emanue, A.E., Orr, J.A.: Current harmonics measurement by means of current transformer. IEEE Trans. Power Deliv. **22**(3), 13, 18–25 (July 2007)
15. Lange, P.K., Yakimov, V.N., Yaroslavkina, E.E., Muratova, V.V.: Method of operational determination of amplitudes of odd harmonics of voltages and currents in power supply circuits of powerful electrical installations. cyber-physical systems: design and application for industry 4.0. In: Kacprzyk, J. (ed.) Systems Research Institute, Polish Academy of Sciences, Warsaw, Poland. Series Title Studies in Systems, Decision, and Control, vol. 342, pp. 311–322. Springer International Publishing (2021). [https://doi.org/10.1007/978-3-030-63563-3\\_11](https://doi.org/10.1007/978-3-030-63563-3_11), pp. 10
16. Efimov, S.V., Zamyatin, S.V., Gayvoronskiy, S.A.: Synthesis of the PID controller with respect to the location of zeros and poles of the system of automatic control. IzvestiyaTomskogopolitekhnikheskogouniversiteta **317**(5), 102–107 (2010). <https://doi.org/10.1088/1757-899X/124/1/012019>
17. Efimov, S.V., Gayvoronskiy, S.A., Zamyatin, S.V.: Root tasks of analysis and synthesis and synthesis of automatic control systems. IzvestiyaTomskogopolitekhnikheskogouniversiteta **316**(5), 16–20 (2010)
18. Wang, X.-H., He, Y.-G.: A new neural network based power system harmonics analysis algorithm with high accuracy. Power Syst. Technol. **3**, 72–75 (2005)
19. Morales-Velazquez, L., Romero-Troncoso R., Herrera-Ruiz G.-R., Morinigo-Sotelo, D., Osornio-Rios, R.A.: Smart sensor network for power quality monitoring in electrical installations. Measurement **103**, 133–142 (2017). <https://doi.org/10.1016/j.measurement.2017.02.032>
20. Kruglova, T.N.: Intelligent diagnosis of the electrical equipment technical condition. Proc. Eng. Int. Conf. Ind. Eng. **129**, 219–224 (2015). <https://doi.org/10.1016/j.proeng.2015.12.036>
21. Ustyugov, N.: Forecast of the cost of electricity and choice of voltage level for the enterprise. In: Kacprzyk, J. (ed.) Cyber-Physical Systems: Design and Application for Industry 4.0. Studies in Systems, Decision. Systems Research Institute, Polish Academy of Sciences, Warsaw, Poland., and Control, vol. 342, pp. 299–310. Springer International Publishing (2021). [https://doi.org/10.1007/978-3-030-63563-3\\_11](https://doi.org/10.1007/978-3-030-63563-3_11), pp. 11



# **Cyber-Physical Systems Intelligent Control**

# On the Possibilities of the Cyber-Physical Approach to Study the Frequency Properties of a Closed-Loop System with Incomplete Information About the Control Plant Model



E. G. Krushel, E. S. Potafeeva, T. P. Ogar, I. V. Stepanchenko,  
and I. M. Kharitonov

**Abstract** The chapter presents a method of reducing the time spent on the experimental study of the frequency properties of a plant with an unknown mathematical model, based on the application of a cyber-physical approach to experiment automation. The processing of experimental data on the response of plant output to an input signal formed as the mixture of harmonic components with different frequencies provides the nonparametric estimation of unknown plant's frequency characteristics. To divide the output signal into components corresponding to each frequency, computer technology is used, which implements an optimization procedure for finding the values of both the real and imaginary frequency characteristics corresponding to the frequencies represented in the harmonic input signal. The method is also suitable for quick estimation of the frequency characteristics of a plant with an unknown time delay. The chapter considers the application of the frequency properties estimation in the problem of stability analysis of closed-loop systems destined for the plant with incomplete information about its model using a serial connected proportion-integral controller. The results of quick frequency characteristics estimation were applied to transfer function parameters identification. To solve the parameterization problem, the facilities of open source software for numerical computation Scilab were applied for the automatic converting the point-wise frequency characteristics to the corresponding transfer function. The example illustrating the design possibilities of the control system with the plant's reduced model shows one of the possible applications of the transfer function's parametric identification results.

**Keywords** Experiment automation · Incomplete information about the plant model · Nonparametric estimates of frequency characteristics · A mixture of input

---

E. G. Krushel (✉) · E. S. Potafeeva · T. P. Ogar · I. V. Stepanchenko · I. M. Kharitonov  
Kamyshin Technological Institute (Branch) of Volgograd State Technical University, Lenin street,  
6a, Kamyshin City 403874, Volgograd Region, Russia

T. P. Ogar  
e-mail: [ogar@kti.ru](mailto:ogar@kti.ru)

and output signal harmonics · Closed-loop system stability · Parametric identification of transfer function · Scilab

## 1 Introduction

One of the important problems of industrial processes control is to ensure the stability of the closed-loop system [1]. Usually, the plant of control is stable, and the controller is stable or neutral. Therefore, instability phenomena can occur only in the corresponding closed-loop system (after closing the open-loop system with a unit feedback loop). The warranty technique allowing the conclusion about closed-loop system stability before closing the feedback loop is based on the analysis of peculiar properties of open-loop system amplitude-phase characteristic (AFC) (Nyquist diagram) (the Nyquist stability criterion [2] or the Bode diagram [3] is used). But to apply this approach, a mathematical model of the control plant should be available; in practice, this requirement often does not hold.

In the presented work, we suppose that it is necessary to conclude about closed-loop control system stability in the absence of some data about control plant characteristics. Particularly, we suppose that the type and parameters of the plant model are unknown but the plant with sufficient accuracy behaves itself as a linear, stable, and inertial one. A plant with such properties suppresses high-frequency harmonic input signals. We assume that approximately known frequency  $\omega^*$  is assigned so that at frequencies  $\omega > \omega^*$  the amplitude of the signal at the plant's output remains less than the predetermined fraction of the input signal amplitude [4].

To conclude on the closed-loop system stability according to the open-loop system AFC, it is necessary to possess more information about the control plant [5]. There are various approaches to such information reception (active experiments, passive observations, adaptive models application, etc.). The presented work is oriented on the methods using the processing of experimental data about the plant frequency properties. In the well-known works [6], the corresponding experiment as a whole consists of a series of experiments, in each of which a sinusoidal signal of a given frequency puts to the input of the plant. After the achievement of the steady-state oscillation mode, the ratio of the signal amplitude at the plant output to the amplitude of the input signal as well as the phase lagging of the output signal with respect to the input one are determined. Such an experiment being notably informative usually requires undesirable time spent for its fulfillment.

## 2 Problem Statement and the Way of Its Decision

The proposed approach to reduce the time spent for the experimental study of the plant frequency properties consists in refusing a series of sequential experiments with a set of single-frequency inputs. Instead, we propose a one-time experiment to study

the reaction of a plant's output to an input signal in the form of a frequencies mixture. Afterward, the proposed sequence of computer processing actions ensures the finding of the amplitude-phase characteristics of the plant estimation at the frequencies used in the mixture [7]. Interpolation of values between these points allows obtaining a nonparametric estimation of the amplitude-phase characteristic of the plant [8]. Since the controller's law is supposed known, the further procedure for closed-loop system stability forecasting possesses no difficulties.

The processing proceeds according to the following scheme:

1. Let an input harmonic signal be a mixture of different frequencies signals with the same amplitude and specified phase lagging (usually zero):

$$u(t) = \sum_{k=1}^K u_k \cdot \sin(\omega_k \cdot t) \quad (1)$$

where  $u_k$  is the amplitude (for the input signal the amplitudes  $u_k$  are equal for each  $k$ ,  $k = 1, \dots, K$ ,  $K$  is the number of sinusoidal signals in the mixture; further, without loss of generality, we suppose  $u_k = 1$ );  $\omega_k$  is the frequencies the input signal,  $k = 1, \dots, K$ .

2. An active experiment consists of the observations at the plant output reaction to the input signal (1) for a period sufficient to achieve steady-state harmonic oscillations. Since the plant shows itself as a linear and inertial one, its output  $y(t)$  will also be obtained in the form of a mixture of signals with the same frequencies, but with diverse amplitudes and phase laggings for different frequencies:

$$y(t) = \sum_{k=1}^K a_k \cdot \sin(\omega_k \cdot t + \psi_k) \quad (2)$$

Here  $a_k, \psi_k, k = 1, \dots, K$ , are the amplitude and phase lagging of the  $k$ th sinusoidal component of the plant's output with respect to the  $k$ th harmonic of the input signal (1), respectively. To compute  $a_k, \psi_k, k = 1, \dots, K$ , an optimization procedure described below is proposed. As a result, the points of the amplitude-frequency characteristic of the plant as well as phase one are obtained, corresponding to the frequencies  $\omega_k, k = 1, \dots, K$ . Further positions of the processing do not differ from the known ones.

3. We assume that in an open-loop system, a commonly used regulator is applied, frequency characteristics of which are determined according to its control law and the setting parameters values. Below, the processing procedure is illustrated by the problem of the stability forecasting of a closed-loop system with a proportional-integral (PI) controller [9] with known setting parameters values.
4. According to the results of items 2 and 3 being carried out, the points of the amplitude-frequency response of the open-loop system are determined as the product of the amplitude-frequency characteristics of the plant and controller at the frequencies corresponding to the frequencies of signals in the mixture (1).

Similarly, the points of phase-frequency response are determined as the sum of the plant and the controller phases at the same frequencies.

5. According to item 4, the values at the points of the amplitude-phase characteristic of the open-loop system are calculated. Further, interpolation by cubic splines [10] allows obtaining a nonparametric estimate of the continuous (in frequencies) amplitude-phase characteristic.
6. According to the Nyquist criterion applied to the stable or neutral open-loop system, the stability of the corresponding closed-loop system will remain stable after the feedback loop closure if the hodograph of the amplitude-phase characteristic of the open-loop system does not cover the critical point on the complex plane with coordinates  $(-1, i_0)$ . For the case when a closed-loop system will be stable, its stability margins in amplitude and phase can be determined [11].
7. With evident additions, the approach is suitable for control systems of linear inertial plants with time delay.

### 3 Optimization Procedure for Determining the Values at the Points of the Plant Amplitude and Phase-Frequency Characteristics

According to (2), it is necessary to obtain  $2K$  relations that allow determining the amplitudes  $a_k$  and phases  $\psi_k$ ,  $k = 1, \dots, K$ . In order to obtain a system of linear equations concerning frequency characteristics parameters, the following formula replaces (2):

$$y(t) = \sum_{k=1}^K [d_{1k} \cdot \sin(\omega_k \cdot t) + d_{2k} \cdot \cos(\omega_k \cdot t)] \quad (3)$$

Here  $d_{1k} = [a_k \cdot \cos(\psi_k)]$ ,  $d_{2k} = [a_k \cdot \sin(\psi_k)]$ .

The system of linear equations for the  $2K$  components of the sought-for block vector  $d^T = [d_1^T; d_2^T]$ ,  $d_1, d_2$  are vectors with components  $d_{1k}, d_{2k}$ ,  $k = 1, \dots, K$ , obtained by minimizing the least-squares criterion  $J(d)$ :

$$J(d) = \sum_{s=0}^{N-1} \left\{ \left[ y[s] - \sum_{k=1}^K d_{1k} \cdot \sin(\omega_k \cdot s \cdot \delta t) + d_{2k} \cdot \cos(\omega_k \cdot s \cdot \delta t) \right] \right\}^2 \rightarrow \min \quad (4)$$

Here  $\delta t$  is a time interval, small enough so that the sampling of the highest-frequency component of the input signal does not lead to noticeable errors.

$N = P_0 \cdot (n_p - n_i) / \delta t$ .  $P_0$  is the period of the lowest frequency component in the mixture of frequencies (1).  $n_i$  is the number of periods of duration  $P_0$  sufficient to achieve the mode of steady-state harmonic oscillations at the output of the plant.  $n_p$

is the number of periods of duration  $P_0$ , for which the experiment was carried out to estimate the frequency characteristics of the plant [12].

Minimization of (4) leads to a  $2K$ -dimensional system of linear equations for the vector  $d$  components:

$$A * d = B \quad (5)$$

$$A = \begin{vmatrix} A_{11} & A_{12} \\ A_{21} & A_{22} \end{vmatrix}; \quad B = \begin{vmatrix} B_1 \\ B_2 \end{vmatrix};$$

$$B_{1i} = \sum_{s=0}^{N-1} y(s \cdot \delta t) \cdot \sin(\omega_i \cdot s \cdot \delta t); \quad B_{2i} = \sum_{s=0}^{N-1} y(s \cdot \delta t) \cdot \cos(\omega_i \cdot s \cdot \delta t)$$

$$A_{11}^{(i,j)} = \sum_{s=0}^{N-1} \sin(\omega_i \cdot s \cdot \delta t) \cdot \sin(\omega_j \cdot s \cdot \delta t); \quad A_{22}^{(i,j)} = \sum_{s=0}^{N-1} \cos(\omega_i \cdot s \cdot \delta t) \cdot \cos(\omega_j \cdot s \cdot \delta t);$$

$$A_{12}^{(i,j)} = \sum_{s=0}^{N-1} \sin(\omega_i \cdot s \cdot \delta t) \cdot \cos(\omega_j \cdot s \cdot \delta t); \quad A_{21}^{(i,j)} = A_{12}^{(i,j)}; \quad i, j = 1, \dots, K$$

The solution of [13] is follows:

$$d = A^{-1} \cdot B; \quad d_{1k} = d_k, \quad k = 1, \dots, K; \quad d_{2k} = d_k, \quad k = K + 1, \dots, 2 \cdot K \quad (6)$$

The  $d_{1k}$  and  $d_{2k}$  components are the values of the real and imaginary frequency characteristics corresponding to the frequencies  $\omega_k$ ,  $k = 1, \dots, K$ . On the complex plane, the abscissa of which is the real frequency response (real frequency response), and the ordinate is the imaginary frequency response (imaginary frequency response), these values are displayed as dots.

From (6) we find, using (3), the values of the amplitudes  $a_k$ ,  $k = 1, \dots, K$  and the phase laggings  $\psi_k$ , corresponding to the frequencies  $\omega_k$ ,  $k = 1, \dots, K$ :

$$a_k = \sqrt{d_{1k}^2 + d_{2k}^2}, \quad \psi_k = \arctan\left(\frac{d_{1k}}{d_{2k}}\right) - \pi * m \quad (7)$$

In (7)  $m = 0, 2, 3, \dots$ , if the vector with abscissa  $d_{1k}$  and ordinate  $d_{2k}$  is displayed in the 1st or 4th quadrants of the complex plane;  $m = 1, 3, 4, \dots$  if this vector is displayed in the 2nd or 3rd quadrants of the complex plane. Next, the AFC values are computed for the frequencies  $\omega_k$ ,  $k = 1, \dots, K$ , after which interpolation is performed (e.g. using cubic splines, as in the example described below).

## 4 Illustrative Example 1

Below, we present the results of the stability estimation of a closed single-loop system. The corresponding open-loop system is represented by a serial connection of a PI controller (setting parameters:  $k_p = 0.5$  (input unit/output unit) and  $k_i = 1.25$  (input unit/(unit of output  $\oplus$  unit of time)) and the inertial self-leveling unit. Therefore, the open-loop system is neutral. Nonparametric estimation of the plant

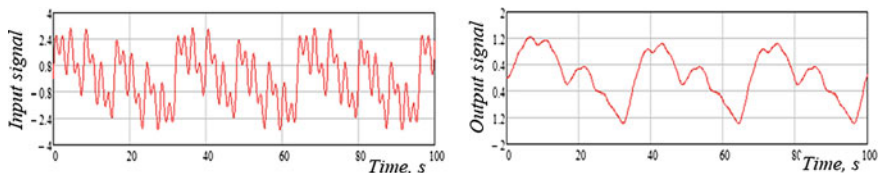


**Fig. 1** Input (on the left) and output (on the right) signals of control plant

AFC is determined using the processing of the corresponding open-loop system output reaction to the input signal formed as a mixture of 5 signals with different frequencies (rad/s):  $\omega = [0.196; 0.393; 0.785; 1.571; 3.142]$ . The amplitudes of the mixture components at all frequencies equal unity. It is required to check whether the system will be stable after closing a feedback unit.

Under the influence of the input signal (Fig. 1 on the left), a harmonic signal arises at the output of the plant (Fig. 1 on the right).

According to (5), the points of the amplitude and phase-frequency characteristics were determined using (7) at the frequencies pointed above:

$$a = [0.802; 0.509; 0.21; 0.063; 0.017]^T;$$

$$\psi = [-0.906; -1.533; -2.174; -2.623; -2.87]^T$$

To verify the obtained values, we have applied a second-order aperiodic unit as a test model with follows parameters of its frequency transfer function:

$$W_{teor}(j\omega) = \frac{k}{[T_1 \cdot T_2 \cdot (j\omega)^2 + (T_1 + T_2) \cdot (j\omega) + 1]}; T_1 = 3(s), T_2 = 2(s), k = 1 \quad (8)$$

For the test model, the theoretical values of  $a^T$  and  $\psi^T$  were determined.

$$a_T = [0.802; 0.509; 0.21; 0.063; 0.017]^T;$$

$$\psi_T = [-0.906; -1.533; -2.174; -2.623; -2.87]^T$$

Figure 2 shows the theoretical graphs of the amplitude (on the left) and phase (on

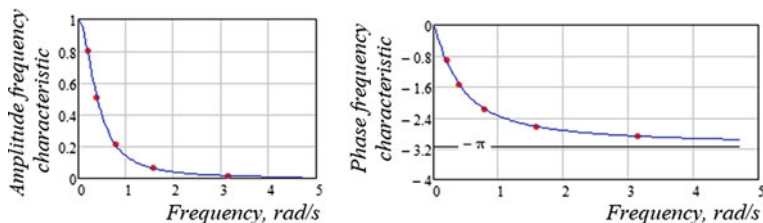


**Fig. 2** Comparison of experimental and test values of control plant frequency characteristics

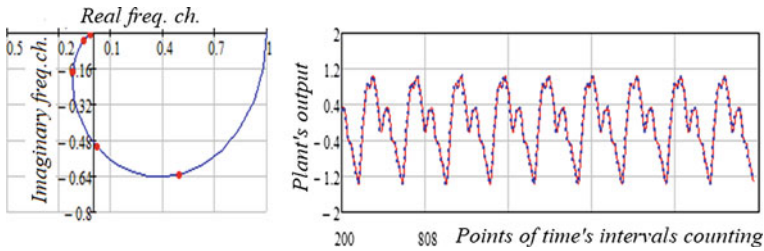


**Fig. 3** Comparison of the experimental and test amplitude-phase characteristics (left) and the graphs of the test and experimental plants outputs (right)

the right) frequency characteristics with the assignment of points determined by the experimental data processing.

The values of the points of amplitude-phase characteristic follow the results of amplitude and phase-frequency characteristics estimation for the frequencies  $\omega_k$ . Figure 3 (on the left) shows these points on the background of the test model AFC hodograph. Figure 3 (on the right) illustrates the closeness of the output of the plant used to estimate the frequency characteristics (shown by dots at Fig. 3) to the output of the test model (shown by the solid curve at Fig. 3).

Since we assume the controller model in this example as given, its amplitude and phase-frequency characteristics are obtainable computationally. Figure 4 shows the amplitude-frequency characteristic (left) and the phase-frequency characteristic (right) of the PI controller with setting parameters  $k_p = 0.5$  and  $k_i = 1.25$ .

At frequencies  $\omega = [0.196; 0.393; 0.785; 1.571; 3.142]$ , used for the experimental estimation of the control plant frequency characteristics, the points of controller's amplitude and phase characteristics are as follows, respectively:

$$a_{reg} = [6.386; 3.222; 1.668; 0.94; 0.639]^T;$$

$$\psi_{reg} = [-1.492; -1.415; -1.266; -1.01; -0.622]^T$$

The components of vector  $a_{open}$  representing the points of the amplitude-frequency characteristic (AFC) are computed as the products of the vectors  $a$  and  $a_{reg}$  components. The components of vector  $\psi_{open}$  representing the points of the phase-frequency

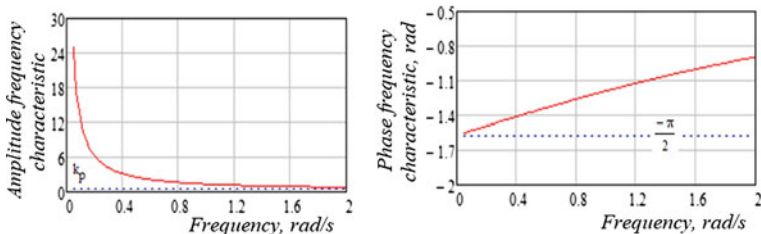
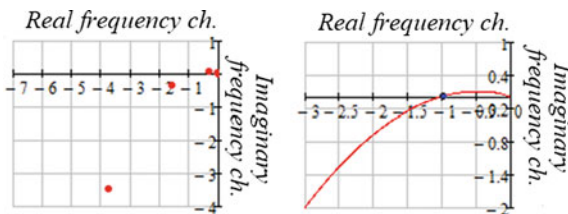


**Fig. 4** Frequency characteristics of PI controller with setting parameters  $k_p = 0.5$  and  $k_i = 1.25$



**Fig. 5** AFC points (left) and the interpolation results (right)



characteristic (PFC) are computed as the sum of the components  $\psi$  and  $\psi_{reg}$  [14]. For the open-loop system, these vectors are:

$$a_{open} = [5.122; 1.639; 0.35; 0.059; 0.011]^T$$

$$\psi_{open} = [-2.399; 2.948; -3.44; -3.633; -3.543]^T$$

According to these data, the values of the open-loop system amplitude-phase characteristic (AFC) points were determined. Figure 5 shows these points on the left; the right of Fig. 5 shows the results of interpolation of the AFC values between these points by cubic splines [10].

Figure 5 on the right shows the critical point with coordinates  $(-1, j_0)$ . The interpolated AFC estimation passes through this point; according to the Nyquist criterion, a closed-loop system with PI controller settings  $k_p = 0.5$  and  $k_i = 1.25$  will be at the stability boundary in the continuous oscillation mode.

## 5 Generalization

Practically without changes, the presented method is suitable for the amplitude-phase characteristics quick estimation if a plant possesses an unknown time delay [15]. The corresponding example shows the results (Fig. 5) being tested by comparing with the frequency characteristics of a plant containing a time delay unit  $\tau = 1.5$  (s), connected in series with a second-order aperiodic unit (8). The AFC of the plant with delay does not differ from that shown in Fig. 2 on the left. The points of the phase-frequency characteristic (Fig. 6 on the left) and the amplitude-phase characteristic (Fig. 6 on the right) of the plant with delay are shown on the background of the corresponding test plant characteristics (good agreement of the computational results with the test is illustrated).

The solid graphs show the corresponding characteristics of the test plant.

If the setting parameters of the PI controller in the system with delay will be the same as for the system with the plant (8), then the closed-loop system will be unstable.

## 6 Parameterization

While the hodograph of the amplitude-phase characteristic of an open-loop system passes through the critical point of the complex plane (as in Fig. 6), then after a negative feedback loop closure, the control process would be unstable. In this case, it will be necessary to solve the problem of the control system design to ensure the required stability margins in amplitude and phase [16]. In design problems, it may be necessary to simulate a plant in an explicit form (either in the form of differential or difference equations or in the form of a transfer function if the plant is linear and stationary). In both cases, it is necessary to receive an estimate of the model numerical parameters values from the approximate graphical representation of its frequency characteristics.

The idea of the estimation is based on determining the vectors of coefficients in the polynomials of the numerator  $num(i\omega)$  and the denominator  $den(i\omega)$  of the frequency transfer function  $W_{appr}(i\omega) = num(i\omega)/den(i\omega)$ . The estimation succeeds the results of computing the vector of coefficients  $d_1$  and  $d_2$  in (6) which represent the points of the real and imaginary frequency characteristics for the frequencies included in the mixture (1). The estimation of the coefficients in the polynomials  $num(i\omega)$  and  $den(i\omega)$  is carried out by the least-squares method to minimize the standard deviation of the  $W_{appr}(i\omega)$  module from the experimental estimate module of the plant frequency transfer function  $W_{exper}(i\omega)$ . The number of frequency points for the computation of standard deviations can be conveniently selected according to the number of frequencies in the mixture (1):

$$W_{exper}(i\omega_k) = d_{1k} + i \cdot d_{2k}, k = 1, \dots, K. \tag{9}$$

The selection of more frequencies is possible. In this case, it will be necessary to approximate the real and imaginary frequency characteristics by cubic splines along with the points  $d_{1k}$  and  $d_{2k}, k = 1, \dots, K$  [17]. However, the testing computations have shown that frequencies number increase improves the accuracy of frequency transfer function coefficients estimation insignificantly.

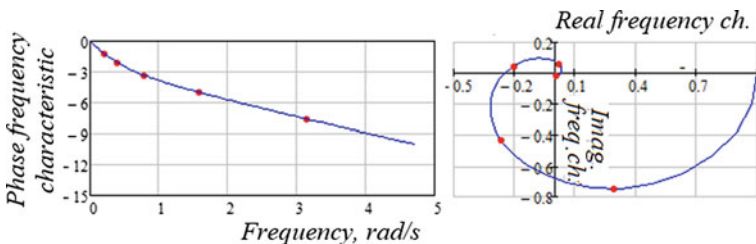


**Fig. 6** Points of phase-frequency characteristic (left) and amplitude-phase characteristic (right) of a plant with time delay

Below, when solving the parameterization problem, we appreciated the advantages of computer mathematics tools, namely the facilities of the open-source software for numerical computation Scilab [18].

The computing process for determining the coefficients of the polynomials  $num(i)$  and  $den(i)$  of the frequency transfer function is carried out in Scilab by the built-in function  $frep2tf(f, W_{exper}(i\omega_k), degree)$ . Here  $f$  is a vector of frequencies with components  $k, k = 1, \dots, K$ , the  $degree$  is the denominator's order of the frequency transfer function  $W_{appr}(i, degree)$ , which is considered as the current approximation to  $W_{exper}(i)$ . The  $degree$  value is used in Scilab to form a  $W_{exper}(i)$  with tunable coefficients, provided the numerator's order is not higher than the denominator's one.

Scilab recommends setting a precise  $degree$  value for the reliable determination of transfer function coefficients. Our computing experiments do not confirm the necessity for an exact  $degree$  value setting. In these experiments the determination of the frequency transfer function denominator's proper order was carried out by iterative search, starting with  $degree = 1$ . For each iteration, the mean square difference between the modules of  $W_{exper}(i\omega)$  and  $W_{appr}(i\omega, degree)$  was computed at  $degree$  values  $= 1, 2, \dots$ . The  $degree^*$  value corresponds to  $degree$  at the iteration in which the mean square difference turns out to be minimum.

You can delete negligibly small values of the coefficients by means of Scilab-function  $clean()$ , which automatically eliminates the coefficients that are less than the specified absolute value of  $e_{abs}$  and/or less than the specified value of  $e_{rel}$  as relative to the maximum coefficient. By default  $e_{abs} = 10^{-10}$ ,  $e_{rel} = 10^{-10}$ .

Since the Laplace transfer function coincides in structure with the frequency transfer function, the result (i.e., the required transfer function with the Laplace variable) is formed by Scilab automatically by means of replacing the frequency complex  $i\omega$  in the found  $W_{appr}(i\omega)$  by the Laplace variable  $s$ .

## 7 Illustrative Example 2

Below, we describe the results of determining the plant transfer function based on the results of real and imaginary frequency characteristics values determination at the points corresponding to the frequencies used in the mixture (1) (these points are represented by the components of the vectors  $d_1$  and  $d_2$  in (6)). Initial data are the same as for illustrative example 1. Results of vectors  $d_1$  and  $d_2$  determination are:

$$d_1 = [0.495; 0.019; -0.119; -0.054; -0.016]^T;$$

$$d_2 = [-0.632; 0.508; 0.173; -0.031; -0.004463]^T.$$

The testing of results consisted in comparison with the theoretical transfer function corresponding to the test function (8) in illustrative example 1. We have compared the found Laplace transfer function with the test transfer function  $W_{test}(s)$  obtained from (8) by replacing the frequency complex ( $i\omega$ ) with the Laplace variable  $s$ :

$$W_{rest}(s) = k/[T_1 \cdot T_2 \cdot s^2 + (T_1 + T_2) \cdot s + 1]; T_1 = 3(c), T_2 = 2(c), k = 1 \quad (10)$$

To take into account the peculiarities of the *freq2tf* () Scilab-function, which transforms the experimental estimates of the real and imaginary frequency characteristics into a parameterized Laplace transfer function, the components of the frequency vector  $f$  in (1) must be expressed in hertz. In this example:

$$f = [1/32; 1/16; 1/8; 1/4; 1/2]^T \quad (11)$$

The processing sequence is as follows:

1. Find the values of the experimental frequency transfer function for each component of the frequency vector by Formula (10) in accordance with  $d_1$  and  $d_2$ ,
2. To calculate the required parametric fractional-rational Laplace transfer function  $H_{appr}(s, degree)$ , it is necessary to specify the order of its denominator. If this order is unknown, the computations are performed iteratively with the sequential values of  $degree = 1, 2, \dots$ . Item 5 specifies the condition for iterations terminating. To define  $H_{appr}(s, degree)$ , the Scilab function *freq2tf* () is applied in the matrix notations accepted in Scilab (as well as in Matlab) [19]:

$$H_{appr} = clean(freq2tf(f, d_1 + i \cdot d_2, degree), e_{abs}, e_{rel}) \quad (12)$$

3. Scilab-function *clean* () eliminates the addends of the transfer function's  $H_{appr}(s, degree)$  numerator and denominator polynomials, if the coefficients in them are less than the specified values  $e_{abs}, e_{rel}$ . In this example,  $e_{abs} = 0.01, e_{rel} = 0.01$ .
4. For each  $degree$  value, estimate the error of the experimental frequency transfer function  $W_{exper}(i\omega)$  restoration by the approximating transfer function  $W_{appr}(i\omega, degree)$ . The obtaining of the last from  $H_{appr}(s, degree)$  consists in replacing the variable  $s$  with the frequency complex ( $i\omega$ ). The replacement process performs by the Scilab-function *repfreq* ():

$$W_{appr} = repfreq(H_{appr}, f).$$

The estimation of mean square error  $error_{degree}$  is follows:

$$error_{degree} = \frac{1}{K} \sum_{k=1}^K (|W_{appr}(i\omega_k, degree)| - |W_{exper}(i\omega_k)|) \quad (13)$$

5. After for some  $degree^*$  the  $error_{degree}$  value becomes the minimum or the denominator of the estimated  $H_{appr}(s, degree)$  consists of the addends with unmatched signs, the calculation terminates. The value  $H_{appr}(s, degree^*)$  is taken as the sought-for fractional-rational Laplace transfer function.

The results of  $H_{appr}(s, degree)$  estimating in this example are:

$$\begin{aligned}
 \text{degree} = 1: H_{appr}(s, 1) &= (-0.34 \cdot s + 1.217)/(5.816 \cdot s + 1); \text{error}_1 = 0.193; \\
 \text{degree} = 2: H_{appr}(s, 2) &= 1.000226/(6.030583 \cdot s^2 + 4.9986741 \cdot s + 1); \\
 &\text{error}_2 = 0.0003734; \\
 \text{degree} = 3: H_{appr}(s, 3) &= (-0.437 \cdot s + 1.192)/(-2.668 \cdot s^3 + 4.97 \cdot s^2 \\
 &+ 5.517 \cdot s + 1.192); \text{error}_3 = 0.0003814;
 \end{aligned}
 \tag{14}$$

With a value of  $degree = 3$ , the signs of the  $H_{appr}(s, 3)$  denominator addends do not coincide, i.e. the estimated transfer function corresponds to an unstable process, which contradicts the initial assumption of plant stability. For  $degree = 2$ , the error is minimal. Therefore, we take the following expression as the required transfer function:

$$H_{appr}(s, 2) = 1.000226/(6.030583 \cdot s^2 + 4.9986741 \cdot s + 1); \tag{15}$$

For the comparison, test transfer function (9) with the parameters  $T_1 = 3(\text{seconds})$ ,  $T_2 = 2(\text{seconds})$ ,  $k = 1$ :  $H_{test}(s) = 1/[6 \cdot s^2 + 5 \cdot s + 1]$ .

Figure 7 (graphs on the left and in the center) illustrates the practical coincidence of the reactions both of the estimated and test transfer functions to the step unit-value input. Figure 7 (on the right, solid line) shows the amplitude-phase characteristic's hodograph corresponding to the transfer function  $H_{appr}(s, 2)$ . Markers show the points of experimental frequency characteristics (components of vectors  $d_1$  and  $d_2$ ). The insignificance of errors of the transfer function determination is illustrated.

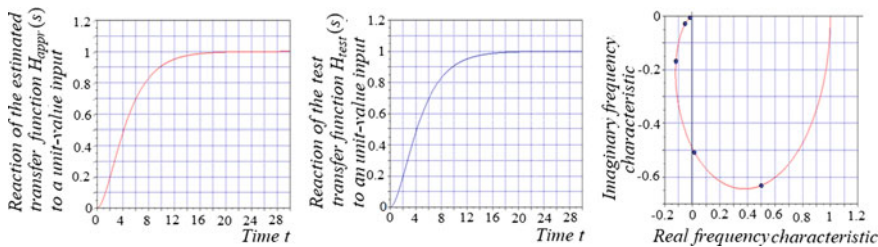


**Fig. 7** Reaction of the estimated transfer function (TF)  $H_{appr}(s, 2)$  to the step unit-value input (left). The reaction of the test TF  $H_{test}(s)$  to the same input (center). Amplitude-phase characteristic of the plant with the estimated TF  $H_{appr}(s, 2)$  (solid line) and the points of experimental characteristics shown by markers (right)

### 8 Illustrative Example 3

The parameters are the same as in illustrative example 2. Estimation of the transfer function with a value of  $degree < degree^*$  may be useful for controlling a high-order process by using control actions of a circuit with a reduced-order process (Fig. 8). The control system is designed to control the output of a plant with a transfer function (14), the denominator of which is second-order polynomial ( $degree = 2$ ). Control actions are formed in the control loop of the reduced-order model with  $degree = 1$ , the denominator of which is the same as in  $H_{appr}(s, 1)$  in (13), and the numerator coincides with the numerator of  $H_{appr}(s, 2)$ . The control loop uses a proportional-integral (PI) controller, the setting parameters of which are selected from the condition of obtaining a 20% overshoot at the output of the feedback loop.

In order to receive the coincidence of the output of the model with  $degree = 2$  and of the circuit for the model with  $degree = 1$ , the system structure includes the unit compensating the distinctions between transfer functions (“Compensator of models’ difference” in Fig. 8) with the transfer function  $H_{comp}(s)$ :

$$H_{comp}(s) = H_{appr}(s, 1)^{-1} \cdot H_{appr}(s, 2) \tag{16}$$

Despite the fact that (15) contains an inverse operator corresponding to the transfer function  $H_{appr}(s, 1)$ , the order of the numerator  $H_{comp}(s)$  remains below the order of the denominator, therefore the condition for the physical feasibility of the compensator is fulfilled.

The purpose of control with the reduced-order model application is to apply “aggressive” PI-controller parameters settings. Those ones increase the control system speed of response, as well as eliminate the oscillation. The same settings in a circuit with a plant of higher-order lead to oscillatory processes in the system up to instability. Figure 9 on the left shows the results of using the control actions generated in the system with a reduced-order model to control a higher-order plant. The system fulfills the target (step function) with high speed, and the plant output process is aperiodic. Application of the same PI controller settings in the control system without using the reduced-order model leads to an oscillating process (Fig. 9 on the right), the time of the transient process is increasing.

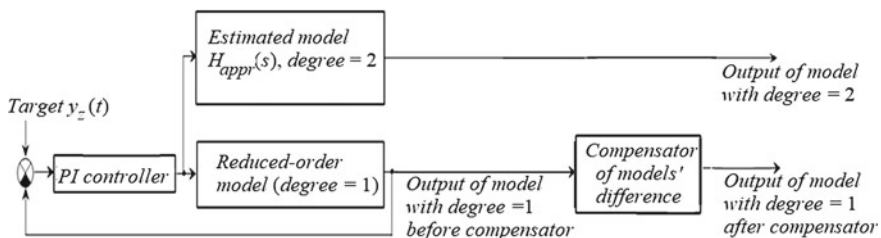
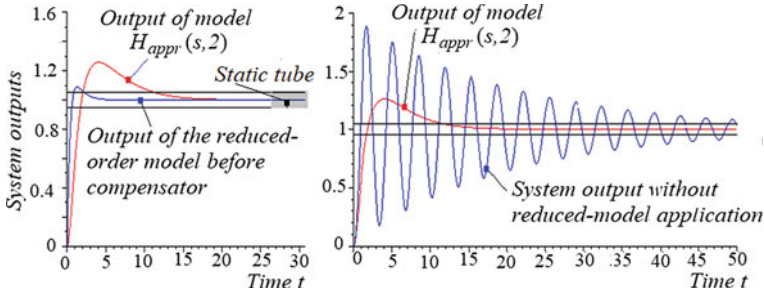
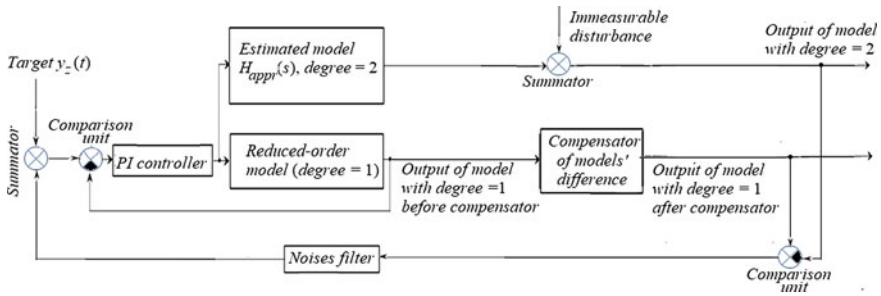


Fig. 8 Control system with reduced-order model application



**Fig. 9** Comparison between the processes of the step target fulfillment in the system (Fig. 8) and the system without reduced-model application



**Fig. 10** Control system with reduced-order model application and with an external feedback loop

The Block diagram in Fig. 10 shows only the proposed control principle itself. This structure is practically unworkable because immeasurable disturbances acting on the  $H_{appr}(s, 2)$  model output do not take into account the control loop with the reduced-order model. Therefore, the control system does not suppress them [20].

Figure 10 shows a more efficient control system structure.

If disturbances are absent, the output of the circuit with  $H_{appr}(s, 2)$  coincides with the output of the contour with a reduced-order model (of course, if the parameters of contours coincide with the prescribed ones). Disturbances are the only reason for distinctions in output signal values. The difference between the output signals with the  $H_{appr}(s, 2)$  and  $H_{appr}(s, 1)$  models gives the estimation of the values of the immeasurable disturbance.

When this difference is not zero, the system corrects the target for the contour of the reduced-order model due to the action of external feedback. Figure 11 illustrates this effect. The process in the system includes two stages. At stage 1, the disturbances are absent, and the outputs of the system with the reduced-order model (after the compensator; the graph is represented by a solid line) and the full-order model  $H_{appr}(s, 2)$  (shown by markers) coincide. At the end of stage 1, the output of the  $H_{appr}(s, 2)$  model receives a stepwise disturbance. Figure 11 (left) illustrates no response of the control system to an immeasurable disturbance when using the structure of Fig. 8.

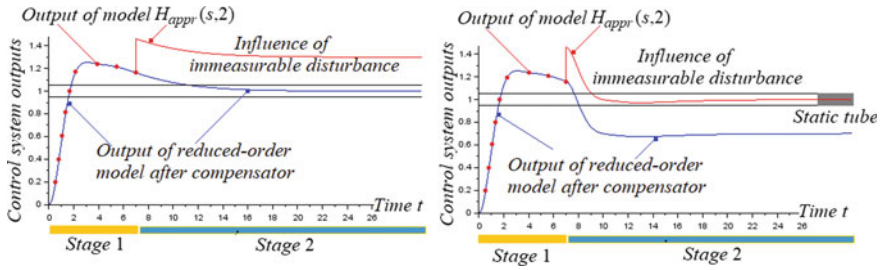


**Fig. 11** Illustration of the influence of immeasurable disturbance on the operation of the systems without external feedback(left) and with the presence of it (right)

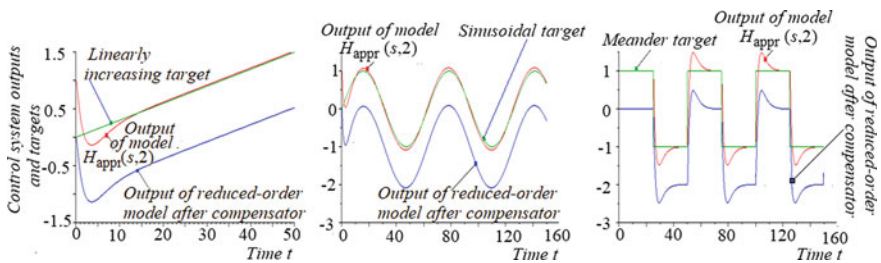


**Fig. 12** The different targets tracking in the control system with the reduced-order model application

Therefore, the effect of working out the target is lost. The right of Fig. 11 illustrates the action of external feedback: when a disturbance appears, the target for a circuit with a reduced-order model redefines. The combined influence of the “artificial” target value and immeasurable disturbance assures correct system reaction to the desired target value (Fig. 12).

## 9 Conclusion

The chapter describes the method of the control plant’s frequency properties quick estimation, based on the processing of data on the plant’s response to a harmonic signal in the form of sinusoidal components mixture.

The example of closed-loop system stability estimation shows the method’s possibilities in the conditions of incomplete information about the plant model.

The results of a quick determination of the plant frequency properties may be useful for its transfer function parametric identification.

The example of the design of the system including the reduced-order model illustrates one of the possible applications of the transfer function’s parametric identification results.



## References

1. Fomin, O., Akimova, A., Akimova, J., Mastepan, A.: The criteria choice of evaluating the effectiveness of the process and automatic control systems. *Procedia Comput. Sci.* **149**, 246–251 (2019). <https://doi.org/10.1016/j.procs.2019.01.130>
2. Brunton, S.L., Kutz L.N.: *Linear Control Theory. Data Driven Science & Engineering: Machine Learning, Dynamical Systems, and Control.* Cambridge (2019)
3. Söderlind, G.: Automatic control and adaptive time-stepping. *Numer. Alg.* **31**, 281–310 (2002). <https://doi.org/10.1023/A:1021160023092>
4. Bamieh, B., Giarré, L.: Identification of linear parameter varying models. *Int. J. Robust Nonlinear Control* 841–853 (2002)
5. Čalasan, M.P., Abdel Aleem, S.H., Bulatović, M., Rubezic, V., Ali, Z.M., Micev, M.: Design of controllers for automatic frequency control of different interconnection structures composing of hybrid generator units using the chaotic optimization approach. *Int. J. Electr. Power Energy Syst.* (2021)
6. Becker, R., King, R., Petz, R., Nitsche, W.: Adaptive closed-loop control on a high-lift configuration using extremum seeking. *AIAA J.* **45**(6), 92–1382 (2007)
7. Xu, J., Wen, C., Xu, D.: Optimal control data scheduling with limited controller-plant communication. *Sci. China Inf. Sci.* **61**, 012202 (2018). <https://doi.org/10.1007/s11432-016-9073-y>
8. Iczkovich, E.L.: Competitiveness of Russian controller manufacturers in the market of production automation. *Industrial automated control systems and controllers* (2), 4–10 (2008)
9. Aleshin, I.Y., Sycheva, A.V., Agisheva, D.K.: Interpolation of unknown functions by cubic splines. *Modern high-tech technologies.* (5–2), 188–189 (2014)
10. Zhang, G., Wu, H.: An all-coefficient adaptive control method for a class of nonlinear time-varying systems. *Sci. China Ser. F-Inf. Sci.* **52**, 1730–1738 (2009). <https://doi.org/10.1007/s11432-009-0176-8>
11. Sha, L., Abdelzaher, T., árzen, K.E., et al.: Real time scheduling theory: a historical perspective. *Real-Time Syst.* **28**, 101–155 (2004). <https://doi.org/10.1023/B:TIME.0000045315.61234.1e>
12. Polyak, B.T., Shcherbakov, P.S.: Hard problems in linear control theory: possible approaches to solution. *Autom. Remote Control* **66**, 681–718 (2005)
13. Barkhatov, V.A.: Identification of patterns of a parametrically specified class. *Russ. J. Nondestruct. Test.* (45), 73–85 (2009)
14. Kurina, G.A.: Invertibility of an operator appearing in the control theory for linear systems. *Math. Notes* (70), 206–212 (2001)
15. Matveev, A.S.: Theory of optimal control in the works of V.A. Yakubovich. *Autom. Remote Control.* (67), 1645–1698 (2006)
16. Grasse, K.A.: Admissible simulation relations, set-valued feedback, and controlled invariance. *Math. Control Sig. Syst.* (20), 199–226 (2008)
17. Stephen, L., Campbell, J.-P., Chancelier, R.: *Modeling and simulation Scilab. Scicos*, 1st edn. Springer (2006)
18. Baresi, L., Delamaro, M., Nardi, P.: Test oracles for Simulink-like models. *Autom. Softw. Eng.* **24**, 369–391 (2017)
19. Schaub, H., Akella, M.R., Junkins, J.L.: Adaptive realization of linear closed-loop tracking dynamics in the presence of large system model errors. *J. Astronaut. Sci.* **48**, 537–551 (2000)
20. Wu, M., Zhou, L., She, J., et al.: Design of robust output-feedback repetitive controller for class of linear systems with uncertainties. *Sci. China Inf. Sci.* **53**, 1006–1015 (2010)

# Combined Control of Technological Processes with Delay



I. V. Gogol, O. A. Remizova, V. V. Syrokvashin, and A. L. Fokin

**Abstract** The chapter considers a control system for objects with delay. Based on traditional regulation laws, an analogy is drawn for the design of complex regulation systems using an additional compensation unit. The chapter presents a technique for obtaining structures of regulators. As a demonstration of the efficiency of the control system, in addition to a single step action, a harmonic oscillation was chosen as a disturbing effect. A comparative analysis of the proposed structures of combined control systems was carried out. The operability of the combined control has been checked under the conditions of disturbances that cannot be measured and in the presence of parametric uncertainty associated with setting the delay value at the input of the control object. It is assumed that the uncertainty in the lag is such that the predictor cannot be applied. It is shown that the system with a traditional estimation of the disturbance is unstable. A structure is proposed that ensures coarseness to parametric uncertainty and provides high-quality stabilization of the output value. For a clear demonstration of the proposed methodology in the work, as an example, the calculation of a control system with a traditional PI regulation law is given. As a test of the operability of the obtained system, a disturbing effect was applied in the form of a sinusoidal signal, and the system was modeled with the application of a disturbance, the types of transient characteristics, which are presented in the work.

**Keywords** Combined control system · Robust system · System robustness · Perturbation

## 1 Introduction

The problem of parrying disturbances is one of the most important tasks of control theory. Perturbations are uncontrolled external or internal effects on the process. They can act at any point in the technological scheme, but most often they are brought to the entrance or exit of the control object. There are also possible cases

---

I. V. Gogol · O. A. Remizova (✉) · V. V. Syrokvashin · A. L. Fokin  
Saint-Petersburg State Institute of Technology, Saint-Petersburg, Russia  
e-mail: [remizova-oa@technolog.edu.ru](mailto:remizova-oa@technolog.edu.ru)

© The Author(s), under exclusive license to Springer Nature Switzerland AG 2022  
A. G. Kravets et al. (eds.), *Cyber-Physical Systems: Modelling and Industrial Application*,  
Studies in Systems, Decision and Control 418,  
[https://doi.org/10.1007/978-3-030-95120-7\\_16](https://doi.org/10.1007/978-3-030-95120-7_16)

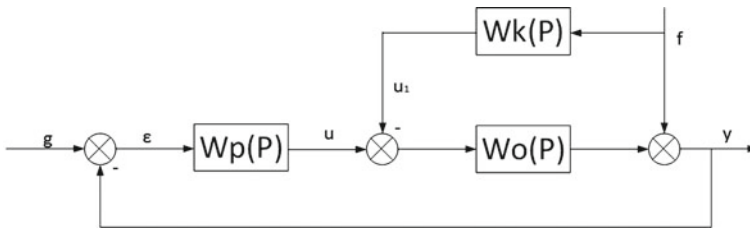


**Fig. 1** Combined control system

when an object is presented in the form of a complex structure, at different points of which disturbing influences can act. But to study the theoretical possibilities of compensating perturbations for simplicity, we will consider perturbations at the input or output of a controlled object.

From a technological point of view, disturbances at the inlet can easily be caused by such interference as uncontrolled changes in the grindability of the milled material at the inlet of the mill, changes in the calorific value of the fuel at the inlet of the burner in the furnace, changes in the concentration or consumption of material at the inlet of the reactor, etc. Uncontrolled changes in the load can be attributed to output disturbances: mechanical, hydraulic, temperature, etc.

For definiteness, in this chapter, we will consider perturbations at the output of the object, which cannot be measured and which can be assigned to the class of bounded functions or the set of functions from the space  $L_2$ , that is, square-integrable functions. It is known [1] that optimal control by the integral quadratic criterion is achieved within the framework of a dual-circuit system of combined control. The structural diagram of such a system is shown in Fig. 1.

Here it is assumed that the disturbance can be measured. Note that under the action of a perturbation from  $L_2$  the stabilization problem is also solved within the framework of single-loop systems. Here optimal solutions are possible within the framework of  $H^2$  and  $H^\infty$  control theory. If an arbitrary bounded disturbance acts, then a combined control is required to solve the stabilization problem. Otherwise, in a steady state, an object will appear in the output of the object.

In our case, the transfer function of the object  $W_0(p)$  contains a delay link; therefore, a predictor is usually used to effectively perturb disturbances [2–12]. A limitation for the use of a structure with a predictor is an exact knowledge of the delay value. In this chapter, we assume a significant uncertainty of delay, which can be defined as the uncertainty in which the scheme with the predictor is inoperative.

Therefore, the urgent task is to build a combined control under the action of an arbitrary non-measurable disturbance from the indicated classes in the presence of significant uncertainty in the value of the delay and parametric uncertainty of the inertial part of the transfer function of the object.

## 2 Formulation of the Problem

If the disturbance cannot be measured, then its estimate is used for control [13–17], which can be obtained if the mathematical model of the object in the form of the transfer function  $W_0^0(p)$  is known. The block diagram is shown in Fig. 2.

In this case, the estimate  $f_1$  contains information about the perturbation  $f$ , as well as the uncertainty of the mathematical model of the object. We show that, given the uncertainty of the delay value, the reduced structure of the system is inoperative.

Statement 1 Compensation circuit (Fig. 2) in the presence of uncertainty of the task of the delay value is unstable.

For proof, we consider the case when there is no parametric uncertainty in the inertial part, and the delay value is known with the uncertainty  $\Delta\tau > 0$ . Then, if  $\tau_0$  is the nominal value of the delay value in the object, then  $W_0(p) = \bar{W}_0(p) \exp(-(\tau_0 + \Delta\tau)p)$ ,  $\bar{W}_0^0(p) \exp(-\tau_0 p)$  and  $\bar{W}_0(p) = \bar{W}_0^0(p)$ .

Grade  $f_1$  can be found by the formula

$$f_1(p) = \Delta W(p)u(p) + f(p), \Delta W(p) = W_0(p) - W_0^0(p), \tag{1}$$

The signal at the input of the object, compensating for the disturbance  $f(p)$  at the output will be

$$u_1 = W_K(p)f_1(p) = W_K(p)(\Delta W(p)u(p) + f(p)). \tag{2}$$

The compensation condition for the two-channel scheme is as follows

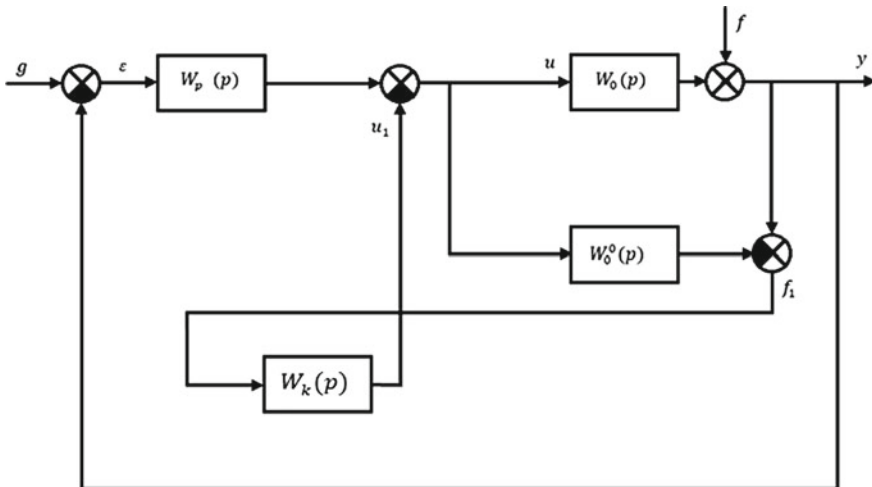


Fig. 2 Combined control with perturbation estimation

$$f(p) - W_0(p)W_K(p)f_1(p) = f(p) - W_0(p)W_K(p)(\Delta W(p)u(p) + f(p)). \quad (3)$$

It is seen that full compensation is impossible since the value of  $\Delta W(p)$  is unknown. With this in mind, we get

$$W_K(p) = (W_0^0(p))^{-1} = (\overline{W_0^0(p)})^{-1} \exp(\tau_0 p). \quad (4)$$

This shows that a predictor is needed for control. If the construction of the predictor is impossible, then instead of (4) in practice, use the formula

$$W_K(p) = (W_0^0(p))^{-1}. \quad (5)$$

Based on (3) we get

$$u_1(p) = (W_0^0(p))^{-1} (\Delta W(p)u(p) + f(p)). \quad (6)$$

Consider the expression (6) in the presence of negative feedback in the loop for estimating the perturbation of  $u = -u_1$  at  $\varepsilon =$ . Then the characteristic equation based on (6) will be

$$1 + (W_0^0(p))^{-1} (\Delta W(p)) = 0. \quad (7)$$

Substituting the transfer functions  $W_0^0(p)$  and  $W(p)$ , we obtain

$$1 + (W_0^0(p)\exp(-p\tau))^{-1} W_0^0(p)(\exp(-p(\tau + \Delta\tau)) - \exp(-p\tau)) = 0. \quad (8)$$

Then

$$1 + \exp(-p\Delta\tau) - 1 = 0.$$

Or

$$\exp(-p\Delta\tau) = 0. \quad (9)$$

We use the Maclaurin expansion, then the left-hand side of (9) can be represented with any degree of accuracy by a polynomial of arbitrary degree, and instead of (9) we get

$$1 - \Delta\tau p + \frac{(\Delta\tau)^2}{2!} p^2 - \dots + (-1)^k \frac{(\Delta\tau)^k}{k!} p^k = 0. \quad (10)$$

For the characteristic Eq. (10), the necessary stability conditions are not satisfied, since the characteristic polynomial has negative coefficients (Stodola stability criterion). Thus, Proposition 1 is proven. The simulation results confirm this.

Next, the task is to build a combined control, operable in the presence of significant uncertainty in setting the value of the delay.

### 3 Research Results

To solve the problem, the structural scheme [18, 19] shown in Fig. 3 is considered in the work.

This block diagram contains a physically feasible additional loop of the servo system to compensate for the disturbance, which does not contain a disturbance predictor. The signal  $u_1$  is used to compensate disturbance. For this, the estimate  $f_1$  for the disturbance  $f$  is used. It is fed to the input of the tracking system, which is the model for the formation of  $f$  in the main circuit. The signal  $u_1$  appears in this model at the input of the object model and is fed to the input of a real object with the opposite sign for compensation.

Consider the model of the object in the form of a transfer function

$$y(p) = W_0(p)u(p) + f(p), \tag{11}$$

where  $f(p)$  disturbance,  $u(p)$  control,  $y(p)$  output quantity.

We consider the transfer function of the following form

$$W_0(p) = k_0 \frac{\beta(p)}{\alpha(p)} \exp(-\tau p), \tag{12}$$

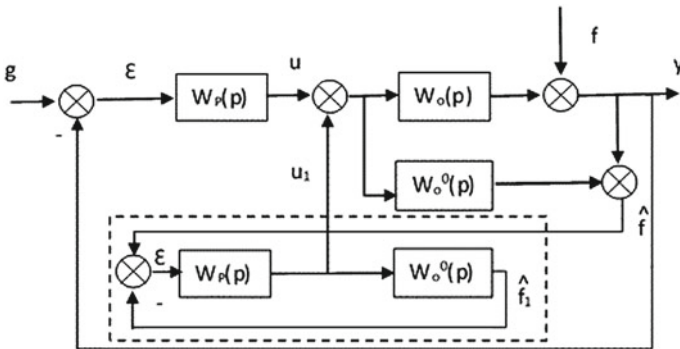


Fig. 3 Combined control with perturbation estimation

where  $\alpha(p)$ ,  $\beta(p)$  polynomials whose roots are located strictly to the left of the imaginary axis,  $\alpha(0) = \beta(0) = 1$ ,  $k_0$  gear ratio,  $\underline{k}_0 \leq k_0 \leq \bar{k}_0$ ,  $\underline{\tau} \leq \tau \leq \bar{\tau}$ .

For disturbance, it is assumed that the restrictions on the magnitude of the absolute value and derivatives

$$|f^k(t)| \leq M_K, k = 0, 1, \dots, K, \quad (13)$$

where  $K$  maximum order of derivative in question.

From the set of transfer functions (12) we single out the nominal transfer function, which has the following form

$$W_0^0(p) = k_0^0 \frac{\beta_0(p)}{\alpha_0(p)} \exp(-\tau_0 p), \quad (14)$$

where  $k_0^0$ ,  $\tau_0$ —nominal values of gear ratio and delay,  $\beta_0(p)$ ,  $\alpha_0(p)$ —nominal polynomials of numerator and denominator,  $\underline{k}_0 \leq k_0^0 \leq \bar{k}_0$ ,  $\underline{\tau} \leq \tau_0 \leq \bar{\tau}$ .

The goal of control is to fulfill inequality

$$|g(t) - y(t)| \leq \delta, \quad (15)$$

where  $g(t)$ —the target value of system input,  $y(t)$ —system output,  $\delta$ —set value of error.

To do this, it is supposed to generate a signal  $u_1(t)$ , that compensates for the disturbance  $f(t)$  with a given accuracy

$$|f(t) - W_0(p)u_1(t)| \leq \delta_1, \quad (16)$$

where  $u_1(t)$ —disturbance compensation signal,  $\delta_1$  compensation error.

Based on the structural diagram, we obtain

$$f_1(p) = W_0(p)u(p) + f(p) - W_0^0(p)u(p) = \Delta W(p)u(p) + f(p), \quad (17)$$

where  $\Delta W(p) = W_0(p) - W_0^0(p)$ .

$$u_1(p) = \frac{W_P(p)}{1 + W_P(p)W_0^0(p)} (\Delta W(p)u(p) + f(p)), \quad (18)$$

where  $u(p) = W_P(p)\varepsilon(p) - u_1(p)$ .

In the nominal system at  $\Delta W(p) = 0$ , from Formula (18) we obtain

$$u_1(p) = \frac{W_P(p)}{1 + W_P(p)W_0^0(p)} f(p). \quad (19)$$

To compensate for the disturbance  $f$  at the output of the object in the nominal system, a signal is used

$$W_0^0(p)u_1(p) = \frac{W_P(p)W_0^0(p)}{1 + W_P(p)W_0^0(p)}f(p). \quad (20)$$

For an object (12), expression (20) exactly coincides with the transfer function of the closed nominal system of the main circuit.

The following statement is true here.

Statement 2 Within the framework of the proposed structure (Fig. 3), the nominal disturbance compensation system  $f$  is described by the transfer function, which coincides with the transfer function of the closed nominal system of the main circuit.

Consequence 1 Both systems have the same robustness, which is numerically evaluated using the  $H^\infty$ —of the sensitivity function [20].

Based on Formula (18) we obtain

$$u_1(p) = \frac{1}{1 + W_P(p)(W_0^0(p) + \Delta W(p))} [W_P(p)(\Delta W(p)W_P(p)\varepsilon(p) + f(p))]. \quad (21)$$

For the error signal, we obtain

$$\varepsilon(p) = g(p) - y(p) = g(p) - (f(p) + W_0(p)W_P(p)\varepsilon(p) - W_0(p)u_1(p)).$$

From this, taking into account (21), we obtain

$$\varepsilon(p) = \frac{1}{a(p)} \{ [1 + W_P(p)(W_0^0(p) + \Delta W(p))] - [1 + W_P(p)(W_0^0(p) + \Delta W(p)) - W_P(p)W_0]f(p) \}, \quad (22)$$

where  $a(p) = (1 + W_P(p)W_0(p))(1 + W_P(p)W_0^0(p)) + W_P(p)\Delta W(p)$ .

From (22) it is clear that for the nominal system with  $\Delta W(p) = 0$  along the channel  $g \rightarrow \varepsilon$  we get

$$\varepsilon(p) = \frac{1}{1 + W_P(p)W_0(p)}g(p). \quad (23)$$

This model coincides with the corresponding model for the main circuit; therefore, the following statement.

Statement 3 The introduction of a compensation system does not affect the dynamics of the main circuit.

Consequence 2 If, together with the slowly varying perturbation under consideration, a random perturbation or function from  $L_2$ , acts, which are traditionally considered in control theory and eliminated by the action of the main circuit, then



the introduction of a compensation system does not affect the compensation of these perturbations.

Based on Formula (22), we can study the accuracy of the system in the steady-state. If the transfer function of the controller  $W_P(p)$  contains an integrator, then in the steady-state  $p \rightarrow 0$  we get  $W_P(p) \rightarrow \infty$ .

Therefore, in the steady-state, based on (22), we obtain  $\varepsilon(p) \rightarrow 0$ , since the transfer function of the controller in the denominator is present in the square, and the numerator only in the first degree. Thus, the first-order astatism occurs. There is no static error for a step disturbance. Under the action of a limited perturbation of an arbitrary shape, an error occurs, and its value depends on the frequency spectrum in which the perturbation signal is located.

To estimate the compensation error (16) after substituting (22) into (21), we obtain

$$u_1(p) = - \left\{ \frac{W_P^2(p) \Delta W(p) [1 + W_P(p)(W_0^0(p) + \Delta W(p) - W_P(p)W_0(p))]}{1 + W_P(p)(W_0^0(p) + \Delta W(p))} \right\} f(p) + \frac{W_P^2(p) \Delta W(p)}{a(p)} g(p). \quad (24)$$

Therefore, taking into account  $W(p) = W_0(p) - W_0^0(p)$  at  $p \rightarrow 0$ ,  $W_P(p) \rightarrow \infty$ , we obtain for the steady-state

$$u_1(t) = \frac{\Delta W(0)}{W_0^0(0)W_0^0} g(t) + \frac{1}{W_0(0)} f(t).$$

Therefore

$$|f(t) - W_0(0)u_1(t)| \leq \frac{|\Delta W(0)|_{max}}{|W_0^0(0)||g(t)|1_{max}}. \quad (25)$$

Thus, the introduction of an additional closed servo system of disturbance compensation in the control loop instead of the predictor makes it possible to construct a robust system with compensation for a varying limited disturbance at the output of the control object with a control delay due to the robust control law in the main circuit and in the compensation system. It is required to provide a five percent error of disturbance compensation. This is achieved in the low-frequency region.

### 4 Example

Consider the nominal transfer function of an object of the form

$$W_0^0(p) = \frac{2exp(-10p)}{15p + 1}. \tag{26}$$

Let the PI law with robust settings be used [21–24]

$$W_P(p) = \frac{0.343}{20} \frac{15p + 1}{p}. \tag{27}$$

In the presence of a sinusoidal disturbance  $f(t) = sin0.005t$  for the system in Fig. 3, we obtain the transition characteristic shown in Fig. 4

If there is uncertainty in setting the value of the delay  $\Delta\tau = 12.5c$  the system is at the stability boundary, this is 125%. With  $\Delta\tau = 4.8c$  the overshoot is 30%. In the steady state, the maximum error is 5%. The transient response is shown in Fig. 5.

Thus, the combined control, which is carried out following the structural diagram shown in Fig. 3, has significant rudeness concerning the uncertainty of setting the delay value, since when the delay increases in the object relative to the nominal value by almost 50%, a 30% value for overshooting is guaranteed and 5% steady-state accuracy. That is, the system under these conditions does not lose operability.

Another advantage of this scheme is that it can be used to compensate for a limited perturbation in the steady-state when solving the stabilization problem, but the accuracy depends on the frequency, and with its increase, the accuracy decreases.

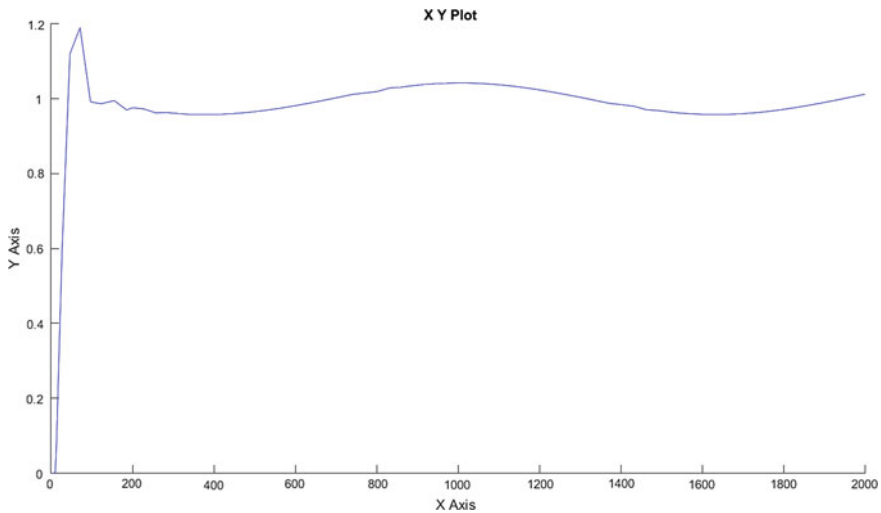


Fig. 4 Transient response in the presence of a sinusoidal disturbance

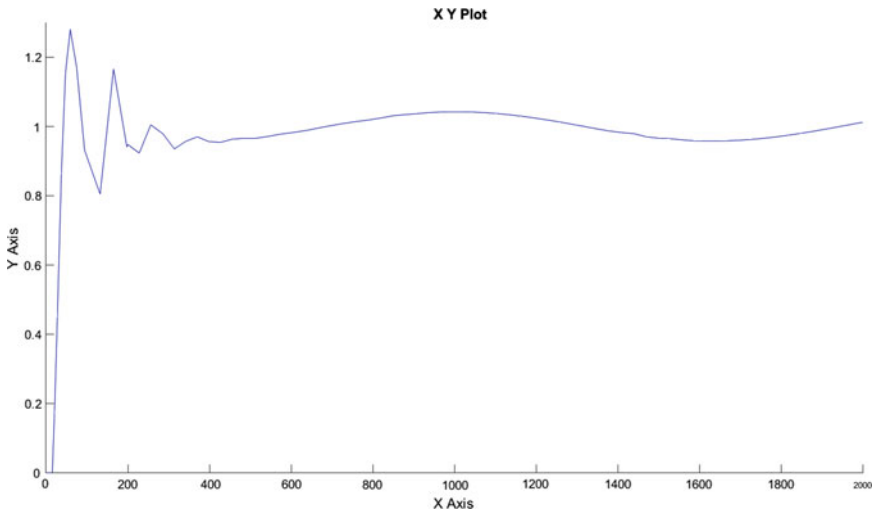


Fig. 5 Transient response in the presence of a 48% delay uncertainty

## 5 Conclusion

The chapter considers the problem of constructing a combined control system under conditions when the perturbation cannot be measured, and the delay value is set with significant uncertainty so that the construction of the predictor is impossible. It is proved that a system with a traditional scheme for estimating perturbations is unstable under these conditions. In the work, another structural scheme of combined control is proposed, which allows one to ensure good quality of compensation of disturbances from the space  $L_2$ , as well as 5% accuracy in the steady-state under the action of a limited disturbance. Moreover, the robustness of the compensation loop is the same as the robustness of the main loop, which in turn depends on the choice of controller. Therefore, the solution to the problem of synthesizing robust control of a control system by mistake simultaneously solves the problem of the rudeness of a control system by perturbation.

## References

1. Pervozvansky, A.A.: Kurs teorii avtomaticheskogo upravlenija [Automatic control theory course], 616p. M.: Nauka (1986) (in Russ.)
2. Bobtsov, A.A., Kolyubin, S.A., Pyrkin, A.A.: Kompensacija neizvestnogo mul'tigarmonicheskogo vozmushhenija dlja nelinejnogo obekta s zapazdyvaniem po upravleniju [Compensation of an unknown multiharmonic disturbance for a nonlinear plant with control delay]. *Avtomatika i telemekhanika* **11**, 136–148 (2010) (in Russ.)
3. Pyrkin, A.A.: Adaptivnyj algoritm kompensacii parametricheski neopredelennogo smeshennogo garmonicheskogo vozmushhenija dlja linejnogo obekta s zapazdyvaniem v kanale

- upravljenija [An adaptive compensation algorithm for a parametrically uncertain shifted harmonic disturbance for a linear plant with a delay in the control channel]. *Avtomatika i telemekhanika* **8**, 62–78 (2010) (in Russ.)
4. Pyrkin, A., Smyshlyaev, A., Bekiaris-Liberis, N., Krstic, M.: Rejection of sinusoidal disturbance of unknown frequency for linear system with input delay. In: American Control Conference, Baltimore, USA (2010)
  5. Pyrkin, A.A., Bobtsov, A.A., Kolyubin, S.A.: Stabilizacija nelinejnogo ob#ekta s vhodnym zapazdyvaniem i sinusoidal' nym vozmushhahushhim vozdejstviem [Stabilization of a nonlinear plant with input lag and sinusoidal disturbance]. *Avtomatika i telemekhanika* **1**, 21–30 (2015) (in Russ.)
  6. Basturk, H., Krstic, M.: Adaptive sinusoidal disturbance cancellation for unknown LTI systems despite input delay. *Automatica* **58**, 131–138 (2015)
  7. Pyrkin, A.A., Bobtsov, A.A., Nikiforov, V.O.: Output adaptive controller for linear system with input delay and multisinusoidal disturbance. In: International Conference on Control Applications, vol. 23, Antibes, pp 1777–1782. IEEE, France (2014)
  8. Pyrkin, A., Wang, J., Vedyakov, A.: Output adaptive controller for a class of MIMO systems with input delay and multisinusoidal disturbance. In: 1st IFAC Conference on Modelling, Identification and Control of Nonlinear Systems, SPb: IFAC, pp. 902–909 (2015)
  9. Pyrkin, A.A., and etc.: Kompensacija poligarmonicheskogo vozmushhenija, dejstvujushhego na sostojanie i vyhod linejnogo objekta s zapazdyvaniem v kanale upravljenija [Compensation of polyharmonic perturbations acting on the state and output of a linear object with a delay in the control channel]. *Avtomatika i telemekhanika* (12), 43–64 (2015) (in Russ.)
  10. Gerasimov, D.N., Paramonov, A.V., Nikiforov, V.O.: Adaptive disturbance compensation in linear systems with input arbitrary delay: internal model approach. In: 8th International Congress on Ultra Modern Telecommunications and Control Systems and Workshops, [S. l.: s. n.], pp. 304–30 (2016)
  11. Gerasimov, D.N., Paramonov, A.V., Nikiforov, V.O.: Algorithms of fast adaptive compensation of disturbance in linear systems with arbitrary input delay. *IFAC-PapersOnLine*, [S. l.: s. n.], vol. 50, no. 1, pp. 12892–12897 (2017)
  12. Gerasimov, D.N., Paramonov, A.V., Nikiforov, V.O.: Adaptive tracking of unknown multi-sinusoidal signal in linear systems with arbitrary input delays and unknown sign of high frequency gain. *IFAC-PapersOnLine*, [S. l.: s. n.], vol. 50, no. 1, pp. 7052–7057 (2017)
  13. O'Dwyer, A.: *Handbook of PI and PID Controller Tuning Rules*, 3rd edn., 411p. Imperial College Press (2009)
  14. Silva, G.J., Datta, A., Bhattacharyya, S.P.: *PID controllers for time-delay systems*, p. 327p. Birkhauser, Boston (2005)
  15. Visioli, A., *Practical, P.I.D.*: Control, p. 286. Springer, London (2006)
  16. Smith, C.A., Corripio, A.B.: *Principles and Practice of Automatic Process Control*, 2nd edn., 573p. Wiley (1997)
  17. Astrom, K.J., Hagglund, T.: *PID Controllers: Theory, Design and Tuning*. 2nd edn., 343p. Instrument Society of America (1995)
  18. Remizova, O.A., Fokin, A.L.: Robastnoe upravlenie ustojchivym tehničeskim obektom pri nalichii zapazdyvanija po upravljeniju s kompensaciej vozmushhenij [Robust control of a stable technical object in the presence of a control delay with compensation of disturbances]. *Izv. vuzov. Priborostroenie* **59**(12), 10–17 (2016) (in Russ.)
  19. Gogol, I.V., Remizova, O.A., Syrokvashin, V.V., Fokin, A.L.: Upravlenie tehničeskimi sistemami s zapazdyvaniem pri pomoshhi tipovyh regulja-torov s kompensaciej vozmushhenij [Control of technical systems with delay using standard controllers with disturbance compensation]. *Izv. vuzov. Priborostroenie* **60**(9), 882–890 (2017) (in Russ.)
  20. Egupov, N.D.: *Metody robastnogo, nejro-nechetkogo i adaptivnogo upravljenija* [Methods of robust, neuro-fuzzy and adaptive control], 744p. M.: BMSTU (2002) (in Russ.)
  21. Remizova, O.A., Syrokvashin, V.V., Fokin, A.L.: Sintez robastnyh sistem upravljenija s tipovymi reguljatorami [Synthesis of robust control systems with standard controllers]. *Izv. vuzov. Priborostroenie* **58**(12), 12–18 (2015) (in Russ.)

22. Fokin, A.L.: Sintez robustnyh sistem upravlenija tehnologicheskimi processami s tipovymi reguljatorami [Synthesis of robust process control systems with standard regulators]. *Izv. Spbsti(TU)* (27), 101–106 (2014) (in Russ.)
23. Kostyukov, V., Medvedev, M., Pavlenko, D., Mayevsky, A., Poluyanovich, N.: The rotor speed controlling possibilities of a promising wind-driven power plant using several variable elements of its geometry. In: Kravets, A.G., Bolshakov, A.A., Shcherbakov, M. (eds.) *Cyber-physical Systems: Design and Application for Industry 4.0. Studies in Systems, Decision and Control. Series, vol. 342*, pp. 49–60 (2020)
24. Demin, S., Panischev, O., Yunusov, V., Timashev, S.: The application of statistical methods for the analysis of multi-parameter data of complex composite objects in the field of cyber-physical systems. In: Kravets, A.G., Bolshakov, A.A., Shcherbakov, M. (eds.) *Cyber-Physical Systems: Digital Technologies and Applications. Studies in Systems, Decision and Control. Series, vol. 350*. pp. 27–38. [https://doi.org/10.1007/978-3-030-67892-0\\_3](https://doi.org/10.1007/978-3-030-67892-0_3)

# Robust Control Objects with Delayed Admission by the Extended Model



I. V. Gogol, I. V. Zhukov, O. A. Remizova, and A. L. Fokin

**Abstract** The problem of robust control of an object with delay is one of the main ones in the automation of technological processes. There are many different approaches to solving the problem of controlling an object with input delay under conditions of uncertainty. In this case, one of the poorly studied problems of robust control in the presence of delay is to provide a compromise between the speed of response and the roughness of the system. When automating, an interesting solution is in the class of traditional regulators. As a rule, an increase in roughness is associated with a decrease in performance. Therefore, the actual task of obtaining the highest performance for a given degree of coarseness. This problem was solved based on the robust Nyquist criterion in the class of traditional regulation laws. In this chapter, we propose another approach to constructing a robust system for an object with delay, which makes it possible to obtain a close to the optimal ratio between roughness and speed, which is confirmed by modeling. This approach is based on the method of using the extended object model. An output regulator is considered, synthesized using the polynomial approach based on the previously obtained optimal distribution of the poles of a closed system based on an extended model of an object that ensures the robustness of the system.

**Keywords** Robustness · Combined control · Uncontrolled perturbation · Limited perturbations

## 1 Introduction

In this work, rough (robust) control will be understood as a control that provides a low sensitivity of the controlled variable to the parametric uncertainty of the object model. Changing the coefficients of the transfer function of the object and the magnitude of the delay when solving stabilization problems leads to the need for frequent readjustment of the controller parameters and reduces the reliability of the control

---

I. V. Gogol · I. V. Zhukov · O. A. Remizova (✉) · A. L. Fokin  
Saint-Petersburg State Institute of Technology, Saint-Petersburg, Russia  
e-mail: [remizova-oa@technolog.edu.ru](mailto:remizova-oa@technolog.edu.ru)

© The Author(s), under exclusive license to Springer Nature Switzerland AG 2022  
A. G. Kravets et al. (eds.), *Cyber-Physical Systems: Modelling and Industrial Application*,  
Studies in Systems, Decision and Control 418,  
[https://doi.org/10.1007/978-3-030-95120-7\\_17](https://doi.org/10.1007/978-3-030-95120-7_17)

system due to a possible loss of stability. With robust control, the interval between reconfigurations and the reliability of the system increase accordingly.

For automation of technological processes, the coarseness of the system is usually sufficient, at which it is possible to change the parameters, including delays, by 3–4 times without loss of stability and by 1.5–2 times while maintaining quality indicators, mainly speed and overshoot. Note that in the literature [1] there is information about a possible change in the delay up to 10 times in a cold rolling mill, and the problem of ensuring maximum roughness is being solved. But in principle, it is always possible to provide maximum robustness with a loss of performance. In the simplest version, it is sufficient to use a small transfer coefficient  $P$  as a component of the regulation law. Therefore, the problem of a simple increase in roughness is not posted here, but only together with the analysis of performance.

In [2], one more problem of designing a robust system by the criterion of aperiodic stability was considered when replacing the delay link with the Padé approximation. The obtained algorithms do not have an optimal compromise between roughness and speed. In terms of speed, these algorithms are inferior to the optimal ones considered in [3]. But the big advantage here is that they practically do not require adjustment—the transfer function of the regulator in the form of PID, PI, PD laws can easily (without calculations on a computer) be obtained directly from the transfer function of the object. This allows you to quickly solve the problem of robust controller tuning in the first approximation. Besides, it should be noted that these algorithms are not inferior to PI and PID laws in the MATLAB package, and in some cases they are superior.

## 2 Problem Statement

At the heart of the proposed methodology, an analytical expression in the generalized form of a mathematical model is considered as a typical automation object, which is a linear inertial object with the delay with one input and one output, which is described by a transfer function

$$y(p) = \frac{\beta_m(p)}{\alpha_n(p)} \exp(-\tau p) \cdot u(p) \quad (1)$$

where  $\beta_m(p)$ ,  $\alpha_n(p)$  are arbitrary polynomials of  $m$ ,  $n$  degree respectively ( $m \leq n$ ), the coefficients of the polynomials  $\beta_m(p)$ ,  $\alpha_n(p)$  can vary in intervals, as well as the delay  $\underline{\tau} \leq \tau \leq \bar{\tau}$ .

To improve the quality indicators of a robust system, it is better to consider a narrower formulation of the problem, when the polynomials  $\beta_m(p)$ ,  $\alpha_n(p)$  are Hurwitz, or there are one or more poles of the transfer function of the object at the point zero—this is a fairly common situation in practice. In addition to the set

of models (1), a nominal model with known polynomials  $\beta_m^0(p)$ ,  $\alpha_n^0(p)$  is considered, the coefficients of which belong to the intervals of variation of the coefficients  $\beta_m(p)$ ,  $\alpha_n(p)$ , and the known value of the delay belongs to the interval  $\underline{\tau} \leq \tau \leq \bar{\tau}$ . It is assumed that the stability conditions are satisfied simultaneously for the pairs of polynomials  $\beta_m(p)$ ,  $\beta_m^0(p)$  and  $\alpha_n(p)$ ,  $\alpha_n^0(p)$ , for the delay link, the Padé approximation is used.

Then not the minimum phase nominal transfer function of the object will have the form

$$y(p) = \frac{\beta_m^0(p)}{\alpha_n^0(p)} \frac{h(p)}{g(p)} \cdot u(p) = \frac{H(p)}{G(p)} u(p) \quad (2)$$

To determine the coefficients of the polynomials  $h(p)$ ,  $g(p)$  the Padé approximation is used. It is known from world practice that it is most rational to use a first-order second-order approximation.

1st order approximation

$$h(p) = 1 - \frac{\tau_0}{2} p, g(p) = 1 + \frac{\tau_0}{2} p. \quad (3)$$

2nd order approximation

$$h(p) = 1 - \frac{\tau_0}{2} p + \frac{\tau_0^2}{12} p^2, g(p) = 1 + \frac{\tau_0}{2} p + \frac{\tau_0^2}{12} p^2. \quad (4)$$

The nominal control object (2) with one input and one output, corresponding to polynomials  $H(p)$ ,  $G(p)$ , is described by the  $(A, B, C, 0)$  representation

$$\dot{x}_0 = A^0 x_0 + b^0 u_0, x_0(0) = x_0^0, \quad (5)$$

$$y_0 = C^0 x_0, \quad (6)$$

Real motion with parametric uncertainty is described by the  $(A, B, C, 0)$  representation

$$\dot{x}' = A' x' + b' u_0, x'(0) = x_0^0, \quad (7)$$

$$y' = C' x' \quad (8)$$

where  $A' = A^0 + \Delta A$ ,  $b' = b^0 + \Delta b$ ,  $C' = C^0 + \Delta C$ ,  $\Delta A$ ,  $\Delta b$ ,  $\Delta C$ , is the parametric uncertainty of the model, which may depend on time. Assumes given intervals:  $\underline{A}' \leq A' \leq \bar{A}'$ ,  $\underline{B}' \leq B' \leq \bar{B}'$ ,  $\underline{C}' \leq C' \leq \bar{C}'$ .

The proposed method is based on the following robust approach mechanism.



Axiom. Suppose that the state vector  $x_0(t)$  for a linear object is divided into two components  $\Delta x_1(t)$  and  $x_1(t)$ , which together for any moment give the initial state vector

$$x_0(t) = \Delta x_1(t) + x_1(t). \quad (9)$$

Let for the nominal model (2) the problem of synthesis of a state regulator is solved, which transfers the nominal object from a nonzero initial state to the origin of coordinates under the additional condition that in this case, mutual partial compensation of the selected components is also carried out during the transient process. Then the resulting control is robust since the mutual compensation  $\Delta x_1(t)$  and  $x_1(t)$  also compensates for the effect of uncertainty on the state vector.

To perform the synthesis procedure, we will use the nominal model. The nominal movement  $x_0$  is forcibly divided using a filter into two components  $(\Delta x_1, x_1)$ , in the general case, not the minimum phase

$$x_1(p) = W_{\phi_1}(p)x_0(p) = \frac{1 - T_{\phi_1}p}{1 + T_{\phi_2}p}x_0(p), \quad (10)$$

$$\Delta x_1 = x_0 - x_1. \quad (11)$$

The nominal model of the object from (2) to (6), (10), (11) expanded after the forced separation of movements has the form

$$\dot{x} = Ax + bu_0, x(0) = \left[ (x_0^0)^T \ 0 \right]^T, \quad (12)$$

$$y = d^T x, \quad (13)$$

where  $A = \begin{bmatrix} \beta A^0 - T_{\phi_2}^{-1}I & \beta A^0 \\ T_{\phi_2}^{-1}(I - T_{\phi_1}A^0) & -T_{\phi_2}^{-1}T_{\phi_1}A^0 \end{bmatrix}$ ,  $b = \begin{bmatrix} \beta b^0 \\ -T_{\phi_2}^{-1}T_{\phi_1}b^0 \end{bmatrix}$ ,  $x = \begin{bmatrix} \Delta x_1 \\ x_1 \end{bmatrix}$  extended object model state vector,  $\beta = 1 + T_{\phi_2}^{-1}T_{\phi_1}$ ,  $d^T = [d_1I \ d_2I]$ ,  $d_1 \neq d_2$ ,  $d_1, d_2 > 0$ .

The result of the introduced new vector variable (13), which is a weighted sum of the components of the extended state vectors  $\Delta x_1(t)$ ,  $x_1(t)$  with unequal positive weights  $d_1, d_2 > 0$ , is its reduction to zero, which will lead to mutual partial compensation of vectors  $\Delta x_1(t)$  and  $x_1(t)$  by solving the problem of the analytical design of optimal controllers (in the simplest case). Next, the spectrum of the closed system is determined and the desired motion of the robust system is formed. In the future, the problem of modal control is solved, as a result of which the output regulator is synthesized. Based on the logarithmic and transient characteristics of the system, quality indicators are determined, and the adjusted parameters are corrected.

### 3 Synthesis of a Robust Output Controller

To ensure partial mutual compensation of the components of the extended state vector, we can consider minimizing the integral quadratic functional of form

$$J = \int_0^{\infty} [y^T(t) Q_0 y(t) + u_0^T(t)] dt = \int_0^{\infty} [x^T(t) Q x(t) + u_0^T(t) R u_0(t)] dt, \quad (14)$$

where  $Q_0^T = Q_0 = \text{diag}\{q_i^2\}_{i=1}^n > 0$ ,  $R^T = R > 0$ ,  $Q = d Q_0 d^T$ .

As a result

$$\begin{aligned} u_0(t) &= -Kx(t) = -K_0 \Delta x_1(t) - K_1 x_1(t) = -K_0 x_0(t) - (K_1 - K_0) x_1(t) \\ &= -K_0 x_0(t) - K_1' x_1(t), \end{aligned} \quad (15)$$

where  $K = R^{-1} (B_1^0)^T P$ .

A symmetric positive definite matrix is obtained as a solution to the Riccati equation

$$A^T P + P A - P b R^{-1} b^T P + Q = 0. \quad (16)$$

The quality of mutual compensation depends on the parameters of the analytical design of optimal controllers problem (12)–(14). Each set of tunable parameters corresponds to its measure of mutual compensation, which can be estimated, for example, using the formula

$$J_m = x^T(0) P x(0), \quad (17)$$

that gives the minimum value of the functional (14).

Another formula can also be used to estimate the mutual compensation measure

$$J_1 = \int_0^{\infty} y^T(t) Q_0 y(t) dt = \int_0^{\infty} \sum_{i=1}^n q_i^2 y_i^2(t) dt = \sum_{i=1}^n q_i^2 \int_0^{\infty} [d_1 \Delta x_{1i}(t) + d_2 x_{1i}(t)]^2 dt. \quad (18)$$

Note that not only a diagonal but also any symmetric positive definite matrix can be considered as  $Q_0$  in (14), (18). In the case of a diagonal matrix, formula (18) is especially clear.

The following provisions can be proved [4].

**Theorem 1.** Stabilization of  $y$  leads to stabilization of  $x_0$ .

**Theorem 2.** Minimization of functional (14) provides mutual partial coordinate-wise compensation of individual components  $\Delta x_1(t)$  and  $x_1(t)$  of the extended state vector  $x(t)$  during the transient process, the quality of which depends on the X tuning  $d_1, d_2, q_i, i = 1, \dots, n$  parameters.

Therefore, further, for each vector of parameters:  $R, T_{\phi 1}, T_{\phi 2}, d_1, d_2, q_i, i = 1, \dots, n$ , the analytical design of optimal controllers problem is solved in the MATLAB system, and, by enumeration, the best solution or solution that suits the developer is sought. This solution, following Theorem 2 and the main axiom, is sought on the set of robust systems. As a result, a certain setting  $R^0, T_{\phi 1}^0, T_{\phi 2}^0, d_1^0, d_2^0, q_i^0, i = 1, \dots, n$  is selected that provides the desired degree of compensation and other quality indicators of the system. At this stage, based on the obtained characteristic numbers of the matrix  $A - bK$ , the proper motion of the desired extended closed-loop system is formed, or rather the characteristic equation of the desired motion

$$G_Z(p) = \det\{pI - (A - bK)\} = p^{2n} + g_{2n-1}^0 p^{2n-1} + \dots + g_1^0 p + g_0^0 = 0. \quad (19)$$

The next step is the synthesis of a modal output controller based on the obtained Eq. (19). Consider the transfer function of the  $n$  order controller with an integrator to ensure astatism.

$$W_P(p) = k_n(p)/l_n(p) = \frac{b_n p^n + \dots + b_1 p + b_0}{p^n + a_{n-1} p^{n-1} + \dots + a_1 p}, \quad (20)$$

where  $b_i, i = 0, \dots, n, a_i, i = 1, \dots, n$  – configurable parameters.

For a system with an output regulator (20) for an object with a transfer function (2), the characteristic equation of the nominal system has the form

$$G(p) = l_n(p)\alpha_n^0(p) + k_n(p)\beta_m^0(p) = p^{2n} + g_{2n-1} p^{2n-1} + \dots + g_1 p + g_0 = 0. \quad (21)$$

The synthesis of the transfer function of the controller  $W_P(p)$  is carried out based on equality

$$G(p) = G_Z(p). \quad (22)$$

The desired characteristic Eq. (19) has  $2n$  known coefficients. If the polynomials  $l_n(p)$  and  $\alpha_n^0(p)$  are normalized so that the coefficient at the leading term is equal to one, as in (19, 21), then the transfer function of controller (20) contains  $2n$  unknown parameters. The coefficients of the polynomial (21) linearly depend on them. Therefore, from condition (22), it is possible to determine  $2n$  unknown parameters of the controller by solving the system  $2n$  of linear equations.

## 4 Example

As a confirmation of the described theory, it is proposed to consider a control object with a nominal transfer function of the object

$$W_0^0(p) = \frac{2 \exp(-10p)}{15p + 1}. \quad (23)$$

For the described transfer function, we synthesize a robust controller using the method described above. As a reference system, it is proposed to consider the system [2], which is optimal according to the aperiodic stability criterion, the regulator of which will have a transfer function

$$W_P(p) = \frac{0.343}{2 \cdot 10} \frac{15p + 1}{p}. \quad (24)$$

As a result of synthesis, a PI regulator was obtained, the regulation time of which is 63 s. That is a sufficiently large value ( $6.3\tau_0$ ), but at the same time, the maximum coarseness is provided for this class of control algorithms. Further, it is assumed that the systems are compared in terms of roughness for a given control time. To estimate the roughness, let us consider two inequalities for the relative variations in the transmission coefficient in (23) and the delay time at which there is no loss of stability.

$$0 < \frac{k_P}{2} \leq k_m, 0 < \frac{\tau}{10} \leq \tau_m, \quad (25)$$

where  $k_m, \tau_m$  – the values of the parameters at which the system is on the stability boundary.

For system (2, 24), with an independent change in one of the parameters at the nominal value of the other parameter, we obtain  $k_m = \tau_m = 4.5$ .

In the proposed technique, the following are used as tunable parameters:  $R, T_{\phi_1}, T_{\phi_2}, d_1, d_2, Q_0$ . This is a fairly wide range of parameters, which does not unambiguously determine the regulation time and roughness, but allows at the same time to provide other quality indicators, for example, the maximum control amplitude, the amount of overshoot. For simplicity, we fix some of them, let  $R = 1, Q_0 = I, d_1 = 5, d_2 = 4.5, T_{\phi_1} = 40s$ . Then, with an increase in  $T_{\phi_2}$ , the regulation time and the coarseness of the system will increase. Some increase in roughness at the same speed can be obtained additionally by varying the matrix  $Q_0$ .

For example,  $Q_0 = \begin{bmatrix} 100 & 0 & 0 \\ 0 & 1 & 0 \\ 0 & 0 & 1 \end{bmatrix}$ .

## References

1. Pradhan, R. Majhi, S.K., Pati, B.B.: Design of PID controller for automatic voltage regulator system using ant lion optimizer. *World J. Eng.* **15**(3), 373–387 (2018)
2. Gogol, I.V., Remizova, O.A., Syrokvashin, V.V., Fokin, A.L.: Sintez robustnykh reguljatorov dlja upravlenija tehnologicheskimi processami v klasse tradicionnykh zakonov regulirovanija [Synthesis of robust regulators to control technological processes in the class of traditional laws of regulation]: *Izv. SPbGTI(TU)*. № 44 P. 98–105. (in Russ.) (2018)
3. O'Dwyer, A.: A summary of PI and PID controller tuning rules for processes with time delay. Part 1: PI tuning rules. In: *Preprints of Proceedings of PID'00: IFAC Workshop on Digital Control*. Terrassa, Spain, April 2000, pp. 175–180. IEEE (2000)
4. Hekimoglu, B.: Sine-cosine algorithm-based optimization for automatic voltage regulator system. *Trans. Inst. Meas. Control.* **41**(6), 1761–1771 (2019)
5. O'Dwyer, A.: *Handbook of PI and PID controller Tuning Rules*, 2nd edn. London, Imperial College Press (2006)
6. O'Dwyer, A.: *Handbook of PI and PID Controller Tuning Rules*, 3rd edn. London, Imperial College Press (2009)
7. Rudposhtii, M.K., Nekoui, M.A., Teshnehlav, M.: Design of robust optimal regulator considering state and control nonlinearities. *Syst. Sci. Control. Eng.* **6**(1), 150–159 (2018)
8. Bortolin, D.C., Gagliardi, G.M., Terra, M.H.: Recursive robust regulator for uncertain linear systems with random state delay based on Markovian jump model. In: *Proceedings of 57th IEEE Conference on Decision and Control (CDC)* (2018)
9. Soliman, M.A., et al.: Linear-quadratic regulator algorithm-based cascaded control scheme for performance enhancement of a variable-speed wind energy conversion system. *Arab. J. Sci. Eng.* **44**(3), 2281–2293 (2019)
10. Ayten, K.K., Dumlu, A., Kaleli, A.: Real-time implementation of self-tuning regulator control technique for coupled tank industrial process system. *Proc. Inst. Mech. Eng. Part I-J. Syst. Control. Eng.* **232**(8), 1039–1052 (2018)
11. Basin, M., Rodriguez-Ramirez, P., Ding, S.X., Daszenies, T., Shtessel, Y.: Continuous fixed-time convergent regulator for dynamic systems with unbounded disturbances. *J. Frankl. Inst. Eng. Appl. Math.* **355**(5), 2762–2778 (2018)
12. Jakovis, L.M.: Prostye sposoby rascheta tipovykh reguljatorov dlja slozhnykh objektov promyshlennoj avtomatizacii [Simple ways to calculate typical regulators for complex industrial automation objects]: *Avtomatizacija v promyshlennosti* № 6, P. 51–56. (in Russ.) (2007)
13. Danik, Y.E., Dmitriev, M.G.: The robustness of the stabilizing regulator for quasilinear discrete systems with state dependent coefficients. In: *Proceedings of International Siberian Conference on Control and Communications (SIBCON)* (2016)
14. Singh, A.K., Pal, B.C.: An extended linear quadratic regulator and its application for control of power system dynamics. In: *Proceedings of IEEE First International Conference on Control, Measurement and Instrumentation (CMI)*, pp. 110–114. IEEE (2016)
15. Lian, K.Y., Liu, C.H., Chiu, C.S.: Simplified robust fuzzy output regulator design for discrete-time nonlinear systems. *J. Intell. Fuzzy Syst* **31**(3), 1499–1511 (2016)
16. Victor, M., Vilanova, R.: *Model-Reference Robust Tuning of PID Controllers*. Springer International Publishing (2016), LNCS Homepage. <http://www.springer.com/lncs>. Last Accessed 21 Nov 2016
17. Dean, S., Mania, H., Manti, N., Recht, B., Tu, S.: Regret bounds for robust adaptive control of the linear quadratic regulator. *Adv. Neural Inf. Process. Syst.* **31**, (2018)
18. Papadopoulos, K.: *PID Controller Tuning Using the Magnitude Optimum Criterion*. Springer International Publishing (2015)
19. Remizova, O.V., Syrokvashin, V.V., Fokin, A.L.: Sintez robustnykh sistem upravlenija s tipovymi reguljatorami [Synthesis of robust control systems with standart controllers]: *Izv. vuzov. Priborostroenie*. V.58. №12. P. 12 – 18. (in Russ.) (2015)

20. Escalante, F.M., Jutinico, A.L., Jaimes, J.C., Siqueira, A.A.G., Terra, M.H.: Robust Kalman filter and robust regulator for discrete-time Markovian jump linear systems: control of series elastic actuators. In: IEEE Conference on Control Technology and Applications, pp. 976–981. IEEE (2018)
21. Ilyushin, Y.V., Novozhilov, I.M.: Development of a technique for the synthesis of a pulsed regulator of a distributed control system. In: Proceedings of IEEE II International Conference on Control in Technical Systems (CTS), pp. 168–171. IEEE (2017)

# Study the Algorithm of Paths Calculation Parallelization in the Problem of Group Control of Robots



Alexandr Krasheninnikov and Serge Popov 

**Abstract** The work is about the development and study of the implementation of a multithreaded flow manager in computing systems for the transport problem of controlling a heterogeneous group of robots. The aim of the work is to investigate the parameters of the thread manager to find a suboptimal configuration for solving the task of managing computation resources and formulating practical recommendations for configuration the developed software as well. In the work, a series of experiments were carried out on the thread manager, experimental dependences of the computing system performance on the manager's configuration parameters were established. In the course of the experiments was established that it is possible to find the suboptimal configuration of the thread manager based on parameters, such as the number of logical threads, the size of the batch of subtasks for computation, the number of the subtasks. The results will be used during the creation of a subsystem for managing computational threads of the general problem and can be used in other applied problems together with portable software in the software of the routes computation threads manager.

**Keywords** Robot · Algorithm · Multithreading · Performance · Optimization · Heterogeneous · Thread · Suboptimal

## 1 Introduction

The multithread method allows us to maximize the use of calculation resources since specially configured software allows us to optimize and dispatch multithread calculations. Based on results of research [1] there was a problem statement about finding suboptimal thread manager settings configuration, since an impact of key parameters,

---

A. Krasheninnikov (✉) · S. Popov  
Peter the Great St. Petersburg Polytechnic University, St. Petersburg 195251, Russia  
e-mail: [Contr239@mail.ru](mailto:Contr239@mail.ru)

S. Popov  
e-mail: [popovserge@spbstu.ru](mailto:popovserge@spbstu.ru)

© The Author(s), under exclusive license to Springer Nature Switzerland AG 2022  
A. G. Kravets et al. (eds.), *Cyber-Physical Systems: Modelling and Industrial Application*,  
Studies in Systems, Decision and Control 418,  
[https://doi.org/10.1007/978-3-030-95120-7\\_18](https://doi.org/10.1007/978-3-030-95120-7_18)

such as task amount in packet в пакете or logic thread amount, provides a significant impact on path calculation time. Manual parameter selection is labor-intensive and does not guarantee the best configuration. In generally submitted researches represents the expansion of studies on automatic thread manager control. That is the resulting fact, that the native parameter configuration of the instrument will result in ineffective usage, and in some cases may slow down calculation speed to a single thread level. In this sense, the problem of automatic finding suboptimal parameter configuration for thread manager on predefined calculation environment is also scientific and technical, and this study is an expansion of studies of automatic thread manager control.

## *1.1 Related Studies*

Multithreading as a factor of performance is estimated like some fixed factor [2]. In considerable tasks of sorting this approach is appropriate, because split by threads happens in a solid task environment. Subtask set becomes consistent and optimal variant is simple simultaneous launch of task amount same as thread amount. Research of different multithread modifications A\* algorithm [3] has resulted in the conclusion of high efficiency of calculating each path in its separate thread, and low efficiency of parallelization multithread calculation of parameters inside a single path. Further proposed modifications of A\* relate only algorithm adaptation to task and simultaneous calculation of several tasks. The idea of combining the multithread approach and partition optimization was not considered in the state but has all chances to improve calculation time.

Interesting variants of the usage multithread approach are based on genetic algorithms [4, 5]. Generally speaking, that algorithm is not parallelizable, because of has an iterative base and clear sequencing. However, nuances of realization allow separating into threads population writing into DB and graphical construction of current iteration for visibility. The timing of calculation on program complex is equal to base algorithm part calculation time.

The question about direct cooperation on low-level with calculation environment is seen as a separated problem [6]. One of the most important conclusions is a summary of the outputs about the non-availability of research of dynamic characteristics of user-created algorithms.

Calculation speed may be affected by direct algorithm realization [7]. Used by many ready-made solutions in the form of a container and built-in algorithm may contain redundant task context information inside and can cause additional resource costs for the calculation system.

Back to mathematical aspects, it is worth considering optimization criteria questions [8]. In research, which is the subject of state the dynamic model is used directly, but criteria selection allows to approve possibility of improving the current static model to dynamic with wider criteria selection.



Considering the problem in terms of control theory also explains many aspects of the target environment [9]. Splitting a task on synthesis and sustainability in a point of state-space using evolution methods allows obtaining high-level control functions, that in a broad sense corresponds to the definition of strategies from the first part of research [10]. Such an approach demonstrates perfect results on synthetic tests but requires an extensive examination of real data for making the decision about its usage in the target problem.

The idea of area exploration from the air is not new, and different options have been suggested [11]. In general, a heterogeneous robot group allows splitting tasks to create a semblance of a pipeline for developing a model towards dynamic. However, in the state considering only one drone is present, that increases costs of equipment to effectively perform tasks, and also decreases the overall MTBF of the system.

The question about splitting tasks on group considering from different angles. An interesting variant with cloud computing usage was proposed [12]. The idea is to decompose the overall task with special programming techniques in algorithm realization usage. Linear distribution, swarm solution, and solution synthesis represent ample opportunities for such an approach. As a result of the state-developed algorithms were successfully tested, but using virtual machines in cloud service raises questions. Refining system attributes in terms of performance is required.

Also for the technical part continuing researches on the use of GPU in applied tasks [13]. It is known, that GPU performance in some tasks far exceeds CPU performance. Pathfinding algorithm somewhat different from used in current research, but realized parallel algorithm on CUDA show significant performance improvement.

The technical aspect in some ways has a more detailed analysis [14]. Consideration in the state affects directly the physical part of the multithread CPU. Researches about architecture were held earlier, from the moment when it was realized that with the current technology level of chip production the limit of working frequency will be made soon. And therefore another characteristic must be scaled—agent number.

The nearest idea to global thought about thread manager can be considered an idea of DDMT (Data-Driven MultiThreading) [15]. This approach is about adopting inside algorithms of the CPU kernel for incoming data. However, the main goal of this study was to improve performance in costs of optimization in different cache levels loading due to calculation.

Directly related with multithreading optimization strategy also became a part of developed [16, 17]. A special operating system was created for multi-agent tasks where the time aspect is critical. The idea of this was in multiple agents functioning with SensorOS on-board.

One of the following steps of current research will be a transition to real data. In such a context some preprocessing may be required to receive data for the pathfinding algorithm. Proposed in state dynamic variant with Delaunay triangulation and modified A\* algorithm [18] can significantly simplify the task of transition from synthetic data to real ones.

In the continuation of the topic theoretic models, the aspect of the multiagent system is worth considering [19]. The question about centralized control emulation

a first sight carries inexplicable benefits. However, the question about the decision-making aspect is raised when talking about a functioning scheme. In conditions and solutions, there is no indication about the central node since those moments are planned to consider in the future. Nevertheless, the subject of state allows to obtain more understanding on realization possibilities earlier and correct the pathfinding algorithm.

Not last aspect in transition to the dynamic system is timely detection of obstacles on the ground robot path. For now, this task handles on drones, but in some tasks, they are not applicable. Area research inside an abandoned factory, for example, does not effectively use air units without special expensive equipment because of obstacles from above. The proposed model of visual obstacle detection [20] allows to digitize obstacles with some accuracy using a standard video camera and then add them into the pathfinding algorithm as preprocessed data. Question about functioning efficiency in difficult environment circumstances remains open and requires full-scale tests.

Returning to questions about the algorithm, it is worth considering the cooperative algorithm variant of  $A^*$ —ICA\* [21]. The main idea is about penalty functions that take into account turn angles and another agent path crossing. As a result of the chapter algorithm show good performance. However, in the context of current research, we should consider an area coverage task solution, that made additional conditions and may negatively affect penalty functions. A possible solution is the alternate usage of  $A^*$  and ICA\*. In this case,  $A^*$  will be used on coverage build trajectory when the radar is active, and ICA\* will be used to move between trajectories.

Thus, in the context of the current research question about creating algorithms and developing a program module that links task solution algorithmic part with an operating system and multithreaded calculations is in demand and important in terms of operating system resource utility optimization.

## 2 Subject Area Problem Statement

Given map  $M$  and heterogeneous robot group  $R$ . For map  $M$  explication for ground robot  $M_g = \{G, Y, R\}$  can be made, where  $G$ —free to move zones,  $Y$ —dangerous zones, that contains zone with large angles of longitudinal/latitudinal roll,  $R$ —closed for movement zones like water, lava or jungle, and explication  $M_f = \{H\}$  for flying robots, where  $H$ —minimal flight height map. Map realization remains in scale that is enough for ground robot pathfinding. Also, the map is not known at the beginning.

Robot group  $R = \{F, G\}$  consists of  $F = \{f_1, \dots, f_n\}$ — subgroup with  $n$  drones, and  $G = \{g_1\}$ —subgroup with one ground robot. Robot  $f = \{C, v, r, h_{max}\}$  has map view radius  $r$ , average flight speed  $v$ , energy consumption per unit of time  $C$  and maximal flight height  $h_{max}$ , caused by external factors: weather or radio transmitters power. Flying robot builds actual large-scale map. Robot  $g = \{C, r, E, \alpha, \beta\}$  with map view radius  $r$ , energy consumption per unit of distance traveled depends on the angle of approach  $\delta C = C(\delta)$ , the energy limit  $E$ , maximal angle of latitudinal roll—the angle of stall  $\alpha$ , maximal angle of approach  $\beta$ .

In this task, it is required to find the path from point  $A$  to point  $B$  for to minimize summary group energy costs and not exceed the angle of stall and approach for the ground robot.

In this case, the common problem statement is a multi-criteria optimization problem:

$$\min_{\underline{x}} \{f_1(\underline{x}), f_2(\underline{x})\}, \underline{x} \in S \quad (1)$$

where  $f_i : R^n \rightarrow R$  are target functions, responsible for energy consumption in flight and admissibility of ground robot movement on angles. Solution vectors  $\underline{x} = (x_1, x_2, \dots, x_n)^T$  belongs to non-empty domain  $S$ .

In cases of multi-criteria optimization, the criteria of satisfaction for different target functions generally conflict, so optimization task frequently has additional conditions as a criteria priority.

### 3 Optimization Problem Statement

While resolving the overall task the subtask of multiple path calculation for each robot in a group. Knowing intermediate control points, we can split the full path into fragments, that can be calculated separately. Under centralized path calculating in a real-time system the question about each part and overall path calculating time appears. For the first iteration, we are interested to launch each drone as soon as possible. Since there can be inaccessible flight zones in the area, let's say that drone starts movement only when the path is completely calculated. In this case, we can formulate suboptimal criteria for chosen path calculation strategy. For  $n$  robots we have an optimization problem:

$$\min_{\text{strat}} \sum_{i=1}^n T_{si}$$

$$\underline{x} \in S$$

where  $T_{si}$ —time of start(S) or time of finish calculating full path  $i$ -th robot. Strat—chosen pathfinding strategy. With that said on previous research steps, strategy is characterized with next points:

- Logic thread amount in target calculating system (h);
- Task packet size for calculation throw thread manager (p);
- Path to subpaths split partitions count (s).

## 4 Task Thread Splitting Method

However, in addition to all of the above, there is another important aspect—the order of tasks for calculation entry into thread manager. Presumably, the impact of that parameter will be minimal on this step with the given impossibility of launching the robot without full calculation. But consideration of this aspect now allows comparing results in the future, when a mathematic model will allow a robot to start moving without full path calculation.

In this case, the formula can be specified:

$$\min_{\{h,p,s\}} \sum_{i=1}^n T_{si}$$

That distribution allows us to take into consideration a greater number of mathematic model parameters and computational system parameters.

## 5 Research of Strategy Affection on Path Readiness

The main idea of the experiment is to find a relationship between path readiness time and path partitions count, logic thread count, the task in packet count. Originally, it is suggested, that the biggest impact on the sum from the formula will have the number of logic threads, as the most evident limiter. In the previous part [1] the impact of logic thread exceedance on OS available threads was checked and obtained result shows the inadvisability of such exceedance because there was no performance increase. However, that variant is worth considering.

The first step of the experiment assumed calculations on standard data set (Table 1) with a variable amount of logical threads. For fairness in calculation amount of ground, robots were equal to 0. Given the principle of thread manager workflow, the task amount in the packet should be larger or equal to the thread

**Table 1** Parameters of experiment 1

Parameter or constant	Value
Map size, points * points	258 × 258
Flying robot amount, units	64
Ground robot amount, units	0
Path length, points	100
Logic thread amount, units	8:2:20
Task amount in packet, units	20
Physical thread count, units	8(16 w/hyper-threading)

count. Otherwise, some logic threads will not be used in the calculation and overall performance will drop (Figs. 1 and 2).

According to obtained results, the smallest time of calculation had been received on the lowest thread count, which is determined by coincidence this amount with logic kernel thread amount. In doing so, if the increasing amount of logic threads, then the overall CPU load will do not change, and yet time costs on system interruptions and the functioning of additional thread manager logic threads are added.

The second step (Table 2) is to consider calculation time for a limited number of logic threads, which is less than the physical thread amount available for OS. The

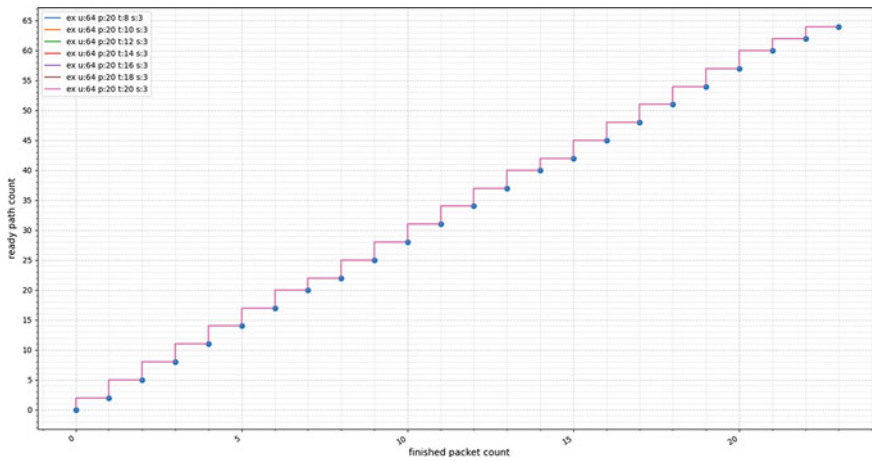


Fig. 1 Computed packet count for variable thread count – Experiment 1

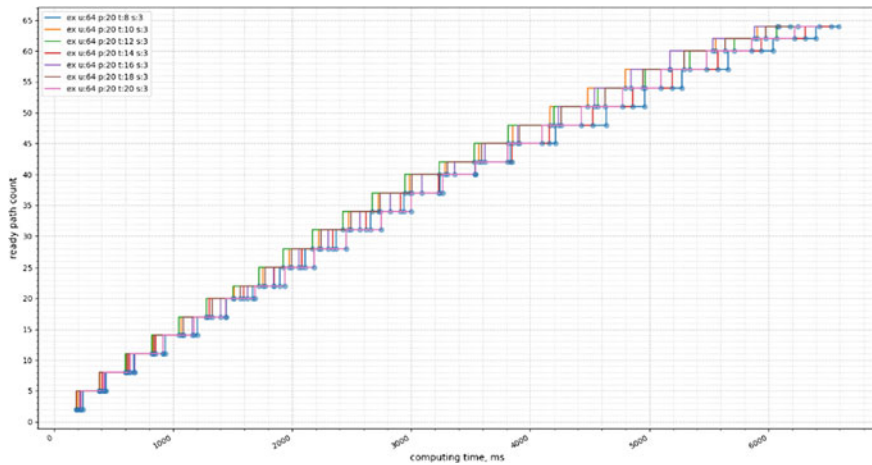


Fig. 2 Computing time for variable thread count – Experiment 1

**Table 2** Parameters of experiment 2

Parameter or constant	Value
Map size, points * points	258 × 258
Flying robot amount, units	64
Ground robot amount, units	0
Path length, points	100
Logic thread amount, units	2:2:8
Task amount in packet, units	8
Physical thread amount, units	8(16 w/hyper-threading)

main thrust is in checking the hypothesis about suboptimal logic thread count that is equal to real or physical kernel core count. That is possible, that Hyper-Threading technology has a negative impact on the same math operations (Figs. 3 and 4).

According to obtained results worst-case time of calculation we get when there is too little amount of threads. However, we are interested more in another two plots, which shows us, that we get an advantage in calculation time when using logic thread count same as CPU kernel core count. In doing so, unlike the experiments in the previous part of the research [1] advantage of time represent a smaller value than two, since for this experiment we are basing our calculations on time to a drone being ready to start moving, instead of the time of overall calculation (Table 3).

Now consider variable task count in a packet with constant logic thread number. The value range on this step includes lesser and greater values regarding thread count (Figs. 5 and 6).

Unlike previous steps difference in counted packet amount on one ready path is noticeable. The most rapid calculation variant implies a usage packet with a maximum size. Originally envisaged, that in some cases it is possible to reach thread manager overloading because of a huge amount of tasks in packet. However, in practice, that

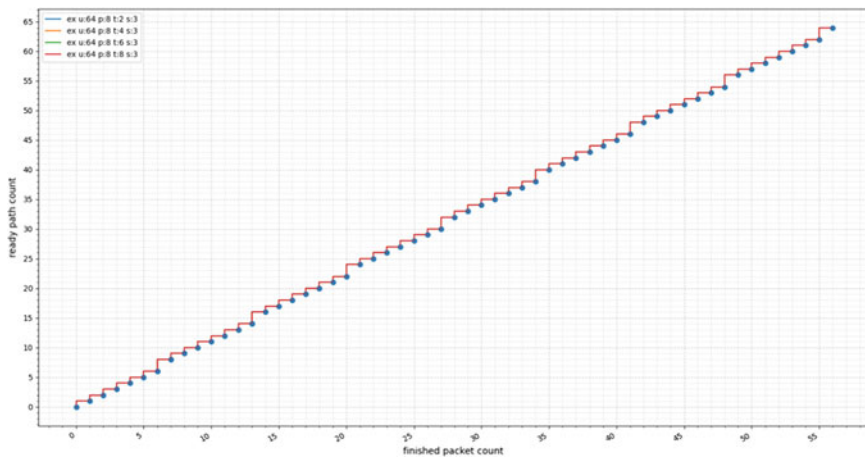


**Fig. 3** Computed packet count for variable thread count – Experiment 2

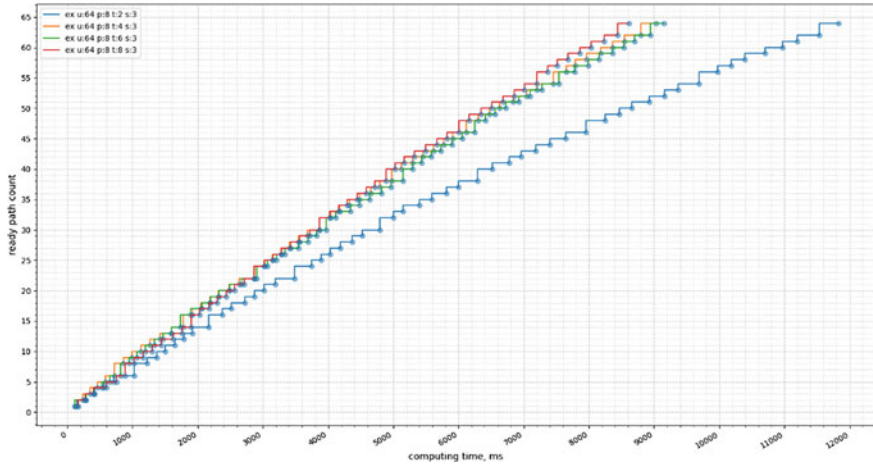


Fig. 4 Computing time for variable thread count – Experiment 2

Table 3 Parameters of experiment 3

Parameter or constant	Value
Map size, points * points	258 × 258
Flying robot amount, units	64
Ground robot amount, units	0
Path length, points	100
Logic thread amount, units	8
Task amount in packet, units	2:2:16
Physical thread amount, units	8(16 w/hyper-threading)

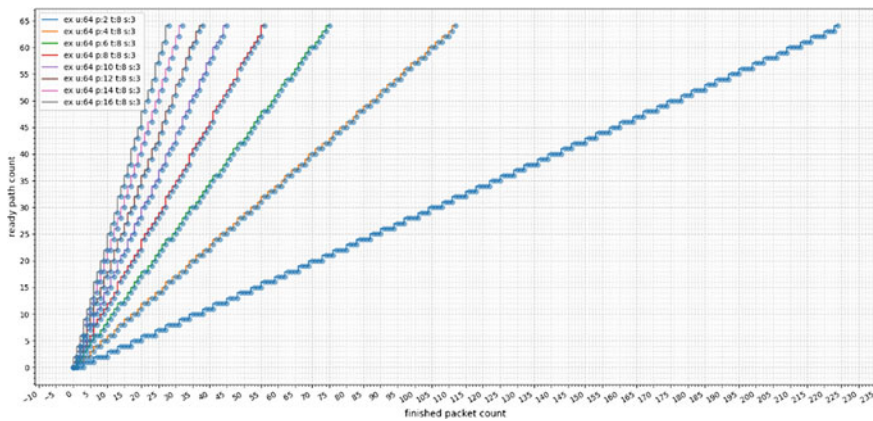
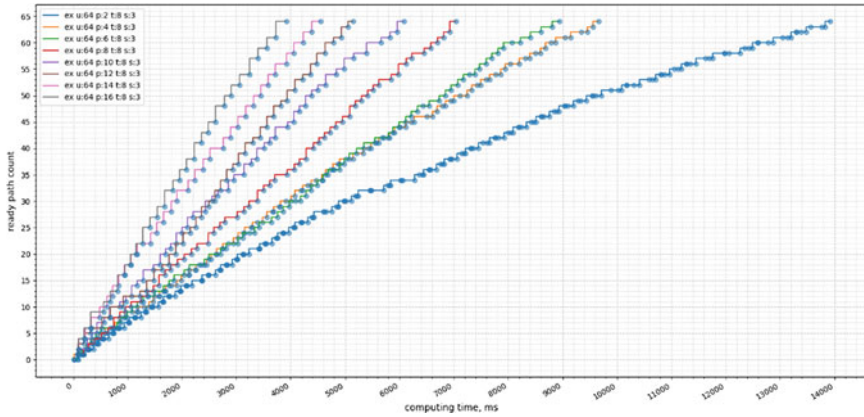


Fig. 5 Computed packet count for variable task count – Experiment 3



**Fig. 6** Computing time for variable task count – Experiment 3

**Table 4** Parameters of experiment 4

Parameter or constant	Value
Map size, points * points	258 × 258
Flying robot amount, units	64
Ground robot amount, units	0
Path length, points	100
Logic thread count, units	8
Task in packet count, units	8
Physical thread amount, units	8(16 w/hyper-threading)
Path split amount, units	0:1:8

case is impossible in our scope of application, so it is better to research that moment in the context of several tasks from different scopes of the appliance (Table 4).

Consider further the influence of the number of partitions on path readiness time. In the current context partition briefly multiplies pathfinding subtask count, but reduces expected path length, and therefore a time of count each shard (Figs. 7 and 8).

During consideration of the area survey strategy, the question about flying robot path split count has been raised. Following the base problem statement, for each drone, any count of control points can be set. In doing so, in the case of the calculation on small parts size of the Li method coverage matrix decreases, which implies counting time reduction. However, under obtained results, minimal counting time was reached without splitting. It should be also noted, that experiment was held on the model map without any obstacles, and obtained time results has comparable order of magnitude. Therefore, on real data more complicated cases are possible, and choosing suboptimal count of partitions is variable depends on location. Also, for creating area coverage by drones with some vision radius, the path might have a control point. Thus, the suboptimal count of partitions is minimally required for the chosen strategy of area exploration.



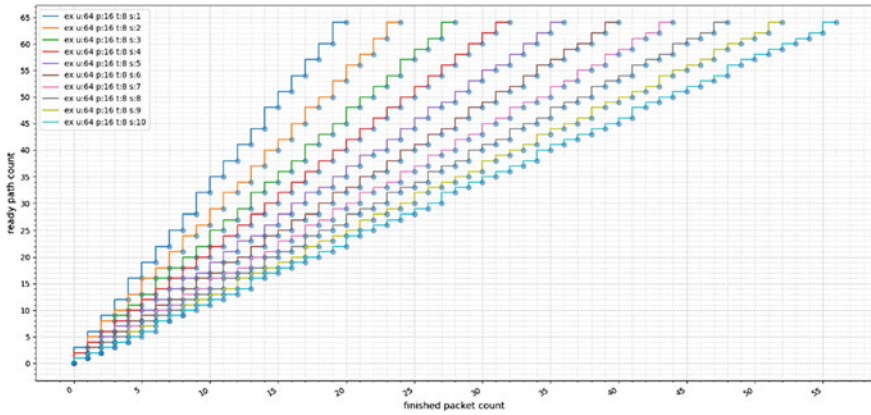


Fig. 7 Computed packet count for variable thread count – Experiment 4

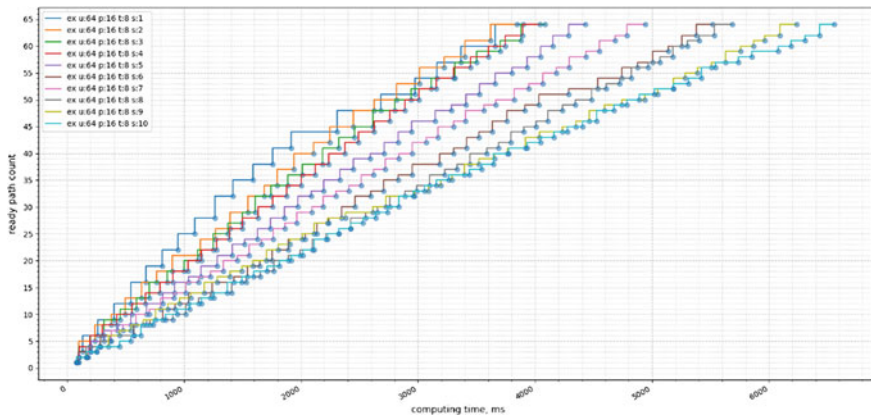


Fig. 8 Computing time for variable thread count – Experiment 4

## 6 Conclusion

Following the results of experiments that have been done the methodology of configuring thread manager parameters were established to produce suboptimal parameters, allowing us to launch area exploration drones as soon as possible. That configuration is oriented on strictly pragmatic usage, because of answering the question «what to do for launch drones as quickly as possible». In the context of general study, this result is a cross-cutting between static and dynamic model, that suppose us in the future to move to path correction «on the fly» in changing external environment with ready parallelization mechanism.

It should also be noted, that the thread manager's source code can be expanded with the configuration module and make it completely alienable, independent from the task. Such construction will be a self-optimizable out-of-the-box solution and allows to minimize implementation time.

**Acknowledgements** The reported study was funded by RFBR according to the research project No 18-2903250 mk.

## References

1. Popov, S.G., Krasheninnikov, A.S., Tuchkov, A.S., Osadchuy, A.I.: Study of the algorithm for multi-thread path search of a heterogeneous group of autonomous mobile robots. *Inf. Space* **4**, 57–65 (2020)
2. Paschenko, D.V., Martushkin, A.I., Perekusihina, A.N.: Multithreading as a factor affecting the speed and performance of a parallel computing system when performing data sorting operations: XXI century. *Results Probl. Present. Plus* **8**(3), 23–29 (2019)
3. Koybash, A.A., Zavadskaya, T.V., Krivosheev, S.V.: Modification of the A\* algorithm for predicting the trajectory of a moving object in distributed computing system. *AI Probl.* **3**(10), (2018)
4. Podvalny, S.L., Vdovin, D.A.: Development of special software for solving transportation problems with a modified genetic algorithm using multi-threading. *Voronezh State Tech. Univ. Bull.* **16**(4), (2020)
5. Yanchin, I.A., Petrov, O.N.: Parallelization of genetic algorithms in pathfinding. In: *International Conference on Soft Computing and Measurements*. Federal State Autonomous Educational Institution of Higher Education V.I. Ulyanov(Lenin) Saint-Petersburg State Electrotechnical University LETI, vol. 1, No. Sections 1–3, pp. 520–523. IEEE (2016)
6. Zyubin V.E., Petukhov A.D.: Distribution of computing resources in environments with multi-threaded implementation of a hyperautomat. In: *IIIrd International Conference «System Identification and Control Tasks» SICPRO*, vol. 4, pp. 446–463. IEEE (2004)
7. Dergachev, S.A., Yakovlev, K.S.: On one issue of the implementation of the trajectory planning algorithm A\*. In: *Fifth All-Russian Scientific and Practical Seminar “Unmanned Vehicles with Artificial Intelligence Elements” (BTS-AI-2019)*, pp. 66–76 (2019)
8. Lavrenov, R.O., Afanasev, I.M., Magid, E.A.: Route planning for an unmanned ground robot taking into account a variety of optimization criteria. In: *Unmanned Vehicles with Artificial Intelligence Elements*, pp. 10–20 (2016)
9. Diveev, A.I., Shamlko, E.U.: Evolutionary computational methods for the synthesis of control of a group of robots and the search for optimal trajectories of their movement. *Cloud Sci.* **4**(3), (2017)
10. Popov, S.G., Krasheninnikov, A.S., Chuvatov, M.V.: The study of the survey algorithm of the heterogeneous group of autonomous mobile robots. In: *Robotics and Technical Cybernetics*, Vol. 7, No. 4, pp. 278–290. Sankt-Peterburg, TsNII RTK (2019)
11. Zenkevich, S.L., Nazarova, A.V., Jianwen, H.: Controlling a group of mobile robots using an escort drone. *Robot. Tech. Cybern.* **7**(3), 208–214 (2019)
12. Darincev, O.V., Migranov, A.B.: Decomposition of tasks in a group of robots using cloud computing technologies. In: *Proceedings of the Institute of Mechanics*. RR Mavlyutova UC RAS, vol. 12. No. 1, pp. 83–88. IEEE (2017)
13. Agafonov, A.A., Maksimov, A.I., Borodinov, A.A.: Investigation the efficiency of computing a reliable shortest path using a GPU, pp. 732–738. *Information Technology and Nanotechnology (ITNT-2020)* (2020)

14. Tullsen, D.M., Eggers, S.J., Levy, H.M.: Simultaneous multithreading: maximizing on-chip parallelism. In: Proceedings of the 22nd Annual International Symposium on Computer Architecture, pp. 392–403. IEEE (1995)
15. Roth, A., Sohi, G.S.: Speculative data-driven multithreading. In: Proceedings HPCA Seventh International Symposium on High-Performance Computer Architecture, pp. 37–48. IEEE (2001)
16. Kim, H., Cha, H.: Multithreading optimization techniques for sensor network operating systems. In: European Conference on Wireless Sensor Networks, pp. 293–308. Springer, Berlin (2007)
17. Kuorilehto, M., et al.: Sensoros: a new operating system for time critical wsn applications. In: International Workshop on Embedded Computer Systems, pp. 431–442. Springer, Berlin (2007)
18. Liu, Z., et al.: A dynamic fusion pathfinding algorithm using delaunay triangulation and improved a-star for mobile robots. *IEEE Access* **9**, 20602–20621 (2021)
19. Chudý, J., Popov, N., Surynek, P.: Emulating centralized control in multi-agent pathfinding using decentralized swarm of reflex-based robots. In: 2020 IEEE International Conference on Systems, Man, and Cybernetics (SMC), pp. 3998–4005. IEEE (2020)
20. Abiyev, R.H., et al.: Robot pathfinding using vision based obstacle detection. In: 2017 3rd IEEE International Conference on Cybernetics (CYBCONF), pp. 1–6. IEEE (2017)
21. Liu, Y., Chen, M., Huang, H.: Multi-agent pathfinding based on improved cooperative A\* in kiva system. In: Proceeding of 2019 5th International Conference on Control, Automation and Robotics (ICCAR), pp. 633–638. IEEE (2019)

# Research of Methods of Decentralized Control of a Group of Robots in the Liquidation of Technogenic Accidents



Leonid M. Kurochkin and Igor R. Muhamedshin

**Abstract** This work analyzes methods for decentralized control of a group of intelligent robots interacting in uncertain environments. Based on the method of collective action planning, an algorithm for decision-making by robots to liquidate technogenic accidents at each moment when the event stream changes is developed to reduce the time to liquidate technogenic accidents in urban infrastructure. A simulation environment is created for the empirical finding of efficiency functions and their corresponding strategic coefficients of the objective function, which sets the goal and strategy of functioning a heterogeneous group of robots. Efficiency functions are empirically selected in the efficiency measure of the target function for solving the problems of protecting security objects, exploring the area, and liquidating sources by a heterogeneous group of robots, interacting in an urban infrastructure with an evolving technogenic accident, using a decentralized group control system. It is shown experimentally that the found efficiency functions reduce the average time required for the complete liquidation of a technogenic accident for a selected set of scenarios. Using the coordinate descent method, a method is shown for finding strategic coefficients in the efficiency measure to minimize the average time for the complete liquidation of technogenic accidents for different parameters of the development of a technogenic accident.

**Keywords** Heterogeneous groups of the intelligent robots · Situational management · Decentralized group control system · Simulation modeling · Model of a technogenic accident · Event stream

## 1 Introduction

The growth in the scale of economic activity and the rapid development of the scientific and technological revolution has led to an increase in the number of emerging technogenic accidents. It is necessary to quickly and correctly make decisions to

---

L. M. Kurochkin (✉) · I. R. Muhamedshin  
Peter the Great St. Petersburg Polytechnic University, Saint-Petersburg, Russia

© The Author(s), under exclusive license to Springer Nature Switzerland AG 2022  
A. G. Kravets et al. (eds.), *Cyber-Physical Systems: Modelling and Industrial Application*,  
Studies in Systems, Decision and Control 418,  
[https://doi.org/10.1007/978-3-030-95120-7\\_19](https://doi.org/10.1007/978-3-030-95120-7_19)

213

liquidate the accident, as they are accompanied by human losses [1]. The problem of analyzing the behavior of controlled complex systems in conditions of uncertainty typical of emergencies, the source of which is a technogenic accident, belongs to the category of difficult-to-formalize problems, and therefore one of the main research methods is the modeling method [1].

To liquidate technogenic accidents in order to reduce the risk for people in the conditions of a dangerous non-deterministic environment, it is necessary to use autonomous mobile robots capable of moving in space [2]. Since the decision-making process in the liquidation of accidents is characterized by a lack of time, incompleteness, and poor quality of information presentation [1], instead of one robot, it is necessary to use a group of robots in the liquidation of a technogenic accident [3].

When robots are used in groups to solve the problem of liquidating a technogenic accident, they interact with each other in a complex environment, when the situation can change unpredictably. Algorithms for planning and controlling group actions of robots should be developed for their implementation in real-time on the basis of onboard computing devices of robots [3]. To achieve the set goals, the actions of each robot should be aimed at obtaining the largest group effect. Group interaction can be effectively implemented only using the methods of decentralized control [3].

**Problem statement.** We need to build the interaction of a group of robots operating in uncertain conditions to minimize the time of liquidating a technogenic accident.

The task of choosing the current action by an individual robot  $R$  included in a group of robots using a decentralized group control system (DGCS) can be formulated as follows:

Find the vector function  $A(t)$  of actions of the robot  $R$  from the group on the time interval  $[t_0, t_k]$  at which the maximum increment of the target function  $\Delta Y = Y(t_0 + \Delta t) - Y(t_0)$  is achieved, taking into account the constraints on possible environment states, actions of robots, the current states of the robots in the group, the current state of the environment, and the initial values of the vector functions of actions for each robot in the group.

The dimension of such a problem is  $n$  times less than the dimension of a problem with a centralized group control system.

To solve this problem, algorithms are considered for solving the problem of distributing the work of a heterogeneous group of robots to liquidate a technogenic accident in urban infrastructure; methods of group control of robots are analyzed; the model of urban infrastructure in which robots operate is developed; method of constructing the objective function is developed; method for calculating the values of the coefficients of the target function is developed; instrumental environment for simulation is developed.

## 2 Analysis of Methods of Group Control of Robots in Uncertain Environments

To build a DGCS, we will consider the main approaches: the method of situational management; the method of potential fields; the market-based methods.

The method of situational management provides for storing in the robot's memory a complete set of situations in which it may find itself, as well as a set of scenarios for achieving the set goals [4–7]. When the environment changes, robots need to analyze the situation with the help of sensors and independently choose a new action corresponding to this situation. Situational management requires large expenditures to create a preliminary database of information about possible situations and methods of management. Consequently, the main drawback of the method is that the current situation usually differs from those envisaged in the scenarios and, as a result, management is often insufficiently effective.

The potential fields method [8–10] assumes to endow obstacles and robots with virtual fields. Objects that should move towards each other are endowed with “charges” of opposite signs, and those that should not approach each other—with “charges” of the same sign. The movement of robots is determined by the influence of the resulting virtual forces generated by the robot's control system. By setting, for example, a “positive” charge for the detected accident source, and for robots and obstacles, a “negative” one, it is possible to form the movement of robots to the source in order to liquidate them and push the robots away from obstacles.

In combination, for example, with the potential field's methods, when organizing the DGCS, to create a more effective control system, one can use the market-based methods [11–15], within which it is possible to solve the problems of planning the actions of robots in an unpredictable environment. The essence of the method is that each robot faced with a new task conducts an auction using information exchanges with other robots in the group, making its own bet on the task. The other robots evaluate the effectiveness of their own solution to this problem, communicating it to others and receiving counter-proposals. The robots revise their bets, taking into account the information received until a final agreement is reached on the rates for the task. The robot with the highest bet starts to solve the problem. The goal of distributing several tasks between robots is to maximize the payoff of the entire group.

In addition, the methods of fuzzy logic [16, 17], swarm algorithms [18], and the method of collective action planning [19] are widely used to control the movement and organize the group actions of robots.

### 3 Robot Group Control Method in Urban Infrastructure

As a result of a comparative analysis of control methods for a group of robots, a method of collective action planning, which considers a group of robots and the environment as a single discrete dynamic system, was chosen to control the movement and to organize group actions of robots for liquidating technogenic accidents in urban infrastructure. This is due to such factors as the cyclical nature of the calculations, the discreteness in the time of obtaining the information generated by the sensor devices, and the discreteness of the data presented in digital computing devices [19].

The problem of controlling a group of robots is formulated as follows:

Let a group of  $n$  robots  $R_1 \div R_n$  operate in the simulated environment  $E$ , the states of which are described by vector functions

$$S_j(t) = \langle s_{1j}, s_{2j}, \dots, s_{mj} \rangle, \quad (j = 1, \dots, n),$$

and the state of the environment surrounding the robot is a vector function

$$E(t) = \langle e_1, e_2, \dots, e_w \rangle.$$

Then the situation (event stream) is a vector

$$P(t) = \langle S_1, S_2, \dots, S_n, E \rangle.$$

The actions of each robot can be described by a vector function

$$A_j(t) = \langle a_{1j}, a_{2j}, \dots, a_{hj} \rangle, \quad (j = 1, \dots, n).$$

Some situations can be prohibited, for example, if the position of the robot coincides with an obstacle. The system of constraints can be represented by a system of inequalities of the form  $\alpha(P) \leq 0$ , which satisfies all valid situations. Similarly, restrictions are imposed on the set of actions of the robot admissible in this situation:  $\beta(A, P) \leq 0$ .

The task of planning the actions of a group of robots is to determine the vector functions of actions  $A_j(t)$  for each robot in the group on the interval  $[t_0, t_k]$ , that satisfy the constraints  $\beta(A, P) \leq 0$ , as a result of which the maximum of the objective function  $Y = F(A_1, A_2, \dots, A_n, P)$  is achieved.

In the method of collective action planning, each robot of the group independently solves the task of planning its actions in the current situation. The optimal actions of the robot are those actions that make the maximum contribution to achieving the overall group goal [19].

Considering the environment and robots as a single discrete dynamic system, considering the actions  $A_j(t)$  as discontinuous vector functions of time, which change abruptly at certain times  $t \cdot \Delta t$  where  $t$  is discrete time (cycle)  $t = 0, 1, 2, \dots$ , and  $\Delta t$  is the time interval through which the next action is selected, and also assuming that

the state of the environment  $E$  and robots  $S_1 \div S_n$  do not change on the interval  $\Delta t$  the task of determining the actions of the robot is simplified to the following form:

Find, as the current action  $A_j^0$  of the robot  $R_j$ , an action  $A_j^{k+1}$  that satisfies the constraints:

$$\beta\left(A_1^{k+1}, \dots, A_{j-1}^{k+1}, A_j^{k+1}, A_{j+1}^k, \dots, A_n^k, S_1^0, S_2^0, \dots, S_n^0, E^0\right) \leq 0$$

$$\alpha\left(S_{1j}^{k+1}, S_{2j}^{k+1}, \dots, S_{nj}^{k+1}, E_j^{k+1}\right) \leq 0,$$

where  $S_{ij}^{k+1} = S_i^0 + \Delta S_{ij}^{k+1}$  and  $E_j^{k+1} = E^0 + \Delta E_j^{k+1}$ ,

$$\Delta S_{ij}^{k+1} = f_i\left(S_1^0, \dots, S_n^0, A_1^{k+1}, \dots, A_{j-1}^{k+1}, A_j^{k+1}, A_{j+1}^k, \dots, A_n^k, E^0\right)\Delta t,$$

$$\Delta E_j^{k+1} = f^*\left(S_1^0, \dots, S_n^0, A_1^{k+1}, \dots, A_{j-1}^{k+1}, A_j^{k+1}, A_{j+1}^k, \dots, A_n^k, E^0\right)\Delta t$$

and gives the maximum increment of the target function:

$$\begin{aligned} \Delta Y_j^{k+1} &= Y_j^{k+1} - Y_{j-1}^{k+1} = \\ &= F\left(S_{1j}^{k+1}, S_{2j}^{k+1}, \dots, S_{nj}^{k+1}, A_1^{k+1}, \dots, A_{j-1}^{k+1}, A_j^{k+1}, A_{j+1}^k, \dots, A_n^k, E_j^{k+1}\right) \\ &\quad - F\left(S_{1j-1}^{k+1}, S_{2j-1}^{k+1}, \dots, S_{nj-1}^{k+1}, A_1^{k+1}, \dots, A_{j-1}^{k+1}, A_j^k, A_{j+1}^k, \dots, A_n^k, E_{j-1}^{k+1}\right), \end{aligned}$$

where  $k = 0, 1, 2, \dots$  is the number of the iteration loop, the values  $\Delta S_{ij}^{k+1}$  and  $\Delta E_j^{k+1}$  determine changes in the current state of the environment and robots in the group as a result of performing actions  $A_1^{k+1}, \dots, A_{j-1}^{k+1}, A_j^{k+1}, A_{j+1}^k, \dots, A_n^k$ .

$Y_{j-1}^{k+1}$ —the value of the target function obtained as a result of performing actions  $A_1^{k+1}, \dots, A_{j-1}^{k+1}, A_j^k, A_{j+1}^k, \dots, A_n^k$  by robots of the group, and  $Y_j^{k+1}$  is the value of the target function obtained as a result of the choice of the action  $A_j^{k+1}$  by the robot  $R_j$  in a  $(k + 1)$  iteration loop.

The idea of the iterative procedure for optimizing the solution is that the robot  $R_j$  at the current time must choose the current action  $A_j^{k+1} = A_j^0$ , the execution of which does not lead to an unacceptable situation and gives maximum increment of the target function  $Y$ , provided that other robots in the group will perform actions  $A_1^{k+1}, \dots, A_{j-1}^{k+1}, A_{j+1}^k, \dots, A_n^k$  [3]. When the robot  $R_j$  chooses a new current action  $A_j^{k+1}$  by solving the posed optimization problem, all the other robots in the group must make a new choice of their optimal actions, since the old choice did not take into account the new action of the robot  $R_j$ , thus resolving the formulated above optimization problem taking into account the new action of the robot  $R_j$ . After that, the robot  $R_j$  must also find a new optimal action again, taking into account changes in the actions of other robots in the group. The procedure is repeated until changes in the



actions of the group's robots lead to a significant increase in the target function. The iterative optimization procedure converges for limited values of the target function, but the method of planning collective actions of robots does not lead to a global maximum of the target function [3].

As one can see, the basis of the described method is the representation of the environment in which robots interact, the states of robots, as well as the event stream in the form of vector functions. Since the full event stream during the implementation of a system for a real physical environment, in which robots interact to liquidate a technogenic accident, can include hundreds of parameters, it is necessary to leave the event stream open for adding new parameters, for example, corresponding to the data read from the robot's sensors.

### 3.1 *Urban Infrastructure Model*

Urban infrastructure model—weighted connected undirected graph  $G(V, E)$ , where:

- $V$ —graph nodes—coordinates of intersections and specified points on the road section. Each node of the graph has a unique sequence number.
- $E$ —edges—road sections between nodes. Sections of roads have their own capacity and at each cycle, they can be blocked with a given probability.

Each node is represented by a pair of coordinates in the Universal Transverse Mercator (UTM) system since in this case, it is possible to use the Euclidean metric within one UTM zone with a small error to calculate the distances.

Security objects are added—arbitrary points with UTM coordinates within the infrastructure.

Each node in the graph  $G(V, E)$  is assigned one of the following types:

- “regular” node;
- “workstation” for replenishing the energy resource of robots;
- “source”—an accident source for liquidation.

### 3.2 *Robot Model*

The developed environment simulates the operation of a finite number of intelligent mobile robots  $R_1 \div R_n$  of three different types (small, large, and medium) with a limited communication area.

The main parameters of the developed robot model:

- serial number ( $\in \mathbb{N}$ );
- travel speed ( $\in \mathbb{R}$ );
- productivity—the amount of energy that the robot can spend on the liquidation of the source within one cycle ( $\in \mathbb{R}$ );

- probability of the robot breaking down;
- current energy resource ( $\in \mathbb{R}$ );
- communication range and range of sensors.

The state of the robot  $R$  corresponds to vector  $S$ . The travel speed, maximum energy resource, productivity, communication range, and range of sensors of different types of robots may vary.

Each robot  $R$  action is specified as a vector  $A$  of the form

$$\langle Ng, At, T \rangle.$$

Action types  $At$ :

- driving to a node with sequence number  $Ng$  of an arbitrary type and “inaction” in it during  $T$  cycles;
- driving to a “workstation” with sequence number  $Ng$  and “replenishing energy resources” in it during  $T$  cycles;
- driving to the visible “source” with sequence number  $Ng$  and “liquidation of the accident source” by robot  $R$  during  $T$  cycles.

Each robot stores up-to-date information about the current situation in the environment.

### 3.3 Accident Source Model

It is known that the development of the emergency process is usually a chain, avalanche-like dynamic process [1]. Therefore, when developing a model of an accident source, the following main parameters are taken into account:

- the radius of the affected area of the accident source ( $\in \mathbb{R}$ );
- source coordinates (unique sequence number in the graph  $G(V, E)$ ) ( $\in \mathbb{N}$ );
- source intensity ( $\in \mathbb{R}$ );
- the rate of increase/decrease in the intensity and radius of the source ( $\in \mathbb{R}$ ).

Also, the probability of changing the type of the “regular” node of the infrastructure graph to the “source” is set when the “regular” node is located within the radius of the affected area of the “source”.

### 3.4 Event Stream Model

Event stream  $P$  is reflecting an instantaneous change in the state of the environment and robots.

A system of information exchanges is organized with the transfer of the following information from the event stream between robots that are at the same time located within the union of their communication range:

- list of blocked edges;
- parameters and coordinates of each source detected by the robot's sensors;
- the state of each robot (coordinates, the current energy resource of the robot).

Robots must interact in subgroups (“components”)—parts of robots that are at the same time located within the union of their communication range. At each cycle, robots in a “component” collect information about the environment with the help of sensors and with information about their own state distribute it among themselves. Thus, each robot in a “component” has up-to-date information about the current state of the environment visible by the subgroup.

### 3.5 Target Function

For the practical implementation of the process of liquidation of technogenic accidents when using the iterative procedure for optimizing the collective solution, the target function is detailed in the form of the sum of the products of the efficiency functions and their corresponding strategic coefficients. This kind of function is used, for example, in [19] to solve the problem of clustering a group of robots.

The target function is presented below:

$$Y = \sum_{R_l \text{ from "component" }} d_{A_l R_l},$$

where  $d_{A_l R_l}$  is the efficiency measure of the choice of the action  $A_l$  by the robot  $R_l$ .

The efficiency measure  $d_{A_l R_l}$  has the following form:

$$\begin{aligned} d_{A_j R_j} = & LIQUIDATE \cdot L(P, A_r, \dots, A_j, \dots A_t) \\ & + TIMEC \cdot T(P, A_r, \dots, A_j, \dots A_t) + ENERGYC \cdot E(P, A_r, \dots, A_j, \dots A_t) \\ & + DISTANCE \cdot D(P, A_r, \dots, A_j, \dots A_t) + REPEATC \\ & \cdot R(P, A_r, \dots, A_j, \dots A_t) \\ & + NOTEMPTYC \cdot N(P, A_r, \dots, A_j, \dots A_t) + OCCUPIEDC \\ & \cdot O(P, A_r, \dots, A_j, \dots A_t) \\ & + SAMEC \cdot S(P, A_r, \dots, A_j, \dots A_t) + GUARDEDC \cdot G(P, A_r, \dots, A_j, \dots A_t), \end{aligned}$$

where  $L, T, E, D, R, N, O, S, G$  are efficiency functions that change their value for different choices of action  $A_j$  by robot  $R_j$  for fixed selected actions of other robots in the iterative optimization procedure.

*LIQUIDATEC, TIMEC, ENERGYC, DISTANCEC, REPEATC,  
NOTEMPTYC, OCCUPIEDC, SAMEC, GUARDED C*

are strategic coefficients to prioritize their respective efficiency functions.

Strategic coefficients and efficiency functions determine the behavior of robots in a “component” in the current situation and, accordingly, the tactics of liquidating a technogenic accident.

Strategic coefficients are predefined and the same for different types of robots and do not change during the simulation of liquidation. A different set of strategic coefficients for each type of robot can reduce the average time for liquidating a technogenic accident by assigning each type of robot a separate “role”; however, this approach requires a long adjustment of these coefficients.

Each efficiency function was selected empirically in order to reduce the number of cycles required for the complete liquidation of a technogenic accident.

- The efficiency function  $L$  allows one to take into account the amount of reduction in the radius and intensity of the source, which is directed by the action  $A_j$  of the “liquidation of the accident source” type of the robot  $R_j$ .  $L$  increases its value with an increase in the energy resource that the robot spends on liquidating the source.
- The efficiency function  $T$  introduces a penalty on the number of cycles that the robot  $R_j$  will spend performing the action  $A_j$  in the infrastructure node.
- The efficiency function  $E$  encourages the robot to replenish the energy resource.
- The efficiency function  $D$  introduces a penalty on the minimum path length that the robot  $R_j$  needs to overcome from its current position to the node corresponding to the action  $A_j$ .
- The efficiency function  $R$  introduces a penalty if the robot has chosen an action to move to an already visited node.
- The efficiency function  $N$  introduces a penalty if the robot, with a non-empty list of visible sources, chooses an action, the type of which is not “liquidation of the accident source”.
- The efficiency function  $O$  introduces a penalty if the robot has chosen action of type “liquidation of the accident source” at a node to which one or more robots have already been sent for liquidation, whose energy resources are sufficient to liquidate the source. Thus,  $O$  forces the robots to disperse over several different sources, each of which is closer to the robot, with an emphasis on the complete liquidation of the source in the node.
- The efficiency function  $G$  introduces a penalty that is directly proportional to the minimum distance between the node to which the robot is directed and the security object in the environment. By changing the GUARDED C coefficient, it is

possible to achieve that the robots will strive to explore the nodes that are closest to the security objects and to liquidate sources in them if they are present.

- The efficiency function  $S$  introduces a penalty if the robot  $R_j$  has chosen to move a node to which one of the visible robots is already heading.

Thus, as the current action, the robot  $R_j$  needs to choose action  $A_j = \arg \left( \max_{A_j \in \{A\}} Y \right)$  at each iteration loop of the iterative procedure for optimizing the collective solution.

The above efficiency functions allow robots to solve the following tasks during the liquidation of a technogenic accident:

- exploring the area—search for coordinates of sources in urban infrastructure;
- protecting security objects—liquidation of accident sources closest to the specified security objects;
- liquidating sources.

It should be noted that robots do not have information about the location of sources and their parameters in advance, so the robots in the created model carry out an iterative optimization procedure in the “component” whenever the event stream is changed, which allows changing the actions of robots, taking into account new changes in the visible parameters of a technogenic accident. Each robot performs assigned actions autonomously. The trajectories of the robots are found using a modification of the Floyd-Warshall algorithm for finding the lengths of the shortest paths between all pairs of nodes, which makes it possible to reconstruct the shortest paths.

## 4 Estimation of the Strategic Coefficients

The above efficiency functions in the target function can be implemented on the basis of expert knowledge about the nature of the development of specific technogenic accidents to develop an optimal strategy for robots during the liquidation of the accident. However, in the absence of experts, the search for efficiency functions and their strategic coefficients can be carried out empirically using the simulation environment to simulate the process of liquidating technogenic accidents with various parameters of the development of a technogenic accident.

The simulation environment will allow one to clearly see the errors in the strategy by which robots interact in the environment and the adequacy of the developed models. Since in the method used, the strategy is completely determined by the efficiency measure, and the model is determined by the vector functions of the parameters, their change should be less time-consuming than when using other approaches.

## 4.1 Simulation Environment

In order to conduct experiments for the developed algorithms for planning the action of a group of robots when using DGCS, changing the event stream and movement of robots, an appropriate program model was developed and created that simulates the process of liquidating a technogenic accident.

The programming model is implemented using the high-level language Kotlin and is designed to work under the Windows 10 operating system.

The software model consists of the following modules:

- module for initialization of the urban infrastructure graph;
- module for rendering infrastructure and robots;
- module for setting parameters of a group of robots and the technogenic accident;
- module for controlling a group of robots and events;
- simulation module.

Third-party free libraries `geojson` and `jgrapht` were used to initialize the urban infrastructure graph. The input to the urban infrastructure graph initialization module receives files in the GeoJSON format intended for storing geographic data structures. The format allows storing primitive types for describing geographic objects, such as points (addresses and locations), segments (streets, highways), polygons (countries, states). Each file contains a set of line segments represented by a list of points with coordinates in the WGS84 system (World Geodetic System 1984). The coordinates of the points in the WGS84 system are translated into the UTM system for the subsequent formation of the infrastructure graph edges. Each segment from the set has its own capacity. The generated data is fed to the input of the `jgrapht` library to create a weighted graph corresponding to the infrastructure, which is the output of the module.

An `OpenStreetMap` and third-party free library `mapjfx` was used to display the urban infrastructure and robots. The result of the rendering module is the generated urban infrastructure. An example of a generated graph of urban infrastructure, robots, and sources is shown in Fig. 1.

The setting of the parameters of a group of robots and the technogenic accident is carried out in the module for setting the parameters of a group of robots and the technogenic accident through the graphical screen of the program, implemented using the `JavaFX` library. By entering various values into the text input fields marked with arrows in Fig. 2 it is possible to change both the tactics of liquidation of the technogenic accident by a group of robots and the scenario of the development of the technogenic accident itself.

In the module for controlling a group of robots and events, a robot, a source, and the environment in which the robots interact are represented by separate classes. It was decided to use the interaction between objects of the classes “Robot”, “Environment” and “Source” to simulate information exchanges between robots and to obtain up-to-date information about the environment by robots. So, different robots are represented by different objects of the “Robot” class. All robots operate in an

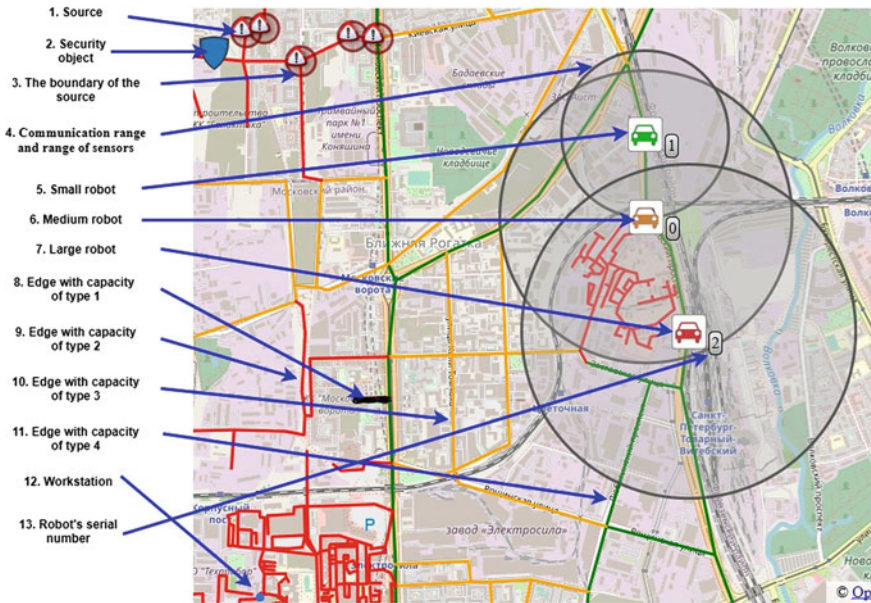


Fig. 1 An example of a generated graph of urban infrastructure, robots, and sources

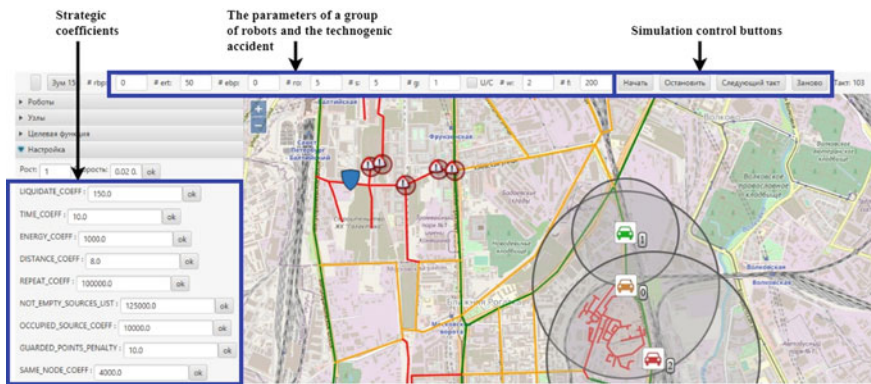


Fig. 2 The main panel of the simulation environment

environment represented by one object of the “Environment” class. The Robot class encapsulates all the parameters of the robot model and the implementation of algorithms for group interaction of robots. The “Environment” class encapsulates all the parameters of the model and the implementation of the algorithm for changing the event stream, and the “Source” class encapsulates the parameters of the source model and the implementation of functions for changing its parameters with an increase in

the number of cycles and the action from the robots. This approach allows one to move away from multi-thread interaction and significantly simplify the implementation.

The simulation module is intended for manual configuration of the infrastructure, parameters of a group of robots, and scenarios for the development of the technogenic accident. The module launches simulations with different parameters, each time keeping the number of cycles required to completely liquidate the technogenic accident.

## 5 Experiments

As it was mentioned earlier, the selection of efficiency functions for the objective function is empirical. However, in order to determine the strategic coefficients corresponding to the introduced efficiency functions, to reduce the number of cycles required for the complete liquidation of technogenic accident and to show that each efficiency function actually reduces the number of cycles for liquidation with different groups of parameters of the accident development, one can use the coordinate descent method by reproducing it steps in a simulation environment.

The following function is optimized:

$$f(\text{LIQUIDATEC}, \text{TIMEC}, \text{ENERGYC}, \text{DISTANCEC}, \\ \text{REPEATC}, \text{NOTEMPTYC}, \text{OCCUPIEDC}, \text{SAMEC}),$$

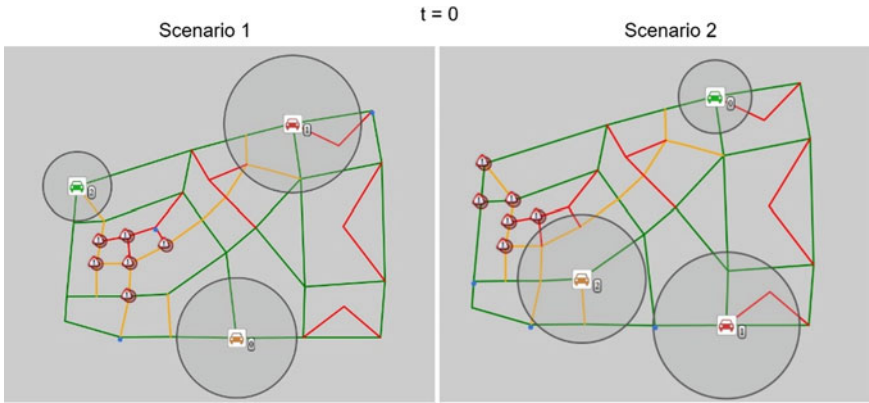
$f$  is equal to the average number of cycles required for the complete liquidation of a technogenic accident, with fixed ranges of changes in the parameters of a group of robots and a technogenic accident, with the number of different scenarios being considered tending to infinity (in the ideal case, however, in the chapter, the number of scenarios considered for each group of accident parameters is 500). An example of two different scenarios of the only group of parameters used for the development of an accident at the initial moment of time is shown in Fig. 3.

Figure 4 shows the state of the environment of the second scenario, presented in Fig. 3, with the number of cycles equal to 61. Scenario 2 from Fig. 3 ends on cycle 68 with the complete liquidation of all accident sources.

One-dimensional optimization is carried out by applying a general search since the nature of the function  $f$  is unknown. Optimization by strategic coefficient  $\text{GUARDED C}$  is not performed. Initial strategic coefficients values were selected empirically.

Figures 5, 6 and 7 below show the dependences of the average number of cycles for the complete liquidation of the accident on the value of the strategic coefficients obtained at the first step of the coordinate descent for one group of parameters, in the following order of one-dimensional optimizations:  $\text{REPEAT C} \rightarrow \text{DISTANCE C} \rightarrow \text{NOTEMPTY C} \rightarrow \text{ENERGY C} \rightarrow \text{LIQUIDATE C} \rightarrow \text{SAME C} \rightarrow \text{TIME C} \rightarrow \text{OCCUPIED C}$ .





**Fig. 3** Two different scenarios of one group of parameters for the development of an accident at the initial moment of time

**Fig. 4** The state of the environment of the second scenario (61 cycles), presented in Fig. 3

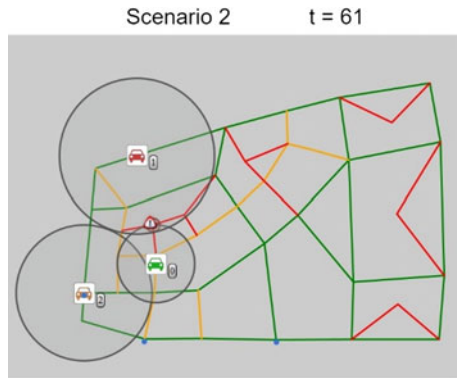


Figure 5 shows that a value exceeding 34,000 should be taken as a new value of strategic coefficient REPEATC, since it corresponds to the minimum average number of cycles for the complete liquidation of an accident for 500 scenarios from a selected group of parameters.

Figure 6 shows that a value equals to 115,200 should be taken as a new value of strategic coefficient NOTEMPTYC, since it corresponds to the minimum average number of cycles for the complete liquidation of an accident for 500 scenarios from a selected group of parameters.

Figure 7 shows that a value equals to 1250 should be taken as a new value of strategic coefficient ENERGYC, since it corresponds to the minimum average number of cycles for the complete liquidation of an accident for 500 scenarios from a selected group of parameters.

Figures 5, 6 and 7 also show that the selected efficiency functions, when changing their priority, affect the strategy of robots and significantly reduce the average number of cycles for liquidating an accident.

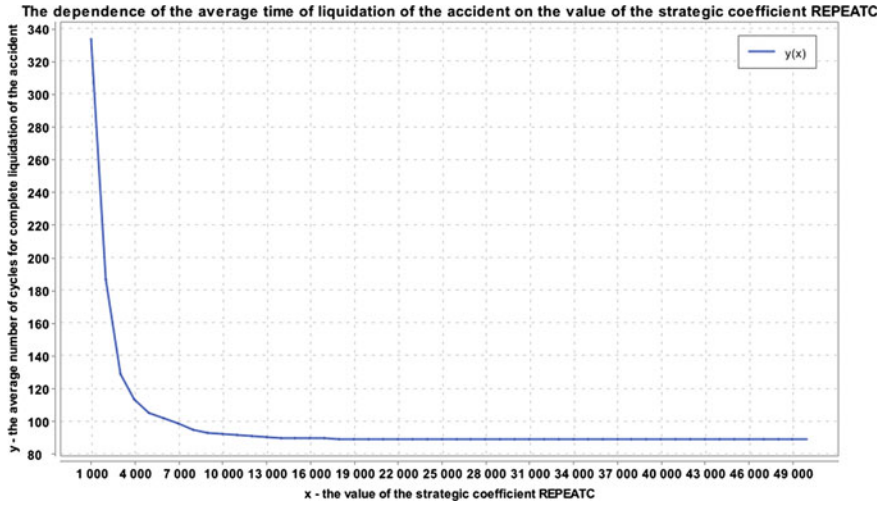


Fig. 5 The dependence of the average time of liquidation of the accident on the value of the strategic coefficient REPEATC

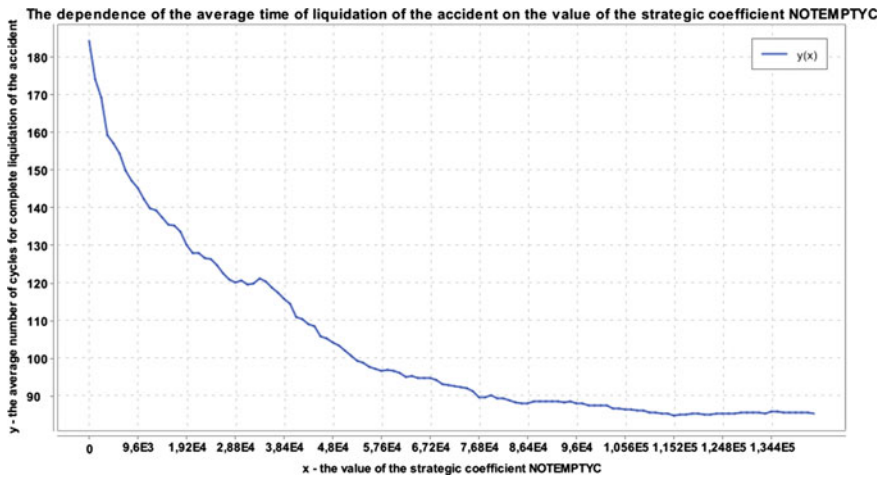


Fig. 6 The dependence of the average time of liquidation of the accident on the value of the strategic coefficient NOTEMPTYC

Similarly, with the help of the simulation environment, it is possible to find the optimal number of iterations of the iterative procedure for optimizing the collective solution necessary to search for robot actions for a selected fixed group of parameters. For each value of the number of iterations of the optimization procedure,

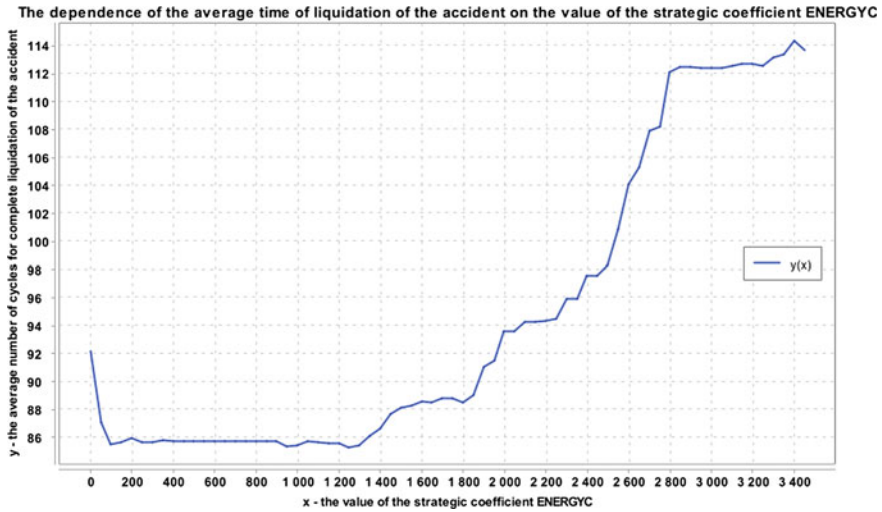


Fig. 7 The dependence of the average time of liquidation of the accident on the value of the strategic coefficient ENERGYC

the average number of cycles for the complete liquidation of the technogenic accident was searched for according to a previously selected set of scenarios (the set of scenarios is the same for different values of the number of iterations).

The dependence of the average number of cycles for the complete liquidation of the accident on the number of iterations of the iterative procedure is shown in Fig. 8.

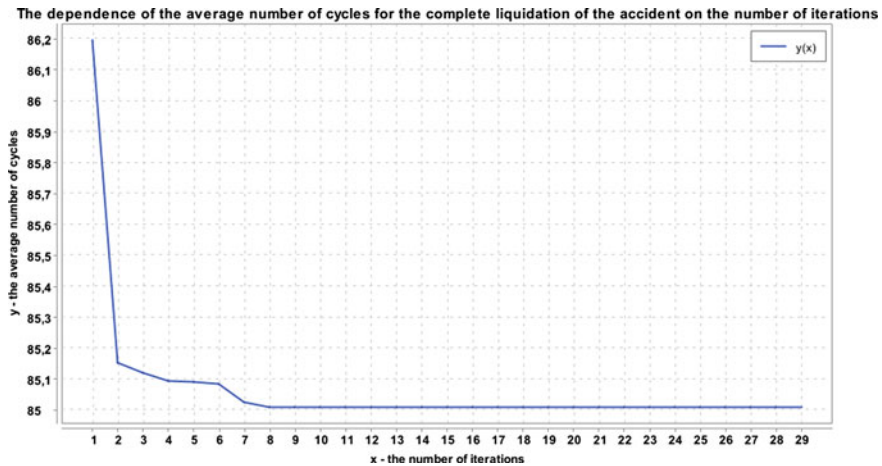
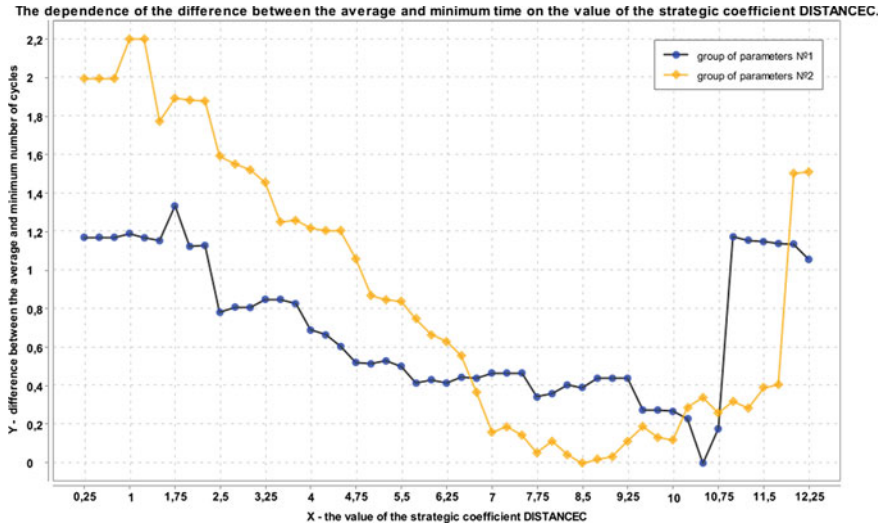


Fig. 8 The dependence of the average number of cycles for the complete liquidation of the accident on the number of iterations of the iterative procedure



**Fig. 9** The dependence of the difference between the average and minimum time for the complete liquidation of the accident on the value of the strategic coefficient DISTANCEC

Figure 8 shows that for the selected 500 scenarios, it is enough to take 10 iterations of the optimization procedure.

To check that different minimum values of strategic coefficients will correspond to different groups of parameters and their corresponding scenarios of a technogenic accident, strategic coefficients by the method of coordinate descent were found for two groups of parameters, one of which includes (group of parameters No 1—500 scenarios) the range of variation of the parameters of the other (group of parameters No 2—500 scenarios). An example of finding one strategic coefficient by the general search method in coordinate descent is shown in Fig. 9.

Figure 9 shows that for the group of parameters No 1, the value 10.5 should be taken as a new value of the strategic coefficient DISTANCEC, whereas for the group of parameters No 2, the value 8.5 should be taken.

Thus, the experiments carried out for the selected scenarios made it possible to determine the values of the strategic coefficients of the target function and the number of iterations of the iterative procedure for optimizing the collective solution that minimizes the time for liquidation of a technogenic accident.

## 6 Conclusion

The following methods were developed in this work:

- method of decentralized control of a group of robots in the liquidation of technogenic accidents;

- method for constructing a target function for controlling robots in order to minimize the number of cycles for liquidating a technogenic accident when using an iterative procedure for optimizing a collective solution;
- method for determining the strategic coefficients of the target function.

An environment for simulation modeling of scenarios of a technogenic accident was developed, which makes it possible to conduct experiments and search for optimal strategic coefficients for various groups of parameters describing scenarios of technogenic accidents.

The proposed solutions to the problem posed to make it possible to reduce the average time to liquidate technogenic accidents for various scenarios of the development of accidents and the composition of a heterogeneous group of robots, which, in turn, will reduce the number of material and human losses.

**Acknowledgements** The reported study was funded by RFBR according to the research project No 18-2903250 mk.

## References

1. Yamalov, I.U.: Modeling of management processes and decision-making in emergency situations. In: Laboratory of Basic Knowledge, p. 288. ISBN 978-5-93208-193-8 (2007)
2. Andreev, A., Zhoga, V., Serov, V., et al.: The control system of the eight-legged mobile walking robot. In: Kravets, A., Shcherbakov, M., Kultsova, M., et al. (eds.) Proceedings of the 11th Joint Conference Knowledge-Based Software Engineering, Volgograd, Russia, 17–20 September 2014, pp. 383–392. Springer, Cham (2014)
3. Kaliaev, I.A., Gaiduk, A.R., Kapustyan, S.G., Phizmathlit, M.: Models and Algorithms of Collective Control in Group of Robots (2009)
4. Fierro, R., Das, A., Spletzer, J., Esposito, J., Kumar, V., Ostrowski, J., et al.: A framework and architecture for multi-robot coordination. *Int. J. Robot. Res.* **21**(10–11), 977–995 (2002)
5. Nicolescu, M., Mataric, M.: Experience-based representation construction: learning from human and robot teachers. In: Proceedings 2001 IEEE/RSJ International Conference on Intelligent Robots and Systems, vol. 2, pp. 740–745. IEEE (2001)
6. Parker, L.: Alliance: an architecture for fault tolerant multi-robot cooperation. *IEEE Trans. Robot. Autom.* **14**(2), 220–240 (1998)
7. Yamada, S., Saito, J.: Adaptive action selection without explicit communication for multirobot box-pushing. *IEEE Trans. Syst. Man, Cybern. Part C: Appl. Rev.* **31**(3), 398–404 (2001)
8. Gazi, V.: Swarm aggregations using artificial potentials and sliding mode control. In: Proceeding of the IEEE Conference on Decision and Control, pp. 2041–2046. Maui, Hawaii (2003)
9. Khatib, M., Chatila, R.: An extended potential field approach for mobile robot-sensor based motions. In: Proceedings of the International Conference on Intelligent Autonomous Systems (IAS'4), pp. 28–35. Karlsruhe, Germany (1995)
10. Sharma, B., Vanualailai, J., Chand, U.: Flocking of multi-agents in constrained environments. *Eur. J. Pure Appl. Math.* **2**(3), 401–425 (2009)
11. Dias, M., Zlot, R., Kalra, N., Stentz, A.: Market-based multirobot coordination: a survey and analysis. *Proc. IEEE* **94**(7), 1257–1270 (2006)
12. Goldberg, D., Cicirello, V., Dias, M., et al.: Market-based Multi-robot planning in distributed layered architecture. In: Proceeding of the 2nd International Workshop on Multi-Robot Systems, pp. 27–38. Washington, DC, USA (2003)

13. Kalra, N., Ferguson, D., Stentz, A.: A market-based framework for planned tight coordination in multirobot teams. In: Proceedings of the IEEE International Conference on Robotics and Automation, pp. 1170–1177. IEEE (2005)
14. Liu, Y., Yang, J., Zheng, Y., Wu, Z., Yao, M.: Multi-robot coordination in complex environment with task and communication constraints. *Int. J. Adv. Robot. Syst.* **10**, 1–14 (2013)
15. Palm, R., Bouguerra, A.: Market-based algorithms and fuzzy methods for the navigation of mobile robots. In: Proceedings of the IEEE International Conference on Fuzzy Systems, pp. 1–8. IEEE (2012)
16. Benbouabdallah, K., Qi-dan, Z.: A fuzzy logic behavior controller for a mobile robot path planning in multi-obstacles environment. *Res. J. Appl. Sci. Eng. Technol.* **5**(14), 3835–3842 (2013)
17. Duman, H., Hu, H.: Fuzzy logic for behavior coordination and multiAgent formation in RoboCup. *Dev. Soft Comput. Adv. Soft Comput.* **9**, 191–198 (2001)
18. Maryasin, O.: Bee-inspired algorithm for groups of cyber-physical robotic cleaners with swarm intelligence. In: Kravets, A., Shcherbakov, M., Bolshakov, A. (eds.) *Cyber-Physical Systems: Modelling and Intelligent Control*, pp.167–177. Springer (2021)
19. Gaiduk, A., Kapustyan, S., Shapovalov, I.: Self-organization in groups of intelligent robots. In: *Robot Intelligence Technology and Applications 3. Advances in Intelligent Systems and Computing*, vol. 345, pp. 171–181 (2015)

# **Cyber-Physical Systems Industrial Implementation**

# Impact of Preventive Measures on Conditions of Risk Insurance in Cyber-Physical System of Industrial Enterprise



Mikhail Geraskin and Elena Rostova

**Abstract** The risks of technical incidents at industrial enterprises are considered. A cyber-physical system for managing such risks, based on the interaction of personnel, a technical device and an insurer, is being investigated. A method for determining the reduction coefficient to the insurance tariff for industrial risk insurance is proposed. This coefficient is proposed to be used as a tool to stimulate the policyholder to carry out preventive measures aimed at reducing the insured risk. The measures include the installation of real-time monitoring systems and other monitoring, control, and production management systems using Industry 4.0 technologies. In production, the use of such systems helps to reduce the industrial risk, and it is stimulated by the insurer. The obtained results allow us to determine the range of values of the reducing coefficient, taking into account the interests of the insurer and the policyholder, i.e. an industrial enterprise.

**Keywords** Industrial risk · Insurance · Preventive measures · Bonus-malus rating · Industry 4.0 technologies

## 1 Introduction

Industrial enterprises face technology-related and artificial risks, which lead to disruption of the production process. Therefore, the enterprise is considered as a cyber-physical system in which management and personnel interact with technical devices to minimize the consequences of technical incidents.

---

M. Geraskin (✉) · E. Rostova  
Samara National Research University, Samara, Russia  
e-mail: [innovation@ssau.ru](mailto:innovation@ssau.ru)

E. Rostova  
e-mail: [el\\_rostova@mail.ru](mailto:el_rostova@mail.ru)



Methods of managing these risks include insurance and the preventive measures aimed at reducing the risk [1–5]. The system includes an insurer who compensates for the consequences of incidents and is interested in preventing incidents.

Many experts note a significant impact of equipment reliability on the likelihood of unforeseen situations in production [6]. The timely diagnostics with a help of the control and monitoring systems reduce production risks and allow us to quickly respond to the occurrence of an emergency and prevent it, or reduce damage. The industrial enterprise can influence the probability of a risk event and the amount of damage through preventive measures and insurance. The insurance company is interested in reducing the insured risk and to encourage the policyholder to reduce the risk, it uses a reducing coefficient—the bonus-malus rating (BMR). The insurance company is interested in collecting statistical information about the object of insurance to form a database and improve underwriting [7].

Many authors consider the problem of industrial risk [8, 9] as the environmental risk and the environmental harm reduction. For risk analysis, the authors use different mathematical methods: the scenario method [10], the multi-agent systems [11, 12], the multi-criteria models [13, 14]. Additionally, this problem was analyzed on various levels: the world market risk [15], the regional economic system risk [16–18], the firm’s risk [19, 20], the technology operation risk [21, 22].

Our research is devoted to determining the boundaries of the values of the BMR, taking into account the interests of the insurer and the industrial enterprise acting as the policyholder.

## 2 Methods

We consider a system that includes an industrial enterprise and an insurance company. We define the conditions for the coordinated interaction of the system agents. We develop a profit function for each agent of the system, which is the objective function of the agent. A detailed justification of the components of the profit function of the industrial enterprise was given in [22].

The profit of the industrial enterprises is

$$\Pi_I = Q_P + W - C_Q - f - X^{res} - V, \quad (1)$$

where the volume of production is  $Q$ , the indemnity is  $W$ , the production cost is  $C_Q$ , the cost to reduce the insured risk is  $f$ , the rest damage of industrial enterprises left to their retention is  $X^{res}$ , the insurance premium is  $V$ .

The profit of the insurance company is

$$\Pi_{II} = (T - \alpha)X^s, \quad (2)$$

where the insurance rate is  $T$ , the ratio of compensation and insured damage is  $\alpha$ , the damage of the industrial enterprise transferred to the insurer is  $X^S$ .

A change in the cost  $\Delta f = \tilde{f} - f > 0$ , which is aimed at reducing the industrial risk, will entail a change in the damage left on its retention  $\Delta X^{res} = X^{res} - \tilde{X}^{res} > 0$ , the insured damage  $\Delta X^S = X^S - \tilde{X}^S > 0$ , the insurance compensation  $W > \tilde{W}$ , and the insurance premium  $V > \tilde{V}$ . The tilde symbol indicates the values corresponding to the parameters of the insurer's system and the industrial enterprise, to increase the cost of reducing the insured industrial risk.

We denote BMR ( $k_T$ ) and write (1) and (2) in the following form:

$$\tilde{\Pi}_I = Q_P + \tilde{W} - C_Q - \tilde{f} - \tilde{X}^{ocm} - \tilde{V},$$

$$\tilde{\Pi}_{II} = (\tilde{T} - \alpha)\tilde{X}^S = (\tilde{T} - k_T - \alpha)\tilde{X}^S.$$

We write the condition for the expediency of carrying out preventive measures for the industrial enterprise and the insurer in the following form:

$$\tilde{\Pi}_I \geq \Pi_I \quad (3)$$

$$\tilde{\Pi}_{II} \geq \Pi_{II} \quad (4)$$

**Proposition 1.** Condition (3) is satisfied if

$$k_T \geq \frac{\Delta f + (\alpha - T)\Delta X^S - \Delta X^{ocm}}{\tilde{X}^S} \quad (5)$$

**Proposition 2.** Condition (4) is satisfied if

$$k_T \leq \frac{\Delta X(\alpha - T)}{\tilde{X}}. \quad (6)$$

We combine constraints (5) and (6) and obtain a set of the possible values of the BMR, taking into account the interests of the agents of the system

$$k_T \in [k_T^-, k_T^+], k_T^- = \frac{\Delta f + (\alpha - T)\Delta X^S - \Delta X^{ocm}}{\tilde{X}^S}, k_T^+ = \frac{\Delta + (\alpha - T)}{\tilde{X}} \quad (7)$$

Minorant (5) and majorant (6) determine the minimum and the maximum possible values of the BMR, taking into account the interests of the industrial enterprise and the insurance company. Restrictions (7) determine the boundaries of the change in the MBR, provided that it is advisable to carry out preventive measures for the insurer and the policyholder.

### 3 Results

We consider various options for transferring risk to the insurer: the all-risk insurance, the proportional insurance, the first risk insurance, and the insurance with the deductible. The insured damage  $X^S$  is the expected damage of the insurer:  $M(X^S) = M(X^S|A) \cdot P(A)$ , where  $M(\cdot)$  is the mathematical expectation of a random variable,  $P(\cdot)$  is the probability of the insurance event  $A$ . We obtain different results of reducing the insured damage for different risk transfer options and different random variable distribution laws. Table 1 demonstrates the results for the exponential distribution.

In Table 1  $C$  is the first risk insurance,  $fr$ —deductible,  $\lambda$  is the exponential distribution parameter that characterizes the frequency of disruption of the production process.

Figure 1 demonstrates the simulation result for the exponential distribution of the insured damage value  $M(X^S|A)$ .

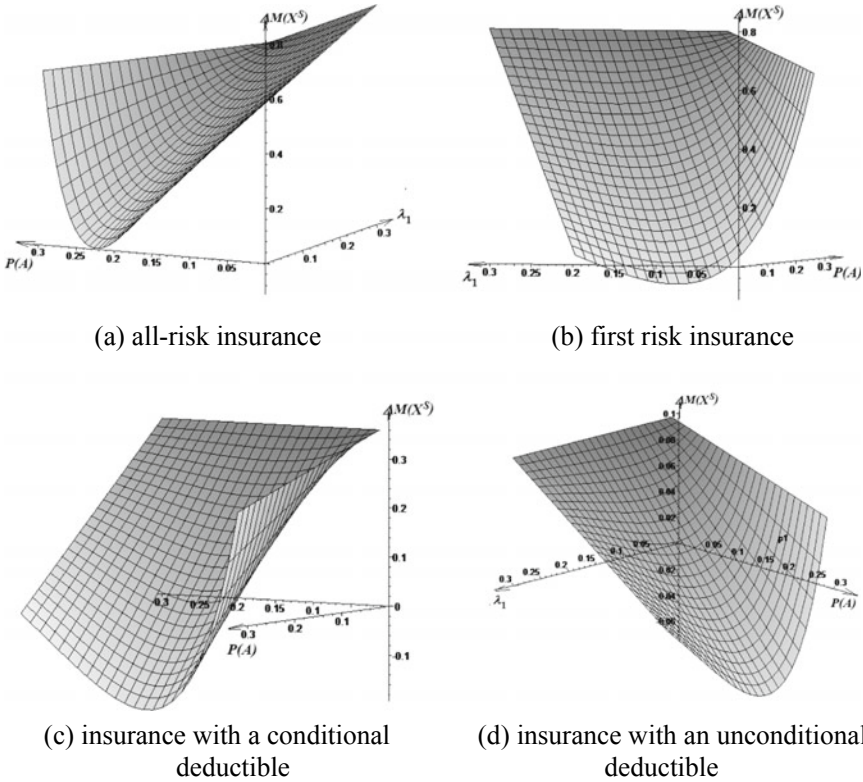
For exponential distribution, there are insurance conditions in which preventive measures will not be profitable. For example, for the first risk insurance and the insurance with a deductible, there are the parameters in which  $M(X^S|A) < 0$ .

Table 2 demonstrates the results for normal distribution.

In Table 2  $C$  is the first risk insurance,  $fr$ —deductible,  $m, \sigma$  are the normal distribution parameters that characterize the average damage value and the deviation from the average.

**Table 1** Reduction of expected insured damage with exponential distribution for various liability systems

Insurance liability system	$M(X^S A)$
All-risk insurance	$\int_0^{X^S} \lambda e^{-\lambda x} dx$
Proportional insurance	$\alpha \int_0^{X^S} \lambda e^{-\lambda x} dx$
First risk insurance	$\int_0^c \lambda e^{-\lambda x} dx + \int_c^{X^S} \lambda e^{-\lambda x} C dx$
Insurance with a conditional deductible	$\int_{fr}^{X^S} \lambda e^{-\lambda x} dx$
Insurance with an unconditional deductible	$\int_{fr}^{X^S} \lambda e^{-\lambda x} (x - fr) dx$



**Fig. 1** Reduction of expected insured damage with exponential distribution for various liability systems

Figure 2 demonstrate the simulation result for the normal distribution of the insured damage value  $M(X^S|A)$ . We see that preventive measures are always beneficial for the all-risk insurance, but for other insurance liability systems, there are the parameters under which  $M(X^S|A) < 0$ .

### 4 Discussion

The obtained results can be used in the formation of the industrial risk insurance tariff, as well as in stimulating the policyholder to reduce the insured risk. The choice of the option of transferring risk to insurance is based on the characteristics of the insured risk. For the all-risk insurance, the numerical experiments demonstrate that the preventive measures are advantageous for any parameter values, because

**Table 2** Reduction of expected insured damage with normal distribution for various liability systems

Insurance liability system	$M(X^S A)$
All-risk insurance	$\int_0^{X^S} \frac{1}{\sigma\sqrt{2\pi}} e^{-\frac{(x-m)^2}{2\sigma^2}} x dx$
Proportional insurance	$\alpha \int_0^{X^S} \frac{1}{\sigma\sqrt{2\pi}} e^{-\frac{(x-m)^2}{2\sigma^2}} x dx$
First risk insurance	$\int_0^c \frac{1}{\sigma\sqrt{2\pi}} e^{-\frac{(x-m)^2}{2\sigma^2}} x dx + \int_c^{X^S} \frac{1}{\sigma\sqrt{2\pi}} e^{-\frac{(x-m)^2}{2\sigma^2}} C dx$
Insurance with a conditional deductible	$\int_{fr}^{X^S} \frac{1}{\sigma\sqrt{2\pi}} e^{-\frac{(x-m)^2}{2\sigma^2}} x dx$
Insurance with an unconditional deductible	$\int_{fr}^{X^S} \frac{1}{\sigma\sqrt{2\pi}} e^{-\frac{(x-m)^2}{2\sigma^2}} (x - fr) dx$

$\Delta M(X^S) > 0$ . For the insurance with the deductible and the first risk insurance, there are parameter values at which preventive measures will not always pay off by reducing damage, because  $\Delta M(X^S) < 0$ . Therefore, the level of cost for preventive measures depends on the specific parameters of the cyber-physical system and the insurance conditions. The theoretical results can be supplemented by considering other laws of distribution of the random value of the insured damage.

## 5 Conclusion

The chapter examines two methods used in risk management—risk reduction and risk transfer. For the system of two agents (the industrial enterprise and the insurer), we deduce the solution to the problem of determining the values of the bonus-malus rating. This solution stimulates the implementation of preventive measures aimed at reducing the insured risk. We obtain the change in the insured damage for various options for transferring responsibility to the insurer and for the exponential distribution and the normal distribution of damage.

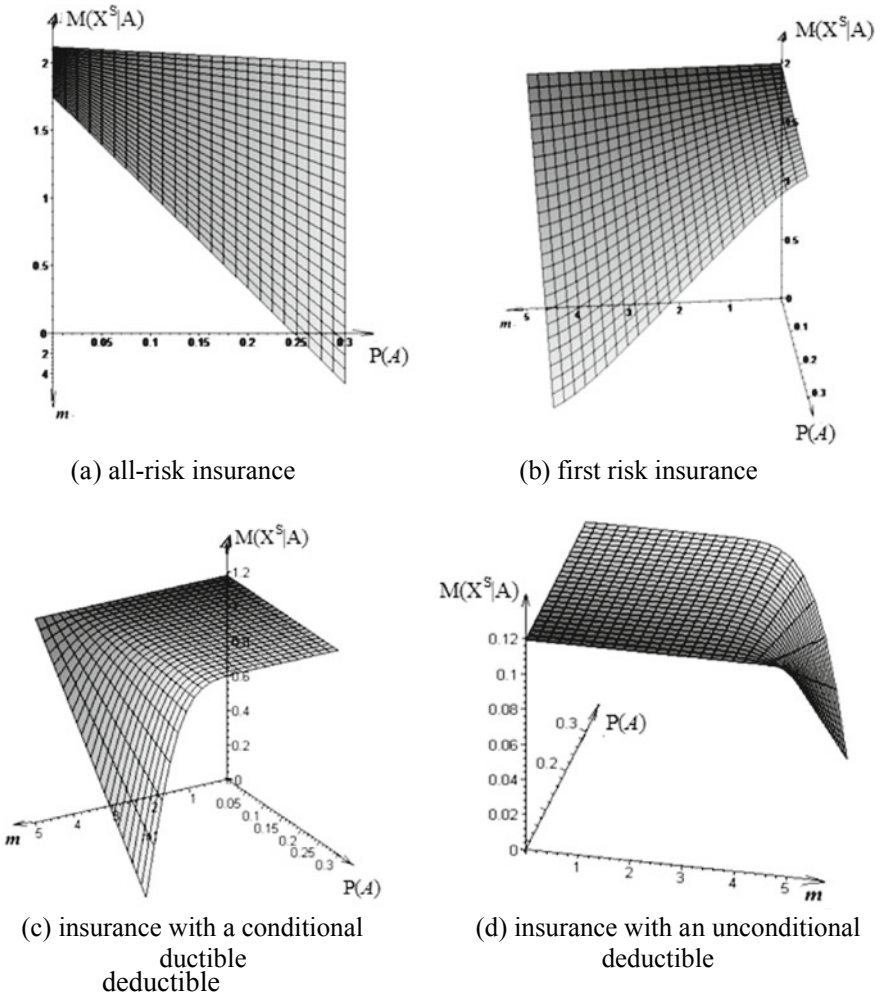


Fig. 2 Reduction of expected insured damage with normal distribution for various liability systems

### References

1. Prokopjeva, E.: Insurance instruments in risk management of the manufacturing sector of a region: the case of the Republic of Khakassia (Russia). *Invest. Manag. Financ. Innov.* **17**(4), 299 (2020)
2. Ovanesyan, N.M., Midler, E.A.: Risk management at the industrial enterprise using business insurance mechanism. *Adv. Eng. Res.* **11**(9), 1719–1725 (2018)
3. Dmitriev, O.N.: Development of risk insurance area for Russian high-technology enterprises. *Eur. Res. Stud. J.* **21**(4), 386–399 (2018)
4. 박중현, 장동환: The Integrated risk management for the fourth industrial revolution-focus on Korea's insurance industry. *유라시아연구* **15**(4), 143–162 (2018)

5. Cays, J.: Life-cycle assessment: reducing environmental impact risk with workflow data you can trust. *Archit. Des.* **87**(3), 96–103 (2017)
6. Shovkun, M.V., Korovin, A.I., Voskovov, V.Y.: On the issue of using the method of element-by-element calculation of the wear of a set of components, mechanisms and aggregates when assessing the frequency of emergency situation at a dangerous object. *Trudy Moskovskogofiziko-technicheskogo institute.* **5**(18), 192–196 (2013)
7. Radanliev, P.: Economic impact of IoT cyber risk—analysing past and present to predict the future developments in IoT risk analysis and IoT cyber insurance (2018)
8. Lee, J., Lee, D.K.: Application of industrial risk management practices to control natural hazards, facilitating risk communication. *ISPRS Int. J. Geo-Inf.* **7**(9), 377 (2018)
9. Samanlioglu, F.: A multi-objective mathematical model for the industrial hazardous waste location-routing problem. *Eur. J. Oper. Res.* **226**(2), 332–340 (2013)
10. Kulba, V., Schelkov, A., Chernov, I., Zaikin, O.: Scenario analysis in the management of regional security and social stability. *Intell. Syst. Ref. Libr.* **98**, 249–268 (2016)
11. Ahn, H.J., Park, S.J.: Modeling of a multi-agent system for coordination of supply chains with complexity and uncertainty. In: Lee, J., Barley, M. (eds.) *Intelligent Agents and Multi-Agent Systems. PRIMA. Lecture Notes in Computer Science*, vol. 2891. Springer, Berlin (2003). [https://doi.org/10.1007/978-3-540-39896-7\\_2](https://doi.org/10.1007/978-3-540-39896-7_2)
12. Finch, P.: Supply chain risk management. *Supply Chain. Manag.* **9**(2), 183–196 (2004). <https://doi.org/10.1108/13598540410527079>
13. Edjossan-Sossou, A.M., Galvez, D., Deck, O., Heib, M.A., Verdel, T., Dupont, L., Chery, O., Camargo, M., Morel, L.: Sustainable risk management strategy selection using a fuzzy multi-criteria decision approach. *Int. J. Disaster Risk Reduct.* **45**, 101474 (2020). <https://doi.org/10.1016/j.ijdr.2020.101474>
14. Yazdani, M., Gonzalez, E.D.R.S., Chatterjee, P.: A multi-criteria decision-making framework for agriculture supply chain risk management under a circular economy context. *Manag. Decis.* (2019). <https://doi.org/10.1108/MD-10-2018-1088>
15. Hanson, D., White, R.: Regimes of risk management in corporate annual reports: a case study of one globalizing Australian company. *J. Risk Res.* **7**, 445–460 (2004)
16. Pazdnikova, N.P., Shipitsyna, S.Y.: Stress analysis in managing the region’s budget risks, risk factors for the regional economic growth. *Econ. Reg.* **3**(39), 208–217 (2014)
17. Sapiro, E.S., Miroljubova, T.V.: Risk factors for the regional economic growth. *Econ. Reg.* **1**, 39–49 (2008)
18. Shorikov, A.F.: Dynamic model of minimax control over economic security state of the region in the presence of risks. *Econ. Reg.* **2**(30), 258–266 (2012)
19. Lee, J., Kim, C.: Multi-agent systems applications in manufacturing systems and supply chain management: a review paper. *Int. J. Prod. Res.* **46**(1), 233–265 (2008). <https://doi.org/10.1080/00207540701441921>
20. Pazdnikova, N.P., Shipitsyna, S.Y.: Stress analysis in managing the region’s budget risks, risk factors for the regional economic growth. *Ekonomika Regiona* **3**(39), 208–217 (2014)
21. Rasmussen, J., Svedung, I.: *Proactive Risk Management in a Dynamic Society*. Swedish Rescue Services Agency (2000)
22. Rostova, E.P., Geraskin, M.I.: Optimization of costs function for prevention of firms’ industrial risks with penalties. In: *The Proceedings of the Third Workshop on Computer Modelling in Decision Making (CMDM 2018)*. *ACSR-Advances in Computer Science Research*, vol. 85, pp. 26–30 (2018)

# A Combined Method for Solving the Problem of Optimizing the Production Schedule of Metal Structure Processing for Use in a Cyber-Physical Control System of a Metallurgical Enterprise



Alexander A. Bolshakov , Lilia Slobodyanyuk, Olga Shashikhina, and Yana Kovalchuk

**Abstract** A generalized diagram of the main stages of the process of forming a production schedule for the processing shop of a metalwork plant is proposed. A scheme for the formation of a production plant with a description of the input and output coordinates, as well as a control variable has been built. The necessity of the process of optimization of the production plan is shown, which will reduce the time of production of products and ensure the maximum load of the equipment of the enterprise. This allows it to be used in a cyber-physical control system in the event of situations that are not foreseen at the initial stage of the formation of an optimal schedule for loading equipment in a processing shop. An informal and formalized statement of the problem of optimization of the production plan of a metalwork plant is given. The target criterion, restrictions on admissible solutions for optimizing the production plan are formulated and investigated. A combined solution algorithm is proposed, including a direct search method for a relatively small dimension and a genetic algorithm for large dimension problems. Testing of the proposed software for the Chelyabinsk plant of metal structures has been carried out. The efficiency of the optimization algorithm and the complexity of programs that implement it has been confirmed. The preferable regions for the parameters of the genetic algorithm were determined: the probabilities of crossing over and mutation, the type of crossing-over, the volume of the initial population.

**Keywords** System analysis · Optimal planning · Metalwork plant · Production scheduling · Genetic algorithm · Cyber-physical system · Control

---

A. A. Bolshakov (✉) · Y. Kovalchuk

Peter the Great St. Petersburg Polytechnic University, 29, Polytechnicheskaya Street, St. Petersburg 195251, Russia

L. Slobodyanyuk · O. Shashikhina

St. Petersburg State Technological Institute (Technical University), 26, Moskovsky pr., St. Petersburg 190013, Russia

e-mail: [rabota1975@74.ru](mailto:rabota1975@74.ru)



## 1 Introduction

Scheduling and planning are considered in various areas, which include: transportation by aviation and rail transport, education, industry. To reduce the time spent to determine the best options, it is necessary to use the appropriate automated systems for planning, as well as to apply methods and algorithms for solving this class of problems [1–6]. This chapter discusses the development of software for solving the automation problem when planning the production load for the processing shop of a metalwork plant [7, 8].

The considered metalwork plant represents a certain type of production, specializing in the production of various metal structures for various purposes, both civil and industrial. At the same time, the technological process of manufacturing metal industrial products is a very laborious and complex procedure. Manufactured metal products are usually unique. Therefore, as a rule, a closed mechanized procedure is required.

The existing systems of management and planning at enterprises have certain resources, such as computers, software, usually with the use of 1C SCP. They contain directories of materials and products, documents (reports). At the same time, 1C UPP allows you to create an integrated information system that provides financial and economic activities at enterprises.

The functions of management and decision-making in the production of metal structures, as a rule, are performed by a person. At the same time, there is a lack of information at the planning stages when forming an optimal production plan at the procurement stage.

To support management decisions and improve their effectiveness, it is necessary to automate the planning procedure at the procurement stage of the production process.

A lot of software products have been developed for planning the production process of serial (repetitive) products. Serial production can be carried out using the “backlog” (blanks used in future orders). When planning this stage of production, it is important to make optimal use of warehouses (reserves).

In our case, the planning procedure is carried out to produce metal products for organizations that produce unique products using individual trajectories. When new customers come into production, new objects “enter”, the product range changes. In this case, a new manufacturing plan is developed and approved, while it is required that it be optimal. For one-off production, this requires a software package that considers the specifics of production and a large, regularly updated product range. Therefore, the developed software complex must have the ability to supplement and update the databases with new products, equipment, technological operations, new manufacturing rules by the specified requirements and perform the required amount of computer calculations in a reasonable time.

## 2 Formulation of the Problem

The study aims to minimize the period for the implementation of orders with the use of appropriate algorithmic and software to determine the optimal load distribution of the equipment available at the plant of the metalwork shop.

To optimize the load plan for the steel structure workshop, it is necessary to solve the following tasks:

1. performing a system analysis [9, 10] and developing an informational description of the technological process for the production of metal structures;
2. the formulation of the task of optimizing the technological process associated with the planning of production in the processing shop of the metal structures plant;
3. building the architecture of the optimal planning system for the processing shop of the metalwork plant;
4. construction of an optimization algorithm for solving the problem of the optimal schedule for distributing the load on the equipment;
5. test approbation of programs based on data from the Chelyabinsk plant of metal structures;
6. analysis and conclusions based on the results of software testing to optimize the planning of the loading of the processing workshop of the metalwork plant.

## 3 System Analysis and Development of an Informational Description of the Technological Process to Produce Metal Structures

Formation of the production plan is an important process in the enterprise. The plan is developed considering the capabilities of the enterprise and the market demand for the products of the enterprise.

Based on the concluded orders, the values associated with the assessment of direct production costs, labor, time labor intensity by type of orders are calculated; indicative dates; production capabilities at various levels of the technological process. The first stage at the plant of metal structures is the implementation of the stage “Plan for a month, taking into account the contractual obligations and transitions in the redistribution of the plant.” This plan describes the main aspects associated with the production of orders for objects.

When forming the “Plan for a month, considering contractual obligations and transitions on the plant’s redistribution”, the following are considered: “portfolio” for the manufacture of structures; contractual terms of delivery of products to customers under concluded contracts; provision of concluded contracts with advance payments, rolled metal, design, and technological documentation; technological capabilities of the main shops, their technical provision.

The stages of forming a production plan for a metalwork processing workshop are described below.

Stage 1. Obtaining input data for production (documentation on orders). At this stage, the necessary documents are formed for approving the order and introducing it into the work process. The following documents are formed: list of orders for the queue; list of metals for the queue; list of hardware for the queue; accompanying route sheets; cutting sheets; drawing development schedules.

Stage 2. Distribution of work on technological equipment. At this stage, tasks are assigned to work centers. These data are recorded in dispatch sheets with an indication of the execution time of each operation. The number of active works centers, their current load, maximum load, priorities for fulfilling orders and drawings are considered. The main task is to decide on the loading of work centers and the possibility of performing work on the necessary equipment. As a result, dispatch lists are formed for each order.

Stage 3. Distribution of work on non-automated equipment. At the third stage, the distribution of tasks for execution on non-automated equipment is carried out. The data is recorded in dispatch sheets with an indication of the time of execution of each operation.

Stage 4. Formation of data on the assembly of queues (dispatch lists). A list of dispatch sheets is formed for each order. Each dispatch sheet contains order numbers, drawing numbers, accompanying sheets, technological equipment, non-automated equipment, and the time it takes to complete the accompanying sheet on the necessary equipment.

Stage 5. Formation of a plan for manufacturing a processing workshop for a week. Based on the completed dispatch sheets, a schedule for the manufacture of metal structures for a week is formed. The priority of the execution of orders and drawings is considered. The order is fulfilled according to its dispatch lists.

Stage 6. Formation of daily assignments for production workshops. At the last stage, a daily schedule for the execution of dispatch sheets is formed. The distribution of work is carried out considering work shifts, the time for completing tasks. The schedule is formed for each section of the shop.

Let us formalize the planning process to produce metal structures in the processing shop and draw up an informational description based on the proposed flow chart for determining the plan to produce metal structures (Fig. 1).

The main indicators that affect the technological process of determining the production plan are the following characteristics: orders, accompanying sheets, queues, drawings, as well as technical operations and work centers (DC).

Production planning for a metalworking workshop as a control object is described by different vectors: (1) input variables  $X: X = (\tilde{Z}, \tilde{C}, \tilde{D}, \tilde{S}, \tilde{R}_c, \tilde{T}, \tilde{P}\tilde{I})$ , where  $\tilde{Z} = \{\overline{Z}_n : \overline{Z} = (N_z, K_z, W_z, Oc_z, D_{oz}, N_{ch}), n = \overline{1, R}\}$ —variables that characterize orders, here  $N_z$  is the order number,  $K_z$ —order code,  $W_z$ —order weight,  $Oc_z$ —order of production of the order,  $D_{oz}$ —order production time,  $N_{ch}$ —numbers of drawings included in the order;  $\tilde{C} = \{\overline{C}_k : \overline{C} = (N_{ch}, K_{ch}, W_{ch}, Oc_{ch}, N_z), k = \overline{1, L}\}$ —variables that characterize the drawings, here  $N_{ch}$  is the drawing number,

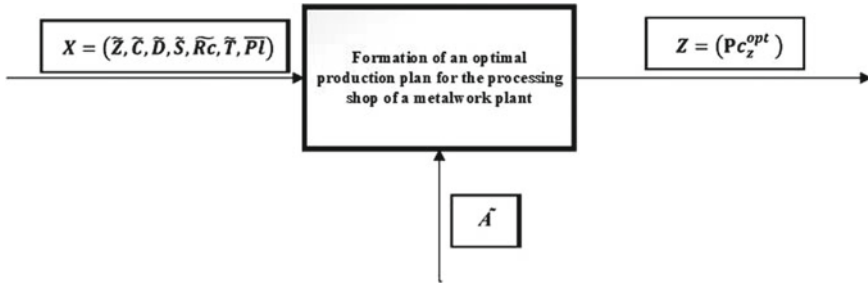


Fig. 1 Diagram of the technological process for determining the production plan

$K_{ch}$ —drawing code,  $W_{sl}$ —drawing weight,  $S_{to}$ —drawing order,  $N_z$ —order number;  $\tilde{D} = \{\overline{D}_i : \overline{D} = (N_{dl}, K_{dl}, Og_{dl}, N_{ch}, N_z), i = \overline{1, N}\}$ —variables that characterize queues (dispatch lists),  $N_{dl}$ —number queue,  $K_{dl}$ —queue code,  $Og_{dl}$ —mark about the readiness of the queue,  $N_{ch}$ —drawing numbers,  $N_z$ —order number;  $\tilde{S} = \{\overline{S}_m : \overline{S} = (N_{sl}, K_{sl}, P_{sl}, W_{sl}, S_{to}, T_{to}, Og_{sl}, N_{dl}), m = \overline{1, P}\}$ —variables that characterize the accompanying sheets,  $W_{sl}$  is the weight of the accompanying sheet,  $S_{to}$  is the set of operations of the technological process in the accompanying sheets,  $P_{sl}$  is the set of working complexes,  $K_{sl}$  is the identifier of the accompanying sheet,  $T_{to}$  is the time period of the technological operation using the accompanying sheets,  $Og_{sl}$  is the indicator of the readiness level of the accompanying sheet,  $N_{dl}$ —identifier (number) of the dispatch sheet,  $N_{sl}$ —identifier (number) of the dispatch sheet;  $\tilde{RC} = \{RC_j : RC = (N_{rc}, K_{rc}, Q_{rc}, Tz_{rc}, \overline{T}_l), j = \overline{1, M}\}$ —variables that characterize work centers,  $Q_{rc}$  is the number of working complexes of a given type,  $\overline{T}_l$  is a set of technological operations performed at a given work center,  $K_{rc}$  is the code of the work center,  $Tz_{rc}$  is the current load of the DC (working hour),  $Norm_{to}$  is the name work center;  $\tilde{T} = \{\overline{T}_l : \overline{T} = (N_{to}, K_{to}, Norm_{to}), l = \overline{1, K}\}$  are variables that characterize technological operations,  $N_{to}$  is the name of the technological operation,  $K_{to}$  is the code of the technological operations,  $\overline{G}_{pl} = [\tau_n, \tau_k]$ —planning horizon,  $Norm_{to}$ —standard production time characteristics for a certain technological operation;  $\overline{Pl} = \{\overline{G}_{pl}, K_o\}$  is the vector of planning parameters,  $\tau_k$  is the end date of the planning period,  $\tau_n$  is the start date of the planning period,  $K_o$  is the optimization criterion; (2) output variables  $Z$ : the resulting production cycle  $Pc_z$ ; (3) control actions  $U$ : optimization algorithm  $\tilde{A}$ .

The formation of an optimal production plan for a metalwork processing workshop includes several steps. At the first stage, orders are selected, as well as work complexes (centers), which are considered in planning. Further, optimization criteria are determined, usually the operating time of a set of dispatch sheets, i.e., production cycle time. Next, an algorithm for calculating the production plan is determined and the values of its parameters are set. A generalized scheme for determining a production plan is shown in Fig. 2.

It is necessary to consider several features that are of certain importance in the formation of a production plan: the emergence of urgent orders; changing the order

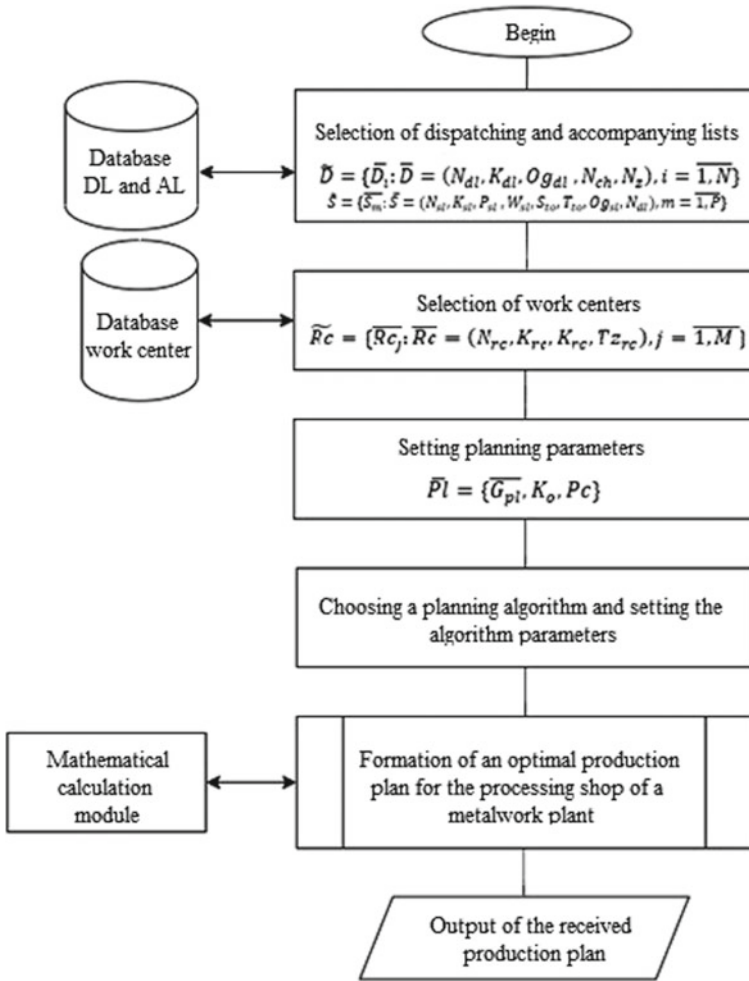


Fig. 2 Generalized scheme of the production plan formation

of production; suspension of dispatch sheets and drawings; the number of works centers when planning.

Currently, the functions of management and decision-making in the production of metal structures are performed by a person. At the same time, the information may be incomplete at the planning stages when optimizing the production plan for the metalworking workshop. To organize support for management decisions, it is necessary to automate the planning procedure at certain stages of the production process.

Optimal planning refers to the use of a set of methods that ensure the selection of the best plan option. When optimizing a production plan, a mathematical model is developed that includes constraints. The latter determines the set of acceptable plan

options. In addition, an objective function is set to select the optimal solution [11, 12]. Formation of an optimal plan usually contains the following steps: (1) problem statement; (2) construction of a mathematical model, an optimization algorithm, and computer programs that implement it; (3) performing calculations; (4) analysis of the results obtained.

Optimization of the production plan is necessary to reduce the production time and maximize the plant equipment utilization. Optimization of the schedule, which allows distributing the load more evenly on the processing centers, will significantly increase the performance of the organization. The optimal plan influences various characteristics of the operation of logistics structures, on the possibility of timely change of tasks for the implementation of repair work, etc. Enterprises that use optimal scheduling, significantly save time and production resources, consider changes in market demand promptly.

#### 4 Statement of the Problem of Optimization of the Technological Process Associated with the Planning of Production in the Processing Shop of a Metalwork Plant

Below is a description of the formulation of the problem of optimization of the technological process associated with the planning of production in the metalworking shop:

A vector of input coordinates  $X = (\tilde{Z}, \tilde{C}, \tilde{D}, \tilde{S}, \tilde{R}c, \tilde{T}, \overline{Pl})$ , is given,  $\tilde{Z} = \{\overline{Z}_i, i = \overline{1}, N\}$  is a set of orders,  $\tilde{C} = \{\overline{C}_k, k = \overline{1}, L\}$  is a set of drawings;  $\tilde{D} = \{\overline{D}_i, i = \overline{1}, N\}$  is the set of queues consisting of given dispatch lists,  $\tilde{S} = \{\overline{S}_m, m = \overline{1}, P\}$  is the set of given accompanying sheets,  $\tilde{R}c = \{\overline{R}c_j, j = \overline{1}, M\}$  is the set of working complexes (centres),  $\tilde{T} = \{\overline{T}_l, l = \overline{1}, K\}$ —a set of specified technological operations. It is required to determine the production plan for  $N$  given dispatch lists on  $M$  specific work complexes for the order  $\llbracket Pc_z$  in the planning period  $\overline{G}_{pl} = [\tau_n, \tau_k]$ , which provides a minimum of the objective function, which represents the total time required to process all dispatch lists:

$$F(Pc_z) \rightarrow \min.$$

In this case, the total processing time is determined as the sum of the values of all maximum time intervals required for processing the  $m$  specified accompanying sheet  $\in$  the  $i$  specific dispatching office at the  $j$  working complex:

$$F(Pc_z) = \sum_i^N \sum_j^M \sum_m^P \max(\tau Rc_j + \tau Sl_{mi}) \rightarrow \min.$$

Here  $\tau Sl_{mi}$  is the processing time of the  $m$  specified accompanying sheet  $\in i$  specific dispatch sheet,  $\tau Rc_j$  is the load of the  $j$  work center. It should be borne in mind that accompanying sheets are placed only on working complexes that can produce specified products. In addition, type II restrictions must be met, any dispatch list is processed no later than the specified date  $T(Pc_{zi}) < Do_i$  in the required time interval  $T(Pc_{zi}) \in [\tau_n, \tau_k]$ .

The vector of control actions is  $\tilde{P}c_z = \{\overline{P}c_z = (j, \tau_o, P_\tau, F, l), i = \overline{1, N}, j = \overline{1, M}, m = \overline{1, P}\}$ , that is, the sequence of processing dispatch lists at the working complexes (centers),  $j$  is the working complex, where the  $m$  accompanying sheet  $\in i$  dispatching center is processed;  $\tau_o$ —start date of dispatching sheet  $i$  processing (date and time of starting the sheet for processing);  $P_\tau$  is the time interval required for processing  $m$  specified accompanying sheet  $\in i$  specific dispatching office in the  $j$  working complex;  $F$  is the number of dispatch lists in a given production cycle  $Pc_z$ ;  $l$  is the ordinal number of processing of the  $i$  dispatch sheet in a given production cycle  $Pc_z$ .

## 5 Building the Architecture of the Optimal Planning System for the Processing Shop of a Metalwork Plant

To solve the problem of forming the optimal processing plan in the metalwork shop, the architecture of the computer planning system has been developed (Fig. 3). The proposed structure of the computer system includes a dispatcher's interface and an administrator's interface; information and software support.

At the beginning of the work, the user enters the order number for which it is necessary to determine the production cycle and the order of execution of dispatch sheets. Further, according to the specified order number, all dispatch lists participating in the order are received from the database.

Further, for each dispatch sheet, the downloads, and names of each work center are determined. Also, the initial load and name of each work center are obtained from the database. Then the program calculates the optimal solution for the task and displays the result to the user.

## 6 Construction of an Optimization Algorithm for Solving the Problem of an Optimal Equipment Distribution Schedule

Due to the generally large dimension of the problem, as well as the need to consider resource constraints and the variety of products, the problem being solved belongs to the so-called NP-complete in the field of discrete optimization. Therefore, it requires large computational costs to solve [13].

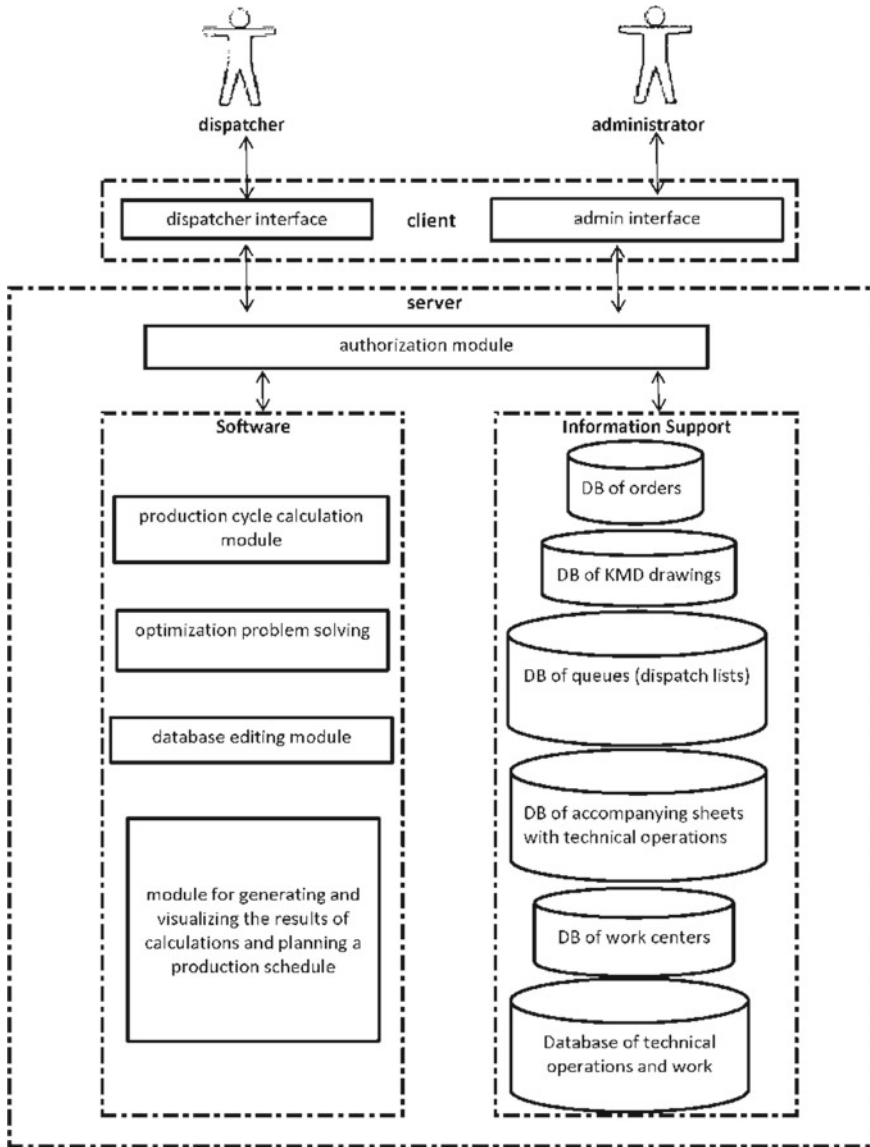


Fig. 3 Planning system architecture

It is expedient to solve the considered planning problem based on optimization methods. In this case, for problems of relatively small dimension, it is advisable to use the exhaustive search method, which guarantees the determination of the global extremum. When solving the planning problem of a relatively large dimension, it is necessary to use evolutionary population methods [14–17], to which the genetic



algorithm belongs. Below is a description of the genetic algorithm used to solve the problem [18–22].

Note that genetic algorithms can implement different target criteria (fitness functions) and constraints. This property is very useful for determining the optimal plan for large-scale production, which requires the fullest possible utilization of work complexes. In the considered problem of optimal production planning, it is necessary to introduce appropriate definitions and assumptions for the use of genetic algorithms. So, everyone is a possible solution to the problem, i.e., production plan. An important advantage of genetic algorithms is the ability to use several points for the search space under consideration, thus parallelization of the search is possible. In this case, the genetic algorithm uses information that is contained in the entire set of feasible solutions [23–26].

The main concepts of the genetic algorithm as a method for solving the problem of optimization of planning the processing of metal structures are as follows.

*Gene.* It represents a unit of so-called hereditary information, i.e., is an integral part of the chromosome, for the internal representation of alternative solutions. The gene is described by the vector  $G_i = (D_i, p_i)$  where  $i$  is the dispatch sheet index corresponding to its index in the original set;  $D_i$ —dispatch sheet;  $p_i$  is the ordinal number of the execution of  $i$  dispatch sheet in the current plan.

*Chromosome.* It is an ordered sequence of genes in the form of a coded data structure that determines a decision. The chromosome includes genes, the number of which is determined by the number of dispatch sheets that need to be placed  $Ch_y = (G_{y,1}, \dots, G_{y,i}, \dots, G_{y,N})$ , where  $y$  is the index placement (chromosomes) in the parental population  $P = \{Ch_y, y = 1, A\}$ , where  $A$  is the number of chromosomes in the population.

Let's consider the main operators of the genetic algorithm.

*Crossbreeding.* To carry out the procedure for crossing the most adapted individuals (the most optimized production plans), the crossover operator is used, which means that for the considered  $y$  variant of assignment of dispatch lists  $Ch_y$ , the index of the second variant of assignment  $t$  is determined from the initial set:  $t : \forall t \in \{1, A\} \wedge t \neq y$ . These two variants ( $Ch_y$  and  $Ch_t$ ) interbreed, resulting in new chromosomes.

In the process of solving the problem, two partially corresponding crossing overs were implemented: one-point and two-point.

For a one-point crossover, two points (boundaries for exchange) of the crossover  $r$  are randomly determined:  $r : \forall r \in \{1, n\} \wedge r > 1 \wedge r < N$ . Crossing over creates a descendant based on selecting a tour from one specific parent and saving the specified dispatch sheet positions from another specified parent when available and in order. So for the parents, for example,  $G_1 = (1\ 2\ 3\ 4\ 5\ |6\ 7\ 8\ 9)$  and  $G_2 = (4\ 5\ 2\ 1\ 8\ |7\ 6\ 9\ 3)$  the descendant is constructed as follows.

We exchange the specified highlighted subtours, and as a result we get  $Ch_1 = (4\ 5\ 2\ 1\ 8\ |X\ X\ X\ X)$  and  $Ch_2 = (1\ 2\ 3\ 4\ 5\ |X\ X\ X\ X)$ , here “X” represents a certain unfilled position, i.e., admitting an arbitrary value. Such an exchange also defines the mapping  $1 \leftrightarrow 4, 2 \leftrightarrow 5, 3 \leftrightarrow 2, 4 \leftrightarrow 1, 5 \leftrightarrow 8$ . Moreover, instead of “X”, certain

dispatch sheets from the initial parents are inserted, for which many conflicts are not absent, there is no cycle:  $Ch_1 = (4\ 5\ 2\ 1\ 8\ | 6\ 7\ X\ 9)$ ,  $Ch_2 = (1\ 2\ 3\ 4\ 5\ | 7\ 6\ 9\ X)$ .

Then the first “X” in  $Ch_1$ , change to “3”. By analogy with the second “X” in the second descendant of  $Ch_2$ , the remaining undefined position “X” is changed by 8, respectively. As a result, we have 2 descendants:  $Ch_1 = (4\ 5\ 2\ 1\ 8\ | 6\ 7\ 3\ 9)$ ,  $Ch_2 = (1\ 2\ 3\ 4\ 5\ | 7\ 6\ 9\ 8)$ .

In the case of a two-point crossover: two points (boundaries for exchange) of the crossover  $r_1, r_2 : \forall r_1, r_2 \in \{1, n\} \wedge r_1, r_2 > 1 \wedge r_1, r_2 < N \wedge r_1 \neq r_2$ . The list of dispatcher sheets from point  $r_1$  to point  $r_2$  will be called a tour. Crossover generates a child based on the selection of the tour from one parent and remembering the order, as well as the position of dispatch sheets from the other parent, if possible. For example, for parents  $G_1 = (1\ 2\ 3\ | 4\ 5\ 6\ 7\ | 8\ 9)$  and  $G_2 = (4\ 5\ 2\ | 1\ 8\ 7\ 6\ | 9\ 3)$  the descendant is constructed as follows.

We exchange the subtours that are highlighted, and we get  $Ch_1 = (X\ X\ X\ | 1\ 8\ 7\ 6\ | X\ X)$  and  $Ch_2 = (X\ X\ X\ | 4\ 5\ 6\ 7\ | X\ X)$ , here “X” represents a position that is not filled, that is allows an arbitrary value. The exchange specifies a display of the  $1 \leftrightarrow 4, 8 \leftrightarrow 5, 7 \leftrightarrow 6$ . Instead of “X” we use the dispatch lists of the initial parents, and there are no conflicts for them, there is no cycle:  $Ch_1 = (X\ 2\ 3\ | 1\ 8\ 7\ 6\ | X\ 9)$ ,  $Ch_2 = (X\ X\ 2\ | 4\ 5\ 6\ 7\ | 9\ 3)$ .

Then the original “X” in  $Ch_1$  is replaced with “4” using map  $1 \leftrightarrow 4$ . Next, the second “X” in the resulting child  $Ch_1$  is changed to “5”, and the second child of  $Ch_2$ , the positions “X” that was left undefined are changed to 1 and 8, respectively. As a result, we get two descendants:  $Ch_1 = (4\ 2\ 3\ | 1\ 8\ 7\ 6\ | 5\ 9)$  and  $Ch_2 = (1\ 8\ 2\ | 4\ 5\ 6\ 7\ | 9\ 3)$ .

*Mutation.* This is a random change in one or more positions on the chromosome. According to the GA scheme, the mutation operator is executed with a given probability  $Pm$ . As a mutation operator for the problem being solved, we used “exchange” and “inverse injection”. In the case of an exchange, the numbers of dispatch sheets (positions) in the chromosome are randomly selected and an exchange is made between these positions. For example, in the round (1-2-3-4-5-6-7-8-9) dispatch sheets 3 and 6 are selected, the exchange of which gives a new chromosome (1-2-6-4-5-3-7-8-9).

*Selection.* To determine the production plans with the best values for the next generation, the so-called fitness function  $F_{change}(Ch_y)$ . As a fitness function, the objective function is used.

$$F(Pc_z) = \sum_i^N \sum_j^M \sum_m^P \max(\tau Rc_j + \tau Sl_{mi}) \rightarrow \min.$$

The algorithm consists of the following steps.

1. User input of order number.
2. Loading all necessary data from the database.
3. Formation of the initial population.

4. Calculation of the fitness function for the initial population.
5. Entering the while loop with the condition of checking the number of populations with the initially specified maximum allowable population value.
6. Application of the operator of reproduction.
7. Application of the crossing-over operator for selected individuals.
8. Mutation of individuals
9. Selection of the best individual according to the lowest value of the fitness function.

The program that implements the genetic algorithm is written in the C # programming language.

To study the influence of the algorithm settings (size of the initial population, crossover probability, mutation probability, stopping criterion) and operator types (selection of the parent pool, selection of parental pairs, type of crossover, type of mutation, formation of a new population), it is advisable to use a low-dimensional problem. For it, using the brute force method, a global extremum is determined, and it is possible to compare the solution obtained based on the genetic algorithm to conclude the dependence of the rate of convergence to the optimal value on the settings of the genetic algorithm.

The developed software module based on the combined optimization method is advisable to use to build a decision support system to optimize the production plan of a metal-structure plant for the functioning of the corresponding cyber-physical system in real-time [27–31].

## **7 Test Approbation of Programs Based on Data from the Chelyabinsk Steel Structures Plant**

For testing, 22 dispatch sheets were loaded into the database. Each dispatch sheet contains the following data:

- order number;
- number of drawings;
- numbers of accompanying sheets;
- the name of the work centers;
- loading of work centers for each accompanying sheet.

The use of the exhaustive search algorithm is possible for up to 7 dispatch sheets, with an increase in the amount of data, the use of the method becomes impractical due to the long execution time of the program, and with 22 dispatch lists, the exhaustive search method requires large computing power. So, for 5 dispatch sheets, the execution time of the genetic algorithm is 0.023 s, and the exhaustive search method is 0.034 s. For 9 dispatch sheets, the execution time of the genetic algorithm is 0.027 s, and the exhaustive search method is 1.3 s. For 22 dispatch sheets, the execution time

**Table 1** The result of the genetic algorithm for different values of the parameters

Crossover type / mutation type	N	Probability crossing over	Mutation probability		
			0,04	0,06	0,08
Single point crossing over / inverse injection	50	0,4	87,1 / 0,033	84,6 / 0,037	85,4 / 0,041
		0,6	86,3 / 0,034	83,6 / 0,036	85,4 / 0,039
		0,8	86,3 / 0,034	84,6 / 0,041	84,6 / 0,047
Point-to-point crossing / exchange	50	0,4	85,4 / 0,042	84,6 / 0,042	86,3 / 0,039
		0,6	85,4 / 0,045	83,6 / 0,047	84,6 / 0,046
		0,8	85,4 / 0,048	84,6 / 0,046	84,6 / 0,048
Single point crossover / exchange	200	0,4	85,4 / 0,074	84,6 / 0,074	85,4 / 0,079
		0,6	83,6 / 0,076	83,6 / 0,076	83,6 / 0,081
		0,8	84,6 / 0,072	83,6 / 0,081	83,6 / 0,085
Two-point crossing over / inverse embedding	200	0,4	84,6 / 0,074	83,6 / 0,073	84,6 / 0,083
		0,6	83,6 / 0,076	83,6 / 0,076	83,6 / 0,078
		0,8	85,4 / 0,081	83,6 / 0,077	83,6 / 0,089

of the genetic algorithm is 0.034 s, and using the brute force method, the result was not obtained due to a lack of computer RAM.

Variable values of the parameters of the genetic algorithm:

- the number of individuals in the population  $N = 50, 200$ ;
- the probability of crossing over  $P_c = 0.4, 0.6, 0.8$ ;
- the probability of mutation  $P_m = 0.04, 0.06, 0.08$ ;
- crossing over: one-point, two-point;
- mutation: exchange, inverse introduction.

Table 1 shows the result of the program using the genetic algorithm.

The cells of the table show the obtained optimal time of the production cycle and the time to find the optimal solution to the problem with the corresponding probabilities of mutation and crossing over, population power, types of mutation, and crossing over. Program execution time is presented in seconds.

With a low probability of mutation, the algorithm does not always provide a result of the required accuracy. So, in some cases, the algorithm reached 50 generations, but the resulting value of the production cycle stopped at 85.4. This can be explained by the fact that the numerical value of the found individuals was concentrated in several points and new points could not appear. It can be noted that the larger the number of individuals in the population, the more accurate the result and the less time it takes to search for it.

In Fig. 4 shows a graph of the dependence of the value of the objective function on the number of iterations.

The value of the objective function is the production cycle time. The number of iterations—50, population power—200, crossing over—two-point, mutation—inverse introduction. The graph shows the distribution of population values at a certain iteration. It can be seen from the graph that by the 30th iteration, the minimum

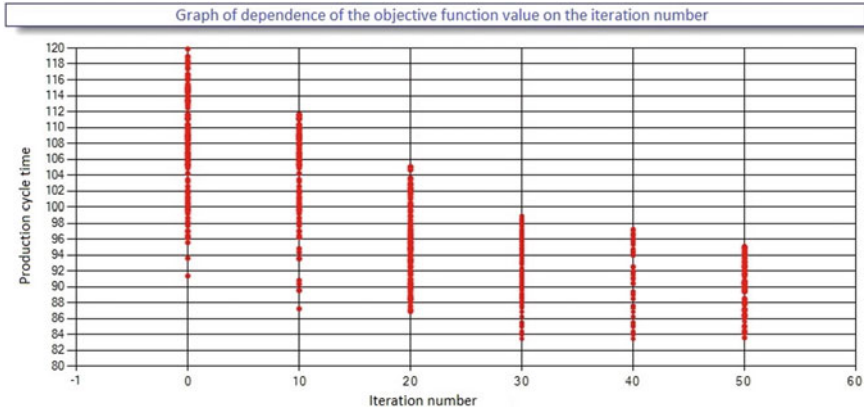


Fig. 4 Graph of dependence of the objective function value on the number of iterations

value has been reached, then the value of 83.6 remains the minimum and is displayed because of the genetic algorithm.

## 8 Analysis and Conclusions Based on the Results of Software Testing to Optimize the Planning of the Loading of the Processing Shop of a Metalwork Plant

During the analysis, the following conclusions were made.

1. For small values of the crossing-over probability ( $P_c = 0.4$ ) and the mutation probability ( $P_m = 0.04$ ), the algorithm did not always find a solution satisfying in terms of accuracy. This can be explained by the fact that solutions converge prematurely to one point, and because of the low probability of mutation, new solutions rarely appear. Both types of mutation (exchange and inverse insertion) provide approximately the same result, so it is not possible to conclude their relative preference.
2. The best results were observed with a crossing-over probability of  $0.6 \div 0.8$ , and a mutation probability of 0.6. Increasing the values further does not improve performance, and sometimes worsens the search result for the optimal solution. A two-point cross-over should be considered more effective.
3. In most cases, the algorithm determines a minimum production cycle of 83.6. The value of the production cycle is calculated without the use of a genetic optimization algorithm. In this case, dispatch sheets are arranged in the order in which they are entered into the database, the production cycle time, in this case, is 91.5, so it can be argued that the algorithm is working correctly.

4. The most effective in terms of the number of generations and the time spent on finding a solution is the use of a population of 200 individuals.
5. The most ineffective is the use of a population of 40 individuals. Due to premature convergence, in most cases, the obtained solution does not satisfy the specified accuracy.

## 9 Conclusions

The chapter describes a systematic analysis of the process of forming a production schedule for the processing shop of a metalwork plant. The substantive and formalized formulation of the production plan optimization problem is presented. A target criterion for optimizing the production plan has been formulated and investigated. A combined solution algorithm is proposed, including a direct enumeration method for problems of relatively small dimension and a genetic algorithm for high dimension. A simple genetic algorithm for the task at hand is described and implemented. The results of the genetic algorithm operation are given for different values of the algorithm parameters, conclusions are drawn about the correct operation of the implemented genetic algorithm. The approbation of the results proves the feasibility of using a simple genetic algorithm for the task of forming an optimal plan for the processing metal structures of the plant shop.

It should be noted that the construction of planning software based on a library of optimization methods increases the economic efficiency of the technological process due to the reduction of time costs for the production cycle, as well as, in the general case, based on fulfilling the contractual terms of production of products, reducing the amount of downtime industrial complexes. At the same time, optimization methods make it possible to consider various characteristics that determine the result associated with technological limitations, equipment malfunction, the cost of work performed and required materials, etc.

It is advisable to use the developed software package in the cyber-physical control system of a metalwork plant for promptly changing the load plan by solving the problem of optimizing the processing of blanks for new operational information.

## References

1. Galkin, A., Istomin, V.: Automation of assembly batches installation in hot rolling mills. In: Kravets, A.G., Bolshakov, A.A., Shcherbakov, M. (eds.) *Cyber-Physical Systems. Digital Technologies and Applications*. Series Title *Studies in Systems, Decision and Control*, vol. 350, pp. 53–62. Publisher Springer International Publishing (2021). [https://doi.org/10.1007/978-3-030-67892-0\\_5](https://doi.org/10.1007/978-3-030-67892-0_5)
2. LaValle, S.M.: *Planning algorithms*. Cambridge University Press (2006)
3. Nikolakis, N., Senington, R., Sipsas, K., Syberfeldt, A., Makris, S.: On a containerized approach for the dynamic planning and control of a cyber-physical production system. *Robot. Comput. Integr. Manuf.* **64**, 101919 (2021)

4. Moshev, M., Meshalkin, V., Romashkin, M.: Development of models and algorithms for intellectual support of life cycle of chemical production equipment. In: Kravets, A.G., Bolshakov, A.A., Shcherbakov, M. (eds.) *Cyber-Physical Systems: Advances in Design & Modelling. Series Title Studies in Systems, Decision and Control*, vol. 259, pp. 153–165. Publisher Springer International Publishing (2020). [https://doi.org/10.1007/978-3-030-32579-4\\_12](https://doi.org/10.1007/978-3-030-32579-4_12)
5. Kerzner, H.: *A systems approach to planning scheduling and controlling* (2017)
6. Yevstratov, S.N., Vozhakov, A.V., Stolbov, V.Y.: Automation of production planning within an integrated information system of a multi-field enterprise. *Autom. Remote Control* **75**(7), 1323–1329 (2014)
7. Belov, V., Moshev, E.: Functional model for the formation of individual metal control programs of boiler equipment. In: Kravets, A.G., Bolshakov, A.A., Shcherbakov, M. (eds.) *Cyber-Physical Systems: Modelling and Intelligent Control. Studies in Systems, Decision and Control*, vol. 338, pp. 323–334. Publisher Springer International Publishing (2021). [https://doi.org/10.1007/978-3-030-66077-2\\_26](https://doi.org/10.1007/978-3-030-66077-2_26)
8. Vinnichenko, M., Noskova, E., Akhmetov, R.: Realization of APS-planning at custom small-scale manufacturing. *J. Phys. Conf. Ser.* **1679** (3), № 032067 (2020). <https://doi.org/10.1088/1742-6596/1679/3/032067>
9. Germashev, I., Derbisher, E., Derbisher, E., Mashihina, T.: Model of paired and solitary influence of ingredients of polymer composition. In: Kravets, A.G., Bolshakov, A.A., Shcherbakov, M. (eds.) *Cyber-physical Systems: Design and Application for Industry 4.0. Studies in Systems, Decision and Control*, vol. 342, pp. 205–217. Copyright 2021 Publisher. Springer International Publishing (2021). [https://doi.org/10.1007/978-3-030-66081-9\\_16](https://doi.org/10.1007/978-3-030-66081-9_16)
10. Dorrer, M., Dorrer, A., Zyryanov, A.: Numerical modeling of business processes using the apparatus of GERT networks. In: Kravets, A.G., Bolshakov, A.A., Shcherbakov, M. (eds.) *Society 5.0: Cyberspace for Advanced Human-Centered Society. Series Title Studies in Systems, Decision and Control*, vol. 333, pp. 47–55. Publisher Springer International Publishing (2021). [https://doi.org/10.1007/978-3-030-63563-3\\_5](https://doi.org/10.1007/978-3-030-63563-3_5)
11. Li, I.H., Chen, Y.H., Wang, W.Y., Kao, Y.F.: Hybrid intelligent algorithm for indoor path planning and trajectory-tracking control of wheeled mobile robot. *Int. J. Fuzzy Syst.* **18**(4), 595–608 (2016)
12. Chistyakova, T.B., Furaev, D.N.: A computer system for training of specialists in design of industrial facilities for petrochemistry and oil processing. In: *Proceedings of 2018 17th Russian Scientific and Practical Conference on Planning and Teaching Engineering Staff for the Industrial and Economic Complex of the Region, PTES*, vol. 17, pp. 92–94. IEEE (2018)
13. Protalinskiy, O., Shvedov, A., Khanova, A.: Life cycle management of power grid companies' equipment. In: Kravets, A.G., Bolshakov, A.A., Shcherbakov, M. (eds.) *Cyber-physical Systems: Design and Application for Industry 4.0. Studies in Systems, Decision and Control*, vol. 342, pp. 265–274. Copyright 2021 Publisher. Springer International Publishing (2021). [https://doi.org/10.1007/978-3-030-66081-9\\_21](https://doi.org/10.1007/978-3-030-66081-9_21)
14. Skobtsov, Y.: Prospects of the interdisciplinary course “Computational Intelligence” in engineering education In: Kravets, A.G., Bolshakov, A.A., Shcherbakov, M. (eds.) *Cyber-physical Systems: Design and Application for Industry 4.0. Studies in Systems, Decision and Control*, vol. 342, pp. 431–441. Copyright 2021 Publisher. Springer International Publishing (2021). [https://doi.org/10.1007/978-3-030-66081-9\\_33](https://doi.org/10.1007/978-3-030-66081-9_33)
15. Skobtsov, Y., Chengar, O., Skobtsov, V., Pavlov, A.: Synthesis production schedules based on ant colony optimization method. In: Kacprzyk J., et al. (eds.) *Proceedings of the 6th Computer Science Online Conference 2017 (CSOC2017)*, in *Advances in Intelligent Systems and Computing*, vol. 1 (573), pp. 456–465. Springer International Publishing Switzerland (2017)
16. Karpenko, A.P., Sviaadze, Z.O.: Meta-optimization based on self-organizing map and genetic algorithm. *Opt. Mem. Neural Netw.* **20**(4), 279–283 (2011)
17. Chistyakova, T.B., et al.: Decision support system for optimal production planning polymeric materials using genetic algorithms. In: *2016 XIX IEEE International Conference on Soft Computing and Measurements (SCM)*, IEEE, pp. 257–259 (2016)

18. Mitra, K.: Genetic algorithms in polymeric material production, design, processing and other applications: a review. *Int. Mater. Rev.* **53**, 275–297 (2008)
19. Man, K.F., Tang, K.S., Kwong, S.: Genetic algorithms in production planning and scheduling problems. In: *Genetic Algorithms. Advanced Textbooks in Control and Signal Processing*. Springer, London (1999)
20. Kucukkoc, I.: Integrating ant colony and genetic algorithms in the balancing and scheduling of complex assembly lines. *Int. J. Adv. Manuf. Technol.* **82**, 265–285 (2016). (Springer)
21. Tahmasebi, P., Hezarkhani, A.A.: Hybrid neural networks-fuzzy logic-genetic algorithm for grade estimation. *Comput. Geosci.* **42**, 18–27 (2012). <https://doi.org/10.1016/j.cageo.2012.02.004>. Accessed 09Mar2021
22. Dagaeva, M., Katasev, A.: Fuzzy rules reduction in knowledge bases of decision support systems by objects state evaluation. In: Kravets, A.G., Bolshakov, A.A., Shcherbakov, M. (eds.) *Cyber-Physical Systems: Modelling and Intelligent Control. Studies in Systems, Decision and Control*, vol. 338, pp. 113–123. Publisher Springer International Publishing (2021). [https://doi.org/10.1007/978-3-030-66077-2\\_9](https://doi.org/10.1007/978-3-030-66077-2_9)
23. Zaborovskij, V., Polyanskiy, V., Popov, S.: On the problem of computability of bounded rationality cognitive solutions. In: Kravets, A.G., Bolshakov, A.A., Shcherbakov, M. (eds.) *Society 5.0: Cyberspace for Advanced Human-Centered Society. Series Title Studies in Systems, Decision and Control*, vol. 333, pp. 15–23. Publisher Springer International Publishing (2021). [https://doi.org/10.1007/978-3-030-63563-3\\_2](https://doi.org/10.1007/978-3-030-63563-3_2)
24. Bolshakov, A., Nikitina, M., Kalimullina, R.: Intelligent system for determining the presence of falsification in meat products based on histological methods. In: Kravets, A.G., Bolshakov, A.A., Shcherbakov, M. (eds.) *Society 5.0: Cyberspace for Advanced Human-Centered Society. Series Title Studies in Systems, Decision and Control*, vol. 333, pp. 179–201. Publisher Springer International Publishing (2021). [https://doi.org/10.1007/978-3-030-63563-3\\_15](https://doi.org/10.1007/978-3-030-63563-3_15)
25. Dykin, V.S., Musatov, V.Y., Varezchnikov, A.S., Bolshakov, A.A., Sysoev, V.V.: Application of genetic algorithm to configure artificial neural network for processing a vector multisensory array signal. In: *International Siberian Conference on Control and Communications, SIBCON*, pp. 719–722 (2015). <https://doi.org/10.1109/sibcon.2015.7147049>. ISBN: 978-147997102-2
26. Valls, V., Ballestín, F., Quintanilla, S.: A hybrid genetic algorithm for the resource constrained project scheduling problem. *Eur. J. Oper. Res.* **185**(2), 495–508 (2008)
27. Kizim, A., Kravets, A.: On systemological approach to intelligent decision-making support in industrial cyber-physical systems. In: Kravets, A.G., Bolshakov, A.A., Shcherbakov, M. (eds.) *Cyber-Physical Systems: Industry 4.0 Challenges. Series Title Studies in Systems, Decision and Control*, vol. 260, pp. 167–183. Publisher Springer International Publishing (2020). [https://doi.org/10.1007/978-3-030-32648-7\\_14](https://doi.org/10.1007/978-3-030-32648-7_14)
28. Meshalkin, V., Bolshakov, A., Petrov, D., Krainov, O.: Algorithms and software system for controlling the quality of glass batch using artificial neural networks. *Theor. Found. Chem. Eng.* **46**(3), 284–287 (2012)
29. Bolshakov, A., Veshneva, I.: Assessment of the effectiveness of decision support in the application of the information system for monitoring the process of forming competences based on status functions. In: *International Conference on Actual Problems of Electron Devices Engineering, APEDE. 2018*, art. no. 8542462, pp. 75–82 (2018). <https://doi.org/10.1109/APEDE.2018.8542462>. ISBN: 978-153864332-7
30. Shashikhina, O., Chistyakova, T., Kohlert, Ch.: Computer system for optimal planning of multi-assortment polymer films industrial production. In: *Proceedings of the 2020 2nd International Conference on Control Systems, Mathematical Modeling, Automation and Energy Efficiency (SUMMA 2020)*, pp. 561–565. Institute of Electrical and Electronics Engineers (2020)
31. Kravets, A.G., Orudjev, N.Y., Salnikova, N.A.: Software for predictive maintenance and repair of the enterprise office equipment. In: *2019 International Multi-Conference on Industrial Engineering and Modern Technologies, FarEastCon 2019*. art. no. 156113 (2019)



# Redmine-Based Approach for Automatic Tasks Distribution in the Industrial Automation Projects



Alla G. Kravets, Alexey Seelantiev, Natalia Salnikova, and Irina Medintseva

**Abstract** The chapter analyzes the Scrum methodology as a method for managing the industrial product development process using the Redmine. In the analysis of the practical use of the Scrum methodology, the need for automation of sprint planning was identified. Using the developed software, it is possible to automatically create a production plan for certain periods, subject to the necessary conditions, such as the availability of a reserve of tasks with a set priority and an approximate estimate of the time for their completion, as well as the schedule of working hours for a group of employees for a given period of time.

**Keywords** Scrum · Production plan · Project management · Redmine · Tasks planning · Project activities · Business processes automation · Resource management

---

A. G. Kravets (✉) · A. Seelantiev  
Volgograd State Technical University, 28 Lenin av., Volgograd 400005, Russia  
e-mail: [agk@gde.ru](mailto:agk@gde.ru)

A. Seelantiev  
e-mail: [leshka.oo@yandex.ru](mailto:leshka.oo@yandex.ru)

A. G. Kravets  
Dubna State University, 19 Universitetskay St., Moscow region, Dubna 141982, Russia

N. Salnikova · I. Medintseva  
Volgograd Institute of Management – branch of the Russian Presidential Academy of National Economy and Public Administration, 8 Gagarin St., Volgograd 400131, Russia  
e-mail: [ns3112@mail.ru](mailto:ns3112@mail.ru)

I. Medintseva  
e-mail: [medinira@yandex.ru](mailto:medinira@yandex.ru)

## 1 Introduction

Before starting any business, it is necessary to carefully think over what, by what date, by what ways, and by what means it is necessary to do. Otherwise, the intentions may be unfulfilled [1, 2]. Therefore, the first and fundamental stage of managing any kind of expedient activity is always the process of setting goals and finding ways to achieve them. It is the stage of setting goals that include foresight, forecasting, planning [3]. The end result of this stage is the construction of an ideal model of the production process aimed at achieving the main goal of the enterprise. Automation of industrial applications is crucial for the entire planning process [4, 5]. After all, the foundation of success and prosperity of any production is a carefully designed, informed plan [6].

When developing software, there are many approaches to development. One of the most common agile development methodologies for industrial applications is Scrum. The Scrum methodology provides a cyclical buildup of product functionality in a short time. The concept is based on sprints. Sprint—a short iteration, strictly limited in time, usually 2–4 weeks. At this time, the duration of the meetings is minimized, but their frequency increases. Thanks to this, control over execution becomes more flexible, and developers respond more quickly to emerging problems [7, 8]. Traditional planning fades into the background, sprint magazine takes its place [9].

The Redmine system implements tools for implementing the Scrum methodology in product development. Redmine displays: sprints, the current state of sprints, percentage of completion, lag behind planned dates with task details, agile task board with an interactive change of task statuses, reports, task combustion charts.

The purpose of the work is to develop software for automatic task distribution in the Redmine system, which ensures the reduction of time and financial costs during planning.

## 2 Overview of the Scrum Methodology and the Redmine System

### 2.1 Scrum Methodology

In most cases, programming is a complex, poorly defined process that requires developers to be creative. Various agile technologies allow you to organize a process of gradual approximation to the project goal by conducting test cycles with the adjustment of subsequent ones based on an analysis of the results of the previous ones. The Scrum methodology is one of the first methodologies for cyclically increasing functionality and adjusting the progress of a project based on an analysis of user feedback. The Scrum methodology sets the rules for managing the development process and allows you to use existing coding practices, adjust requirements, or make tactical changes. Using this methodology makes it possible to identify and eliminate deviations from the desired result at earlier stages of software product development. The

basis of the Scrum methodology is the theory of empirical control—empiricism. According to this theory, experience is the source of knowledge, and real data is the solution. In order to improve the predictability and effectiveness of risk management, the Scrum methodology uses an iterative and incremental approach. The empirical management process is based on the “three pillars”:

1. transparency, important elements of the process should be available to those who are responsible for its result. Moreover, these aspects of the system can be included in common standards that will allow all participants to have their common understanding;
2. inspection, process participants should regularly inspect the artifacts of Scrum and the progress towards the Sprint Goal, which is necessary for the timely detection of unwanted deviations. The frequency of inspections should not interfere with work. Inspections are most beneficial if performed by professionals with the appropriate skills;
3. adaptation, if deviations from the permissible limits of one or more elements of the process or product are detected, appropriate changes should be made. It can be both changes in the process itself and the materials used in it. The sooner the changes are made, the lower the risk of further deviations [10].

## 2.2 *Redmine System*

Redmine is a web-based project management information system (online), which includes a complete set of tools for collaborating on projects. The system allows you to run several projects simultaneously, track their status, manage project steps, tasks, priorities, and flexibly assign roles to participants [11].

Projects are one of the basic concepts in the subject area of project management systems. Thanks to this essence, it is possible to organize collaboration and planning of several projects simultaneously with differentiation of access for different users. Projects allow hierarchical nesting.

Trackers are the main classification by which tasks in a project are sorted. The term “tracker” itself goes back to error accounting systems, each representing one project individually. In Redmine, trackers are an analog of subclasses of the Task class and are the basis for the polymorphism of various kinds of tasks, allowing you to define different fields for each type. Examples of trackers are “Improvement”, “Error”, “Documentation”, “Support”.

Tasks are the central concept of the whole system, describing a certain task that must be completed. Each task has a description and an author without fail, without fail the task is tied to a tracker. Each task has a status. Statuses are a separate entity with the ability to determine the rights to assign a status for various roles or determine the relevance of a task (for example, “open”, “assigned”—relevant, but “closed”, “rejected”—no). For each project, a set of development stages and a set of task categories are separately determined. Among other fields, the “estimated time”, which serves as the basis for constructing management charts, as well as the field for

selecting observers for a task, is also interesting. You can attach files to tasks (there is a separate entity called “Application”). Values of other enumerated properties (for example, priority) are stored in a separate general table.

### ***2.3 Tracking the Changes in Task Settings***

Two entities are responsible for tracking changes in task parameters by users in the system: “Recording the changelog” and “Changed parameter”. A log entry displays one user action for editing task parameters and/or adding a comment to it. That is, it serves both as a tool for conducting the history of the task and a tool for conducting a dialogue.

The entity “Modified parameter” is tied to a separate journal entry and is intended to store the old and new values of the parameter changed by the user.

Tasks can be interconnected: for example, one task is a subtask for another or precede it. This information may be useful during the planning of program development; a separate entity is responsible for its storage in Redmine.

Accounting for the time spent on the project supports accounting for the time spent due to the essence of the “time spent” associated with users and the task. The essence allows you to store the time spent, the type of user activity (development, design, support), and a brief comment on the work. This data can be used, for example, to analyze the contribution of each participant to the project or to assess the actual complexity and cost of development.

Receiving user notifications about changes occurring on the site is carried out using the entity “Observers”, which connects users with objects of various classes (projects, tasks, forums, etc.). The database also stores RSS access keys to receive notifications using this technology, and notifications are also sent via email [11].

## **3 Redmine Planning Plugin Design**

In the Redmine system, the standard functions do not include a list of tasks that require automation:

- Import of production calendar;
- Calculation of the working hours of an employee or group;
- Automatically filling the operational plan with time-bound tasks that do not exceed the group’s temporary resources for the period of the operational plan [12].

But the Redmine system is under an open license [13]. This means that you can write your own plugin that implements certain tasks and connect it to the main project (Table 1). A REST API is also available, which provides integration with other systems [14].

**Table 1** Comparison of module implementation methods

Module implementation methods	Programming language for implementation	Redmine Failover
Development of a module integrated through REST API	API supported by languages: Python, Ruby, Delphi, .NET, Java, PHP, Perl, C++, C#	High
Developing an embedded plugin for Redmine	Ruby	Low

To implement the plugin, a method was selected in which a third-party web service is required to interact with the Redmine system through the REST API, for the following reasons.

When writing a plugin, it is possible to use only the specific programming language in which Redmine itself is written—the Ruby language. When developing a third-party web service, the language does not matter, because the interaction of systems will occur according to uniform rules provided by the Redmine REST API.

When introducing a plugin, there is a high probability of an application regression when the plugin, in addition to solving the main task, can affect the integrity of the program in other modules and its data. When approaching through the REST API, there can be no such problem, since the limited functionality of the application is provided through the API.

Libraries for using the REST API Redmine have already been written for many programming languages, which allows you to immediately begin to implement the tasks without thinking about designing the architecture of interaction between systems [15].

To implement the module, the Python programming language was chosen. The library for interacting with the Redmine REST API is Python-Redmine [16, 17].

### 3.1 Redmine Data Model Classes

Data models imported from the Redmine system (Fig. 1), such as employees (user), groups, projects, tasks, statuses, priorities, trackers, versions have general data structure, therefore, the basic interface (Redmine Base Model) will be implemented, which will be endowed with logic:

- converting the imported data of one structure into the structure required for working with Django models, i.e. into instances of model objects. Method `convert_to_model`;
- correspondence of fields between different data structures. Property `FIELDS_MAPPING_WITH_REDMINE`;
- saving data to the database, by updating existing objects or adding new ones. `Save_object` method.

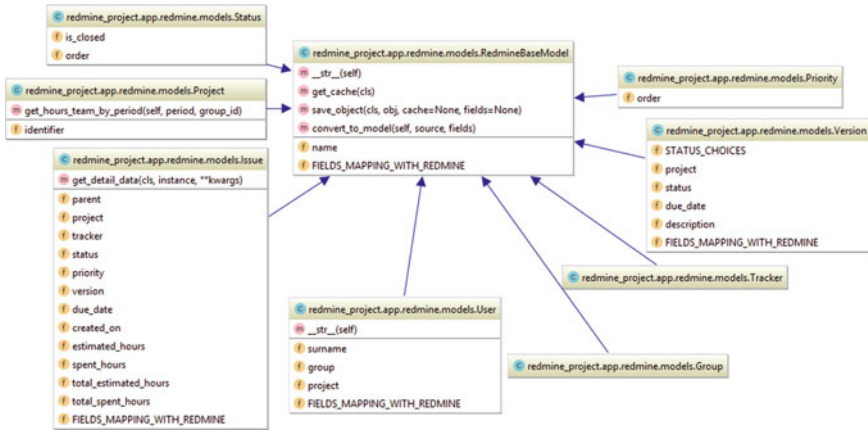


Fig. 1 Class Diagram of data models imported from the Redmine system

Derived classes of data models will inherit the logic of the RedmineBase Model and describe the types of fields needed to store data [18, 19].

### 3.2 Conceptual and Logical Data Models

As a result of the analysis of the Redmine system, a number of data models were identified that would be required to implement the application.

Figure 2 shows the conceptual model of the application database. Figure 3 shows the logical database model.

Employees (*redmine\_user*)—an imported data model, the table structure is identical to the table in the Redmine system. It contains personal information about employees, to which group they belong and to which project they are assigned. In Redmine, the many-to-many relationship between employees and groups.

Working hours (*business\_time\_workhours*)—the data model stores the working days of the week and the number of hours in each day for each employee.

Non-working/Shortened days/Holidays of employees (*business\_time\_holidays*)—the data model stores date intervals at which the employee may not work, or work for a reduced time. It involves storing common holiday dates that apply to all employees.

Norm of working hours (*business\_time\_userperformance*)—the data model stores the norm of working hours of an employee by month.

Groups (*redmine\_group*)—an imported data model, the table structure is identical to the table in the Redmine system. Stores the name of groups that include employees.

Projects (*redmine\_project*)—an imported data model, the structure of the table is identical to the table in the Redmine system. Stores project information, is a key model, stands at the top of the model hierarchy referenced by child models.

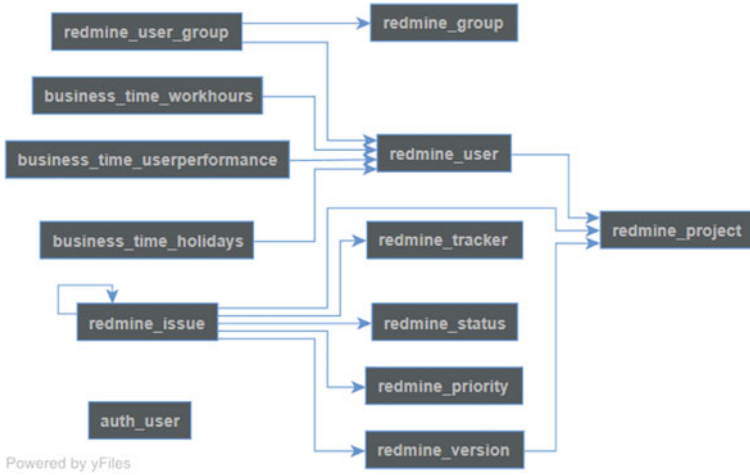


Fig. 2 Conceptual database model

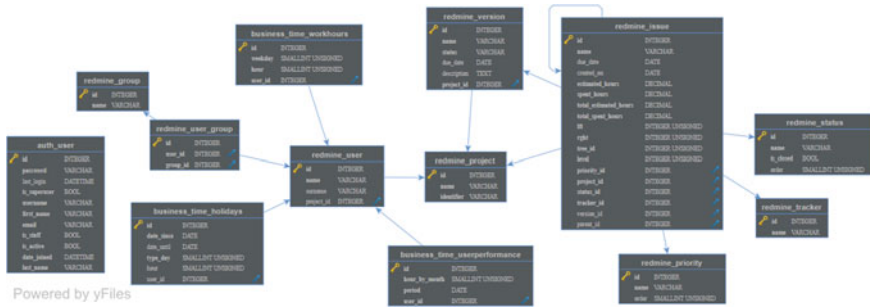


Fig. 3 Logical database model

Versions (redmine\_version)—an imported data model, the table structure is identical to the table in the Redmine system. Stores the name, deadlines, and a list of tasks to the version. It reflects information about the released versions of the project; in the user interface of the Redmine system, this menu is called the “Operational Plan”.

Tasks (redmine\_issue)—an imported data model, the table structure is identical to the table in the Redmine system. It stores detailed information on the task: name, description, which project is attached to, task category, what status is at the given time, who is responsible for the implementation, start date, completion dates, total time spent on the task. It is a key model, it also stands at the top of the model hierarchy, after the redmine\_project table.

Priority (redmine\_priority)—the imported data model, the table structure is identical to the table in the Redmine system. The dependent model on the redmine\_issue table, stores information about the priorities of the task.

Tracker (`redmine_tracker`)—an imported data model, the table structure is identical to the table in the Redmine system. The dependent model on the `redmine_issue` table, stores information about trackers.

Status (`redmine_status`)—an imported data model, the table structure is identical to the table in the Redmine system. The dependent model on the `redmine_issue` table, stores information about the status of the task.

User (`auth_user`)—the standard table from the Django framework, designed to authorize users in the application.

## 4 Automatic Tasks Distribution Plugin Development

The REST API provides access to Redmine system resources. Tasks are special cases of problems that belonged to the project. Projects—an object of the system that describes the current state, problems, forecasted plans for the future, the real project of the company. Users tied to the project. Users—accounts of company employees. Labor costs—a register of time tracking of each employee of the company. News—recording news feeds of projects. Relationships between tasks—keeping relationships between tasks. Versions—an operational plan that includes deadlines and a list of tasks. Reference information—a directory that stores various types of literature on projects. Requests—saved task filters. Attachments—Uploaded files to the Redmine system. Task statuses—a list of possible task states. Trackers—a list of possible task trackers. Priorities—a list of possible task priorities. Types of activity (Labor) —a list of types of activities of company employees. Categories of documents—a list of possible categories of documents. Roles—a set of user access rights to Redmine system objects. Groups—grouping Redmine system users into groups. Custom fields—additional fields that add additional information to the tasks [20, 21].

### 4.1 Working Hours Accounting Algorithm

Based on the date range of the operational plan for each employee, its working time is calculated. The date range is broken down into a list of days in the date range.

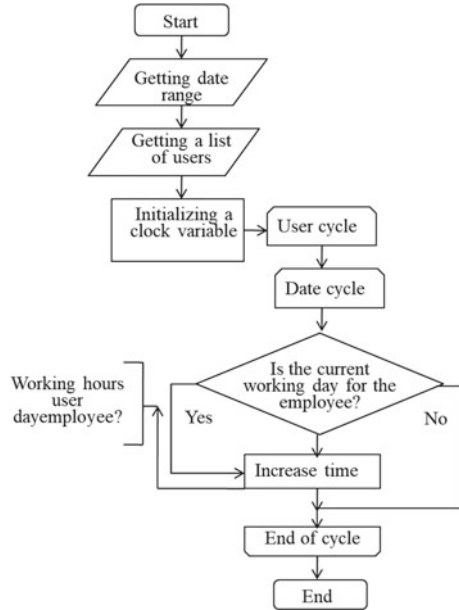
A variable is created in which the total working hours for the team employees will be stored, by default the value is zero.

Obtaining a list of team employees with their working hours, and non-working dates.

For each employee of the team, a cycle is launched according to the list of days of the operational plan, where the condition is checked: is the current day the working day of the employee of the team? If so, then the variable that contains the total hours for each employee of the team is incremented by a value that is equal to the value—the number of working hours of the employee of the team on that day, otherwise—the transition to the next iteration of the day.



**Fig. 4** Working hours accounting algorithm



After going through all the team employees in a cycle, the value of the variable will contain the value of the sum of the team’s working hours, which can work out during the operational plan period [22, 23]. The block diagram of the algorithm is shown below (Fig. 4).

### 4.2 Tasks Distribution Algorithm

An important criterion for the distribution of tasks is the availability of estimated time for solving the problem and its priority [24].

The entire list of tasks is sorted by priority, tasks with high priority are at the top of the list. A variable is created that will store the total number of evaluation hours for each task, by default, the value is zero. The cycle starts according to the list of tasks, in the body of the cycle checks the condition that the variable with the total score of the hours plus the estimated time of the current task is less than or equal to the value of the variable in which the total working hours for the team employees are stored. If the condition is fulfilled, then the task falls into the operational plan, otherwise, the task does not fall into the operational plan and the cycle stops because the limit of the estimated time for tasks has already been exceeded. The list of tasks that fell into the operational plan is tied to the “Version” of the project. The block diagram of the algorithm is shown below (Fig. 5).

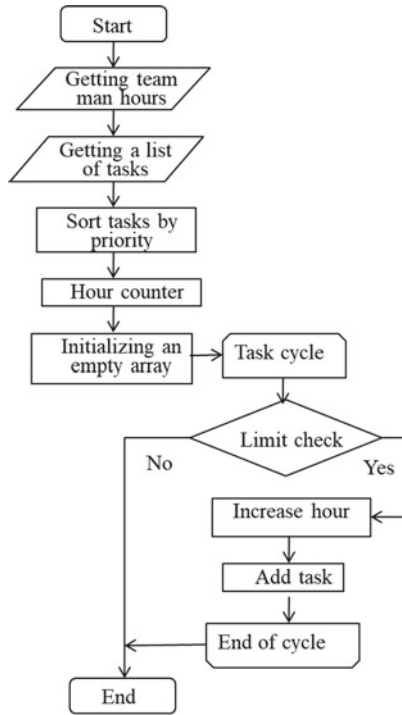


Fig. 5 Tasks Distribution Algorithm

Model classes Holidays, WorkHours, UserPerformance describe the types of fields needed to store data. Figure 6 shows the UML class diagram of a time tracking application.

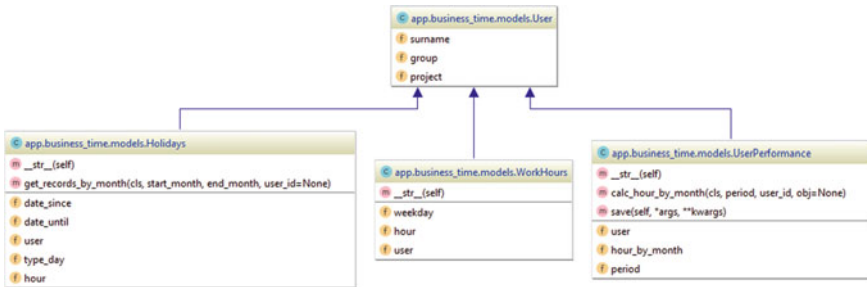
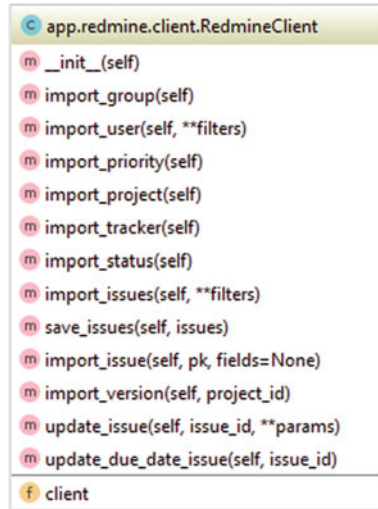


Fig. 6 Logical database model of a time tracking application

Fig. 7 UML diagram of the RedmineClient class



### 4.3 Redmine Sync API

RedmineClient—a class that implements the interface between the application and Redmine. Class methods can be divided into two groups: data import methods and data export methods. Figure 7 shows the UML diagram of the RedmineClient class.

Methods implementing data import:

- import\_user—import of all employees;
- import\_group—import of all groups;
- import\_project—import of all projects;
- import\_version—importing versions filtering by the project;
- import\_issue—import tasks by the filter;
- import\_status—import of all statuses;
- import\_priority—import of all priorities;
- import\_tracker—import of all trackers.

Methods implementing data export:

- update\_issue—update task parameters;
- export\_version—creating a version in the Redmine system.

### 4.4 Test Results

During testing, measurements were made of the execution time of the main processes of the module. Synchronizing the module with the Redmine system to receive updated resource data takes less than one second of time for each resource, this indicator

**Table 2** Comparison of time costs for the distribution of tasks

Distribution methods	Module synchronization	Algorithm execution	Export tasks	Total
Automated (sec.)	8	1	1	10
Manual (sec.)	–	900	–	900

directly depends on Internet speed and data size, the module stores eight synchronized resources, if rounded to seconds, it takes about 8 to complete synchronization seconds. Running the algorithms for distributing tasks by version, 13 tasks were used in the test example, their distribution also took less than one second, the execution time of the algorithm depends on the number of tasks, and a noticeable time difference will only be when the number of tasks exceeds three-digit numbers. Exporting distributed tasks back to the Redmine system takes as much time as importing a single resource. When manually distributing tasks by version, it is known that the manager took an average of 15 min. The measurement results are shown below (Table 2).

## 5 Conclusion

This work is devoted to the application of the Scrum methodology in the Redmine system when developing software products. The application of this methodology increases the efficiency of planning work on a product, due to short-term plans that quickly bring new functionality to the product and quickly respond to changing product requirements under the influence of an external environment that affects it.

**Acknowledgements** The reported study was funded by RFBR according to the research project # 19-07-01200.

## References

1. Salnikova, N.A., Lempert, B.A., Lempert, M.B.: Integration of methods to quantify the quality of medical care in the automated processing systems of medical and economic information. In: Communications in Computer and Information Science (CCIS-2015), vol. 535, pp. 307–319. Volgograd, Russia (2015)
2. Kravets, A.G., Salnikova, N.A., Mikhnev, I.P., Orudjev, N.Y., Poplavskaya, O.V.: Web portal for project management in electronics design software development. In: 2019 International Seminar on Electron Devices Design and Production (SED-2019), art. No 8798472 (2019)
3. Kravets, A., Kozunova, S.: The risk management model of design department's PDM information system. In: Communications in Computer and Information Science, (CCIS-2017), vol. 754, pp. 490–500 (2017)
4. Kravets, A.G., Bui, N.D., Nguyen, L.T.T.: Resource-oriented architecture of mobile devices QoS-based management system. In: 2017 8th International Conference on Information, Intelligence, Systems and Applications, IISA 2017, 2018-January, art. No. 135267 (2018)

5. Kravets, A.G., Skorobogatchenko, D.A., Salnikova, N.A., Orudjev, N.Y., Poplavskaya, O.V.: The traffic safety management system in urban conditions based on the C4.5 algorithm, In: Moscow Workshop on Electronic and Networking Technologies (MWENT-2018), art. No. 8337254, pp. 1–7 (2018)
6. Shcherbakov, M., Groumpos, P.P., Kravets, A.: A method and IR4I index indicating the readiness of business processes for data science solutions, In: Communications in Computer and Information Science (CCIS-2017), vol. 754, pp. 21–34 (2017)
7. Kravets, A., Shumeiko, N., Lempert, B., Salnikova, N., Shcherbakova, N.: “Smart Queue” approach for new technical solutions discovery in patent applications, In: Communications in Computer and Information Science (CCIS-2017), vol. 754, pp. 37–47. Volgograd, Russia (2017)
8. Saltykov, S., Rusyaeva, E., Kravets, A.G.: Typology of scientific constructions as an instrument of conceptual creativity, In: Communications in Computer and Information Science (CCIS-2015), vol. 535, pp. 41–57. Volgograd, Russia (2015)
9. Kravets, A.G., Kanavina, M.A., Salnikova, N.A.: Development of an integrated method of placement of solar and wind energy objects in the Lower Volga, In: International Conference on Industrial Engineering, Applications and Manufacturing (ICIEAM-2017), pp.1–5 (2017)
10. Scrum Guide [Electronic resource]. <https://www.scrumguides.org/docs/scrumguide/v2016/2016-scrum-guide-russian.pdf>. (Date of the application 20.05.2021)
11. Redmine [Electronic resource]. <https://www.redmine.org/>. (Date of the application 20.05.2021)
12. Agile Redmine Plugin [Electronic resource]. [https://www.redmine.org/plugins/redmine\\_agile](https://www.redmine.org/plugins/redmine_agile). (Date of the application 20.05.2021)
13. Redmine License [Electronic resource]. <https://en.wikipedia.org/wiki/Redmine>. (Date of the application 20.05.2021)
14. API Redmine Documentation [Electronic resource]. [http://www.redmine.org/projects/redmine/wiki/Rest\\_api](http://www.redmine.org/projects/redmine/wiki/Rest_api). (Date of the application 20.05.2021)
15. Redmine API Clients [Electronic resource]. [http://www.redmine.org/projects/redmine/wiki/Rest\\_api#API-Usage-in-various-languagertools](http://www.redmine.org/projects/redmine/wiki/Rest_api#API-Usage-in-various-languagertools). (Date of the application 20.05.2021)
16. Python Overview [Electronic resource]. <http://python-3.ru/page/nedostatki-python-i-ih-opisanie>. (Date of the application 20.05.2021)
17. Postgre SQL DBMS [Electronic resource]. <https://postgrespro.ru/docs/postgresql/9.6/intro-what-is>. (Date of the application 20.05.2021)
18. Python library for working with http requests [Electronic resource]. <http://docs.python-requests.org/en/master/>. (Date of the application 20.05.2021)
19. Celery, an asynchronous Python framework [Electronic resource]. <http://www.celeryproject.org/>. (Date of the application 20.05.2021)
20. Django Features [Electronic resource]. <https://web-creator.ru/articles/django>. (Date of the application 20.05.2021)
21. Django, a Python framework [Electronic resource]. <https://www.djangoproject.com/>. (Date of the application 20.05.2021)
22. Python library for integration with Redmine system [Electronic resource]. <https://python-redmine.com/>. (Date of the application 20.05.2021)
23. REST specification [Electronic resource]. <https://docs.swagger.io/spec.html>. (Date of the application 20.05.2021)
24. JSON Specification: API [Electronic resource]. <https://jsonapi.org/format>. (Date of the application 20.05.2021)

# Development of a Tool for Extracting and Analyzing Software Development Process Models



Aleksandr Kushchenko  and Aleksandr Samochadin

**Abstract** The chapter describes an extensible set of tools aimed at extracting processes from the event logs of information systems used in the process of software development and building models of these processes. The features of the software development area include the fact that software developers interact with several information systems at once during their activities and, accordingly, events describing the development process are distributed between these systems, stored in different formats, and described in different ways. The developed tools can expand the ways of specifying sources and parameters for extracting events. Based on the event log generated from several sources, a process model is created using the methods of Process Mining, which can be used for their analysis and improvement. The chapter demonstrates the application of the developed complex for cases when the sources of events are two information systems used in software development (YouTrack and GitLab). Based on the events extracted from the logs of these systems, a model is built, and the resulting model is analyzed.

## 1 Introduction

Analysis of technological or business processes occurring in organizations is a difficult task, especially when it comes to large enterprises with many employees. Performance and efficiency can be affected by many factors that are not always possible to detect manually. Extraction and analysis of process models make it possible to simplify the tasks of finding bottlenecks, violations of regulations, and errors in the process itself.

---

A. Kushchenko (✉) · A. Samochadin  
Peter the Great St.Petersburg Polytechnic University, Polytechnicheskaya, 29, Russia 195251  
St.Petersburg  
e-mail: [kutshenko.ae@edu.spbstu.ru](mailto:kutshenko.ae@edu.spbstu.ru)

A. Samochadin  
e-mail: [samochadin\\_av@spbstu.ru](mailto:samochadin_av@spbstu.ru)

Specialized information systems (personnel accounting systems, order management systems, logistics systems, etc.) function in almost all organizations and generate large amounts of data, including information about events occurring during the operation of the systems. The sequences of such events make up a log that can describe the behavior of processes occurring in the organization.

Process Mining technology is a set of methods aimed at extracting knowledge about the structure and behavior of processes based on data about events recorded in logs. For example, discovery methods allow you to automatically build a process model.

One of the areas in which Process Mining methods are used is software development. The quality of the software significantly depends on the efficiency of the development processes used by the developers and on compliance with the organizational requirements adopted by the company. Many companies have great difficulties since most approaches to the organization of the development process are still based on personal experience and do not use effective methods. There are problems with tracking the activity of developers to optimize and improve the development process. Flexible development methodologies (Agile methodology) allow the integration of Process Mining technology during the implementation of a software development project. Many of these methodologies involve dividing the development process into iterations or "sprints" (using Scrum terminology), in between which the development process can be formally analyzed to identify weak points and take steps to improve it.

Difficulties in extracting a model of the software development process arise since event data is distributed in several information systems and most cases is not stored in the event format supported by Process Mining methods. Therefore, the task arises of extracting event data from several information systems and integrating them into a single event log for further construction and analysis of software development process models.

The purpose of the tools described in this work is to extract and analyze models of the software development process to use the obtained models for improving the development process. The tools being developed should be able to expand and set parameters for event extraction and log construction.

## 2 Related Works

There are many works devoted to the application of Process Mining technology in software development. Let's look at the most interesting publications and determine their distinctive features.

In [1], the authors talk about the real experience of implementing Process Mining in the IT department of a large automobile company. The authors demonstrate the list of information systems but did not specify which events were extracted and how. The Heuristic Miner algorithm was used to detect the process model. They described a specific list of approaches to analyzing and improving the model, but they did not apply them in practice to the existing model.

In the publication [2], attention is paid to the data collected from two Jira Software systems that follow the Scrum methodology. The authors focused on identifying deviations from following the Scrum requirements.

In [3] considered events related to the creation, modification, and deletion of documents, files, and other large amounts of information stored in data management systems. A distinctive feature of this work is that it offers its own incremental approach to process improvement, which assumes continuous monitoring and improvement of the process based on a regularly rebuilt model extracted from the event log.

The work [4] differs from our task in that the authors apply the Process Mining methods not to the development process, but during the development process. They demonstrated how the Process Mining methods allow us to quickly identify problems in the developed product and simplify its testing.

In all the above works, the authors pay attention to the detection of the process and take steps to improve it, but they do not consider one of the most important stages before the Process Mining and it is the preparation of the event log. It is possible that information systems already have an open-access journal in the required format, but this happens quite rarely. Basically, the log is extracted using a specially developed tool for each business system, which is responsible for collecting data and generating the log.

In this work, an important place is occupied by the development of a tool that can be configured for different log formats. Each organization has its own list of business information systems, and there is a need to develop an extensible tool for collecting source data, filtering it, and creating a log.

Process extraction tools are widely used in various fields, including in the software development process. However, a distinctive feature of the extraction of the development process is that to obtain the most correct and complete model of the process, it is necessary to extract event data from as many systems as possible with which developers interact.

### **3 Problem Statement**

The purpose of the software package development is to create tools for automated data extracting from a given list of information systems that developers interact with.

Information systems are understood as business systems of organizations, such as task management systems, version control systems, integrated development environments, data management systems, business messengers, and others. This list may vary depending on the organization.

One of the components of the developed complex is the component of adapting data extracted from information services to build models of the software development process. This component is designed to interact with one or more information systems to extract event data and generate a log. Log construction includes sorting, filtering, and splitting events into sequences representing process instances.



To perform these tasks, the component must convert the internal representation of requests to services into the format of events supported by Process Mining methods.

Most external information systems do not store data in the form necessary for extracting events (indicating the type of event, timestamp, resource, etc.), but form entities in popular text data exchange formats, for example, JSON or XML. To extract data, most often systems provide an open REST API interface, interaction with which is performed under the HTTP protocol.

## 4 Technologies and Tools

To identify the process models, we have developed our own tools and applied existing approaches. Next, we will consider each of them.

### 4.1 *The Petri Net as a Representation of the Process Model*

There are many methods aimed at creating process models from the sequence of actions performed in the organization. Such sequences are stored in event logs generated by business information systems operating in companies. Such models are most convenient to represent in the form of a transition system, where the transition is the actions of the process. In most cases, the detection of the process model is reduced to the construction of a Petri net [5]. A Petri net is defined as a bipartite-oriented multigraph consisting of two types of nodes—places and transitions. The places can contain tokens (markers) that can move around the network. An event is called a transition trigger, in which the labels from the input places of this transition are moved to the output places [6]. This view has become a standard in the field of Process Mining, as it clearly shows the parallelism, choice, and causal relationships between events. In addition to Petri nets, a well-known extension of the Petri net, called workflow net, is used to represent the model [7]. Workflow nets unlike Petri nets have one source node and one receiver node. Consequently, all nodes represent the path from the source to the receiver.

### 4.2 *Process Mining Technology*

The work is based on the technology of Process Mining—a research area that focuses on the analysis of processes using event data. Classical Data Mining methods, such as classification, clustering, regression, and sequence analysis, do not focus on business process models and are often used only to analyze a specific step in the overall process [8]. Process Mining focuses on the process from start to finish.

Process models are used for analysis (for example, modeling [9] and validation) and are consistent with BPM/WFM systems. Previously, process models were usually created manually without using event data. However, actions performed by people, machines, and software leave a trail in the event logs. Each event in such a log is associated with an activity (i.e., a defined step in a process) and is associated with a specific case (i.e., an instance of the process). Events related to the case can be considered as a single "run" of the process. Event logs can store additional information about events, such as the resource (i.e., the person or device that initiated the action), the timestamp of the event, or other data that is recorded with the event (for example, the size of the order). In Process Mining methods, event logs are used to solve three main tasks [10]: discovery of the process model, conformance checking that the model matches the event log, and enhancement of the model to change or expand it [11].

### ***4.3 Approaches to Improving the Software Development Process***

For intelligent analysis and improvement of the process, it is proposed to use Social Network methods and clustering algorithms. Clustering allows us to use information about resources to identify roles, i.e. groups of people who often perform related actions [8]. Social networks built based on the control flow in the Petri net allow analyzing the performance of resources (for example, the ratio between workload and service time) [11].

In addition, the waiting time between actions is analyzed by measuring the time difference between causally related events and calculating statistics such as mean, variance, and confidence intervals. Thus, it is possible to determine the main weakness of the process [12].

Standard classification methods are used to analyze the decision points in the process model [13]. As an example, consider activity  $x$ , which has two possible outcomes ( $y, z$ ). Using the data known before the decision is made, we can construct a decision tree that explains the observed behavior. In addition, process improvement is not limited to offline analysis and can also be used for forecasts and online recommendations [14].

In addition to Process Mining methods, it is proposed to use business process management (BPM) approaches to analyze and improve process models. For example, [15] describes the ISEA method, which introduces 4 stages: identification, modeling, evaluation, and improvement. These stages are supported by interaction with the end-users of the business system. Thus, this approach is perfectly suited for improving the efficiency of the development process itself in the organization, as well as the activities of individual employees.

#### **4.4 *Open-Source Framework ProM***

In [16], a comparison of software for solving Process Mining problems was made. Based on the literature and testing, the authors identified a set of criteria for evaluating the tools. The paper focuses on commercial software for Process Mining. However, the authors did not ignore the open-source ProM tool, which we decided to use for current tasks. In ProM, almost all the main Process Mining tools are implemented in the form of plugins, of which there are more than 200 [17].

ProM works with logs presented in the MXML format and its parent, XES. XES is an XML-like format approved by the IEEE Task Force on Process Mining and described in [18]. This imposes additional difficulties, since most information systems record information in more familiar document formats, such as JSON and XML, or in a relational database. The ProM extension library includes several plugins for extracting the event log from various systems and data structures. In the current implementation, event information is stored in a PostgreSQL relational database and the XESame extension is used to retrieve the log. The extension eliminates the need to develop a relational model converter in XES and does not require programming skills at all since it has a convenient graphical interface [19].

#### **4.5 *Spring Framework***

The development of a tool for extracting source event data and building a log is carried out in the Java language using the Spring framework.

Most information business systems have an open REST API, which allows us to request entities that contain information about events using the HTTP protocol.

Webflux library is used to interact with the API. Webflux includes the WebClient class, which methods allow you to form HTTP requests. The methods and input parameters are described in the official WebFlux library documentation [20].

All extracted entities are stored in the Postgres database. To interact with entities (tables, columns) of a relational database, the Spring Data JPA extension is used. To work with a database, a data schema is described in the form of regular Java classes, where fields correspond to columns in tables. Thus, Spring Data JPA maps the object data model to a relational one.

### **5 Implementation Details and Architecture of the Developed Complex**

Figure 1 schematically shows the architecture of the complex of tools. There is a tool (Event log extractor) for extracting event data and building an event log in the format familiar to Process Mining methods. The Process Mining methods are used to

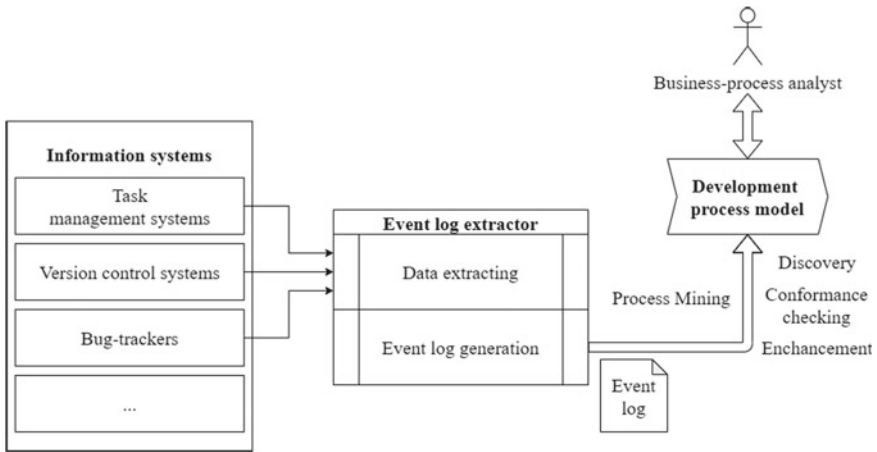


**Fig. 1** Process Mining in the software development process

solve the problems of discovering the process model, checking the conformance of this model and its enhancement. Further, based on the results obtained, the business process analyst can take steps to optimize the development process.

The developed tool (Event log extractor) consists of two interconnected components.

The first component is designed to extract initial data about events from a predefined list of business information systems. It is an application that runs in the background and periodically polls the APIs of various business systems to get and save the event data. A convenient mechanism for expanding event sources is provided, which is based on the “Factory” design pattern, which allows you to add new classes to the project in a convenient way. This template defines an interface for creating instances of one of several possible classes. In this interface, the method responsible for creating objects is defined, and it is commonly called the factory method. The class (a specific factory) that inherits this interface determines which instance of the class to initialize. For each individual API resource, a different method is added for polling it and the fields that need to be saved for further logging are specified.

The second component uses the extracted data to generate an event log, which later gets to the input of the Process Mining methods. As is known from the definition, the log should be divided into cases (process examples). The project provides a configuration file that sets the parameters for generating the log. The “sources” parameter lists the business information systems, the events from which will participate in the formation of the log. The “events” parameter lists the types of events that will be logged. In this way, we can build a log of a specific subprocess, for example, by specifying events related to testing or continuous integration settings. Both components consist of ETL procedures (Extract, Transform, Load) [21].

## 6 Data Sources for the Event Log

Before applying the Process Mining methods to the software development process, you should define data sources with events.

In the course of their work, programmers interact with several information systems that can store information that is characteristic of the development process. The main systems used in the development process include:

- Version control systems (e.g., GitLab, BitBucket)
- Task management systems and bug trackers (e.g., YouTrack, Jira)
- Internet browsers (e.g., Google Chrome, Edge)
- etc.

The list can be expanded by any systems operating in the organization that may contain information reflecting the development process.

The following entities can be used as source data for building the event log:

- Branches (event for creating, deleting, merging a branch).
- Commits (events related to committing changes to any files included in the repository)
- Repositories (repository initialization events).
- Wiki (events for creating or editing a wiki page).
- Tasks (information about changing the status of tasks in the corporate task management system).
- Timetrack—elapsed time (adding the elapsed time to the task).
- Attachments (comments and attachments to the task that play the role of feedback from the employee or management).
- Visit history—the history of site visits through the Chrome web browser.

As noted earlier, events in the log should be split into cases. Figure 2 shows an example of how we can split the events. In this case, a sequence of events related to a single Issue is considered as a case. Accordingly, any case should start with the task opening event and end with its closing.

## 7 Example of a Built Model

As a result of the application of the developed complex to the GitLab and YouTrack information systems, experimental data for a period of 7 days were collected and an event log was built. A model is constructed based on the extracted data (see Fig. 3) in the form of a Petri net. The well-known  $\alpha$ -miner was used as an algorithm for discovering the model.

The number of transitions of the constructed model corresponds to the number of unique events in the log, which means that not one event is ignored by the algorithm, and this is one of the indicators indicating the completeness and correctness of the

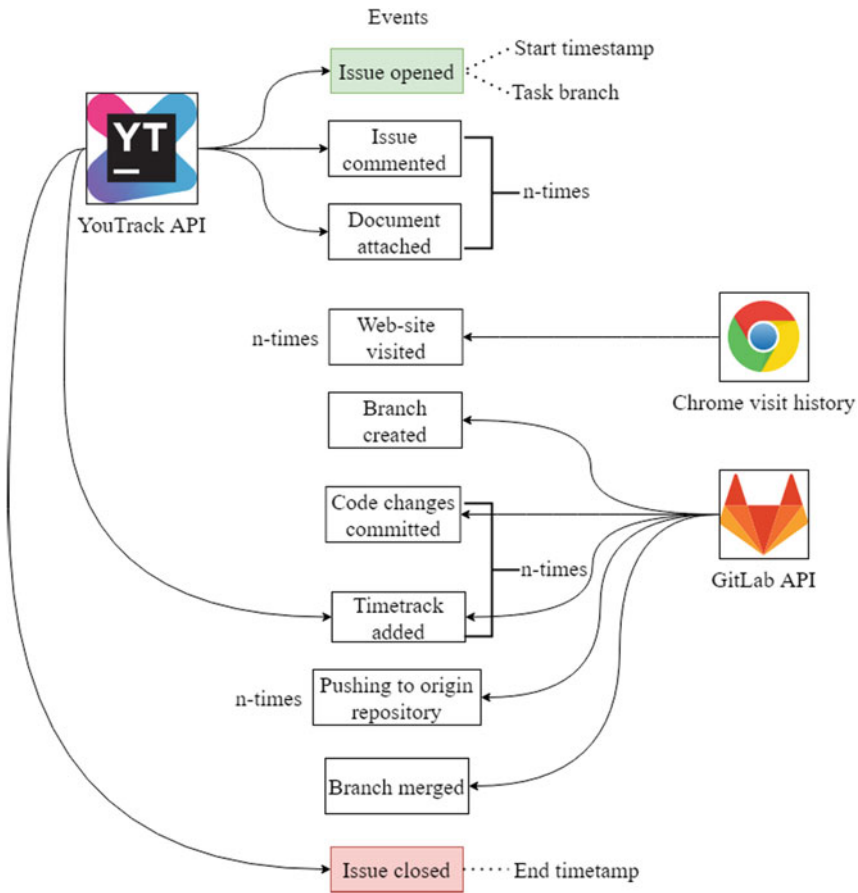
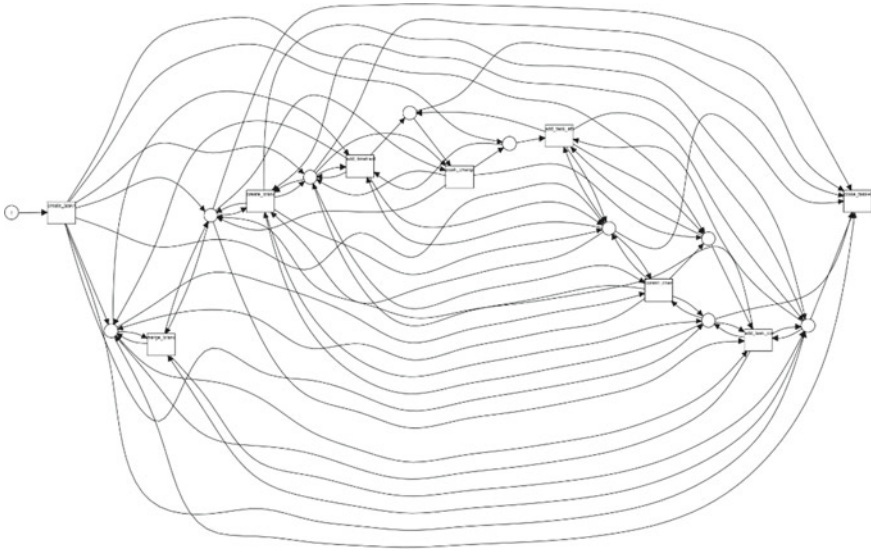


Fig. 2 An approach to generating the event log

model. But to make more accurate conclusions about the suitability of the model, it is necessary to check conformance with the log.

To check conformance, the method of reproducing process instances from the log on the detected model, widely used in Process Mining, is used. Events are assigned weights that are remembered when the event was not reproduced by the model, or vice versa if the model had a transition that was not in the log. According to the results of the conformance check, most of the events were reproduced in a log, which indicates a high precision.

The improvement of the discovered model and the corresponding development process is the main direction for future work. Based on the extracted model, it is planned to solve the following tasks aimed at optimizing and improving the development process:



**Fig. 3** The process model discovered by  $\alpha$ -miner

- Adjustment of the requirements for the development regulations.
- Reallocation of tasks.
- Detect employees who, do not follow the requirements for the organization of the development process.
- Identify weaknesses in the process.

## 8 Conclusion

In this chapter, we considered an approach for intelligent analysis of the software development process, based on the information available in the information business systems that software developers interact with during their activities.

The goal has been achieved, the extensible tool has been developed for extracting event data from several sources and building a log that is used by Process Mining methods.

The chapter demonstrates the integration of the tool with two information systems (YouTrack and GitLab), with which developers interact. An algorithm for generating process instances based on events that occur as part of working on a task in the project management system and the version control system is developed. A process model was built based on the extracted data, and model conformance was checked. The resulting model has high precision and clearly displays the behavior of the process.

## References

1. Sebu, M.L., Ciocarlie, H.: Applied process mining in software development, pp. 55–60 (2014). <https://doi.org/10.1109/SACL.2014.6840098>
2. Marques, R., Mira da Silva, M., Ferreira, D.: Assessing Agile Software Development Processes with Process Mining: A Case Study, pp. 109–118 (2018)
3. Rubin, V., Günther, C., Aalst, W., Kindler, E., Dongen, B., Schäfer, W.: Process Mining Framework for Software Processes, pp 169–181 (2007)
4. Rubin, V., Lomazova, I., Aalst, W.: Agile development with software process mining. In: ACM International Conference Proceeding Series (2014)
5. Thamizhara, R., Appavoo, K.: A review on software process mining using petri nets. Asian J. Appl. Sci. **9**, 131–142 (2016)
6. Aalst, W., Stahl, C.: Modeling Business Processes: A Petri Net Oriented Approach (2011)
7. Aalst, W.: The application of petri nets to workflow management. J. Circuits Syst. Comput. **8**, 21–66 (1998)
8. Aalst, W.: Process mining: overview and opportunities. ACM Trans. Manag. Inf. Sys. **3**, 7.1–7.17 (2012)
9. Dorrer, M., Dorrer, A., Zyryanov, A.: Numerical modeling of business processes using the apparatus of GERT networks. In: Society 5.0: Cyberspace for Advanced Human-Centered Society, vol. 333, pp. 47–55. Springer, Berlin (2021)
10. Aalst, W.: Process Mining: Discovery, Conformance and Enhancement of Business Processes (2011)
11. Song, M., Aalst, W., Choi, I.: Mining Social Networks for Business Process Logs (2004)
12. Peil, S.: A Systematic Methodology for Process Analysis based on Process Mining, Machine Learning and Complexity Theory (2018)
13. Aalst, W., Schonenberg, H., Song, M.: Time prediction based on process mining. Inf. Syst. **36**, 450–475 (2011)
14. Ho, G.T.S., Lau, H., Lee, C., Ip, W.H.: Real-time process mining system for supply chain network: OLAP-based fuzzy approach. Int. J. Enterp. Netw. Manag. (2008)
15. Front, A., Rieu, D., Santórum G.M., Movahedian, F.: A participative end-user method for multi-perspective business process elicitation and improvement. Softw. Syst. Model. 691–714 (2015)
16. Viner, D., Stierle, M., Matzner, M.: A Process Mining Software Comparison (2020)
17. Aalst, W., Dongen, B., Günther, C., Rozinat, A., Verbeek, E., Weijters, A.: ProM: The Process Mining Toolkit. Allergy. onstration Track 2010. In: Rosa, M.L. (ed.) CEUR Workshop Proceedings Series, vol. 615, pp 34–39 (2009)
18. XES Standart (2021). <http://www.xes-standard.org/>. Accessed 1 May 2021
19. XESame user interface (2021). <http://www.promtools.org/doku.php?id=gettingstarted:xesameui>. Accessed 21 Apr 2021
20. Spring WebFlux (2021). <https://docs.spring.io/spring-framework/docs/current/reference/html/web-reactive.html#webflux-config>. Accessed 15 Apr 2021
21. Protalinskiy, O., Sachenko, N., Khanova, A.: Data mining integration of power grid companies enterprise asset management. In: Cyber-Physical Systems: Industry 4.0 Challenges, vol. 260, pp. 39–49. Springer, Berlin (2020)



# Models and Algorithms for Determining the Safety Valves Critical Flow at Petrochemical Facilities



A. V. Nikolin and E. R. Moshev

**Abstract** The chapter deals with the problem of automating the process of determining the critical flow of safety valves. The analysis of normative-technical and scientific-technical literature on the object of research is given. It is shown that in the available literature there are no models and algorithms that allow automating the process of determining the critical flow rate of safety valves. With the help of a systematic approach, the analysis of the process of determining the emergency flow rate of safety valves as an object of computerization is carried out. As a result of the analysis, it was found that this process contains heuristic knowledge and can be formalized using the methods of the theory of artificial intelligence. A functional model for determining the critical flow rate of safety valves as an organizational and technological process is presented, and the necessary heuristic and computational algorithms are provided. The developed models and algorithms make it possible to create a cyber-physical system that will ensure the determination of the critical flow of safety valves in an automated mode.

**Keywords** Safety valve · Relief pressure · Critical flow · Overpressure · Functional model · Heuristic-computational algorithm · Cyber-physical system

## 1 Introduction

To prevent emergencies, special technical devices called safety valves (SV) are installed on the equipment and pipelines of petrochemical plants. They are designed to relieve the pressure that exceeds the value allowed by industrial safety rules. The most important parameter that ensures the correct choice of the brand and size of the valve is the value of the critical flow rate of the substance in the device. The critical

---

A. V. Nikolin (✉) · E. R. Moshev  
Perm National Research Polytechnic University, Komsomolsky Prospekt 29, Perm 614990, Russia  
e-mail: [aletrof@mail.ru](mailto:aletrof@mail.ru)

E. R. Moshev  
e-mail: [erm@pstu.ru](mailto:erm@pstu.ru)

flow rate here means the minimum throughput of the SV, which guarantees that the pressure in the vessel or pipeline does not rise more than the value allowed by the normative and technical documentation.

The critical flow rate of safety valves must be determined in strict accordance with the requirements of industrial safety rules and it is a complex engineering and technical problem [1], the solution of which depends on many factors, e.g. chemical composition, pressure, temperature, and volume of the substance in the apparatus; the parameters and type of the technological process taking place in specific equipment for which it is necessary to select an SV. At the same time, the process of determining the critical SV consumption takes a long time, which is due to the presence of a large number of various routine operations related to the search for reference data, their processing, as well as the procedures for making intelligent decisions [2, 3]. It is possible to simplify and accelerate the determination of critical SV consumption if you create and apply special software - a cyber-physical system (CPS) [4–7]. Analysis of scientific and technical literature did not reveal models [8–13] and algorithms [14–16] that can be used without correction for the development indicated by the CPS. Based on the foregoing, the purpose of this study was to create models and algorithms that automate the determination of critical SV consumption.

To achieve this goal, the following tasks were formulated:

- to analyze the process of determining the critical consumption of an SV as an object of computerization;
- to develop a functional model (FM) for determining critical SV consumption as an organizational and technological process;
- to develop algorithms that formalize the procedures for determining critical SV consumption.

## **2 The Process of Determining the Critical Flow of Safety Valves as an Object of Computerization**

The analysis of the normative and technical documentation and scientific and technical literature established that the process of determining critical SV consumption consists of three main stages: determining the characteristics for calculating critical SV consumption; calculating critical SV consumption; checking the critical SV consumption for a fire condition. In this case, the most difficult stage in terms of computerization is the second stage—the calculation of the critical flow rate. This is because the critical flow has complex relationships with the parameters of a specific technological process and its hardware design, and engineering and technical calculations require good knowledge of chemical technology. At the same time, there are dependencies between the SV characteristics and the working environment, which are discrete in most cases. The analysis of the procedures for determining critical SV consumption showed that they can be formalized using the methods of the theory of artificial intelligence [2, 3], which allows them to be automated.

### 3 Development of a Functional Model for Determining the Critical Flow of Safety Valves

As a result of the analysis of knowledge about the subject of research, carried out using a systematic approach [17, 18], a logical-informational model was developed that formalizes the definition of critical SV consumption as an organizational and technological process. The model is described following the methodology of structural analysis and design SADT (Structured Analysis & Design Technique) (Fig. 1). The SADT methodology [19, 20] was chosen since it is often used in the development of complex systems and many cases are considered an integral part of CALS technologies [21, 22]. In the Russian Federation, it is also widely known as a functional modelling methodology.

The developed functional model (FM) is distinguished by the use of a systematic approach and account of the complex relationships between the various stages of determining the critical consumption of an SV, as well as the connection with data- and knowledgebases, which allows automating the execution of the steps indicated above, and, at the same time, ensure a high information exchange rate. As an example of FM detailing, the decomposition of block A12 (Fig. 2) of diagram A1 is presented, which shows the relationship between various functions of the procedure for calculating the critical consumption of SVs installed on technological equipment. In Fig. 2  $P_1$  is the full opening pressure of the valve;  $G_{SUP}^{CR}$  is power flow of the column in the emergency mode during  $P_1$ ;  $e$  is a mass fraction of steam in the feed (fraction of distillate);  $i_{SUP}^{LN}$  is heat content of liquid feed in the normal mode at  $P_P$ ;  $P_P$  is

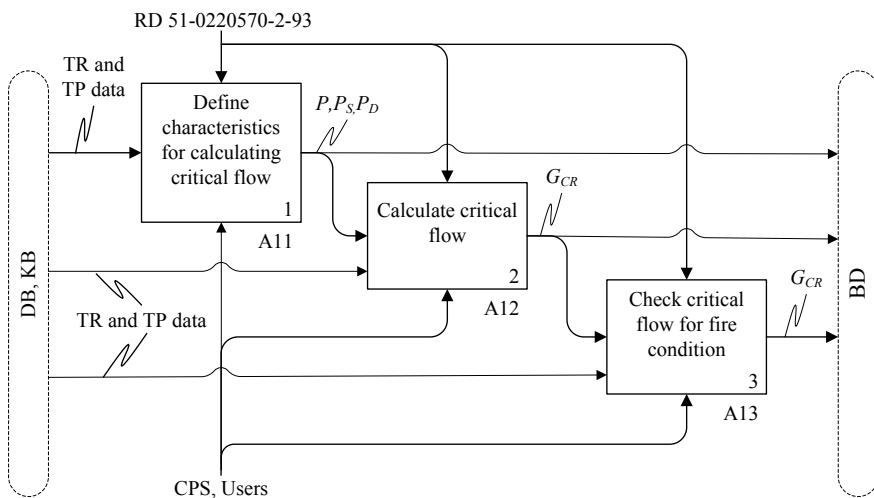


**Fig. 1** Diagram A1 of the functional model for determining the critical flow of safety valves: TR is technological regulations; TP is a technical passport of the vessel;  $G_{CR}$  is the critical flow of the working medium;  $P$  is the SV working pressure;  $P_D$  is the SV design pressure;  $P_S$  is the SV setting pressure; DB is database; KB is knowledge base

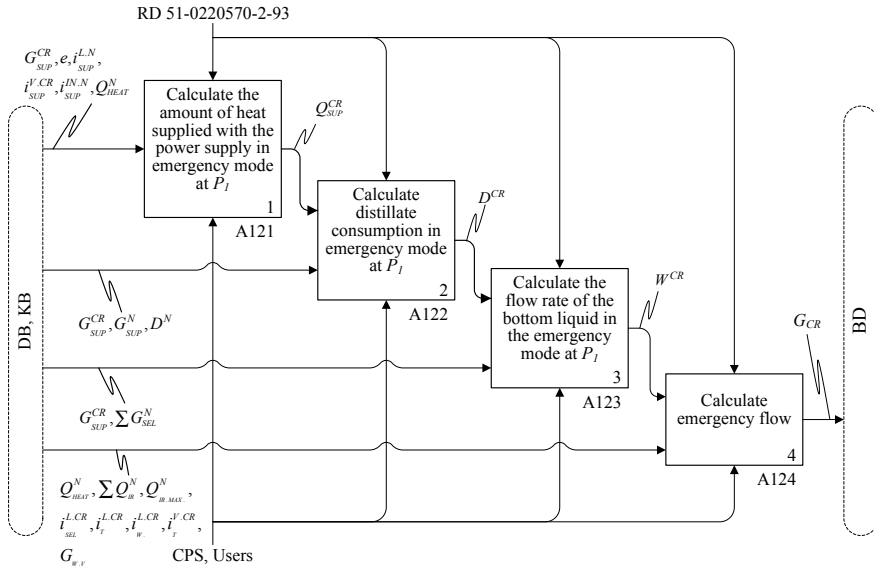


Fig. 2 Decomposition of block A12 of diagram A1

process pressure;  $i_{SUP}^{V,CR}$  is heat content of supply vapour in the emergency mode during  $P_I$ ;  $i_{SUP}^{IN,N}$  is heat content of the feed at the input to the feed heater in the normal mode at  $P_P$  (adopted according to the project);  $Q_{HEAT}^N$  is thermal load of the power heater in the normal mode at  $P_P$ ;  $Q_{SUP}^{CR}$  is the amount of heat supplied with feed in the emergency mode during  $P_I$ ;  $G_{SUP}^N$  is power consumption of the column in the normal mode at  $P_P$  (adopted according to the project);  $D^N$  is distillate consumption in the normal mode at  $P_P$  (adopted according to the project);  $D^{CR}$  is distillate consumption in the emergency mode during  $P_I$ ;  $\sum G_{SEL}^N$  is the sum of the intermediate selection flow rates in the normal mode at  $P_P$  (adopted according to the project);  $W^{CR}$  is consumption of bottom liquid in the emergency mode during  $P_I$ ;  $\sum Q_{IR}^N$  is the total heat load of intermediate circulating irrigation in normal mode;  $Q_{IR,MAX}^N$  is the heat load of one of the intermediate circulating irrigations, which has the highest value, in normal mode at  $P_P$  (adopted according to the project);  $i_{SEL}^{L,CR}$  is the heat content of the intermediate withdrawal fluid in emergency mode at  $P_I$ ;  $i_T^{L,CR}$  is the heat content of the liquid product at the top of the column in emergency mode  $P_I$ ;  $i_W^{L,CR}$  is the heat content of the liquid vat residue in emergency mode at  $P_I$ ;  $i_T^{V,CR}$  is the heat content of steam at the top of the column in emergency mode at  $P_I$ ;  $G_{WV}$  is the flow of water vapour (inert gas) supplied to the column for stripping (taken into account only if the pressure of water vapour is higher than  $P_I$ ).

## 4 Algorithms to Automate the Determination of Critical Flow of Safety Valves

As a mechanism for the implementation of the functions specified in the FM blocks, the corresponding algorithms have been developed. Examples of algorithms that make it possible to automate the execution of block A12 for different types of equipment are shown in Figs. 3 and 4. Figure 3 shows an algorithm for determining the critical flow rate of SVs installed on distillation columns.

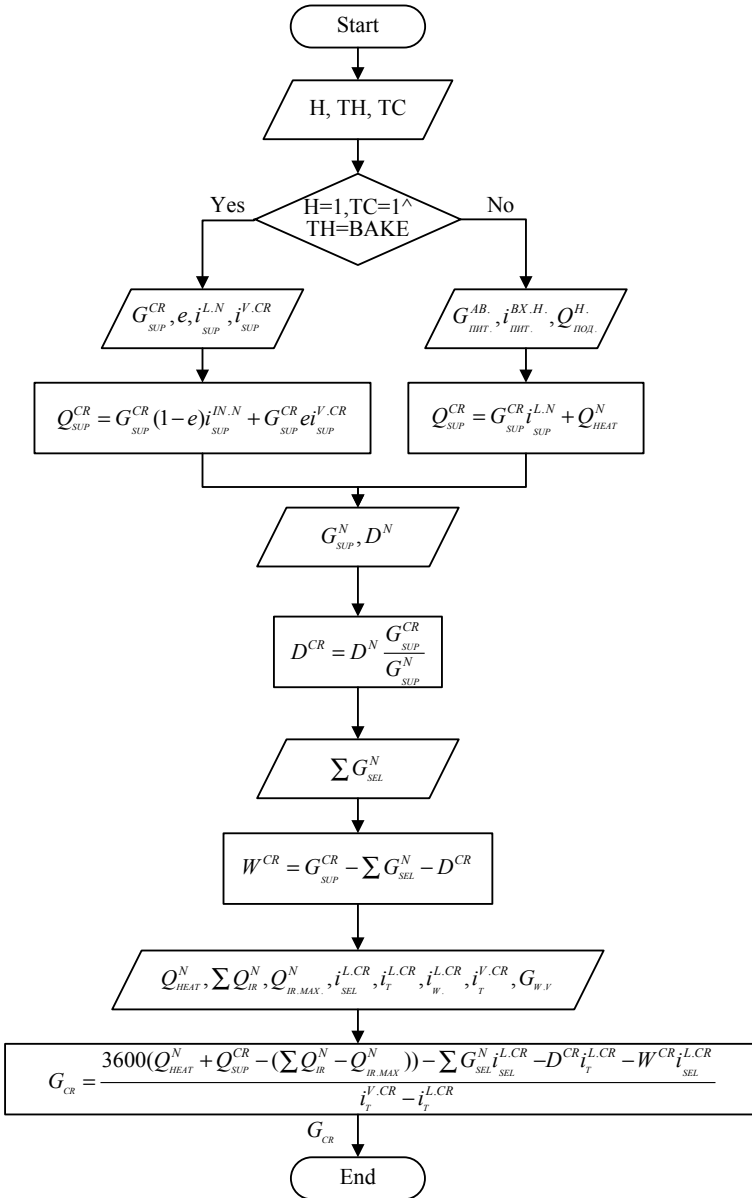
This algorithm formalizes the process of determining the critical flow rate of the SV installed on the rectification columns, as well as the following characteristics: the amount of heat supplied with the power supply in the emergency mode (at  $P_I$ )  $Q_{SUP}^{CR}$ ; distillate consumption in the emergency mode (during  $P_I$ )  $D^{CR}$ ; the flow rate of bottom liquid in the emergency mode (at  $P_I$ )  $W^{CR}$ . The algorithm differs in that with the help of the given initial data (a heater at the power supply H, the type of heater at the power supply TH, regulation of the supply temperature at the outlet), it allows us to automate computational and intelligent decision-making procedures when determining the critical consumption of SVs installed on the distillation columns, following the requirements of the normative and technical documentation.

Figure 4 shows an algorithm for determining the critical flow rate of the SVs installed on other (not rectification columns) process vessels and pipelines, in particular, tanks; separators; degassers; absorbers; adsorbers; phase separators; liquid pipelines, and vessels filled with liquid and designed for the pressure of the supply source; pipelines on the lower pressure side downstream of the pressure regulators; discharge lines after a pump or compressor.

The following designations are used in the algorithm (Fig. 4): Lis SV location (for example, LPis liquid pipeline; IP is injection pipeline); TE is the type of equipment (for example, PT is process tank; SPR is separator; DGS is degasser; ABR is absorber; ABR is adsorber; ADR is adsorber; VCFLis vessel filled with liquid);  $T_1$  is the working temperature of the liquid in the neighbour (pipeline);  $T_2$  is the maximum temperature of the liquid in the vessel (pipeline) (taken equal to 50 °C);  $V_V$  is the initial volume of liquid in the vessel (pipeline) at temperature  $T_1$ ;  $\rho_L$  is the density of the liquid at temperature  $T_1$ ;  $\beta_L$  is the coefficient of volumetric expansion of the liquid.

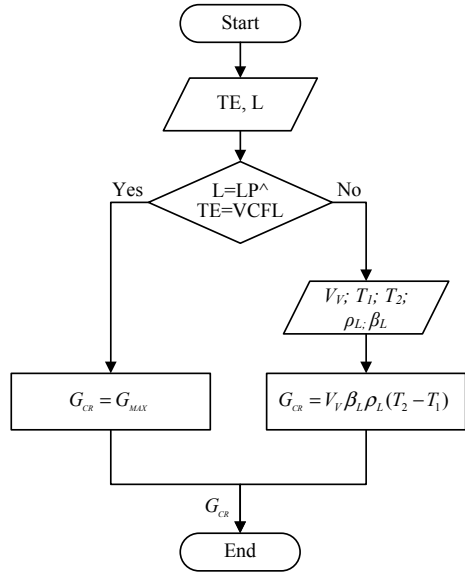
An example of a heuristic-computational algorithm that automates the execution of block A13 is shown in Fig. 5.

In the algorithm (Fig. 5), the following designations are used: SAM is the medium aggregation state (where L is liquid, G is gas, G/L is gas/liquid); TC is the type of medium (where FL is flammable liquids, LG is liquefied gas, CG is combustible gas, etc.); L is the SV location (for example, BSV is between the shut-off valves); TE is the type of equipment; RE is refrigeration equipment; PH is pipeline heating; TI is thermal insulation;  $r$  is the latent heat of vaporization of a liquid at discharge pressure  $P_D$  (for safety valves installed on a heated pipeline with flammable liquids or liquefied gases between shut-off valves), or the latent heat of vaporization of a liquid at temperature  $t_L$  (for vessels completely filled with a liquid phase or containing a



**Fig. 3** Block diagram of a heuristic-computational algorithm for determining the critical consumption of SVs installed on rectification columns

**Fig. 4** Block diagram of a heuristic-computational algorithm for determining the critical consumption of SVs installed on process vessels and pipelines



liquid and vapor phase);  $t_s$  is satellite temperature;  $t_{BPL}$  is the boiling point of the liquid at discharge pressure  $P_D$ ;  $K$  is heat transfer coefficient when heating with a steam or water satellite;  $F_H$  is the surface of the heated pipeline section between the shut-off valves;  $F_{WS}$  is wetted surface of the apparatus;  $t_G$  is the temperature of the gas-air mixture that washes the outer surface of the apparatus in case of fire;  $t_{BL}$  is the boiling point of the liquid at the full opening pressure of the safety valve;  $K_L$  is the overall coefficient of heat transfer from the ambient air through the apparatus wall to the liquid;  $F_O$  is total outer surface of the apparatus;  $t_V$  is the temperature of gases (vapors) in the apparatus during normal operation;  $C_V$  is the heat capacity of gas (vapor) at the discharge pressure  $P_D$ ;  $K_V$  is the overall coefficient of heat transfer from the ambient air through the apparatus wall to the gas (vapor).

The developed algorithm formalizes the verification process of the calculated critical flow rate of a spring-loaded safety valve for a fire condition. The algorithm differs in that with the help of the given initial characteristics, it allows automating computational and intelligent decision-making procedures when checking the calculated critical SV consumption for a fire condition following the requirements of regulatory and technical documentation.

## 5 Conclusion

Thus, as a result of this study, by analyzing the regulatory and technical documentation and scientific and technical literature, as well as using a systematic approach to the process of determining critical SV consumption, the following were developed:

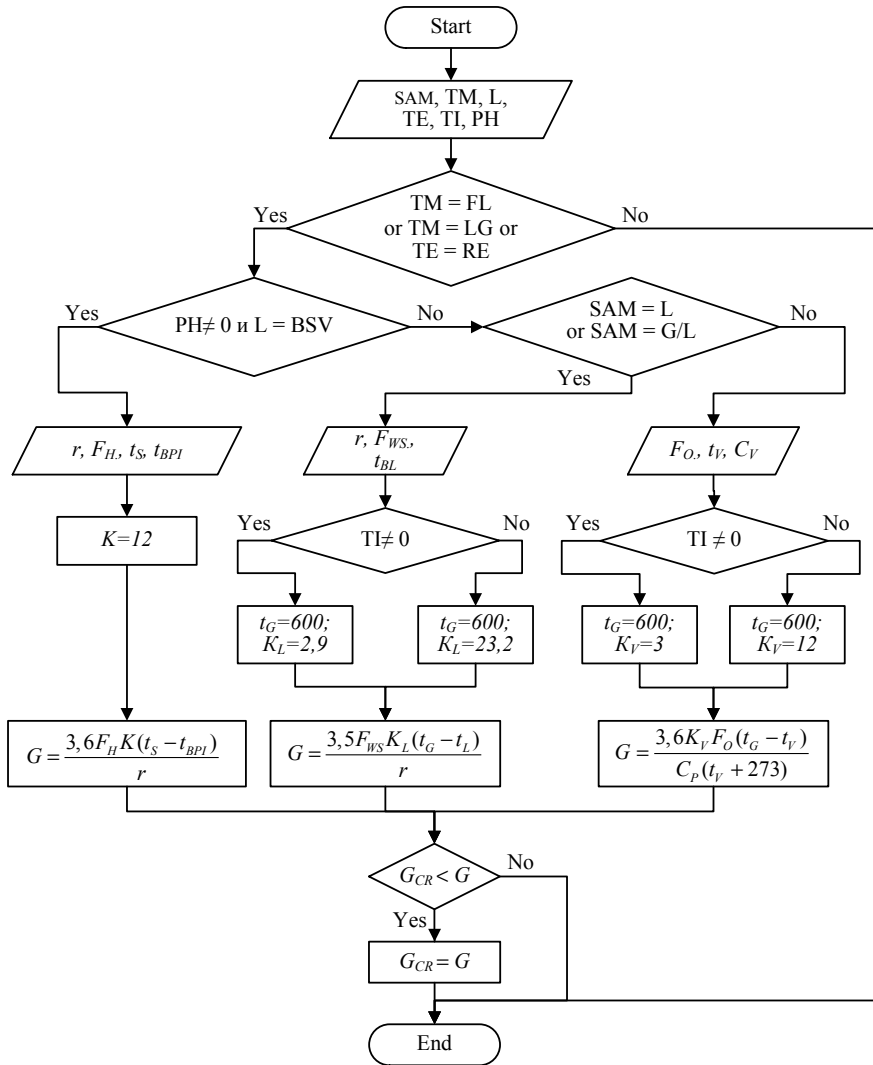


**Fig. 5** Block diagram of a heuristic-computational algorithm for checking critical SV consumption for a fire condition

- A functional model for determining the critical flow rate of safety valves as an organizational and technological process, which is distinguished by the systematic approach and account of complex relationships between various stages of characterization for calculating the SV critical flow rate, as well as by connection with data- and knowledge bases, which allows automating the procedure for determining the critical flow of an SV while providing a high speed of data exchange.



- Heuristic-computational algorithms allow automating computational and intelligent decision-making procedures when performing the functions specified in the functional model block and when determining critical SV consumption, following the requirements of the normative and technical documentation.

The developed models and algorithms make it possible to create a CPS, the use of which will accelerate the search and data processing procedures, as well as reduce the number of subjective errors in determining critical SV consumption, which will increase the quality of SV selection, and, consequently, the industrial safety and economic efficiency of petrochemical facilities in general.

## References

1. Horlacher, H.-B., Helbig (Hrsg.), U.: Rohrleitungsplanung–Grundsätze, Vorschriften, Regelwerke//Rohrleitungen 1, Springer Reference Technik 2016. C. 35–43 (2016)
2. Wu, D., Olson, D.L., Dolgui, A.: Artificial intelligence in engineering risk analytics. *Eng. Appl. Artif. Intell.* **65**, 433–435 (2017)
3. Russell, S.J., Norvig, P.: *Artificial Intelligence: A Modern Approach*, 3rd edn. Prentice Hall, New Jersey (2010)
4. Buldakova T.I., Suyatinov S.I.: Assessment of the State of production system components for Digital Twins Technology. In: Kravets, A., Bolshakov, A., Shcherbakov, M. (eds.) *Cyber-Physical Systems: Advances in Design & Modelling. Studies in Systems, Decision and Control*, vol. 259. Springer, Cham (2020)
5. Stepanov, M., Musatov, V., Egorov, I., Pchelintzeva, S., Stepanov, A.: Cyber-physical control system of hardware-software complex of anthropomorphous robot: architecture and models. In: Kravets, A., Bolshakov, A., Shcherbakov, M. (eds.) *Cyber-Physical Systems: Advances in Design & Modelling. Studies in Systems, Decision and Control*, vol. 259. Springer, Cham (2020)
6. Alekseev, A.P.: Conceptual approach to designing efficient cyber-physical systems in the presence of uncertainty. In: Kravets, A., Bolshakov, A., Shcherbakov, M. (eds.) *Cyber-Physical Systems: Advances in Design & Modelling. Studies in Systems, Decision and Control*, vol. 259. Springer, Cham (2020)
7. Moshev, E., Meshalkin, V., Romashkin, M.: Development of models and algorithms for intellectual support of life cycle of chemical production equipment. In: Kravets, A., Bolshakov, A., Shcherbakov, M. (eds.) *Cyber-Physical Systems: Advances in Design & Modelling. Studies in Systems, Decision and Control*, vol. 259. Springer, Cham.(2020)
8. Guo, F., Zou, F., Liu, J., Wang, Z.: Working mode in aircraft manufacturing based on digital coordination model. In: *The International Journal of Advanced Manufacturing Technology*, vol. 98, pp. 1547–1571. Springer, Cham (2018). <https://doi.org/10.1007/s00170-018-2048-0>
9. Kim, H., Han, S.: Interactive 3d building modeling method using panoramic image sequences and digital map. In: *Multimedia Tools and Applications*, vol. 77, №20, pp. 27387–27404. Springer, Cham (2018). <https://doi.org/10.1007/s11042-018-5926-4>
10. Cheng J., Liu Z., Yu X., Feng Q., Zeng X.: Research on dynamic modeling and electromagnetic force centering of piston/piston rod system for labyrinth piston compressor. *Proceedings of the institution of mechanical engineers. Part I J. Syst. Control Eng.* **230**(8), 786–798 (2016)
11. Comelli, M., Gourgand, M., Lemoine, D.: A review of tactical planning models. *J. Syst. Sci. Syst. Eng.* **17**(2), 204–229 (2008)
12. Moshev, E.R., Romashkin, M.A.: Development of a conceptual model of a piston compressor for automating the information support of dynamic equipment. *Chem. Pet. Eng.* **49**(9–10), 679–685. Springer, Cham (2014). <https://doi.org/10.1007/s10556-014-9818-9>

13. Elena, N.M.: A Cost model for integrated logistic support activities. *Adv. Oper. Res.* **2013**, 1–6 (2013)
14. Menshikov, V., Meshalkin, V., Obratsov, A.: Heuristic algorithms for 3D optimal chemical plant layout design. In: *Proceedings of 19th International Congress of Chemical and Process Engineering (CHISA-2010)*, vol. 4, pp. 1425, Prague (2010)
15. Kravets, A.G., Bolshakov, A.A., Shcherbakov, M.V.: *Cyber-Physical Systems: Industry 4.0 Challenges*, p. 334. Springer, Berlin (2019). <https://doi.org/10.1007/978-3-030-32648-7>
16. Lu, J., Zhu, Q., Wu, Q.: A novel data clustering algorithm using heuristic rules based on k-nearest neighbors' chain. *Eng. Appl. Artif. Intell.* **72**, 213–227 (2018)
17. Bertoni, M., Bertoni, A., Isaksson, O.: A value-driven concept selection method for early system design. *J. Syst. Sci. Syst. Eng.* **27**(1), 46–77 (2018)
18. Martin, P., Kolesár, J.: Logistic support and computer aided acquisition. *J. Logist. Manag.* **1**, 1–5 (2012)
19. Bogomolov, B.B., Bykov, E.D., Men'shikov, V.V., et al.: Organizational and technological modeling of chemical process systems. *Theor. Found. Chem. Eng.* **51**, 238–246 (2017). <https://doi.org/10.1134/S0040579517010043>
20. Marca, D.A.: SADT/IDEF0 for augmenting UML, agile and usability engineering methods. In: Escalona, M.J., Cordeiro, J., Shishkov, B. (eds.) *Software and Data Technologies. ICSoft 2011. Communications in Computer and Information Science*, vol. 303. Springer, Berlin, Heidelberg (2013)
21. Meshalkin, V.P., Moshev, E.R.: Modes of functioning of the automated system “Pipeline” with integrated logistical support of pipelines and vessels of industrial enterprises. *J. Mach. Manuf. Reliab.* **44**(7), 580–592 (2015)
22. Moshev, E. R., Meshalkin, V. P.: Computer-based logistics support system for the maintenance of chemical plant equipment. *Theor. Found. Chem. Eng.* **48**(6), 855–863 (2014)

# **New Materials Production for Cyber-Physical Systems**

# Analysis of the Efficiency of the Rotary Method for Producing a Mixture of Granular Raw Materials in the Preparation of a Cyber-Physical Platform



A. B. Kapranova , D. V. Stenko , D. D. Bahaeva , A. A. Vatagin, and A. E. Lebedev

**Abstract** The actual problem of creating rational methods for processing industrial waste includes the problem of mixing granular raw materials and can be successfully solved within the framework of a cyber-physical system. In this work, an analysis of the efficiency of the rotary method of obtaining a mixture from the indicated components is carried out using two rows of elastic rectangular blades fixed in one direction tangentially to the outer cylindrical surface of the mixing drum. The assessment of this efficiency was carried out taking into account the degree of overlapping of the intervals of variation of the peak values for the characteristic geometric parameters of the mixing process of the tested working materials. The data obtained using the energy method on the laws of particle distribution in the flows formed to connect the sets of input and output parameters of the technological process at the stage of preparing the cyber-physical platform.

**Keywords** Cyber-physical system · Rotary mixing · Granular raw materials · Mixture · Elastic blades · Modeling · Parameters

## 1 Introduction

An increase in the total volume of waste is a negative consequence of the accelerated development of the chemical industry, energy complexes, and construction industry facilities. The need to process significant flows of secondary raw materials, including of a technogenic nature [1], leads to the problem of finding new forms and methods of achieving energy and resource efficiency indicators. One of the types of secondary industrial raw materials is granular materials, the further use of which or their disposal

---

A. B. Kapranova (✉) · D. V. Stenko · D. D. Bahaeva · A. A. Vatagin · A. E. Lebedev  
Yaroslavl State Technical University, Moskovskiy Prospect, 88, Yaroslavl 150023, Russia

D. V. Stenko  
e-mail: [dvs3d@yandex.ru](mailto:dvs3d@yandex.ru)

A. A. Vatagin  
e-mail: [vatagerr@bk.ru](mailto:vatagerr@bk.ru)

© The Author(s), under exclusive license to Springer Nature Switzerland AG 2022  
A. G. Kravets et al. (eds.), *Cyber-Physical Systems: Modelling and Industrial Application*,  
Studies in Systems, Decision and Control 418,  
[https://doi.org/10.1007/978-3-030-95120-7\\_25](https://doi.org/10.1007/978-3-030-95120-7_25)

is often associated with preliminary high-quality mixing. Achievement of indicators of homogeneity [2, 3] of the resulting granular mixture, in this case, is considered a priority. Involvement of the principles of operation of cyber-physical systems makes it possible to successfully cope with such tasks [4]. At the same time, the preparatory stage of the formation of a cyber-physical platform requires the establishment of sufficiently complete sets of parameters that determine the information variables of the designed constructive solution for the technological process of mixing technogenic raw materials. For example, the composition of such mixtures for construction purposes [5] may include slag sand, as a product of combustion at thermal power plants (TPP) of fuel from solid materials [6, 7]. However, the lack of stability of the characteristic mechanical properties of these processed products leads to additional difficulties in obtaining the corresponding high-quality granular mixtures, free from the segregation effect [7] at a given routine granulometric composition [8].

The organization of a continuous mode of mixing granular materials in rarefied flows requires the fulfillment of some conditions for the technical characteristics of the apparatus, which include, for example, sets [3, 9, 10]:

- design parameters (geometric dimensions of the main mixing elements, working chamber);
- performance indicators (drum rotation frequency, heights of component layers, and the gap between the drum and the reference plane for the specified layers);
- characteristics of properties of mixed components and materials of construction (mechanical, physical).

The efficiency of using mixing elements in the form of elastic blades [11, 12] or brushes [2, 4, 13] of various shapes and methods of fixing on a rotating drum (external [2, 4, 12, 13] or internal [11] way) significantly depends on their design parameters [11], the dosing system [14]. The purpose of this work is to evaluate the efficiency of rotary mixing of granular materials by the degree of closeness of the ranges of variation of the extreme values of the angles characterizing the resulting fluxes of component particles, based on the corresponding stochastic model. In this case, the basic principles of the system-structural analysis of the process under study [15, 16] and the energy modeling method Yu were used. Klimontovich [17, 18] for the specified process of rotary mixing of granular raw materials at the stage of preparation of the corresponding cyber-physical platform.

## **2 Some Design Features of the Rotary Mixing Process of Granular Raw Materials**

At the stage of formation of a cyber-physical platform, a special role is played by information parameters [3] of the studied process of obtaining a free-flowing mixture, including from industrial waste [12]. Let us briefly dwell on the issue of some design features of the process of rotary mixing of granular raw materials, for example,

implemented in an apparatus with a moving belt [19] or in a working chamber with a cylindrical body for the specified mixing unit. In particular, mixing drums with resilient blades are used to form flows of free-flowing components in a rarefied state. These rectangular blades are fixed in two rows in the same direction tangentially to the outer cylindrical surface of this drum at equal angular intervals. The described rows of blades have the same number, while angular displacements of the rows concerning each other in the cross-sectional plane to the drum axis are observed. For further modeling, we denote the entire set of design parameters of the main mixing unit of the apparatus in the form of the following set  $\{A, B, X(t), Y(t)\} \equiv Z(t)$ , where  $A \equiv \{A_{k_1} = \overline{cont}\}$ ;  $B \equiv \{B_{k_2} = \overline{cont}\}$ ;  $X(t) \equiv \{X_1, X_2\} = \{X_i\}$ ;  $Y(t) \equiv \{V_C, X_i\}$ . Here, respectively, are indicated:  $A$ —parameters for the mixing unit of the structure ( $k_1 = \overline{1, s_1}$ );  $B$ —parameters for a given mode of continuous processing of granular raw materials ( $k_2 = \overline{1, s_2}$ );  $X(t)$ —input parameters for the component  $i = \overline{1, 2}$ ;  $Y(t)$ —output parameters at the required value of the coefficient of heterogeneity of the finished product  $V_C$ . Then the complete sets of the components of the set  $Z$  represent the view:

$$A = \{R_b, L_b, R_C, l_b, q_b, h_b, K_s, K_r, \varepsilon\}, B = \{H_0, H_{Li}, \omega\}, \quad (1)$$

$$X = \{C_{Vi}, Q_{Vi}\}, Y = \{V_C^{reg}, \Delta V_C, C_{Vi}, Q_{Vi}\}. \quad (2)$$

Expressions (1), (2) contain the notation:  $R_b, L_b$  are radius and length of the mixing drum;  $R_C$  is the characteristic size of the working chamber (for example, the width of the moving belt or the radius of the cylindrical body for the mixing drum);  $l_b, q_b, h_b$  are length, width, and height of a rectangular blade;  $K_s, K_r$  are number of elastic blades of each row and number of rows (let  $K_r = 2$ );  $\varepsilon$  is angular displacements for the  $K_r$  rows relative to each other in the cross-sectional plane to the drum axis; to the drum axis;  $H_0$  is the height of the gap between the drum and the support surface for the layers of granular raw materials;  $H_{Li}$  is the total height of the layer  $i$  at the entrance to the specified gap;  $\omega$  is the angular speed of rotation of the mixing element (drum);  $C_{Vi}$ —volume fractions of the mixed bulk components;  $Q_{Vi}$  is the value of the volumetric flow rate of the granular material  $i$ ;  $V_C^{reg}$  are regulations for assessing the quality of the mixture according to the criterion in the form of the coefficient of heterogeneity  $V_C$ ;  $\Delta V_C$  is the specified absolute error for the value  $V_C^{reg}$ .

Therefore, taking into account the fact that the resulting mixture is a two-component ( $i = \overline{1, 2}$ ) total number of information variables  $K_z = 19$ . Besides a special place among the factors affecting the nature of mixing of granular components is occupied by their physical and mechanical characteristics, for example, included in the set  $Q = \{D_i, \rho_i\}$ . Here are designated:  $D_i$  is particle diameters of the mixed granular raw materials ( $i = \overline{1, 2}$ );  $\rho_i$  is the density of the corresponding substances.

Note that when designing a mixing apparatus of a rotary type, the formation of an optimization problem for finding the corresponding optimal values of parameters

is multifactorial. However, when solving practical problems, it is often sufficient to identify rational intervals of change in the parameters of class  $Z$  based on mathematical modeling of the process under study, taking into account its most significant factors, which also require establishment.

### 3 Basic Provisions of Stochastic Modeling of the Process of Rotary Mixing of Granular Raw Materials

As already noted in the introduction, the basis for the design of a rotary apparatus for mixing granular raw materials is the modeling of the formation of flows of components in a rarefied state from the standpoint of the stochastic approach [20, 21]. The latter, among other things, includes many methods of a cybernetic nature [22], the use of time series [23, 24], and Markov [25] with some modifications [26–30].

Thus, there are all the prerequisites for applying the methodology of a cyber-physical system to the study of the specified random mixing process and the development of an engineering methodology for calculating its parameters. The level of control of the mixing process of granular raw materials (in the ratio of the volume fractions of the components  $C_{V1} : C_{V2}$ ) is achieved through a set of information variables  $Z$  due to feedback according to (1), (2). The latter is manifested, for example, in the form of comparative calculations of the predicted  $V_C$  and regulations  $V_C^{reg}$  values of the heterogeneity coefficient of the finished mixture. The feasibility of using a probabilistic description of the distribution pattern of particles of bulk materials in the resulting flows follows from the random nature of the specified mixing process. In this case, preference is given to the energy method of Klimontovich [17, 18], already tested for solving similar problems [2, 9, 13].

An attempt to simulate the process of mixing granular materials for a drum with a single-row set of elastic non-radial blades ( $K_r = 1$  can be extended to the cases of two-row ( $K_r = 2$ ) or multi-row mounting [12]. We use it in the second case, when  $K_r = 2$ .

The layers of the mixed components of granular raw materials ( $i = \overline{1, 2}$ ) after dosing and vertical loading, fall into the gap of the rotating drum and the supporting surface (for a moving belt or a coaxial cylindrical chamber). Then the particles from these layers interact with the elastic blades, detach from them and pass into a rarefied state, forming unidirectional flows of granular media.

Taking into account the randomness of the behavior of the set of particles of each component, it is assumed that the following provisions of the energy method are fulfilled [17, 18].

- The granular raw material to be processed has particles that are close in shape to spherical with a diameter  $D_i$ , equal to the average value for the available fractions.
- Due to the unidirectionality of the motion of these flows ( $i = \overline{1, 2}$ ) it is assumed that these macrosystems are free from macroscale fluctuations of their states.

- The behavior of the particles of these components corresponds to energetically closed macrosystems.

Then the description of the stationary case for the solution of the kinetic Fokker–Planck equation for a homogeneous, stationary random process by A. A. Markov is performed using phase variables ( $V_{xij}, V_{yij}$ ) or in polar coordinates ( $r_{ij}, \varphi_{ij}$ ).

Using the approximations adopted above and expressing the velocity of the center of mass of the particle of each component ( $i = \overline{1, 2}$ ) depending on the position of the endpoints of the elastic blades as they move along the Archimedes spiral, an expression is formed for the energy of stochastic motion of the particle  $E_{ij}(r_{ij}, \theta_{ij}, \cdot)$ . Note that the indicated dependence  $E_{ij}(r_{ij}, \theta_{ij}, \cdot)$  corresponds to an element of the phase volume  $d\Omega_{ij} = -\omega^2 r_{ij} dr_{ij} d\theta_{ij}$  and takes into account the set of parameters from expression (1):  $A$  for the mixing unit of the structure ( $k_1 = \overline{1, s_1}$ );  $B$  for a given mode of continuous processing of granular raw materials ( $k_2 = \overline{1, s_2}$ ). above equation for the Archimedes spiral  $r_{Aij}(\theta_{ij}) = \lambda_0 + \lambda_1 \theta_{ij}$  additionally takes into account the parameter  $H_0$  from the set (1) and the presence of the second row of blades ( $K_r = 2$ ). Here the coefficients  $\lambda_0, \lambda_1$  depend on the sets  $A, B$  from expressions (1):  $\lambda_0 = R_b(1 - \cos\varphi_0) + H_0$ ;  $\lambda_1 = \{([R_b(1 + \cos\varphi_0)]^2 + (R_b + l_b)^2)^{1/2} - \lambda_0 - H_0/3\}/\theta_\delta$ ;  $\varphi_\delta = \pi + \arctg\{(R_b + l_b)/[R_b(1 + \cos\varphi_0)]\}$ ;  $\varphi_0 = 2\pi/K_s$ . The general view of the energy of stochastic motion of a particle  $E_{ij}$  at  $i = \overline{1, 2}$  is given by the expression:

$$E_{ij} = a_i D_i \omega^2 [10s_{30} w_{ij}(\theta_{ij}) + D_i^2] w_{ij}(\theta_{ij}) + k_u \theta_{ij}^2 / 2 \tag{3}$$

where  $w_{ij}(\theta_{ij}) \equiv (\mu_0 + \mu_1 \theta_{ij})^4 / \{\mu_0^2 [(s_0 + s_1 \theta_{ij})^2 + s_{20}^2]\}$ ;  $a_i = \pi \rho_i / 12$ ;  $s_0 = \cos\{(1/2)\arctg[\lambda_1/\lambda_0]\}$ ;  $s_1 = (\lambda_1^2 / 2n_4) \sin\{(1/2)\arctg[\lambda_1/\lambda_0]\}$ ;  $n_4 = \lambda_0^2 + \lambda_1^2$ ;  $\mu_0 = n_0 + n_1$ ;  $n_0 = \lambda_0 \cos\{(3/2)\arctg[\lambda_1/\lambda_0]\}$ ;  $n_1 = (\lambda_0^2 - n_0^2 + R_b^2) / 2$ ;  $\mu_1 = \{3n_2 / (2\lambda_0^3) + n_0 n_4 \lambda_1 / \lambda_0 + \lambda_0^3 \lambda_1 [2n_4(n_0^2 - \lambda_0^2) + n_3] / (8n_1)\} / n_4$ ;  $n_3 = (3/2)\lambda_0 \lambda_1 \sin\{3\arctg[\lambda_1/\lambda_0]\}$ ;  $s_{20} = [s_0(1 - s_0)]^{1/2}$ ;  $s_{30} = (s_0^2 + s_{20}^2)^2$ ;  $n_2 = \lambda_1^2 \sin\{(3/2)\arctg[\lambda_1/\lambda_0]\}$ .

Differential distribution functions  $p_{ij}(\theta_{ij})$  for the number of particles  $N_{ij}$  in the flows of granular components after the operation of the mixing unit “drum-elastic blades” are obtained depending on the scattering angle  $\theta_{ij}$

$$p_{ij}(\theta_{ij}) = (1/N_{ij}) dN_{ij} / d\theta_{ij}, \tag{4}$$

$$P_i(\theta_{ij}) = \prod_{j=1}^{K_r} p_i(\theta_{ij}). \tag{5}$$

where the total distribution functions  $P_i(\theta_{ij})$  are determined by independent random processes of interaction of the particles of the mixed components with elastic blades of different rows located with angular displacements  $\varepsilon$ .



When finding  $p_{ij}(\theta_{ij})$  and  $P_i(\theta_{ij})$  following (4), (5), the following form of the stationary solution of the kinetic Fokker–Planck equation was used [17, 18]

$$f_{ij} = \alpha_{ij} \exp\left(-\frac{E_{ij}}{E_{0ij}}\right). \quad (6)$$

Here, the parameters  $\alpha_{ij}$  and  $E_{0ij}$  are determined, respectively, by the normalization operations and the energy balance at the stages of the capture of granular particles by the blades in the gap of the drum and their dispersion in the flows. The obtained analytical expressions for the functions  $p_{ij}(\theta_{ij})$  and  $P_i(\theta_{ij})$  are not presented due to their cumbersomeness.

## 4 Simulation Results

The results of the operation of the mixing unit with two rows of blades are illustrated by the example of obtaining a preliminary composition for a construction mixture from granular raw materials with two components (Figs. 1, 2 and 3): slag sand GOST 3344–83 ( $i = 1$ ;  $\rho_1 = 1.30 \times 10^3 \text{ kg/m}^3$ ;  $D_1 = 2.25 \times 10^{-4} \text{ m}$ ) and natural sand GOST 8736–93 ( $i = 2$ ;  $\rho_2 = 1.80 \times 10^3 \text{ kg/m}^3$ ;  $D_2 = 2.0 \times 10^{-4} \text{ m}$ ).

Analysis of the results allows us to identify the main factors that make the greatest contribution to the behavior of the sought functions  $p_{ij}(\theta_{ij})$  and  $P_i(\theta_{ij})$ . In particular, these include the following parameters of a rotary mixer: regime (angular velocity  $\omega$ ; the number of rows of blades  $K_r$ ; angular displacement of blades  $\varepsilon$ ). In this case, the complex design parameter is of particular importance (the degree of deformation of the blades is  $\delta = H_0/l_b$ ). As can be seen from the graphs (Figs. 1, 2 and 3), an important consequence of the studies carried out is the coincidence of the regions for the extreme values of the scattering angles of particles of both components. The specified picture of their distributions can be considered as the fulfillment of the condition of the efficiency of the designed apparatus for mixing granular raw materials.

This fact is observed for the differential distribution functions  $p_{ij}(\theta_{ij})$  of the number of particles  $N_{ij}$  in the flows of granular components after the operation of the mixing unit “drum-elastic blades” (for example, graphs 1, Fig. 1a and graphs 1, Fig. 1b). Similarly, for complete functions  $P_i(\theta_{ij})$ , including in Fig. 2b (graphs 2) and Fig. 3b (graphs 2). The use of rows of blades with an angular displacement  $\varepsilon$  makes it possible to orient the scattered stream of particles in a narrower area near the most probable angle of dispersion of the mixed granular components (in particular, graphs 1 and 3, Fig. 2c; graphs 1 and 3, Fig. 3c). The results of the study of the effectiveness of the rotary mixing process are part of the corresponding system-structural analysis of this technological operation.

It is shown that the presence of angular displacement ( $\varepsilon \neq 0$ ; graphs 2, 3; Fig. 2a–c and graphs 2, 3; Fig. 3a–c) for the second row of elastic blades in comparison with its absence ( $\varepsilon = 0$ ; graph 1; Fig. 2a–c and graph 1; Fig. 3a–c) decreases the likelihood of

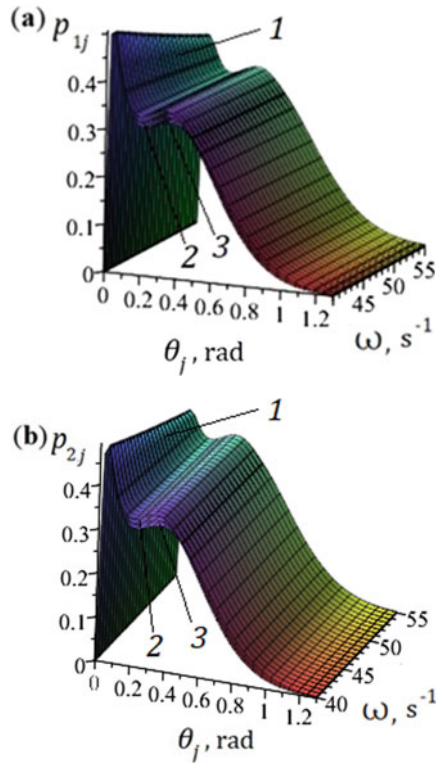


**Fig. 1** Dependence  $p_{ij}(\theta_{ij}, \omega)$ : **a** slag sand GOST 3344–83 ( $i = 1$ ); **b** natural sand GOST 8736–93 ( $i = 2$ );  $K_s = 8$ ;  $K_r = 2$ ;  $\delta = 0.67$ ;  $\varepsilon = 0$  (1);  $\varepsilon = 0.3927$  rad (2);  $\varepsilon = 0.5236$  rad (3)

additional dropping of granular particles from the surfaces of elastic elements during their gradual straightening. And the larger this angular displacement  $\varepsilon$ , the less the local maximum of the function  $P_i(\theta_{ij})$  becomes expressed. For example, an increase in the value of  $\varepsilon$  by 1.33 times leads to a decrease in the values of the function  $P_i(\theta_{ij})$  near the scattering angle region  $0.3 \text{ rad} \leq \theta_{ij} \leq 0.4 \text{ rad}$  by a factor of 1.04 for slag sand (graphs 2; Fig. 2b and graphs 2; Fig. 2c) and 1.07 times for natural sand (graphs 2; Fig. 3b and graphs 2; Fig. 3c).

However, an increase in the values of the degree of deformation of elastic blades ( $\delta = H_0/l_b$ ), on the contrary, leads to a more pronounced peak for the function  $P_i(\theta_{ij})$  within the scattering angle  $0.3 \text{ rad} \leq \theta_{ij} \leq 0.4 \text{ rad}$  (graphs 1, 3; Fig. 2a and graphs 1, 3; Fig. 3a). Here, against the background of a fall in the maximum value of  $P_i(\theta_{ij})$  by 1.68 times for slag sand (graphs 1, 3; Fig. 2a) and by 1.65 times for natural sand (graphs 1, 3; Fig. 3a), there is an increase in the local maximum of the function  $P_i(\theta_{ij})$  by 1.17 times and 1.14 times, respectively. The effect of changing the angular speed of rotation of the mixing drum on the behavior of the functions  $p_{ij}(\theta_{ij})$  can be traced using graphs 1–3; Fig. 1a and graphs 1–3; Fig. 1b. These descriptions will

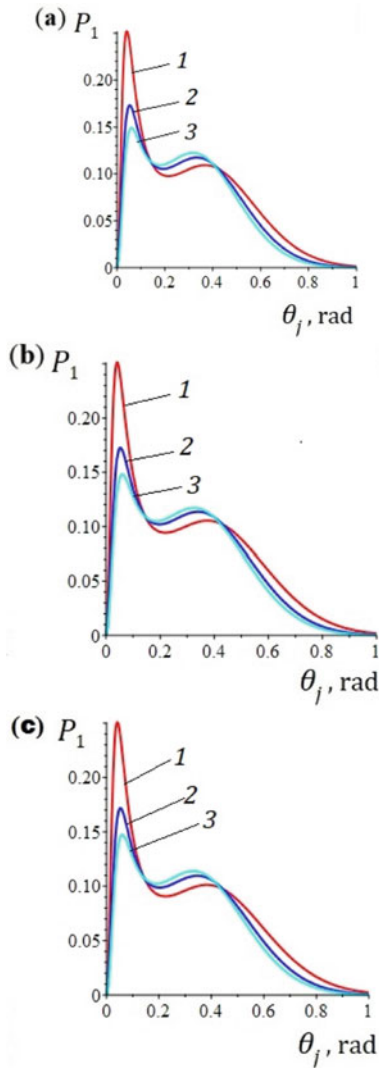


**Fig. 2** Dependence  $P_1(\theta_j, \omega)$  for slag sand GOST 3344-83 ( $i = 1$ ):  $K_s = 8$ ;  $K_r = 2$ ;  $\omega = 57.6 \text{ s}^{-1}$ ; **a**  $\varepsilon = 0$ ;  $1 - \delta = 0.60$ ;  $E_{011} = 1.34 \times 10^{-4} \text{ J}$ ;  $2 - \delta = 0.67$ ;  $E_{012} = 1.13 \times 10^{-4} \text{ J}$ ;  $3 - \delta = 0.70$ ;  $E_{012} = 1.04 \times 10^{-4} \text{ J}$ ; **b**  $\varepsilon = 0.3927 \text{ rad}$ ;  $1 - \delta = 0.60$ ;  $E_{011} = 1.45 \times 10^{-4} \text{ J}$ ;  $2 - \delta = 0.67$ ;  $E_{012} = 1.23 \times 10^{-4} \text{ J}$ ;  $3 - \delta = 0.70$ ;  $E_{012} = 1.16 \times 10^{-4} \text{ J}$ ; **c**  $\varepsilon = 0.5236 \text{ rad}$ ;  $1 - \delta = 0.60$ ;  $E_{011} = 1.58 \times 10^{-4} \text{ J}$ ;  $2 - \delta = 0.67$ ;  $E_{012} = 1.33 \times 10^{-4} \text{ J}$ ;  $3 - \delta = 0.70$ ;  $E_{012} = 1.23 \times 10^{-4} \text{ J}$

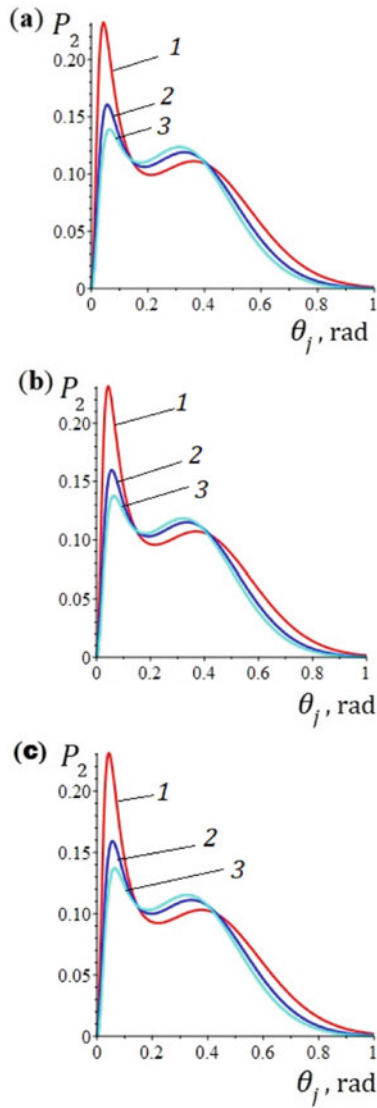


**Fig. 3** Dependence  $P_2(\theta_j, \omega)$  for natural sand GOST 8736–93 ( $i = 2$ ):  $K_s = 8$ ;  $K_r = 2$ ;  $\omega = 57.6 \text{ s}^{-1}$ ; **a**  $\varepsilon = 0$ ;  $1 - \delta = 0.60$ ;  $E_{011} = 1.30 \times 10^{-4} \text{ J}$ ;  $2 - \delta = 0.67$ ;  $E_{012} = 1.11 \times 10^{-4} \text{ J}$ ;  $3 - \delta = 0.70$ ;  $E_{012} = 1.03 \times 10^{-4} \text{ J}$ ; **b**  $\varepsilon = 0.3927 \text{ rad}$ ;  $1 - \delta = 0.60$ ;  $E_{011} = 1.41 \times 10^{-4} \text{ J}$ ;  $2 - \delta = 0.67$ ;  $E_{012} = 1.19 \times 10^{-4} \text{ J}$ ;  $3 - \delta = 0.70$ ;  $E_{012} = 1.12 \times 10^{-4} \text{ J}$ ; **c**  $\varepsilon = 0.5236 \text{ rad}$ ;  $1 - \delta = 0.60$ ;  $E_{011} = 1.54 \times 10^{-4} \text{ J}$ ;  $2 - \delta = 0.67$ ;  $E_{012} = 1.29 \times 10^{-4} \text{ J}$ ;  $3 - \delta = 0.70$ ;  $E_{012} = 1.19 \times 10^{-4} \text{ J}$

allow in the future; to analyze the achievement of the regulatory productivity of the process of mixing granular raw materials including taking into account the additional stage of impact mixing.

## 5 Conclusion

Thus, the process of mixing granular raw materials, including technogenic ones, using a rotary method using two rows of elastic rectangular blades is considered from the standpoint of preparing a cyber-physical platform. These elastic elements are fixed in one direction tangentially to the outer cylindrical surface of the mixing drum.

The formation of this platform corresponds to the choice of a set of information variables  $Z(t) \equiv \{A, B, X(t), Y(t)\}$ , which includes the process parameters: input  $X(t)$ , output  $Y(t)$ , constructive  $A$ , regime  $B$ . Note that the total number of these parameters as information variables is  $K_z = 19$ . Additional considered parameters are the characteristics of the physical and mechanical properties of working substances (mixed granular raw materials, elastic elements). The use of stochastic modeling made it possible to evaluate the efficiency of the rotary process of obtaining granular mixtures by the degree of closeness of the ranges of variation of the extreme values of the angles characterizing the resulting fluxes of the component particles.

In particular, when using the energy method, the following main conclusions and results were obtained.

- The significant operating parameters of the rotary mixer (angular velocity  $\omega$ ; the number of rows of blades  $K_r$ ; angular displacement of the blades  $\varepsilon$ ) and its complex design characteristic (the degree of deformation of the blades  $\delta$ ) have been established.
- The influence of these parameters on the distribution of particles in scattered flows in the working volume of a rotary apparatus using two rows of elastic rectangular blades has been analyzed.
- It has been shown that the use of two rows of blades with angular displacement allows to orient the scattered particle flux to a narrower area near the most probable angle of scattering of the mixed granular components.
- In the presence of an angular displacement of the location of the elastic blades, the probability of additional dropping of granular particles from the surfaces of elastic elements decreases when they are gradually straightened. For example, an increase in the value of  $\varepsilon$  by a factor of 1.33 leads to a decrease in the values of the function  $P_i(\theta_{ij})$  near the scattering angle region  $0.3 \text{ rad} \leq \theta_{ij} \leq 0.4 \text{ rad}$  within (1.04–1.07) times for the tested granular materials.
- At the same time, for the described test components of a construction mixture made from technogenic raw materials, there is an increase in the local maximum of the function  $P_i(\theta_{ij})$  by a factor of (1.14–1.17) with an increase in the values of the degree of deformation of elastic blades  $\delta$ .

## References

1. Yan, J., Bäverman, C., Moreno, L., Neretnieks, I.: The long-term acid neutralizing capacity of steel slag. *Stud. Environ. Sci.* **71**, 631–640 (1997). [https://doi.org/10.1016/S0166-1116\(97\)80246-4](https://doi.org/10.1016/S0166-1116(97)80246-4)
2. Kapranova, A.B., Bakin, M.N., Verloka, I.I.: Simulation of the quality criterion of a mixture in a drum-belt apparatus. *Chem. Pet. Eng.* **54**(5), 287–297 (2018). <https://doi.org/10.1007/s10556-018-0477-0>
3. Kapranova, A.B., Verloka, I.I., Yakovlev, P.A., Bahaeva, D.D.: Investigation of the quality of the mixture at the first stage of operation of a gravitational apparatus. *Russ. J. Gen. Chem.* **90**(6), 1178–1179 (2020). <https://doi.org/10.1134/S1070363220060341>
4. Kapranova, A.B., Verloka, I.I., Bahaeva, D.D.: About preparation of the analytical platform for creation of a cyber-physical system of industrial mixture of loose components. In: *Cyber-Physical Systems: Advances in Design & Modelling. Studies in Systems, Decision, and Control*, vol. 259, pp. 81–91 (2020). [https://doi.org/10.1007/978-3-030-32579-4\\_7](https://doi.org/10.1007/978-3-030-32579-4_7)
5. Zhang, H. (ed.): *Building Materials in Civil Engineering, Series: Woodhead Publishing Series in Civil and Structural Engineering* Published, 1st ed., p. 440. Elsevier (9th May 2011)
6. Shaul, S., Rabinovich, E., Kalman, H.: Generalized flow regime diagram of fluidized beds based on the height to bed diameter ratio. *Powder Technol.* **228**, 264–271 (2012). <https://doi.org/10.1016/j.powtec.2012.05.029>
7. Bauman, I., Curic, D., Boban, M.: Mixing of solids in different mixing devices. *Sadhana* **33**(6), 721–731 (2008). <https://doi.org/10.1007/s12046-008-0030-5> (Springer)
8. Makarov, Y.I.: *Devices for Mixing Bulk Materials*. 216 p. Mechanical Engineering, Moscow (1973)
9. Kapranova, A.B., Verloka, I.I., Bahaeva, D.D., Tarshis, M.Yu., Cherpitsky, S.N.: To the calculation of the average value of the volume fraction of the key bulk component at the intermediate stage of mixing with an inclined bump. *Front. Energy Res. Process Energy Syst.* **8**, 1–11 (07 August 2020). Article 135. <https://doi.org/10.3389/fenrg.2020.00135>
10. Zaslavskiy, V., Shved, S., Shepelenko, M., Suslo, N.: Modeling the horizontal movement of bulk material in the system “conveyor–rotary mixer”. In: *E3S Web Conference*, vol. 166, p. 06008 (2020). <https://doi.org/10.1051/e3sconf/202016606008>
11. Zeren, Z., Neau, H., Fede, P., Simonin, O., Bernard, D., Williams, S.: Numerical study of solid particle axial mixing in a fixed cylindrical drum with rotating paddles: modeling and simulation of reacting multiphase flows at industrial scales. In: *2012 AIChE Annual Meeting*, (28 October 2012–02 November 2012) (Pittsburgh, United States). [https://www.researchgate.net/publication/282212762\\_Numerical\\_study\\_of\\_solid\\_particle\\_axial\\_mixing\\_in\\_a\\_fixed\\_cylindrical\\_drum\\_with\\_rotating\\_paddles](https://www.researchgate.net/publication/282212762_Numerical_study_of_solid_particle_axial_mixing_in_a_fixed_cylindrical_drum_with_rotating_paddles)
12. Kapranova, A., Bahaeva, D., Stenko, D., Vatagin, A., Lebedev, A., Lichak, D.: Distribution of the components of the building mixture in the presence of secondary raw materials during rotary mixing. In: *E3s Web of Conference*, vol. 220, p. 01060 (16 December 2020). <https://doi.org/10.1051/e3sconf/202022001060>
13. Verloka, I., Kapranova, A., Tarshis, M., Cherpitsky, S.: Stochastic modeling of bulk components batch mixing process in gravity apparatus. *Int. J. Mech. Eng. Technol.* **9**(2), 438–444 (2018). Article ID: IJMET\_09\_02\_045. <http://www.iaeme.com/IJMET/issues.asp?JType=IJMET&VType=9&IType=2>
14. Zhang, L., Nie, G.Y.: ODS analysis on the rack of batching system mixer. *Appl. Mech. Mater.* **437**, 257–260 (2013). [0.4028/www.scientific.net/AMM.437.257](https://doi.org/10.4028/www.scientific.net/AMM.437.257)
15. Kafarov, V.V., Dorokhov, I.N., Arutyunov, S.Y.: *System Analysis of Processes of Chemical Engineering*, 440 p. Science, Moscow (1985)
16. Bogomolov, B., Boldyrev, V., Zubarev, A., Meshalkin, V., Men'shikov, V.: Intelligent logical information algorithm for choosing energy- and resource-efficient chemical technologies. *Theor. Found. Chem. Eng.* **53**(5), 709–718 (2019). <https://doi.org/10.1134/S0040579519050270>

17. Klimontovich, Y.L.: *Turbulent Motion and the Structure of Chaos: A New Approach to the Statistical Theory of Open Systems*, 328 p. LENAND, Moscow (2014)
18. Klimontovich, Y.L.: Turbulent motion and the structure of chaos. *Ser. Fund. Theor. Phys.* **42**, p. 401 (1991). <https://doi.org/10.1007/978-94-011-3426-2>
19. Lebedev, A.E., Vatagin, A.A., Borisovsky, M.E., Romanova, M.N., Badaeva, N.V., Sheronina, I.S.: *Utility Model Patent: 2624698 Russian Federation, B01F3/18. Unit for mixing and compaction of bulk materials* (2017)
20. Bharucha-Reid, A.T.: *Elements of the Theory of Markov Processes and Their Applications*. McGraw-Hill, New York (1960)
21. Röpke, G.: *Statistical Mechanics for Non-Equilibrium*. German Publishing House of Sciences, Berlin (1987)
22. Geng, T., Sau, L.L., Xiaochuan, Ya. Moo, S.H.: A dimensionless analysis of residence time distributions for continuous powder mixing. *Powder Technol.* **315**, 332–338 (2017). <https://doi.org/10.1016/j.powtec.2017.04.007>
23. Johnson, N., Kendal, L.M., Stuar, T.A.: *J. R. Stat. Soc. Ser. D (The Statistician)* **12**(2), 138 (1962)
24. Ghaderi, A.: Continuous mixing of particulate materials. In: *Proceedings of the 4th International Conference for Conveying and Handling of particulate solids, At Budapest, Hungary, vol. 2* (January 2003). <https://doi.org/10.13140/2.1.3487.6801>
25. Leonchik, B.I., Mayakin, V.P.: *Measurements in Dispersed Flows*. Energy, Moscow, 248 p. (1985)
26. Dehling, H.G., Gottschalk, T., Hoffmann, A.C.: *Stochastic Modeling in Process Technology*, 279 p. Elsevier Science, London (2007)
27. Mizonov, V., Balagurov, I., Berthiaux, H., Gatumel, C.: Gatumel Markov chain model of mixing kinetics for a ternary mixture of dissimilar particulate solids. *Particuology* **31**, 80–86 (2016). <https://doi.org/10.1016/j.partic.2016.05.006>
28. Akhmadiev, F.G., Gizzyatov, R.F.: Modeling of separation of granular materials on multiple-deck classifiers using the theory of stochastic processes. *Theor. Found. Chem. Eng.* **52**(3), 360–370 (2018)
29. Zhuang, Y., Chen, X., Liu, D.: Stochastic bubble developing model combined with Markov process of particles for bubbling fluidized beds. *Chem. Eng. J.* **291**, 206–214 (2016) <https://doi.org/10.1016/j.cej.2016.01.095>
30. Zhukov, V.P., Belyakov, A.N.: Simulation of combined heterogeneous processes based on discrete models of the Boltzmann equation. *Theor. Found. Chem. Eng.* **51**(1), 88–93 (2017). <https://doi.org/10.1134/S0040579517010158> (Springer)

# Optimization of Ingredients of a Polymeric Composition Under the Conditions of a Paired Interaction of Active Additives



I. V. Germashev, E. F. Feoktistov, E. V. Derbisher, and V. E. Derbisher

**Abstract** The main aspects of the use of polymer composite materials are considered. The urgency of the task of developing methods for assessing properties and controlling them by ranking the concentrations of the polymer matrix's tenants has been substantiated. The main methods for studying polymer compositions are presented, their systematization is considered according to the principle of controlling properties at different stages of material synthesis. The problem of optimization of the composition of the polymer composition is proposed. The solution is based on a mathematical model that describes the manifestation of both individual properties of the polymer composition and pair interactions of ingredients. Not only the positive but also the negative influence of the ingredients on the entire composition of the polymer matrix is taken into account. A mathematical model has been built for a fuzzy criterion of consumer requirements for the final product under the conditions of known interactions of the components of the composition. The model is presented and solved as a quadratic programming problem using a specific example. Various cut-off values for the content of the ingredients have been used. The analyzed results obtained illustrate the dependence of the properties of a chemical system on the concentration of specific ingredients.

**Keywords** Optimization · Composite materials · Fuzzy criterion · Mathematical model · Quadratic programming

---

I. V. Germashev (✉) · E. F. Feoktistov  
Volgograd State University, 100, Universitetsky Avenue, Volgograd 400062, Russia  
e-mail: [germashev@volsu.ru](mailto:germashev@volsu.ru)

E. V. Derbisher · V. E. Derbisher  
Volgograd State Technical University, 28, Lenin Avenue, Volgograd 400006, Russia  
e-mail: [derbisher2@vstu.ru](mailto:derbisher2@vstu.ru)



## 1 Introduction

Composite materials (composites) are complex multicomponent systems. The creation and synthesis of new compositions have been constantly growing in recent years due to the requirements and requests of technical industries. Identification and management of certain properties is a multi-criteria task that is solved using experimental, mathematical, and quantum-chemical methods [1]. The use of polymers as modern materials is due to a complex of unique physicochemical and physicochemical properties, which are a consequence of the chain structure of macromolecules. As an example, one can cite high elasticity moduli, flexibility, reversible deformations at high temperatures, viscosity, the ability to convert chemical energy into mechanical energy, and so on.

Products made of composite polymer materials, especially structural ones, are widely used in various industries: construction, mechanical engineering, space and aviation technology, radio electronics, etc. many factors. These factors are often difficult to take into account since the very nature and properties of the polymer matrix can interact with an active and passive filler, which is added in order to obtain certain properties, their amount, and functionality, as well as parameters for controlling technological operations.

The advancement of new synthesized materials and substances to the technological market is complicated by the fact that the physicochemical and other properties of polymer compositions depend on the above factors. Today, the creation of new materials and the assessment of the reliability of products made from them requires, along with a preliminary experiment, a theoretical analysis of the deformation-strength and other operational characteristics, an assessment of the reliability of structures with a further transition to theoretical tests, as well as the study of the possibility of using mathematical tools and methods for modeling compositions and shortening the path from design to technology. In this regard, the theoretical analysis of polymers by constructing mathematical models and identifying the properties of materials is relevant.

The most widespread polymers were synthesized more than half a century ago, now more and more works are being done to optimize the properties of already known materials. Of course, work is underway on new ones as well. In this regard, one of the most important tasks is to determine the properties of chemical systems in solving various problems. Sometimes it is suggested to conduct property management experimentally, which often requires expensive equipment, a complex and materially expensive technical process. Nowadays, the approaches that use mathematical and informational methods and computational chemistry to predict the properties of polymer composite materials are important [2–4].

Here one cannot do without laws linking the structure of a material with its physical and chemical properties. However, the nature of this connection in most cases is not clear and this forces researchers to delve deeper into the establishment of the relationship “structure–property”. The description of the behavior of composite materials as deformable multicomponent and multifactorial solids with a complex

structure, the determination of effective chemical and physical–mechanical characteristics is one of the trends of the present time. Therefore, polymer materials science has moved to a qualitatively new way of development—the use of highly intelligent methods, including mathematical and information technologies, in particular, solving problems of identification. Here, the research tool is the methods of system analysis, mathematical, and information modeling. And given the similarity of the models of the structure of materials of natural and artificial origin from the point of view of the chemical composition and the degree of ordering in the structure of the polymer, we can talk about the prospects for describing natural phenomena.

Materials obtained on the basis of polymer composites also fall into this circle, being extremely complex heterogeneous systems, which, according to processing technology and structural features, can be divided in accordance with the prevailing views on approximately the following groups:

- fiber-filled;
- dispersedly filled;
- with interpenetrating structures of continuous phases;
- mixed;
- volumetric (“3D”);
- layered (“2D”).

The creation of polymers takes place in several stages, and at each of these stages, it is possible to change their properties. In some works, the “structure–property” approach is used, in which the predicted properties of the polymer composition are simulated by the structure of the monomer [5]. Neural networks are often used at this stage of control. This technology is used to search for relationships between the properties of chemical systems and their structures. Among the methods, the generalized Widrow-Hoff delta rule and the flexible propagation method are distinguished [6]. The use of a feedforward multilayer neural network, which is trained by the backpropagation method [7], is widely used. Using this method in polymer compositions, for example, the autoignition temperature, viscosity and density are studied [8].

Modern developments in the field of materials science cannot do without nanocomposites—multicomponent materials, for example, consisting of a plastic polymer base and a filler—organomodified nanoclay [9]. Nanocomposites have improved properties as compared to conventional polymers; therefore, the problem of identifying these properties is now especially urgent [10–12]. For example, the model of thermal conductivity of polymers, developed in different approximations, which makes it possible to evaluate various properties using a system of linear and differential equations, has become widespread. This effect is achieved by reinforcing nanocomposites with carbon nanotubes [13].

Then the stage of controlling the properties during polymerization is distinguished [14–16]. Most of the works are devoted to the determination of properties during free polymerization. In the process of polymerization, mathematical modeling is used to describe, for example, the kinetics or the effect of other substances on the chemical system as a whole [17].

The development of computational approaches aimed at studying the addition of large radicals and the effect of chain length led to the study of copolymer systems. Computational methods for studying the copolymerization reaction were first applied in the early 2000s. The first computational experiments with a copolymer system date back to the same time. As a result, the kinetics of propagation reactions involved in the free polymerization process was modeled. Since then, free polymerization has been described by the fundamental equations of the terminal model and the model of the penultimate unit [18].

In addition, with the help of active and passive additives, the properties of polymer compositions are also controlled [19–21, 24, 25]. This is one of the most common approaches in modern scientific literature. However, in this case, almost no mathematical methods are used. So, for example, the methods of quantum chemistry, if used in this approach, are often used to calculate the results of polymerization when controlling certain of its characteristics, but not to calculate the interaction of active additives.

Particular attention should be paid to integrated approaches to assessing the properties of composite materials. These approaches include preliminary processing of the material using methods for analyzing the effect of structure on properties, then mathematical and computational support of the polymer synthesis process, and, finally, evaluation of the results and the possibility of further processing of the finished polymer with active and passive additives. This is followed by the optimization of the ingredients of the entire polymer matrix, taking into account the chemical interactions of the ingredients and their positive and negative influence on the properties. The formation of the main task of optimizing the composition of the polymer composition and its solution is based on the platform of dependence “composition—property—quality—application” and provides for the selection of a certain number of ingredients with the necessary technical functions, often using fuzzy modeling. However, such an integrated approach has not yet been developed and seems to be extremely promising. Improving the quality of the material, reducing the cost of production, and spreading the use of polymers is just a small part of the advantages that such an approach can provide.

Mathematical modeling of the interaction of chemical structures based on several polymer matrices is rarely covered. More often, one polymer matrix is presented as the analyzed system, in which the processes of interaction of monomers and ingredients within it are studied. The development of quantum-chemical methods for the analysis of a more complex system, consisting of several high-molecular compounds, is still an unexplored field for experiments, both empirical and analytical methods. This approach can help in synthesizing new properties, new materials, predicting interaction processes, and a more detailed study of the chemical properties of the system as a whole.

The planning of ingredients to obtain the required characteristics of the target composite and the identification of the properties of a complex composite system are problems that still do not have an acceptable solution. Quite often, the complexity of chemical systems is described by fuzzy mathematics. This is due, for example, to the absence or uncertainty of data, a huge number of possible different formulations

of compositions, conflicting opinions of experts, and linguistic descriptions of data. All this leads to a multitude of particular solutions and the absence of a universal model [22, 23].

In addition to the influence of individual components on the properties of the polymer composition of interest, it is necessary to take into account the complex systemic interactions of the entire composition as a whole. At this stage, it is proposed to adopt a coarser, approximate model, in which we restrict ourselves to the interaction between the various components of a given chemical system, in particular, pair interaction. Similar models have already been built and used to solve other problems [22].

This chapter formulates the problem of optimizing the set of ingredients and additives to obtain the required properties of the polymer composition. Moreover, the constructed model takes into account paired interactions between all additives and ingredients.

## 2 Problem Statement

The identification of the properties of a composite polymer material today can be carried out on three sites: empirical, semi-empirical, and non-empirical. The last two require mathematical modeling.

Since it is often possible to speak only about the final properties of a polymer composition, many important details of the very process of building a chemical system are usually unknown: how additives and ingredients interacted with each other in the synthesis process, the functions of each of the ingredients and its properties can be different manifest itself in different polymer compositions, the function of the influence of each ingredient on the composition depends not only on its concentration in the substance but also on other factors, etc.

Most of these data can only be obtained experimentally, however, conducting such a number of experiments for a deep understanding of this subject area is impossible in a conceivable short period of time and for acceptable means. Here there is a need for preliminary, at least approximate, modeling.

So, consider the following problem.

Let polymer P be given. P is a polymer matrix not including additives and ingredients. P has a basic set of properties  $Q_1, \dots, Q_m$ , where  $m$  is the number of properties of the polymer P. The values of the manifestation of these properties are set through  $x_1, \dots, x_m$ , respectively.

As for  $s_1, \dots, s_n$ , we denote the ingredients that, together with the polymer matrix P, form the polymer composition C. Ingredients  $s_1, \dots, s_n$  have a concentration of  $c_1, \dots, c_n$ .

The general research problem is the need to find such values of  $c_1, \dots, c_n$ , which provide an optimal set of properties  $Q_1, \dots, Q_m$ .

Within the framework of this work, we solve a narrower problem: optimizing the composition, we determine the concentration  $c_1, \dots, c_n$ , of additives and ingredients for the greatest manifestation of one specific property  $Q_j$ , where  $j$ —is a fixed value, and in the future, we will consider one property  $Q_j$ .

### 3 Mathematical Model

Let us introduce the following notation.

Let  $x_j$  be the manifestation of the  $Q_j$  property of the polymer P. After the polymer is modified with additives  $s_{i_1}$  and  $s_{i_2}$ , the manifestation of the  $Q_j$  property will change. To reflect such a change, we introduce the coefficient  $a_{i_1 i_2 j}$  of the pairing effect of additives:

$$a_{i_1 i_2 j} = \frac{x_{i_1 i_2 j}}{x_j}$$

where  $x_{i_1 i_2 j}$  is the manifestation of the property  $Q_j$  of the composition after introduction into the polymer. In this case, the coefficient  $a_{i_1 i_2 j}$  takes values from 0 to 1, if the property  $Q_j$  worsens, while improving the values will be greater than 1. But to solve the proposed problem, it is necessary that when the property deteriorates, there are negative values, and when the property improves, they are positive. To do this, we introduce the reduced coefficient  $q_{i_1 i_2 j}$ , which will take positive values when the property improves and negative values when it deteriorates:

$$q_{i_1 i_2 j} = a_{i_1 i_2 j} - 1$$

General manifestation of the property  $Q_j$  of the entire composition, after the introduction of all the ingredients, we denote as  $x'_j$ . For  $x'_j$  we also introduce the reduced coefficient  $q_j$ , reflecting the effect of the entire complex of additives on the property  $Q_j$ .

$$q_j = \frac{x'_j}{x_j} - 1$$

To estimate the value of  $q_j$ , it is proposed to use a fuzzy value  $\hat{q}_j$ , which is calculated on the basis of a complex of paired effects of additives on the polymer. The details of calculating  $\hat{q}_j$  are given in [3], where it is proposed to use the fuzzy value:

$$\hat{q}_j(x_j) = \exp\left(-\frac{(x_j - \tilde{q}_j)}{\delta_j^2} \ln 2\right),$$

where  $\tilde{q}_j = \frac{\bar{q}_j + q_j}{2}$ ,  $\delta_j = \frac{\bar{q}_j - q_j}{2}$ ,  $\bar{q}_j = \sum_{i_1=1}^n \sum_{i_2=i_1+1}^n q_{i_1 i_2 j}$ , and  $q_j = \frac{1}{n} \sum_{i_1=1}^n \sum_{i_2=i_1+1}^n q_{i_1 i_2 j}$ .

Each additive has its own concentration in the overall composition system. Moreover, in formulations, the concentration of substances is often set not by an exact value, but by a range, therefore it makes sense to introduce a fuzzy  $\hat{c}_i$ , which means the concentration of the ingredient  $s_i$ . At the same time, we add to the model the ability to control the maximum and minimum content of ingredients using fuzzy values: by  $\hat{p}_i^{\min}$  we denote the minimum possible content of  $s_i$ ; by  $\hat{p}_i^{\max}$  we denote the maximum possible content of  $s_i$ ; by  $\hat{p}$  we denote the maximum total content of all additives, i.e.

$$\sum_{i=1}^n \hat{c}_i \leq \hat{p}, \hat{c}_i \leq \hat{p}_i^{\max}, \hat{c}_i \geq \hat{p}_i^{\min}, i = \overline{1, n} \tag{1}$$

These restrictions allow you to adjust the following ratios. An excessive increase in the content of additives can lead to a negligible content of the polymer matrix, which, in principle, will change the formulation of the problem and, therefore, is unacceptable.

The second limitation allows you to stop the increase in the content of the additive, for example, if a further increase in concentration leads to too weak an effect or for other reasons. When solving certain consumer problems, the content of any additive in the composition may seem important. This condition is tracked by the third constraint.

By varying the concentration  $\hat{c}_i$  it is possible to manage the manifestation  $\hat{q}_j$  of property  $Q_j$  of the polymer composition, which is described by the following relationship:

$$\hat{q}_j = -\frac{1}{2} \hat{c}^T D \hat{c} + l^T \hat{c}$$

where the elements of the matrix  $D = (d_{i_1 i_2})$  show the specific (per concentration unit) interaction of the pair of additives  $s_{i_1}$  and  $s_{i_2}$ , and the elements of the vector  $l = (l_i)$  show the specific effect of the additive  $s_i$  on the manifestation of the property  $Q_j$ .

Thus, we get a fuzzy programming problem.

$$r(\hat{c}) = -\frac{1}{2} \hat{c}^T D \hat{c} + l^T \hat{c} \rightarrow \max_{\hat{c}}$$

subject to constraints (1). We will assume that the matrix  $D$  and vector  $l$  are given.

## 4 Computational Experiment

To solve the problem, defuzzification was carried out to pass to the quadratic programming problem. As a result, we have obtained the following quadratic programming problem

$$r(c) = -\frac{1}{2}c^T Dc + l^T c \rightarrow \max_c,$$

where  $c$  is the vector of de-fuzzified concentration values of the corresponding additives.

Take the following matrix  $D$

$$D = \begin{pmatrix} 1 & 0.5 & 0.75 & 0 \\ 0.5 & 0.5 & 1.3 & 0.6 \\ 0.75 & 1.3 & 1.5 & 0.85 \\ 0 & 0.6 & 0.85 & 1.05 \end{pmatrix},$$

and as for  $l$  the following:

$$l = (0.25; 1.25; 0.375; 0.5).$$

First, let us assume that the total share of all ingredients is small, and imagine that it is limited to 30%, that is,  $\hat{p} = 0.3$ . Each ingredient will have an upper and lower bound

$$\hat{p}_i^{\max} = 0.2 \text{ and } \hat{p}_i^{\min} = 0.001.$$

Solving the resulting quadratic programming problem, we obtain the following results for the optimal concentration of ingredients:

$$c^* = (0.19; 0.001; 0.001; 0.09)^T, \quad r(c^*) = 0.107$$

Thus, the best effect will be achieved by adding 19% of the first and 9% of the fourth, respectively.

However, at low concentrations, some active additives are not able to fully manifest their positive effect, therefore, in order to continue the experiment, the possible boundary values should be increased.

Let us assume that the total share of all ingredients is limited to  $\hat{p} = 0.7$ . Each active additive also has the boundary values  $\hat{p}_i^{\max} = 0.5$  and  $\hat{p}_i^{\min} = 0.001$ .

Solving the same quadratic programming problem, we get:

$$c^* = (0.21; 0.001; 0.175; 0.298)^T, \quad r(c^*) = 0.3322$$

Thus, the best effect will be achieved by adding 21% of the first, 17.5% of the third, and 29.8% of the fourth, respectively. The level  $r(c)$  of the beneficial effect of the additives increased by about 3 times.

From this computational experiment, it follows that for the adopted matrix  $D$ , a high concentration of additives, in particular the third additive, which exhibits properties only with an increase in the proportion of the content in the total composition, will be more optimal. However, such an increase does not always bring a positive result. It should be borne in mind that too high a concentration of one or another ingredient can entail negative consequences of exposure to the entire polymer matrix, for example, breaking chemical bonds, causing a reaction with another element, or simply stopping a positive effect on the properties of the composition. These factors are not taken into account in the proposed model but can be added if necessary. These modifications can be considered as one of the directions of the model's development.

## 5 Conclusion

The use of mathematical models and methods of quantum chemistry makes it possible to predict various properties of the polymer, the time and conditions of its polymerization, and the structure after interaction with additives and fillers. Often, such calculations are accompanied by an experiment that can immediately show the relevance and accuracy of the model or method. However, it is not possible to check empirically more often due to the high cost of equipment, complexity, energy consumption of the process, or its long periods.

Today, polymer compositions are an integral component of a promising direction for the use of nanocomposites and hybrid nanomaterials. Further development of the scientific and technological principles of nanochemistry and nanotechnology opens up great opportunities for expanding the areas of the practical application of polymer systems. The ability to synthesize high-performance products, however, requires more detailed modeling and elaboration of the model presented in this chapter.

In view of the wide variability of the polymers themselves and their properties, it is rather difficult to single out a unified system for determining the best method or model for assessing the properties and pair interactions of elements of the chemical structure. Even similar theoretical structure–property approaches use rather different models and methods.

With the help of this model, it is possible to solve both the direct problem of assessing the specified properties of the polymer composition and the reverse, the selection of the optimal composition of the ingredients. But there are two important points in the proposed model that require a quite significant improvement.

First, the values of the matrix  $D$  and the vector  $l$  are usually unknown. It is possible to obtain them experimentally, or to calculate them, for example, using the methods of quantum chemistry or machine learning based on known recipes.



Secondly, the consumer is interested not in just one, even a very important, property, but in a whole complex of properties that reflects all the requirements for the final product. Therefore, it is necessary for the future in the model to take into account the multicriteria nature of this problem.

This information will further allow formalizing the initial data of the subject area by means of mathematical modeling, when, upon receiving an order from the consumer, a set of requirements for the composite material is automatically generated, and then the assessments of compliance with the formed requirements for specific candidates for the components of the polymer composition are calculated. Then the technical aspect of the composition of the chemical structure is worked out, which ensures the high quality of the material obtained. The model presented here is given as a possible prospect for the development of the applied use of mathematical modeling tools in technological production processes in order to improve the synthesis of new materials, optimize their composition, and, accordingly, properties. Further development will take into account the economic, environmental, and many other aspects of the development of polymer composite materials.

## References

1. Bobryshev, A.N., Yerofeev, V.T., Kozomazov, V.N.: *Polymernie Compositsonnie Materialy: Ucheb. Posobie* (Polymer composite materials: textbook). ASV, Moscow (In Russian) (2013)
2. Wang, G.: Modelling of thermal transport through a nanocellular polymer foam toward the generation of a new superinsulating material. *Nanoscale* **9**, 5996–6009 (2017)
3. Rentería-Baltierrez, F.Y., Reyes-Melo, M.E., Puente-Córdova, J.G., López-Walle B.: Correlation between the mechanical and dielectric responses in polymer films by a fractional calculus approach. *Appl. Polym.* **138**(7) (2021)
4. Grigoriev, I.V.: Chislennoe issledovanie processa polimerizatsii butadiena metodami matematicheskogo modelirovaniya (Numerical study of the butadiene polymerization process by methods of mathematical modeling). Paper presented at *Differentsialnie Uravneniya I Smezhnye Problemi* (Differential Equations and Related Problems), Bashkir State University, Sterlitamak, June 25–29 (2018)
5. Morita, A., Matsuba, G., Fujimoto, M.: Evaluation of hydrophilic cellulose nanofiber dispersions in a hydrophobic isotactic polypropylene composite. *Appl. Polym.* **138**(8) (2021)
6. Patnaik, L.M., Rajan, K.: Target detection through image processing and resilient propagation algorithms. *Neurocomputing* **35**(1–4), 123–125 (2000)
7. Zhang, J., et al.: Inferential estimation of polymer quality using stacked neural networks. *Comput. Chem. Eng.* **21**, S1025–S1030 (1997)
8. Gakh, A.A., Gakh, E.G., Sumpter, B.G., Noid, D.W.: Neural network-graph theory approach to the prediction of the physical properties of organic compounds. *J. Chem. Inf. Comput. Sci.* **34**(4), 832–839 (1994)
9. Brzakański, D., Przekop, R.E., Dobrosielska, M., Sztorch, B., Marciniak, P., Marciniak, B.: Highly bulky spherosilicates as functional additives for polyethylene processing—Influence on mechanical and thermal properties. *Polym. Compos.* **41**, 3389–3402 (2020)
10. Abbasi, H., Antunes, M., Velasco, J.I.: Enhancing the electrical conductivity of polyetherimide-based foams by simultaneously increasing the porosity and graphene nanoplatelets dispersion. *Polym. Compos.* **40**, E1416–E1425 (2019)

11. Bouknaitir, I., Panniello, A., Teixeira, S.S., Kreit, L., Corricelli, M., Striccoli, M., Costa, L.C., Achour, M.E.: Optical and dielectric properties of PMMA (poly(methyl methacrylate))/carbon dots composites. *Polym. Compos.* **40**, E1312–E1319 (2019)
12. Jiang, J., Mei, C., Pan, M., Cao, J.: Improved mechanical properties and hydrophobicity on wood flour reinforced composites: incorporation of silica/montmorillonite nanoparticles in polymers. *Polym. Compos.* **41**, 1090–1099 (2020)
13. Zare, Y., Rhee, K.Y.: Advancement of a model for electrical conductivity of polymer nanocomposites reinforced with carbon nanotubes by a known model for thermal conductivity. *Eng. Comput.* **2020**, 1–11 (2020)
14. Goli, E., et al.: Frontal polymerization of unidirectional carbon-fiber-reinforced composites. *Compos. Part A. Appl. Sci. Manuf.* **130**, 105689 (2020)
15. De Keer, L., et al.: Benchmarking stochastic and deterministic kinetic modeling of bulk and solution radical polymerization processes by including six types of factors two. *Macromol. Theory Simul.* **29**(6), 2000065 (2020)
16. López-Domínguez, P., Clemente-Montes, D.A., Vivaldo-Lima, E.: Modeling of reversible deactivation radical polymerization of vinyl monomers promoted by redox initiation using NHPI and Xanthone. *Macromol. React. Eng.* **14**(6), 2000020 (2020)
17. Wendel, R., et al.: Anionic polymerization of  $\epsilon$ -caprolactam under the influence of water: 2. Kinetic model. *J. Compos. Sci.* **4**(1), 8 (2020)
18. Mavrouidakis, E., Cuccato, D., Moscatelli, D.: On the use of quantum chemistry for the determination of propagation, copolymerization, and secondary reaction kinetics in free radical polymerization. *Polymers* **7**, 1789–1819 (2015)
19. Akgul, Y., Ahlatci, H., Turan, M.E., Simsir, H., Erden, M.E., Sun, Y., Kilic, A.: Mechanical, tribological, and biological properties of carbon fiber/hydroxyapatite reinforced hybrid composites. *Polym. Compos.* **41**, 2426–2432 (2020)
20. Wu, M.C., et al.: Polymer additives for morphology control in high-performance lead-reduced perovskite solar cells. *Solar RRL* **4**(6), 2000093 (2020)
21. Chen, Q., et al.: Thermal management of polymer electrolyte membrane fuel cells: A review of cooling methods, material properties, and durability. *Appl. Energy* **286**, 116496 (2021)
22. Germashev, I.V., Derbisher, E.V., Derbisher, V.E., Mashihina, T.P.: Model of paired and solitary influence of ingredients of polymer composition. *Stud. Syst. Decis. Control* **342**, 205–217 (2021)
23. Derbisher, E.V., Derbisher, V.E.: Application of computational methods for the creation and selection of polymer compositions with specified properties. *Matematicheskaya Fizika I Kompyuternoe Modelirovanie (Mathematical Physics and Computer Modeling)* **1**(22), 35–53. (In Russian) (2019)
24. Germashev, I.V., Derbisher, V.E., Orlova, S.A.: Evaluation of activity of the fireproofing compounds in elastomer compositions by means of fuzzy sets. *Kauchuk i Rezina* **6**, 15–17. (In Russian) (2001)
25. Germashev, I.V., Derbisher, V.E., Vasil'ev, P.M.: Prediction of the activity of low-molecular organics in polymer compounds using probabilistic methods. *Theor. Found. Chem. Eng.* **32**(5), 514–517 (1998)

# Mathematical Model of the Heat Transfer Process in Multilayer Fencing Structures



Fail Akhmadiev , Renat Gizzyatov , and Ilshat Nazipov 

**Abstract** The process of non-stationary heat transfer through multilayer building envelopes is considered based on the heat conduction equation with asymmetric boundary conditions of the third kind and with an unknown indoor air temperature. Heat transfer coefficients on the inner and outer surfaces of the building envelope in the boundary conditions are calculated taking into account radiation and convection. In this case, natural convection is considered near the inner surface of the fence, caused by the difference in air and surface temperatures. At the outer surface of the fence, forced convection is considered, which is determined by the action of the wind. The influence of radiant heat transfer on the heat transfer coefficient on the inner and outer surfaces of the enclosing structure is determined based on the Stefan-Boltzmann law. To determine the temperature change inside the room, which is the basis for the choice of materials for the enclosing structures, the Cauchy problem is considered. To solve the problem, numerical methods were used; in the process of its numerical solution, an analysis of the stability of the constructed design scheme was carried out. The process of non-stationary heat transfer through multilayer structures depends on a large number of different factors, parameters and, therefore, to control the temperature regime inside the room, it must be considered as a cyber-physical system. Based on computer modeling, the modes of the process of unsteady heat transfer through various multilayer enclosing structures, which is a large and complex distributed system, are studied, i.e. cyber-physical system.

**Keywords** Mathematical modeling · Non-stationary heat transfer · Enclosing structures · Large systems · Computer modeling · Cyber-physical systems

---

F. Akhmadiev (✉) · R. Gizzyatov · I. Nazipov  
Kazan State University of Architecture and Engineering, 1 Zelenaya, Kazan 420043, Russia  
e-mail: [akhmadiev@kgasu.ru](mailto:akhmadiev@kgasu.ru)

I. Nazipov  
e-mail: [nilshat@inbox.ru](mailto:nilshat@inbox.ru)

© The Author(s), under exclusive license to Springer Nature Switzerland AG 2022  
A. G. Kravets et al. (eds.), *Cyber-Physical Systems: Modelling and Industrial Application*,  
Studies in Systems, Decision and Control 418,  
[https://doi.org/10.1007/978-3-030-95120-7\\_27](https://doi.org/10.1007/978-3-030-95120-7_27)

323

## 1 Introduction

Numerous theoretical and experimental works are devoted to the study of heat transfer processes in enclosing structures, in products with multilayer coatings of various functional purposes, for example, [1–8]. Despite the obvious achievements in the field of quantitative description of these processes, which was facilitated by the development of mathematical modeling and the widespread use of computer technology, their modeling, taking into account the mutual influence of a large number of different factors, the emergence of new materials for fencing and material costs is insufficiently studied for construction and related industries. Studies of heat transfer processes are currently being intensively continued both by experimental and theoretical methods, for example, [1, 2, 6, 8].

Obtaining accurate analytical solutions for non-stationary heat conduction problems for multilayer enclosing structures with different thermophysical properties of fencing materials causes certain difficulties associated with the need to fulfill the conjugation conditions in the form of equality of temperatures and heat fluxes. Such solutions are represented by infinite series, including the Bessel functions, and when passing through the discontinuity points, they make a jump and converge poorly in the initial period. Theoretically, the exact solution turns out to be approximate, therefore, in practice, they are of little use for engineering calculations.

Approximate methods are also used to study thermal processes in multilayer enclosing structures, for example, [4, 9, 10]. In this case, for small values of the time variable in orthogonal methods, it is necessary to write down a large number of terms of the series, which leads to a system of algebraic equations of large dimension for the eigenvalues of the boundary value problem. The accuracy of their solution may be insufficient.

For the numerical solution of equations with discontinuous coefficients, special through-counting schemes have also been developed that use information about the position of the breakpoints, for example, the balance method or the integro-interpolation method [11]. Reducing heat loss in a multilayer enclosing structure, selecting the optimal design option, taking into account its cost, as well as other economic indicators, in particular, energy consumption for heating buildings is an urgent task. The heat transfer process is strongly influenced by changes in weather conditions, i.e. the process is non-stationary. It becomes necessary to solve the non-stationary heat conduction equation with discontinuous coefficients and conjugation conditions at the interfaces with the subsequent formulation and solution of some optimization problems to select the appropriate materials for the fence. The solution is further complicated by the fact that the indoor air temperature is an unknown quantity that must be determined at each step of the calculations from the solution of the corresponding Cauchy problem. Thus, the heat transfer process can be considered a cyber-physical system. At the same time, the key in the cyber-physical system is a mathematical model of the heat transfer process, which allows you to control the temperature conditions inside the room and select the materials for the enclosing structures.

The aim of the work is the mathematical modeling of the process of non-stationary heat transfer through multilayer enclosing structures and conducting a computational experiment for the subsequent selection of the optimal version of the enclosing structure and process control taking into account non-stationary thermal conditions inside the room.

## 2 Mathematical Modeling

The process of unsteady heat transfer through multilayer enclosing structures is considered, taking into account the thermophysical characteristics of the materials used for each layer, which is described by the generalized one-dimensional unsteady heat conduction equation [5]:

$$c(x) \cdot \rho(x) \frac{\partial T}{\partial t} = \frac{\partial}{\partial x} \left( \lambda(x) \frac{\partial T}{\partial x} \right) \pm j_F c_B \frac{\partial T}{\partial x} + P_T, \quad 0 \leq x \leq \delta,$$

where

$$c(x) \cdot \rho(x) = \begin{cases} c_1 \rho_1, \\ c_2 \rho_2, \\ \dots \\ c_m \rho_m, \end{cases} \quad \lambda(x) = \begin{cases} \lambda_1, & 0 \leq x < \delta_1, \\ \lambda_2, & \delta_1 \leq x < \delta_2, \\ \dots & \dots \\ \lambda_m, & \delta_{m-1} \leq x \leq \delta_m, \end{cases} \quad (1)$$

$c_k, \rho_k, \lambda_k$ —accordingly, the specific heat capacity, density, thermal conductivity of the material of the  $k$ -th layer of the fence;  $\delta_k$ —distance from the outer surface of the fence to the end of the  $k$ -th layer,  $k = \overline{1, m}$ ;  $\delta = \delta_k$ —fence thickness;  $m$ —number of layers;  $P_T$ —specific power of heat sources in the fence;  $c_B$ —specific heat of air;  $j_F$ —filtered air flow through the unit of the enclosure surface. In Eq. (1), the  $\pm j_F c_B \frac{\partial T}{\partial x}$  term takes into account the convective heat transfer due to air filtration, which occurs, as a rule, in winter through an external fence. Thermophysical characteristics of fencing materials do not depend on temperature and are constant within the layer.

For an enclosure with a heat source of the “heating cable” type, the specific power of the source can be calculated on the assumption that it is a point source, using the formula:  $P_T = \delta(x - x_p)P(t)$ , where  $\delta(x - x_p)$  is the Dirac delta function;  $x_p$  is the distance from the outer surface of the enclosure to the plane of the source location;  $P(t)$  is the power of the source.

To study the processes of heat transfer through the building envelope, Eq. (1) is considered under boundary conditions of the third kind, which set the law of heat transfer with the environment:

$$-\lambda_1 \frac{\partial T}{\partial x} = \alpha_O (T_O - T_{OS}), \quad x = 0; \quad -\lambda_m \frac{\partial T}{\partial x} = \alpha_I (T_{IS} - T_I), \quad x = \delta, \quad (2)$$

where  $\alpha_O, \alpha_I$ —respectively, the coefficients of heat transfer from the outer and inner surfaces of the fence;  $T_O, T_I$ —outside and inside air temperatures;  $T_{OS}, T_{IS}$ —temperatures of the outer and inner surfaces of the fence. The initial temperature values for Eq. (1) can be determined from the solution of the stationary problem at fixed values of  $T_O$  and  $T_I$  at the initial moment of time.

To simplify the problem being solved, the process of heat transfer in multilayer enclosing structures will be considered without taking into account the heat source and air filtration. Taking them into account presents no mathematical difficulties. Then the thermal regime of the building can be described by the model:

$$c(x) \cdot \rho(x) \frac{\partial T}{\partial t} = \frac{\partial}{\partial x} \left( \lambda(x) \frac{\partial T}{\partial x} \right), \quad 0 \leq x \leq \delta, \quad (3)$$

$$T(x, 0) = T^0(x), \quad 0 \leq x \leq \delta, \quad (4)$$

$$-\lambda_1 \frac{\partial T}{\partial x} = \alpha_O(T_O(t) - T(0, t)), \quad -\lambda_m \frac{\partial T}{\partial x} = \alpha_I(T(\delta, t) - T_I(t)), \quad (5)$$

$$\lim_{\varepsilon \rightarrow 0} [T(\delta_j - \varepsilon, t) = T(\delta_j + \varepsilon, t)], \quad (6)$$

$$\lim_{\varepsilon \rightarrow 0} [\lambda_j \frac{\partial T(\delta_j - \varepsilon, t)}{\partial x} = \lambda_{j+1} \frac{\partial T(\delta_j + \varepsilon, t)}{\partial x}], \quad j = \overline{1, m-1}, \quad (7)$$

$$c_B m_B \frac{dT_I(t)}{dt} = -\alpha_I S_F (T_I(t) - T(\delta, t)) - \alpha_W S_W (T_I(t) - T_O(t)), \quad (8)$$

$$T_I(0) = T_I^0, \quad (9)$$

where  $S_F$  and  $S_W$  are the areas of the inner surface of the enclosure and the windows of the room,  $m_B$  is the air mass in the room,  $\alpha_W$  is the heat transfer coefficient of the windows. Problem (3)–(9) is solved taking into account the conjugation conditions at the interface (joint) of the enclosing structures (6) and (7), specified in the form of equality of temperatures and heat fluxes. Equation (8) describes the change in indoor air temperature over time, depending on the temperature of the inner surface of the fence and heat transfer through the windows of the room. In each specific case, it is necessary to determine your own law of changes in the temperature inside the room over time (Eq. (8)), since in real conditions the change in the air temperature inside the room will depend not only on the inertial capacity of the outer wall but also on the design features of the room itself [6]. Here, the  $T_O(t)$  function sets the change in the ambient temperature depending on weather conditions. In real conditions, linear, sinusoidal, cyclic, and other laws of change in external temperature can be used for this.

The heat transfer coefficients on the internal ( $\alpha_I = \alpha_{IR} + \alpha_{IC}$ ) and external ( $\alpha_E = \alpha_{ER} + \alpha_{EC}$ ) surfaces of the enclosing structure in Formulas (5) and (8) are

determined taking into account radiation and convection. The heat transfer coefficient by radiation on the inner surface of the fence is determined on the basis of the Stefan-Boltzmann law [7, 12–14]:  $\alpha_{IR} = \varepsilon \cdot c_0 \cdot \theta$ , where  $c_0$  is the emissivity of a blackbody,  $\varepsilon$  is the relative emissivity of the surface. In this case, the temperature coefficient on the inner surface of the fence, taking into account the non-stationarity of the thermal process, can be determined by the expression:

$$\theta(t) = \left[ \left( \frac{T_I(t) + 273}{100} \right)^4 - \left( \frac{T(\delta, t) + 273}{100} \right)^4 \right] / (T_I(t) - T(\delta, t))$$

Heat transfer by radiation on the outer surface of the enclosing structure is determined not only by the thermal radiation emitted by the surface of the enclosing structure itself. It also depends on the daily change in solar radiation falling on the surface of the fence, its geographical coordinates of the location, its orientation to the cardinal points, the time of day, weather conditions, and a number of other factors [15]. Under the influence of solar radiation in the daytime, an overheated area of the air environment is formed near the outer surface of the fence, and at night—a supercooled area. All these processes affect the thermal regime of the building. The coefficient of radiant heat transfer on the outer surface of the  $\alpha_{ER}$  fence is determined similarly to the coefficient on its inner surface based on the Stefan-Boltzmann law. In this case, the influence of solar radiation on the thermal regime of the building is taken into account by an increase in the outside air temperature  $T_O(t)$  by an amount equivalent to solar irradiation. Simplifying assumptions made in the simulation of radiant heat transfer on the surface of the fence are formulated in [5]. Calculations of this coefficient for some practical cases are given, for example, in [1, 7].

Difficulties associated with determining the amount of heat transferred by convective heat transfer are in calculating the heat transfer coefficients at the surfaces of the fence. Based on the generalization of experimental data and using the similarity theory, criterion equations are obtained for solving specific practical problems [7, 13]. At the inner surface of the fence, natural convection is considered, caused by the temperature difference between the air and the surface. At the outer surface of the fence, forced convection takes place, which is mainly determined by the action of the wind.

The intensity of the natural convective flow in a generalized form is determined by the product of the Grashof criteria  $Gr$  and Prandtl  $Pr$  [13]. Indoors, natural heat exchange occurs mainly in a laminar air flow at the surface of the fence [12, 13]. From the criterion expression  $Nu = 0,356(Gr)^{0,25}$ , which determines the intensity of heat transfer by convection for the value of the criterion  $Pr = 0,709$ , the coefficient of heat transfer by convection  $\alpha_{IC} = Nu \cdot \lambda_a / \ell$  on the inner surface is determined by the expression [12]:  $\alpha_{IC} = 1,39 \cdot (\Delta t / \ell)^{0,25}$ , where  $Nu$  is the Nusselt criterion;  $\lambda_a$ —coefficient of thermal conductivity of air, determined depending on the arithmetic mean temperature of air and surface;  $\Delta t$  is the temperature difference between the internal air and the surface of the fence;  $\ell$  is the defining size of the surface in the direction of air flow.

Heat transfer by convection in the interaction of a building with the environment is a complex task. The process of unsteady heat transfer is considered as a complex cyber-physical system. The direction of the wind, the shape, and the location of the building form rather complex flows near the surface along with the height of the building. Therefore, the distribution of air temperature along the height of the fence is uneven. On the outer surface of the fence, convection heat transfer occurs mainly due to the wind blowing over the surface. In engineering calculations, the wind speed is determined from the reference material [13, 16]. The heat transfer coefficient  $\alpha_{EC} = Nu \cdot \lambda_a / \ell$  on the outer surface of the enclosure for forced convection is determined at the value of the Nusselt criterion  $Nu = 0,032Re^{0,8}$  [13], where  $Re = v_0 \cdot \ell / \nu$  is the Reynolds criterion;  $v_0$  is the wind speed;  $\nu$ —coefficient of kinematic viscosity of air;  $\ell$  is the defining size of the surface in the direction of the wind. To calculate the coefficient, the empirical formula proposed by Frank is often used:  $\alpha_{EC} = 7,34 \cdot v_0^{0,656} + 3,78 \cdot \exp(-1,91 \cdot v_0)$ , as well as other empirical formulas, for example,  $\alpha_{EC} = 5,9 \cdot v_0^{0,8} / \ell^{0,2}$ , which are given, for example, in the reference material [13]. The calculation of the heat transfer coefficient by convection  $\alpha_{EC}$  for some practical cases is given, for example, in [1]. In engineering calculations for a stationary heat transfer mode for external surfaces in direct contact with the outside air, the value of the heat transfer coefficient is taken as  $\alpha_E = 23 \text{ W}/(\text{m}^2 \cdot \text{C}^0)$  [13]. All the above dependences and the calculation algorithm for determining the coefficients  $\alpha_I$  and  $\alpha_E$  in the mathematical model (3)–(9) were subsequently used in its numerical implementation.

For the numerical solution of problem (3)–(5), an implicit difference scheme was constructed based on the law of conservation of energy balance for a cell [11]. On each partial segment  $[\delta_{j-1}; \delta_j]$ , where  $j = \overline{1, m}$  and  $\delta_0 = 0$ , a uniform grid of nodal points with a step  $h_j = (\delta_j - \delta_{j-1}) / m_j$  is constructed, where  $m_j$  is the number of partitions of the  $j$ -th segment. Thus, a piecewise-uniform grid of nodal points is considered on the segment  $[0; \delta]$ . Then two grids are introduced:  $S_1$  with nodes  $(x_i; t_k)$ - the main grid and  $S_2$  with nodes  $(x_{i+1/2}; t_k)$ —auxiliary grid. In this case, the temperature is determined at the nodes of the main mesh  $S_1$ , and heat fluxes—at the nodes of the auxiliary mesh  $S_2$ .

Integration of Eq. (3) over the difference cell leads to the expression:

$$\int_{x_{i-1/2}}^{x_{i+1/2}} \int_{t_k}^{t_{k+1}} \left[ \rho(x) \cdot c(x) \frac{\partial T}{\partial t} \right] dt dx = - \int_{t_k}^{t_{k+1}} \int_{x_{i-1/2}}^{x_{i+1/2}} \left[ \frac{\partial Q}{\partial x} \right] dx dt \tag{10}$$

where  $Q(x, t) = -\lambda(x) \frac{\partial T(x, t)}{\partial x}$  is the heat flow. For each elementary cell of the grid, a balance equation is written, which contains integrals of the flow function and its derivatives along the cell boundaries. This makes it possible to take into account the conjugation conditions (6) and (7) at the joints of the layers of multilayer enclosing structures. In this case, the approximation of the discontinuous coefficients is carried out on the basis of integral averaging.

Calculation of the integrals gives:



$$\int_{x_{i-1/2}}^{x_{i+1/2}} [\rho(x) \cdot c(x)[T(x, t_{k+1}) - T(x, t_k)]] dx = \int_{t_k}^{t_{k+1}} [Q(x_{i+1/2}, t) - Q(x_{i-1/2}, t)] dt \tag{11}$$

Expression (11) is the energy conservation law written for the different cell. The heat conduction equation is obtained by calculating the heat balance over a certain interval  $[x_{i-1/2}; x_{i+1/2}]$  for a certain period of time  $[t_k; t_{k+1}]$ . Equation (11) is the heat conduction equation in integral form.

To solve Eq. (11), some approximations are carried out. Let  $T(x, t_k) = T_i^k$  at values  $x \in [x_{i-1/2}; x_{i+1/2}]$ , and the value of the flow  $Q(x_{i-1/2}, t)$  at each interval  $[t_k; t_{k+1}]$  is represented as:

$$Q(x_{i-1/2}, t) = \gamma \cdot Q(x_{i-1/2}, t_{k+1}) + (1 - \gamma) \cdot Q(x_{i-1/2}, t_k), \text{ where } 0 \leq \gamma \leq 1. \tag{12}$$

The introduction of an additional parameter  $\gamma$  allows one to control the properties of the difference scheme, but this leads to implicit difference equations.

Further, on the segment  $[x_{i-1}; x_i]$ , the heat flux is expressed through the temperature in the form:

$$Q(x_{i-1/2}, t) = -\bar{\lambda}_i \frac{T(x_i, t) - T(x_{i-1}, t)}{h_i}, \text{ where } h_i = x_i - x_{i-1} \text{ и } \bar{\lambda}_i = \left[ \frac{1}{2} \left( \frac{1}{\lambda_i} + \frac{1}{\lambda_{i-1}} \right) \right]^{-1}.$$

The designations are introduced:  $\tau = t_{k+1} - t_k$  and  $r_i = x_{i+1/2} - x_{i-1/2}$ . Since on the segment,  $[0; \delta]$  a piecewise-uniform mesh of nodal points is considered, and the dimensions of the layers of the enclosing structures in width can differ greatly. Consequently, at the joints of the  $h_i \neq r_i$  fence and if this is not taken into account, then additional errors may arise. Then Eq. (11), taking into account dependencies (12), is written in the form:

$$\begin{aligned} & \rho_i \cdot c_i (T_i^{k+1} - T_i^k) \cdot r_i \\ & = - \left[ \int_{t_k}^{t_{k+1}} \gamma \cdot (Q_{i+1/2}^{k+1} - Q_{i-1/2}^{k+1}) dt + \int_{t_k}^{t_{k+1}} (1 - \gamma) \cdot (Q_{i+1/2}^k - Q_{i-1/2}^k) dt \right] \end{aligned} \tag{13}$$

Taking into account dependencies (12), to determine the heat flux at the nodes of the auxiliary grid, we can write the relations

$$\begin{aligned} Q_{i-1/2}^k &= -\bar{\lambda}_i \cdot \frac{T_i^k - T_{i-1}^k}{h_i}, & Q_{i-1/2}^{k+1} &= -\bar{\lambda}_i \cdot \frac{T_i^{k+1} - T_{i-1}^{k+1}}{h_i}, \\ Q_{i+1/2}^k &= -\bar{\lambda}_{i+1} \cdot \frac{T_{i+1}^k - T_i^k}{h_{i+1}}, & Q_{i+1/2}^{k+1} &= -\bar{\lambda}_{i+1} \cdot \frac{T_{i+1}^{k+1} - T_i^{k+1}}{h_{i+1}}. \end{aligned} \tag{14}$$

Knowing the temperature distribution at time  $t_k$  and taking into account dependencies (14), to calculate the temperature distribution in multilayer enclosing structures at the time  $t_{k+1}$ , we can write a difference scheme, which, depending on the value of the parameter  $\gamma$ , can have both explicit and implicit forms:

$$\rho_i \cdot c_i \frac{T_i^{k+1} - T_i^k}{\tau} = \gamma \cdot \left[ \frac{\lambda_{i+1} T_{i+1}^{k+1} - T_i^{k+1}}{h_{i+1} \cdot r_i} - \frac{\lambda_i T_i^{k+1} - T_{i-1}^{k+1}}{h_i \cdot r_i} \right] + (1 - \gamma) \cdot \left[ \frac{\lambda_{i+1} T_{i+1}^k - T_i^k}{h_{i+1} \cdot r_i} - \frac{\lambda_i T_i^k - T_{i-1}^k}{h_i \cdot r_i} \right] \tag{15}$$

where  $i = \overline{1, n - 1}$  are internal nodal points. The missing equations are determined from the boundary conditions (5).

Next, a finite-difference analog of the heat balance of the enclosure is constructed at  $x_0 = 0$  and  $x_n = \delta$ , i.e. the boundary conditions are approximated (5).

The amount of heat in the section  $[x_0; x_{1/2}]$  is determined from the equation:

$$\int_{x_0}^{x_{1/2}} \frac{\partial T(x,t)}{\partial x} dx = - \int_{x_0}^{x_{1/2}} \frac{Q(x,t)}{\lambda_1(x)} dx, \text{ the solution of which gives } Q_o^{k+1} = -\lambda_1 \frac{T_1^{k+1} - T_0^{k+1}}{h_1}.$$

Thus, the left boundary condition (5) at the point  $x_0 = 0$  is approximated in the form:

$$\left( \frac{\lambda_1}{h_1} + \alpha_E \right) \cdot T_0^{k+1} - \frac{\lambda_1}{h_1} \cdot T_1^{k+1} = \alpha_E \cdot T_O(t_{k+1}) \tag{16}$$

An approximation of the right boundary condition (5) at a point  $x_n = \delta$  gives:

$$-\frac{\lambda_m}{h_n} \cdot T_{n-1}^{k+1} + \left( \frac{\lambda_m}{h_n} + \alpha_I \right) \cdot T_n^{k+1} = \alpha_I \cdot T_I(t_{k+1}) \tag{17}$$

The different system of Eqs. (15)–(17) with respect to the temperature values at the nodal points can be written:

$$A_i \cdot T_{i-1}^{k+1} + B_i \cdot T_i^{k+1} + C_i \cdot T_{i+1}^{k+1} = D_i, \quad i = \overline{0, n}, \tag{18}$$

where  $A_0 = 0, B_0 = \frac{\lambda_1}{h_1} + \alpha_E, C_0 = -\frac{\lambda_1}{h_1}, D_0 = \alpha_E \cdot T_O(t_{k+1}),$

$$A_i = -\gamma \frac{\overline{\lambda_i} \cdot \tau}{\rho_i \cdot c_i \cdot h_i \cdot r_i}, B_i = 1 + \gamma \cdot \left( \frac{\overline{\lambda_{i+1}}}{h_{i+1}} + \frac{\overline{\lambda_i}}{h_i} \right) \frac{\tau}{\rho_i \cdot c_i \cdot r_i}, C_i = -\gamma \frac{\overline{\lambda_{i+1}} \cdot \tau}{\rho_i \cdot c_i \cdot h_{i+1} \cdot r_i},$$

$$D_i = T_i^k + (1 - \gamma) \left[ \frac{\overline{\lambda_{i+1}} \cdot \tau}{\rho_i \cdot c_i \cdot h_{i+1} \cdot r_i} (T_{i+1}^k - T_i^k) - \frac{\overline{\lambda_i} \cdot \tau}{\rho_i \cdot c_i \cdot h_i \cdot r_i} (T_i^k - T_{i-1}^k) \right], i = \overline{1, n - 1},$$

$$A_n = -\frac{\lambda_m}{h_n}, B_n = \frac{\lambda_m}{h_n} + \alpha_I, C_n = 0, D_n = \alpha_I \cdot T_I(t_{k+1}).$$

The matrix of coefficients of the system (11) has a three-diagonal view and the sweep method is used to solve it. For the numerical solution of system (11), it is necessary to set the initial temperature distribution and the values of the temperatures of the outside and inside air at the moment of time  $t_{k+1}$ , if the temperatures of the outside and inside air at the moment of the beginning of observation  $T_O(0)$  and  $T_I(0)$  are known. The value of the outdoor air temperature at any time is considered to be known depending on weather conditions, and the indoor air temperature  $T_I(t)$  at each discrete time is determined from the solution of problem (8)–(9).

The first approximation of the temperature of the internal air  $T_I(t_{k+1})$  at the moment of time  $t = t_{k+1}$ , where  $k = 0, 1, \dots$  is determined from the solution of problem (8) and (9), taking into account the value of the temperature at the inner boundary at the previous moment of time  $T(\delta, t_k)$ . At the same time, in the calculations, the value of the coefficient  $\alpha_I$ , found at temperature  $T_I(t_k)$ , is used. Then two problems are successively solved: the non-stationary heat transfer problem (3)–(5) and the Cauchy problem (8) and (9). In this case, from the solution of the non-stationary heat transfer problem (3)–(5), the temperature value at the inner boundary of the  $T(\delta, t_{k+1})$  is determined, and from the solution of the problem (8) and (9) the temperature of the  $T_I(t_{k+1})$  is determined. The value of the coefficient  $\alpha_I$  before each new stage of calculations is refined using the value of the air temperature found in the previous stage. Further, the entire process of solving the non-stationary problem (3)–(5) is repeated with a new value of the internal air temperature  $T_I(t_{k+1})_i$  until the temperature value on the inner surface of the fence stops changing within the accuracy of  $|T(\delta, t_{k+1})_{i+1} - T(\delta, t_{k+1})_i| < \varepsilon_0$  interest to us, where epsilon is the specified accuracy of the solution of the problem,  $T(\delta, t_{k+1})_i$ ,  $T_I(t_{k+1})_i$ —respectively, the values of temperatures on the inner surface of the fence and internal air at the  $i$ -th iteration at a time  $t = t_{k+1}$ .

The initial temperature distribution  $T_i^0$  at the nodal points is determined from the solution of the stationary problem (the notation  $T(x, 0) = T(x)$  is adopted):

$$\frac{d}{dx} \left( \lambda(x) \frac{dT(x)}{dx} \right) = 0, \tag{19}$$

$$-\lambda_1 \frac{dT}{dx} = \alpha_E(T_O(0) - T(0)), \quad -\lambda_m \frac{dT}{dx} = \alpha_I(T(\delta) - T_I(0)). \tag{20}$$

Taking into account the expression for the heat flow  $Q(x) = -\lambda(x) \frac{dT(x)}{dx}$ , Eq. (1) in Chap. 12 after integration on the segment  $[x_{i-1/2}; x_{i+1/2}]$  can be written as:

$$\int_{x_{i-1/2}}^{x_{i+1/2}} \left[ \frac{dQ(x)}{dx} \right] dx = Q(x_{i+1/2}) - Q(x_{i-1/2}) = 0.$$

The last equation shows that in the stationary mode for a multilayer wall, the heat flux passing through the layers of the fence is the same. Further, the heat flux is expressed through the temperature as well as for the non-stationary case:  $Q_{i-1/2} =$

$\overline{\lambda}_i \frac{T_i - T_{i-1}}{h_i}$ . As a result, to determine the temperature value at the grid nodes, a system of linear algebraic equations is obtained:  $\overline{\lambda}_i T_{i-1} - \left( \frac{\overline{\lambda}_i}{h_i} + \frac{\overline{\lambda}_{i+1}}{h_{i+1}} \right) \cdot T_i + \overline{\lambda}_{i+1} T_{i+1} = 0$ ,  $i = \overline{1, n - 1}$ .

The missing two equations are determined from boundary conditions (20) in the same way as for the non-stationary case:

$$\begin{aligned} \left( \frac{\lambda_1}{h_1} + \alpha_E \right) \cdot T_0 - \frac{\lambda_1}{h_1} \cdot T_1 &= \alpha_E \cdot T_O(0) \text{ and} \\ - \frac{\lambda_m}{h_n} \cdot T_{n-1} + \left( \frac{\lambda_m}{h_n} + \alpha_I \right) \cdot T_n &= \alpha_I \cdot T_I(0). \end{aligned}$$

The resulting system for determining the temperature distribution in the fence in a stationary mode is solved by the sweep method.

For the numerical implementation of the constructed mathematical model, a corresponding software package was developed. In the process of numerically solving problems (3)–(9) and (19) and (20), an analysis of the stability of the constructed difference scheme was carried out. These questions are considered quite full, for example, in works [11, 17–21]. For the implicit scheme, with the value of the parameter  $\gamma$  in the interval  $1/2 \leq \gamma \leq 1$ , the stability of the system of obtained Eqs. (15)–(17) is provided under the condition  $\beta > 0$ , where  $\beta = (p \cdot \tau)/(h \cdot r)$  is  $p = \max_i \lambda_i/(\rho_i \cdot c_i)$ ,  $h = \min_i h_i$ ,  $r = \min_i r_i$ . The implicit scheme approximation error is proportional to  $\tau$  and  $h \cdot r$ . The study of the convergence of the solution of the difference problem was checked by changing the step of approximation of the derivatives and by analyzing the stability of the difference scheme [17, 18].

### 3 Results and Discussion

Based on the constructed mathematical model and its numerical solution, a computational experiment was carried out for several variants of multilayer enclosing structures (Table 1).

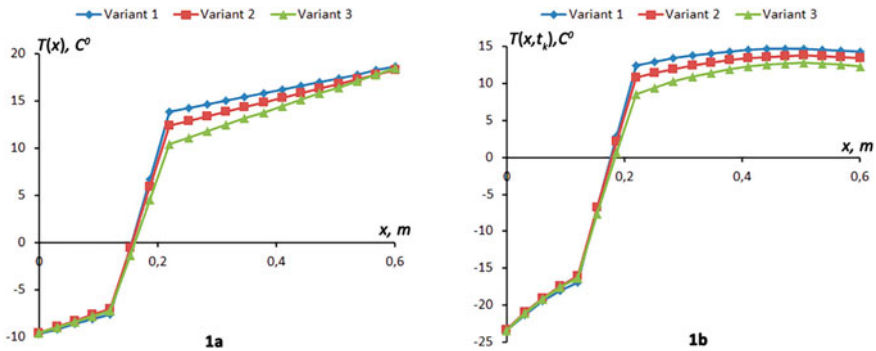
The results of a computational experiment in a particular case are consistent with the results of experimental studies of other authors and correspond to a real process, for example, [6].

Figure 1 shows the temperature distribution over the wall thickness of the enclosing structures before the start of the thermal process and 24 h after its start with a decrease in the outside air temperature according to a linear law, and Fig. 2 shows how, under these conditions, the air temperature inside changes over time premises.

In real conditions, the change in the air temperature inside the room depends not only on the temperature on the inner surface of the wall but also on the internal structures of the premises, in particular, on the area of the windows in the room, on their heat transfer coefficients. Therefore, in each specific case, it is necessary to

**Table 1** Thermophysical characteristics of materials of enclosing constructions

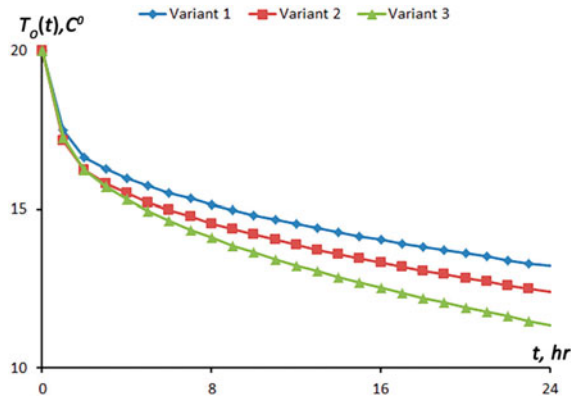
Layer material	Layer thickness $\delta$ , m	Density $\rho$ , kg/m <sup>3</sup>	Thermal conductivity $\lambda$ , W/(m,C <sup>0</sup> )	Specific heat C, J/(kg · C <sup>0</sup> )
<i>Variant 1</i> ( $R = 3.45 \text{ m}^2 \cdot \text{C}^0/\text{W}$ )				
Facing brick	0.12	1350	0.47	880
Basalt insulation	0.10	120	0.038	880
Full-bodied red brick	0.38	1800	0.65	880
Cement-sand mortar	0.02	1700	0.87	840
<i>Variant 2</i> ( $R = 3.15 \text{ m}^2 \cdot \text{C}^0/\text{W}$ )				
Facing brick	0.12	1350	0.47	880
Basalt insulation	0.10	200	0.052	840
Full-bodied red brick	0.38	1800	0.65	880
Cement-sand mortar	0.02	1700	0.87	840
<i>Variant 3</i> ( $R = 3.27 \text{ m}^2 \cdot \text{C}^0/\text{W}$ )				
Facing brick	0.12	1350	0.47	880
Basalt insulation	0.10	200	0.052	840
Full-bodied red brick	0.38	1450	0.44	840
Cement-sand mortar	0.02	1700	0.87	840



**Fig. 1** Temperature distribution over the wall thickness for various variants of multilayer enclosing structures (Table 1): 1a-at  $t = 0$  and 1b-24 h after the start of the thermal process

determine your law of temperature variation (8) inside the room over time, taking into account the design features of the indoor space. Calculations show that the temperature distribution is influenced by a large number of factors: the properties of materials, their thickness and the number of layers, weather conditions, especially the characteristics of insulation, the low thermal conductivity of which allows us to restrict ourselves to their small thickness of 0.1–0.2 m. Therefore, to meet modern requirements thermal protection of a building without the use of effective insulation is almost impossible. Thus, for the design of multilayer building envelopes, it is

**Fig. 2** Change in indoor air temperature over time when the outdoor temperature decreases linearly from  $-10$  to  $-25$  °C within 24 h



necessary to carry out computer modeling of heat transfer processes for various options of fence materials to control the temperature inside the room and select the best option for maintaining the thermal regime, taking into account the total financial costs.

## 4 Conclusion

In engineering calculations, the thermophysical characteristics of the enclosing structures, as a rule, are determined for a stationary thermal regime. In real conditions, the process of heat transfer through the enclosing structures is unsteady, because weather conditions change: the outside air temperature, the intensity of solar radiation, the strength and direction of the wind, and therefore the temperature inside the room. Therefore, the process of heat transfer through the enclosing structures should be considered unsteady. In addition, the process depends on the type and quantity of the enclosing materials and the thickness of the layers, on their thermophysical properties. Thus, multilayer building envelopes and the heat transfer process depend on a large number of factors and parameters, i.e. are large and complex distributed systems and can be thought of as a cyber-physical system. At the same time, the key to a cyber-physical system is the mathematical model of the process. Computer simulation of the heat transfer process allows you to control the temperature conditions inside the room and select materials for the enclosing structures, heating devices, their power and regulate the temperature inside the room. As a result, it is possible to formulate an optimization problem taking into account the type, quantity, and cost of materials, construction work, and energy consumption for heating buildings.

## References

1. Basok, B.I., Noviko, V.G., Davydenko, B.V., Belyaeva, T.G., Novitskaya, M.P., Sorokovoi, R.Y.: Radiative-convective heat exchange of a building with the environment on exposure to solar radiation. *J. Eng. Phys. Thermophys.* **93**(1), 45–53 (2020). <https://doi.org/10.1007/s10891-020-02089-5>
2. Gusev, S.A.: Application of SDEs to estimating solutions to heat conduction equations with discontinuous coefficients. *Numer. Anal. Appl.* **8**(2), 122–134 (2015). <https://doi.org/10.1134/S1995423915020044>
3. Sadykov, R.A.: Transfer process in multilayered shielding constructions and facilities. *News KGASU* **1**(14), 66–70 (2014)
4. Tarasova, V.V.: Mathematical modeling of unsteady processes in the building envelope. *Modern High-Tech Technol.* **8**(2), 265–269 (2016)
5. Tabunchikov, Y.A., Hrometc, D.Y., Matrosov, Yu.: *Thermal Protection of Enclosing Structures of Buildings and Structures*. Stroyizdat, Moscow (1986)
6. Pastushkov, P.P.: Numerical and experimental investigation of the cooling of building envelopes after turning off the heating system. *Vestnik MGSU* **7**, 312–318 (2011). <https://doi.org/10.31659/0585-430X-2019-769-4-57-63>
7. Melnik, A.P., Chuvashv, S.N., Zorina, I.G.: Simulation of heat transfer for determination of actual thermal characteristics of buildings. *Inf. Technol.* **11**, 46–51 (2008)
8. Shevchuk, V.A., Gavris, A.P.: Nonstationary heat-conduction problem for a half-space with a multilayer coating upon cyclic change in the ambient temperature. *J. Eng. Phys. Thermophys.* **93**(6), 1543–1551 (2020)
9. Patankar, S.V.: *Numerical Heat Transfer and Fluid Flow*, p. 197. Hemisphere Publishing Corporation, McGraw-Hill (1980)
10. Fletcher, C.A.: *Computational Galerkin Methods*. Springer, New York (1984)
11. Tikhonov, A.N., Samarskii, A.A.: *Equations of Mathematical Physics*, p. 800. Courier Corporation (2013)
12. Bogoslovsky, V.N., Samarin, O.D.: Research and modeling of the natural thermal regime of a building during commissioning. *Install. Spec. Works Constr.* **6**, 19–22 (2001)
13. Malyavina, E.G.: *Heat Loss of the Building*, p. 144. Avok-Press, Moscow (2007)
14. Umnyakova, N.P.: Heat transfer through enclosing structures taking into account the radiation coefficients of the internal surfaces of the room. *Hous. Constr.* **6**, 14–17 (2014)
15. Duffie, J.A., Beckman, W.A.: *Solar Engineering of Thermal Processes*, p. 910. Wiley, New Jersey (2013)
16. SP 131.13330.2018 SNiP 23-01-99 \* *Construction climatology*. Ministry of Construction of Russia, Moskov (2018)
17. Godunov, S.K., Ryabenky, V.S.: *Difference Schemes*, p. 440. Nauka, Moskov (1973)
18. Samarsky, A.A.: *Introduction to the Theory of Difference Schemes*, p. 553. Nauka, Moskov (1971)
19. Livshits, MYu., Nenashev, A.V., Borodulin, B.B.: Efficient computational procedure for the alternance method of optimizing the temperature regimes of structures of autonomous objects. *Stud. Syst. Decis. Control* **260**, 79–90 (2020)
20. Starodub, Y., Veselivskyy, R., Vasylenko, O.: Simulation process of the heat transfer in multilayered structures. In: *MATEC Web of Conferences*, vol. 247, p. 00048 (2018) <https://doi.org/10.1051/mateconf/201824700048>
21. Gamayunova, O., Petrichenko, M., Mottaeva, A.: Thermotechnical calculation of enclosing structures of a standard type residential building. *J. Phys. Conf. Ser.* **1614**, 012066 (2020). <https://doi.org/10.1088/1742-6596/1614/1/012066>

# Calculation Features for the Heat and Power Balance in the Cyber-Physical System of Pellets Roasting on the Roasting Machine Conveyor



Vladimir Bobkov  and Maksim Dli

**Abstract** The chapter investigates chemical and power engineering processes for the production of pellets from fine-dispersed apatite-nepheline raw materials: moisture removal, dissociation of carbonates, taking into account the thermal and technological features of the roasting conveyor machines operation as complex and energy-intensive cyber-physical systems. It has been determined that in the technological zones of heating, roasting, and recuperation, the same physicochemical processes take place, differing in quantitative characteristics. The need of the charge in the heat carrier gas for the appropriate zones, the content of carbon dioxide, iron oxide, and carbon in dry pellets, which depend on the chemical composition, the degree of emission of carbon dioxide, oxidation of iron oxide, and combustion of carbon, are taken into account. For each of the zones, depending on the composition of the charge, according to the results of experimental data, the following is calculated: heat consumption for the decomposition of limestone, the specific volume of carbon dioxide, heat output during oxidation of iron oxide; oxygen consumption for oxidation of iron oxide, heat introduced by carbon dioxide, initial and final heat of the heat carrier gas. A mathematical description of the heat-and-power features for the cyber-physical systems–roasting conveyor machines operation is proposed, taking into account the thermally activated chemical and power engineering processes occurring in apatite-nepheline technogenic raw materials when heated, based on the energy- balance mathematical models.

**Keywords** Pellets · Conveyor roasting machine · Modelling · Roasting · Heat exchange · Temperature · Drying

---

V. Bobkov (✉) · M. Dli

National Research University “Moscow Power Engineering Institute” (Branch) in Smolensk, Smolensk 214013, Russia



## 1 Introduction

The most important and significant direction to ensure sustainable development of the mining and processing industry in modern Russia is the creation of energy and resource-saving technologies based on the widespread use of cyber-physical systems and digital twins [1–3]. Obviously, the greatest efficiency of energy and resource-saving should be expected in industries that consume mineral resources, which, of course, include the production of pellets from fine ore waste of mining and processing plants [4]. Tough competition in the market for pelletized enriched raw materials, especially pellets, forces mining and processing enterprises to reduce production costs and improve product quality [5, 6]. Thermal hardening of the pellets allows using fuel, which is not scarce, to improve the technological properties of the pellets, to reduce fuel and energy costs in the subsequent redistribution [7, 8]. The next important factor is the rise in the cost of heat and electrical energy spent on the production of pellets from apatite-nepheline ore waste, which leads to their constant rise in price. All the above factors determined the search for optimal energy and resource efficiency modes of the roasting conveyor machines operation for roasting pellets, based on the creation of mathematical models, taking into account the main chemical-engineering and heat and mass transfer processes occurring in the dynamic layer of pellets on the roasting machine conveyor [9, 10]. The presented work sets a problem to complete the information necessary for the mathematical description of the heat and power features of the conveyor roasting machines operation as complex cyber-physical systems, taking into account thermally activated chemical and power engineering processes occurring in the apatite-nepheline raw material, based on the energy balance mathematical models. The considered models of heat and mass transfer processes can be used to optimize the operation modes for the existing roasting conveyor machines and create their digital twins, as well as to calculate parameters in the design of cyber-physical systems [11, 12].

## 2 Heat and Power Features of the Conveyor Roasting Machine Operation

The productivity of the roasting machine, t/h for the finished pellets is  $Q_r = qF$ , where  $q$ —the specific productivity of the roasting machine,  $t/(m^2 \cdot h)$ ;  $F$ —area,  $m^2$ ;  $q = 1/(q_s^{-1} + q_c^{-1} + q_m^{-1})$ , where  $q_s, q_c, q_m$ —the specific productivity of the drying, roasting, cooling zones,  $t/(m^2 \cdot h)$  is determined by the heat demand of the pellet layer and the heat supply rate to the layer:  $q = 3600 w/v$ , where  $w$ —the specific filtration rate of the zone heat carrier gas,  $m^3/(m^2 \cdot s)$ ;  $v$ —the specific demand of the pellet layer for the zone heat carrier gas,  $m^3/t$  of the finished product.

The specific rate for the heat carrier gas filtration by zones is as follows,  $m^3/(m^2 \cdot s)$  (Table 1).

**Table 1** Specific rate

Drying with blowing	1,76
Drying with sucking	1,76
Recuperation	1
Heating I	1,6
Heating II	1,7
Roasting I	1,2
Roasting II	1,9

The specific filtration rate of each zone is taken based on practical data. The specific demand of the pellets for the heat carrier gas is determined from the heat balance of each zone. For the drying zone  $v$ ,  $m^3/t$ :

$$v_c = 1000 \Delta i_{OK} / K_1 (10W\beta_{H_2O} / K_2) (q_{H_2O} + 1, 24i_{H_2O}) / (i_r^H + i_r^K)$$

where 1000—mass for the finished product, kg;  $\Delta i_p$ —heat gain for dry pellets, J/kg;  $W$ —moister content in raw pellets, unit fraction, 0,1 is accepted for calculation; —heat consumption for water heating from 20 to 100 °C and its evaporation is taken equal to 620·4,1868 kJ/kg;  $i_{H_2O}$ —the heat of water vapour leaving the layer with exhaust gases is taken equal to 36·4,1868 kJ/m<sup>3</sup>; 1,24—specific volume of water vapor, m<sup>3</sup>/kg;  $i_g^n, i_g^k$ —initial and final heat content of the heat carrier gas, J/m;  $\beta_{H_2O}$ —the degree of moister removal in the drying zone, fraction unit, according to the practical data 100% of moister is removed;  $K_1$ —yield factor for good pellets from dry ones;  $K_2$ —coefficient of the output for roasted pellets from raw ones;  $\Delta i_p = C_k t_k - C_n t_n$ ,  $C_k, C_n$ —final and initial mass heat capacity of pellets, J/kg;  $t_k, t_n$ —final and initial pellets temperature at the beginning and end of the zone, °C (Table 1 in Chap. 2);  $K_1 = 1 - \Pi$ ,  $\Pi$ —the total quantity of losses during calcination, fines content, spills on the machine, according to the practical data [13, 14] is taken for 0,09;  $K_2 = 1 - W$  (Table 2).

In the zones of heating, roasting, and recuperation, the same physical and chemical processes take place, differing in quantitative characteristics, therefore, the specific demand of the charge for the heat carrier gas in the corresponding zones  $v_h, v_c, v_r$ ,  $m^3/t$ , is determined by the formula:

$$v_{h,c,r} = \frac{1000}{\kappa_1} \left( \frac{\Delta i_r + (972 + 0, 51 i_{CO_2} \beta_{CO_2} [CO_2])}{i_{g.n.} - i_{g.k.}} - \frac{371 - 0, 778 i_{FeO}^H [FeO] + 8100 \beta_C [C]}{i_{g.n.} - i_{g.k.}} \right)$$

where  $[CO_2], [FeO], [C]$ —respectively, the content of carbon dioxide, iron oxide and carbon in dry pellets, units fraction, is taken depending on the chemical composition of the pellets;  $\beta_{CO_2}, \beta_{FeO}, \beta_C$ —respectively, the degree of evolution of carbon dioxide, carbon combustion, units fraction, for each technological zone is taken according to the results of the experimental data for each specific case depending on the charge

**Table 2** Temperature for pellets and heat carrier gas in the technological zones of the conveyor roasting machine

Technological zone	$t_{p.n.}$ , °C	$t_{p.k.}$ , °C	$t_{g.n.}$ , °C	$t_{g.k.}$ , °C
	Pellets		Heat carrier	
Drying I (blowing)	20	70	350	170
Drying II (sucking)	10	100	350	150
Heating	100	490	720	250
Roasting	490	1200	1250	1500
Recuperation	1200	1000	850	550
Cooling I (blowing)	1000	350	–	850
Cooling II (blowing)	350	100	–	250

composition; 972.4, 1868 kJ/kg CO<sub>2</sub>—heat consumption for the limestone decomposition; 0,51 m<sup>3</sup>/kg—specific volume CO<sub>2</sub>; 371.4, 1868 kJ/kg FeO—heat output during oxidation of iron oxide; 0,778 m<sup>3</sup>/kg—oxygen consumption for oxide iron oxidation FeO;  $i_{CO_2}$ —heat contributed by CO<sub>2</sub>, J/m<sup>3</sup>;  $i_{g.n.}$ ,  $i_{g.k.}$ —initial and final heat of the heat carrier gas, J/m<sup>3</sup>.

Specific consumption of the charge in the heat carrier gas in the cooling zone, m<sup>3</sup>/t:

$$v_m = 1000(i_{p.n.} - i_{p.k.}) / K_1(i_{v.k.} - i_{v.n.}),$$

where  $i_{p.n.}$ ,  $i_{p.k.}$ —pellets heat at the beginning and the end of the cooling zone, J/kg;  $i_{v.n.}$ ,  $i_{v.k.}$ —air heat before and after the pellets layer, J/m<sup>3</sup>.

Roasting machine area, m<sup>2</sup>:  $F = F_s + F_h + F_c + F_r + F_m$ .

The area of the drying zone, m<sup>2</sup>:  $F_s = (0, 1 Q_s W E) / b$ , where  $Q_c$ —the productivity of the machine for raw pallets, t/h, with a known value of productivity for the finished product is determined by the formula:  $Q_s = Q_p(K_1 - K_2)$ ;  $W$ —pellets moister, %, is taken equal to 9,5–10,5%;  $E$ —drying efficiency, %, for zone I (blowing) is equal to 65–70%, for zone II (sucking) it is 35–30%;  $b$ —evaporation coefficient, which is equal to  $b = I_s / (x_n - x_p)$ , where  $I_s$ —drying intensity, kg/(m<sup>3</sup>·h);  $x_n$ —moister content for the saturated off-gas from the layer, kg/m<sup>3</sup>, in the calculation it is taken equal to 0,122 kg/m<sup>3</sup>;  $x_p$ —moister content of the supplied heat carrier gas, kg/m<sup>3</sup>, in calculations it is taken equal to 0,016 kg/0,3.

$$I_s = 0, 2445V(1 - m)w_f^{0,8} \varphi(x_n - x_p) / \alpha(x_n + 0, 804),$$

where  $V$ —pellets volume for 1 m<sup>2</sup> of a pallet area, m<sup>3</sup>/m<sup>2</sup>, with the pellets layer height of 0,3 m  $V = 0,3$  m<sup>3</sup>/m<sup>2</sup>;  $m$ —porosity of the pellets layer, m<sup>3</sup>/m<sup>3</sup>, in the calculation is taken equal to 0,45 m<sup>3</sup>/m<sup>3</sup>;  $w_f$ —specific filtration rate of the heat carrier, m<sup>3</sup>/(m<sup>2</sup>·c).

The length of the drying zone, m:  $l = F_c/B$ , where  $B$ —the machine width, m.

The area of the heating zone:  $l = F_s/B$ , where  $l_h$ —the length of the heating zone:  $l_h = v\tau_h$ ,  $v$ —travel velocity of the roasting pallet, m/min;  $v = Q_h/60HB\gamma_h$ ,  $H$ —the height of the raw pellets layer on the machine, m;  $\gamma$ —buck density of the raw pellets,  $t/3$ ;  $\tau_h$ —residence time of the pellets in the heating zone, min;  $\tau_h = (t_k - t_n)v_t$ ;  $t_k$ ,  $t_n$ —pellets temperature at the beginning and the end of the heating zone, respectively, °C;  $v_t$ —the heating rate of the pellets layer in the given temperature range, °C/min; taken according to the results of the experimental data; at  $t_n - t_k = 100 - 500$  °C,  $v_t = 150$  °C/min.

The area of the roasting zone, m<sup>2</sup>:  $F_c = Bl_c$ , where  $l_c$ —the length of the roasting zone, m;  $l_c = v(\tau_{c1} + \tau_{c2} + \tau_{c3})$ , where  $\tau_{c1}$ ,  $\tau_{c2}$ ,  $\tau_{c3}$ —the duration of pellets heating at permissible heating rates in a given temperature range, min;  $\tau_{c1} = (1000 - t_{c.n.})v'_t$ ,  $t_{c.n.}$ —pellets temperature at the beginning of the roasting zone, °C;  $v'_t$ —the heating rate of the pellets layer in the temperature range of 500–1000 °C;  $v'_t = 250-300$  °C/min;  $\tau_{c2} = (t_{c.max} - 1000)v''_t$ ,  $t_{c.max}$ —maximum temperature of pellets in the roasting zone, °C;  $v''_t$ —the heating rate of the pellets layer in the temperature range of 1000–1350 °C;  $v''_t = 125$  °C/min;  $\tau_{c3} = 3-5$  min—holding time of the pellets layer at the maximum temperature, taken according to the results of the experimental data depending on the required strength of the pellets.

The area of the recuperation zone, m<sup>2</sup>:  $F_r = Bl_r$ , where  $l_r$ —the length of the recuperation zone, m;  $l_r = v\tau_r$ ,  $\tau_r$ —heat treatment duration of the pellets layer in the recuperation zone, min, equal to  $\tau_r = H/v_{t.v}$ , where  $H$ —the height of the raw pellets layer, mm;  $v_{t.v}$ —velocity rate of the heatwave, mm/min, determined by the formula:  $v_{t.v} = kw_f C_t 60/\gamma_p C_M^2 (1 - m)$ , where  $k$ —the proportionality coefficient, representing the ratio of the heat capacity of the pellets flow and the heat carrier, taken equal to 1,55;  $C_M$ ,  $C_t$ —specific mass and volumetric heat capacity of the pellets and heat carrier gas, respectively, is taken equal to  $J/(kg \cdot K)$ ,  $J/(m^3 \cdot K)$  at the given temperatures;  $w_f$ —specific filtration rate, m<sup>3</sup>/(m<sup>2</sup>·c);  $\gamma_p$ —bulk density of the roasted pellets is taken equal to 0,45.

The area of the cooling zone, m<sup>2</sup>:  $F_m = Bl_m$ , where  $l_m$ —the length of the cooling zone, m;  $l_m = v\tau_m$ ,  $\tau_m$ —the duration of cooling the pellets layer to the given temperature  $t$ , min, determined from the ration of the temperature non-dimensional coefficient for the pellets and heat carrier gas— $Y = \alpha_{\Sigma V} H/3600VC_g$  and  $Z = \alpha_V \tau_0/60C_M \gamma_p$ ; where  $C_g$ —specific volumetric heat capacity of the heat carrier gas (air) at the given temperature,  $C_M$ —specific mass heat capacity of the pellets,  $J/(kg \cdot K)$  shown in Fig. 1;  $\alpha_{\Sigma V}$ —total heat transfer volumetric coefficient,  $W/(m^3 \cdot K)$ ,  $V$ —the quantity of air entering the zone, m<sup>3</sup> [16, 17].

$1/\alpha_{\Sigma V} = 1/\alpha_V + R^2/15(1 - m)\lambda$ , where  $\alpha_V$ —external heat transfer coefficient,  $W/(m^2 \cdot K)$ ,  $R$ —pellet radius is taken equal to 0,0065 m,  $\lambda$ —heat conductivity of pellets,  $W/(m \cdot K)$ , is taken according to the results of the experimental data, shown in Fig. 2.

The external heat transfer coefficient  $\alpha_V = Aw_f^{0,9} T_v^{0,3} M/d^{0,75}$ , where  $A$ —dependence coefficient for the properties of mining and processing plants wastes during their heat treatment, with the range of variation 150–219, a low value is taken during roasting, a higher value is taken during cooling;  $M$ —the coefficient considers the

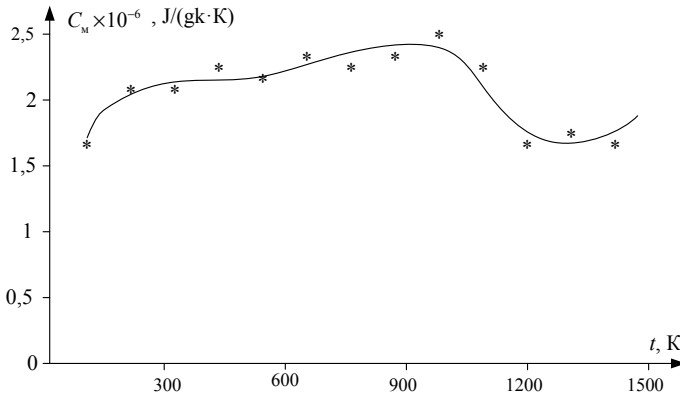


**Fig. 1** Dependence for the specific mass heat capacity of pellets from apatite-nepheline ores waste on temperature

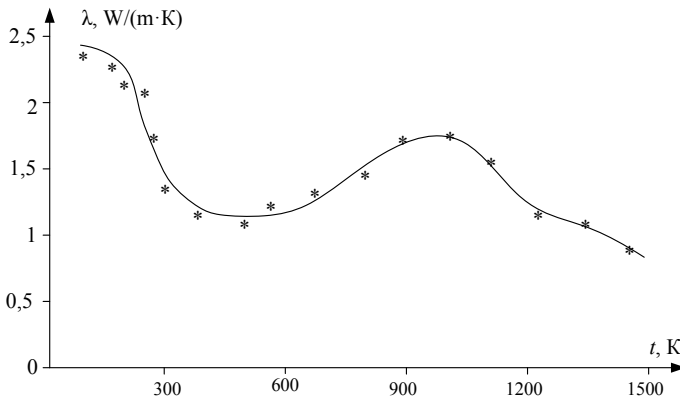


**Fig. 2** Dependence for the thermal conductivity coefficient of pellets from apatite-nepheline ores waste on temperature

presence of a fine fraction is taken within 0,7–0,9;  $d$ —the pellet average diameter, in the calculation is taken equal to 0,013 m;  $T_v$ —the air average temperature in a layer, K [18, 19].

The quantity of the bottom bed,  $t/h$ :  $Q_d = 60vH_dB_1\gamma$ , where  $H_d$ —the height of the bottom bed, m, is taken equal to 0,07–0,1 m.

The quantity of the side bed:  $Q_b = 60vH_bB_1\gamma$ , where  $H_b$ —the height of the side bed, m, is taken equal to 0,4 m;  $B_1$ —the width of the side bed layer, m, is taken equal to 0,08 for both sides [20, 21].

### 3 Results Analysis

The developed mathematical description for the heat and power engineering features of the conveyor roasting machines operation allows performing the following functions:

1. Automatize the control for the parameters of the engineering processes (centralized collection and information primary processing), as well as control over the state of technological objects (processes, devices).
2. Technical control and accounting of the apatite-nepheline pellets production.
3. Determination of the operational technical and economic indicators.
4. Managing the chemical and power engineering processes: stabilization of parameters at a given level; optimal control in transient technological modes; optimal control for the steady modes of engineering processes.
5. Operational analysis and control of pellets production.

At the pelletizing plants of modern Russia, the automation level of the production processes for pelletizing fine-dispersed technogenic raw materials is significantly different. Table 3 shows the parameters of various types for roasting machines, which are possible (plus) or impossible (minus) to control and adjust automatically.

Based on the developed mathematical description for the heat and power features of the conveyor roasting machines operation, taking into account the thermally activated chemical and power engineering processes occurring in the apatite-nepheline raw materials, based on energy-balance mathematical models, computational experiments were carried out using the developed computer programs complex [22, 23]. The temperature results for the heat carrier gas and the rate of its supply in the corresponding vacuum chambers of the conveyor roasting machine are presented in Table 4.

Using the developed mathematical and computer models, a complex of computer programs, experiments were carried out to determine the operating parameters of roasting at various physicochemical characteristics of the initial apatite-nepheline fine-dispersed raw materials in raw pellets and the external flow of the heat carrier gas, which showed good agreement between calculated and experimental data [24, 25].

The scientific novelty of the obtained research results consists in the developed mathematical and computer models, a complex of computer programs that differ

**Table 3** Adjustable and controlled parameters for the conveyor roasting machines

Parameters	Roasting machine type			
	OK-108	OK-306	OK-520	OK-520/536
Material flow	–	+	+	+
Machine thermal condition	+	+	+	+
Gas flows	–	–	+	+
Consumption, pressure and temperature of the cooling water	+	+	+	+

**Table 4** The temperature of the heat carrier gas and the rate of its supply in the vacuum chambers of the OK-520/536 conveyor roasting machine in the scheduled mode

	№ vacuum chambers	The supply rate of the heat carrier gas, m/s	The temperature of the heat carrier gas, °C			
			Above the pellets layer	At a pellets layer depth of 17sm	At a pellets layer depth of 34sm	In vacuum chambers
Zero camera	1	0.5 ↓	200	79	57	51
Drying I	2	1.1 ↑	42	63	101	230
	3		51	74	109	240
	4		63	81	115	250
Drying II	5	1.0 ↑	65	93	122	330
	6		68	99	129	340
	7		71	101	134	345
	8		78	108	142	350
	9		82	114	149	355
Drying III	10	0.65 ↓	325	271	245	212
	11		400	299	263	251
Heating	12	0.65 ↓	800	408	313	288
	13		900	473	417	332
Roasting	14	0.65 ↓	950	508	491	367
	15		1000	601	532	405
	16		1050	677	593	443
	17		1100	714	621	465
	18		1150	753	669	478
	19		1200	789	696	485
	20		1200	813	737	493
	21		1200	837	761	499
Recuperation	22	0.65 ↓	1000	854	796	503
	23		900	881	832	517
Cooling I	24	1.05 ↑	824	819	801	200
	25		811	788	753	195
	25		802	745	706	190
	27		791	709	652	185
	28		733	687	608	180

(continued)

**Table 4** (continued)

	№ vacuum chambers	The supply rate of the heat carrier gas, m/s	The temperature of the heat carrier gas, °C			
			Above the pellets layer	At a pellets layer depth of 17sm	At a pellets layer depth of 34sm	In vacuum chambers
Cooling II	29	1.2 ↑	620	549	502	40
	30		417	403	399	35
	31		334	312	245	30
	32		198	181	124	25
	33		163	92	71	20

from the known ones [26, 27], taking into account the indicators dependence of the apatite-nepheline pellets on the characteristics of the initial fine-dispersed raw materials, as well as the influence of these indicators on the quality of roasted pellets arriving for melting in ore-thermal furnaces.

## 4 Conclusion

The results presented are significant for the methods development of the processes analysis and modelling of the roasting pelletized apatite-nepheline raw materials in the conveyor multi-chamber roasting machines and can be used in the algorithmic support of decision-making systems when optimizing the energy consumption of the entire technological system for the production of finished pellets and especially when designing cyber-physical systems and digital twins for roasting conveyor machines.

The developed mathematical model gives qualitative and quantitative dependences of the thermal parameters of apatite-nepheline pellets roasting and allows analyzing the effect of any of them on the behaviour of a complex chemical and power engineering system for the pellets production from technogenic fine-dispersed waste from apatite-nepheline ore mining and processing plants, to reveal the energy-saving potential, and finally, to increase its energy and resource efficiency, based on the optimization of the described chemical and power engineering processes.

**Acknowledgements** The study was funded by RFBR according to the research project No 18-29-24094 MK and with financial support within government research activities, project No FSWF-2020-0019.



## References

1. Bolshakov, A., Kulik, A., Sergushov, I., Scripal, E.: Decision support algorithm for parrying the threat of an accident. In: Kravets, A.G., et al. (eds.) *Cyber-Physical Systems: Industry4.0 Challenges, Studies in Systems, Decision and Control*, vol. 260, pp. 237–247. Springer NatureSwitzerland AG (2020)
2. Gaiduk, A.R., Neydorf, R.A., Kudinov, N.V.: Application of cut-glue approximation in analytical solution of the problem of nonlinear control design. In: *Cyber-Physical Systems: Industry4.0 Challenges*, pp. 117–132. Springer (2020)
3. Kizim, A.V., Kravets, A.G.: On systemological approach to intelligent decision-making support in industrial cyber-physical systems. *Stud. Syst. Decis. Control* **260**, 167–183 (2020)
4. Leontyev, L.I., Grigorovich, K.V., Kostina, M.V.: Fundamental research as a base of creating new materials and technologies in the field of metallurgy. Part 1. *Institution News. Ferr. Metall.* **61**(1), 11–22 (2018)
5. Gurin, I.A., Lavrov, V.V., Spirin, N.A., Nikitin, A.G.: Web technologies for building information-modelling systems for technological processes in metallurgy. *Higher education news. Ferr. Metall.* **60**(7), 573–579 (2017)
6. Nayak, D., Ray, N., Dash, N., Pati, S., De, P.S.: Induration aspects of low-grade ilmenite pellets: Optimization of oxidation parameters and characterization for direct reduction application. *Powder Technol.* **380**, 408–420 (2021)
7. Bragin, V.V., Bokovikov, B.A., Naidich, M.I., Gruzdev, A.I., Shvydkii, V.S.: Relation between the productivity and fuel consumption in roasting machines. *Steel Transl.* **44**(8), 590–594 (2014)
8. Wang, S., Guo, Y., Zheng, F., Chen, F., Yang, L.: Improvement of roasting and metallurgical properties of fluorine-bearing iron concentrate pellets. *Powder Technol.* **376**, 126–135 (2020)
9. Matkarimov, S.T., Berdiyarov, B.T., Yusupkhodjayev, A.A.: Technological parameters of the process of producing metallized iron concentrates from poor raw material. *Int. J. Innov. Technol. Explor. Eng.* **8**(11), 600–603 (2019)
10. Li, J., An, H.F., Liu, W.X., Yang, A.M., Chu, M.S.: Effect of basicity on metallurgical properties of magnesium fluxed pellets. *J. Iron. Steel Res. Int.* **27**(3), 239–247 (2020)
11. Shishov, A.A., Bogomolov, A.V.: Physiological justification of an adequate way out of an emergency situation in high-altitude flight. *Aerosp. Environ. Med.* **54**(2), 65–71 (2020)
12. Kravets, A.G., Bolshakov, A.A., Shcherbakov, M.V.: *Cyber-Physical Systems: Advances in Design & Modelling*, 340 p. Springer (2019). <https://doi.org/10.1007/978-3-030-32579-4>
13. Tian, H., Pan, J., Zhu, D., Wang, D., Xue, Y.: Utilization of ground sinter feed for oxidized pellet production and its effect on pellet consolidation and metallurgical properties. In: *Minerals, Metals and Materials Series. 11th International Symposium on High-Temperature Metallurgical Processing*, pp. 857–866 (2020)
14. Bobkov, V.I., Borisov, V.V., Dli, M.I., Meshalkin, V.P.: Multicriterial optimization of the energy efficiency of the thermal preparation of raw materials. *Theor. Found. Chem. Eng.* **49**(6), 842–846 (2015)
15. Bobkov, V.I., Borisov, V.V., Dli, M.I., Meshalkin, V.P.: Intensive technologies for drying a lump material in a dense bed. *Theor. Found. Chem. Eng.* **51**(1), 70–75 (2017)
16. Bokovikov, B.A., Bragin, V.V., Shvydkii, V.S.: Role of the thermal-inertia zone in conveyer roasting machines. *Steel Transl.* **44**(8), 595–601 (2014)
17. Akberdin, A.A., Kim, A.S., Sultangaziev, R.B.: Planning of numerical and physical experiment in the simulation of technological processes. *Institution news. Ferr. Metall.* **61**(9), 737–742 (2018)
18. Shvydkii, V.S., Fakhudinov, A.R., Devyatykh, E.A., Spirin, N.A.: To the mathematical modeling of layered metallurgical furnaces and units. *Institution news. Ferr. Metall.* **60**(1), 19–23 (2018)
19. Yuryev, B.P., Goltsev, V.A.: Change in the equivalent porosity of the pellet bed along the length of the indurating machine. *Institution news. Ferr. Metall.* **60**(2), 116–123 (2018)

20. Shvydkii, V.S., Yaroshenko, Y.G., Spirin, N.A., Lavrov, V.V.: Mathematical model of roasting process of ore and coal pellets in a indurating machine. *Institution news. Ferr. Metall.* **60**(4), 329–335 (2018)
21. Novichikhin, A.V., Shorokhova, A.V.: Control procedures for the step-by-step processing of iron ore mining waste. *Institution news. Ferr. Metall.* **60**(7), 565–572 (2018)
22. Tian, Y., Qin, G., Zhang, Y., Zhao, L., Yang, T.: Experimental research on pellet production with boron-containing concentrate. In: *Characterization of Minerals, Metals, and Materials*, pp. 91–102 (2020)
23. Yaroshenko, Y.G.: Thermal physics as the basis for energy and resource conservation in steelmaking. *Steel Transl.* **47**(8), 505–516 (2017)
24. Yang, C.C., Zhu, D.Q., Pan, J., Zhou, B.Z., Xun, H.: Oxidation and induration characteristics of pellets made from western Australian ultrafine magnetite concentrates and its utilization strategy. *J. Iron. Steel Res. Int.* **23**(9), 924–932 (2017)
25. Zhuravlev, F.M., Lyalyuk, V.P., Tarakanov, A.K., Chuprinov, E.V., Kassim, D.A.: Metallurgical characteristics of unfluxed pellets produced from concentrates with different mineral content. *Steel Transl.* **46**(6), 419–427 (2016)
26. Qing, G., Tian, Y., Zhang, W., Wang, X., Huang, W., Dong, X., Li, M.: Study on application of iron ore fine in pelletizing. In: *Minerals, Metals and Materials Series, Part F8*, pp. 279–285 (2018)
27. Gan, M., Ji, Z., Fan, X., Lv, W., Zheng, R., Chen, X., Liu, S., Jiang, T.: Preparing high-strength titanium pellets for ironmaking as furnace protector: optimum route for ilmenite oxidation and consolidation. *Powder Technol.* **333**, 385–393 (2018)